

**Ongoing Face Recognition  
Vendor Test (FRVT)**  
**Part 1: Verification**

Patrick Grother  
Mei Ngan  
Kayee Hanaoka  
Joyce C. Yang  
Austin Hom

*Information Access Division  
Information Technology Laboratory*

This publication is available free of charge from:  
<https://www.nist.gov/programs-projects/face-recognition-vendor-test-frvt-ongoing>

2022/01/20

## ACKNOWLEDGMENTS

The authors are grateful for the long-standing support and collaboration of the the Department of Homeland Security's Science & Technology Directorate (S&T) and the Office of Biometric Identity Management (OBIM).

Additionally, the authors are grateful to staff in the NIST Biometrics Research Laboratory for infrastructure supporting rapid evaluation of algorithms.

## DISCLAIMER

Specific hardware and software products identified in this report were used in order to perform the evaluations described in this document. In no case does identification of any commercial product, trade name, or vendor, imply recommendation or endorsement by the National Institute of Standards and Technology, nor does it imply that the products and equipment identified are necessarily the best available for the purpose.

## INSTITUTIONAL REVIEW BOARD

The National Institute of Standards and Technology's Research Protections Office reviewed the protocol for this project and determined it is not human subjects research as defined in Department of Commerce Regulations, 15 CFR 27, also known as the Common Rule for the Protection of Human Subjects (45 CFR 46, Subpart A).

## FRVT STATUS

**This report** is a draft NIST Interagency Report, and is open for comment. It is the thirty sixth edition of the report since the first was published in June 2017. Prior editions of this report are maintained on the FRVT [website](#), and may contain useful information about older algorithms and datasets no longer used in FRVT.

**FRVT remains open:** All [four tracks](#) of the FRVT are open to new algorithm submissions.

**2022-01-20** changes since 2021-12-18:

- ▷ We have added results for first algorithms from four developers: Armatura, Beyne.AI, One More Security, and VinBigData
- ▷ We have added results for new algorithms from 19 returning developers: AuthenMetric, BOE Technology Group, Cybercore, Cyberlink, Dahua Technology, FaceTag Co, Innovatrics, Megvii, Mobbeel Solutions, Neurotechnology, Oz Forensics, Rank One Computing, Regula Forensics, Samsung S1, Securif AI, Sensetime Group, TigerIT Americas, Videmo Intelligente Videoanalyse, and YooniK.
- ▷ We have retired results for 14 algorithms per our policy to only list results for two algorithms per developer. Results for retired algorithms appear in prior versions of this report in the [archive](#).

**2021-12-16** changes since 2021-11-22:

- ▷ We have added results for first algorithms from five developers: Alfabeta, Cloudmatrix, Euronovate SA, FaceOnLive Inc, and Mobicin Technology.
- ▷ We have added results for new algorithms from ten returning developers: ACI Software, ITMO University, NEO Systems, Guangzhou Pixel Solutions, Panasonic R+D Center Singapore, Qnap Security, Scanovate, Tevian, Unissey, and Vietnam Posts and Telecommunications Group.
- ▷ We have retired results for eight algorithms per our policy to only list results for two algorithms per developer. Results for retired algorithms appear in prior versions of this report in the [archive](#).
- ▷ We have revamped Figure 19 showing performance on 20 pairs of open-source images. It now color-codes false negatives and positives against a default threshold value.

**2021-11-22** changes since 2021-10-28:

- ▷ We have added results to the [website](#) for kiosk-collected images where the design and geometry configuration mean that many images have considerable downward pitch angle. In some images, the face is partially cropped. Some images have other background faces.
- ▷ We have stopped using child exploitation images in FRVT, as we lost access to the imagery. All results for that set have been removed from the [website](#), and will be removed from future PDF reports.
- ▷ We have added results for first algorithms from seven new developers: CUDO Communication, Daon, KuKe3D Technology, Mantra Softtech India, Maxvision Technology, Multi-Modality Intelligence, and Samsung-SDS.
- ▷ We have added results for new algorithms from seven returning developers: Acer Incorporated, Cloudwalk-Moontime Smart Technology, Gorilla Technology, ID3 Technology, Incode Technologies, NSENSE Corp., and SQIssoft.
- ▷ We have retired results for six algorithms per our policy to only list results for two algorithms per developer. Results for retired algorithms appear in prior versions of this report in the [archive](#).

**2021-10-28 changes since 2021-09-08:**

- ▷ We have substantially revised the algorithm-specific report cards that are linked from the [FRVT results page](#). (Example: [HTML](#)).
- ▷ We have added results for first algorithms from eight new developers: Beijing Mendaxia Technology, Beijing Hisign Technology, Biocube Matrics, Clearview AI, Reveal Media, Toppan ID Gate, Verigram, and Viettel High Technology.
- ▷ We have added results for new algorithms from thirty returning developers: 20Face, 3divi, Canon Inc Chunghwa Telecom, Corsight, Decatur Industries, Deepglint, Dermalog, FaceTag, Fiberhome Telecommunication Technologies, GeoVision, ICM Airport Technics, Imagus Technology, InsightFace AI, Kakao Enterprise, Kookmin University, Line Corporation, N-Tech Lab, NotionTag Technologies, Realnetworks, Suprema ID, Taiwan-Certificate Authority, Toshiba, Tripleize, Trueface.ai, Veridas Digital Authentication, Visidon, VisionLabs, YooniK, and Yuan High-Tech Development.
- ▷ We have retired results for twenty algorithms per our policy to only list results for two algorithms per developer. Results for retired algorithms appear in prior versions of this report in the [archive](#).

**2021-09-08 changes since 2021-08-02:**

- ▷ We have added results for first algorithms from seven new developers: Griaule, SQISoft, Qnap Security, Techsign, Smart Engines, Verihubs, and Wuhan Tianyu Information Industry.
- ▷ We have added results for new algorithms from sixteen returning developers: ADVANCE.AI, AuthenMetric, CloudSmart Consulting, Code Everest Pvt, Cognitec Systems, Thales Gemalto Cogent, Intel Research Group, Omnidarde, Oz Forensics, Rank One Computing, Samsung S1 Corp, Securif AI, Tevian, TigerIT Americas, Universidade de Coimbra, and Vigilant Solutions
- ▷ We have retired results for eleven algorithms per our policy to only list results for two algorithms per developer. Results for retired algorithms appear in prior versions of this report in the [archive](#).

**2021-08-02 changes since 2021-06-25:**

- ▷ We have added results for first algorithms from eight new developers: Bee the Data, Closeli Inc, Coretech Knowledge Inc, Deepsense (France), ioNetworks Inc, Kakao Pay Corp, Seventh Sense Artificial Intelligence, and SK Telecom.
- ▷ We have added results for new algorithms from fifteen returning developers: Alchera Inc, Adera Global PTE, Aware, Bresee Technology, Cyberlink Corp, Expasoft LLC, Fujitsu Research and Development Center, Gorilla Technology, Idemia, Neurotechnology, NEO Systems, NHN Corp, Paravision, Panasonic R+D Center Singapore, and Shenzhen University-Macau University of Science and Technology.
- ▷ We have retired results for twelve algorithms per our policy to only list results for two algorithms per developer. Results for retired algorithms appear in prior versions of this report in the [archive](#).

**2021-06-25 changes since 2021-05-21:**

- ▷ We have added results for first algorithms from six new developers: Alice Biometrics, BOE Technology Group, Fincore, Neosecu, Sodec App, and Yuntu Data and Technology.

- ▷ We have added results for new algorithms from seven returning developers: Incode Technologies, HyperVerge, Mobbeel Solutions, Guangzhou Pixel Solutions, Remark Holdings, Sensetime, and Vietnam Posts and Telecommunications Group.
- ▷ We have retired results for four algorithms per our policy to only list results for two algorithms per developer. Results for retired algorithms appear in prior versions of this report in the [archive](#).

**2021-05-21** changes since 2021-04-26:

- ▷ We have added results for first algorithms from five new developers: Ekin Smart City Technologies, Suprema ID, Tripleize, Taiwan-Certificate Authority, and Vision Intelligence Center of Meituan.
- ▷ We have added results for new algorithms from eight returning developers: ID3 Technology, Imagus Technology, Momentum Digital, N-Tech Lab, NSENSE, Shanghai Jiao Tong University, Vision-Box, and Yuan High-Tech Development
- ▷ We have retired results for seven algorithms per our policy to only list results for two algorithms per developer. Results for retired algorithms appear in prior versions of this report in the [archive](#).

**2021-04-26** changes since 2021-04-16:

- ▷ We have added results for first algorithms from three new developers: Quantasoft, Rendip, and NEO Systems.
- ▷ We have added results for new algorithms from four returning developers: 3Divi, Realnetworks, Veridas Digital Authentication Solutions, and Universidade de Coimbra.
- ▷ We have retired results for three algorithms per our policy to only list results for two algorithms per developer. Results for retired algorithms appear in prior versions of this report in the [archive](#).

**2021-04-16** changes since 2021-03-19:

- ▷ We have added results for first algorithms from six new developers: 20Face, Beijing DeepSense Technologies, BitCenter UK, Enface, FaceTag, InsightFace AI, Line Corporation, Lema Labs, Nanjing Kiwi Network Technology, Omnidarde, Regula Forensics, and Suprema.
- ▷ We have added results for new algorithms from ten returning developers: CloudSmart Consulting, Dermalog, GeoVision, Neurotechnology, Panasonic R+D Center Singapore, Samsung S1, Securif AI, Trueface.ai, Vigilant Solutions, and Visidon.
- ▷ We have retired results for ten algorithms per our policy to only list results for two algorithms per developer. Results for retired algorithms appear in prior versions of this report in the [archive](#).

**2021-03-19** changes since 2021-03-05:

- ▷ We have added results for first algorithms from six new developers: Ajou University, AuthenMetric, Code Everest, Corsight, Papilon Savunma, and NHN Corp
- ▷ We have added results for new algorithms from seven returning developers: Alchera, Deepglint, Fiber-home Telecommunication Technologies, Kakao Enterprise, Kookmin University, Megvii/Face++, and NotionTag Technologies.

- ▷ We have updated many of the hyperlinked HTML report-cards to include seven figures on demographic dependence. Figures of this kind first appeared, and are documented in, the December 2019 document, [NIST Interagency Report 8280](#) on demographic differentials in face recognition. The figures quantify false negative dependence on demographics using “visa-border” comparisons, and false positive dependence using comparisons of “application” photos that uniformly of quality and similar to visa photos.

**2021-03-05** changes since 2021-01-19:

- ▷ We have added results for first algorithms from three new developers: IVA Cognitive, Mobbeel, and MoreDian Technology.
- ▷ We have added results for new algorithms from returning developers: Ability Enterprise - Andro Video, ACI Software, Adera Global, AnyVision, BioID Technologies, China Electronics Import-Export, Cognitec Systems, Fujitsu Research and Development Center, Glory, Guangzhou Pixel Solutions, Hengrui AI Technology, Incode Technologies, Intel Research, iQIYI, Mobai, Oz Forensics, Paravision, VisionLabs, and Xforward AI Technology.
- ▷ We have added a new “resources” tab to the main [webpage](#). It includes sortable columns for data related to speed, model size, storage, and memory consumption.
- ▷ We have retired results for 13 algorithms per our policy to only list results for two algorithms per developer. Results for retired algorithms appear in prior versions of this report in the [archive](#).

**2021-01-19** changes since 2020-12-18:

- ▷ This report adds results for first algorithms from four developers: Herta Security, Irex AI, Shenzhen University-Macau University of Science and Technology, and Vietnam Posts and Telecommunications Group. See Table 6 for more information.
- ▷ The report also includes results for thirteen developers who have previously submitted algorithms: Bresee Technology, Canon (previously Canon Information Technology (Beijing)), Cyberlink, CSA IntelliCloud Technology, Dahua Technology, ID3 Technology, Imagus Technology (Vixvizon), Moontime Smart Technology, N-Tech Lab, Thales Cogent, Veridas Digital Authentication Solutions, Vocord, and Yuan High-Tech Development.
- ▷ We have retired results for ten algorithms per our policy to only list results for two algorithms per developer. Results for retired algorithms appear in prior versions of this report in the [archive](#).

**2020-12-18** changes since 2020-10-09:

- ▷ This report adds results for first algorithms from ten developers: BitCenter UK, CloudSmart Consulting, Cubox, Institute of Computing Technology, Naver Corp, Minivision, NSENSE Corp, Viettel Group, Visage Technologies, and Xiamen University. See Table 6 for more information.
- ▷ The report also includes results for eighteen developers who have previously submitted algorithms: ADVANCE.AI, Awidit Systems, Chosun University, Dermalog, GeoVision, ICM Airport Technics, Idemia, Institute of Information Technologies, Kakao Enterprise, Neurotechnology, Panasonic R+D Center Singapore, Rank One Computing, SenseTime Group, Shanghai Jiao Tong University, TigerIT Americas LLC, Vigilant Solutions, Winsense, and YooniK

- ▷ We have retired results for twelve algorithms per our policy to only list results for two algorithms per developer. Results for retired algorithms appear in prior versions of this report in the [archive](#).

#### **Changes since September 18, 2020:**

- ▷ This report adds results for first algorithms from five developers: Aigen, Cortica, Kookmin University, Securif AI and Vinai.
- ▷ The report also includes results for three developers who have previously submitted algorithms: Fujitsu Laboratories, Hengrui AI, and X-Forward AI.
- ▷ In the per-algorithm report-cards linked from tables and the main webpage, we have added a chart to showing reduction in error rates over the course of FRVT i.e. from 2017 onwards for all algorithms supplied by that developer. Similarly we have added a chart showing error rate reductions for our test of protective face mask verification.
- ▷ We plan to continue evaluating algorithms on various mask datasets. We hold that algorithms should be capable of detecting masks and verifying identity of all combinations of masked and unmasked faces. We have accordingly increased the amount of time allowed to extract those features from 1.0 to 1.5 seconds.

#### **Changes since August 25, 2020:**

- ▷ This report adds results for first algorithms from eight new developers. Akurat Satu Indonesia, Cybercore, Decatur Industries, Innef Labs, Satellite Innovation/Eocortex, Expasoft, and Mobai.
- ▷ The report includes results for seven developers who have previously submitted algorithms: 3Divi, BioID Technologies, Incode Technologies, Innovatrics, iSAP Solution, Synology, and Tevian.
- ▷ We have retired results for five algorithms per our policy to only list results for two algorithms per developer. Results for retired algorithms appear in prior versions of this report in the [archive](#).

#### **Changes since July 27, 2020:**

- ▷ We have introduced per-algorithm report sheets. These are HTML documents linked from the accuracy tables in this report (i.e. Table 24) and on the FRVT 1:1 [homepage](#). The sheets contain interactive graphics allowing, for example, mouseover exploration of FNMR(T) and FMR(T). Some of their content had previously appeared in this document.
- ▷ This report adds results for algorithms from six new developers. ACI Software, Bresee Technology, Fiberhome Telecommunication Technologies, Imageware Systems, Oz Forensics, and Pensees.
- ▷ The report includes results for thirteen developers who have previously submitted algorithms: Canon Information Technology (Beijing), Cyberlink, Dahua Technology, Gorilla Technology, ID3 Technology, Intel Research Group, iQIYI Inc, Momentum Digital, Netbridge Technology, Tech5 SA, Shenzhen AiMall Tech, Vigilant Solutions, and VisionLabs.
- ▷ We have retired results for nine algorithms per our policy to only list results for two algorithms per developer. Results for retired algorithms appear in prior versions of this report in the [archive](#).

#### **Changes since May 18, 2020:**

- ▷ The report is the first FRVT update since the pandemic closed it from March to June 2020.

- ▷ This report includes results for algorithms from nine new developers: GeoVision Inc, Su Zhou NaZhi-TianDi Intelligent Technology, YooniK, AYF Technology, PXL Vision AG, Yuan High-Tech Development, Beihang University-ERCACAT, ICM Airport Technics, and Staqu Technologies
- ▷ This report includes results for algorithms from 15 returning developers Acer Incorporated, Antheus Technologia, Chosun University, Chunghwa Telecom, Idemia, Moontime Smart Technology, Neurotechnology, Guangzhou Pixel Solutions, Panasonic R+D Center Singapore, Rank One Computing, Scanovate, Shanghai University - Shanghai Film Academy, Synesis, Trueface.ai, and Veridas Digital Authentication Solutions
- ▷ We have retired results for ten algorithms per our policy to only list results for two algorithms per developer. Results for retired algorithms appear in prior versions of this report in the [archive](#).
- ▷ We separated timing and other resource consumption from the main participation table. The new Table 15 includes template generation durations for four kinds of images, not just mugshots.
- ▷ We have published a separate report, [NIST Interagency Report 8311](#) on accuracy of pre-pandemic algorithms on subjects wearing face masks. We plan to track improvements in accuracy on masked images going forward. In particular, we invite submission of algorithms that can detect whether a person is wearing a mask, extract features from the full face or the exposed periocular region, and do appropriate comparison. We do not intend to evaluate algorithms that assume 100% of images will be of masked individuals.

#### **Changes since March 25, 2020:**

- ▷ The report is a maintenance release - it does not add any new algorithms, and FRVT has been closed to new algorithms since mid March 2020.
- ▷ We modified the primary accuracy summary, Table 24, as follows:
  - ▷▷ For visa images, the column for FNMR at FMR = 0.0001 has been removed. The visa images are so highly controlled that the error rates for the most accurate algorithms are dominated by false rejection of very young children and by the presence of a few noisy greyscale images. For now, two visa columns remain: FNMR at  $FMR = 10^{-6}$  and, for matched covariates, FNMR at  $FMR = 10^{-4}$ .
  - ▷▷ We have inserted a new column labelled "BORDER" giving accuracy for comparison of moderately poor webcam border-crossing photos that exhibit pose variations, poor compression, and low contrast due to strong background illumination. The accuracies are the worst from all cooperative image datasets used in FRVT.
- ▷ Accordingly, we updated the failure-to-template rates in Table 31.
- ▷ We withdrew a figure showing how false matches are concentrated in certain visa images used in cross-comparison, because it didn't attempt to include demographic information.

#### **Changes since February 27, 2020:**

- ▷ The report adds results algorithms from two new developers: Beijing Alleyes Technology, and the Chinese University of Hong Kong. Results for newly submitted algorithms from two other developers will appear in the next report.
- ▷ The report adds results for algorithms from thirteen returning developers: ASUSTek Computer, Aware, Cyberlink Corp, Gorilla Technology, Innovative Technology, Kakao Enterprise, Lomonosov Moscow State University, Panasonic R+D Center Singapore, Shenzhen AiMall Technology, Shenzhen Intellifusion Technologies, Synology, Tech5 SA, and Via Technologies.

- ▷ Per policy to only list results for two algorithms per developer, we have dropped results for algorithms from Aware, Cyberlink, Gorilla Technology, Kakao Enterprise, Lomonosov Moscow State University, Panasonic R+D Center Singapore, and Tech5 SA.

### **Changes since January 20, 2020:**

- ▷ The report adds results for five new developers: Ability Enterprise (Andro Video), Chosun University, Fujitsu Research and Development Center, University of Coimbra, and Xforward AI Technology.
- ▷ The report adds results for algorithms from six returning developers: AlphaSSTG, Incode Technologies, Kneron, Shanghai Jiao Tong University, Vocord, and X-Laboratory.
- ▷ We have corrected template comparison timing numbers for algorithms submitted September 2019 to January 2020. The values reported previously were slower due to a software bug.
- ▷ We have dropped results for algorithms from Vocord and Incode per policy to only list results for two algorithms per developer.
- ▷ The [FRVT 1:1 homepage](#) has been updated with latest accuracy results.
- ▷ The [FRVT 1:N homepage](#) now includes an update to the September 2019 NIST Interagency Report 8271. The new report adds results for one-to-many search algorithms submitted to NIST from June 2019 to January 2020.

### **Changes since January 6, 2020:**

- ▷ Section 2 has been updated to better describe the Visa and Border images. The caption for Table 24 has been updated to better relate the accuracy values to particular image comparisons.
- ▷ The report adds results for five new developers: Acer, Advance.AI, Expasoft, Netbridge Technology, and Videmo Intelligent Videoanalyse.
- ▷ The report adds results for algorithms from 7 returning developers: China Electronics Import-Export Corp, Intel Research Group, ITMO University, Neurotechnology, N-Tech Lab, Rokid, and VisionLabs.
- ▷ We have dropped results from this edition of the report per policy to only list results for two algorithms per developer: N-Tech Lab, Neurotechnology, ITMO, Visionlabs, and CEIEC.
- ▷ The [FRVT homepage](#) has been updated with latest accuracy results.

### **Changes since November 11, 2019:**

- ▷ Table 15 has been updated to include runtime memory usage. This is the first time such a quantity has been reported. The value is the peak size of the resident set size logged during enrollment of single images.
- ▷ We have migrated summary results table to a new platform that supports sortable tables:  
<https://pages.nist.gov/frvt/html/frvt11.html>
- ▷ The report adds results for four new developers: Antheus Technologia, BioID Technologies SA, Canon Information Tech. (Beijing), Samsung S1 (listed in the tables as S1), and Taiwan AI Labs.
- ▷ The report adds results for algorithms from 13 returning developers: Anke Investments, Chunghwa Telecom, Deepglint, Institute of Information Technologies, iQIYI, Kneron, Ping An Technology, Paravision, KanKan Ai, Rokid Corporation, Shanghai Universiy - Shanghai Film Academy, Veridas Digital Authentication Solutions, and Videonetics Technology.

- ▷ We have dropped results from this edition of the report per policy to only list results for two algorithms per developer: remarkai-000, veridas-001, sensetime-001, iit-000, anke-003, and everai-002. Results for these are available in prior editions of this report linked from the FRVT page.
- ▷ We issued [NIST Interagency Report 8280: FRVT Part 3: Demographics](#) on 2019-12-19. It includes results for many of the algorithms covered by this report.

#### Changes since October 16, 2019:

- ▷ The report adds results for ten new developers: Ai-Union Technology, ASUSTek Computer, DiDi ChuXing Technology, Innovative Technology, Luxand, MVision, Pyramid Cyber Security + Forensic, Scanovate, Shenzhen AiMall Tech, and TUPU Technology.
- ▷ The report adds results for 12 returning developers: CTBC Bank Glory Gorilla Technology Guangzhou Pixel Solutions Imagus Technology Incode Technologies Lomonosov Moscow State University Rank One Computing Samtech InfoNet Shanghai Ulucu Electronics Technology Synesis, and Winsense.
- ▷ We have dropped results from this edition of the report per policy to only list results for two algorithms per developer: glory-000, gorilla-002, incode-003, rankone-006, and synesis-004.
- ▷ Results for five recently submitted algorithms will appear in the next report.

#### Changes since September 11, 2019:

- ▷ The report adds results for five new participants: Awidit Systems (Awiros), Momenmtum Digital (Sertis), Trueface AI, Shanghai Jiao Tong University, and X-Laboratory.
- ▷ The reports adds results for five new algorithms from returning developers: Cyberlink, Hengrui AI Technology, Idemia, Panasonic R+D Singapore, and Tevian. This causes three algorithm, to be de-listed from the report per policy to list results for two algorithms per developer.

#### Changes since July 31 2019:

- ▷ The HTML table on the [FRVT 1:1 homepage](#) has been updated to include a column for cross-domain Visa-Border verification. Results for this new dataset appeared in the July 29 report under the name "CrossEV" - these are now renamed "Visa-Border".
- ▷ The [FRVT 1:1 homepage](#) lists algorithms according to lowest mean rank accuracy:
 
$$\begin{aligned} & \text{Rank(FNMR}_{\text{VISA}} \text{ at FMR} = 0.000001) + \\ & \text{Rank(FNMR}_{\text{VISA-BORDER}} \text{ at FMR} = 0.000001) + \\ & \text{Rank(FNMR}_{\text{MUGSHOT}} \text{ at FMR} = 0.00001 \text{ after 14 years}) + \\ & \text{Rank(FNMR}_{\text{WILD}} \text{ at FMR} = 0.00001) \end{aligned}$$

This ordering rewards high accuracy across all datasets.
- ▷ The main results in Table 24 is now in landscape format to accomodate extra columns for the Visa-Border set, and mugshot comparisons after at least 12 years.
- ▷ The report adds results for nine new participants: Alpha SSTG, Intel Research, ULSee, Chungwa Telecon, iSAP Solution, Rokid, Shenzhen EI Networks, CSA Intellicloud, Shenzhen Intellifusion Technologies.
- ▷ The reports adds results for six new algorithms from returning developers: Innovatrics, Dahua Technology, Tech5 SA, Intellivision, Nodeflux and Imperial College, London. One algorithm, from Imperial has been retired, per policy to list results for two algorithms per developer.
- ▷ The cross-country false match rate heatmaps have been replotted to reveal more structure by listing countries by region instead of alphabetically.

- ▷ The next version of this report will be posted around October 18, 2019.

#### **Changes since July 3 2019:**

- ▷ The HTML table on the [FRVT 1:1 homepage](#) has been updated to list the 20 most accurate developers rather than algorithms, choosing the most accurate algorithm from each developer based on visa and mugshot results. Also, the algorithms are ordered in terms of lowest mean rank across mugshot, visa and wild datasets, rewarding broad accuracy over a good result on one particular dataset.
- ▷ This report includes results for a new dataset - see the column labelled "visa-border" in Table 5. It compares a new set of high quality visa-like portraits with a set webcam border-crossing photos that exhibit moderately poor pose variations and background illumination. The two new sets are described in sections [2.2](#) and [2.3](#). The comparisons are "cross-domain" in that the algorithm must compare "visa" and "wild" images. Results for other algorithms will be added in future reports as they become available.
- ▷ This report adds results for algorithms from 9 developers submitted in early July 2019. These are from 3DiVi, Camvi, EverAI-Paravision, Facesoft, Farbar (F8), Institute of Information Technologies, Shanghai U. Film Academy, Via Technologies, and Ulucu Electronics Tech. Six of these are new participants.
- ▷ Several other algorithms have been submitted and are being evaluated. Results will be released in the next report, scheduled for September 5. That report will include results for new datasets.
- ▷ Older algorithms from Everai, Camvi and 3DiVi, have been retired, per the policy to list only two algorithms per developer.

#### **Changes since June 20 2019:**

- ▷ This report adds results for algorithms from 18 developers submitted in early June 2019. These are from CTBC Bank, Deep Glint, Thales Cogent, Ever AI Paravision, Gorilla Technology, Imagus, Incode, Kneron, N-Tech Lab, Neurotechnology, Notiontag Technologies, Star Hybrid, Videonetics, Vigilant Solutions, Winsense, Anke Investments, CEIEC, and DSK. Nine of these are new participants.
- ▷ Several other algorithms have been submitted and are being evaluated. Results will be released in the next report, scheduled for August 1.
- ▷ Older algorithms from Everai, Thales Cogent, Gorilla Technology, Incode, Neurotechnology, N-Tech Lab and Vigilant Solutions have been retired, per the policy to list only two algorithms per developer.

#### **Changes since April 2019:**

- ▷ This report adds results for nine algorithms from nine developers submitted in early June 2019. These are from Tencent Deepsea, Hengrui, Kedacom, Moontime, Guangzhou Pixel, Rank One Computing, Synesis, Sensetime and Vocord.
- ▷ Another 23 algorithms have been submitted and are being evaluated. Results will be released in the next report, scheduled for July 3.
- ▷ Older algorithms for Rank One, Synesis, and Vocord have been retired, per the policy to list only two algorithms per developer.

#### **Changes since February 2019:**

- ▷ This report adds results for 49 algorithms from 42 developers submitted in early March 2019.
- ▷ This report omits results for algorithms that we retired. We retired for three reasons: 1. The developer submitted a new algorithm, and we only list two. 2. The algorithm needs a GPU, and we no longer allow GPU-based algorithms. 3. Inoperable algorithms.
- ▷ Previous results for retired algorithms are available in older editions of this report linked [here](#).
- ▷ The mugshot database used from February 2017 to January 2019 has been replaced with an extract of the mugshot database documented in NIST Interagency Report 8238, November 2018. The new mugshot set is described in section [2.4](#) and is adopted because:

- ▷▷ It has much better identity label integrity, so that false non-match rates are substantially lower than those reported in FRVT 1:1 reports to date - see Figure 77.
- ▷▷ It includes images collected over a 17 year period such that ageing can be much better characterized - - see Figure 277.
- ▷ Using the new mugshot database, Figure 277 shows accuracy for four demographic groups identified in the biographic metadata that accompanies the data: black females, black males, white females and white males.
- ▷ The report adds Figure 19 with results for the twenty human-difficult pairs used in the May 2018 paper *Face recognition accuracy of forensic examiners, superrecognizers, and face recognition algorithms* by Phillips et al. [1].
- ▷ The report uses an update to the wild image database that corrects some ground truth labels.
- ▷ Some results for the child exploitation database are not complete. They are typically updated less frequently than for other image sets.

## Contents

<b>ACKNOWLEDGMENTS</b>	<b>1</b>
<b>DISCLAIMER</b>	<b>1</b>
<b>INSTITUTIONAL REVIEW BOARD</b>	<b>1</b>
<b>1 METRICS</b>	<b>45</b>
1.1 CORE ACCURACY . . . . .	45
<b>2 DATASETS</b>	<b>46</b>
2.1 VISA IMAGES . . . . .	46
2.2 APPLICATION IMAGES . . . . .	46
2.3 BORDER CROSSING IMAGES . . . . .	46
2.4 MUGSHOT IMAGES . . . . .	47
2.5 WILD IMAGES . . . . .	47
<b>3 RESULTS</b>	<b>47</b>
3.1 TEST GOALS . . . . .	47
3.2 TEST DESIGN . . . . .	48
3.3 FAILURE TO ENROLL . . . . .	51
3.4 RECOGNITION ACCURACY . . . . .	58
3.5 GENUINE DISTRIBUTION STABILITY . . . . .	277
3.5.1 EFFECT OF BIRTH PLACE ON THE GENUINE DISTRIBUTION . . . . .	277
3.5.2 EFFECT OF AGEING . . . . .	310
3.5.3 EFFECT OF AGE ON GENUINE SUBJECTS . . . . .	335
3.6 IMPOSTOR DISTRIBUTION STABILITY . . . . .	369
3.6.1 EFFECT OF BIRTH PLACE ON THE IMPOSTOR DISTRIBUTION . . . . .	369
3.6.2 EFFECT OF AGE ON IMPOSTORS . . . . .	373

## List of Tables

1 PARTICIPANT INFORMATION . . . . .	19
2 PARTICIPANT INFORMATION . . . . .	20
3 PARTICIPANT INFORMATION . . . . .	21
4 PARTICIPANT INFORMATION . . . . .	22
5 PARTICIPANT INFORMATION . . . . .	23
6 PARTICIPANT INFORMATION . . . . .	24
7 ALGORITHM SUMMARY . . . . .	25
8 ALGORITHM SUMMARY . . . . .	26
9 ALGORITHM SUMMARY . . . . .	27
10 ALGORITHM SUMMARY . . . . .	28
11 ALGORITHM SUMMARY . . . . .	29
12 ALGORITHM SUMMARY . . . . .	30
13 ALGORITHM SUMMARY . . . . .	31
14 ALGORITHM SUMMARY . . . . .	32
15 ALGORITHM SUMMARY . . . . .	33
16 FALSE NON-MATCH RATE . . . . .	34
17 FALSE NON-MATCH RATE . . . . .	35
18 FALSE NON-MATCH RATE . . . . .	36
19 FALSE NON-MATCH RATE . . . . .	37
20 FALSE NON-MATCH RATE . . . . .	38
21 FALSE NON-MATCH RATE . . . . .	39

22	FALSE NON-MATCH RATE	40
23	FALSE NON-MATCH RATE	41
24	FALSE NON-MATCH RATE	42
25	FAILURE TO ENROL RATES	51
26	FAILURE TO ENROL RATES	52
27	FAILURE TO ENROL RATES	53
28	FAILURE TO ENROL RATES	54
29	FAILURE TO ENROL RATES	55
30	FAILURE TO ENROL RATES	56
31	FAILURE TO ENROL RATES	57

## List of Figures

1	PERFORMANCE SUMMARY: FNMR VS. TEMPLATE SIZE TRADEOFF	43
2	PERFORMANCE SUMMARY: FNMR VS. TEMPLATE TIME TRADEOFF	44
3	EXAMPLE IMAGES	48
(A)	VISA	48
(B)	MUGSHOT	48
(C)	WILD	48
(D)	BORDER	48
4	PERFORMANCE ON 20 HUMAN-DIFFICULT PAIRS	59
5	PERFORMANCE ON 20 HUMAN-DIFFICULT PAIRS	60
6	PERFORMANCE ON 20 HUMAN-DIFFICULT PAIRS	61
7	PERFORMANCE ON 20 HUMAN-DIFFICULT PAIRS	62
8	PERFORMANCE ON 20 HUMAN-DIFFICULT PAIRS	63
9	PERFORMANCE ON 20 HUMAN-DIFFICULT PAIRS	64
10	PERFORMANCE ON 20 HUMAN-DIFFICULT PAIRS	65
11	PERFORMANCE ON 20 HUMAN-DIFFICULT PAIRS	66
12	PERFORMANCE ON 20 HUMAN-DIFFICULT PAIRS	67
13	PERFORMANCE ON 20 HUMAN-DIFFICULT PAIRS	68
14	PERFORMANCE ON 20 HUMAN-DIFFICULT PAIRS	69
15	PERFORMANCE ON 20 HUMAN-DIFFICULT PAIRS	70
16	PERFORMANCE ON 20 HUMAN-DIFFICULT PAIRS	71
17	PERFORMANCE ON 20 HUMAN-DIFFICULT PAIRS	72
18	PERFORMANCE ON 20 HUMAN-DIFFICULT PAIRS	73
19	PERFORMANCE ON 20 HUMAN-DIFFICULT PAIRS	74
20	ERROR TRADEOFF CHARACTERISTIC: VISA IMAGES	75
21	ERROR TRADEOFF CHARACTERISTIC: VISA IMAGES	76
22	ERROR TRADEOFF CHARACTERISTIC: VISA IMAGES	77
23	ERROR TRADEOFF CHARACTERISTIC: VISA IMAGES	78
24	ERROR TRADEOFF CHARACTERISTIC: VISA IMAGES	79
25	ERROR TRADEOFF CHARACTERISTIC: VISA IMAGES	80
26	ERROR TRADEOFF CHARACTERISTIC: VISA IMAGES	81
27	ERROR TRADEOFF CHARACTERISTIC: VISA IMAGES	82
28	ERROR TRADEOFF CHARACTERISTIC: VISA IMAGES	83
29	ERROR TRADEOFF CHARACTERISTIC: VISA IMAGES	84
30	ERROR TRADEOFF CHARACTERISTIC: VISA IMAGES	85
31	ERROR TRADEOFF CHARACTERISTIC: VISA IMAGES	86
32	ERROR TRADEOFF CHARACTERISTIC: VISA IMAGES	87
33	ERROR TRADEOFF CHARACTERISTIC: VISA IMAGES	88
34	ERROR TRADEOFF CHARACTERISTIC: VISA IMAGES	89
35	ERROR TRADEOFF CHARACTERISTIC: VISA IMAGES	90
36	ERROR TRADEOFF CHARACTERISTIC: VISA IMAGES	91
37	ERROR TRADEOFF CHARACTERISTIC: VISA IMAGES	92
38	ERROR TRADEOFF CHARACTERISTIC: VISA IMAGES	93

39	ERROR TRADEOFF CHARACTERISTIC: VISA IMAGES	94
40	ERROR TRADEOFF CHARACTERISTIC: VISA IMAGES	95
41	ERROR TRADEOFF CHARACTERISTIC: VISA IMAGES	96
42	ERROR TRADEOFF CHARACTERISTIC: VISA IMAGES	97
43	ERROR TRADEOFF CHARACTERISTIC: VISA IMAGES	98
44	ERROR TRADEOFF CHARACTERISTIC: VISA IMAGES	99
45	ERROR TRADEOFF CHARACTERISTIC: VISA IMAGES	100
46	ERROR TRADEOFF CHARACTERISTIC: VISA IMAGES	101
47	ERROR TRADEOFF CHARACTERISTIC: VISA IMAGES	102
48	ERROR TRADEOFF CHARACTERISTIC: VISA IMAGES	103
49	ERROR TRADEOFF CHARACTERISTIC: VISA IMAGES	104
50	ERROR TRADEOFF CHARACTERISTIC: VISA IMAGES	105
51	ERROR TRADEOFF CHARACTERISTIC: VISA IMAGES	106
52	ERROR TRADEOFF CHARACTERISTIC: VISA IMAGES	107
53	ERROR TRADEOFF CHARACTERISTIC: VISA IMAGES	108
54	ERROR TRADEOFF CHARACTERISTIC: VISA IMAGES	109
55	ERROR TRADEOFF CHARACTERISTIC: VISA IMAGES	110
56	ERROR TRADEOFF CHARACTERISTIC: VISA IMAGES	111
57	ERROR TRADEOFF CHARACTERISTIC: VISA IMAGES	112
58	ERROR TRADEOFF CHARACTERISTIC: VISA IMAGES	113
59	ERROR TRADEOFF CHARACTERISTIC: MUGSHOT IMAGES	114
60	ERROR TRADEOFF CHARACTERISTIC: MUGSHOT IMAGES	115
61	ERROR TRADEOFF CHARACTERISTIC: MUGSHOT IMAGES	116
62	ERROR TRADEOFF CHARACTERISTIC: MUGSHOT IMAGES	117
63	ERROR TRADEOFF CHARACTERISTIC: MUGSHOT IMAGES	118
64	ERROR TRADEOFF CHARACTERISTIC: MUGSHOT IMAGES	119
65	ERROR TRADEOFF CHARACTERISTIC: MUGSHOT IMAGES	120
66	ERROR TRADEOFF CHARACTERISTIC: MUGSHOT IMAGES	121
67	ERROR TRADEOFF CHARACTERISTIC: MUGSHOT IMAGES	122
68	ERROR TRADEOFF CHARACTERISTIC: MUGSHOT IMAGES	123
69	ERROR TRADEOFF CHARACTERISTIC: MUGSHOT IMAGES	124
70	ERROR TRADEOFF CHARACTERISTIC: MUGSHOT IMAGES	125
71	ERROR TRADEOFF CHARACTERISTIC: MUGSHOT IMAGES	126
72	ERROR TRADEOFF CHARACTERISTIC: MUGSHOT IMAGES	127
73	ERROR TRADEOFF CHARACTERISTIC: MUGSHOT IMAGES	128
74	ERROR TRADEOFF CHARACTERISTIC: MUGSHOT IMAGES	129
75	ERROR TRADEOFF CHARACTERISTIC: MUGSHOT IMAGES	130
76	ERROR TRADEOFF CHARACTERISTIC: MUGSHOT IMAGES	131
77	ERROR TRADEOFF CHARACTERISTIC: MUGSHOT IMAGES	132
78	ERROR TRADEOFF CHARACTERISTIC: WILD IMAGES	133
79	ERROR TRADEOFF CHARACTERISTIC: WILD IMAGES	134
80	ERROR TRADEOFF CHARACTERISTIC: WILD IMAGES	135
81	ERROR TRADEOFF CHARACTERISTIC: WILD IMAGES	136
82	ERROR TRADEOFF CHARACTERISTIC: WILD IMAGES	137
83	ERROR TRADEOFF CHARACTERISTIC: WILD IMAGES	138
84	ERROR TRADEOFF CHARACTERISTIC: WILD IMAGES	139
85	ERROR TRADEOFF CHARACTERISTIC: WILD IMAGES	140
86	ERROR TRADEOFF CHARACTERISTIC: WILD IMAGES	141
87	ERROR TRADEOFF CHARACTERISTIC: WILD IMAGES	142
88	ERROR TRADEOFF CHARACTERISTIC: WILD IMAGES	143
89	ERROR TRADEOFF CHARACTERISTIC: WILD IMAGES	144
90	ERROR TRADEOFF CHARACTERISTIC: WILD IMAGES	145
91	ERROR TRADEOFF CHARACTERISTIC: WILD IMAGES	146
92	ERROR TRADEOFF CHARACTERISTIC: WILD IMAGES	147
93	ERROR TRADEOFF CHARACTERISTIC: WILD IMAGES	148
94	FALSE MATCH RATES WITHIN AND ACROSS DEMOGRAPHIC GROUPS	149
95	FALSE MATCH RATES WITHIN AND ACROSS DEMOGRAPHIC GROUPS	150

96	FALSE MATCH RATES WITHIN AND ACROSS DEMOGRAPHIC GROUPS	151
97	FALSE MATCH RATES WITHIN AND ACROSS DEMOGRAPHIC GROUPS	152
98	FALSE MATCH RATES WITHIN AND ACROSS DEMOGRAPHIC GROUPS	153
99	FALSE MATCH RATES WITHIN AND ACROSS DEMOGRAPHIC GROUPS	154
100	FALSE MATCH RATES WITHIN AND ACROSS DEMOGRAPHIC GROUPS	155
101	FALSE MATCH RATES WITHIN AND ACROSS DEMOGRAPHIC GROUPS	156
102	FALSE MATCH RATES WITHIN AND ACROSS DEMOGRAPHIC GROUPS	157
103	FALSE MATCH RATES WITHIN AND ACROSS DEMOGRAPHIC GROUPS	158
104	FALSE MATCH RATES WITHIN AND ACROSS DEMOGRAPHIC GROUPS	159
105	FALSE MATCH RATES WITHIN AND ACROSS DEMOGRAPHIC GROUPS	160
106	FALSE MATCH RATES WITHIN AND ACROSS DEMOGRAPHIC GROUPS	161
107	FALSE MATCH RATES WITHIN AND ACROSS DEMOGRAPHIC GROUPS	162
108	FALSE MATCH RATES WITHIN AND ACROSS DEMOGRAPHIC GROUPS	163
109	FALSE MATCH RATES WITHIN AND ACROSS DEMOGRAPHIC GROUPS	164
110	FALSE MATCH RATES WITHIN AND ACROSS DEMOGRAPHIC GROUPS	165
111	FALSE MATCH RATES WITHIN AND ACROSS DEMOGRAPHIC GROUPS	166
112	FALSE MATCH RATES WITHIN AND ACROSS DEMOGRAPHIC GROUPS	167
113	SEX AND RACE EFFECTS: MUGSHOT IMAGES	168
114	SEX AND RACE EFFECTS: MUGSHOT IMAGES	169
115	SEX AND RACE EFFECTS: MUGSHOT IMAGES	170
116	SEX AND RACE EFFECTS: MUGSHOT IMAGES	171
117	SEX AND RACE EFFECTS: MUGSHOT IMAGES	172
118	SEX AND RACE EFFECTS: MUGSHOT IMAGES	173
119	SEX AND RACE EFFECTS: MUGSHOT IMAGES	174
120	SEX AND RACE EFFECTS: MUGSHOT IMAGES	175
121	SEX AND RACE EFFECTS: MUGSHOT IMAGES	176
122	SEX AND RACE EFFECTS: MUGSHOT IMAGES	177
123	SEX AND RACE EFFECTS: MUGSHOT IMAGES	178
124	SEX AND RACE EFFECTS: MUGSHOT IMAGES	179
125	SEX AND RACE EFFECTS: MUGSHOT IMAGES	180
126	SEX AND RACE EFFECTS: MUGSHOT IMAGES	181
127	SEX AND RACE EFFECTS: MUGSHOT IMAGES	182
128	SEX AND RACE EFFECTS: MUGSHOT IMAGES	183
129	SEX AND RACE EFFECTS: MUGSHOT IMAGES	184
130	SEX AND RACE EFFECTS: MUGSHOT IMAGES	185
131	SEX AND RACE EFFECTS: MUGSHOT IMAGES	186
132	SEX EFFECTS: VISA IMAGES	187
133	SEX EFFECTS: VISA IMAGES	188
134	SEX EFFECTS: VISA IMAGES	189
135	SEX EFFECTS: VISA IMAGES	190
136	SEX EFFECTS: VISA IMAGES	191
137	SEX EFFECTS: VISA IMAGES	192
138	SEX EFFECTS: VISA IMAGES	193
139	SEX EFFECTS: VISA IMAGES	194
140	SEX EFFECTS: VISA IMAGES	195
141	SEX EFFECTS: VISA IMAGES	196
142	SEX EFFECTS: VISA IMAGES	197
143	SEX EFFECTS: VISA IMAGES	198
144	SEX EFFECTS: VISA IMAGES	199
145	SEX EFFECTS: VISA IMAGES	200
146	SEX EFFECTS: VISA IMAGES	201
147	SEX EFFECTS: VISA IMAGES	202
148	SEX EFFECTS: VISA IMAGES	203
149	SEX EFFECTS: VISA IMAGES	204
150	SEX EFFECTS: VISA IMAGES	205
151	SEX EFFECTS: VISA IMAGES	206
152	SEX EFFECTS: VISA IMAGES	207

153 SEX EFFECTS: VISA IMAGES . . . . .	208
154 SEX EFFECTS: VISA IMAGES . . . . .	209
155 SEX EFFECTS: VISA IMAGES . . . . .	210
156 SEX EFFECTS: VISA IMAGES . . . . .	211
157 SEX EFFECTS: VISA IMAGES . . . . .	212
158 SEX EFFECTS: VISA IMAGES . . . . .	213
159 SEX EFFECTS: VISA IMAGES . . . . .	214
160 SEX EFFECTS: VISA IMAGES . . . . .	215
161 SEX EFFECTS: VISA IMAGES . . . . .	216
162 SEX EFFECTS: VISA IMAGES . . . . .	217
163 SEX EFFECTS: VISA IMAGES . . . . .	218
164 FALSE MATCH RATE CALIBRATION: MUGSHOT IMAGES . . . . .	219
165 FALSE MATCH RATE CALIBRATION: MUGSHOT IMAGES . . . . .	220
166 FALSE MATCH RATE CALIBRATION: MUGSHOT IMAGES . . . . .	221
167 FALSE MATCH RATE CALIBRATION: MUGSHOT IMAGES . . . . .	222
168 FALSE MATCH RATE CALIBRATION: MUGSHOT IMAGES . . . . .	223
169 FALSE MATCH RATE CALIBRATION: MUGSHOT IMAGES . . . . .	224
170 FALSE MATCH RATE CALIBRATION: MUGSHOT IMAGES . . . . .	225
171 FALSE MATCH RATE CALIBRATION: MUGSHOT IMAGES . . . . .	226
172 FALSE MATCH RATE CALIBRATION: MUGSHOT IMAGES . . . . .	227
173 FALSE MATCH RATE CALIBRATION: MUGSHOT IMAGES . . . . .	228
174 FALSE MATCH RATE CALIBRATION: MUGSHOT IMAGES . . . . .	229
175 FALSE MATCH RATE CALIBRATION: MUGSHOT IMAGES . . . . .	230
176 FALSE MATCH RATE CALIBRATION: MUGSHOT IMAGES . . . . .	231
177 FALSE MATCH RATE CALIBRATION: MUGSHOT IMAGES . . . . .	232
178 FALSE MATCH RATE CALIBRATION: MUGSHOT IMAGES . . . . .	233
179 FALSE MATCH RATE CALIBRATION: MUGSHOT IMAGES . . . . .	234
180 FALSE MATCH RATE CALIBRATION: MUGSHOT IMAGES . . . . .	235
181 FALSE MATCH RATE CALIBRATION: MUGSHOT IMAGES . . . . .	236
182 FALSE MATCH RATE CALIBRATION: MUGSHOT IMAGES . . . . .	237
183 FALSE MATCH RATE CALIBRATION: VISA IMAGES . . . . .	238
184 FALSE MATCH RATE CALIBRATION: VISA IMAGES . . . . .	239
185 FALSE MATCH RATE CALIBRATION: VISA IMAGES . . . . .	240
186 FALSE MATCH RATE CALIBRATION: VISA IMAGES . . . . .	241
187 FALSE MATCH RATE CALIBRATION: VISA IMAGES . . . . .	242
188 FALSE MATCH RATE CALIBRATION: VISA IMAGES . . . . .	243
189 FALSE MATCH RATE CALIBRATION: VISA IMAGES . . . . .	244
190 FALSE MATCH RATE CALIBRATION: VISA IMAGES . . . . .	245
191 FALSE MATCH RATE CALIBRATION: VISA IMAGES . . . . .	246
192 FALSE MATCH RATE CALIBRATION: VISA IMAGES . . . . .	247
193 FALSE MATCH RATE CALIBRATION: VISA IMAGES . . . . .	248
194 FALSE MATCH RATE CALIBRATION: VISA IMAGES . . . . .	249
195 FALSE MATCH RATE CALIBRATION: VISA IMAGES . . . . .	250
196 FALSE MATCH RATE CALIBRATION: VISA IMAGES . . . . .	251
197 FALSE MATCH RATE CALIBRATION: VISA IMAGES . . . . .	252
198 FALSE MATCH RATE CALIBRATION: VISA IMAGES . . . . .	253
199 FALSE MATCH RATE CALIBRATION: VISA IMAGES . . . . .	254
200 FALSE MATCH RATE CALIBRATION: VISA IMAGES . . . . .	255
201 FALSE MATCH RATE CALIBRATION: VISA IMAGES . . . . .	256
202 FALSE MATCH RATE CALIBRATION: VISA IMAGES . . . . .	257
203 FALSE MATCH RATE CALIBRATION: VISA IMAGES . . . . .	258
204 FALSE MATCH RATE CALIBRATION: VISA IMAGES . . . . .	259
205 FALSE MATCH RATE CALIBRATION: VISA IMAGES . . . . .	260
206 FALSE MATCH RATE CALIBRATION: VISA IMAGES . . . . .	261
207 FALSE MATCH RATE CALIBRATION: VISA IMAGES . . . . .	262
208 FALSE MATCH RATE CALIBRATION: VISA IMAGES . . . . .	263
209 FALSE MATCH RATE CALIBRATION: VISA IMAGES . . . . .	264

210	FALSE MATCH RATE CALIBRATION: VISA IMAGES	265
211	FALSE MATCH RATE CALIBRATION: VISA IMAGES	266
212	FALSE MATCH RATE CALIBRATION: VISA IMAGES	267
213	FALSE MATCH RATE CALIBRATION: VISA IMAGES	268
214	FALSE MATCH RATE CALIBRATION: VISA IMAGES	269
215	FALSE MATCH RATE CALIBRATION: VISA IMAGES	270
216	FALSE MATCH RATE CALIBRATION: VISA IMAGES	271
217	FALSE MATCH RATE CALIBRATION: VISA IMAGES	272
218	FALSE MATCH RATE CALIBRATION: VISA IMAGES	273
219	FALSE MATCH RATE CALIBRATION: VISA IMAGES	274
220	FALSE MATCH RATE CALIBRATION: VISA IMAGES	275
221	FALSE MATCH RATE CALIBRATION: VISA IMAGES	276
222	EFFECT OF COUNTRY OF BIRTH ON FNMR	278
223	EFFECT OF COUNTRY OF BIRTH ON FNMR	279
224	EFFECT OF COUNTRY OF BIRTH ON FNMR	280
225	EFFECT OF COUNTRY OF BIRTH ON FNMR	281
226	EFFECT OF COUNTRY OF BIRTH ON FNMR	282
227	EFFECT OF COUNTRY OF BIRTH ON FNMR	283
228	EFFECT OF COUNTRY OF BIRTH ON FNMR	284
229	EFFECT OF COUNTRY OF BIRTH ON FNMR	285
230	EFFECT OF COUNTRY OF BIRTH ON FNMR	286
231	EFFECT OF COUNTRY OF BIRTH ON FNMR	287
232	EFFECT OF COUNTRY OF BIRTH ON FNMR	288
233	EFFECT OF COUNTRY OF BIRTH ON FNMR	289
234	EFFECT OF COUNTRY OF BIRTH ON FNMR	290
235	EFFECT OF COUNTRY OF BIRTH ON FNMR	291
236	EFFECT OF COUNTRY OF BIRTH ON FNMR	292
237	EFFECT OF COUNTRY OF BIRTH ON FNMR	293
238	EFFECT OF COUNTRY OF BIRTH ON FNMR	294
239	EFFECT OF COUNTRY OF BIRTH ON FNMR	295
240	EFFECT OF COUNTRY OF BIRTH ON FNMR	296
241	EFFECT OF COUNTRY OF BIRTH ON FNMR	297
242	EFFECT OF COUNTRY OF BIRTH ON FNMR	298
243	EFFECT OF COUNTRY OF BIRTH ON FNMR	299
244	EFFECT OF COUNTRY OF BIRTH ON FNMR	300
245	EFFECT OF COUNTRY OF BIRTH ON FNMR	301
246	EFFECT OF COUNTRY OF BIRTH ON FNMR	302
247	EFFECT OF COUNTRY OF BIRTH ON FNMR	303
248	EFFECT OF COUNTRY OF BIRTH ON FNMR	304
249	EFFECT OF COUNTRY OF BIRTH ON FNMR	305
250	EFFECT OF COUNTRY OF BIRTH ON FNMR	306
251	EFFECT OF COUNTRY OF BIRTH ON FNMR	307
252	EFFECT OF COUNTRY OF BIRTH ON FNMR	308
253	EFFECT OF COUNTRY OF BIRTH ON FNMR	309
254	ERROR TRADEOFF CHARACTERISTIC: MUGSHOT IMAGES	311
255	ERROR TRADEOFF CHARACTERISTIC: MUGSHOT IMAGES	312
256	ERROR TRADEOFF CHARACTERISTIC: MUGSHOT IMAGES	313
257	ERROR TRADEOFF CHARACTERISTIC: MUGSHOT IMAGES	314
258	ERROR TRADEOFF CHARACTERISTIC: MUGSHOT IMAGES	315
259	ERROR TRADEOFF CHARACTERISTIC: MUGSHOT IMAGES	316
260	ERROR TRADEOFF CHARACTERISTIC: MUGSHOT IMAGES	317
261	ERROR TRADEOFF CHARACTERISTIC: MUGSHOT IMAGES	318
262	ERROR TRADEOFF CHARACTERISTIC: MUGSHOT IMAGES	319
263	ERROR TRADEOFF CHARACTERISTIC: MUGSHOT IMAGES	320
264	ERROR TRADEOFF CHARACTERISTIC: MUGSHOT IMAGES	321
265	ERROR TRADEOFF CHARACTERISTIC: MUGSHOT IMAGES	322
266	ERROR TRADEOFF CHARACTERISTIC: MUGSHOT IMAGES	323

267	ERROR TRADEOFF CHARACTERISTIC: MUGSHOT IMAGES . . . . .	324
268	ERROR TRADEOFF CHARACTERISTIC: MUGSHOT IMAGES . . . . .	325
269	ERROR TRADEOFF CHARACTERISTIC: MUGSHOT IMAGES . . . . .	326
270	ERROR TRADEOFF CHARACTERISTIC: MUGSHOT IMAGES . . . . .	327
271	ERROR TRADEOFF CHARACTERISTIC: MUGSHOT IMAGES . . . . .	328
272	ERROR TRADEOFF CHARACTERISTIC: MUGSHOT IMAGES . . . . .	329
273	ERROR TRADEOFF CHARACTERISTIC: MUGSHOT IMAGES . . . . .	330
274	ERROR TRADEOFF CHARACTERISTIC: MUGSHOT IMAGES . . . . .	331
275	ERROR TRADEOFF CHARACTERISTIC: MUGSHOT IMAGES . . . . .	332
276	ERROR TRADEOFF CHARACTERISTIC: MUGSHOT IMAGES . . . . .	333
277	ERROR TRADEOFF CHARACTERISTIC: MUGSHOT IMAGES . . . . .	334
278	EFFECT OF SUBJECT AGE ON FNMR . . . . .	336
279	EFFECT OF SUBJECT AGE ON FNMR . . . . .	337
280	EFFECT OF SUBJECT AGE ON FNMR . . . . .	338
281	EFFECT OF SUBJECT AGE ON FNMR . . . . .	339
282	EFFECT OF SUBJECT AGE ON FNMR . . . . .	340
283	EFFECT OF SUBJECT AGE ON FNMR . . . . .	341
284	EFFECT OF SUBJECT AGE ON FNMR . . . . .	342
285	EFFECT OF SUBJECT AGE ON FNMR . . . . .	343
286	EFFECT OF SUBJECT AGE ON FNMR . . . . .	344
287	EFFECT OF SUBJECT AGE ON FNMR . . . . .	345
288	EFFECT OF SUBJECT AGE ON FNMR . . . . .	346
289	EFFECT OF SUBJECT AGE ON FNMR . . . . .	347
290	EFFECT OF SUBJECT AGE ON FNMR . . . . .	348
291	EFFECT OF SUBJECT AGE ON FNMR . . . . .	349
292	EFFECT OF SUBJECT AGE ON FNMR . . . . .	350
293	EFFECT OF SUBJECT AGE ON FNMR . . . . .	351
294	EFFECT OF SUBJECT AGE ON FNMR . . . . .	352
295	EFFECT OF SUBJECT AGE ON FNMR . . . . .	353
296	EFFECT OF SUBJECT AGE ON FNMR . . . . .	354
297	EFFECT OF SUBJECT AGE ON FNMR . . . . .	355
298	EFFECT OF SUBJECT AGE ON FNMR . . . . .	356
299	EFFECT OF SUBJECT AGE ON FNMR . . . . .	357
300	EFFECT OF SUBJECT AGE ON FNMR . . . . .	358
301	EFFECT OF SUBJECT AGE ON FNMR . . . . .	359
302	EFFECT OF SUBJECT AGE ON FNMR . . . . .	360
303	EFFECT OF SUBJECT AGE ON FNMR . . . . .	361
304	EFFECT OF SUBJECT AGE ON FNMR . . . . .	362
305	EFFECT OF SUBJECT AGE ON FNMR . . . . .	363
306	EFFECT OF SUBJECT AGE ON FNMR . . . . .	364
307	EFFECT OF SUBJECT AGE ON FNMR . . . . .	365
308	EFFECT OF SUBJECT AGE ON FNMR . . . . .	366
309	EFFECT OF SUBJECT AGE ON FNMR . . . . .	367
310	WORST CASE REGIONAL EFFECT FNMR . . . . .	370
311	IMPOSTOR DISTRIBUTION SHIFTS FOR SELECT COUNTRY PAIRS . . . . .	372

	Location	Developer Name	Short Name	Seq. Num.	Validation Date
1	NL	20Face	20face-000	000	2021-04-12
2	NL	20Face	20face-001	001	2021-09-29
3	US	3Divi	3divi-006	006	2021-04-14
4	US	3Divi	3divi-007	007	2021-09-27
5	TH	ACI Software	acisw-003	003	2020-08-03
6	TH	ACI Software	acisw-007	007	2021-11-15
7	SG	ADVANCE.AI	advance-002	002	2019-12-19
8	SG	ADVANCE.AI	advance-003	003	2021-08-05
9	TW	ASUSTek Computer Inc	asusaics-000	000	2019-10-24
10	TW	ASUSTek Computer Inc	asusaics-001	001	2020-02-25
11	CN	AYF Technology	ayftech-001	001	2020-07-06
12	TW	Ability Enterprise - Andro Video	androvideo-000	000	2021-01-25
13	TW	Acer Incorporated	acer-001	001	2020-06-30
14	TW	Acer Incorporated	acer-002	002	2021-11-10
15	SG	Adera Global PTE	adera-002	002	2021-02-16
16	SG	Adera Global PTE	adera-003	003	2021-07-12
17	TH	Ai First	aifirst-001	001	2019-11-21
18	TW	AiUnion Technology	aiunionface-000	000	2019-10-22
19	TH	Aigen	aigen-001	001	2020-10-06
20	TH	Aigen	aigen-002	002	2021-03-15
21	KR	Ajou University	ajou-001	001	2021-03-08
22	ID	Akurat Satu Indonesia	ptakuratsatu-000	000	2020-09-11
23	KR	Alchera Inc	alchera-002	002	2021-03-05
24	KR	Alchera Inc	alchera-003	003	2021-07-13
25	ID	Alfabeta	alfabeta-001	001	2021-12-02
26	ES	Alice Biometrics	alice-000	000	2021-06-15
27	RU	Alivia / Innovation Sys	isystems-001	001	2018-06-12
28	RU	Alivia / Innovation Sys	isystems-002	002	2018-10-18
29	IN	AllGoVision	allgovision-000	000	2019-03-01
30	CN	AlphaSTG	alphaface-001	001	2019-09-03
31	CN	AlphaSTG	alphaface-002	002	2020-02-20
32	GB	Amplified Group	amplifiedgroup-001	001	2019-03-01
33	CN	Anke Investments	anke-004	004	2019-06-27
34	CN	Anke Investments	anke-005	005	2019-11-21
35	BR	Antheus Technologia	antheus-000	000	2019-12-05
36	BR	Antheus Technologia	antheus-001	001	2020-06-25
37	GB	AnyVision	anyvision-004	004	2018-06-15
38	GB	AnyVision	anyvision-005	005	2021-02-03
39	CN	AuthenMetric	authenmetric-002	002	2021-03-10
40	CN	AuthenMetric	authenmetric-003	003	2021-08-09
41	CN	AuthenMetric	authenmetric-004	004	2022-01-03
42	US	Aware	aware-005	005	2020-02-27
43	US	Aware	aware-006	006	2021-07-03
44	IN	Awidit Systems	awirovs-001	001	2019-09-23
45	IN	Awidit Systems	awirovs-002	002	2020-10-28
46	JP	Ayonix	ayonix-000	000	2017-06-22
47	CN	BOE Technology Group	boetech-001	001	2021-06-22
48	CN	BOE Technology Group	boetech-002	002	2021-12-21
49	ES	Bee the Data	beethedata-000	000	2021-07-26
50	CN	Beihang University-ERCACAT	ercacat-001	001	2020-07-06
51	CN	Beijing Alleyes Technology	alleyes-000	000	2020-03-09
52	CN	Beijing DeepSense Technologies	deepsense-000	000	2021-03-19
53	CN	Beijing Hisign Technology	hisign-001	001	2021-09-24
54	CN	Beijing Mendaxia Technology	mendaxiatech-000	000	2021-09-15
55	CN	Beijing Vion Technology Inc	vion-000	000	2018-10-19
56	CH	BioID Technologies SA	bioidechswiss-001	001	2020-08-28
57	CH	BioID Technologies SA	bioidechswiss-002	002	2021-02-17
58	IN	Biocube Matrics	biocube-001	001	2021-09-08
59	UK	BitCenter UK	farfaces-001	001	2021-04-09
60	CN	Bitmain	bm-001	001	2018-10-17
61	CN	Bresee Technology	bresee-001	001	2020-12-30
62	CN	Bresee Technology	bresee-002	002	2021-06-30
63	CN	CSA IntelliCloud Technology	intellicloudai-001	001	2019-08-13
64	CN	CSA IntelliCloud Technology	intellicloudai-002	002	2020-12-17
65	TW	CTBC Bank	ctbcbank-000	000	2019-06-28
66	TW	CTBC Bank	ctbcbank-001	001	2019-10-28
67	KR	CUDO Communication	cudocommunication-001	001	2021-10-20
68	US	Camvi Technologies	camvi-002	002	2018-10-19
69	US	Camvi Technologies	camvi-004	004	2019-07-12
70	CN	Canon Inc	canon-002	002	2020-12-29

Table 1: Summary of participant information included in this report.

	Location	Developer Name	Short Name	Seq. Num.	Validation Date
71	JP	Canon Inc	canon-003	003	2021-09-15
72	CN	China Electronics Import-Export Corp	ceiec-003	003	2020-01-06
73	CN	China Electronics Import-Export Corp	ceiec-004	004	2021-01-18
74	CN	China University of Petroleum	upc-001	001	2019-06-05
75	CN	Chinese University of Hong Kong	cuhkee-001	001	2020-03-18
76	KR	Chosun University	chosun-001	001	2020-07-01
77	KR	Chosun University	chosun-002	002	2020-11-25
78	TW	Chunghwa Telecom	chtface-003	003	2020-06-24
79	TW	Chunghwa Telecom	chtface-004	004	2021-10-08
80	US	Clearview AI Inc	clearviewai-000	000	2021-09-22
81	CN	Closeli Inc	closeli-001	001	2021-07-15
82	US	CloudSmart Consulting LLC	csc-002	002	2021-03-24
83	US	CloudSmart Consulting LLC	csc-003	003	2021-08-26
84	TW	Cloudmatrix	cloudmatrix-000	000	2021-10-22
85	CN	Cloudwalk - Hengrui AI Technology	cloudwalk-hr-003	003	2020-09-25
86	CN	Cloudwalk - Hengrui AI Technology	cloudwalk-hr-004	004	2021-02-10
87	CN	Cloudwalk - Hengrui AI Technology	cloudwalk-mt-004	004	2021-11-09
88	CN	Cloudwalk - Moontime Smart Technology	cloudwalk-mt-003	003	2020-12-22
89	IN	Code Everest Pvt	facex-001	001	2021-03-08
90	IN	Code Everest Pvt	facex-002	002	2021-08-24
91	DE	Cognitec Systems GmbH	cognitec-002	002	2021-02-24
92	DE	Cognitec Systems GmbH	cognitec-003	003	2021-07-30
93	TW	Coretech Knowledge Inc	coretech-000	000	2021-07-12
94	IL	Corsight	corsight-001	001	2021-03-11
95	IL	Corsight	corsight-002	002	2021-09-01
96	IL	Cortica	cor-001	001	2020-09-24
97	KR	Cubox	cubox-001	001	2020-12-07
98	KR	Cubox	cubox-002	002	2021-08-24
99	JP	Cybercore	cybercore-000	000	2020-08-26
100	JP	Cybercore	cybercore-001	001	2021-12-15
101	US	Cyberextruder	cyberextruder-001	001	2017-08-02
102	US	Cyberextruder	cyberextruder-002	002	2018-01-30
103	TW	Cyberlink Corp	cyberlink-006	006	2021-01-08
104	TW	Cyberlink Corp	cyberlink-007	007	2021-07-16
105	TW	Cyberlink Corp	cyberlink-008	008	2022-01-07
106	CN	DSK	dsk-000	000	2019-06-28
107	CN	Dahua Technology	dahua-005	005	2020-08-13
108	CN	Dahua Technology	dahua-006	006	2020-12-30
109	CN	Dahua Technology	dahua-007	007	2021-12-20
110	IE	Daon	daon-000	000	2021-11-03
111	US	Decatur Industries Inc	decatur-000	000	2020-08-18
112	US	Decatur Industries Inc	decatur-001	001	2021-09-27
113	CN	Deepglint	deepglint-003	003	2021-03-03
114	CN	Deepglint	deepglint-004	004	2021-09-17
115	FR	Deepsense	dps-000	000	2021-07-16
116	DE	Dermalog	dermalog-008	008	2021-03-25
117	DE	Dermalog	dermalog-009	009	2021-10-06
118	CN	DiDi ChuXing Technology	didiglobalface-001	001	2019-10-23
119	GB	Digital Barriers	digitalbarriers-002	002	2019-03-01
120	TR	Ekin Smart City Technologies	ekin-002	002	2021-05-04
121	RU	Enface	enface-000	000	2021-04-09
122	RU	Enface	enface-001	001	2021-12-17
123	CH	Euronovate SA	euronovate-001	001	2021-11-15
124	RU	Expasoft LLC	expasoft-001	001	2020-09-03
125	RU	Expasoft LLC	expasoft-002	002	2021-07-26
126	DE	FaceOnLive Inc	faceonlive-001	001	2021-11-23
127	GB	FaceSoft	facesoft-000	000	2019-07-10
128	KR	FaceTag Co	facetag-000	000	2021-03-22
129	KR	FaceTag Co	facetag-001	001	2021-08-17
130	KR	FaceTag Co	facetag-002	002	2022-01-06
131	TW	FarBar Inc	f8-001	001	2019-07-11
132	CN	Fiberhome Telecommunication Technologies	fiberhome-nanjing-003	003	2021-03-12
133	CN	Fiberhome Telecommunication Technologies	fiberhome-nanjing-004	004	2021-09-14
134	UK	Fincore Ltd	fincore-000	000	2021-06-07
135	CN	Fujitsu Research and Development Center	fujitsulab-002	002	2021-02-24
136	CN	Fujitsu Research and Development Center	fujitsulab-003	003	2021-07-12
137	US	Gemalto Cogent	cogent-005	005	2020-12-29
138	US	Gemalto Cogent	cogent-006	006	2021-07-28
139	TW	GeoVision Inc	geo-002	002	2021-04-01
140	TW	GeoVision Inc	geo-003	003	2021-09-15

Table 2: Summary of participant information included in this report.

	Location	Developer Name	Short Name	Seq. Num.	Validation Date
141	JP	Glory	glory-002	002	2019-11-12
142	JP	Glory	glory-003	003	2021-01-15
143	TW	Gorilla Technology	gorilla-007	007	2021-06-28
144	TW	Gorilla Technology	gorilla-008	008	2021-11-08
145	US	Griaule	griaule-000	000	2021-08-20
146	CN	Guangzhou Pixel Solutions	pixelall-006	006	2021-06-17
147	CN	Guangzhou Pixel Solutions	pixelall-007	007	2021-12-01
148	ES	Herta Security	hertasecurity-000	000	2021-01-05
149	CN	Hikvision Research Institute	hik-001	001	2019-03-01
150	IN	HyperVerge Inc	hyperverge-001	001	2020-12-13
151	IN	HyperVerge Inc	hyperverge-002	002	2021-05-27
152	AU	ICM Airport Technics	icm-002	002	2020-11-13
153	AU	ICM Airport Technics	icm-003	003	2021-09-06
154	FR	ID3 Technology	id3-006	006	2020-12-17
155	FR	ID3 Technology	id3-008	008	2021-11-10
156	RU	ITMO University	itmo-007	007	2020-01-06
157	RU	ITMO University	itmo-008	008	2021-11-19
158	RU	IVA Cognitive	ivacognitive-001	001	2021-01-29
159	FR	Idemia	idemia-007	007	2020-12-04
160	FR	Idemia	idemia-008	008	2021-07-07
161	US	Imageware Systems	iws-000	000	2020-08-12
162	AU	Imagus Technology Pty	imagus-002	002	2020-12-31
163	AU	Imagus Technology Pty	imagus-004	004	2021-09-20
164	GB	Imperial College London	imperial-000	000	2019-03-01
165	GB	Imperial College London	imperial-002	002	2019-08-28
166	US	Incode Technologies Inc	incode-009	009	2021-06-22
167	US	Incode Technologies Inc	incode-010	010	2021-10-22
168	IN	Innef Labs	innefulabs-000	000	2020-09-04
169	GB	Innovative Technology	innovativetechnologyltd-001	001	2019-10-22
170	GB	Innovative Technology	innovativetechnologyltd-002	002	2020-02-26
171	SK	Innovatrics	innovatrics-006	006	2019-08-13
172	SK	Innovatrics	innovatrics-007	007	2020-08-19
173	SK	Innovatrics	innovatrics-008	008	2021-12-15
174	CN	InsightFace AI	insightface-000	000	2021-03-17
175	CN	InsightFace AI	insightface-001	001	2021-09-27
176	CN	Institute of Computing Technology	icthtc-000	000	2020-11-29
177	RU	Institute of Information Technologies	iit-002	002	2019-12-04
178	RU	Institute of Information Technologies	iit-003	003	2020-12-01
179	IS	Intel Research Group	intelresearch-003	003	2021-01-18
180	IS	Intel Research Group	intelresearch-004	004	2021-08-24
181	US	Intellivision	intellivision-001	001	2017-10-10
182	US	Intellivision	intellivision-002	002	2019-08-23
183	US	IrexAI	irex-000	000	2020-12-17
184	IL	Is It You	isityou-000	000	2017-06-26
185	KR	Kakao Enterprise	kakao-005	005	2021-03-09
186	KR	Kakao Pay Corp	kakaopay-001	001	2021-07-06
187	SG	Kedacom International Pte	kedacom-000	000	2019-06-03
188	US	Kneron Inc	kneron-003	003	2019-07-01
189	US	Kneron Inc	kneron-005	005	2020-02-21
190	KR	Kookmin University	kookmin-002	002	2021-03-05
191	CN	KuKe3D Technology	kuke3d-001	001	2021-10-28
192	IN	Lema Labs	lemalabs-001	001	2021-04-13
193	JP	Line Corporation	line-000	000	2021-03-31
194	JP	Line Corporation	line-001	001	2021-09-26
195	RU	Lomonosov Moscow State University	intsysmsu-001	001	2019-10-22
196	RU	Lomonosov Moscow State University	intsysmsu-002	002	2020-03-12
197	IN	Lookman Electroplast Industries	lookman-002	002	2018-06-13
198	IN	Lookman Electroplast Industries	lookman-004	004	2019-06-03
199	US	Luxand Inc	luxand-000	000	2019-11-07
200	RU	MVision	mvision-001	001	2019-11-12
201	IN	Mantra Softech India	mantra-000	000	2021-10-28
202	CN	Maxvision Technology	maxvision-000	000	2021-10-27
203	CN	Megvii/Face++	megvii-003	003	2021-03-08
204	GB	MicroFocus	microfocus-001	001	2018-06-13
205	GB	MicroFocus	microfocus-002	002	2018-10-17
206	CN	Minivision	minivision-000	000	2020-10-28
207	NO	Mobai	mobai-000	000	2020-08-26
208	NO	Mobai	mobai-001	001	2021-02-17
209	ES	Mobbeel Solutions	mobbl-000	000	2021-01-28
210	ES	Mobbeel Solutions	mobbl-001	001	2021-06-16

Table 3: Summary of participant information included in this report.

	Location	Developer Name	Short Name	Seq. Num.	Validation Date
211	ES	Mobbeel Solutions	mobbil-002	002	2021-12-16
212	KR	Mobipin Technology	mobipintech-000	000	2021-11-23
213	TH	Momentum Digital	sertis-000	000	2019-10-07
214	TH	Momentum Digital	sertis-002	002	2021-05-13
215	CN	MoreDian Technology	moredian-000	000	2021-02-24
216	CN	Multi-Modality Intelligence	multimodality-000	000	2021-10-19
217	RU	N-Tech Lab	ntechlab-010	010	2021-04-30
218	RU	N-Tech Lab	ntechlab-011	011	2021-09-13
219	CA	NEO Systems	neosystems-002	002	2021-07-03
220	CA	NEO Systems	neosystems-003	003	2021-11-11
221	KR	NHN Corp	nhn-001	001	2021-03-15
222	KR	NHN Corp	nhn-002	002	2021-07-15
223	KR	NSENSE Corp	nsensecorp-002	002	2021-05-06
224	KR	NSENSE Corp	nsensecorp-003	003	2021-10-29
225	CN	Nanjing Kiwi Network Technology	kiwitech-000	000	2021-03-19
226	KR	Naver Corp	clova-000	000	2020-10-21
227	KR	Neosecu Co	openface-001	001	2021-06-15
228	TW	Netbridge Technology Incoporation	netbridgetech-001	001	2020-01-08
229	TW	Netbridge Technology Incoporation	netbridgetech-002	002	2020-08-11
230	LT	Neurotechnology	neurotechnology-011	011	2021-03-26
231	LT	Neurotechnology	neurotechnology-012	012	2021-07-26
232	LT	Neurotechnology	neurotechnology-013	013	2022-01-07
233	ID	Nodeflux	nodeflux-002	002	2019-08-13
234	IN	NotionTag Technologies Private Limited	notiontag-001	001	2021-03-04
235	IN	NotionTag Technologies Private Limited	notiontag-002	002	2021-09-17
236	US	Omnigarde Ltd	omnigarde-000	000	2021-04-05
237	US	Omnigarde Ltd	omnigarde-001	001	2021-08-23
238	RU	Oz Forensics LLC	oz-002	002	2021-01-18
239	RU	Oz Forensics LLC	oz-003	003	2021-08-09
240	RU	Oz Forensics LLC	oz-004	004	2021-12-13
241	CH	PXL Vision AG	pxl-001	001	2020-06-30
242	SG	Panasonic R+D Center Singapore	psl-008	008	2021-07-21
243	SG	Panasonic R+D Center Singapore	psl-009	009	2021-12-08
244	TR	Papilon Savunma	papsav1923-001	001	2021-03-10
245	US	Paravision (EverAI)	paravision-004	004	2019-12-11
246	US	Paravision (EverAI)	paravision-008	008	2021-06-30
247	SG	Pensees Pte	pensees-001	001	2020-08-17
248	IN	Pyramid Cyber Security + Forensic (P)	pyramid-000	000	2019-11-04
249	TW	Qnap Security	qnap-000	000	2021-08-09
250	TW	Qnap Security	qnap-001	001	2021-12-09
251	CZ	Quantasoft	quantasoft-003	003	2021-04-19
252	US	Rank One Computing	rankone-010	010	2020-11-05
253	US	Rank One Computing	rankone-011	011	2021-08-27
254	US	Rank One Computing	rankone-012	012	2021-12-27
255	US	Realnetworks Inc	realnetworks-004	004	2021-04-15
256	US	Realnetworks Inc	realnetworks-005	005	2021-09-27
257	US	Regula Forensics	regula-000	000	2021-04-13
258	US	Regula Forensics	regula-001	001	2021-12-14
259	CN	Remark Holdings	remarkai-001	001	2019-03-01
260	CN	Remark Holdings	remarkai-003	003	2021-06-22
261	SG	Rendip	rendip-000	000	2021-04-19
262	UK	Reveal Media Ltd	revealmedia-005	005	2021-09-24
263	CN	Rokid Corporation	rokid-000	000	2019-08-01
264	CN	Rokid Corporation	rokid-001	001	2019-12-13
265	KR	SK Telecom	sktelecom-000	000	2021-07-09
266	KR	SQIsoft	sqisoft-001	001	2021-07-27
267	KR	SQIsoft	sqisoft-002	002	2021-11-03
268	DE	Saffe	saffe-001	001	2018-10-19
269	DE	Saffe	saffe-002	002	2019-03-01
270	KR	Samsung S1 Corp	s1-002	002	2021-03-24
271	KR	Samsung S1 Corp	s1-003	003	2021-08-24
272	KR	Samsung S1 Corp	s1-004	004	2022-01-04
273	KR	Samsung-SDS	samsungsds-000	000	2021-10-28
274	IN	Samtech InfoNet Limited	samtech-001	001	2019-10-15
275	RU	Satellite Innovation/Eocortex	eocortex-000	000	2020-08-26
276	IL	Scanovate	scanovate-002	002	2020-06-26
277	IL	Scanovate	scanovate-003	003	2021-11-15
278	RO	Securif AI	securifai-001	001	2020-10-06
279	RO	Securif AI	securifai-003	003	2021-08-03
280	RO	Securif AI	securifai-004	004	2021-12-21

Table 4: Summary of participant information included in this report.

	Location	Developer Name	Short Name	Seq. Num.	Validation Date
281	CN	Sensetime Group	sensetime-004	004	2020-11-20
282	CN	Sensetime Group	sensetime-005	005	2021-05-24
283	CN	Sensetime Group	sensetime-006	006	2021-12-28
284	SG	Seventh Sense Artificial Intelligence	sevensense-000	000	2021-06-29
285	US	Shaman Software	shaman-000	000	2017-12-05
286	US	Shaman Software	shaman-001	001	2018-01-13
287	CN	Shanghai Jiao Tong University	sjtu-003	003	2020-11-02
288	CN	Shanghai Jiao Tong University	sjtu-004	004	2021-05-13
289	CN	Shanghai Ulucu Electronics Technology	uluface-002	002	2019-07-10
290	CN	Shanghai Ulucu Electronics Technology	uluface-003	003	2019-11-12
291	CN	Shanghai University - Shanghai Film Academy	shu-002	002	2019-12-10
292	CN	Shanghai University - Shanghai Film Academy	shu-003	003	2020-06-24
293	CN	Shanghai Yitu Technology	yitu-003	003	2019-03-01
294	CN	Shenzhen AiMall Tech	aimall-002	002	2020-03-12
295	CN	Shenzhen AiMall Tech	aimall-003	003	2020-08-12
296	CN	Shenzhen EI Networks	einetworks-000	000	2019-08-13
297	CN	Shenzhen Inst Adv Integrated Tech CAS	siat-002	002	2018-06-13
298	CN	Shenzhen Inst Adv Integrated Tech CAS	siat-004	004	2019-03-01
299	CN	Shenzhen Intellifusion Technologies	intellifusion-001	001	2019-08-22
300	CN	Shenzhen Intellifusion Technologies	intellifusion-002	002	2020-03-18
301	CN	Shenzhen University-Macau University of Science and Technology	sztu-000	000	2020-12-17
302	CN	Shenzhen University-Macau University of Science and Technology	sztu-001	001	2021-07-13
303	RU	Smart Engines	smartengines-000	000	2021-08-25
304	DE	Smilart	smilart-002	002	2018-02-06
305	DE	Smilart	smilart-003	003	2018-06-18
306	TR	Sodec App Inc	sodec-000	000	2021-06-02
307	IN	StaQu Technologies	staqu-000	000	2020-07-15
308	CN	Star Hybrid Limited	starhybrid-001	001	2019-06-19
309	CN	Su Zhou NaZhiTianDi intelligent technology	nazhai-000	000	2020-06-25
310	KR	Suprema	suprema-000	000	2021-03-31
311	KR	Suprema ID Inc	suprema-001	001	2021-09-23
312	KR	Suprema ID Inc	supremaid-001	001	2021-05-04
313	RU	Synesis	synesis-006	006	2019-10-10
314	RU	Synesis	synesis-007	007	2020-06-24
315	TW	Synology Inc	synology-000	000	2019-10-23
316	TW	Synology Inc	synology-002	002	2020-08-20
317	CN	TUPU Technology	tuputech-000	000	2019-10-11
318	TW	Taiwan AI Labs	ailabs-001	001	2019-12-18
319	TW	Taiwan-Certificate Authority Incorporation	twface-000	000	2021-05-14
320	TW	Taiwan-Certificate Authority Incorporation	twface-001	001	2021-09-14
321	CH	Tech5 SA	tech5-004	004	2020-03-09
322	CH	Tech5 SA	tech5-005	005	2020-07-24
323	TR	Techsign	techsign-000	000	2021-08-25
324	CN	Tencent Deepsea Lab	deepsea-001	001	2019-06-03
325	RU	Tevian	tevian-007	007	2021-08-06
326	RU	Tevian	tevian-008	008	2021-12-06
327	US	TigerIT Americas LLC	tiger-003	003	2018-10-16
328	US	TigerIT Americas LLC	tiger-005	005	2021-07-29
329	US	TigerIT Americas LLC	tiger-006	006	2021-12-13
330	RU	Tinkoff Bank	tinkoff-001	001	2021-05-13
331	CN	TongYi Transportation Technology	tongyi-005	005	2019-06-12
332	TW	Toppan ID Gate	toppanidgate-000	000	2021-09-28
333	JP	Toshiba	toshiba-003	003	2019-03-01
334	JP	Toshiba	toshiba-004	004	2021-09-27
335	JP	Tripleize	aize-001	001	2021-04-23
336	JP	Tripleize	aize-002	002	2021-10-08
337	US	Trueface.ai	trueface-002	002	2021-03-29
338	US	Trueface.ai	trueface-003	003	2021-09-30
339	CN	ULSee Inc	ulsee-001	001	2019-07-31
340	FR	Unissey	unissey-001	001	2021-11-29
341	PT	Universidade de Coimbra	visteam-001	001	2021-03-16
342	PT	Universidade de Coimbra	visteam-002	002	2021-08-20
343	US	VCognition	vcog-002	002	2017-06-12
344	ES	Veridas Digital Authentication Solutions S.L.	veridas-006	006	2021-04-15
345	ES	Veridas Digital Authentication Solutions S.L.	veridas-007	007	2021-09-02
346	KZ	Verigram	verigram-000	000	2021-09-06
347	ID	Verihubs	verihubs-inteligensia-000	000	2021-07-27
348	TW	Via Technologies Inc	via-000	000	2019-07-08
349	TW	Via Technologies Inc	via-001	001	2020-01-08
350	DE	Videmo Intelligent Videoanalyse	videmo-000	000	2019-12-19

Table 5: Summary of participant information included in this report.

	Location	Developer Name	Short Name	Seq. Num.	Validation Date
351	DE	Videmo Intelligent Videoanalyse	videmo-001	001	2021-12-22
352	IN	Videonetics Technology Pvt	videonetics-001	001	2019-06-19
353	IN	Videonetics Technology Pvt	videonetics-002	002	2019-11-21
354	VN	Vietnam Posts and Telecommunications Group	vnpt-002	002	2021-06-08
355	VN	Vietnam Posts and Telecommunications Group	vnpt-003	003	2021-12-01
356	VN	Viettel Group	vts-000	000	2020-11-04
357	VN	Viettel High Technology	viettelhightech-000	000	2021-08-04
358	US	Vigilant Solutions	vigilantsolutions-010	010	2021-04-07
359	US	Vigilant Solutions	vigilantsolutions-011	011	2021-08-07
360	VN	VinAI Research VietNam	vinai-000	000	2020-09-24
361	SE	Visage Technologies	visage-000	000	2020-12-09
362	FI	Visidon	vd-002	002	2021-04-12
363	FI	Visidon	vd-003	003	2021-10-12
364	CN	Vision Intelligence Center of Meituan	meituan-000	000	2021-05-14
365	PT	Vision-Box	visionbox-001	001	2019-03-01
366	PT	Vision-Box	visionbox-002	002	2021-04-29
367	RU	VisionLabs	visionlabs-010	010	2021-01-25
368	RU	VisionLabs	visionlabs-011	011	2021-10-13
369	RU	Vocord	vocord-008	008	2020-01-31
370	RU	Vocord	vocord-009	009	2020-12-28
371	CN	Winsense	winsense-001	001	2019-10-16
372	CN	Winsense	winsense-002	002	2020-11-20
373	CN	Wuhan Tianyu Information Industry	wuhantianyu-001	001	2021-08-05
374	CN	X-Laboratory	x-laboratory-000	000	2019-09-03
375	CN	X-Laboratory	x-laboratory-001	001	2020-01-21
376	CN	Xforward AI Technology	xforwardai-001	001	2020-09-25
377	CN	Xforward AI Technology	xforwardai-002	002	2021-02-10
378	CN	Xiamen Meiya Pico Information	meiya-001	001	2019-03-01
379	CN	Xiamen University	xm-000	000	2020-10-19
380	PT	YooniK	yoonik-001	001	2020-10-26
381	PT	YooniK	yoonik-002	002	2021-09-06
382	PT	YooniK	yoonik-003	003	2022-01-06
383	TW	Yuan High-Tech Development	yuan-002	002	2021-05-17
384	TW	Yuan High-Tech Development	yuan-003	003	2021-09-17
385	CN	Yuntu Data and Technology	ytu-000	000	2021-06-16
386	CN	Zhuhai Yisheng Electronics Technology	yisheng-004	004	2018-06-12
387	[**Developer country**]	[**Developer name**]	armatura-001	001	2022-01-04
388	[**Developer country**]	[**Developer name**]	beyneai-000	000	2022-01-03
389	[**Developer country**]	[**Developer name**]	omsecurity-000	000	2021-12-15
390	[**Developer country**]	[**Developer name**]	vinbigdata-001	001	2022-01-06
391	CN	iQIYI Inc	iqface-000	000	2019-06-04
392	CN	iQIYI Inc	iqface-003	003	2021-02-23
393	TW	iSAP Solution Corporation	isap-001	001	2019-08-07
394	TW	iSAP Solution Corporation	isap-002	002	2020-09-01
395	TW	ioNetworks Inc	ionetworks-000	000	2021-07-20

Table 6: Summary of participant information included in this report.

ALGORITHM				CONFIG	LIBRARY	TEMPLATE					COMPARISON <sup>4</sup>		
NAME		DATA	DATA	MEMORY	SIZE	GENERATION TIME (ms) <sup>4</sup>					TIME (ns) <sup>5</sup>		
		(KB) <sup>1</sup>	(KB) <sup>2</sup>	(MB) <sup>3</sup>	(B)	MUGSHOT	480x720	960x1440	1600x2400	3000x4500	GENUINE	IMPOSTOR	
1	20face-000	117155	324083	183 <sup>905</sup>	144 <sup>2048</sup> ± 0	31 <sup>232</sup> ± 1	20 <sup>223</sup> ± 1	15 <sup>226</sup> ± 4	13 <sup>222</sup> ± 1	10 <sup>224</sup> ± 1	354 <sup>44880</sup> ± 134	353 <sup>44462</sup> ± 163	
2	20face-001	226824	324119	304 <sup>1940</sup>	351 <sup>4096</sup> ± 0	41 <sup>279</sup> ± 2	24 <sup>266</sup> ± 1	18 <sup>266</sup> ± 1	17 <sup>267</sup> ± 1	13 <sup>267</sup> ± 0	281 <sup>5553</sup> ± 54	279 <sup>5541</sup> ± 65	
3	3divi-006	273866	52656	73 <sup>472</sup>	126 <sup>2048</sup> ± 0	177 <sup>654</sup> ± 1	141 <sup>651</sup> ± 0	125 <sup>660</sup> ± 1	109 <sup>678</sup> ± 2	111 <sup>759</sup> ± 13	93 <sup>775</sup> ± 19	92 <sup>770</sup> ± 22	
4	3divi-007	483115	24723	243 <sup>1285</sup>	234 <sup>2048</sup> ± 0	162 <sup>615</sup> ± 1	133 <sup>616</sup> ± 1	111 <sup>623</sup> ± 1	98 <sup>644</sup> ± 1	101 <sup>727</sup> ± 5	78 <sup>707</sup> ± 31	81 <sup>712</sup> ± 25	
5	acer-001	36650	66086	59 <sup>417</sup>	17 <sup>512</sup> ± 0	28 <sup>199</sup> ± 0	21 <sup>237</sup> ± 28	16 <sup>229</sup> ± 26	16 <sup>242</sup> ± 37	12 <sup>259</sup> ± 21	212 <sup>2453</sup> ± 44	214 <sup>2461</sup> ± 62	
6	acer-002	43922	624858	28 <sup>187</sup>	150 <sup>2048</sup> ± 0	25 <sup>184</sup> ± 0	16 <sup>184</sup> ± 0	10 <sup>185</sup> ± 0	8 <sup>185</sup> ± 0	8 <sup>186</sup> ± 0	248 <sup>3370</sup> ± 47	248 <sup>3350</sup> ± 54	
7	acisw-003	282029	35664	40 <sup>282</sup>	379 <sup>18467</sup> ± 8	32 <sup>232</sup> ± 1	25 <sup>267</sup> ± 22	67 <sup>488</sup> ± 28	204 <sup>990</sup> ± 24	308 <sup>2977</sup> ± 129	380 <sup>847908</sup> ± 16757	380 <sup>851850</sup> ± 17018	
8	acisw-007	267619	36111	41 <sup>286</sup>	172 <sup>2048</sup> ± 0	46 <sup>283</sup> ± 0	34 <sup>293</sup> ± 3	40 <sup>414</sup> ± 0	28 <sup>404</sup> ± 0	36 <sup>484</sup> ± 1	143 <sup>1316</sup> ± 22	143 <sup>1297</sup> ± 23	
9	ader-a-002	0	749797	188 <sup>921</sup>	369 <sup>5120</sup> ± 0	370 <sup>1394</sup> ± 11	325 <sup>1381</sup> ± 1	322 <sup>1393</sup> ± 1	297 <sup>1403</sup> ± 1	254 <sup>1464</sup> ± 2	202 <sup>2163</sup> ± 32	203 <sup>2158</sup> ± 28	
10	ader-a-003	0	749778	186 <sup>917</sup>	370 <sup>5120</sup> ± 0	366 <sup>1381</sup> ± 12	327 <sup>1385</sup> ± 1	323 <sup>1394</sup> ± 1	295 <sup>1401</sup> ± 1	255 <sup>1469</sup> ± 1	201 <sup>2148</sup> ± 34	200 <sup>2130</sup> ± 32	
11	advance-002	257173	20434	45 <sup>295</sup>	183 <sup>2048</sup> ± 0	232 <sup>811</sup> ± 2	189 <sup>803</sup> ± 2	140 <sup>696</sup> ± 2	115 <sup>699</sup> ± 4	97 <sup>718</sup> ± 1	109 <sup>987</sup> ± 10	107 <sup>988</sup> ± 45	
12	advance-003	258867	78699	90 <sup>518</sup>	92 <sup>2048</sup> ± 0	143 <sup>586</sup> ± 0	118 <sup>584</sup> ± 0	97 <sup>583</sup> ± 0	78 <sup>588</sup> ± 0	63 <sup>591</sup> ± 1	183 <sup>1813</sup> ± 17	179 <sup>1788</sup> ± 26	
13	aifirst-001	224157	808777	76 <sup>485</sup>	221 <sup>2048</sup> ± 0	147 <sup>587</sup> ± 2	113 <sup>568</sup> ± 2	98 <sup>584</sup> ± 3	85 <sup>601</sup> ± 6	109 <sup>755</sup> ± 5	128 <sup>1099</sup> ± 14	127 <sup>1087</sup> ± 45	
14	aigen-001	256958	595227	224 <sup>1136</sup>	198 <sup>2048</sup> ± 0	378 <sup>1448</sup> ± 9	337 <sup>1451</sup> ± 8	339 <sup>1759</sup> ± 6	337 <sup>2594</sup> ± 4	325 <sup>5691</sup> ± 44	261 <sup>3772</sup> ± 57	260 <sup>3736</sup> ± 56	
15	aigen-002	205300	1316138	178 <sup>874</sup>	256 <sup>2048</sup> ± 0	146 <sup>586</sup> ± 24	117 <sup>582</sup> ± 4	206 <sup>920</sup> ± 4	319 <sup>1758</sup> ± 5	323 <sup>5427</sup> ± 17	258 <sup>3678</sup> ± 44	256 <sup>3646</sup> ± 48	
16	ailabs-001	1054663	338989	238 <sup>1252</sup>	240 <sup>2048</sup> ± 0	184 <sup>664</sup> ± 4	183 <sup>774</sup> ± 50	270 <sup>1145</sup> ± 12	325 <sup>1972</sup> ± 74	321 <sup>5205</sup> ± 272	371 <sup>104034</sup> ± 661	371 <sup>103415</sup> ± 7722	
17	aimall-002	370156	25210	276 <sup>1576</sup>	170 <sup>2048</sup> ± 0	222 <sup>776</sup> ± 4	238 <sup>927</sup> ± 27	215 <sup>940</sup> ± 21	196 <sup>955</sup> ± 34	167 <sup>1003</sup> ± 75	368 <sup>72811</sup> ± 7399	367 <sup>71216</sup> ± 6286	
18	aimall-003	504324	171935	300 <sup>1913</sup>	63 <sup>1024</sup> ± 0	182 <sup>662</sup> ± 1	173 <sup>740</sup> ± 51	157 <sup>752</sup> ± 62	131 <sup>741</sup> ± 46	121 <sup>807</sup> ± 47	349 <sup>34565</sup> ± 93	350 <sup>34598</sup> ± 118	
19	aiunionface-000	241642	840295	54 <sup>402</sup>	167 <sup>2048</sup> ± 0	171 <sup>637</sup> ± 13	177 <sup>754</sup> ± 41	240 <sup>1025</sup> ± 28	247 <sup>1179</sup> ± 29	268 <sup>1639</sup> ± 47	119 <sup>1072</sup> ± 19	125 <sup>1080</sup> ± 47	
20	aize-001	268456	168970	263 <sup>1436</sup>	214 <sup>2048</sup> ± 0	88 <sup>437</sup> ± 10	66 <sup>440</sup> ± 8	84 <sup>542</sup> ± 17	136 <sup>756</sup> ± 27	264 <sup>1583</sup> ± 53	191 <sup>1937</sup> ± 22	188 <sup>1919</sup> ± 23	
21	aize-002	257106	182517	108 <sup>586</sup>	246 <sup>2048</sup> ± 0	98 <sup>467</sup> ± 1	79 <sup>479</sup> ± 1	159 <sup>756</sup> ± 1	307 <sup>1477</sup> ± 1	319 <sup>4617</sup> ± 41	48 <sup>597</sup> ± 16	52 <sup>598</sup> ± 14	
22	ajou-001	363257	31734	65 <sup>442</sup>	230 <sup>2048</sup> ± 0	120 <sup>530</sup> ± 0	99 <sup>536</sup> ± 0	82 <sup>535</sup> ± 0	71 <sup>549</sup> ± 0	60 <sup>577</sup> ± 0	47 <sup>597</sup> ± 19	50 <sup>596</sup> ± 13	
23	alchera-002	405409	22275	236 <sup>1233</sup>	157 <sup>2048</sup> ± 0	294 <sup>968</sup> ± 1	248 <sup>976</sup> ± 2	227 <sup>979</sup> ± 1	203 <sup>988</sup> ± 1	171 <sup>1025</sup> ± 2	254 <sup>3488</sup> ± 63	252 <sup>3430</sup> ± 63	
24	alchera-003	487718	24613	252 <sup>1376</sup>	243 <sup>2048</sup> ± 0	253 <sup>854</sup> ± 3	209 <sup>862</sup> ± 2	186 <sup>870</sup> ± 1	169 <sup>882</sup> ± 2	147 <sup>918</sup> ± 1	251 <sup>3426</sup> ± 57	249 <sup>3383</sup> ± 53	
25	alfabeta-001	128232	21780	67 <sup>73</sup>	36 <sup>512</sup> ± 0	38 <sup>271</sup> ± 0	29 <sup>276</sup> ± 0	55 <sup>459</sup> ± 2	171 <sup>886</sup> ± 2	299 <sup>2547</sup> ± 9	34 <sup>470</sup> ± 25	36 <sup>458</sup> ± 20	
26	alice-000	1741293	19355	288 <sup>1732</sup>	319 <sup>4096</sup> ± 0	287 <sup>950</sup> ± 2	240 <sup>933</sup> ± 1	220 <sup>949</sup> ± 1	210 <sup>1011</sup> ± 3	217 <sup>1264</sup> ± 8	323 <sup>14975</sup> ± 201	322 <sup>14890</sup> ± 229	
27	alleyes-000	507636	997090	175 <sup>857</sup>	197 <sup>2048</sup> ± 0	225 <sup>784</sup> ± 1	246 <sup>970</sup> ± 61	225 <sup>974</sup> ± 62	192 <sup>943</sup> ± 69	180 <sup>1057</sup> ± 23	142 <sup>1298</sup> ± 34	144 <sup>1303</sup> ± 51	
28	algovision-000	172509	155862	103 <sup>561</sup>	200 <sup>2048</sup> ± 0	71 <sup>384</sup> ± 8	52 <sup>395</sup> ± 17	39 <sup>413</sup> ± 14	49 <sup>471</sup> ± 14	93 <sup>710</sup> ± 21	347 <sup>29903</sup> ± 406	348 <sup>29735</sup> ± 194	
29	alphaface-001	259849	81636	93 <sup>527</sup>	180 <sup>2048</sup> ± 0	159 <sup>612</sup> ± 1	128 <sup>613</sup> ± 3	108 <sup>612</sup> ± 1	90 <sup>619</sup> ± 1	76 <sup>640</sup> ± 2	114 <sup>1008</sup> ± 10	114 <sup>1002</sup> ± 19	
30	alphaface-002	768995	70692	262 <sup>1434</sup>	123 <sup>2048</sup> ± 0	168 <sup>628</sup> ± 2	174 <sup>746</sup> ± 19	156 <sup>751</sup> ± 18	142 <sup>779</sup> ± 22	127 <sup>828</sup> ± 40	104 <sup>945</sup> ± 25	103 <sup>935</sup> ± 17	
31	amplifiedgroup-001	0	47053	10 <sup>81</sup>	52 <sup>866</sup> ± 2	8 <sup>93</sup> ± 0	-	-	-	-	363 <sup>57803</sup> ± 4210	360 <sup>56365</sup> ± 1196	
32	androvideo-000	174847	585063	55 <sup>403</sup>	125 <sup>2048</sup> ± 0	40 <sup>277</sup> ± 0	32 <sup>285</sup> ± 0	23 <sup>314</sup> ± 0	26 <sup>372</sup> ± 1	69 <sup>620</sup> ± 0	229 <sup>2860</sup> ± 28	229 <sup>2847</sup> ± 22	
33	anke-004	349388	410776	140 <sup>706</sup>	296 <sup>2056</sup> ± 0	166 <sup>625</sup> ± 1	134 <sup>627</sup> ± 2	119 <sup>635</sup> ± 3	103 <sup>653</sup> ± 2	163 <sup>982</sup> ± 8	63 <sup>633</sup> ± 22	65 <sup>632</sup> ± 34	
34	anke-005	328553	429160	223 <sup>1134</sup>	286 <sup>2056</sup> ± 0	148 <sup>590</sup> ± 2	123 <sup>594</sup> ± 5	104 <sup>601</sup> ± 3	97 <sup>638</sup> ± 4	125 <sup>821</sup> ± 24	74 <sup>685</sup> ± 19	77 <sup>687</sup> ± 26	
35	antheus-000	119453	41994	16 <sup>116</sup>	43 <sup>520</sup> ± 0	12 <sup>109</sup> ± 1	17 <sup>187</sup> ± 1	12 <sup>189</sup> ± 1	9 <sup>195</sup> ± 1	11 <sup>236</sup> ± 2	297 <sup>6901</sup> ± 268	297 <sup>6936</sup> ± 103	
36	antheus-001	119453	41962	17 <sup>118</sup>	42 <sup>520</sup> ± 0	14 <sup>120</sup> ± 1	23 <sup>265</sup> ± 13	61 <sup>468</sup> ± 22	257 <sup>1223</sup> ± 27	300 <sup>2660</sup> ± 87	293 <sup>6218</sup> ± 47	292 <sup>6216</sup> ± 45	
37	anyvision-004	401001	630797	220 <sup>1102</sup>	62 <sup>1024</sup> ± 0	61 <sup>355</sup> ± 1	-	-	-	-	189 <sup>1891</sup> ± 51	183 <sup>1829</sup> ± 85	
38	anyvision-005	190979	116595	196 <sup>963</sup>	61 <sup>1024</sup> ± 0	297 <sup>985</sup> ± 1	251 <sup>997</sup> ± 1	237 <sup>1004</sup> ± 1	205 <sup>995</sup> ± 1	168 <sup>995</sup> ± 1	84 <sup>733</sup> ± 14	86 <sup>733</sup> ± 16	
39	armatura-001	0	374608	225 <sup>1151</sup>	117 <sup>2048</sup> ± 0	195 <sup>688</sup> ± 1	153 <sup>689</sup> ± 1	138 <sup>693</sup> ± 1	119 <sup>708</sup> ± 3	110 <sup>756</sup> ± 13	14 <sup>270</sup> ± 17	17 <sup>268</sup> ± 11	
40	asusaics-000	257418	245320	116 <sup>605</sup>	189 <sup>2048</sup> ± 0	106 <sup>484</sup> ± 13	93 <sup>506</sup> ± 21	181 <sup>850</sup> ± 26	320 <sup>1789</sup> ± 61	327 <sup>6305</sup> ± 188	279 <sup>5455</sup> ± 78	278 <sup>5422</sup> ± 112	
41	asusaics-001	257418	245330	113 <sup>595</sup>	331 <sup>4096</sup> ± 0	250 <sup>842</sup> ± 17	254 <sup>1008</sup> ± 20	318 <sup>1377</sup> ± 28	336 <sup>2423</sup> ± 90	332 <sup>7284</sup> ± 277	308 <sup>8618</sup> ± 42	308 <sup>8638</sup> ± 136	
42	authenmetric-003	293599	39492	201 <sup>982</sup>	237 <sup>2048</sup> ± 0	300 <sup>992</sup> ± 1	253 <sup>1006</sup> ± 1	236 <sup>1003</sup> ± 2	209 <sup>1002</sup> ± 1	174 <sup>1036</sup> ± 1	172 <sup>1757</sup> ± 19	171 <sup>1755</sup> ± 19	
43	authenmetric-004	381165	39492	230 <sup>1214</sup>	235 <sup>2048</sup> ± 0	272 <sup>910</sup> ± 1	231 <sup>909</sup> ± 1	203 <sup>915</sup> ± 1	183 <sup>921</sup> ± 2	156 <sup>950</sup> ± 1	168 <sup>1724</sup> ± 14	165 <sup>1691</sup> ± 29	
44	aware-005	300017	26320	240 <sup>1265</sup>	83 <sup>1572</sup> ± 0	268 <sup>886</sup> ± 23	265 <sup>1038</sup> ± 21	263 <sup>1121</sup> ± 22	279 <sup>1337</sup> ± 58	284 <sup>2195</sup> ± 144	155 <sup>1475</sup> ± 63	151 <sup>1427</sup> ± 115	

Table 7: Summary of algorithms and properties included in this report. The red superscripts give ranking for the quantity in that column.

Notes												
1	The configuration size does not capture static data included											

	ALGORITHM	CONFIG	LIBRARY	TEMPLATE								COMPARISON <sup>4</sup>								
				NAME	DATA	DATA	MEMORY	SIZE (B)	GENERATION TIME (ms) <sup>4</sup>				TIME (ns) <sup>5</sup>							
									MUGSHOT	480x720	960x1440	1600x2400	3000x4500	GENUINE	IMPOSTOR					
		(KB) <sup>1</sup>	(KB) <sup>2</sup>	(MB) <sup>3</sup>																
45	aware-006	298543	14124	194 <sup>943</sup>	14 <sup>352</sup>	0 ±	328	1148 ± 3	287	1146 ± 2	281	1190 ± 2	271	1306 ± 20	275 <sup>1754</sup>	± 84	221 <sup>2598</sup>	± 42	221 <sup>2559</sup>	± 60
46	awiros-001	15499	87480	12 <sup>88</sup>	29 <sup>512</sup>	0 ±	9	97 ± 6	5	98 ± 4	6	138 ± 6	14	225 ± 7	56	556 ± 8	121 <sup>1079</sup>	± 44	120 <sup>1050</sup>	± 45
47	awiros-002	289016	203723	104 <sup>562</sup>	166 <sup>2048</sup>	0 ±	102	479 ± 0	91	500 ± 0	81	534 ± 0	89	618 ± 0	165	946 ± 1	192 <sup>1966</sup>	± 31	192 <sup>1957</sup>	± 25
48	ayftech-001	195423	43580	149 <sup>731</sup>	22 <sup>512</sup>	0 ±	77	408 ± 23	78	476 ± 52	170	814 ± 108	321	1827 ± 384	322	5412 ± 1029	56	615 ± 16	103 <sup>885</sup>	± 44
49	ayonix-000	58505	5252	5 <sup>69</sup>	68 <sup>1036</sup>	0 ±	2	18 ± 2	-	-	-	-	-	-	-	58	621 ± 23	60 <sup>620</sup>	± 26	
50	beethedata-000	227849	1087592	102 <sup>555</sup>	255 <sup>2048</sup>	0 ±	96	465 ± 0	77	467 ± 0	59	468 ± 0	48	467 ± 0	31	467 ± 0	199 <sup>2121</sup>	± 34	199 <sup>2110</sup>	± 38
51	beyneai-000	256958	591433	221 <sup>1124</sup>	131 <sup>2048</sup>	0 ±	91	451 ± 8	69	449 ± 1	161	767 ± 7	314	1603 ± 25	320	4669 ± 124	260 <sup>3730</sup>	± 57	258 <sup>3668</sup>	± 54
52	biocube-001	25030	6192987	69 <sup>458</sup>	339 <sup>4096</sup>	0 ±	45	282 ± 22	33	292 ± 24	79	521 ± 57	110	684 ± 59	220	1282 ± 68	336 <sup>21812</sup>	± 109	336 <sup>21812</sup>	± 109
53	bioditechswiss-001	1178769	120811	265 <sup>1455</sup>	31 <sup>512</sup>	0 ±	293	966 ± 4	309	1270 ± 270	301	1294 ± 96	298	1409 ± 157	277	1793 ± 79	222 <sup>2610</sup>	± 25	223 <sup>2624</sup>	± 32
54	bioditechswiss-002	744786	114842	204 <sup>993</sup>	35 <sup>512</sup>	0 ±	275	917 ± 2	239	930 ± 2	221	952 ± 2	194	947 ± 3	181	1058 ± 11	203 <sup>2177</sup>	± 29	204 <sup>2170</sup>	± 31
55	bm-001	287734	38076	22 <sup>148</sup>	1	64 ± 0	89	444 ± 88	-	-	-	-	-	-	-	188	1887 ± 31	187 <sup>1877</sup>	± 26	
56	boetech-001	261376	88710	255 <sup>1384</sup>	241 <sup>2048</sup>	0 ±	37	271 ± 1	26	268 ± 1	19	273 ± 0	18	286 ± 1	16	318 ± 1	365 <sup>68519</sup>	± 1921	365 <sup>67648</sup>	± 822
57	boetech-002	294347	88710	268 <sup>1489</sup>	165 <sup>2048</sup>	0 ±	51	305 ± 4	36	296 ± 1	21	302 ± 1	19	313 ± 1	19	348 ± 2	366 <sup>68921</sup>	± 2137	366 <sup>69473</sup>	± 2104
58	bresee-001	287880	23227	231 <sup>1214</sup>	223 <sup>2048</sup>	0 ±	342	1223 ± 3	298	1216 ± 1	312	1331 ± 1	260	1227 ± 1	234	1360 ± 1	350 <sup>37240</sup>	± 655	351 <sup>37167</sup>	± 584
59	bresee-002	313627	30902	306 <sup>1956</sup>	140 <sup>2048</sup>	0 ±	211	743 ± 4	285	1143 ± 2	271	1146 ± 2	241	1148 ± 2	205	1176 ± 2	174 <sup>1778</sup>	± 22	174 <sup>1775</sup>	± 23
60	camvi-002	236278	225285	150 <sup>737</sup>	56 <sup>1024</sup>	0 ±	189	677 ± 7	167	726 ± 36	185	869 ± 28	235	1129 ± 43	305	2785 ± 113	55 <sup>612</sup>	± 26	54 <sup>603</sup>	± 20
61	camvi-004	280733	615819	187 <sup>919</sup>	220 <sup>2048</sup>	0 ±	215	759 ± 10	208	861 ± 17	231	986 ± 34	267	1279 ± 51	307	2891 ± 158	105 <sup>948</sup>	± 40	106 <sup>963</sup>	± 31
62	canon-002	446491	130232	181 <sup>891</sup>	335 <sup>4096</sup>	0 ±	358	1308 ± 2	317	1315 ± 1	310	1326 ± 2	282	1345 ± 1	253	1452 ± 1	292 <sup>6211</sup>	± 25	291 <sup>6194</sup>	± 25
63	canon-003	2550850	101378	368 <sup>5472</sup>	373 <sup>6180</sup>	0 ±	349	1263 ± 3	307	1263 ± 1	294	1283 ± 1	277	1320 ± 1	258	1482 ± 2	272 <sup>4783</sup>	± 17	269 <sup>4780</sup>	± 19
64	ceiec-003	260371	88707	63 <sup>430</sup>	174 <sup>2048</sup>	0 ±	237	817 ± 4	220	883 ± 57	195	897 ± 60	176	899 ± 72	153	944 ± 72	207 <sup>2256</sup>	± 38	207 <sup>2241</sup>	± 54
65	ceiec-004	263476	67011	56 <sup>408</sup>	134 <sup>2048</sup>	0 ±	304	1024 ± 1	258	1027 ± 1	242	1027 ± 1	213	1030 ± 1	179	1055 ± 1	185 <sup>1844</sup>	± 26	184 <sup>1836</sup>	± 20
66	chosun-001	765615	707	80 <sup>491</sup>	128 <sup>2048</sup>	0 ±	224	783 ± 2	196	826 ± 4	338	1662 ± 13	342	3679 ± 67	339	11694 ± 243	111 <sup>998</sup>	± 25	119 <sup>1035</sup>	± 11
67	chosun-002	234001	31875	66 <sup>450</sup>	159 <sup>2048</sup>	0 ±	33	248 ± 3	28	273 ± 3	334	1495 ± 14	343	7920 ± 90	340	80302 ± 1349	60 <sup>623</sup>	± 17	67 <sup>634</sup>	± 13
68	chtface-003	363153	369529	227 <sup>1178</sup>	87 <sup>2048</sup>	0 ±	153	594 ± 16	165	720 ± 33	250	1050 ± 41	324	1884 ± 90	324	5606 ± 334	198 <sup>2110</sup>	± 37	206 <sup>2219</sup>	± 65
69	chtface-004	409656	311027	267 <sup>1487</sup>	205 <sup>2048</sup>	0 ±	56	332 ± 0	35	323 ± 1	26	329 ± 1	21	335 ± 1	22	377 ± 1	169 <sup>1727</sup>	± 17	168 <sup>1720</sup>	± 16
70	clearviewai-000	342491	211852	334 <sup>2750</sup>	164 <sup>2048</sup>	0 ±	373	1402 ± 1	331	1403 ± 1	325	1412 ± 1	301	1420 ± 1	248	1418 ± 1	159 <sup>1592</sup>	± 37	158 <sup>1561</sup>	± 37
71	closeli-001	420342	9851	154 <sup>773</sup>	345 <sup>4096</sup>	0 ±	249	839 ± 1	203	843 ± 1	179	841 ± 1	159	845 ± 1	137	865 ± 1	278 <sup>5404</sup>	± 17	277 <sup>5400</sup>	± 25
72	cloudmatrix-000	309939	542141	146 <sup>727</sup>	105 <sup>2048</sup>	0 ±	213	754 ± 10	175	750 ± 2	158	754 ± 4	140	764 ± 1	118	793 ± 2	358 <sup>49192</sup>	± 206	358 <sup>49275</sup>	± 176
73	cloudwalk-hr-003	383739	144263	203 <sup>984</sup>	298 <sup>2057</sup>	0 ±	156	606 ± 0	120	588 ± 0	100	594 ± 0	120	612 ± 1	-	-	300 <sup>6982</sup>	± 80	299 <sup>6972</sup>	± 84
74	cloudwalk-hr-004	502916	520169	257 <sup>1394</sup>	260 <sup>2049</sup>	0 ±	262	873 ± 1	218	877 ± 1	190	876 ± 1	168	879 ± 1	143	902 ± 3	315 <sup>11652</sup>	± 127	314 <sup>11608</sup>	± 123
75	cloudwalk-mt-003	490365	494959	248 <sup>1342</sup>	261 <sup>2049</sup>	0 ±	278	923 ± 1	233	918 ± 1	211	926 ± 1	184	925 ± 1	151	936 ± 1	314 <sup>11620</sup>	± 179	316 <sup>11661</sup>	± 128
76	cloudwalk-mt-004	1384602	512628	367 <sup>5426</sup>	239 <sup>2048</sup>	0 ±	279	923 ± 2	234	919 ± 1	205	918 ± 0	182	919 ± 0	148	927 ± 1	316 <sup>11744</sup>	± 170	315 <sup>11631</sup>	± 126
77	clova-000	198420	6824	71 <sup>464</sup>	161 <sup>2048</sup>	0 ±	87	437 ± 0	62	431 ± 0	47	435 ± 0	41	452 ± 2	40	508 ± 7	177 <sup>1794</sup>	± 16	180 <sup>1795</sup>	± 19
78	cogent-005	1876796	75276	336 <sup>2806</sup>	310 <sup>2523</sup>	0 ±	341	1221 ± 2	303	1236 ± 1	296	1289 ± 2	300	1420 ± 4	269	1602 ± 5	342 <sup>24854</sup>	± 69	342 <sup>24858</sup>	± 71
79	cogent-006	1078167	58108	272 <sup>1547</sup>	71 <sup>1062</sup>	0 ±	219	768 ± 0	186	789 ± 1	177	831 ± 2	186	930 ± 1	161	971 ± 1	179 <sup>1802</sup>	± 17	181 <sup>1797</sup>	± 23
80	cognitec-002	394088	62354	119 <sup>624</sup>	268 <sup>2052</sup>	0 ±	26	192 ± 6	19	219 ± 6	17	233 ± 8	15	241 ± 6	10	314 ± 10	246 <sup>3250</sup>	± 41	246 <sup>3241</sup>	± 48
81	cognitec-003	471458	62502	165 <sup>817</sup>	267 <sup>2052</sup>	0 ±	67	366 ± 9	54	403 ± 9	37	408 ± 9	34	424 ± 9	41	509 ± 13	250 <sup>3417</sup>	± 51	253 <sup>3433</sup>	± 53
82	cor-001	1194948	11240	237 <sup>1249</sup>	301 <sup>2060</sup>	0 ±	200	699 ± 3	211	863 ± 76	183	865 ± 80	165	872 ± 89	157	952 ± 39	376 <sup>270145</sup>	± 2259	376 <sup>282686</sup>	± 11788
83	coretech-000	186423	43964	53 <sup>393</sup>	19 <sup>512</sup>	0 ±	155	602 ± 15	142	659 ± 12	268	1139 ± 24	242	1149 ± 25	201	1165 ± 23	22	333 ± 14	22 <sup>321</sup>	± 13
84	corsight-001	1437763	31525	312 <sup>2040</sup>	302 <sup>2064</sup>	0 ±	355	1291 ± 3	310	1285 ± 1	299	1293 ± 1	270	1303 ± 2	233	1379 ± 3	375 <sup>249340</sup>	± 1713	375 <sup>248929</sup>	± 1909
85	corsight-002	1474921	32093	313 <sup>2061</sup>	305 <sup>2080</sup>	0 ±	354	1290 ± 1	311	1287 ± 1	297	1290 ± 1	272	1307 ± 2	240	1388 ± 4	343 <sup>24953</sup>	± 637	341 <sup>24263</sup>	± 578
86	csc-002	0	519768	253 <sup>1376</sup>	47 <sup>544</sup>	0 ±	100	473 ± 0	88	494 ± 0	63	481 ± 1	55	490 ± 1	44	514 ± 5	27	367 ± 11	28 <sup>371</sup>	± 10
87	csc-003	0	400435	281 <sup>1609</sup>	46 <sup>544</sup>	0 ±	111	499 ± 0	90	500 ± 1	72	502 ± 0	59	508 ± 1	48	535 ± 4	30	393 ± 8	31 <sup>397</sup>	± 7
88	ctcbcbank-000	257208	599238	106 <sup>570</sup>	139 <sup>2048</sup>	0 ±	137	568 ± 43	126	606 ± 38	136	690 ± 53	121	711 ± 50	128	831 ± 51	255 <sup>3551</sup>	± 87	271 <sup>4805</sup>	± 209

Notes

- The configuration size does not capture static data included in libraries.
- The library size is the combined total of all files provided in the submission lib folder. These libraries e.g. OpenCV may or may not be installed on any end user's platform natively and would not need to be

ALGORITHM		CONFIG		LIBRARY	TEMPLATE					COMPARISON <sup>4</sup>		
NAME		DATA	DATA	MEMORY	SIZE	GENERATION TIME (ms) <sup>4</sup>				TIME (ns) <sup>5</sup>		
		(KB) <sup>1</sup>	(KB) <sup>2</sup>	(MB) <sup>3</sup>	(B)	MUGSHOT	480x720	960x1440	1600x2400	3000x4500	GENUINE	IMPOSTOR
89	ctbcbank-001	275511	599238	114 603	179 2048 ± 0	175 652 ± 35	185 781 ± 30	189 875 ± 43	175 898 ± 51	172 1030 ± 47	262 3926 ± 45	262 3924 ± 56
90	cubox-001	369627	75427	122 649	191 2048 ± 0	271 907 ± 1	229 902 ± 1	193 903 ± 0	180 917 ± 0	149 931 ± 0	145 1379 ± 37	150 1417 ± 38
91	cubox-002	542254	90975	307 1964	116 2048 ± 0	276 921 ± 1	235 921 ± 1	208 922 ± 1	188 933 ± 1	168 1003 ± 1	194 2008 ± 72	194 1969 ± 57
92	cudocommunication-001	385258	341277	215 1077	135 2048 ± 0	280 925 ± 1	236 923 ± 1	213 928 ± 1	187 932 ± 0	159 964 ± 1	216 2534 ± 20	218 2537 ± 20
93	cuuhkee-001	787853	74917	325 2515	263 2052 ± 0	295 977 ± 31	-	-	-	-	223 2719 ± 60	227 2783 ± 56
94	cybercore-000	86008	55441	33 200	27 512 ± 0	179 655 ± 3	154 689 ± 71	123 649 ± 6	100 648 ± 8	85 680 ± 6	322 14800 ± 75	324 15757 ± 782
95	cybercore-001	166096	7791	327 2574	115 2048 ± 0	108 487 ± 0	83 486 ± 0	53 487 ± 0	39 502 ± 0	359 52119 ± 111	359 52127 ± 111	
96	cyberextruder-001	121211	13629	27 178	3 256 ± 0	270 893 ± 25	-	-	-	-	122 1083 ± 16	124 1079 ± 19
97	cyberextruder-002	168909	13924	32 194	228 2048 ± 0	122 532 ± 6	-	-	-	-	180 1803 ± 14	176 1779 ± 22
98	cyberlink-007	380046	102446	289 1743	374 6212 ± 0	204 725 ± 1	170 732 ± 1	152 734 ± 1	129 736 ± 1	116 767 ± 1	19 304 ± 19	20 304 ± 16
99	cyberlink-008	380047	102470	290 1748	375 6212 ± 0	206 729 ± 1	166 725 ± 0	149 727 ± 0	127 732 ± 0	112 760 ± 0	13 263 ± 17	16 255 ± 13
100	dahua-006	831641	119261	365 5068	203 2048 ± 0	371 1398 ± 2	330 1397 ± 1	324 1404 ± 1	296 1402 ± 1	243 1402 ± 1	11 249 ± 13	14 250 ± 11
101	dahua-007	1578737	119418	374 7237	332 4096 ± 0	369 1393 ± 2	324 1373 ± 1	319 1378 ± 1	289 1378 ± 1	236 1379 ± 2	28 367 ± 102	33 434 ± 108
102	daon-000	280726	2307	311 2013	303 2065 ± 0	133 562 ± 3	116 581 ± 5	164 791 ± 9	155 838 ± 15	178 1055 ± 32	325 16052 ± 88	325 16041 ± 85
103	decatur-000	350495	171271	184 907	357 4100 ± 0	306 1024 ± 2	-	-	-	-	312 11439 ± 80	312 11418 ± 112
104	decatur-001	342866	253734	269 1507	275 2052 ± 0	319 1103 ± 2	270 1064 ± 2	254 1063 ± 2	223 1067 ± 2	185 1084 ± 2	53 610 ± 19	53 602 ± 8
105	deepglint-003	838065	262081	320 2374	371 6144 ± 0	330 1159 ± 1	286 1145 ± 1	272 1148 ± 1	240 1148 ± 1	200 1163 ± 1	327 17227 ± 41	327 17210 ± 51
106	deepglint-004	1073382	261571	346 3084	177 2048 ± 0	379 1470 ± 1	340 1474 ± 1	333 1485 ± 1	306 1474 ± 1	259 1492 ± 2	280 5961 ± 34	287 5955 ± 29
107	deepsea-001	147497	336250	51 358	58 1024 ± 0	169 630 ± 7	176 752 ± 37	155 746 ± 30	125 727 ± 32	124 820 ± 32	149 1401 ± 37	152 1467 ± 50
108	deeppsense-000	357113	936618	375 7618	250 2048 ± 0	185 664 ± 3	140 645 ± 1	127 660 ± 2	112 687 ± 2	122 808 ± 3	35 480 ± 22	37 459 ± 34
109	dermalog-008	0	937895	364 4989	20 512 ± 0	74 404 ± 2	55 410 ± 3	44 424 ± 5	36 430 ± 5	34 477 ± 5	33 468 ± 31	24 328 ± 13
110	dermalog-009	0	319363	126 664	28 512 ± 0	60 349 ± 0	44 351 ± 0	28 352 ± 0	24 357 ± 0	23 389 ± 0	36 487 ± 34	30 385 ± 29
111	didiglobalface-001	259849	70680	92 527	207 2048 ± 0	158 612 ± 1	137 633 ± 3	118 634 ± 3	101 650 ± 15	82 666 ± 4	107 973 ± 20	108 988 ± 20
112	digitalbarriers-002	83002	598577	302 1930	291 2056 ± 0	29 209 ± 11	22 250 ± 19	38 411 ± 37	146 808 ± 72	286 2236 ± 123	319 13409 ± 228	320 13267 ± 206
113	dps-000	0	22118182	210 1058	336 4096 ± 0	250 868 ± 2	226 893 ± 6	329 1445 ± 9	339 2910 ± 38	335 9345 ± 17	154 1473 ± 37	154 1479 ± 37
114	dsk-000	11967	782905	36 252	16 512 ± 0	50 304 ± 47	37 317 ± 33	235 1001 ± 96	338 2660 ± 170	337 10451 ± 832	304 7152 ± 115	302 7134 ± 111
115	einetworks-000	372608	219883	179 880	287 2056 ± 0	173 645 ± 3	-	-	-	-	274 4876 ± 66	274 5156 ± 77
116	ekin-002	51434	278	19 139	313 3072 ± 0	337 1186 ± 13	293 1180 ± 12	278 1181 ± 11	253 1191 ± 11	210 1207 ± 8	266 4294 ± 80	281 5569 ± 112
117	enface-000	369598	153781	125 662	59 1024 ± 0	132 555 ± 4	111 558 ± 4	129 669 ± 6	202 987 ± 15	291 2349 ± 54	302 7059 ± 62	300 6980 ± 65
118	enface-001	370710	173609	129 670	54 1024 ± 0	130 550 ± 4	109 555 ± 3	128 668 ± 7	199 981 ± 15	295 2416 ± 59	295 6734 ± 68	296 6766 ± 69
119	eocortex-000	255937	59432	35 224	249 2048 ± 0	52 305 ± 22	43 341 ± 25	51 440 ± 47	45 464 ± 45	42 513 ± 44	103 923 ± 11	104 918 ± 11
120	ercacat-001	811623	58012	337 2816	277 2052 ± 0	314 1052 ± 3	-	-	-	-	217 2551 ± 62	215 2501 ± 81
121	euronovate-001	0	1774966	246 1308	73 1177 ± 0	310 1034 ± 2	288 1165 ± 3	274 1160 ± 3	246 1177 ± 3	204 1172 ± 2	370 81294 ± 591	370 81631 ± 931
122	expasoft-001	39057	983064	20 142	201 2048 ± 0	670 ± 0	374 ± 0	377 ± 0	373 ± 0	374 ± 0	162 1660 ± 35	162 1676 ± 48
123	expasoft-002	38760	59825	241 168	152 2048 ± 0	434 ± 0	234 ± 0	234 ± 0	134 ± 0	134 ± 0	309 8870 ± 78	309 8838 ± 77
124	f8-001	272977	19668	241 1276	242 2048 ± 0	242 822 ± 39	-	-	-	-	324 15262 ± 139	323 15277 ± 212
125	faceonline-001	0	71529	470 302	284 2056 ± 0	22 179 ± 0	12 179 ± 0	14 190 ± 0	12 217 ± 0	18 343 ± 1	118 1064 ± 37	118 1033 ± 35
126	facesoft-000	370120	10612	158 796	133 2048 ± 0	188 675 ± 18	146 669 ± 3	134 686 ± 3	107 675 ± 5	88 687 ± 2	206 2239 ± 28	208 2277 ± 96
127	facetag-000	1232331	4022	198 965	51 684 ± 0	62 355 ± 17	49 369 ± 8	233 989 ± 33	335 2408 ± 91	333 7930 ± 316	367 72003 ± 625	368 71912 ± 612
128	facetag-002	819806	4021	145 726	93 2048 ± 0	126 544 ± 1	103 544 ± 0	85 542 ± 0	69 545 ± 0	55 554 ± 0	170 1730 ± 25	169 1733 ± 25
129	facex-001	305074	930372	344 2931	96 2048 ± 0	81 422 ± 4	64 434 ± 4	78 520 ± 7	130 737 ± 13	269 1670 ± 27	186 1871 ± 23	185 1846 ± 29
130	facex-002	305074	928334	347 3095	173 2048 ± 0	82 426 ± 5	61 429 ± 4	76 516 ± 8	126 730 ± 12	274 1738 ± 36	61 631 ± 25	58 614 ± 19
131	farfaces-001	346494	44581	37 261	24 512 ± 0	333 1179 ± 1	292 1180 ± 1	277 1180 ± 0	250 1185 ± 1	211 1209 ± 2	101 855 ± 25	100 860 ± 31
132	fiberhome-nanjing-003	352895	1482309	172 845	204 2048 ± 0	324 1136 ± 7	282 1134 ± 4	267 1132 ± 3	238 1139 ± 3	196 1154 ± 5	124 1097 ± 38	126 1083 ± 42

#### Notes

- 1 The configuration size does not capture static data included in libraries.
- 2 The library size is the combined total of all files provided in the submission lib folder. These libraries e.g. OpenCV may or may not be installed on any end user's platform natively and would not need to be installed with the algorithm. Some developers put neural network models in their libraries.
- 3 The memory usage is the peak resident set size reported by the ps system call during template generation.
- 4 The median template creation times are measured on Intel®Xeon®CPU E5-2630 v4 @ 2.20GHz processors.
- 5 The comparison durations, in nanoseconds, are estimated using std::chrono::high\_resolution\_clock which on the machine in (2) counts 1ns clock ticks. Precision is somewhat worse than that however. The ± value is the median absolute deviation times 1.48 for Normal consistency.

Table 9: Summary of algorithms and properties included in this report. The red superscripts give ranking for the quantity in that column.

	ALGORITHM	CONFIG	LIBRARY	TEMPLATE								COMPARISON <sup>4</sup>		
				NAME	DATA		MEMORY	SIZE	GENERATION TIME (ms) <sup>4</sup>				TIME (ns) <sup>5</sup>	
					(KB) <sup>1</sup>	(KB) <sup>2</sup>			(B)	MUGSHOT	480x720	960x1440	1600x2400	3000x4500
133	fiberhome-nanjing-004	443779	1482313	<sup>207</sup> 1048	<sup>341</sup> 4096 ± 0	<sup>361</sup> 1321 ± 5	<sup>314</sup> 1304 ± 3	<sup>304</sup> 1307 ± 2	<sup>273</sup> 1308 ± 3	<sup>231</sup> 1326 ± 5	<sup>141</sup> 1276 ± 40	<sup>141</sup> 1265 ± 38		
134	fincore-000	256615	19409	<sup>96</sup> 535	<sup>146</sup> 2048 ± 0	<sup>115</sup> 508 ± 3	<sup>92</sup> 505 ± 0	<sup>73</sup> 508 ± 1	<sup>61</sup> 513 ± 2	<sup>49</sup> 535 ± 1	<sup>173</sup> 1765 ± 31	<sup>172</sup> 1763 ± 22		
135	fujitsulab-002	0	1088887	<sup>282</sup> 1613	<sup>360</sup> 4104 ± 0	<sup>345</sup> 1237 ± 2	<sup>300</sup> 1222 ± 2	<sup>288</sup> 1236 ± 1	<sup>262</sup> 1251 ± 2	<sup>232</sup> 1327 ± 2	<sup>227</sup> 2836 ± 25	<sup>228</sup> 2809 ± 44		
136	fujitsulab-003	662263	318209	<sup>373</sup> 6907	<sup>361</sup> 4104 ± 0	<sup>289</sup> 951 ± 20	<sup>242</sup> 941 ± 19	<sup>223</sup> 952 ± 19	<sup>198</sup> 971 ± 20	<sup>176</sup> 1045 ± 21	<sup>228</sup> 2855 ± 16	<sup>230</sup> 2849 ± 19		
137	geo-002	369903	98667	<sup>205</sup> 1018	<sup>145</sup> 2048 ± 0	<sup>228</sup> 791 ± 1	<sup>187</sup> 793 ± 0	<sup>165</sup> 794 ± 0	<sup>143</sup> 795 ± 1	<sup>119</sup> 803 ± 1	<sup>249</sup> 3407 ± 45	<sup>251</sup> 3422 ± 65		
138	geo-003	371712	102175	<sup>235</sup> 1224	<sup>148</sup> 2048 ± 0	<sup>351</sup> 1283 ± 1	<sup>313</sup> 1290 ± 1	<sup>295</sup> 1285 ± 1	<sup>269</sup> 1292 ± 1	<sup>223</sup> 1302 ± 1	<sup>110</sup> 997 ± 13	<sup>112</sup> 1001 ± 20		
139	glory-002	0	385177	<sup>200</sup> 982	<sup>308</sup> 2106 ± 0	<sup>152</sup> 594 ± 3	<sup>177</sup> 740 ± 3	<sup>219</sup> 948 ± 3	<sup>328</sup> 2168 ± 6	<sup>9</sup> 191 ± 15	<sup>296</sup> 6787 ± 85	<sup>295</sup> 6551 ± 249		
140	glory-003	0	536910	<sup>258</sup> 1400	<sup>365</sup> 4234 ± 0	<sup>109</sup> 489 ± 0	<sup>112</sup> 565 ± 0	<sup>151</sup> 732 ± 0	<sup>323</sup> 1876 ± 2	<sup>334</sup> 8941 ± 20	<sup>288</sup> 6020 ± 90	<sup>290</sup> 6003 ± 72		
141	gorilla-007	441058	708166	<sup>283</sup> 1691	<sup>376</sup> 6288 ± 0	<sup>150</sup> 592 ± 1	<sup>122</sup> 592 ± 1	<sup>105</sup> 603 ± 1	<sup>94</sup> 625 ± 2	<sup>99</sup> 722 ± 9	<sup>259</sup> 3686 ± 37	<sup>259</sup> 3709 ± 36		
142	gorilla-008	450175	707000	<sup>293</sup> 1789	<sup>378</sup> 8338 ± 0	<sup>154</sup> 595 ± 1	<sup>121</sup> 590 ± 0	<sup>103</sup> 600 ± 1	<sup>92</sup> 621 ± 2	<sup>98</sup> 720 ± 9	<sup>269</sup> 4530 ± 44	<sup>267</sup> 4524 ± 38		
143	griaule-000	0	598214	<sup>209</sup> 1054	<sup>269</sup> 2052 ± 0	<sup>80</sup> 416 ± 6	<sup>59</sup> 425 ± 7	<sup>163</sup> 770 ± 14	<sup>318</sup> 1749 ± 43	<sup>329</sup> 6406 ± 189	<sup>263</sup> 3987 ± 42	<sup>263</sup> 3938 ± 38		
144	hertasecurity-000	0	780014	<sup>89</sup> 516	<sup>5</sup> 256 ± 0	<sup>10</sup> 99 ± 0	<sup>6</sup> 98 ± 0	<sup>5</sup> 100 ± 0	<sup>5</sup> 107 ± 0	<sup>5</sup> 139 ± 0	<sup>80</sup> 710 ± 31	<sup>73</sup> 667 ± 28		
145	hik-001	667866	9290	<sup>371</sup> 6597	<sup>78</sup> 1408 ± 0	<sup>174</sup> 651 ± 0	<sup>140</sup> 667 ± 8	<sup>131</sup> 677 ± 16	<sup>111</sup> 686 ± 13	<sup>104</sup> 737 ± 12	<sup>37</sup> 488 ± 19	<sup>38</sup> 477 ± 22		
146	hisign-001	732412	167488	<sup>273</sup> 1553	<sup>304</sup> 2080 ± 0	<sup>357</sup> 1306 ± 1	<sup>319</sup> 1320 ± 1	<sup>306</sup> 1315 ± 1	<sup>276</sup> 1312 ± 1	<sup>229</sup> 1325 ± 1	<sup>9</sup> 201 ± 10	<sup>6</sup> 185 ± 13		
147	hyperverge-001	260819	88624	<sup>84</sup> 507	<sup>158</sup> 2048 ± 0	<sup>191</sup> 682 ± 20	<sup>156</sup> 695 ± 17	<sup>284</sup> 1196 ± 37	<sup>334</sup> 2400 ± 68	<sup>331</sup> 7178 ± 204	<sup>290</sup> 6026 ± 40	<sup>289</sup> 5984 ± 38		
148	hyperverge-002	2951900	198832	<sup>308</sup> 1975	<sup>53</sup> 1024 ± 0	<sup>282</sup> 938 ± 1	<sup>241</sup> 939 ± 1	<sup>217</sup> 941 ± 1	<sup>193</sup> 945 ± 1	<sup>162</sup> 975 ± 1	<sup>289</sup> 6023 ± 37	<sup>288</sup> 5966 ± 40		
149	icm-002	621586	903	<sup>75</sup> 484	<sup>141</sup> 2048 ± 0	<sup>309</sup> 1031 ± 7	-	-	-	-	<sup>340</sup> 24052 ± 118	<sup>339</sup> 24049 ± 124		
150	icm-003	1513988	940	<sup>82</sup> 500	<sup>208</sup> 2048 ± 0	<sup>190</sup> 681 ± 6	<sup>148</sup> 672 ± 4	<sup>146</sup> 714 ± 11	<sup>151</sup> 837 ± 41	<sup>237</sup> 1381 ± 131	<sup>341</sup> 24351 ± 161	<sup>340</sup> 24227 ± 146		
151	ichthc-000	172459	1471004	<sup>295</sup> 1805	<sup>225</sup> 2048 ± 0	<sup>59</sup> 338 ± 11	<sup>42</sup> 338 ± 9	<sup>48</sup> 437 ± 16	<sup>118</sup> 705 ± 24	<sup>273</sup> 1719 ± 44	<sup>277</sup> 5284 ± 63	<sup>276</sup> 5290 ± 54		
152	id3-006	210116	7706	<sup>202</sup> 082	<sup>41</sup> 520 ± 0	<sup>192</sup> 683 ± 0	<sup>273</sup> 1088 ± 1	<sup>282</sup> 1192 ± 1	<sup>256</sup> 1209 ± 1	<sup>218</sup> 1270 ± 1	<sup>280</sup> 5547 ± 34	<sup>280</sup> 5563 ± 34		
153	id3-008	242416	8151	<sup>213</sup> 1068	<sup>9</sup> 264 ± 0	<sup>238</sup> 819 ± 0	<sup>296</sup> 1209 ± 2	<sup>302</sup> 1297 ± 2	<sup>278</sup> 1329 ± 1	<sup>251</sup> 1433 ± 1	<sup>283</sup> 5658 ± 44	<sup>283</sup> 5624 ± 40		
154	idemia-007	353242	67485	<sup>208</sup> 1051	<sup>15</sup> 468 ± 0	<sup>72</sup> 384 ± 0	<sup>51</sup> 389 ± 0	<sup>34</sup> 393 ± 1	<sup>29</sup> 405 ± 2	<sup>26</sup> 441 ± 8	<sup>244</sup> 3243 ± 63	<sup>244</sup> 3202 ± 63		
155	idemia-008	374017	69922	<sup>228</sup> 1194	<sup>13</sup> 348 ± 0	<sup>93</sup> 457 ± 1	<sup>74</sup> 461 ± 0	<sup>58</sup> 466 ± 1	<sup>60</sup> 476 ± 2	<sup>43</sup> 513 ± 10	<sup>239</sup> 3080 ± 41	<sup>236</sup> 3046 ± 56		
156	iit-002	259579	52070	<sup>148</sup> 731	<sup>213</sup> 2048 ± 0	<sup>116</sup> 514 ± 1	<sup>90</sup> 531 ± 2	<sup>89</sup> 547 ± 1	<sup>74</sup> 583 ± 1	<sup>102</sup> 733 ± 2	<sup>116</sup> 1023 ± 7	<sup>115</sup> 1011 ± 66		
157	iit-003	261288	53791	<sup>16</sup> 817	<sup>118</sup> 2048 ± 0	<sup>104</sup> 482 ± 0	<sup>86</sup> 493 ± 0	<sup>74</sup> 509 ± 0	<sup>67</sup> 541 ± 0	<sup>80</sup> 661 ± 0	<sup>21</sup> 324 ± 17	<sup>23</sup> 326 ± 8		
158	imagus-002	227766	318409	<sup>58</sup> 411	<sup>100</sup> 2048 ± 0	<sup>226</sup> 786 ± 1	<sup>179</sup> 766 ± 2	<sup>192</sup> 885 ± 3	<sup>302</sup> 1430 ± 3	<sup>316</sup> 4080 ± 10	<sup>70</sup> 676 ± 16	<sup>62</sup> 630 ± 20		
159	imagus-004	254405	380049	<sup>137</sup> 697	<sup>171</sup> 2048 ± 0	<sup>165</sup> 624 ± 1	<sup>119</sup> 587 ± 10	<sup>112</sup> 626 ± 3	<sup>83</sup> 592 ± 3	<sup>96</sup> 717 ± 6	<sup>89</sup> 760 ± 22	<sup>80</sup> 703 ± 28		
160	imperial-000	370120	10623	<sup>159</sup> 796	<sup>138</sup> 2048 ± 0	<sup>186</sup> 669 ± 1	<sup>149</sup> 675 ± 3	<sup>138</sup> 683 ± 17	<sup>108</sup> 676 ± 2	<sup>89</sup> 689 ± 2	<sup>200</sup> 2130 ± 32	<sup>197</sup> 2052 ± 100		
161	imperial-002	472327	16134	<sup>296</sup> 1826	<sup>147</sup> 2048 ± 0	<sup>138</sup> 569 ± 1	<sup>115</sup> 581 ± 15	<sup>95</sup> 575 ± 5	<sup>73</sup> 576 ± 2	<sup>62</sup> 588 ± 3	<sup>208</sup> 2278 ± 90	<sup>201</sup> 2131 ± 44		
162	incode-009	266103	21014	<sup>192</sup> 039	<sup>193</sup> 2048 ± 0	<sup>112</sup> 503 ± 0	<sup>88</sup> 490 ± 1	<sup>71</sup> 498 ± 0	<sup>58</sup> 505 ± 0	<sup>50</sup> 537 ± 0	<sup>126</sup> 1102 ± 28	<sup>129</sup> 1113 ± 29		
163	incode-010	627808	21014	<sup>329</sup> 2628	<sup>258</sup> 2048 ± 0	<sup>335</sup> 1180 ± 2	<sup>290</sup> 1178 ± 1	<sup>279</sup> 1182 ± 1	<sup>248</sup> 1184 ± 1	<sup>212</sup> 1221 ± 1	<sup>132</sup> 1164 ± 32	<sup>132</sup> 1144 ± 32		
164	innefulabs-000	370588	162172	<sup>64</sup> 439	<sup>86</sup> 2048 ± 0	<sup>302</sup> 1006 ± 3	<sup>257</sup> 1025 ± 3	<sup>244</sup> 1030 ± 4	<sup>217</sup> 1041 ± 2	<sup>194</sup> 1135 ± 3	<sup>284</sup> 5782 ± 41	<sup>280</sup> 5741 ± 45		
165	innovativetechnologyltd-001	177232	335757	<sup>49</sup> 341	<sup>187</sup> 2048 ± 0	<sup>85</sup> 433 ± 7	<sup>68</sup> 446 ± 8	<sup>49</sup> 439 ± 4	<sup>40</sup> 452 ± 4	<sup>37</sup> 485 ± 7	<sup>187</sup> 1877 ± 42	<sup>189</sup> 1924 ± 97		
166	innovativetechnologyltd-002	173939	372324	<sup>185</sup> 912	<sup>151</sup> 2048 ± 0	<sup>180</sup> 661 ± 2	<sup>168</sup> 726 ± 4	<sup>228</sup> 981 ± 27	<sup>206</sup> 997 ± 40	<sup>115</sup> 766 ± 3	<sup>184</sup> 1841 ± 50	<sup>186</sup> 1857 ± 59		
167	innovatrics-007	0	493269	<sup>303</sup> 1937	<sup>72</sup> 1064 ± 0	<sup>381</sup> 1485 ± 7	<sup>342</sup> 1785 ± 184	<sup>341</sup> 2078 ± 24	<sup>327</sup> 2123 ± 15	<sup>285</sup> 2210 ± 42	<sup>287</sup> 5978 ± 88	<sup>289</sup> 5690 ± 102		
168	innovatrics-008	307323	59842	<sup>260</sup> 1424	<sup>45</sup> 538 ± 0	<sup>223</sup> 778 ± 6	<sup>180</sup> 767 ± 3	<sup>162</sup> 770 ± 3	<sup>144</sup> 803 ± 3	<sup>134</sup> 853 ± 10	<sup>236</sup> 3021 ± 66	<sup>224</sup> 2673 ± 88		
169	insightface-000	806953	16606	<sup>358</sup> 3912	<sup>325</sup> 4096 ± 0	<sup>303</sup> 1009 ± 1	<sup>256</sup> 1019 ± 2	<sup>238</sup> 1017 ± 2	<sup>211</sup> 1020 ± 2	<sup>173</sup> 1032 ± 2	<sup>175</sup> 1778 ± 31	<sup>173</sup> 1773 ± 35		
170	insightface-001	776777	16606	<sup>355</sup> 3852	<sup>90</sup> 2048 ± 0	<sup>364</sup> 1366 ± 2	<sup>322</sup> 1368 ± 3	<sup>288</sup> 1375 ± 5	<sup>239</sup> 1386 ± 4	<sup>128</sup> 1119 ± 29	<sup>128</sup> 1108 ± 34			
171	intellicloudai-001	220831	868246	<sup>123</sup> 655	<sup>181</sup> 2048 ± 0	<sup>99</sup> 468 ± 2	<sup>71</sup> 456 ± 1	<sup>57</sup> 466 ± 3	<sup>56</sup> 492 ± 1	<sup>70</sup> 632 ± 2	<sup>117</sup> 1056 ± 4	<sup>121</sup> 1051 ± 72		
172	intellicloudai-002	259047	58559	<sup>351</sup> 3584	<sup>359</sup> 4100 ± 0	<sup>251</sup> 847 ± 1	<sup>204</sup> 847 ± 2	<sup>180</sup> 849 ± 1	<sup>161</sup> 853 ± 1	<sup>139</sup> 878 ± 4	<sup>98</sup> 822 ± 28	<sup>98</sup> 818 ± 23		
173	intellifusion-001	271872	289387	<sup>152</sup> 762	<sup>142</sup> 2048 ± 0	<sup>216</sup> 764 ± 38	<sup>182</sup> 774 ± 39	<sup>166</sup> 797 ± 42	<sup>145</sup> 803 ± 34	<sup>120</sup> 805 ± 33	<sup>127</sup> 1112 ± 28	<sup>130</sup> 1128 ± 41		
174	intellifusion-002	762731	385841	<sup>193</sup> 941	<sup>350</sup> 4096 ± 0	<sup>288</sup> 950 ± 2	<sup>277</sup> 1096 ± 42	<sup>258</sup> 1088 ± 33	<sup>244</sup> 1168 ± 31	<sup>202</sup> 1171 ± 10	<sup>166</sup> 1713 ± 57	<sup>161</sup> 1665 ± 87		
175	intellivision-001	43692	11649	<sup>8</sup> 74	<sup>282</sup> 2056 ± 0	<sup>5</sup> 62 ± 2	-	-	-	-	<sup>220</sup> 2573 ± 91	<sup>219</sup> 2544 ± 38		
176	intellivision-002	43692	14505	<sup>11</sup> 81	<sup>285</sup> 2056 ± 0	<sup>54</sup> 322 ± 1	<sup>48</sup> 355 ± 2	<sup>32</sup> 372 ± 1	<sup>33</sup> 422 ± 2	<sup>65</sup> 600 ± 1	<sup>320</sup> 13525 ± 134	<sup>319</sup> 12782 ± 278		

**Notes**

- 1 The configuration size does not capture static data included in libraries.
- 2 The library size is the combined total of all files provided in the submission lib folder. These libraries e.g. OpenCV may or may not be installed on any end user's platform natively and would not need to be installed with the algorithm. Some developers put neural network models in their libraries.
- 3 The memory usage is the peak resident set size reported by the ps system call during template generation.
- 4 The median template creation times are measured on Intel®Xeon®CPU E5-2630 v4 @ 2.20GHz processors.
- 5 The comparison durations, in nanoseconds, are estimated using std::chrono::high\_resolution\_clock which on the machine in (2) counts 1ns clock ticks. Precision is somewhat worse than that however. The ± value is the median absolute deviation times 1.48 for Normal consistency.

Table 10: Summary of algorithms and properties included in this report. The red superscripts give ranking for the quantity in that column.

	ALGORITHM	CONFIG	LIBRARY	TEMPLATE								COMPARISON <sup>4</sup>	
	NAME	DATA	DATA	MEMORY	SIZE		GENERATION TIME (ms) <sup>4</sup>					TIME (ns) <sup>5</sup>	
		(KB) <sup>1</sup>	(KB) <sup>2</sup>	(MB) <sup>3</sup>	(B)	MUGSHOT	480x720	960x1440	1600x2400	3000x4500	GENUINE	IMPOSTOR	
177	intelresearch-003	401343	85085	226 1177	184 2048 ± 0	343 1232 ± 3	304 1237 ± 2	289 1242 ± 2	265 1263 ± 2	228 1324 ± 3	268 4443 ± 75	266 4374 ± 77	
178	intelresearch-004	646918	85290	299 1856	119 2048 ± 0	360 1319 ± 2	320 1322 ± 3	311 1330 ± 3	281 1345 ± 3	246 1411 ± 5	270 4696 ± 63	268 4692 ± 66	
179	intsysmsu-001	384409	172480	157 789	91 2048 ± 0	161 614 ± 2	131 615 ± 2	121 642 ± 2	134 750 ± 3	199 1159 ± 4	59 621 ± 8	56 611 ± 31	
180	intsysmsu-002	765921	172298	156 786	60 1024 ± 0	151 593 ± 1	188 793 ± 2	172 827 ± 1	166 875 ± 104	222 1293 ± 3	41 549 ± 25	43 548 ± 29	
181	ionetworks-000	287609	51236	51 351	89 2048 ± 0	84 430 ± 0	65 435 ± 0	46 433 ± 0	37 432 ± 0	28 444 ± 0	298 6913 ± 102	303 7150 ± 160	
182	iqface-000	268819	596337	139 704	367 4750 ± 32	124 538 ± 26	87 494 ± 2	87 543 ± 3	128 734 ± 4	242 1393 ± 4	379 636433 ± 38446	379 632654 ± 85615	
183	iqface-003	370803	963398	164 817	368 4763 ± 37	118 529 ± 1	96 532 ± 2	102 599 ± 8	160 850 ± 2	270 1694 ± 2	378 575924 ± 2601	378 576653 ± 2051	
184	irex-000	741899	47419	314 2086	316 3080 ± 0	252 852 ± 2	206 850 ± 1	188 874 ± 2	190 939 ± 1	215 1249 ± 5	7 201 ± 11	9 208 ± 8	
185	isap-001	99049	204201	1 18	343 4096 ± 0	1 0 ± 0	-	-	-	-	32 459 ± 17	35 456 ± 11	
186	isap-002	256765	49931	43 288	254 2048 ± 0	220 769 ± 3	259 1027 ± 2	191 877 ± 2	139 761 ± 1	145 912 ± 2	237 3045 ± 94	232 2973 ± 66	
187	isityou-000	48010	36621	14 110	380 19200 ± 0	13 113 ± 5	-	-	-	-	374 237517 ± 1318	374 237374 ± 1279	
188	isystems-001	274621	639268	219 1091	143 2048 ± 0	47 291 ± 9	-	-	-	-	43 557 ± 16	45 564 ± 22	
189	isystems-002	358984	803389	279 1595	98 2048 ± 0	241 822 ± 8	-	-	-	-	86 749 ± 31	64 632 ± 28	
190	itmo-007	415979	245376	318 2199	103 2048 ± 0	210 741 ± 2	-	-	-	-	218 2551 ± 50	217 2529 ± 80	
191	itmo-008	726866	318238	254 1377	340 4096 ± 0	315 1060 ± 1	269 1058 ± 1	252 1059 ± 1	225 1072 ± 4	189 1104 ± 1	256 3578 ± 25	255 3580 ± 28	
192	ivacognitive-001	256958	62791	195 947	232 2048 ± 0	356 1292 ± 3	312 1289 ± 4	298 1292 ± 4	268 1292 ± 3	227 1321 ± 4	265 4228 ± 41	264 4226 ± 41	
193	iws-000	30875	3063	9 77	21 512 ± 0	39 277 ± 5	31 283 ± 1	69 494 ± 3	201 984 ± 3	309 2987 ± 39	112 999 ± 40	110 992 ± 22	
194	kakao-005	414316	152216	277 1581	272 2052 ± 0	316 1068 ± 1	272 1073 ± 1	256 1079 ± 0	226 1077 ± 1	187 1089 ± 1	197 2067 ± 26	196 2043 ± 34	
195	kakaopay-001	397864	179869	131 684	348 4096 ± 0	90 448 ± 0	102 542 ± 0	85 542 ± 0	68 542 ± 0	53 555 ± 0	62 633 ± 22	63 630 ± 22	
196	kedacom-000	245292	37401	380 23574	11 292 ± 0	113 506 ± 3	106 547 ± 10	110 614 ± 9	79 588 ± 10	81 665 ± 24	73 684 ± 14	75 682 ± 16	
197	kiwitech-000	369711	21375	162 808	188 2048 ± 0	149 591 ± 0	124 594 ± 0	101 595 ± 1	84 596 ± 0	66 609 ± 0	171 1755 ± 20	170 1734 ± 16	
198	kneron-003	58366	1747	29 188	121 2048 ± 0	42 281 ± 3	30 280 ± 1	24 315 ± 13	25 365 ± 7	214 1224 ± 30	276 5237 ± 63	275 5274 ± 99	
199	kneron-005	375374	13633	68 457	153 2048 ± 0	117 518 ± 2	94 522 ± 4	92 556 ± 5	137 757 ± 19	276 1760 ± 25	190 1922 ± 11	190 1926 ± 20	
200	kookmin-002	371771	30734	167 827	101 2048 ± 0	312 1038 ± 2	267 1047 ± 1	248 1045 ± 1	222 1061 ± 1	190 1116 ± 1	63 638 ± 19	68 636 ± 20	
201	kuke3d-001	403462	68786	94 530	342 4096 ± 0	234 814 ± 2	191 811 ± 2	169 814 ± 2	147 814 ± 1	131 834 ± 1	294 6412 ± 57	294 6413 ± 51	
202	lemalabs-001	748400	198794	333 2738	195 2048 ± 0	231 810 ± 0	192 812 ± 0	168 813 ± 0	149 819 ± 0	133 844 ± 1	318 11930 ± 35	318 11913 ± 37	
203	line-000	264443	407003	110 590	155 2048 ± 0	144 586 ± 0	127 612 ± 0	107 609 ± 1	87 611 ± 0	68 618 ± 1	226 2753 ± 19	226 2745 ± 23	
204	line-001	944355	407058	319 2373	106 2048 ± 0	247 833 ± 10	199 830 ± 3	173 828 ± 4	156 838 ± 8	130 833 ± 4	224 2696 ± 23	225 2677 ± 35	
205	lookman-002	138200	25410	378 16518	48 548 ± 0	20 173 ± 1	-	-	-	-	54 610 ± 19	57 612 ± 22	
206	lookman-004	244775	37401	379 23548	49 548 ± 0	114 507 ± 5	104 545 ± 12	109 613 ± 12	81 590 ± 11	77 656 ± 16	102 871 ± 29	102 878 ± 29	
207	luxand-000	0	57908	251 1366	69 1040 ± 0	75 407 ± 23	63 433 ± 11	52 444 ± 14	44 464 ± 14	58 562 ± 25	99 828 ± 28	99 828 ± 32	
208	mantra-000	471458	62566	151 749	262 2052 ± 0	78 413 ± 18	84 487 ± 19	70 494 ± 18	60 511 ± 18	64 598 ± 19	242 3151 ± 51	240 3127 ± 63	
209	maxvision-000	133114	56426	294 1791	25 512 ± 0	68 359 ± 0	47 356 ± 0	30 359 ± 0	23 356 ± 0	21 370 ± 1	213 2461 ± 20	212 2452 ± 17	
210	megvii-003	4430290	42790	363 4878	338 4096 ± 0	339 1210 ± 1	301 1223 ± 0	314 1356 ± 4	312 1582 ± 7	302 2727 ± 23	373 225342 ± 3574	373 225413 ± 6344	
211	megvii-004	3962505	44019	362 4436	354 4097 ± 0	353 1287 ± 1	323 1369 ± 2	305 1310 ± 2	291 1384 ± 3	252 1436 ± 5	356 46801 ± 204	356 46832 ± 207	
212	meitu-an-000	259514	333178	100 554	113 2048 ± 0	86 436 ± 4	67 441 ± 1	113 626 ± 5	229 1098 ± 15	311 3126 ± 53	66 638 ± 17	66 633 ± 16	
213	meiya-001	280055	264913	85 507	259 2049 ± 0	164 622 ± 12	-	-	-	-	307 8356 ± 615	307 8134 ± 97	
214	mendaxiatech-000	1941475	45484	349 3195	353 4097 ± 0	346 1243 ± 2	305 1255 ± 1	317 1373 ± 2	313 1598 ± 3	301 2689 ± 8	357 46906 ± 275	357 46872 ± 217	
215	microfocus-001	104524	27242	30 190	4 256 ± 0	36 264 ± 18	-	-	-	-	10 215 ± 8	10 217 ± 10	
216	microfocus-002	96288	27362	26 176	6 256 ± 0	34 259 ± 18	-	-	-	-	23 337 ± 34	12 230 ± 25	
217	minivision-000	836697	16597	360 4013	323 4096 ± 0	311 1035 ± 1	263 1033 ± 2	247 1035 ± 1	215 1037 ± 1	182 1059 ± 2	214 2466 ± 26	213 2460 ± 25	
218	mobai-000	365451	80573	155 786	372 6144 ± 0	218 766 ± 8	213 869 ± 6	286 1205 ± 31	322 1867 ± 45	315 3549 ± 190	326 16458 ± 333	326 16423 ± 1473	
219	mobai-001	265297	60164	90 534	194 2048 ± 0	157 612 ± 3	130 614 ± 3	135 687 ± 9	170 886 ± 31	271 1707 ± 103	146 1386 ± 25	146 1377 ± 26	
220	mobbl-001	231160	58706	34 223	107 2048 ± 0	24 183 ± 32	15 184 ± 25	29 354 ± 76	152 823 ± 396	304 2781 ± 1166	317 11832 ± 109	317 11851 ± 88	

## Notes

- 1 The configuration size does not capture static data included in libraries.
- 2 The library size is the combined total of all files provided in the submission lib folder. These libraries e.g. OpenCV may or may not be installed on any end user's platform natively and would not need to be installed with the algorithm. Some developers put neural network models in their libraries.
- 3 The memory usage is the peak resident set size reported by the ps system call during template generation.
- 4 The median template creation times are measured on Intel®Xeon®CPU E5-2630 v4 @ 2.20GHz processors.
- 5 The comparison durations, in nanoseconds, are estimated using std::chrono::high\_resolution\_clock which on the machine in (2) counts 1ns clock ticks. Precision is somewhat worse than that however. The ± value is the median absolute deviation times 1.48 for Normal consistency.

Table 11: Summary of algorithms and properties included in this report. The red superscripts give ranking for the quantity in that column.

	ALGORITHM	CONFIG	LIBRARY	TEMPLATE							COMPARISON <sup>4</sup>			
				NAME		DATA	MEMORY	SIZE	GENERATION TIME (ms) <sup>4</sup>			TIME (ns) <sup>5</sup>		
				(KB) <sup>1</sup>	(KB) <sup>2</sup>				(B)	MUGSHOT	480x720	960x1440	1600x2400	3000x4500
221	mobbbl-002	242920	60119	<sup>44</sup> 288	<sup>224</sup> 2048 ± 0	<sup>183</sup> 663 ± 6	<sup>143</sup> 660 ± 5	<sup>126</sup> 662 ± 5	<sup>105</sup> 663 ± 5	<sup>84</sup> 676 ± 5	<sup>313</sup> 11616 ± 78	<sup>313</sup> 11588 ± 97		
222	mobipintech-000	370514	303291	<sup>222</sup> 1130	<sup>88</sup> 2048 ± 0	<sup>347</sup> 1245 ± 1	<sup>302</sup> 1234 ± 1	<sup>292</sup> 1264 ± 1	<sup>287</sup> 1360 ± 1	<sup>272</sup> 1707 ± 1	<sup>321</sup> 14506 ± 214	<sup>321</sup> 14433 ± 197		
223	moreidian-000	525259	21374	<sup>190</sup> 932	<sup>252</sup> 2048 ± 0	<sup>198</sup> 694 ± 0	<sup>157</sup> 698 ± 0	<sup>142</sup> 699 ± 0	<sup>116</sup> 700 ± 0	<sup>98</sup> 713 ± 1	<sup>181</sup> 1803 ± 11	<sup>177</sup> 1779 ± 23		
224	multimodality-000	0	503924	<sup>259</sup> 1417	<sup>136</sup> 2048 ± 0	<sup>79</sup> 416 ± 0	<sup>58</sup> 420 ± 0	<sup>42</sup> 423 ± 0	<sup>35</sup> 427 ± 0	<sup>30</sup> 463 ± 0	<sup>100</sup> 848 ± 25	<sup>96</sup> 800 ± 28		
225	mvision-001	227502	149531	<sup>144</sup> 723	<sup>26</sup> 512 ± 0	<sup>196</sup> 691 ± 21	<sup>159</sup> 702 ± 19	<sup>141</sup> 697 ± 24	<sup>120</sup> 708 ± 29	<sup>94</sup> 710 ± 27	<sup>129</sup> 1123 ± 40	<sup>133</sup> 1154 ± 38		
226	nazhiai-000	547484	16141	<sup>330</sup> 2716	<sup>230</sup> 2048 ± 0	<sup>193</sup> 683 ± 3	<sup>152</sup> 687 ± 2	<sup>176</sup> 835 ± 27	<sup>158</sup> 840 ± 31	<sup>132</sup> 834 ± 34	<sup>205</sup> 2230 ± 34	<sup>202</sup> 2133 ± 81		
227	neosystems-002	599441	349942	<sup>234</sup> 1222	<sup>233</sup> 2048 ± 0	<sup>323</sup> 1135 ± 2	<sup>344</sup> 1855 ± 3	<sup>342</sup> 2258 ± 5	<sup>331</sup> 2238 ± 3	<sup>287</sup> 2247 ± 3	<sup>329</sup> 18752 ± 167	<sup>330</sup> 18610 ± 213		
228	neosystems-003	599442	349942	<sup>232</sup> 1215	<sup>218</sup> 2048 ± 0	<sup>326</sup> 1143 ± 2	<sup>343</sup> 1836 ± 7	<sup>343</sup> 2260 ± 3	<sup>333</sup> 2273 ± 6	<sup>288</sup> 2273 ± 3	<sup>332</sup> 19130 ± 223	<sup>332</sup> 19167 ± 186		
229	netbridge-tech-001	133108	205875	<sup>86</sup> 508	<sup>346</sup> 4096 ± 0	<sup>7</sup> 85 ± 1	<sup>4</sup> 83 ± 0	<sup>4</sup> 84 ± 0	<sup>4</sup> 92 ± 0	<sup>113</sup> 84 ± 4	<sup>310</sup> 9280 ± 74	<sup>310</sup> 9446 ± 512		
230	netbridge-tech-002	257687	49931	<sup>46</sup> 299	<sup>114</sup> 2048 ± 0	<sup>248</sup> 838 ± 6	<sup>202</sup> 838 ± 2	<sup>178</sup> 839 ± 1	<sup>157</sup> 839 ± 3	<sup>135</sup> 859 ± 3	<sup>230</sup> 2893 ± 65	<sup>237</sup> 3050 ± 123		
231	neurotechnology-012	147830	51395	<sup>163</sup> 814	<sup>2</sup> 256 ± 0	<sup>70</sup> 384 ± 0	<sup>50</sup> 387 ± 0	<sup>36</sup> 404 ± 1	<sup>39</sup> 435 ± 1	<sup>61</sup> 583 ± 7	<sup>3</sup> 119 ± 7	<sup>3</sup> 116 ± 7		
232	neurotechnology-013	474749	85552	<sup>343</sup> 2894	<sup>39</sup> 514 ± 0	<sup>301</sup> 1000 ± 1	<sup>252</sup> 1006 ± 2	<sup>239</sup> 1022 ± 2	<sup>220</sup> 1053 ± 2	<sup>206</sup> 1195 ± 8	<sup>2</sup> 109 ± 4	<sup>1</sup> 110 ± 4		
233	nhn-001	336391	817674	<sup>124</sup> 662	<sup>330</sup> 4096 ± 0	<sup>308</sup> 1027 ± 3	<sup>261</sup> 1029 ± 1	<sup>243</sup> 1029 ± 1	<sup>218</sup> 1044 ± 1	<sup>188</sup> 1090 ± 1	<sup>361</sup> 56650 ± 260	<sup>362</sup> 56639 ± 210		
234	nhn-002	363471	817674	<sup>128</sup> 667	<sup>321</sup> 4096 ± 0	<sup>325</sup> 1141 ± 3	<sup>283</sup> 1138 ± 2	<sup>269</sup> 1141 ± 2	<sup>243</sup> 1151 ± 6	<sup>207</sup> 1203 ± 2	<sup>360</sup> 56608 ± 579	<sup>361</sup> 56549 ± 606		
235	nodeflux-002	774668	690213	<sup>72</sup> 466	<sup>217</sup> 2048 ± 0	<sup>203</sup> 708 ± 4	<sup>161</sup> 709 ± 4	<sup>147</sup> 716 ± 5	<sup>124</sup> 716 ± 7	<sup>103</sup> 736 ± 3	<sup>253</sup> 3475 ± 62	<sup>250</sup> 3408 ± 143		
236	notiontag-001	92753	427967	<sup>105</sup> 566	<sup>50</sup> 584 ± 0	<sup>281</sup> 929 ± 35	<sup>274</sup> 1092 ± 39	<sup>344</sup> 3709 ± 81	<sup>344</sup> 10233 ± 180	-	<sup>352</sup> 43636 ± 286	<sup>352</sup> 43724 ± 330		
237	notiontag-002	271987	967207	<sup>339</sup> 2840	<sup>309</sup> 2120 ± 0	<sup>92</sup> 453 ± 2	<sup>70</sup> 453 ± 3	<sup>53</sup> 453 ± 3	<sup>42</sup> 458 ± 2	<sup>32</sup> 471 ± 3	<sup>335</sup> 20278 ± 194	<sup>335</sup> 20195 ± 186		
238	nsensecorp-002	187421	122407	<sup>101</sup> 554	<sup>162</sup> 2048 ± 0	<sup>58</sup> 333 ± 0	<sup>40</sup> 333 ± 0	<sup>27</sup> 337 ± 0	<sup>22</sup> 338 ± 0	<sup>20</sup> 351 ± 0	<sup>355</sup> 45965 ± 213	<sup>355</sup> 45988 ± 158		
239	nsensecorp-003	199895	117041	<sup>142</sup> 710	<sup>219</sup> 2048 ± 0	<sup>181</sup> 661 ± 0	<sup>144</sup> 664 ± 0	<sup>127</sup> 662 ± 1	<sup>104</sup> 659 ± 1	<sup>78</sup> 659 ± 0	<sup>353</sup> 44658 ± 51	<sup>354</sup> 44654 ± 72		
240	ntechlab-010	698591	217167	<sup>345</sup> 2991	<sup>75</sup> 1280 ± 0	<sup>332</sup> 1177 ± 2	<sup>294</sup> 1180 ± 2	<sup>285</sup> 1197 ± 2	<sup>258</sup> 1224 ± 1	<sup>230</sup> 1326 ± 3	<sup>31</sup> 405 ± 13	<sup>32</sup> 416 ± 31		
241	ntechlab-011	786933	209458	<sup>372</sup> 6867	<sup>76</sup> 1280 ± 0	<sup>329</sup> 1148 ± 2	<sup>284</sup> 1142 ± 1	<sup>273</sup> 1159 ± 1	<sup>249</sup> 1185 ± 1	<sup>221</sup> 1290 ± 3	<sup>4</sup> 179 ± 11	<sup>5</sup> 173 ± 11		
242	omnigarde-000	264057	32882	<sup>91</sup> 523	<sup>55</sup> 1024 ± 0	<sup>285</sup> 944 ± 0	<sup>223</sup> 887 ± 0	<sup>194</sup> 888 ± 1	<sup>174</sup> 892 ± 0	<sup>144</sup> 902 ± 0	<sup>223</sup> 2671 ± 35	<sup>222</sup> 2620 ± 29		
243	omnigarde-001	200523	32882	<sup>70</sup> 464	<sup>34</sup> 512 ± 0	<sup>283</sup> 941 ± 0	<sup>221</sup> 883 ± 1	<sup>193</sup> 886 ± 1	<sup>173</sup> 891 ± 1	<sup>141</sup> 898 ± 0	<sup>150</sup> 1405 ± 31	<sup>147</sup> 1379 ± 26		
244	openface-001	0	40111	<sup>13</sup> 100	<sup>168</sup> 2048 ± 0	<sup>17</sup> 148 ± 1	<sup>10</sup> 154 ± 0	<sup>31</sup> 365 ± 3	<sup>31</sup> 409 ± 9	<sup>67</sup> 616 ± 31	<sup>52</sup> 608 ± 14	<sup>55</sup> 604 ± 13		
245	oz-003	484147	519652	<sup>377</sup> 11949	<sup>279</sup> 2053 ± 0	<sup>365</sup> 1375 ± 12	<sup>328</sup> 1388 ± 3	<sup>340</sup> 1773 ± 16	<sup>326</sup> 2039 ± 6	<sup>313</sup> 3209 ± 5	<sup>369</sup> 73905 ± 456	<sup>369</sup> 73892 ± 444		
246	oz-004	373982	1075452	<sup>376</sup> 8071	<sup>280</sup> 2053 ± 0	<sup>246</sup> 832 ± 7	<sup>214</sup> 871 ± 6	<sup>196</sup> 899 ± 10	<sup>227</sup> 1078 ± 12	<sup>266</sup> 1608 ± 10	<sup>364</sup> 61654 ± 418	<sup>363</sup> 61749 ± 450		
247	papsav1923-001	279210	52652	<sup>74</sup> 473	<sup>202</sup> 2048 ± 0	<sup>167</sup> 626 ± 1	<sup>135</sup> 628 ± 1	<sup>115</sup> 630 ± 1	<sup>99</sup> 648 ± 2	<sup>107</sup> 744 ± 3	<sup>83</sup> 725 ± 25	<sup>85</sup> 731 ± 28		
248	paravision-004	556670	145440	<sup>275</sup> 1572	<sup>349</sup> 4096 ± 0	<sup>241</sup> 829 ± 2	<sup>201</sup> 834 ± 6	<sup>173</sup> 832 ± 2	<sup>153</sup> 833 ± 4	<sup>129</sup> 833 ± 2	<sup>85</sup> 737 ± 31	<sup>83</sup> 718 ± 38		
249	paravision-008	542190	204400	<sup>264</sup> 1448	<sup>347</sup> 4096 ± 0	<sup>207</sup> 699 ± 0	<sup>158</sup> 700 ± 0	<sup>143</sup> 701 ± 0	<sup>117</sup> 702 ± 1	<sup>92</sup> 702 ± 0	<sup>24</sup> 337 ± 17	<sup>25</sup> 330 ± 13		
250	pensees-001	1619431	408932	<sup>301</sup> 1922	<sup>377</sup> 8200 ± 0	<sup>321</sup> 1108 ± 3	<sup>336</sup> 1448 ± 17	<sup>327</sup> 1439 ± 10	<sup>305</sup> 1464 ± 5	<sup>263</sup> 1546 ± 9	<sup>241</sup> 3151 ± 34	<sup>241</sup> 3143 ± 25		
251	pixelall-006	0	746305	<sup>191</sup> 934	<sup>311</sup> 2560 ± 0	<sup>305</sup> 1024 ± 3	<sup>260</sup> 1028 ± 2	<sup>245</sup> 1033 ± 1	<sup>214</sup> 1032 ± 1	<sup>177</sup> 1054 ± 2	<sup>87</sup> 754 ± 14	<sup>84</sup> 722 ± 10		
252	pixelall-007	0	444912	<sup>250</sup> 1349	<sup>97</sup> 2048 ± 0	<sup>307</sup> 1026 ± 4	<sup>264</sup> 1038 ± 2	<sup>259</sup> 1089 ± 2	<sup>228</sup> 1087 ± 2	<sup>191</sup> 1124 ± 2	<sup>79</sup> 708 ± 14	<sup>79</sup> 701 ± 19		
253	psl-008	954351	524525	<sup>334</sup> 3807	<sup>317</sup> 3144 ± 0	<sup>375</sup> 1412 ± 4	<sup>334</sup> 1415 ± 3	<sup>326</sup> 1416 ± 2	<sup>299</sup> 1418 ± 2	<sup>247</sup> 1418 ± 2	<sup>12</sup> 259 ± 22	<sup>18</sup> 252 ± 22		
254	psl-009	411027	411504	<sup>366</sup> 5369	<sup>364</sup> 4168 ± 0	<sup>367</sup> 1382 ± 2	<sup>326</sup> 1381 ± 1	<sup>320</sup> 1383 ± 1	<sup>290</sup> 1383 ± 2	<sup>238</sup> 1385 ± 1	<sup>20</sup> 316 ± 14	<sup>19</sup> 289 ± 14		
255	ptakuratsatu-000	0	585434	<sup>249</sup> 1347	<sup>44</sup> 538 ± 0	<sup>263</sup> 875 ± 3	<sup>210</sup> 863 ± 48	<sup>214</sup> 928 ± 9	<sup>197</sup> 958 ± 17	<sup>184</sup> 1066 ± 26	<sup>285</sup> 5900 ± 103	<sup>284</sup> 5687 ± 167		
256	pxl-001	110116	78231	<sup>23</sup> 168	<sup>30</sup> 512 ± 0	<sup>11</sup> 101 ± 5	<sup>7</sup> 104 ± 5	<sup>13</sup> 189 ± 12	<sup>30</sup> 408 ± 27	<sup>256</sup> 1470 ± 144	<sup>282</sup> 5598 ± 45	<sup>282</sup> 5590 ± 68		
257	pyramid-000	372608	219883	<sup>160</sup> 804	<sup>295</sup> 2056 ± 0	<sup>141</sup> 583 ± 2	-	-	-	-	<sup>303</sup> 7147 ± 59	<sup>305</sup> 7586 ± 425		
258	qnap-000	186731	15598	<sup>39</sup> 272	<sup>102</sup> 2048 ± 0	<sup>205</sup> 726 ± 9	<sup>72</sup> 457 ± 1	<sup>54</sup> 458 ± 0	<sup>46</sup> 464 ± 1	<sup>35</sup> 482 ± 2	<sup>69</sup> 660 ± 25	<sup>71</sup> 654 ± 29		
259	qnap-001	196210	13399	<sup>42</sup> 286	<sup>109</sup> 2048 ± 0	<sup>160</sup> 614 ± 1	<sup>132</sup> 615 ± 1	<sup>114</sup> 627 ± 1	<sup>93</sup> 623 ± 1	<sup>72</sup> 634 ± 2	<sup>67</sup> 649 ± 11	<sup>69</sup> 648 ± 14		
260	quantasoft-003	370518	211354	<sup>211</sup> 1058	<sup>176</sup> 2048 ± 0	<sup>170</sup> 632 ± 2	<sup>138</sup> 634 ± 0	<sup>117</sup> 632 ± 0	<sup>95</sup> 631 ± 1	<sup>71</sup> 634 ± 0	<sup>8</sup> 201 ± 7	<sup>8</sup> 203 ± 8		
261	rankone-011	0	179209	<sup>21</sup> 146	<sup>7</sup> 261 ± 0	<sup>135</sup> 567 ± 1	<sup>110</sup> 557 ± 1	<sup>94</sup> 567 ± 1	<sup>77</sup> 586 ± 1	<sup>86</sup> 682 ± 3	<sup>16</sup> 283 ± 14	<sup>11</sup> 220 ± 19		
262	rankone-012	0	264182	<sup>18</sup> 134	<sup>8</sup> 261 ± 0	<sup>134</sup> 564 ± 3	<sup>108</sup> 554 ± 1	<sup>93</sup> 564 ± 1	<sup>76</sup> 586 ± 1	<sup>90</sup> 695 ± 1	<sup>15</sup> 273 ± 17	<sup>13</sup> 231 ± 14		
263	realnetworks-004	172335	913988	<sup>323</sup> 2467	<sup>294</sup> 2056 ± 0	<sup>55</sup> 330 ± 4	<sup>41</sup> 333 ± 3	<sup>33</sup> 402 ± 7	<sup>75</sup> 585 ± 15	<sup>244</sup> 1402 ± 51	<sup>134</sup> 1210 ± 29	<sup>137</sup> 1202 ± 17		
264	realnetworks-005	172253	56755	<sup>136</sup> 697	<sup>289</sup> 2056 ± 0	<sup>30</sup> 211 ± 4	<sup>18</sup> 205 ± 3	<sup>20</sup> 290 ± 6	<sup>62</sup> 515 ± 17	<sup>224</sup> 1312 ± 78	<sup>133</sup> 1213 ± 17	<sup>138</sup> 1207 ± 16		

Table 12: Summary of algorithms and properties included in this report. The red superscripts give ranking for the quantity in that column.

Notes
1 The configuration size does not capture static data included in libraries.
2 The library size is the combined total of all files provided in the submission lib folder. These libraries e.g. OpenCV may or may not be installed on any end user's platform natively and would not need to be installed with the algorithm. Some developers put neural network models in their libraries.
3 The memory usage is the peak resident set size reported by the ps system call during template generation.
4 The median template creation times are measured on Intel®Xeon®CPU E5-2630 v4 @

	ALGORITHM	CONFIG	LIBRARY	TEMPLATE								COMPARISON <sup>4</sup>									
				NAME				GENERATION TIME (ms) <sup>4</sup>				TIME (ns) <sup>5</sup>									
				DATA (KB) <sup>1</sup>		DATA (KB) <sup>2</sup>		MEMORY (MB) <sup>3</sup>		SIZE (B)		MUGSHOT	480x720	960x1440	1600x2400	3000x4500	GENUINE	IMPOSTOR			
265	regula-000	262444	29384	117	610	227	2048 ± 0	338	1187 ± 1	281	1126 ± 1	266	1129 ± 0	236	1132 ± 1	198	1159 ± 1	39	491 ± 16	40	500 ± 22
266	regula-001	256075	25980	199	976	111	2048 ± 0	352	1284 ± 1	299	1220 ± 1	287	1222 ± 1	259	1226 ± 1	216	1255 ± 1	26	361 ± 10	26	342 ± 25
267	remarkai-001	241857	868314	147	730	266	2052 ± 0	245	831 ± 6	205	849 ± 18	251	1055 ± 25	254	1198 ± 34	261	1519 ± 38	139	1229 ± 20	97	805 ± 56
268	remarkai-003	280516	58559	357	3896	355	4100 ± 0	298	986 ± 1	250	993 ± 1	234	992 ± 1	207	999 ± 3	170	1019 ± 2	95	787 ± 20	94	793 ± 22
269	rendip-000	0	437653	130	682	209	2048 ± 0	93	464 ± 2	73	458 ± 0	62	473 ± 0	51	483 ± 1	57	556 ± 4	44	576 ± 13	46	573 ± 11
270	revealmedia-005	293933	202465	153	763	356	4100 ± 0	83	428 ± 0	60	428 ± 0	45	430 ± 0	38	433 ± 0	27	442 ± 0	195	2023 ± 38	195	2009 ± 26
271	rokid-000	258612	396624	233	1218	290	2056 ± 0	127	546 ± 3	101	542 ± 2	88	545 ± 1	63	522 ± 3	59	563 ± 4	252	3457 ± 62	254	3463 ± 77
272	rokid-001	641223	413733	214	1071	300	2060 ± 0	273	911 ± 2	228	901 ± 5	197	899 ± 2	177	900 ± 3	142	901 ± 3	247	3345 ± 50	247	3346 ± 149
273	s1-003	145509	95446	166	817	344	4096 ± 0	286	947 ± 0	244	959 ± 0	222	952 ± 0	195	952 ± 1	158	955 ± 1	257	3652 ± 19	257	3652 ± 16
274	s1-004	246514	202623	138	700	206	2048 ± 0	233	815 ± 0	193	818 ± 1	171	818 ± 1	150	820 ± 1	126	828 ± 1	245	3245 ± 100	242	3161 ± 88
275	saffe-001	85973	62488	25	168	77	1280 ± 0	43	281 ± 1	-	-	-	-	-	-	-	140	1274 ± 19	142	1277 ± 26	
276	saffe-002	260622	28285	174	855	110	2048 ± 0	236	817 ± 11	190	805 ± 15	167	809 ± 19	148	815 ± 29	123	813 ± 23	81	717 ± 7	82	714 ± 29
277	samsungsd-000	0	307431	217	1083	192	2048 ± 0	53	316 ± 0	39	326 ± 5	25	328 ± 4	20	327 ± 1	17	343 ± 0	338	23722 ± 295	338	23874 ± 305
278	samtech-001	288082	219883	115	605	281	2056 ± 0	49	294 ± 3	-	-	-	-	-	-	-	306	7694 ± 59	306	7678 ± 91	
279	scanovate-002	256986	457227	173	850	186	2048 ± 0	199	696 ± 32	162	713 ± 33	153	738 ± 28	141	779 ± 32	203	1172 ± 53	235	3021 ± 38	239	3120 ± 163
280	scanovate-003	135585	89469	161	808	211	2048 ± 0	142	585 ± 1	129	613 ± 12	99	591 ± 1	86	610 ± 2	87	684 ± 1	231	2926 ± 22	231	2925 ± 20
281	securifai-003	303794	13512	341	2868	362	4104 ± 0	128	549 ± 7	107	550 ± 7	90	549 ± 7	70	546 ± 6	51	546 ± 6	167	1714 ± 26	167	1713 ± 37
282	securifai-004	282177	12027	121	636	94	2048 ± 0	257	869 ± 1	212	867 ± 1	184	867 ± 1	164	867 ± 1	138	865 ± 1	165	1711 ± 19	166	1705 ± 29
283	sesenseit-005	765353	37673	370	6133	65	1028 ± 0	363	1361 ± 27	315	1304 ± 1	308	1319 ± 1	286	1360 ± 1	260	1514 ± 1	138	1223 ± 28	136	1184 ± 29
284	sesenseit-006	765353	37673	369	5994	64	1028 ± 0	362	1352 ± 17	316	1311 ± 1	309	1323 ± 1	284	1357 ± 1	262	1523 ± 2	133	1179 ± 28	135	1157 ± 29
285	sertis-000	265572	68770	61	427	251	2048 ± 0	214	754 ± 0	178	759 ± 0	160	764 ± 0	138	760 ± 0	113	763 ± 0	156	1497 ± 29	159	1582 ± 38
286	sertis-002	460790	68929	256	1391	99	2048 ± 0	336	1181 ± 1	289	1178 ± 0	280	1183 ± 0	252	1187 ± 0	213	1221 ± 0	123	1086 ± 32	122	1076 ± 31
287	seventhsense-000	369850	1561668	168	824	276	2052 ± 0	348	1250 ± 3	306	1257 ± 1	290	1261 ± 1	264	1259 ± 1	219	1272 ± 2	178	1800 ± 35	178	1787 ± 32
288	shaman-000	0	120033	83	507	324	4096 ± 0	176	653 ± 16	-	-	-	-	-	-	-	29	380 ± 25	29	379 ± 31	
289	shaman-001	0	174446	88	511	327	4096 ± 0	48	294 ± 2	-	-	-	-	-	-	-	64	635 ± 19	34	441 ± 25	
290	shu-002	731250	148309	180	890	320	4096 ± 0	212	751 ± 2	181	769 ± 4	209	922 ± 4	303	1431 ± 9	314	3489 ± 47	381	2930763 ± 47355	381	2929759 ± 39149
291	shu-003	428774	146940	87	511	129	2048 ± 0	239	820 ± 6	198	828 ± 3	210	941 ± 9	274	1308 ± 15	310	3045 ± 44	215	2506 ± 26	216	2512 ± 38
292	siat-002	486842	7738	321	2434	265	2052 ± 0	139	579 ± 0	-	-	-	-	-	-	-	92	769 ± 13	89	750 ± 13	
293	siat-004	940063	6984	356	3860	358	4100 ± 0	187	670 ± 0	147	671 ± 7	137	693 ± 10	133	742 ± 10	150	935 ± 17	264	4013 ± 45	261	3782 ± 173
294	sjtu-003	480795	148243	97	538	216	2048 ± 0	240	821 ± 2	194	820 ± 2	210	923 ± 3	255	1201 ± 3	292	2373 ± 9	158	1560 ± 20	157	1560 ± 14
295	sjtu-004	1953267	241108	331	2727	366	4608 ± 0	344	1236 ± 2	297	1209 ± 2	300	1294 ± 4	310	1554 ± 5	303	2738 ± 8	238	3057 ± 14	238	3070 ± 20
296	sktelecom-000	527132	298496	247	1311	79	1536 ± 0	322	1110 ± 1	278	1113 ± 1	262	1114 ± 1	232	1120 ± 1	197	1155 ± 1	346	26583 ± 128	345	26508 ± 126
297	smartengines-000	1711	3025	3	50	10	288 ± 0	19	168 ± 7	13	180 ± 1	11	188 ± 3	11	217 ± 3	14	275 ± 1	6	197 ± 5	4	167 ± 11
298	smilart-002	111826	87805	38	263	57	1024 ± 0	21	176 ± 16	-	-	-	-	-	-	-	330	18784 ± 136	331	18795 ± 151	
299	smilart-003	67339	91670	31	192	33	512 ± 0	23	180 ± 12	14	181 ± 10	22	313 ± 22	106	665 ± 49	289	2299 ± 196	147	1395 ± 74	117	1027 ± 66
300	sodec-000	836592	13142	348	3186	333	4096 ± 0	313	1041 ± 2	262	1032 ± 1	216	1035 ± 1	182	1037 ± 2	183	1061 ± 2	176	1794 ± 37	175	1775 ± 23
301	sqisoft-001	278968	386291	133	688	297	2056 ± 0	101	477 ± 5	321	1348 ± 18	313	1353 ± 26	280	1340 ± 14	241	1393 ± 28	96	797 ± 22	93	788 ± 22
302	sqisoft-002	278039	386291	127	666	292	2056 ± 0	97	466 ± 8	76	466 ± 2	60	468 ± 11	43	461 ± 6	33	472 ± 4	88	758 ± 11	90	760 ± 23
303	stagu-000	879661	624676	212	1064	326	4096 ± 0	233	813 ± 25	-	-	-	-	-	-	-	232	2979 ± 31	235	3007 ± 75	
304	starhybrid-001	100509	289356	171	845	190	2048 ± 0	64	358 ± 82	46	355 ± 49	33	379 ± 58	27	401 ± 79	24	393 ± 67	120	1075 ± 51	123	1078 ± 53
305	suprema-000	246761	38507	120	625	149	2048 ± 0	221	771 ± 2	184	778 ± 1	182	864 ± 2	231	1109 ± 2	283	2150 ± 4	164	1690 ± 17	164	1688 ± 13
306	suprema-001	373423	41460	287	1731	122	2048 ± 0	227	788 ± 1	197	826 ± 2	202	914 ± 2	239	1146 ± 7	297	2443 ± 4	243	3212 ± 16	245	3220 ± 22
307	supremaid-001	258193	23479	98	541	212	2048 ± 0	103	479 ± 1	81	481 ± 0	64	481 ± 0	54	490 ± 0	47	522 ± 0	77	704 ± 19	70	652 ± 19
308	synesis-006	731941	21817	266	1472	363	4094 ± 0	129	549 ± 1	109	546 ± 1	91	552 ± 1	72	558 ± 2	75	639 ± 28	76	697 ± 32	78	688 ± 31

#### Notes

- 1 The configuration size does not capture static data included in libraries.
- 2 The library size is the combined total of all files provided in the submission lib folder. These libraries e.g. OpenCV may or may not be installed on any end user's platform natively and would not need to be installed with the algorithm. Some developers put neural network models in their libraries.
- 3 The memory usage is the peak resident set size reported by the ps system call during template generation.
- 4 The median template creation times are measured on Intel®Xeon®CPU E5-2630 v4 @ 2.20GHz processors.
- 5 The comparison durations, in nanoseconds, are estimated using std::chrono::high\_resolution\_clock which on the machine in (2) counts 1ns clock ticks. Precision is somewhat worse than that however. The ± value is the median absolute deviation times 1.48 for Normal consistency.

Table 13: Summary of algorithms and properties included in this report. The red superscripts give ranking for the quantity in that column.

	ALGORITHM	CONFIG	LIBRARY	TEMPLATE								COMPARISON <sup>4</sup>		
				NAME	DATA	DATA	MEMORY	SIZE	GENERATION TIME (ms) <sup>4</sup>				TIME (ns) <sup>5</sup>	
									(KB) <sup>1</sup>	(KB) <sup>2</sup>	(MB) <sup>3</sup>	(B)	MUGSHOT	480x720
309	synthesis-007		1442961	24145	<sup>322</sup> 2443	<sup>315</sup> 3080 ± 0		<sup>340</sup> 1215 ± 5	<sup>308</sup> 1268 ± 30	<sup>303</sup> 1306 ± 67	<sup>275</sup> 1311 ± 58	<sup>249</sup> 1423 ± 52	<sup>72</sup> 684 ± 32	<sup>76</sup> 686 ± 25
310	synology-000		221021	25809	<sup>67</sup> 453	<sup>222</sup> 2048 ± 0		<sup>76</sup> 407 ± 14	<sup>56</sup> 415 ± 14	<sup>139</sup> 694 ± 31	<sup>294</sup> 1396 ± 58	<sup>318</sup> 4568 ± 211	<sup>334</sup> 19720 ± 203	<sup>333</sup> 19767 ± 379
311	synology-002		256713	25943	<sup>78</sup> 488	<sup>238</sup> 2048 ± 0		<sup>269</sup> 886 ± 4	<sup>225</sup> 892 ± 3	<sup>207</sup> 920 ± 2	<sup>208</sup> 1000 ± 5	<sup>225</sup> 1317 ± 12	<sup>153</sup> 1466 ± 32	<sup>155</sup> 1496 ± 45
312	sztu-000		338637	15871	<sup>244</sup> 1298	<sup>257</sup> 2048 ± 0		<sup>121</sup> 531 ± 0	<sup>97</sup> 532 ± 0	<sup>80</sup> 533 ± 0	<sup>64</sup> 537 ± 0	<sup>52</sup> 548 ± 0	<sup>45</sup> 585 ± 11	<sup>49</sup> 592 ± 13
313	sztu-001		338650	15871	<sup>245</sup> 1298	<sup>132</sup> 2048 ± 0		<sup>123</sup> 535 ± 0	<sup>100</sup> 537 ± 0	<sup>83</sup> 538 ± 0	<sup>66</sup> 540 ± 0	<sup>54</sup> 553 ± 0	<sup>50</sup> 599 ± 10	<sup>51</sup> 598 ± 10
314	tech5-004		2410272	118858	<sup>332</sup> 2733	<sup>12</sup> 321 ± 0		<sup>260</sup> 872 ± 2	<sup>279</sup> 1117 ± 164	<sup>261</sup> 1114 ± 182	<sup>237</sup> 1134 ± 179	<sup>166</sup> 999 ± 44	<sup>46</sup> 597 ± 13	<sup>48</sup> 592 ± 16
315	tech5-005		1178769	120517	<sup>261</sup> 1426	<sup>32</sup> 512 ± 0		<sup>350</sup> 1272 ± 109	<sup>266</sup> 1038 ± 63	<sup>249</sup> 1046 ± 39	<sup>233</sup> 1124 ± 38	<sup>233</sup> 1351 ± 44	<sup>219</sup> 2573 ± 37	<sup>220</sup> 2545 ± 32
316	techsign-000		0	1101622	<sup>305</sup> 1955	<sup>229</sup> 2048 ± 0		<sup>68</sup> 366 ± 1	<sup>53</sup> 398 ± 1	<sup>275</sup> 1172 ± 3	<sup>341</sup> 3065 ± 18	<sup>338</sup> 10460 ± 65	<sup>271</sup> 4758 ± 112	<sup>270</sup> 4789 ± 93
317	tevian-007		779934	19523	<sup>286</sup> 1714	<sup>66</sup> 1032 ± 0		<sup>140</sup> 583 ± 1	<sup>114</sup> 579 ± 0	<sup>96</sup> 580 ± 0	<sup>80</sup> 588 ± 1	<sup>74</sup> 636 ± 0	<sup>275</sup> 4894 ± 65	<sup>273</sup> 4841 ± 83
318	tevian-008		847177	19519	<sup>350</sup> 3490	<sup>67</sup> 1032 ± 0		<sup>267</sup> 884 ± 2	<sup>230</sup> 903 ± 1	<sup>198</sup> 903 ± 1	<sup>179</sup> 911 ± 1	<sup>154</sup> 946 ± 1	<sup>273</sup> 4828 ± 40	<sup>272</sup> 4811 ± 41
319	tiger-005		342866	253734	<sup>271</sup> 1531	<sup>274</sup> 2052 ± 0		<sup>317</sup> 1097 ± 2	<sup>271</sup> 1065 ± 2	<sup>255</sup> 1066 ± 2	<sup>224</sup> 1067 ± 3	<sup>186</sup> 1088 ± 3	<sup>57</sup> 620 ± 19	<sup>59</sup> 615 ± 16
320	tiger-006		421186	394688	<sup>141</sup> 707	<sup>271</sup> 2052 ± 0		<sup>368</sup> 1392 ± 16	<sup>332</sup> 1411 ± 10	<sup>328</sup> 1444 ± 10	<sup>308</sup> 1531 ± 11	<sup>278</sup> 1848 ± 10	<sup>182</sup> 1810 ± 20	<sup>182</sup> 1801 ± 13
321	tinkoff-001		274660	389272	<sup>112</sup> 592	<sup>154</sup> 2048 ± 0		<sup>331</sup> 1176 ± 3	<sup>291</sup> 1179 ± 3	<sup>276</sup> 1178 ± 3	<sup>245</sup> 1169 ± 2	<sup>209</sup> 1203 ± 3	<sup>267</sup> 4361 ± 74	<sup>265</sup> 4364 ± 75
322	tongyi-005		1140701	138919	<sup>315</sup> 2121	<sup>307</sup> 2089 ± 0		<sup>18</sup> 165 ± 1	-	-	-	-	<sup>331</sup> 18924 ± 65	<sup>334</sup> 20158 ± 103
323	toppanidgate-000		671181	711850	<sup>292</sup> 1786	<sup>337</sup> 4096 ± 0		<sup>274</sup> 915 ± 1	<sup>232</sup> 916 ± 1	<sup>204</sup> 916 ± 1	<sup>181</sup> 917 ± 1	<sup>146</sup> 917 ± 1	<sup>344</sup> 25262 ± 84	<sup>343</sup> 25264 ± 97
324	toshiba-003		984125	114264	<sup>229</sup> 1197	<sup>82</sup> 1560 ± 0		<sup>125</sup> 540 ± 0	-	-	-	-	<sup>211</sup> 2390 ± 41	<sup>211</sup> 2407 ± 81
325	toshiba-004		599297	27880	<sup>280</sup> 1595	<sup>283</sup> 2056 ± 0		<sup>377</sup> 1447 ± 3	<sup>338</sup> 1453 ± 2	<sup>332</sup> 1457 ± 9	<sup>304</sup> 1457 ± 3	<sup>257</sup> 1479 ± 4	<sup>115</sup> 1020 ± 25	<sup>111</sup> 998 ± 32
326	trueface-002		253947	123116	<sup>77</sup> 486	<sup>85</sup> 2000 ± 0		<sup>66</sup> 360 ± 0	<sup>48</sup> 361 ± 0	<sup>43</sup> 423 ± 0	<sup>82</sup> 590 ± 1	-	<sup>6</sup> 192 ± 14	<sup>7</sup> 186 ± 19
327	trueface-003		346530	24308	<sup>359</sup> 3915	<sup>253</sup> 2048 ± 0		<sup>320</sup> 1107 ± 22	<sup>150</sup> 677 ± 3	<sup>150</sup> 732 ± 7	<sup>178</sup> 905 ± 5	-	<sup>1</sup> 103 ± 11	<sup>2</sup> 112 ± 29
328	tuputech-000		11476	17185	<sup>23</sup> 33	<sup>175</sup> 2048 ± 0		<sup>15</sup> 122 ± 4	<sup>8</sup> 120 ± 1	<sup>7</sup> 142 ± 2	<sup>10</sup> 196 ± 5	<sup>25</sup> 411 ± 14	<sup>339</sup> 23893 ± 406	<sup>344</sup> 25279 ± 406
329	twface-000		661735	11782	<sup>328</sup> 2610	<sup>215</sup> 2048 ± 0		<sup>258</sup> 871 ± 1	<sup>216</sup> 873 ± 2	<sup>187</sup> 873 ± 2	<sup>167</sup> 876 ± 2	<sup>140</sup> 898 ± 1	<sup>157</sup> 1504 ± 29	<sup>156</sup> 1510 ± 34
330	twface-001		671511	11782	<sup>340</sup> 2855	<sup>112</sup> 2048 ± 0		<sup>277</sup> 923 ± 1	<sup>237</sup> 925 ± 2	<sup>212</sup> 926 ± 1	<sup>185</sup> 929 ± 2	<sup>152</sup> 940 ± 2	<sup>148</sup> 1400 ± 32	<sup>148</sup> 1402 ± 37
331	ulsee-001		370519	57261	-	<sup>231</sup> 2048 ± 0		<sup>178</sup> 654 ± 2	-	-	-	-	<sup>291</sup> 6065 ± 94	<sup>293</sup> 6228 ± 77
332	uluface-002		0	480761	<sup>218</sup> 1088	<sup>163</sup> 2048 ± 0		<sup>261</sup> 873 ± 42	<sup>207</sup> 855 ± 9	<sup>226</sup> 978 ± 24	<sup>266</sup> 1271 ± 40	<sup>290</sup> 2333 ± 68	<sup>333</sup> 19207 ± 1114	<sup>329</sup> 18501 ± 274
333	uluface-003		97357	529422	<sup>239</sup> 1264	<sup>314</sup> 3072 ± 0		<sup>292</sup> 965 ± 11	<sup>248</sup> 968 ± 10	<sup>257</sup> 1087 ± 20	<sup>292</sup> 1387 ± 36	<sup>298</sup> 2469 ± 86	<sup>342</sup> 26057 ± 195	<sup>347</sup> 26865 ± 566
334	unissey-001		0	1956593	<sup>278</sup> 1584	<sup>352</sup> 4096 ± 0		<sup>265</sup> 880 ± 3	<sup>224</sup> 892 ± 3	<sup>331</sup> 1452 ± 8	<sup>340</sup> 3048 ± 12	<sup>336</sup> 10017 ± 387	<sup>132</sup> 1463 ± 35	<sup>153</sup> 1471 ± 34
335	upc-001		0	89914	<sup>216</sup> 1077	<sup>70</sup> 1052 ± 0		<sup>131</sup> 551 ± 15	<sup>160</sup> 703 ± 56	<sup>148</sup> 724 ± 51	<sup>135</sup> 751 ± 49	<sup>136</sup> 863 ± 33	<sup>240</sup> 3114 ± 44	<sup>243</sup> 3165 ± 97
336	vcog-002		3229434	118946	<sup>352</sup> 3666	<sup>381</sup> 61504 ± 5		<sup>63</sup> 357 ± 25	-	-	-	-	<sup>377</sup> 296154 ± 3077	<sup>377</sup> 296436 ± 4183
337	vd-002		254498	34389	<sup>134</sup> 688	<sup>40</sup> 516 ± 0		<sup>194</sup> 684 ± 5	<sup>151</sup> 679 ± 4	<sup>130</sup> 676 ± 5	<sup>114</sup> 693 ± 5	<sup>108</sup> 754 ± 5	<sup>18</sup> 300 ± 14	<sup>21</sup> 319 ± 32
338	vd-003		254505	44051	<sup>135</sup> 696	<sup>278</sup> 2052 ± 0		<sup>197</sup> 691 ± 5	<sup>155</sup> 690 ± 5	<sup>132</sup> 683 ± 4	<sup>113</sup> 691 ± 5	<sup>100</sup> 722 ± 5	<sup>113</sup> 1003 ± 11	<sup>113</sup> 1001 ± 7
339	veridas-006		355669	896424	<sup>310</sup> 1990	<sup>245</sup> 2048 ± 0		<sup>266</sup> 880 ± 8	<sup>222</sup> 885 ± 8	<sup>293</sup> 1271 ± 18	<sup>332</sup> 2242 ± 38	<sup>330</sup> 6414 ± 156	<sup>362</sup> 56940 ± 149	<sup>364</sup> 66077 ± 194
340	veridas-007		355105	891492	<sup>326</sup> 2527	<sup>196</sup> 2048 ± 0		<sup>259</sup> 872 ± 9	<sup>217</sup> 875 ± 8	<sup>291</sup> 1261 ± 18	<sup>330</sup> 2238 ± 38	<sup>328</sup> 6374 ± 147	<sup>68</sup> 655 ± 16	<sup>72</sup> 660 ± 19
341	verigram-000		256209	7798	<sup>297</sup> 1842	<sup>247</sup> 2048 ± 0		<sup>229</sup> 807 ± 1	<sup>195</sup> 821 ± 1	<sup>224</sup> 972 ± 2	<sup>285</sup> 1358 ± 3	<sup>306</sup> 2848 ± 13	<sup>137</sup> 1222 ± 17	<sup>139</sup> 1219 ± 17
342	verihubs-inteligensia-000		209562	51877	<sup>62</sup> 427	<sup>130</sup> 2048 ± 0		<sup>136</sup> 567 ± 0	<sup>341</sup> 1558 ± 8	<sup>337</sup> 1560 ± 8	<sup>311</sup> 1568 ± 8	<sup>267</sup> 1621 ± 8	<sup>337</sup> 22351 ± 91	<sup>337</sup> 22371 ± 81
343	via-000		124422	11151	<sup>197</sup> 964	<sup>185</sup> 2048 ± 0		<sup>202</sup> 707 ± 8	<sup>172</sup> 740 ± 5	<sup>200</sup> 906 ± 41	<sup>191</sup> 941 ± 40	<sup>175</sup> 1040 ± 5	<sup>106</sup> 966 ± 28	<sup>110</sup> 1021 ± 44
344	via-001		370255	11151	<sup>284</sup> 1697	<sup>178</sup> 2048 ± 0		<sup>291</sup> 964 ± 3	<sup>255</sup> 1011 ± 3	<sup>241</sup> 1026 ± 4	<sup>219</sup> 1045 ± 3	<sup>195</sup> 1137 ± 28	<sup>108</sup> 983 ± 31	<sup>109</sup> 989 ± 40
345	videmo-000		139643	39470	<sup>52</sup> 390	<sup>248</sup> 2048 ± 0		<sup>16</sup> 142 ± 5	<sup>9</sup> 150 ± 4	<sup>150</sup> 151 ± 6	<sup>6</sup> 151 ± 4	<sup>40</sup> 513 ± 16	<sup>41</sup> 523 ± 38	
346	videmo-001		212051	95063	<sup>48</sup> 304	<sup>108</sup> 2048 ± 0		<sup>27</sup> 199 ± 0	<sup>11</sup> 164 ± 0	<sup>9</sup> 164 ± 0	<sup>7</sup> 164 ± 0	<sup>17</sup> 296 ± 17	<sup>18</sup> 288 ± 16	
347	videoenetcs-001		30875	5963	<sup>4</sup> 61	<sup>23</sup> 512 ± 0		<sup>36</sup> 262 ± 3	<sup>27</sup> 273 ± 1	<sup>50</sup> 439 ± 3	<sup>151</sup> 820 ± 3	<sup>293</sup> 2393 ± 43	<sup>130</sup> 1153 ± 38	<sup>131</sup> 1142 ± 65
348	videonetcs-002		121981	6289	<sup>15</sup> 115	<sup>273</sup> 2052 ± 0		<sup>44</sup> 282 ± 5	<sup>35</sup> 295 ± 1	<sup>75</sup> 513 ± 4	<sup>212</sup> 1029 ± 3	<sup>312</sup> 3151 ± 46	<sup>136</sup> 1219 ± 57	<sup>140</sup> 1262 ± 56
349	viettelhightech-000		259471	215557	<sup>60</sup> 419	<sup>199</sup> 2048 ± 0		<sup>94</sup> 461 ± 1	<sup>75</sup> 461 ± 2	<sup>56</sup> 461 ± 1	<sup>47</sup> 467 ± 2	<sup>38</sup> 494 ± 0	<sup>49</sup> 599 ± 11	<sup>47</sup> 591 ± 13
350	vigilantsolutions-010		348798	49973	<sup>170</sup> 840	<sup>81</sup> 1548 ± 0		<sup>163</sup> 615 ± 0	<sup>136</sup> 631 ± 0	<sup>116</sup> 632 ± 0	<sup>96</sup> 636 ± 0	<sup>79</sup> 659 ± 0	<sup>38</sup> 490 ± 13	<sup>39</sup> 488 ± 11
351	vigilantsolutions-011		255661	49973	<sup>111</sup> 591	<sup>80</sup> 1548 ± 0		<sup>73</sup> 402 ± 0	<sup>57</sup> 418 ± 0	<sup>41</sup> 418 ± 0	<sup>32</sup> 422 ± 0	<sup>29</sup> 445 ± 0	<sup>25</sup> 339 ± 20	<sup>27</sup> 366 ± 37
352	vinal-000		402391	866522	<sup>206</sup> 1032	<sup>226</sup> 2048 ± 0		<sup>318</sup> 1099 ± 1	<sup>276</sup> 1095 ± 1	<sup>260</sup> 1093 ± 1	<sup>230</sup> 1099 ± 1	<sup>193</sup> 1126 ± 1	<sup>233</sup> 2996 ± 20	<sup>234</sup> 2993 ± 26

Notes

1 The configuration size does not capture static data included in libraries.

2 The library size is the combined total of all files provided in the submission lib folder. These libraries e.g. OpenCV may or may not be installed on any end user's platform natively and would not need to be installed with the algorithm. Some developers put neural network models in their libraries.

3 The memory usage is the peak resident set size reported by the ps system call during template generation.

4 The median template creation times are measured on Intel®Xeon®CPU E5-2630 v4 @ 2.20GHz processors.

5 The comparison durations, in nanoseconds, are estimated using std::chrono::high\_resolution\_clock which on the machine in (2) counts 1ns clock ticks. Precision is somewhat worse than that however. The ± value is the median absolute deviation times 1.48 for Normal consistency.

	ALGORITHM	CONFIG	LIBRARY	TEMPLATE								COMPARISON <sup>4</sup>									
				NAME	DATA		MEMORY	SIZE	GENERATION TIME (ms) <sup>4</sup>				TIME (ns) <sup>5</sup>								
					(KB) <sup>1</sup>	(KB) <sup>2</sup>			(B)	MUGSHOT	480x720	960x1440	1600x2400	3000x4500	GENUINE	IMPOSTOR					
353	vinbigdata-001	271405	44746	109	589	169	2048 ± 0	372	1400 ± 5	329	1393 ± 2	321	1391 ± 2	293	1393 ± 1	245	1404 ± 1	144	1351 ± 50	145	1310 ± 38
354	vion-000	228219	7533	81	498	264	2052 ± 0	57	333 ± 1	-	-	-	-	-	351	39839 ± 3561	346	26830 ± 2241			
355	visage-000	49218	70150	7	73	18	512 ± 0	3	27 ± 0	1	27 ± 0	1	31 ± 0	2	38 ± 0	2	63 ± 0	204	2220 ± 14	205	2218 ± 14
356	visionbox-001	256869	190645	107	579	160	2048 ± 0	296	983 ± 7	275	1093 ± 46	315	1360 ± 68	329	2181 ± 105	326	5955 ± 281	131	1161 ± 22	134	1154 ± 20
357	visionbox-002	259063	135281	118	612	299	2059 ± 0	105	482 ± 1	82	482 ± 0	65	484 ± 1	57	492 ± 1	45	517 ± 3	193	1969 ± 44	191	1931 ± 42
358	visionlabs-010	1067280	19357	182	902	37	513 ± 0	207	730 ± 0	163	717 ± 1	144	709 ± 0	122	713 ± 1	105	739 ± 0	51	600 ± 41	61	626 ± 35
359	visionlabs-011	1067280	19353	176	862	38	513 ± 0	208	731 ± 1	164	717 ± 1	145	710 ± 1	123	714 ± 1	106	741 ± 1	42	556 ± 26	44	559 ± 25
360	visteam-001	186440	30878	57	410	328	4096 ± 0	256	869 ± 7	215	872 ± 6	264	1121 ± 15	317	1719 ± 38	317	4375 ± 157	301	7054 ± 108	301	7025 ± 109
361	visteam-002	186440	30888	99	547	329	4096 ± 0	243	829 ± 5	200	832 ± 6	177	839 ± 7	162	853 ± 6	169	1013 ± 14	299	6952 ± 118	298	6970 ± 120
362	vnpt-002	271649	3203296	79	489	244	2048 ± 0	209	739 ± 2	169	731 ± 2	154	740 ± 1	132	742 ± 2	114	763 ± 2	91	766 ± 13	91	762 ± 13
363	vnpt-003	369956	297799	143	714	334	4096 ± 0	359	1315 ± 4	318	1315 ± 4	307	1318 ± 2	283	1350 ± 3	250	1428 ± 3	305	7397 ± 31	304	7384 ± 29
364	vocord-008	603867	345047	274	1559	312	2688 ± 0	290	962 ± 2	247	976 ± 2	253	1061 ± 3	261	1236 ± 23	279	1851 ± 9	234	3015 ± 50	233	2988 ± 62
365	vocord-009	1380132	201560	361	4162	84	1920 ± 0	380	1472 ± 2	339	1472 ± 1	336	1549 ± 1	315	1667 ± 2	282	2064 ± 2	196	2052 ± 50	198	2056 ± 39
366	vts-000	256589	169760	285	1704	156	2048 ± 0	107	486 ± 1	80	481 ± 0	66	484 ± 0	52	485 ± 1	46	517 ± 0	372	124209 ± 352	372	123652 ± 358
367	winsense-001	264428	32035	189	922	74	1280 ± 0	217	766 ± 7	268	1058 ± 47	229	983 ± 97	221	1053 ± 119	226	1320 ± 84	160	1631 ± 28	193	1964 ± 171
368	winsense-002	281379	25780	291	1781	120	2048 ± 0	110	494 ± 2	89	498 ± 1	77	519 ± 1	65	537 ± 1	73	634 ± 1	163	1683 ± 8	163	1685 ± 7
369	wuhantianyu-001	465118	66457	177	866	95	2048 ± 0	172	642 ± 1	139	642 ± 1	122	644 ± 0	102	652 ± 0	91	697 ± 0	311	9502 ± 151	311	9920 ± 253
370	x-laboratory-000	520020	197310	270	1524	293	2056 ± 0	230	808 ± 7	227	897 ± 113	201	907 ± 103	172	886 ± 103	83	673 ± 39	82	725 ± 19	88	749 ± 34
371	x-laboratory-001	625140	398792	298	1844	288	2056 ± 0	145	586 ± 2	125	596 ± 5	106	603 ± 6	91	620 ± 7	117	793 ± 14	97	813 ± 28	101	872 ± 32
372	xforwardai-001	340100	51163	316	2173	124	2048 ± 0	334	1180 ± 2	295	1182 ± 1	283	1194 ± 1	251	1186 ± 2	208	1203 ± 1	94	779 ± 17	95	797 ± 13
373	xforwardai-002	707715	51163	309	1989	322	4096 ± 0	284	944 ± 1	243	942 ± 1	218	943 ± 4	189	935 ± 1	160	967 ± 1	151	1406 ± 8	149	1405 ± 13
374	xm-000	578041	148920	132	688	270	2052 ± 0	264	878 ± 2	219	882 ± 1	232	988 ± 2	263	1258 ± 3	296	2434 ± 7	161	1634 ± 17	160	1632 ± 20
375	yisheng-004	486351	38653	242	1279	318	3704 ± 0	69	378 ± 12	-	-	-	-	-	-	76	693 ± 137	42	526 ± 34		
376	yitu-003	1525719	138919	333	3737	306	2082 ± 0	254	860 ± 0	-	-	-	-	-	-	328	18305 ± 71	328	18286 ± 62		
377	yoonik-002	453720	265415	335	2755	182	2048 ± 0	327	1145 ± 4	280	1123 ± 2	265	1124 ± 2	234	1125 ± 2	192	1126 ± 3	90	761 ± 32	87	736 ± 32
378	yoonik-003	346691	265415	317	2196	210	2048 ± 0	299	991 ± 3	249	980 ± 1	230	984 ± 4	200	982 ± 1	164	983 ± 1	71	684 ± 45	74	678 ± 41
379	ytu-000	1477360	44032	324	2484	104	2048 ± 0	119	530 ± 0	98	533 ± 0	120	640 ± 0	163	861 ± 2	281	1949 ± 8	348	31797 ± 131	349	31794 ± 133
380	yuan-002	370472	165662	338	2838	137	2048 ± 0	376	1420 ± 3	335	1429 ± 4	335	1511 ± 4	316	1695 ± 4	294	2408 ± 5	209	2297 ± 23	210	2310 ± 31
381	yuan-003	370419	147783	342	2885	127	2048 ± 0	374	1405 ± 2	333	1413 ± 3	330	1446 ± 3	309	1547 ± 5	280	1878 ± 5	210	2320 ± 32	209	2287 ± 34

## Notes

- 1 The configuration size does not capture static data included in libraries.
- 2 The library size is the combined total of all files provided in the submission lib folder. These libraries e.g. OpenCV may or may not be installed on any end user's platform natively and would not need to be installed with the algorithm. Some developers put neural network models in their libraries.
- 3 The memory usage is the peak resident set size reported by the ps system call during template generation.
- 4 The median template creation times are measured on Intel®Xeon®CPU E5-2630 v4 @ 2.20GHz processors.
- 5 The comparison durations, in nanoseconds, are estimated using std::chrono::high\_resolution\_clock which on the machine in (2) counts 1ns clock ticks. Precision is somewhat worse than that however. The ± value is the median absolute deviation times 1.48 for Normal consistency.

Table 15: Summary of algorithms and properties included in this report. The red superscripts give ranking for the quantity in that column.

Algorithm	FALSE NON-MATCH RATE (FNMR)																		
	CONSTRAINED, COOPERATIVE												LESS CONSTRAINED, NON-COOP.						
	Name	VISAMC	VISA	MUGSHOT	MUGSHOT12+YRS	VISABORDER	BORDER	BORDER	WILD	CHILDEXP									
	FMR	0.0001	1E-06	1E-05	1E-05	1E-06	1E-06	1E-05	0.0001	0.01									
1	20face-000	0.1268	325	0.1828	322	0.1748	331	0.2768	330	0.1765	319	0.1864	267	0.0927	294	0.0405	230	-	
2	20face-001	0.0521	307	0.0732	307	0.1414	326	0.2549	328	0.0769	301	0.1354	263	0.0419	261	0.0295	135	-	
3	3divi-006	0.0064	134	0.0094	132	0.0047	112	0.0066	115	0.0091	119	0.0191	138	0.0113	120	0.0289	115	-	
4	3divi-007	0.0024	28	0.0038	32	0.0028	27	0.0034	27	0.0046	39	0.0101	57	0.0082	68	0.0300	146	-	
5	acer-001	0.0294	289	0.0504	295	0.0240	288	0.0463	288	0.0436	283	0.0622	234	0.0360	254	0.0307	157	-	
6	acer-002	0.0169	260	0.0262	262	0.0103	217	0.0167	229	0.0182	222	0.0281	182	0.0159	177	0.0297	140	-	
7	acisw-003	0.9682	380	0.9971	380	0.7892	368	0.8738	367	0.8752	362	0.8275	329	0.6698	351	0.4470	353	-	
8	acisw-007	0.4276	356	0.5493	358	0.8425	369	0.9185	368	0.8424	357	0.9976	351	0.9930	365	0.4963	357	-	
9	adera-002	0.0052	100	0.0071	96	0.0047	110	0.0064	111	0.0087	111	0.0159	108	0.0136	149	0.0990	292	-	
10	adera-003	0.0043	78	0.0059	76	0.0036	70	0.0043	57	0.0076	92	0.0151	96	0.0128	141	0.0989	291	-	
11	advance-002	0.0089	181	0.0137	183	0.0073	175	0.0115	178	0.0400	276	0.0722	241	0.0593	277	0.0498	252	-	
12	advance-003	0.0060	128	0.0087	123	0.0052	126	0.0067	116	0.0389	275	0.4914	298	0.1291	303	0.0508	254	-	
13	aifirst-001	0.0119	220	0.0170	215	0.0084	196	0.0127	190	0.0131	179	0.0212	147	0.0138	152	0.0432	238	0.4301	8
14	aigen-001	0.0124	226	0.0219	237	0.0143	256	0.0217	251	0.0236	246	0.8960	332	0.3255	326	0.0681	274	-	
15	aigen-002	0.0192	272	0.0343	277	0.0256	289	0.0402	283	0.0389	274	0.9196	335	0.3876	332	0.1096	299	-	
16	ailabs-001	0.0158	254	0.0276	267	0.0192	275	0.0317	276	0.0352	268	0.0608	231	0.0434	265	0.0338	195	-	
17	aimall-002	0.0119	222	0.0167	213	0.0224	283	0.0411	284	0.0233	244	0.0373	210	0.0235	231	0.0327	184	-	
18	aimall-003	0.0033	49	0.0041	38	0.0033	61	0.0035	32	0.0056	63	0.0109	64	0.0087	79	0.0312	167	-	
19	aiunionface-000	0.0104	206	0.0154	203	0.0082	193	0.0122	181	0.0141	188	0.0243	163	0.0169	186	0.0306	155	-	
20	aize-001	0.0223	280	0.0344	278	0.0199	276	0.0313	274	0.0367	270	0.0522	224	0.0359	253	0.0446	243	-	
21	aize-002	0.0210	278	0.0327	273	0.0280	292	0.0489	291	0.0504	288	0.0692	238	0.0434	264	0.0854	286	-	
22	ajou-001	0.0093	190	0.0147	194	0.0071	172	0.0126	185	0.0173	219	0.0274	177	0.0186	202	0.0348	202	-	
23	alchera-002	0.0107	209	0.0157	205	0.0104	221	0.0229	254	0.0144	193	0.0246	164	0.0198	214	0.0328	186	-	
24	alchera-003	0.0044	80	0.0055	70	0.0031	44	0.0039	47	0.0042	29	0.0077	26	0.0065	27	0.0339	197	-	
25	alfabeta-001	0.4867	365	0.5831	362	0.6855	357	0.8156	360	0.8253	356	0.7765	325	0.6416	350	0.3427	345	-	
26	alice-000	0.0119	223	0.0192	226	0.0106	224	0.0170	230	0.0167	211	0.0265	173	0.0150	169	0.0288	108	-	
27	alleyes-000	0.0058	118	0.0090	126	0.0055	136	0.0087	154	0.0068	86	0.0105	62	0.0076	55	0.0282	69	-	
28	allgovision-000	0.0346	296	0.0527	298	0.0232	284	0.0339	277	0.0372	273	0.0620	233	0.0443	267	0.0607	268	-	
29	alphaface-001	0.0065	137	0.0097	140	0.0039	85	0.0063	110	0.0083	105	-	-	-	0.0280	56	-		
30	alphaface-002	0.0052	102	0.0075	106	0.0030	34	0.0044	60	1.0000	372	0.0115	73	0.0084	74	0.0279	48	-	
31	amplifiedgroup-001	0.5034	367	0.5848	363	0.6973	361	0.8316	361	0.7807	351	0.7724	323	0.6354	347	0.4250	350	-	
32	androvideo-000	0.0243	283	0.0438	291	0.0239	286	0.0365	281	0.0483	287	0.1870	268	0.0635	280	0.1163	302	-	
33	anke-004	0.0080	171	0.0154	202	0.0073	174	0.0112	176	0.0102	146	0.0178	127	0.0118	127	0.0288	110	0.3577	3
34	anke-005	0.0070	148	0.0109	163	0.0059	147	0.0094	160	0.0105	149	0.0142	86	0.0102	101	0.0289	114	0.3337	2
35	antheus-000	0.2564	339	0.3776	343	0.7240	363	0.8699	364	0.8899	363	0.9872	342	0.9483	360	0.7668	362	0.9233	45
36	antheus-001	0.1311	326	0.2306	328	0.5113	348	0.6797	348	0.8748	361	0.9908	346	0.9649	363	0.7586	361	-	
37	anyvision-004	0.0267	287	0.0385	285	0.0258	290	0.0487	290	0.0234	245	0.0301	187	0.0191	207	0.0470	247	0.4633	9
38	anyvision-005	0.0023	26	0.0037	30	0.0027	26	0.0035	31	0.0049	45	0.0084	35	0.0069	39	0.0285	87	-	
39	armatura-001	0.0033	50	0.0042	44	0.0031	42	0.0037	39	0.0056	62	0.0110	65	0.0092	87	0.0815	285	-	
40	asusaics-000	0.0125	229	0.0209	232	0.0085	197	0.0134	199	0.0143	191	0.7189	317	0.0285	244	0.0295	134	-	
41	asusaics-001	0.0125	231	0.0210	233	0.0085	199	0.0134	200	0.0143	192	0.7437	320	0.0289	245	0.0295	133	-	
42	authenmetric-003	0.0036	60	0.0053	67	0.0039	89	0.0051	78	0.0095	135	0.9930	347	0.5932	345	0.0290	120	-	
43	authenmetric-004	0.0027	37	0.0042	43	0.0033	58	0.0036	36	0.0083	107	0.9879	344	0.4058	335	0.0290	122	-	
44	aware-005	0.0457	304	0.0643	302	0.0603	312	0.1094	313	0.0613	294	0.1075	257	0.0491	269	0.0314	170	-	

Table 16: FNMR is the proportion of mated comparisons below a threshold set to achieve the FMR given in the header on the fourth row. FMR is the proportion of impostor comparisons at or above that threshold. The light grey values give rank over all algorithms in that column. The pink columns use only same-sex impostors; others are selected regardless of demographics. The exception, in the green column, uses “matched-covariates” i.e. impostors of the same sex, age group, and country of birth. The second pink column includes effects of extended ageing. Missing entries for border, visa, mugshot and wild images generally mean the algorithm did not run to completion. For child exploitation, missing entries arise because NIST executes those runs only infrequently. The VISA columns compare images described in section 2.1. The MUGSHOT columns compare images described in section 2.4. The VISA-BORDER column compare images described in section 2.2 with those of section 2.3. The BORDER column compares images described in section 2.3. The WILD columns compare images described in section 2.5. The CHILD-EXPLOITATION columns compare images described in section ??.

	Algorithm	FALSE NON-MATCH RATE (FNMR)										LESS CONSTRAINED, NON-COOP.							
		CONSTRAINED, COOPERATIVE																	
		Name	ViSAMC	VISA	MUGSHOT	MUGSHOT12+YRS	VISABORDER	BORDER	BORDER	WILD	CHILDEXP								
FMR	0.0001	1E-06	1E-05	1E-05	1E-06	1E-06	1E-06	1E-05	0.0001	0.01									
45	aware-006	0.0487	305	0.0819	311	0.0529	308	0.1090	312	0.1011	311	0.1058	253	0.0502	271	0.0317	173	-	
46	awiros-001	0.4044	353	0.4622	350	0.5530	349	0.6518	347	0.2008	323	0.1994	272	0.1386	306	0.5584	359	-	
47	awiros-002	0.1990	333	0.2561	331	0.3319	339	0.4411	338	0.3821	336	0.9938	348	0.2634	321	0.0997	293	-	
48	ayftech-001	0.0946	321	0.1941	323	0.2438	336	0.3625	334	0.1558	317	0.1589	264	0.0936	295	0.0785	281	-	
49	ayonix-000	0.4351	359	0.4872	351	0.6150	354	0.7510	353	0.6557	345	0.6361	310	0.4981	339	0.3635	346	0.8434	39
50	beethedata-000	0.0127	232	0.0195	227	0.0092	209	0.0157	221	0.0171	216	0.0306	189	0.0204	215	0.0285	89	-	
51	beyneai-000	0.0071	153	0.0107	160	0.0104	222	0.0131	197	0.0170	215	0.9837	341	0.6171	346	0.0597	267	-	
52	biocube-001	0.5596	370	0.6834	368	0.7700	367	0.8712	365	0.8446	358	0.9661	339	0.7922	355	0.2377	331	-	
53	bioidechswiss-001	0.0054	110	0.0072	98	0.0069	166	0.0124	184	0.0060	70	0.0094	46	0.0065	31	0.0313	168	-	
54	bioidechswiss-002	0.0049	91	0.0067	91	0.0064	154	0.0116	179	0.0067	84	0.0117	74	0.0086	77	0.0279	41	-	
55	bm-001	0.7431	375	0.9494	376	0.9586	372	0.9843	370	0.9049	364	0.9021	334	0.8395	358	0.9935	371	0.8845	42
56	boetech-001	0.0662	315	0.0802	310	0.0493	305	0.0791	305	0.0682	298	0.1074	256	0.0758	289	0.1719	317	-	
57	boetech-002	0.0535	309	0.0565	300	0.0114	239	0.0136	202	0.0403	277	0.0650	235	0.0606	278	0.1697	316	-	
58	bresee-001	0.0085	178	0.0143	190	0.0086	203	0.0153	219	0.0108	154	0.0168	117	0.0115	124	0.0355	213	-	
59	bresee-002	0.0079	170	0.0101	151	0.0065	159	0.0079	138	0.0129	175	0.0263	171	0.0224	227	0.0327	185	-	
60	camvi-002	0.0125	230	0.0221	239	0.0089	207	0.0145	211	0.0142	189	0.2650	283	0.0166	185	0.0288	106	0.5760	18
61	camvi-004	0.0171	264	0.0316	272	0.0042	98	0.0049	75	0.0097	140	0.6636	312	0.0141	156	0.0284	80	0.5788	19
62	canon-002	0.0034	57	0.0050	60	0.0026	19	0.0033	26	0.0043	31	0.0182	130	0.0065	30	0.0279	45	-	
63	canon-003	0.0041	75	0.0059	77	0.0030	33	0.0040	49	0.0040	24	0.0073	19	0.0059	19	0.0274	18	-	
64	ceiec-003	0.0071	154	0.0107	159	0.0061	150	0.0079	140	0.0160	203	0.0316	192	0.0260	239	0.0308	162	-	
65	ceiec-004	0.0038	67	0.0051	61	0.0045	109	0.0053	82	0.0062	77	0.3939	292	0.0104	107	0.0325	181	-	
66	chosun-001	0.0525	308	0.0936	313	0.0742	316	0.1263	316	0.0978	310	1.0000	368	0.9354	359	0.4446	352	-	
67	chosun-002	0.0390	299	0.0646	303	0.0339	299	0.0576	299	0.0455	285	0.6904	314	0.1746	313	0.0696	276	-	
68	chtface-003	0.0091	185	0.0146	193	0.0083	195	0.0128	192	0.0132	180	0.0220	154	0.0149	167	0.0301	147	-	
69	chtface-004	0.0046	86	0.0062	84	0.0052	125	0.0080	142	0.0088	116	0.0152	97	0.0106	110	0.0306	156	-	
70	clearviewai-000	0.0010	4	0.0019	7	0.0024	5	0.0028	13	0.0030	6	0.0058	7	0.0050	6	0.0271	4	-	
71	closedli-001	0.0136	234	0.0163	208	0.0039	87	0.0054	84	0.0072	89	1.0000	362	0.0094	91	0.0318	174	-	
72	cloudmatrix-000	0.0192	273	0.0340	276	0.0133	250	0.0220	252	0.9837	366	1.0000	365	0.0281	243	0.0668	272	-	
73	cloudwalk-hr-003	0.0026	34	0.0041	40	0.0040	93	0.0058	94	0.0060	75	0.9992	354	0.0094	89	0.7206	360	-	
74	cloudwalk-hr-004	0.0009	2	0.0018	5	0.0034	63	0.0028	17	0.0052	52	0.9992	355	0.0093	88	0.1625	315	-	
75	cloudwalk-mt-003	0.0013	8	0.0022	8	0.0026	15	0.0027	10	0.0039	20	0.0076	22	0.0067	33	0.0347	199	-	
76	cloudwalk-mt-004	0.0009	3	0.0013	1	0.0024	7	0.0021	2	0.0028	4	0.0054	4	0.0050	7	0.0285	91	-	
77	clova-000	0.0099	200	0.0150	197	0.0094	213	0.0147	214	0.0136	182	0.0213	149	0.0152	173	0.0307	158	-	
78	cogent-005	0.0060	126	0.0112	167	0.0064	157	0.0070	120	0.0095	134	0.0184	133	0.0135	146	0.0423	236	-	
79	cogent-006	0.0046	84	0.0059	80	0.0036	67	0.0047	66	0.0058	68	0.0113	70	0.0091	84	0.0343	198	-	
80	cognitec-002	0.0066	139	0.0101	150	0.0079	184	0.0108	172	0.0181	221	0.0317	193	0.0237	232	0.0372	219	-	
81	cognitec-003	0.0038	66	0.0052	63	0.0054	135	0.0057	92	0.0225	241	0.0416	215	0.0388	257	0.0348	203	-	
82	cor-001	0.0075	163	0.0113	169	0.0055	139	0.0084	148	0.0091	121	0.0148	92	0.0092	86	0.0277	34	-	
83	coretech-000	0.7699	377	1.0000	384	1.0000	381	-	1.0000	384	1.0000	373	1.0000	383	1.0000	378	-		
84	corsight-001	0.0040	73	0.0057	74	0.0033	60	0.0047	65	0.0045	34	0.0095	49	0.0063	25	0.0276	25	-	
85	corsight-002	0.0053	105	0.0068	93	0.0030	38	0.0041	51	0.0039	22	0.0079	28	0.0054	14	0.0276	30	-	
86	csc-002	0.0099	202	0.0132	181	0.0077	179	0.0142	208	0.0126	173	0.0195	140	0.0146	163	0.1779	320	-	
87	csc-003	0.0053	104	0.0065	88	0.0037	74	0.0047	68	0.0074	90	0.0124	80	0.0112	119	0.1773	319	-	
88	ctbcbank-000	0.0168	258	0.0250	255	0.0146	259	0.0224	253	0.0211	238	0.8964	333	0.3779	331	1.0000	380	0.8803	41

Table 17: FNMR is the proportion of mated comparisons below a threshold set to achieve the FMR given in the header on the fourth row. FMR is the proportion of impostor comparisons at or above that threshold. The light grey values give rank over all algorithms in that column. The pink columns use only same-sex impostors; others are selected regardless of demographics. The exception, in the green column, uses “matched-covariates” i.e. impostors of the same sex, age group, and country of birth. The second pink column includes effects of extended ageing. Missing entries for border, visa, mugshot and wild images generally mean the algorithm did not run to completion. For child exploitation, missing entries arise because NIST executes those runs only infrequently. The VISA columns compare images described in section 2.1. The MUGSHOT columns compare images described in section 2.4. The VISA-BORDER column compare images described in section 2.2 with those of section 2.3. The BORDER column compares images described in section 2.3. The WILD columns compare images described in section 2.5. The CHILD-EXPLOITATION columns compare images described in section ??.

	Algorithm	FALSE NON-MATCH RATE (FNMR)												LESS CONSTRAINED, NON-COOP.					
		CONSTRAINED, COOPERATIVE								BORDER									
		Name	VISAMC	VISA	MUGSHOT	MUGSHOT12+YRS	VISABORDER	BORDER	BORDER	WILD	CHILDEXP								
FMR	0.0001	1E-06	1E-05	1E-05	1E-06	1E-06	1E-06	1E-05	0.0001	0.01									
89	ctcbcbank-001	0.0155	252	0.0235	248	0.0148	264	0.0243	259	0.0207	235	0.9279	336	0.3469	328	1.0000	381	-	
90	cubox-001	0.0064	136	0.0080	113	0.0037	73	0.0055	87	0.0060	71	0.0111	67	0.0077	56	0.0300	144	-	
91	cubox-002	0.0034	56	0.0041	39	0.0025	12	0.0025	8	0.0033	10	0.0064	12	0.0058	18	0.0480	250	-	
92	cudocommunication-001	0.4777	363	1.0000	383	0.4373	344	0.5360	341	1.0000	380	1.0000	370	1.0000	384	1.0000	379	-	
93	cuhkee-001	0.0036	59	0.0045	50	0.0031	48	0.0046	63	0.0051	51	0.0095	50	0.0079	59	0.1492	311	-	
94	cybercore-000	0.0728	317	0.1110	316	0.1521	328	0.2375	325	0.1874	322	0.1907	269	0.1178	301	0.1191	304	-	
95	cybercore-001	0.3759	351	0.5677	360	0.6928	360	0.7926	356	0.8118	354	0.9291	338	0.7080	353	0.3811	347	-	
96	cyberextruder-001	0.1972	331	0.2547	330	0.4686	347	0.6387	346	0.3807	335	0.3806	290	0.2582	317	0.1747	318	0.7804	38
97	cyberextruder-002	0.0811	319	0.1336	318	0.1465	327	0.2266	324	0.2086	326	1.0000	376	1.0000	380	0.1000	294	0.6105	20
98	cyberlink-007	0.0032	46	0.0053	65	0.0041	96	0.0043	55	0.0052	55	0.0243	162	0.0084	75	0.0280	55	-	
99	cyberlink-008	0.0042	77	0.0056	72	0.0038	83	0.0048	70	0.0053	56	0.0099	54	0.0074	50	0.0274	15	-	
100	dahua-006	0.0027	35	0.0039	34	0.0031	46	0.0039	48	0.0039	21	0.0067	15	0.0058	17	0.0280	50	-	
101	dahua-007	0.0017	17	0.0023	10	0.0026	17	0.0032	25	0.0033	9	0.0060	9	0.0054	13	0.0278	38	-	
102	daon-000	0.0095	195	0.0117	171	0.0068	163	0.0077	135	0.0092	126	0.0174	123	0.0137	151	0.0331	189	-	
103	decatur-000	0.0714	316	0.1115	317	0.0608	313	0.1106	314	0.0866	305	1.0000	366	0.0714	286	0.0658	271	-	
104	decatur-001	0.0424	301	0.0711	305	0.0237	285	0.0458	287	0.0447	284	1.0000	360	0.9969	367	0.0280	54	-	
105	deepglint-003	0.0027	36	0.0038	31	0.0030	37	0.0032	24	0.0043	30	0.0082	33	0.0076	54	0.0279	42	-	
106	deepglint-004	0.0025	32	0.0034	27	0.0039	88	0.0061	107	0.0050	49	0.0091	42	0.0082	67	0.0285	93	-	
107	deepsea-001	0.0136	237	0.0215	236	0.0142	255	0.0214	250	0.0163	207	0.0250	166	0.0192	208	0.0347	201	0.5606	17
108	deepsense-000	0.0145	243	0.0265	263	0.0113	237	0.0196	243	0.0151	196	0.0215	151	0.0129	142	0.0290	119	-	
109	dermalog-008	0.0096	197	0.0166	212	0.0086	201	0.0133	198	0.0165	209	0.0586	228	0.0226	228	0.0277	33	-	
110	dermalog-009	0.0067	142	0.0094	133	0.0051	123	0.0069	118	0.0116	165	0.0312	190	0.0177	194	0.0270	3	-	
111	didiglobalface-001	0.0055	112	0.0092	128	0.0030	35	0.0045	61	0.0088	114	0.0119	77	0.0085	76	0.0282	68	0.4270	6
112	digitalbarriers-002	0.3360	348	0.3690	341	0.0877	318	0.1557	317	0.0971	309	0.0951	249	0.0497	270	0.0436	240	-	
113	dps-000	0.0115	215	0.0176	219	0.0149	266	0.0185	239	0.0173	218	0.0275	179	0.0180	197	0.1067	297	-	
114	dsk-000	0.1526	328	0.2169	326	0.3787	341	0.5426	343	0.3115	329	0.3089	286	0.1994	314	0.2201	327	0.7313	31
115	einetworks-000	0.0099	201	0.0180	221	0.0088	206	0.0140	206	0.0130	177	0.0225	157	0.0147	165	0.0293	128	-	
116	ekin-002	0.1168	323	0.2042	324	0.1530	329	0.2524	327	0.1777	321	0.2773	284	0.1347	305	0.4801	356	-	
117	enface-000	0.0028	40	0.0049	56	0.0043	101	0.0072	122	0.0058	69	0.0150	94	0.0090	83	0.0290	124	-	
118	enface-001	0.0072	157	0.0107	158	0.0071	168	0.0138	203	0.0068	87	0.0515	222	0.0094	92	0.0284	84	-	
119	eocortex-000	0.3485	349	0.6943	369	0.1122	321	0.1574	318	0.2155	328	0.2257	279	0.1606	312	0.2546	338	-	
120	ercacat-001	0.0036	62	0.0044	48	0.0033	57	0.0047	69	0.0106	151	0.0202	144	0.0184	200	0.0258	1	-	
121	euronorate-001	0.2786	342	0.3608	340	0.4489	346	0.6105	345	0.5010	340	0.5392	303	0.3769	330	0.4333	351	-	
122	expasoft-001	0.0328	295	0.0488	293	0.0211	280	0.0342	279	0.0629	297	0.6483	311	0.2816	323	0.0552	262	-	
123	expasoft-002	0.0170	261	0.0274	265	0.0787	317	0.0768	304	0.1629	318	0.9996	356	0.9631	362	0.0337	193	-	
124	f8-001	0.0249	284	0.0336	274	0.0178	273	0.0232	255	0.0303	263	0.0615	232	0.0408	260	0.0475	249	0.5272	14
125	faceonlive-001	0.0269	288	0.0359	281	0.0387	302	0.0721	303	0.0246	254	0.0349	204	0.0220	222	0.0548	260	-	
126	facesoft-000	0.0085	179	0.0112	168	0.0064	156	0.0107	171	0.0091	120	0.0171	120	0.0107	111	0.0275	20	0.4992	11
127	facetag-000	0.2836	343	0.4081	347	0.2933	338	0.4303	337	0.3448	331	0.6312	309	0.3530	329	0.2087	326	-	
128	facetag-002	0.0098	199	0.0147	195	0.0064	158	0.0110	173	0.0116	164	0.0190	137	0.0119	131	0.0675	273	-	
129	facex-001	1.0000	384	1.0000	382	1.0000	376	-	1.0000	375	1.0000	378	1.0000	373	1.0000	374	-		
130	facex-002	0.0803	318	0.1404	319	0.1283	323	0.1979	321	0.1440	316	0.1952	271	0.1299	304	0.2377	330	-	
131	farfaces-001	0.4890	366	0.5860	364	0.5650	350	0.7268	351	0.8015	353	0.7511	321	0.5892	344	0.1976	324	-	
132	fiberhome-nanjing-003	0.0090	182	0.0139	187	0.0082	192	0.0144	209	0.0110	158	0.0174	121	0.0107	112	0.0272	9	-	

Table 18: FNMR is the proportion of mated comparisons below a threshold set to achieve the FMR given in the header on the fourth row. FMR is the proportion of impostor comparisons at or above that threshold. The light grey values give rank over all algorithms in that column. The pink columns use only same-sex impostors; others are selected regardless of demographics. The exception, in the green column, uses “matched-covariates” i.e. impostors of the same sex, age group, and country of birth. The second pink column includes effects of extended ageing. Missing entries for border, visa, mugshot and wild images generally mean the algorithm did not run to completion. For child exploitation, missing entries arise because NIST executes those runs only infrequently. The VISA columns compare images described in section 2.1. The MUGSHOT columns compare images described in section 2.4. The VISA-BORDER column compare images described in section 2.2 with those of section 2.3. The BORDER column compares images described in section 2.3. The WILD columns compare images described in section 2.5. The CHILD-EXPLOITATION columns compare images described in section ??.

	Algorithm	FALSE NON-MATCH RATE (FNMR)										LESS CONSTRAINED, NON-COOP.							
		CONSTRAINED, COOPERATIVE																	
		Name	VISAMC	VISA	MUGSHOT	MUGSHOT12+YRS	VISABORDER	BORDER	BORDER	WILD	CHILDEXP								
FMR		0.0001	1E-06	1E-05	1E-05	1E-06	1E-06	1E-06	1E-05	0.0001	0.01								
133	fiberhome-nanjing-004	0.0037	65	0.0056	73	0.0031	43	0.0043	56	0.0043	32	0.0083	34	0.0061	23	0.0272	7	-	
134	fincore-000	0.0309	293	0.0502	294	0.0281	293	0.0510	293	0.0521	290	0.0815	243	0.0522	272	0.0681	275	-	
135	fujitsulab-002	0.0091	187	0.0124	175	0.0105	223	0.0156	220	0.0169	214	0.0345	202	0.0146	164	0.0282	65	-	
136	fujitsulab-003	0.0045	82	0.0065	89	0.0057	144	0.0083	146	0.0080	98	0.0154	102	0.0101	98	0.0280	49	-	
137	geo-002	0.0171	263	0.0187	224	0.0035	66	0.0051	80	0.0064	79	0.0117	75	0.0083	72	0.0302	150	-	
138	geo-003	0.0180	267	0.0313	271	0.0239	287	0.0552	294	0.0319	267	0.0487	220	0.0222	225	0.0308	164	-	
139	glory-002	0.0241	282	0.0311	270	0.0116	242	0.0151	218	0.0157	200	0.0264	172	0.0188	205	0.1265	305	-	
140	glory-003	0.0076	165	0.0125	176	0.0077	181	0.0103	168	0.0130	176	0.0205	145	0.0143	160	0.0763	279	-	
141	gorilla-007	0.0074	161	0.0111	166	0.0065	160	0.0126	186	0.0100	144	0.0151	95	0.0102	100	0.0278	35	-	
142	gorilla-008	0.0058	119	0.0091	127	0.0049	116	0.0079	139	0.0079	97	0.0126	82	0.0091	85	0.0278	40	-	
143	griaule-000	0.0071	152	0.0099	143	0.0050	119	0.0072	121	0.0160	201	0.0304	188	0.0267	241	0.0338	194	-	
144	hertasecurity-000	0.0630	313	0.0780	309	0.0503	307	0.0898	307	0.0738	299	0.0693	240	0.0420	262	0.0575	265	-	
145	hiik-001	0.0096	196	0.0125	178	0.0093	212	0.0164	227	0.0108	155	0.0937	247	0.0127	138	0.0271	5	-	
146	hisign-001	0.0036	63	0.0050	59	0.0034	62	0.0046	62	0.0079	96	0.0153	101	0.0133	144	0.0286	99	-	
147	hyperverge-001	1.0000	382	1.0000	381	1.0000	377	-	1.0000	379	1.0000	384	1.0000	376	1.0000	384	-	-	
148	hyperverge-002	0.0050	92	0.0066	90	0.0035	65	0.0051	77	0.0062	76	0.0107	63	0.0074	51	0.0276	29	-	
149	icm-002	0.0143	241	0.0249	254	0.0144	257	0.0256	260	0.0236	248	0.0386	212	0.0263	240	0.0339	196	-	
150	icm-003	0.0138	238	0.0222	240	0.0149	265	0.0282	269	0.0227	242	0.0384	211	0.0257	237	0.0333	191	-	
151	icthtc-000	0.0260	286	0.0396	286	0.0207	279	0.0339	278	0.0291	260	0.0474	218	0.0346	251	0.0459	246	-	
152	id3-006	0.0072	159	0.0103	153	0.0049	117	0.0074	128	0.0095	133	0.0165	116	0.0119	130	0.9938	372	-	
153	id3-008	0.0039	69	0.0055	71	0.0032	53	0.0042	52	0.0081	102	0.0155	103	0.0134	145	0.8856	366	-	
154	idemia-007	0.0024	29	0.0039	35	0.0032	55	0.0038	45	0.0046	38	0.0092	44	0.0070	43	0.0288	112	-	
155	idemia-008	0.0023	27	0.0032	22	0.0023	4	0.0028	12	0.0034	13	0.0067	14	0.0056	16	0.0290	121	-	
156	iit-002	0.0111	213	0.0177	220	0.0085	198	0.0140	205	0.0193	231	0.0332	198	0.0260	238	0.1373	307	-	
157	iit-003	0.0082	177	0.0151	200	0.0053	128	0.0084	149	0.0122	170	0.0199	142	0.0137	150	0.0407	231	-	
158	imagus-002	0.0062	129	0.0086	120	0.0053	130	0.0075	129	0.0121	168	0.0207	146	0.0161	179	0.0735	278	-	
159	imagus-004	0.0063	131	0.0094	134	0.0055	138	0.0081	144	0.0098	141	0.0157	106	0.0111	116	0.0283	76	-	
160	imperial-000	0.0067	143	0.0108	162	0.0080	188	0.0134	201	0.0087	112	0.0581	226	0.0102	102	0.0281	60	-	
161	imperial-002	0.0058	120	0.0081	117	0.0055	137	0.0085	151	0.0083	106	0.0157	105	0.0103	103	0.0273	12	0.5151	12
162	incode-009	0.0044	81	0.0067	92	0.0034	64	0.0051	76	0.0049	46	0.0091	41	0.0067	34	0.0296	138	-	
163	incode-010	0.0041	74	0.0063	86	0.0028	29	0.0043	54	0.0047	43	0.0077	25	0.0061	22	0.0296	139	-	
164	innefulabs-000	0.0122	224	0.0199	228	0.0112	236	0.0197	244	0.0222	240	0.0372	209	0.0271	242	0.0348	204	-	
165	innovativetechnologyltd-001	0.0578	311	0.0938	314	0.0501	306	0.0981	308	0.0592	293	0.0779	242	0.0422	263	0.0449	245	-	
166	innovativetechnologyltd-002	0.0451	303	0.0716	306	0.0541	309	0.1009	310	0.0506	289	0.0682	236	0.0371	255	0.0804	284	-	
167	innovatrictrs-007	0.0040	71	0.0054	68	0.0057	143	0.0078	136	0.0079	95	0.0123	78	0.0088	80	0.0282	70	-	
168	innovatrictrs-008	0.0047	88	0.0064	87	0.0038	82	0.0052	81	0.0053	57	0.0088	39	0.0069	40	0.0287	100	-	
169	insightface-000	0.0018	19	0.0027	19	0.0029	30	0.0030	23	0.0038	19	0.0077	24	0.0068	36	0.0276	27	-	
170	insightface-001	0.0009	1	0.0014	2	0.0027	23	0.0024	4	0.0035	14	0.0070	17	0.0065	28	0.0279	44	-	
171	intellicloudai-001	0.0142	240	0.0234	246	0.0092	211	0.0145	210	0.0162	205	0.0371	208	0.0171	188	0.0409	232	-	
172	intellicloudai-002	0.0059	123	0.0085	119	0.0060	149	0.0069	119	0.0108	153	0.2477	282	0.0171	187	0.0303	151	-	
173	intellifusion-001	0.0072	156	0.0094	136	0.0056	142	0.0085	152	0.0111	160	0.0212	148	0.0143	159	0.0289	113	0.5454	15
174	intellifusion-002	0.0059	122	0.0077	109	0.0040	92	0.0074	127	0.0085	110	0.5352	302	0.0104	108	0.0305	154	-	
175	intellivision-001	0.1335	327	0.2205	327	0.1090	319	0.1670	319	0.1385	313	0.1676	265	0.1170	300	0.2445	333	0.7766	37
176	intellivision-002	0.1000	322	0.1775	321	0.0610	314	0.1009	309	0.0805	303	0.1074	255	0.0682	281	0.0768	280	-	

Table 19: FNMR is the proportion of mated comparisons below a threshold set to achieve the FMR given in the header on the fourth row. FMR is the proportion of impostor comparisons at or above that threshold. The light grey values give rank over all algorithms in that column. The pink columns use only same-sex impostors; others are selected regardless of demographics. The exception, in the green column, uses “matched-covariates” i.e. impostors of the same sex, age group, and country of birth. The second pink column includes effects of extended ageing. Missing entries for border, visa, mugshot and wild images generally mean the algorithm did not run to completion. For child exploitation, missing entries arise because NIST executes those runs only infrequently. The VISA columns compare images described in section 2.1. The MUGSHOT columns compare images described in section 2.4. The VISA-BORDER column compare images described in section 2.2 with those of section 2.3. The BORDER column compares images described in section 2.3. The WILD columns compare images described in section 2.5. The CHILD-EXPLOITATION columns compare images described in section ??.

	Algorithm	FALSE NON-MATCH RATE (FNMR)																	
		CONSTRAINED, COOPERATIVE								LESS CONSTRAINED, NON-COOP.									
		Name	ViSAMC	VISA	MUGSHOT	MUGSHOT12+YRS	VISABORDER	BORDER	BORDER	WILD	CHILDEXP								
		FMR	0.0001	1E-06	1E-05	1E-05	1E-05	1E-06	1E-06	1E-05	0.0001	0.01							
177	intelresearch-003	0.0046	83	0.0062	82	0.0038	79	0.0060	102	0.0088	115	0.0168	118	0.0136	147	0.0304	153	-	
178	intelresearch-004	0.0025	30	0.0035	28	0.0032	51	0.0038	43	0.0049	47	0.0094	45	0.0072	44	0.0290	123	-	
179	intsysmsu-001	0.9543	379	0.9888	378	0.9923	373	-	0.9977	367	0.9955	349	0.9892	364	0.7871	363	-		
180	intsysmsu-002	0.0130	233	0.0254	257	0.0137	253	0.0267	267	0.0160	202	0.0267	175	0.0145	162	0.0289	117	-	
181	ionetworks-000	0.0060	127	0.0087	121	0.0044	102	0.0058	96	0.0080	101	0.0144	90	0.0112	117	0.0319	175	-	
182	iqface-000	0.0091	186	0.0143	188	0.0075	178	0.0110	174	0.0171	217	0.2234	277	0.0359	252	0.0381	222	0.6490	22
183	iqface-003	0.0058	117	0.0079	111	0.0051	124	0.0058	97	0.0104	148	0.0200	143	0.0193	209	0.0402	228	-	
184	irex-000	0.0052	99	0.0099	146	0.0056	141	0.0083	147	0.0137	185	0.0163	114	0.0078	57	0.0285	88	-	
185	isap-001	0.5092	368	0.6588	366	0.6899	359	0.7978	357	0.7200	347	0.7253	318	0.5373	341	0.1931	323	-	
186	isap-002	0.0114	214	0.0186	223	0.0087	204	0.0151	217	0.0156	199	0.5134	301	0.0333	247	0.0354	212	-	
187	isityou-000	0.5682	371	0.7033	370	1.0000	379	-	1.0000	378	1.0000	382	1.0000	375	1.0000	382	1.0000	359	
188	isystems-001	0.0149	249	0.0245	252	0.0138	254	0.0210	248	0.0209	237	0.0332	197	0.0223	226	0.0524	258	0.5152	13
189	isystems-002	0.0118	218	0.0182	222	0.0111	233	0.0162	225	0.0166	210	0.0284	183	0.0195	211	0.0516	255	0.4876	10
190	itmo-007	0.0080	172	0.0125	177	0.0107	225	0.0185	237	0.0167	212	0.0222	156	0.0144	161	0.0300	145	-	
191	itmo-008	0.0090	183	0.0150	198	0.0058	146	0.0059	101	0.0187	227	0.0355	205	0.0339	248	0.1498	312	-	
192	ivacognitive-001	0.0189	270	0.0351	279	0.0123	245	0.0235	256	0.0198	233	0.0274	178	0.0155	174	0.0296	137	-	
193	iws-000	0.4824	364	0.5801	361	0.6859	358	0.8155	359	0.8251	355	0.7756	324	0.6400	349	0.3251	344	-	
194	kakao-005	0.0040	70	0.0059	78	0.0036	72	0.0057	91	0.0085	109	0.0239	160	0.0125	136	0.0280	53	-	
195	kakaopay-001	0.0152	251	0.0252	256	0.0145	258	0.0270	268	0.0232	243	0.0344	201	0.0194	210	0.0416	235	-	
196	kedacom-000	0.0055	111	0.0081	116	0.0111	235	0.0120	180	0.0415	279	0.0966	251	0.0686	282	0.2511	336	0.7650	35
197	kiwitech-000	0.0076	166	0.0105	155	0.0081	190	0.0128	193	0.0096	136	0.0163	113	0.0101	99	0.0279	47	-	
198	kneron-003	0.0542	310	0.0902	312	0.0346	300	0.0562	297	0.0919	307	0.1251	261	0.0973	296	0.3053	343	0.6962	27
199	kneron-005	0.0157	253	0.0259	259	0.0126	248	0.0212	249	0.0406	278	0.0693	239	0.0542	274	0.0471	248	-	
200	kookmin-002	0.0054	109	0.0077	107	0.0043	100	0.0065	112	0.0123	171	0.7591	322	0.0198	213	0.0285	90	-	
201	kuke3d-001	0.0058	115	0.0104	154	0.0083	194	0.0093	159	0.0270	257	0.9901	345	0.8341	357	0.0404	229	-	
202	lemalabs-001	0.0111	212	0.0175	217	0.0088	205	0.0142	207	0.0143	190	0.0228	158	0.0140	154	0.0281	57	-	
203	line-000	0.0172	265	0.0236	249	0.0109	229	0.0194	242	0.0183	223	0.0291	184	0.0204	216	0.0298	141	-	
204	line-001	0.0025	31	0.0040	36	0.0026	22	0.0034	30	0.0045	36	0.4127	294	0.0080	63	0.0283	75	-	
205	lookman-002	0.0297	291	0.0547	299	0.0339	298	0.0562	296	0.0614	295	0.0960	250	0.0790	290	0.2640	340	-	
206	lookman-004	0.0074	162	0.0099	145	0.0124	247	0.0149	215	0.0430	282	0.0866	245	0.0694	283	0.2516	337	0.7664	36
207	luxand-000	0.2056	334	0.2814	334	0.4053	343	0.5365	342	0.3497	332	0.3743	289	0.2605	319	0.2222	329	-	
208	mantra-000	0.0037	64	0.0052	64	0.0054	133	0.0056	89	0.0097	139	0.0181	129	0.0151	170	0.0350	208	-	
209	maxvision-000	0.0078	169	0.0106	157	0.0110	231	0.0147	213	0.0368	272	1.0000	379	0.1545	309	0.0445	242	-	
210	megvii-003	0.0064	133	0.0094	131	0.0136	252	0.0260	262	0.0050	48	0.0080	29	0.0059	21	0.0288	103	-	
211	megvii-004	0.0020	22	0.0033	25	0.0028	28	0.0035	33	0.0037	18	0.0074	20	0.0068	38	0.0283	77	-	
212	meituan-000	0.0197	274	0.0424	289	0.0078	182	0.0074	126	0.0103	147	0.0193	139	0.0164	182	0.1063	296	-	
213	meiya-001	0.0171	262	0.0275	266	0.0159	270	0.0261	265	0.0311	264	0.2250	278	0.0245	235	0.0363	218	-	
214	mendaxiatech-000	0.0027	38	0.0036	29	0.0029	31	0.0036	37	0.0031	7	0.0057	6	0.0051	9	0.0275	21	-	
215	microfocus-001	0.4482	361	0.5524	359	0.7256	364	0.8416	362	0.7301	348	0.6926	315	0.5180	340	0.2567	339	0.6890	26
216	microfocus-002	0.3605	350	0.5057	353	0.5783	352	0.7223	350	0.5909	341	0.5963	308	0.4160	336	0.1582	314	0.6517	23
217	minivision-000	0.0033	51	0.0048	55	0.0038	80	0.0049	73	0.0055	61	0.0094	48	0.0079	61	0.0273	10	-	
218	mobai-000	0.0360	298	0.0439	292	0.0372	301	0.0700	301	0.0367	271	0.0939	248	0.0795	291	0.2640	341	-	
219	mobai-001	0.0199	276	0.0219	238	0.0047	111	0.0061	104	0.0093	131	0.0174	122	0.0138	153	0.1045	295	-	
220	mobbl-001	0.3208	345	0.4375	348	0.5680	351	0.7193	349	0.6282	343	0.5783	306	0.3984	333	0.1866	321	-	

Table 20: FNMR is the proportion of mated comparisons below a threshold set to achieve the FMR given in the header on the fourth row. FMR is the proportion of impostor comparisons at or above that threshold. The light grey values give rank over all algorithms in that column. The pink columns use only same-sex impostors; others are selected regardless of demographics. The exception, in the green column, uses “matched-covariates” i.e. impostors of the same sex, age group, and country of birth. The second pink column includes effects of extended ageing. Missing entries for border, visa, mugshot and wild images generally mean the algorithm did not run to completion. For child exploitation, missing entries arise because NIST executes those runs only infrequently. The VISA columns compare images described in section 2.1. The MUGSHOT columns compare images described in section 2.4. The VISA-BORDER column compare images described in section 2.2 with those of section 2.3. The BORDER column compares images described in section 2.3. The WILD columns compare images described in section 2.5. The CHILD-EXPLOITATION columns compare images described in section ??.

Algorithm	FALSE NON-MATCH RATE (FNMR)									
	CONSTRAINED, COOPERATIVE								LESS CONSTRAINED, NON-COOP.	
	Name	ViSAMC	VISA	MUGSHOT	MUGSHOT12+YRS	ViSABORDER	BORDER	BORDER	WILD	CHILDEXP
FMR	0.0001	1E-06	1E-05	1E-05	1E-06	1E-06	1E-06	1E-05	0.0001	0.01
221 <b>mobbl-002</b>	0.9914	381	0.9970	379	0.9355	370	-	1.0000	371	1.0000
222 <b>mobilpintech-000</b>	0.0090	184	0.0149	196	0.0039	91	0.0057	90	0.0115	163
223 <b>moreedian-000</b>	0.3874	352	0.4912	352	0.9988	374	-	0.9990	368	0.9999
224 <b>multimodality-000</b>	0.0034	55	0.0047	54	0.0036	71	0.0044	59	0.0077	93
225 <b>mvision-001</b>	0.0191	271	0.0233	244	0.0204	278	0.0356	280	0.0198	234
226 <b>nazhai-000</b>	0.0040	72	0.0059	79	0.0036	68	0.0048	72	0.0057	65
227 <b>neosystems-002</b>	0.2905	344	0.4077	346	0.2028	334	0.3252	332	0.4088	338
228 <b>neosystems-003</b>	0.2429	336	0.3349	337	0.1844	332	0.2999	331	0.5942	342
229 <b>netbridge-tech-001</b>	0.4749	362	0.6599	367	0.4438	345	0.5676	344	0.4491	339
230 <b>netbridge-tech-002</b>	0.0101	204	0.0166	210	0.0077	180	0.0127	189	0.0133	181
231 <b>neurotechnology-012</b>	0.0051	98	0.0070	95	0.0038	76	0.0056	88	0.0066	83
232 <b>neurotechnology-013</b>	0.0032	48	0.0045	51	0.0026	21	0.0036	34	0.0037	17
233 <b>rhn-001</b>	0.0066	141	0.0098	141	0.0053	129	0.0079	141	0.0093	127
234 <b>rhn-002</b>	0.0068	146	0.0096	139	0.0057	145	0.0087	155	0.0136	184
235 <b>nodeflux-002</b>	0.0186	269	0.0340	275	0.0261	291	0.0451	286	0.0548	291
236 <b>notiontag-001</b>	0.6846	373	0.8006	373	0.3955	342	0.5247	340	0.8669	360
237 <b>notiontag-002</b>	0.0066	138	0.0089	124	0.0045	108	0.0061	105	0.0077	94
238 <b>nsensecorp-002</b>	0.4277	357	0.5375	356	0.6734	356	0.7924	355	0.7194	346
239 <b>nsensecorp-003</b>	0.0251	285	0.0295	269	0.0212	281	0.0305	272	0.0131	178
240 <b>ntechlab-010</b>	0.0013	9	0.0017	3	0.0024	11	0.0029	21	0.0031	8
241 <b>ntechlab-011</b>	0.0012	5	0.0019	6	0.0024	9	0.0028	19	0.0029	5
242 <b>omnigarde-000</b>	0.0633	314	0.1002	315	0.1109	320	0.2042	323	0.1288	312
243 <b>omnigarde-001</b>	0.0168	259	0.0260	260	0.0203	277	0.0402	282	0.0243	251
244 <b>omsecurity-000</b>	0.2573	340	0.3835	344	0.3590	340	0.4903	339	0.3956	337
245 <b>openface-001</b>	0.1804	330	0.2921	335	0.2878	337	0.3906	336	0.2054	325
246 <b>oz-003</b>	0.0095	194	0.0143	189	0.0054	134	0.0077	134	0.0096	137
247 <b>oz-004</b>	0.0033	53	0.0049	58	0.0038	84	0.0055	86	0.0081	103
248 <b>papsav1923-001</b>	0.0078	168	0.0130	180	0.0068	164	0.0105	170	0.0119	166
249 <b>paravision-004</b>	0.0030	43	0.0046	52	0.0030	36	0.0036	35	0.0091	123
250 <b>paravision-008</b>	0.0018	18	0.0025	15	0.0024	6	0.0025	7	0.0036	15
251 <b>pensees-001</b>	0.0087	180	0.0133	182	0.0071	170	0.0122	183	0.0145	194
252 <b>pixelall-006</b>	0.0032	47	0.0042	42	0.0032	50	0.0039	46	0.0063	78
253 <b>pixelall-007</b>	0.0036	61	0.0049	57	0.0039	86	0.0044	58	0.0068	85
254 <b>psl-008</b>	0.0026	33	0.0040	37	0.0024	8	0.0028	18	0.0041	26
255 <b>psl-009</b>	0.0161	256	0.0294	268	0.0023	3	0.0025	5	0.0036	16
256 <b>ptakuratsatu-000</b>	0.0060	125	0.0089	125	0.0070	167	0.0104	169	0.0096	138
257 <b>pxl-001</b>	0.0488	306	0.0752	308	0.0586	311	0.1087	311	0.0946	308
258 <b>pyramid-000</b>	0.0136	236	0.0233	245	0.0117	243	0.0192	241	0.0185	226
259 <b>qnap-000</b>	0.0149	246	0.0228	242	0.0155	268	0.0267	266	0.0238	250
260 <b>qnap-001</b>	0.0148	245	0.0215	235	0.0103	218	0.0162	224	0.0183	225
261 <b>quantasoft-003</b>	0.0081	175	0.0113	170	0.0056	140	0.0076	132	0.0091	122
262 <b>rankone-011</b>	0.0049	90	0.0075	105	0.0038	75	0.0048	71	0.0060	74
263 <b>rankone-012</b>	0.0043	79	0.0058	75	0.0031	49	0.0038	42	0.0047	41
264 <b>realnetworks-004</b>	0.0075	164	0.0101	149	0.0066	161	0.0097	165	0.0108	157

Table 21: FNMR is the proportion of mated comparisons below a threshold set to achieve the FMR given in the header on the fourth row. FMR is the proportion of impostor comparisons at or above that threshold. The light grey values give rank over all algorithms in that column. The pink columns use only same-sex impostors; others are selected regardless of demographics. The exception, in the green column, uses “matched-covariates” i.e. impostors of the same sex, age group, and country of birth. The second pink column includes effects of extended ageing. Missing entries for border, visa, mugshot and wild images generally mean the algorithm did not run to completion. For child exploitation, missing entries arise because NIST executes those runs only infrequently. The VISA columns compare images described in section 2.1. The MUGSHOT columns compare images described in section 2.4. The VISA-BORDER column compare images described in section 2.2 with those of section 2.3. The BORDER column compares images described in section 2.3. The WILD columns compare images described in section 2.5. The CHILD-EXPLOITATION columns compare images described in section ??.

		FALSE NON-MATCH RATE (FNMR)																	
	Algorithm	CONSTRAINED, COOPERATIVE								LESS CONSTRAINED, NON-COOP.									
	Name	ViSAMC	VISA	MUGSHOT	MUGSHOT12+YRS	VISABORDER	BORDER	BORDER	WILD	CHILDEXP									
	FMR	0.0001	1E-06	1E-05	1E-05	1E-06	1E-06	1E-05	0.0001	0.01									
265	realnetworks-005	0.0070	147	0.0093	130	0.0063	153	0.0089	157	0.0092	125	0.0161	111	0.0104	106	0.0289	116	-	
266	regula-000	0.0184	268	0.0376	284	0.0103	219	0.0185	236	0.0120	167	0.9983	353	0.0231	229	0.0273	13	-	
267	regula-001	0.0072	158	0.0107	161	0.0102	216	0.0179	234	0.0123	172	0.0333	199	0.0174	190	0.0295	132	-	
268	remarkai-001	0.0144	242	0.0256	258	0.0102	215	0.0159	222	0.0162	206	0.0582	227	0.0185	201	0.0308	161	-	
269	remarkai-003	0.0047	87	0.0063	85	0.0033	59	0.0049	74	0.0054	58	0.0100	56	0.0072	45	0.0275	24	-	
270	rendip-000	0.0055	113	0.0077	108	0.0048	114	0.0060	103	0.0080	99	0.0142	88	0.0110	115	0.0433	239	-	
271	revealmedia-005	0.0050	94	0.0074	104	0.0050	120	0.0068	117	0.0075	91	0.0124	79	0.0104	109	0.3960	349	-	
272	rokid-000	0.0093	191	0.0145	191	0.0073	176	0.0102	167	0.0164	208	0.0280	181	0.0214	220	0.0857	287	-	
273	rokid-001	0.0105	208	0.0162	207	0.0094	214	0.0163	226	0.0181	220	0.0276	180	0.0165	184	0.0325	182	-	
274	s1-003	0.0051	97	0.0073	100	0.0044	104	0.0063	109	0.0052	54	0.0096	52	0.0070	41	0.1321	306	-	
275	s1-004	0.0053	103	0.0080	115	0.0038	77	0.0059	100	0.0057	64	0.0103	58	0.0073	47	0.0281	59	-	
276	saffe-001	0.4339	358	0.5261	354	0.7539	366	0.8736	366	0.7977	352	0.9810	340	0.7435	354	0.3887	348	0.8973	43
277	saffe-002	0.0119	221	0.0206	229	0.0107	228	0.0177	232	0.0244	252	0.9998	357	0.2785	322	0.0308	160	-	
278	samsungsds-000	0.0046	85	0.0069	94	0.0132	249	0.0081	143	0.0099	142	0.0179	128	0.0162	180	0.1874	322	-	
279	samtech-001	0.0197	275	0.0365	282	0.0146	262	0.0241	258	0.0238	249	0.0394	213	0.0251	236	0.0337	192	-	
280	scanovate-002	0.0175	266	0.0355	280	0.0146	260	0.0286	270	0.0269	256	0.0301	185	0.0178	195	0.0301	148	-	
281	scanovate-003	0.0054	107	0.0080	114	0.0054	131	0.0072	124	0.0312	265	0.0599	229	0.0568	275	0.0283	71	-	
282	securifai-003	0.4086	354	0.7577	372	0.7233	362	0.8070	358	0.7787	350	1.0000	369	0.9988	368	0.8326	365	-	
283	securifai-004	0.0136	235	0.0192	225	0.0064	155	0.0099	166	0.0115	162	0.0272	176	0.0127	139	0.0347	200	-	
284	sensetime-005	0.0019	20	0.0029	20	0.0022	2	0.0021	3	0.0023	2	0.0044	2	0.0039	2	0.0273	11	-	
285	sensetime-006	0.0014	10	0.0024	13	0.0021	1	0.0020	1	0.0021	1	0.0040	1	0.0036	1	0.0272	8	-	
286	sertis-000	0.0118	219	0.0208	231	0.0080	186	0.0127	188	0.0110	159	0.0176	126	0.0114	122	0.0285	92	-	
287	sertis-002	0.0049	89	0.0061	81	0.0039	90	0.0061	108	0.0055	60	0.0099	55	0.0070	42	0.0281	58	-	
288	seventhsense-000	0.0067	145	0.0099	148	0.0045	106	0.0065	113	0.0093	128	0.0169	119	0.0124	135	0.0275	23	-	
289	shaman-000	0.9297	378	0.9774	377	0.9990	375	-	-	0.9999	369	1.0000	364	0.9999	371	0.9575	368	0.9618	47
290	shaman-001	0.3346	347	0.4616	349	0.2368	335	0.3723	335	0.3574	333	0.3527	288	0.2304	316	0.1498	313	0.8990	44
291	shu-002	-	-	0.0079	112	0.0146	261	0.0308	273	1.0000	370	0.0183	131	0.0115	123	0.0284	82	-	
292	shu-003	0.0028	39	0.0041	41	0.0050	118	0.0088	156	0.0081	104	0.0133	84	0.0094	90	0.0283	78	-	
293	siat-002	0.0091	188	0.0126	179	0.0109	230	0.0190	240	0.0276	259	0.0516	223	0.0464	268	0.0520	257	0.4277	7
294	siat-004	0.0067	144	0.0099	144	0.0152	267	-	-	0.0275	258	0.4823	297	0.4823	338	1.0000	373	-	
295	sjtu-003	0.0017	15	0.0033	23	0.0030	39	0.0037	40	0.0058	66	0.0104	59	0.0081	66	0.0284	86	-	
296	sjtu-004	0.0014	11	0.0025	14	0.0027	24	0.0028	20	0.0046	37	0.0086	37	0.0073	46	0.0272	6	-	
297	sktelecom-000	0.0038	68	0.0054	69	0.0031	40	0.0051	79	0.0042	27	0.3418	287	0.0061	24	0.0293	130	-	
298	smartengines-000	0.6240	372	0.7562	371	0.9552	371	0.9784	369	0.9515	365	0.9288	337	0.8200	356	0.8037	364	-	
299	smilart-002	0.2440	337	0.3532	339	-	-	-	-	0.3785	334	0.4145	295	0.2611	320	-	0.6999	28	
300	smilart-003	0.6944	374	0.8836	374	0.0695	315	0.1193	315	0.0894	306	0.1221	260	0.0737	288	0.1190	303	-	
301	sodec-000	0.0033	52	0.0044	49	0.0040	94	0.0053	83	0.0054	59	0.0096	51	0.0080	62	0.0274	16	-	
302	sqisoft-001	0.1220	324	0.2088	325	0.1978	333	0.3386	333	0.2111	327	0.2798	285	0.1474	308	0.0519	256	-	
303	sqisoft-002	0.0082	176	0.0124	173	0.0051	122	0.0086	153	0.0102	145	0.0183	132	0.0122	133	0.0287	102	-	
304	stazu-000	0.0139	239	0.0208	230	0.0104	220	0.0145	212	0.0156	198	0.8063	326	0.1408	307	0.0332	190	-	
305	starhybrid-001	0.0108	210	0.0138	184	0.0081	189	0.0113	177	0.0152	197	0.0265	174	0.0189	206	0.0350	209	0.5584	16
306	suprema-000	0.0064	135	0.0092	129	0.0081	191	0.0096	164	0.0139	187	0.0254	170	0.0220	223	0.1131	301	-	
307	suprema-001	0.0041	76	0.0053	66	0.0038	81	0.0047	67	0.0060	73	0.0111	66	0.0095	93	0.0382	223	-	
308	supremaid-001	0.0053	106	0.0073	101	0.0045	107	0.0066	114	0.0099	143	0.0186	134	0.0148	166	0.0352	211	-	

Table 22: FNMR is the proportion of mated comparisons below a threshold set to achieve the FMR given in the header on the fourth row. FMR is the proportion of impostor comparisons at or above that threshold. The light grey values give rank over all algorithms in that column. The pink columns use only same-sex impostors; others are selected regardless of demographics. The exception, in the green column, uses “matched-covariates” i.e. impostors of the same sex, age group, and country of birth. The second pink column includes effects of extended ageing. Missing entries for border, visa, mugshot and wild images generally mean the algorithm did not run to completion. For child exploitation, missing entries arise because NIST executes those runs only infrequently. The VISA columns compare images described in section 2.1. The MUGSHOT columns compare images described in section 2.4. The VISA-BORDER column compare images described in section 2.2 with those of section 2.3. The BORDER column compares images described in section 2.3. The WILD columns compare images described in section 2.5. The CHILD-EXPLOITATION columns compare images described in section ??.

	Algorithm	FALSE NON-MATCH RATE (FNMR)																	
		CONSTRAINED, COOPERATIVE								LESS CONSTRAINED, NON-COOP.									
		Name	VISAMC	VISA	MUGSHOT	MUGSHOT12+YRS	VISABORDER	BORDER	BORDER	WILD	CHILDEXP								
	FMR	0.0001	1E-06	1E-05	1E-05	1E-05	1E-06	1E-06	1E-05	0.0001	0.01								
309	synesis-006	0.0070	149	0.0096	137	0.0107	226	0.0166	228	-	0.0128	83	0.0089	81	0.0292	126	-		
310	synesis-007	0.0050	95	0.0073	103	0.0062	152	0.0076	131	-	0.0105	60	0.0080	65	0.0288	104	-		
311	synology-000	0.0149	248	0.0238	250	0.0148	263	0.0261	263	0.0221	239	0.0331	196	0.0209	219	0.0330	188	-	
312	synology-002	0.0104	207	0.0153	201	0.0107	227	0.0184	235	0.0189	229	0.02032	273	0.0180	196	0.0312	166	-	
313	sztu-000	0.0092	189	0.0139	186	0.0091	208	0.0201	246	0.0136	183	0.0685	237	0.0118	129	0.0270	2	-	
314	sztu-001	0.0031	44	0.0043	47	0.0025	13	0.0028	16	0.0051	50	0.0113	71	0.0089	82	0.0275	19	-	
315	tech5-004	0.0123	225	0.0234	247	0.0086	202	0.0162	223	0.0065	82	0.0112	68	0.0082	69	0.0281	62	-	
316	tech5-005	0.0054	108	0.0072	97	0.0069	165	0.0122	182	0.0060	72	0.0094	47	0.0066	32	0.0349	206	-	
317	techsign-000	0.0325	294	0.0511	296	0.0435	304	0.0710	302	0.0746	300	0.1104	258	0.0841	292	0.0639	270	-	
318	tevian-007	0.0019	21	0.0027	18	0.0032	54	0.0041	50	0.0045	33	0.0086	36	0.0078	58	0.0310	165	-	
319	tevian-008	0.0012	7	0.0017	4	0.0033	56	0.0042	53	0.0042	28	0.0081	30	0.0068	37	0.0290	118	-	
320	tiger-005	0.0624	312	0.2450	329	0.0292	296	0.0556	295	0.0430	281	1.0000	359	0.9964	366	0.0278	37	-	
321	tiger-006	0.0066	140	0.0101	152	0.0050	121	0.0075	130	0.0089	118	0.0158	107	0.0117	126	0.0290	125	-	
322	tinkoff-001	0.0145	244	0.0244	251	0.0318	297	0.0636	300	0.0236	247	1.0000	375	0.0339	249	0.0563	264	-	
323	tongyi-005	0.0073	160	0.0146	192	0.0187	274	0.0421	285	0.0161	204	0.0215	150	0.0149	168	0.0399	226	0.6195	21
324	toppanidgate-000	0.0021	24	0.0033	24	0.0026	16	0.0028	14	0.0039	23	0.0075	21	0.0068	35	0.0376	221	-	
325	toshiba-003	0.0125	228	0.0214	234	0.0085	200	0.0131	196	-	0.0241	161	0.0151	172	0.0282	63	-		
326	toshiba-004	0.0030	42	0.0042	45	0.0025	14	0.0027	11	0.0034	12	0.0063	11	0.0053	12	0.0278	36	-	
327	trueface-002	0.0060	124	0.0096	138	0.0048	113	0.0061	106	0.0112	161	0.0198	141	0.0155	175	0.0793	283	-	
328	trueface-003	0.0070	150	0.0094	135	0.0053	127	0.0081	145	0.0122	169	0.0217	153	0.0159	178	0.0785	282	-	
329	tuputech-000	0.3218	346	0.3696	342	-	-	-	0.3237	330	0.4304	296	0.2973	325	0.9415	367	-		
330	twface-000	0.0051	96	0.0072	99	0.0041	97	0.0058	93	0.0071	88	0.0153	100	0.0100	95	0.0276	28	-	
331	twface-001	0.0036	58	0.0051	62	0.0031	47	0.0038	41	0.0049	44	0.0091	43	0.0075	53	0.0277	31	-	
332	ulsee-001	0.0151	250	0.0246	253	0.0113	238	0.0185	238	0.0187	228	0.6766	313	0.0181	198	0.0316	172	-	
333	ultinous-000	0.2343	335	0.3484	338	-	-	-	-	-	-	-	-	-	0.9447	46	-		
334	ultinous-001	0.2485	338	0.4003	345	-	-	-	-	-	-	-	-	-	0.6847	25	-		
335	uluface-002	0.0081	174	0.0123	172	0.0071	169	0.0095	163	0.0107	152	1.0000	374	0.0140	155	0.0444	241	0.6729	24
336	uluface-003	0.0100	203	0.0150	199	0.0079	183	0.0128	191	-	-	-	-	-	0.0635	269	-		
337	unissey-001	0.0095	193	0.0160	206	0.0134	251	0.0150	216	0.0147	195	0.0253	169	0.0163	181	0.0946	290	-	
338	upc-001	0.0234	281	0.0519	297	0.0291	295	0.0490	292	0.0294	261	0.2316	280	0.0389	258	0.0314	169	0.4224	5
339	vcog-002	0.7522	376	0.9033	375	-	-	-	-	-	-	-	-	-	0.7523	33	-		
340	vd-002	0.0429	302	0.0704	304	0.0569	310	0.0844	306	0.0801	302	0.0937	246	0.0577	276	0.0556	263	-	
341	vd-003	0.0199	277	0.0222	241	0.0115	241	0.0130	195	0.0138	186	0.0239	159	0.0177	193	0.0389	224	-	
342	veridas-006	0.0098	198	0.0167	214	0.0079	185	0.0127	187	0.0127	174	0.0217	152	0.0151	171	0.0286	98	-	
343	veridas-007	0.0063	132	0.0083	118	0.0044	103	0.0058	95	0.0080	100	0.0152	98	0.0120	132	0.0284	83	-	
344	verigram-000	0.0032	45	0.0043	46	0.0031	41	0.0034	28	0.0093	130	0.0175	124	0.0164	183	0.0276	26	-	
345	verihubs-inteligensia-000	0.0070	151	0.0098	142	0.0048	115	0.0076	133	0.0092	124	0.0160	109	0.0117	125	0.0283	74	-	
346	via-000	0.0216	279	0.0365	283	0.0177	272	0.0287	271	0.0296	262	0.0572	225	0.0290	246	0.0349	205	0.7638	34
347	via-001	0.0149	247	0.0229	243	0.0114	240	0.0177	233	0.0183	224	0.4056	293	0.0176	191	0.0373	220	-	
348	videmo-000	0.0298	292	0.0423	288	0.0155	269	0.0260	261	0.0246	253	0.0397	214	0.0239	233	0.0541	259	-	
349	videmo-001	0.0295	290	0.0417	287	0.0164	271	0.0261	264	0.0355	269	0.0603	230	0.0442	266	0.1473	310	-	
350	videonetics-001	0.5483	369	0.6446	365	0.7517	365	0.8607	363	0.8664	359	0.8255	328	0.6956	352	0.2986	342	0.7297	30
351	videonetics-002	0.4274	355	0.5329	355	0.6081	353	0.7438	352	0.7775	349	0.7297	319	0.5756	343	0.1976	325	0.7435	32
352	viettelhightech-000	0.0117	217	0.0166	211	0.0110	232	0.0198	245	0.0167	213	0.0249	165	0.0158	176	0.0409	233	-	

Table 23: FNMR is the proportion of mated comparisons below a threshold set to achieve the FMR given in the header on the fourth row. FMR is the proportion of impostor comparisons at or above that threshold. The light grey values give rank over all algorithms in that column. The pink columns use only same-sex impostors; others are selected regardless of demographics. The exception, in the green column, uses "matched-covariates" i.e. impostors of the same sex, age group, and country of birth. The second pink column includes effects of extended ageing. Missing entries for border, visa, mugshot and wild images generally mean the algorithm did not run to completion. For child exploitation, missing entries arise because NIST executes those runs only infrequently. The VISA columns compare images described in section 2.1. The MUGSHOT columns compare images described in section 2.4. The VISA-BORDER column compare images described in section 2.2 with those of section 2.3. The BORDER column compares images described in section 2.3. The WILD columns compare images described in section 2.5. The CHILD-EXPLOITATION columns compare images described in section ??.

	Algorithm	FALSE NON-MATCH RATE (FNMR)										LESS CONSTRAINED, NON-COOP.							
		CONSTRAINED, COOPERATIVE																	
		Name	VISAMC	VISA	MUGSHOT	MUGSHOT12+YRS	VISABORDER	BORDER	BORDER	WILD	CHILDEXP								
	FMR	0.0001	1E-06	1E-05	1E-05	1E-06	1E-06	1E-06	1E-05	0.0001	0.01								
353	vigilantsolutions-010	0.0109	211	0.0164	209	0.0074	177	0.0095	162	0.0209	236	0.0365	207	0.0233	230	0.0277	32	-	
354	vigilantsolutions-011	0.0124	227	0.0176	218	0.0073	173	0.0095	161	0.0196	232	0.0360	206	0.0221	224	0.0274	14	-	
355	vinai-000	0.0081	173	0.0124	174	0.0045	105	0.0072	123	0.0089	117	0.1814	266	0.0112	118	0.0274	17	-	
356	vinbigdata-001	0.2576	341	0.2763	332	0.1404	325	0.1988	322	0.1407	315	0.1150	259	0.0703	285	0.9767	369	-	
357	vion-000	0.0419	300	0.0590	301	0.0422	303	0.0478	289	0.0581	292	0.0968	252	0.0847	293	0.2479	335	0.8765	40
358	visage-000	0.0933	320	0.1441	320	0.1316	324	0.2416	326	0.1395	314	0.1920	270	0.1001	297	0.0500	253	-	
359	visionbox-001	0.0159	255	0.0270	264	0.0111	234	0.0173	231	0.0190	230	0.0315	191	0.0205	217	0.0389	225	-	
360	visionbox-002	0.0058	116	0.0079	110	0.0060	148	0.0074	125	0.0084	108	0.0149	93	0.0113	121	0.0447	244	-	
361	visionlabs-010	0.0017	16	0.0024	12	0.0026	18	0.0030	22	0.0033	11	0.0061	10	0.0052	10	0.0282	67	-	
362	visionlabs-011	0.0012	6	0.0022	9	0.0024	10	0.0026	9	0.0028	3	0.0053	3	0.0046	3	0.0280	52	-	
363	visteam-001	0.4417	360	0.5385	357	0.6410	355	0.7788	354	0.6386	344	0.5904	307	0.4023	334	0.1413	309	-	
364	visteam-002	0.1564	329	0.2789	333	0.1581	330	0.2567	329	0.1776	320	0.2090	275	0.1021	298	0.0349	207	-	
365	vnpt-002	0.0351	297	0.0424	290	0.0220	282	0.0316	275	0.0471	286	0.0817	244	0.0698	284	0.0400	227	-	
366	vnpt-003	0.0117	216	0.0138	185	0.0040	95	0.0058	98	0.0087	113	0.0161	112	0.0126	137	0.0284	79	-	
367	vocord-008	0.0029	41	0.0038	33	0.0042	99	0.0055	85	0.0045	35	0.0086	38	0.0073	48	0.0286	96	-	
368	vocord-009	0.0022	25	0.0029	21	0.0036	69	0.0046	64	0.0052	53	0.0098	53	0.0086	78	0.0284	85	-	
369	vts-000	0.0103	205	0.0174	216	0.0080	187	0.0129	194	0.0250	255	0.0450	216	0.0372	256	0.0596	266	-	
370	winsense-001	0.0062	130	0.0099	147	0.0092	210	0.0210	247	0.0093	129	0.0144	91	0.0098	94	0.0320	177	0.4155	4
371	winsense-002	0.0050	93	0.0073	102	0.0038	78	0.0059	99	0.0064	80	0.0118	76	0.0084	73	0.0307	159	-	
372	wuhantianyu-001	0.0163	257	0.0262	261	0.0281	294	0.0569	298	0.0316	266	0.0486	219	0.0344	250	0.0324	180	-	
373	x-laboratory-000	0.0071	155	0.0106	156	0.0123	246	0.0138	204	0.0419	280	0.5629	305	0.2852	324	0.0295	136	0.9686	48
374	x-laboratory-001	0.0059	121	0.0110	164	0.0054	132	0.0078	137	0.0094	132	0.0142	87	0.0100	97	0.0294	131	-	
375	xforwardai-001	0.0021	23	0.0034	26	0.0027	25	0.0028	15	0.0046	40	0.0088	40	0.0079	60	0.0281	61	-	
376	xforwardai-002	0.0016	14	0.0023	11	0.0026	20	0.0025	6	0.0040	25	0.0081	32	0.0074	49	0.0282	64	-	
377	xm-000	0.0015	12	0.0026	17	0.0031	45	0.0038	44	0.0058	67	0.0105	61	0.0082	70	0.0282	66	-	
378	yisheng-004	0.1988	332	0.3329	336	0.1147	322	0.1849	320	0.2044	324	-	-	-	0.0908	289	0.7152	29	
379	yitu-003	0.0015	13	0.0026	16	0.0066	162	0.0085	150	0.0064	81	0.0114	72	0.0103	104	0.0325	183	-	
380	yoonik-002	0.0052	101	0.0062	83	0.0029	32	0.0034	29	0.0615	296	0.1279	262	0.1166	299	0.0549	261	-	
381	yoonik-003	0.0034	54	0.0047	53	0.0032	52	0.0037	38	0.0816	304	0.2033	274	0.1601	311	0.0699	277	-	
382	ytu-000	0.0057	114	0.0087	122	0.0121	244	0.0238	257	0.0047	42	0.0078	27	0.0059	20	0.0286	97	-	
383	yuan-002	0.0094	192	0.0154	204	0.0071	171	0.0110	175	0.0108	156	0.0348	203	0.0127	140	0.0319	176	-	
384	yuan-003	0.0078	167	0.0111	165	0.0062	151	0.0091	158	0.0106	150	0.0511	221	0.0123	134	0.0320	178	-	

Table 24: FNMR is the proportion of mated comparisons below a threshold set to achieve the FMR given in the header on the fourth row. FMR is the proportion of impostor comparisons at or above that threshold. The light grey values give rank over all algorithms in that column. The pink columns use only same-sex impostors; others are selected regardless of demographics. The exception, in the green column, uses “matched-covariates” i.e. impostors of the same sex, age group, and country of birth. The second pink column includes effects of extended ageing. Missing entries for border, visa, mugshot and wild images generally mean the algorithm did not run to completion. For child exploitation, missing entries arise because NIST executes those runs only infrequently. The VISA columns compare images described in section 2.1. The MUGSHOT columns compare images described in section 2.4. The VISA-BORDER column compare images described in section 2.2 with those of section 2.3. The BORDER column compares images described in section 2.3. The WILD columns compare images described in section 2.5. The CHILD-EXPLOITATION columns compare images described in section ??.

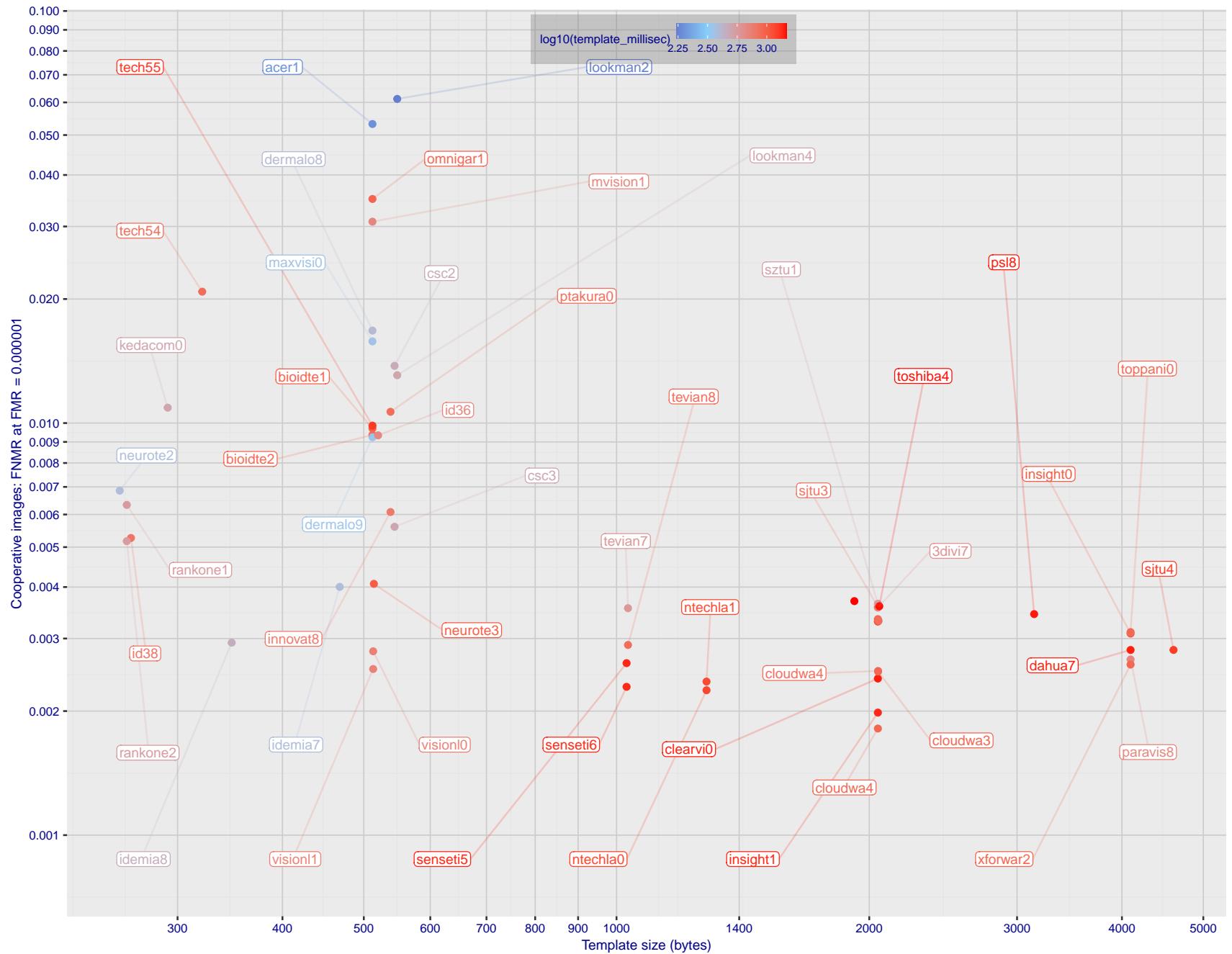


Figure 1: The points show false non-match rates (FNMR) versus the size of the encoded template. FNMR is the geometric mean of FNMR values for visa and mugshot images (from Figs. 58 and 77) at the false match rate (FMR) given in the y-axis label. The color of the points encodes template generation time - which spans at least one order of magnitude. Durations are measured on a single core of a c. 2016 Intel Xeon CPU E5-2630 v4 running at 2.20GHz. Algorithms with poor FNMR are omitted.

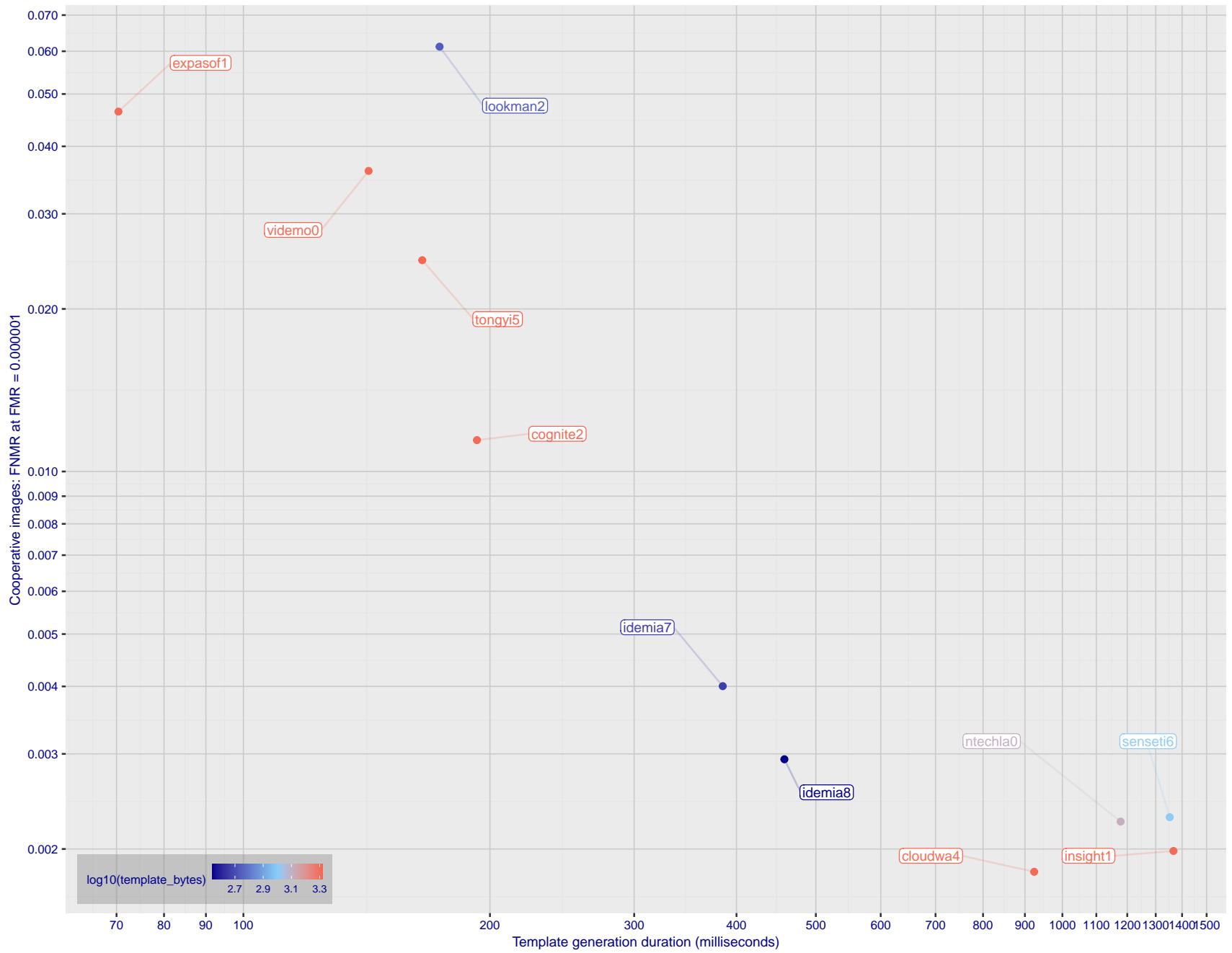


Figure 2: The points show false non-match rates (FNMR) versus the duration of the template generation operation. FNMR is the geometric mean of FNMR values for visa and mugshot images (from Figs. 58 and 77) at a false match rate (FMR) given in the y-axis label. Template generation time is a median estimated over 640 x 480 pixel portraits. It is measured on a single core of a c. 2016 Intel Xeon CPU E5-2630 v4 running at 2.20GHz. The color of the points encodes template size - which span two orders of magnitude. Algorithms with poor FNMR are omitted.

# 1 Metrics

## 1.1 Core accuracy

Given a vector of N genuine scores,  $u$ , the false non-match rate (FNMR) is computed as the proportion below some threshold, T:

$$\text{FNMR}(T) = 1 - \frac{1}{N} \sum_{i=1}^N H(u_i - T) \quad (1)$$

where  $H(x)$  is the unit step function, and  $H(0)$  taken to be 1.

Similarly, given a vector of N impostor scores,  $v$ , the false match rate (FMR) is computed as the proportion above T:

$$\text{FMR}(T) = \frac{1}{N} \sum_{i=1}^N H(v_i - T) \quad (2)$$

The threshold, T, can take on any value. We typically generate a set of thresholds from quantiles of the observed impostor scores,  $v$ , as follows. Given some interesting false match rate range,  $[\text{FMR}_L, \text{FMR}_U]$ , we form a vector of K thresholds corresponding to FMR measurements evenly spaced on a logarithmic scale

$$T_k = Q_v(1 - \text{FMR}_k) \quad (3)$$

where  $Q$  is the quantile function, and  $\text{FMR}_k$  comes from

$$\log_{10} \text{FMR}_k = \log_{10} \text{FMR}_L + \frac{k}{K} [\log_{10} \text{FMR}_U - \log_{10} \text{FMR}_L] \quad (4)$$

Error tradeoff characteristics are plots of FNMR(T) vs. FMR(T). These are plotted with  $\text{FMR}_U \rightarrow 1$  and  $\text{FMR}_L$  as low as is sustained by the number of impostor comparisons, N. This is somewhat higher than the “rule of three” limit  $3/N$  because samples are not independent, due to re-use of images.

## 2 Datasets

### 2.1 Visa images

- ▷ The number of images is on the order of  $10^5$ .
- ▷ The number of subjects is on the order of  $10^5$ .
- ▷ The number of subjects with two images is on the order of  $10^4$ .
- ▷ The images have geometry in reasonable conformance with the ISO/IEC 19794-5 Full Frontal image type. Pose is generally excellent.
- ▷ The images are of size 252x300 pixels. The mean interocular distance (IOD) is 69 pixels.
- ▷ The images are of subjects from greater than 100 countries, with significant imbalance due to visa issuance patterns.
- ▷ The images are of subjects of all ages, including children, again with imbalance due to visa issuance demand.
- ▷ Many of the images are live capture. A substantial number of the images are photographs of paper photographs.
- ▷ When these images are input to the algorithm, they are labelled as being of type "ISO" - see Table 4 of the FRVT API.

### 2.2 Application images

- ▷ The number of images is on the order of  $10^6$ .
- ▷ The number of subjects is on the order of  $10^6$ .
- ▷ The number of subjects with two images is on the order of  $10^6$ .
- ▷ The images have geometry in good conformance with the ISO/IEC 19794-5 Full Frontal image type. Pose is generally excellent.
- ▷ The images are of size 300x300 pixels. The mean interocular distance (IOD) is 61 pixels.
- ▷ The images are of subjects from greater than 100 countries, with significant imbalance due to population and immigration patterns.
- ▷ The images are of subjects of adults with imbalance due to population and immigration patterns and demand.
- ▷ All of the images are live capture.
- ▷ When these images are input to the algorithm, they are labelled as being of type "ISO" - see Table 4 of the FRVT API.

### 2.3 Border crossing images

- ▷ The number of images is on the order of  $10^6$ .
- ▷ The number of subjects is on the order of  $10^6$ .
- ▷ The number of subjects with two images is on the order of  $10^6$ .
- ▷ The images are taken with a camera oriented by an attendant toward a cooperating subject. This is done under time constraints so there are roll, pitch and yaw angle variations. Also background illumination is sometimes strong, so the face is under-exposed. There is some perspective distortion due to close range images. Some faces are partially cropped.
- ▷ The images are of subjects from greater than 100 countries, with significant imbalance due to population and immigration patterns.
- ▷ The images are of subjects of adults with imbalance due to population and immigration patterns and demand.

- ▷ The images have mean IOD of 38 pixels.
- ▷ The images are all live capture.
- ▷ When these images are input to the algorithm, they are labelled as being of type "WILD" - see Table 4 of the FRVT API.

## 2.4 Mugshot images

- ▷ The number of images is on the order of  $10^6$ .
- ▷ The number of subjects is on the order of  $10^6$ .
- ▷ The number of subjects with two images is on the order of  $10^6$ .
- ▷ The images have geometry in reasonable conformance with the ISO/IEC 19794-5 Full Frontal image type.
- ▷ The images are of variable sizes. The median IOD is 105 pixels. The mean IOD is 113 pixels. The 1-st, 5-th, 10-th, 25-th, 75-th, 90-th and 99-th percentiles are 34, 58, 70, 87, 121, 161 and 297 pixels.
- ▷ The images are of subjects from the United States.
- ▷ The images are of adults.
- ▷ The images are all live capture.
- ▷ When these images are input to the algorithm, they are labelled as being of type "mugshot" - see Table 4 of the FRVT API.

## 2.5 Wild images

- ▷ The number of images is on the order of  $10^5$ .
- ▷ The number of subjects is on the order of  $10^3$ .
- ▷ The number of subjects with two images on the order of  $10^3$ .
- ▷ The images include many photojournalism-style images. Images are given to the algorithm using a variable but generally tight crop of the head. Resolution varies very widely. The images are very unconstrained, with wide yaw and pitch pose variation. Faces can be occluded, including hair and hands.
- ▷ The images are of adults.
- ▷ All of the images are live capture, none are scanned.
- ▷ When these images are input to the algorithm, they are labelled as being of type "WILD" - see Table 4 of the FRVT API.

## 3 Results

### 3.1 Test goals

- ▷ To state absolute accuracy for different kinds of images, including those with and without subject cooperation.
- ▷ To state comparative accuracy, across algorithms.

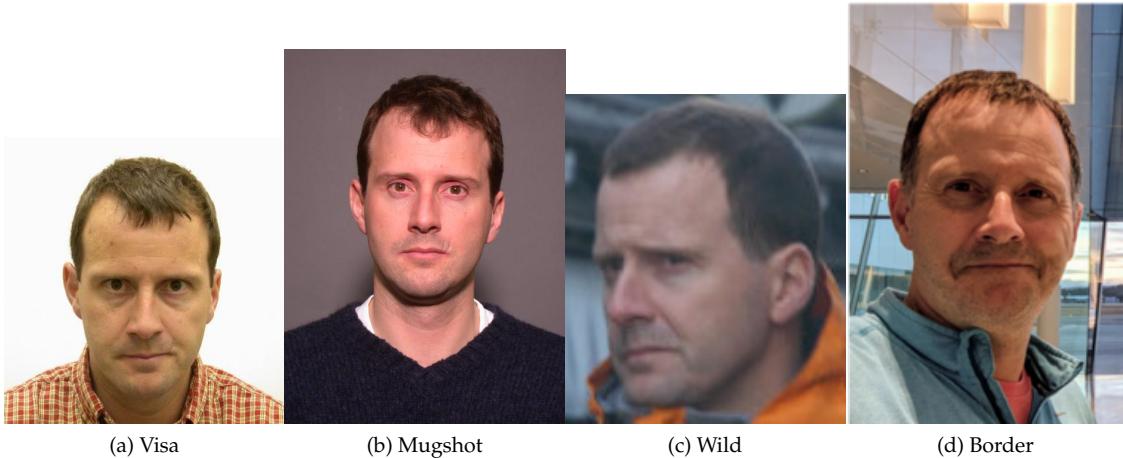


*Figure 3: The figure gives simulated samples of image types used in this report.*

### 3.2 Test design

**Method:** For visa images:

- ▷ The comparisons are of visa photos against visa photos.
- ▷ The number of genuine comparisons is on the order of  $10^4$ .
- ▷ The number of impostor comparisons is on the order of  $10^{10}$ .
- ▷ The comparisons are fully zero-effort, meaning impostors are paired without attention to sex, age or other covariates. However, later analysis is conducted on subsets.
- ▷ The number of persons is on the order of  $10^5$ .
- ▷ The number of images used to make 1 template is 1.
- ▷ The number of templates used to make each comparison score is two corresponding to simple one-to-one verification.

**Method:** For mugshot images:

- ▷ The comparisons are of mugshot photos against mugshot photos.
- ▷ The number of genuine comparisons is on the order of  $10^6$ .
- ▷ The number of impostor comparisons is on the order of  $10^8$ .
- ▷ The impostors are paired by sex, but not by age or other covariates.
- ▷ The number of persons is on the order of  $10^6$ .
- ▷ The number of images used to make 1 template is 1.
- ▷ The number of templates used to make each comparison score is two corresponding to simple one-to-one verification.

**Method:** For visa-border comparisons:

- ▷ The comparisons are of visa-like frontals against border crossing webcam photos.
- ▷ The number of genuine comparisons is on the order of  $10^6$ .
- ▷ The number of impostor comparisons is on the order of  $10^8$ .

- ▷ The impostors are paired by sex, but not by age or other covariates.
- ▷ The number of persons is on the order of  $10^6$ .
- ▷ The number of images used to make 1 template is 1.
- ▷ The number of templates used to make each comparison score is two corresponding to simple one-to-one verification.

**Method:** For border-border comparisons:

- ▷ The comparisons are of border crossing webcam photos.
- ▷ The number of genuine comparisons is on the order of  $10^6$ .
- ▷ The number of impostor comparisons is on the order of  $10^8$ .
- ▷ The impostors are paired by sex, but not by age or other covariates.
- ▷ The number of persons is on the order of  $10^6$ .
- ▷ The number of images used to make 1 template is 1.
- ▷ The number of templates used to make each comparison score is two corresponding to simple one-to-one verification.

**Method:** For wild images:

- ▷ The comparisons are of wild photos against wild photos.
- ▷ The number of genuine comparisons is on the order of  $10^6$ .
- ▷ The number of impostor comparisons is on the order of  $10^7$ .
- ▷ The comparisons are fully zero-effort, meaning impostors are paired without attention to sex, age or other covariates.
- ▷ The number of persons is on the order of  $10^4$ .
- ▷ The number of images used to make 1 template is 1.
- ▷ The number of templates used to make each comparison score is two corresponding to simple one-to-one verification.

**Method:** For child exploitation images:

- ▷ The comparisons are of unconstrained child exploitation photos against others of the same type.
- ▷ The number of genuine comparisons is on the order of  $10^4$ .
- ▷ The number of impostor comparisons is on the order of  $10^7$ .
- ▷ The comparisons are fully zero-effort, meaning impostors are paired without attention to sex, age or other covariates.
- ▷ The number of persons is on the order of  $10^3$ .
- ▷ The number of images used to make 1 template is 1.
- ▷ The number of templates used to make each comparison score is two corresponding to simple one-to-one verification.
- ▷ We produce two performance statements. First, is a DET as used for visa and mugshot images. The second is a cumulative match characteristic (CMC) summarizing a simulated one-to-many search process. This is done as follows.
  - We regard  $M$  enrollment templates as items in a gallery.

- These  $M$  templates come from  $M > N$  individuals, because multiple images of a subject are present in the gallery under separate identifiers.
- We regard the verification templates as search templates.
- For each search we compute the rank of the highest scoring mate.
- This process should properly be conducted with a 1:N algorithm, such as those tested in NIST IR 8009. We use the 1:1 algorithms in a simulated 1:N mode here to a) better reflect what a child exploitation analyst does, and b) to show algorithm efficacy is better than that revealed in the verification DETs.

### 3.3 Failure to enroll

	Algorithm Name	Failure to Enrol Rate <sup>1</sup>											
		APPLICATION	BORDER	CHILD-EXPLOIT	MUGSHOT	VISA	WILD	SEC. 2.2	SEC. 2.3	SEC. ??	SEC. 2.4	SEC. 2.1	SEC. 2.5
1	20face-000	0.0000	229	0.0008	196	-	286	0.0000	116	0.0004	207	0.0004	164
2	20face-001	0.0000	208	0.0008	195	-	67	0.0000	120	0.0004	209	0.0004	162
3	3divi-006	0.0000	219	0.0007	173	-	343	0.0001	202	0.0002	122	0.0005	205
4	3divi-007	0.0000	205	0.0007	171	-	50	0.0001	204	0.0002	124	0.0005	203
5	acer-001	0.0000	176	0.0011	237	-	158	0.0001	182	0.0004	228	0.0004	172
6	acer-002	0.0000	313	0.0008	190	-	350	0.0003	268	0.0004	224	0.0011	254
7	acisw-003	0.0000	56	0.0000	1	-	124	0.0000	88	0.0000	85	0.0001	110
8	acisw-007	0.0000	123	0.0000	65	-	291	0.0000	24	0.0000	29	0.0000	50
9	adera-002	0.0000	295	0.0034	308	-	105	0.0003	276	0.0005	315	0.0505	347
10	adera-003	0.0000	294	0.0034	309	-	178	0.0003	275	0.0005	312	0.0505	348
11	advance-002	0.0000	227	0.0013	258	-	287	0.0000	166	0.0004	225	0.0009	244
12	advance-003	0.0000	284	0.0012	247	-	298	0.0001	219	0.0004	263	0.0011	250
13	aifirst-001	0.0000	161	0.0000	66	0.0000	13	0.0000	49	0.0000	49	0.0000	88
14	aigen-001	0.0000	97	0.0000	84	-	356	0.0000	6	0.0000	7	0.0000	76
15	aigen-002	0.0000	108	0.0000	99	-	338	0.0000	15	0.0000	16	0.0000	80
16	ailabs-001	0.0000	179	0.0090	347	-	163	0.0007	324	0.0005	287	0.0016	267
17	aimall-002	0.0000	296	0.0043	321	-	167	0.0012	339	0.0005	307	0.0005	214
18	aimall-003	0.0000	278	0.0012	252	-	227	0.0004	290	0.0005	281	0.0004	185
19	aiunionface-000	0.0000	47	0.0000	9	-	107	0.0000	80	0.0000	82	0.0000	91
20	aize-001	0.0001	338	0.0040	316	-	352	0.0026	359	0.0022	362	0.0058	295
21	aize-002	0.0000	137	0.0014	262	-	274	0.0005	311	0.0004	208	0.0071	302
22	ajou-001	0.0000	226	0.0020	283	-	319	0.0001	205	0.0004	269	0.0045	289
23	alchera-002	0.0000	192	0.0008	201	-	140	0.0001	226	0.0004	183	0.0003	150
24	alchera-003	0.0001	349	0.0013	256	-	366	0.0002	253	0.0004	233	0.0036	283
25	alfabeta-001	0.0005	358	0.0650	377	-	101	0.0024	354	0.0018	358	0.1071	366
26	alice-000	0.0000	159	0.0006	150	-	235	0.0000	128	0.0004	180	0.0004	186
27	alleyes-000	0.0000	213	0.0010	222	-	362	0.0002	232	0.0004	244	0.0004	192
28	allgovision-000	0.0007	362	0.0062	339	-	161	0.0026	358	0.0052	375	0.0131	316
29	alphaface-001	0.0000	180	0.0012	243	-	172	0.0000	170	0.0004	248	0.0004	168
30	alphaface-002	0.0000	241	0.0012	244	-	234	0.0000	168	0.0004	247	0.0004	170
31	amplifiedgroup-001	0.0114	376	0.1023	379	-	215	0.0189	378	0.0279	383	0.1390	375
32	androvideo-000	0.0000	122	0.0000	64	-	290	0.0000	23	0.0000	28	0.0002	114
33	anke-004	0.0000	236	0.0011	234	0.0944	29	0.0001	211	0.0004	250	0.0006	226
34	anke-005	0.0000	195	0.0012	245	0.1228	31	0.0001	222	0.0004	261	0.0007	229
35	antheus-000	0.0000	60	0.0000	27	0.0000	2	0.0000	91	0.0000	96	0.0242	330
36	antheus-001	0.0000	14	0.0000	35	-	192	0.0000	59	0.0000	57	0.0242	331
37	anyvision-004	0.0000	281	0.0017	273	0.1660	34	0.0001	223	0.0004	221	0.0080	305
38	anyvision-005	0.0000	234	0.0013	253	-	265	0.0000	146	0.0004	179	0.0004	188
39	armatura-001	0.0000	304	0.0021	286	-	62	0.0005	305	0.0005	294	0.0357	343
40	asusaics-000	0.0000	25	0.0000	33	-	198	0.0000	62	0.0000	60	0.0000	37
41	asusaics-001	0.0000	142	0.0000	78	-	244	0.0000	34	0.0000	39	0.0000	58
42	authenmetric-003	0.0000	43	0.0000	12	-	131	0.0000	76	0.0000	74	0.0000	3
43	authenmetric-004	0.0000	36	0.0000	48	-	141	0.0000	69	0.0000	70	0.0000	46
44	aware-005	0.0000	266	0.0020	281	-	279	0.0001	231	0.0004	251	0.0011	247
45	aware-006	0.0000	232	0.0009	209	-	306	0.0000	147	0.0004	214	0.0006	223
46	awiroes-001	0.0039	367	0.0369	371	-	371	0.0386	379	0.0872	384	0.3415	379
47	awiroes-002	0.0000	314	0.0038	314	-	174	0.0007	323	0.0012	350	0.0208	326
48	ayftech-001	0.0002	351	0.0046	327	-	289	0.0043	369	0.0011	339	0.0091	309
49	ayonix-000	0.0053	370	0.0341	368	0.0000	19	0.0113	376	0.0137	379	0.1194	370
50	beethedata-000	0.0005	357	0.0042	320	-	219	0.0002	239	0.0010	334	0.0006	218
51	beyneai-000	0.0000	89	0.0000	91	-	376	0.0000	1	0.0000	1	0.0000	71
52	biocube-001	0.0006	360	0.0391	372	-	90	0.0015	344	0.0020	361	0.0253	335
53	bioidechtechswiss-001	0.0000	239	0.0007	167	-	261	0.0000	134	0.0004	240	0.0025	278
54	bioidechtechswiss-002	0.0000	178	0.0007	170	-	164	0.0000	142	0.0004	234	0.0005	215
55	bm-001	0.0000	24	0.0000	32	0.0000	10	0.0000	109	0.0000	59	0.0000	38
56	boetech-001	0.0087	374	0.0272	361	-	355	0.0032	365	0.0160	380	0.0946	363
57	boetech-002	0.0087	373	0.0272	360	-	143	0.0032	366	0.0160	381	0.0946	362
58	bresee-001	0.0000	187	0.0010	227	-	153	0.0002	240	0.0003	153	0.0003	125

Table 25: FTE is the proportion of failed template generation attempts. Failures can occur because the software throws an exception, or because the software electively refuses to process the input image. This would typically occur if a face is not detected. FTE is measured as the number of function calls that give EITHER a non-zero error code OR that give a “small” template. This is defined as one whose size is less than 0.3 times the median template size for that algorithm. This second rule is needed because some algorithms incorrectly fail to return a non-zero error code when template generation fails.

<sup>1</sup>The effects of FTE are included in the accuracy results of this report by regarding any template comparison involving a failed template to produce a low similarity score. Thus higher FTE results in higher FNMR and lower FMR.

	Algorithm	Failure to Enrol Rate <sup>1</sup>						
		APPLICATION	BORDER	CHILD-EXPLOIT	MUGSHOT	VISA	WILD	
Name	SEC. 2.2	SEC. 2.3	SEC. ??	SEC. 2.4	SEC. 2.1	SEC. 2.5		
59 bressee-002	0.0000	287	0.0020	284	- 146	0.0008 325	0.0004 199	0.0031 282
60 camvi-002	0.0000	129	0.0000	61	0.0000 17	0.0000 27	0.0000 31	0.0000 53
61 camvi-004	0.0000	44	0.0000	105	0.0000 5	0.0000 79	0.0000 79	0.0000 7
62 canon-002	0.0000	58	0.0000	3	- 122	0.0000 87	0.0000 83	0.0000 12
63 canon-003	0.0000	204	0.0008	185	- 54	0.0000 165	0.0004 232	0.0003 152
64 ceiec-003	0.0000	73	0.0013	259	- 92	0.0001 189	0.0004 243	0.0004 161
65 ceiec-004	0.0000	64	0.0008	194	- 87	0.0000 145	0.0004 188	0.0004 191
66 chosun-001	0.0000	74	0.0000	20	- 102	0.0000 98	0.0000 97	0.0000 21
67 chosun-002	0.0000	4	0.0000	43	- 202	0.0000 51	0.0000 51	0.0000 28
68 chtface-003	0.0000	289	0.0018	276	- 318	0.0001 193	0.0006 319	0.0010 245
69 chtface-004	0.0000	115	0.0017	270	- 310	0.0000 154	0.0004 245	0.0020 274
70 clearviewwai-000	0.0000	207	0.0003	128	- 59	0.0000 158	0.0003 140	0.0003 124
71 closeli-001	0.0000	61	0.0000	28	- 75	0.0000 89	0.0000 95	0.0001 111
72 cloudmatrix-000	0.0000	257	0.0012	248	- 382	0.0001 183	0.0004 173	0.0004 181
73 cloudwalk-hr-003	0.0000	168	0.0008	197	- 225	0.0001 192	0.0004 182	0.0113 312
74 cloudwalk-hr-004	0.0000	233	0.0011	241	- 302	0.0004 292	0.0003 162	0.0129 315
75 cloudwalk-mt-003	0.0000	196	0.0007	162	- 82	0.0002 248	0.0004 256	0.0004 165
76 cloudwalk-mt-004	0.0000	167	0.0009	202	- 221	0.0002 256	0.0004 265	0.0004 178
77 clova-000	0.0000	305	0.0022	287	- 111	0.0006 318	0.0005 283	0.0019 270
78 cogent-005	0.0000	106	0.0000	100	- 328	0.0000 13	0.0000 17	0.0000 79
79 cogent-006	0.0000	30	0.0000	51	- 165	0.0000 65	0.0000 64	0.0000 43
80 cognitec-002	0.0001	333	0.0069	341	- 120	0.0003 285	0.0005 290	0.0050 293
81 cognitec-003	0.0001	334	0.0194	356	- 200	0.0003 282	0.0005 292	0.0039 285
82 cor-001	0.0000	224	0.0006	154	- 314	0.0002 262	0.0004 212	0.0004 201
83 coretech-000	0.0000	107	0.0000	98	- 337	0.0000 14	0.0000 15	0.0000 81
84 corsight-001	0.0000	199	0.0006	159	- 78	0.0001 228	0.0004 200	0.0004 180
85 corsight-002	0.0000	235	0.0005	148	- 264	0.0001 212	0.0004 203	0.0003 153
86 csc-002	0.0015	365	0.0033	305	- 323	0.0006 319	0.0006 324	0.0968 365
87 csc-003	0.0015	364	0.0033	304	- 223	0.0006 320	0.0006 325	0.0968 364
88 ctcbank-000	0.0001	336	0.0051	332	0.3285 41	0.0011 337	0.0019 359	0.0868 359
89 ctcbank-001	0.0000	315	0.0036	313	- 266	0.0005 308	0.0010 332	0.0844 356
90 cubox-001	0.0000	113	0.0000	95	- 309	0.0000 18	0.0000 23	0.0000 84
91 cubox-002	0.0000	262	0.0006	157	- 294	0.0002 263	0.0005 310	0.0016 266
92 cudocommunication-001	0.0000	49	0.0000	7	- 113	0.0000 82	0.0000 81	0.0000 90
93 cuhkee-001	0.0000	216	0.0011	240	- 329	0.0000 115	0.0004 201	0.1278 372
94 cybercore-000	0.0000	170	0.0073	344	- 190	0.0001 200	0.0005 289	0.0383 344
95 cybercore-001	0.0000	299	0.0001	116	- 351	0.0002 235	0.0002 118	0.0018 269
96 cyberextruder-001	0.0029	366	0.0293	362	0.5338 47	0.0024 352	0.0029 372	0.0597 352
97 cyberextruder-002	0.0013	363	0.0840	378	0.2672 40	0.0027 360	0.0028 369	0.0335 341
98 cyberlink-007	0.0000	42	0.0003	122	- 132	0.0000 113	0.0003 154	0.0001 96
99 cyberlink-008	0.0000	140	0.0004	138	- 281	0.0000 111	0.0003 152	0.0002 123
100 dahua-006	0.0000	69	0.0000	102	- 85	0.0000 163	0.0003 164	0.0000 15
101 dahua-007	0.0000	45	0.0000	101	- 136	0.0000 161	0.0003 163	0.0000 6
102 daon-000	0.0000	319	0.0028	296	- 195	0.0014 343	0.0015 354	0.0030 281
103 decatur-000	0.0000	259	0.0020	280	- 331	0.0004 298	0.0005 280	0.0236 329
104 decatur-001	0.0000	238	0.0009	214	- 275	0.0001 196	0.0004 197	0.0004 194
105 deepglint-003	0.0000	228	0.0004	139	- 288	0.0002 255	0.0004 190	0.0003 140
106 deepglint-004	0.0000	242	0.0005	143	- 239	0.0002 259	0.0004 185	0.0003 142
107 deepsea-001	0.0000	70	0.0000	22	0.0000 4	0.0000 97	0.0000 98	0.0000 20
108 deepsense-000	0.0000	135	0.0006	160	- 278	0.0000 127	0.0004 167	0.0003 145
109 dermalog-008	0.0000	310	0.0031	302	- 384	0.0006 313	0.0003 128	0.0002 113
110 dermalog-009	0.0000	307	0.0031	301	- 205	0.0006 315	0.0003 131	0.0002 112
111 didiglobalface-001	0.0000	206	0.0012	242	0.2175 36	0.0000 172	0.0004 249	0.0004 166
112 digitalbarriers-002	0.0001	341	0.0045	324	- 272	0.0028 362	0.0027 366	0.0071 301
113 dps-000	0.0000	112	0.0000	96	- 348	0.0000 17	0.0000 18	0.0000 83
114 dsk-000	0.0000	126	0.0000	62	0.0000 16	0.0000 25	0.0000 27	0.0000 52
115 einetworks-000	0.0000	316	0.0017	272	- 273	0.0002 250	0.0005 304	0.0008 241
116 ekin-002	0.0000	22	0.0000	107	- 196	0.0000 112	0.0000 108	0.0019 271

Table 26: FTE is the proportion of failed template generation attempts. Failures can occur because the software throws an exception, or because the software electively refuses to process the input image. This would typically occur if a face is not detected. FTE is measured as the number of function calls that give EITHER a non-zero error code OR that give a “small” template. This is defined as one whose size is less than 0.3 times the median template size for that algorithm. This second rule is needed because some algorithms incorrectly fail to return a non-zero error code when template generation fails.

<sup>1</sup> The effects of FTE are included in the accuracy results of this report by regarding any template comparison involving a failed template to produce a low similarity score. Thus higher FTE results in higher FNMR and lower FMR.

	Algorithm	Failure to Enrol Rate <sup>1</sup>						
		APPLICATION	BORDER	CHILD-EXPLOIT	MUGSHOT	VISA	WILD	
Name	SEC. 2.2	SEC. 2.3	SEC. ??	SEC. 2.4	SEC. 2.1	SEC. 2.5		
117	enface-000	0.0000	86	0.0012	251	-	69	0.0000
118	enface-001	0.0000	1	0.0012	250	-	210	0.0000
119	eocortex-000	0.0095	375	0.0602	375	-	106	0.0094
120	ercacat-001	0.0000	6	0.0005	144	-	212	0.0000
121	euronovate-001	0.0255	380	0.0102	349	-	271	0.0021
122	expasoft-001	0.0000	15	0.0000	37	-	185	0.0000
123	expasoft-002	0.0000	27	0.0000	53	-	157	0.0000
124	f8-001	0.0003	354	0.0059	338	0.2026	35	0.0035
125	faceonline-001	0.0000	325	0.0029	299	-	123	0.0013
126	facesoft-000	0.0000	80	0.0000	18	0.0000	1	0.0000
127	facetag-000	0.0000	79	0.0000	17	-	61	0.0000
128	facetag-002	0.0000	50	0.0000	8	-	108	0.0000
129	facex-001	0.0001	347	0.0360	369	-	209	0.0047
130	facex-002	0.0001	348	0.0360	370	-	320	0.0047
131	farfaces-001	0.0000	312	0.0007	169	-	137	0.0003
132	fiberhome-nanjing-003	0.0000	143	0.0004	136	-	247	0.0000
133	fiberhome-nanjing-004	0.0000	144	0.0004	137	-	249	0.0000
134	fincore-000	0.0000	189	0.0008	198	-	127	0.0001
135	fujitsulab-002	0.0000	88	0.0009	207	-	374	0.0001
136	fujitsulab-003	0.0000	19	0.0008	188	-	189	0.0001
137	geo-002	0.0000	209	0.0015	263	-	68	0.0001
138	geo-003	0.0000	200	0.0010	221	-	94	0.0000
139	glory-002	0.0003	352	0.0045	323	-	76	0.0015
140	glory-003	0.0000	276	0.0027	293	-	312	0.0004
141	gorilla-007	0.0000	185	0.0009	218	-	151	0.0001
142	gorilla-008	0.0000	214	0.0009	219	-	369	0.0001
143	griaule-000	0.0000	322	0.0026	291	-	104	0.0004
144	hertasecurity-000	0.0133	377	0.0077	346	-	139	0.0025
145	hik-001	0.0000	77	0.0000	109	-	58	0.0000
146	hisign-001	0.0000	153	0.0000	72	-	258	0.0000
147	hyperverge-001	0.0000	330	0.0072	342	-	297	0.0015
148	hyperverge-002	0.0000	94	0.0008	187	-	378	0.0002
149	icm-002	0.0000	125	0.0001	113	-	285	0.0000
150	icm-003	0.0000	76	0.0001	112	-	57	0.0000
151	icthtc-000	0.0001	346	0.0047	330	-	181	0.0028
152	id3-006	0.0000	271	0.0009	217	-	100	0.0004
153	id3-008	0.0000	87	0.0006	158	-	373	0.0001
154	idemia-007	0.0000	124	0.0004	140	-	284	0.0000
155	idemia-008	0.0000	154	0.0004	141	-	259	0.0000
156	iit-002	0.0000	320	0.0021	285	-	168	0.0009
157	iit-003	0.0000	173	0.0008	199	-	197	0.0000
158	imagus-002	0.0000	269	0.0018	274	-	110	0.0000
159	imagus-004	0.0000	145	0.0000	75	-	250	0.0000
160	imperial-000	0.0000	32	0.0000	50	-	173	0.0000
161	imperial-002	0.0000	38	0.0000	45	0.0000	6	0.0000
162	incode-009	0.0000	251	0.0009	210	-	154	0.0002
163	incode-010	0.0000	260	0.0009	211	-	336	0.0002
164	innefulabs-000	0.0000	217	0.0024	288	-	333	0.0003
165	innovativetechnologyltd-001	0.0001	345	0.0050	331	-	191	0.0024
166	innovativetechnologyltd-002	0.0000	272	0.0046	325	-	65	0.0057
167	innovatrics-007	0.0000	163	0.0007	178	-	206	0.0001
168	innovatrics-008	0.0000	211	0.0009	213	-	353	0.0000
169	insightface-000	0.0000	155	0.0000	68	-	229	0.0000
170	insightface-001	0.0000	102	0.0000	83	-	360	0.0000
171	intellicloudai-001	0.0000	104	0.0000	79	-	367	0.0000
172	intellicloudai-002	0.0000	117	0.0008	191	-	317	0.0000
173	intellifusion-001	0.0000	212	0.0005	146	0.0949	30	0.0001
174	intellifusion-002	0.0000	62	0.0000	106	-	74	0.0000

Table 27: FTE is the proportion of failed template generation attempts. Failures can occur because the software throws an exception, or because the software electively refuses to process the input image. This would typically occur if a face is not detected. FTE is measured as the number of function calls that give EITHER a non-zero error code OR that give a “small” template. This is defined as one whose size is less than 0.3 times the median template size for that algorithm. This second rule is needed because some algorithms incorrectly fail to return a non-zero error code when template generation fails.

<sup>1</sup>The effects of FTE are included in the accuracy results of this report by regarding any template comparison involving a failed template to produce a low similarity score. Thus higher FTE results in higher FNMR and lower FMR.

	Algorithm	Failure to Enrol Rate <sup>1</sup>											
		APPLICATION	BORDER	CHILD-EXPLOIT	MUGSHOT	VISA	WILD	SEC. 2.2	SEC. 2.3	SEC. ??	SEC. 2.4	SEC. 2.1	SEC. 2.5
175	intellivision-001	0.0042	368	0.0296	363	0.5495	48	0.0048	373	0.0042	374	0.1358	373
176	intellivision-002	0.0000	331	0.0046	326	-	361	0.0012	338	0.0005	317	0.0146	318
177	intelresearch-003	0.0000	182	0.0006	152	-	176	0.0000	131	0.0004	187	0.0003	154
178	intelresearch-004	0.0000	169	0.0006	153	-	180	0.0000	129	0.0004	186	0.0003	144
179	intsysmsu-001	0.0000	82	0.0010	224	-	70	0.0001	208	0.0004	222	0.0004	189
180	intsysmsu-002	0.0000	148	0.0010	226	-	253	0.0001	206	0.0004	216	0.0004	190
181	ionetworks-000	0.0000	33	0.0016	268	-	171	0.0004	288	0.0005	288	0.0004	193
182	iqface-000	0.0000	20	0.0000	34	0.0000	8	0.0000	60	0.0000	62	0.0000	36
183	iqface-003	0.0000	317	0.0076	345	-	324	0.0006	314	0.0005	316	0.0069	299
184	irex-000	0.0000	280	0.0009	216	-	73	0.0000	157	0.0005	282	0.0003	151
185	isap-001	0.0000	52	0.0000	5	-	118	0.0000	85	0.0000	87	0.0000	10
186	isap-002	0.0000	68	0.0000	26	-	84	0.0000	92	0.0000	89	0.0000	16
187	isityou-000	0.0068	372	0.0316	366	0.4714	44	0.0023	351	0.0010	336	0.0663	353
188	isystems-001	0.0000	324	0.0035	311	0.1421	33	0.0010	334	0.0007	326	0.0128	314
189	isystems-002	0.0000	323	0.0035	310	0.1421	32	0.0010	335	0.0007	327	0.0128	313
190	itmo-007	0.0000	114	0.0009	206	-	315	0.0003	286	0.0000	22	0.0004	174
191	itmo-008	0.0000	103	0.0135	353	-	370	0.0024	355	0.0000	11	0.0836	355
192	ivacognitive-001	0.0000	250	0.0011	236	-	145	0.0001	185	0.0004	260	0.0011	248
193	iws-000	0.0005	359	0.0650	376	-	56	0.0024	353	0.0012	346	0.0936	361
194	kakao-005	0.0000	11	0.0000	103	-	224	0.0000	53	0.0000	109	0.0000	31
195	kakapay-001	0.0000	264	0.0013	257	-	269	0.0001	187	0.0004	264	0.0078	304
196	kedacom-000	0.0000	101	0.0000	82	0.0000	20	0.0000	9	0.0000	12	0.0000	78
197	kiwitech-000	0.0000	230	0.0009	203	-	295	0.0004	295	0.0005	284	0.0004	199
198	kneron-003	0.0239	378	0.0306	364	0.4883	46	0.0044	370	0.0016	357	0.1823	377
199	kneron-005	0.0000	326	0.0226	357	-	179	0.0006	312	0.0005	296	0.0097	310
200	kookmin-002	0.0000	134	0.0000	59	-	268	0.0000	30	0.0000	32	0.0000	55
201	kuke3d-001	0.0000	81	0.0000	19	-	60	0.0000	101	0.0000	103	0.0000	23
202	lemalabs-001	0.0000	83	0.0005	147	-	71	0.0002	249	0.0004	178	0.0004	167
203	line-000	0.0000	31	0.0000	52	-	166	0.0000	66	0.0000	63	0.0000	94
204	line-001	0.0000	99	0.0000	86	-	359	0.0000	8	0.0000	6	0.0001	105
205	lookman-002	0.0000	130	0.0000	60	-	299	0.0000	28	0.0000	30	0.0000	54
206	lookman-004	0.0000	116	0.0000	94	0.0000	18	0.0000	19	0.0000	21	0.0000	85
207	luxand-000	0.0000	95	0.0000	88	-	383	0.0000	4	0.0000	2	0.0000	73
208	mantra-000	0.0001	335	0.0041	319	-	347	0.0003	277	0.0004	273	0.0037	284
209	maxvision-000	0.0000	156	0.0000	104	-	231	0.0000	47	0.0000	48	0.0000	68
210	megvii-003	0.0000	164	0.0010	231	-	207	0.0002	260	0.0004	252	0.0011	255
211	megvii-004	-	381	-	382	-	170	0.0002	244	0.0004	229	0.0011	249
212	meituan-000	0.0000	120	0.0001	115	-	321	0.0000	121	0.0002	120	0.0001	106
213	meiya-001	0.0000	321	0.0028	297	-	142	0.0004	299	0.0010	337	0.0025	277
214	mendaxiatech-000	0.0000	223	0.0010	220	-	313	0.0002	258	0.0004	246	0.0011	251
215	microfocus-001	0.0001	344	0.0053	334	0.0791	27	0.0008	328	0.0016	356	0.0220	328
216	microfocus-002	0.0001	343	0.0053	335	0.0791	28	0.0008	327	0.0016	355	0.0220	327
217	minivision-000	0.0000	96	0.0000	87	-	354	0.0000	5	0.0000	8	0.0000	74
218	mobai-000	0.0000	292	0.0114	351	-	251	0.0003	281	0.0012	348	0.1242	371
219	mobai-001	0.0000	255	0.0040	315	-	53	0.0001	213	0.0012	347	0.0523	349
220	mobbl-001	0.0000	318	0.0052	333	-	218	0.0002	237	0.0005	306	0.0181	325
221	mobbl-002	0.0000	327	0.0029	300	-	233	0.0002	254	0.0009	331	0.0026	279
222	mobipintech-000	0.0000	157	0.0000	69	-	226	0.0000	44	0.0000	46	0.0000	67
223	moreedian-000	0.0000	247	0.0009	204	-	242	0.0004	296	0.0005	285	0.0004	200
224	multimodality-000	0.0000	35	0.0000	47	-	144	0.0000	70	0.0000	71	0.0000	47
225	mvision-001	0.0000	57	0.0000	2	-	121	0.0000	86	0.0000	84	0.0000	13
226	nazhiai-000	0.0000	34	0.0000	49	-	177	0.0000	68	0.0000	67	0.0000	45
227	neosystems-002	0.0000	40	0.0000	13	-	128	0.0000	74	0.0000	75	0.0000	2
228	neosystems-003	0.0000	13	0.0000	39	-	183	0.0000	55	0.0000	58	0.0000	33
229	netbridge-001	0.0000	41	0.0000	14	-	129	0.0000	75	0.0000	76	0.0000	1
230	netbridge-002	0.0000	118	0.0000	92	-	326	0.0000	20	0.0000	24	0.0000	87
231	neurotechnology-012	0.0000	308	0.0010	233	-	149	0.0001	221	0.0004	220	0.0005	210
232	neurotechnology-013	0.0000	54	0.0008	200	-	114	0.0000	118	0.0001	110	0.0004	179

Table 28: FTE is the proportion of failed template generation attempts. Failures can occur because the software throws an exception, or because the software electively refuses to process the input image. This would typically occur if a face is not detected. FTE is measured as the number of function calls that give EITHER a non-zero error code OR that give a “small” template. This is defined as one whose size is less than 0.3 times the median template size for that algorithm. This second rule is needed because some algorithms incorrectly fail to return a non-zero error code when template generation fails.

<sup>1</sup> The effects of FTE are included in the accuracy results of this report by regarding any template comparison involving a failed template to produce a low similarity score. Thus higher FTE results in higher FNMR and lower FMR.

	Algorithm	Failure to Enrol Rate <sup>1</sup>							
		Name	APPLICATION	BORDER	CHILD-EXPLOIT	MUGSHOT	VISA	WILD	
	Name	SEC. 2.2	SEC. 2.3	SEC. ??	SEC. 2.4	SEC. 2.1	SEC. 2.5		
233	nhn-001	0.0000	188	0.0019	277	-	125	0.0001	198
234	nhn-002	0.0000	29	0.0004	142	-	159	0.0000	141
235	nodeflux-002	0.0000	165	0.0261	359	-	213	0.0008	326
236	notiontag-001	0.0000	105	0.0000	80	-	368	0.0027	361
237	notiontag-002	0.0000	84	0.0000	15	-	64	0.0000	104
238	nsensecorp-002	0.0000	202	0.0009	205	-	96	0.0003	269
239	nsensecorp-003	0.0000	18	0.0000	111	-	188	0.0000	130
240	ntechlab-010	0.0000	222	0.0005	145	-	349	0.0001	209
241	ntechlab-011	0.0000	3	0.0003	124	-	203	0.0000	160
242	omnigarde-000	0.0000	225	0.0008	184	-	316	0.0000	133
243	omnigarde-001	0.0000	243	0.0008	183	-	236	0.0000	135
244	omsecurity-000	0.0000	133	0.0000	58	-	263	0.0000	29
245	openface-001	0.0000	301	0.0104	350	-	301	0.0004	293
246	oz-003	0.0000	48	0.0002	118	-	112	0.0000	114
247	oz-004	0.0000	306	0.0003	126	-	304	0.0000	117
248	papsav1923-001	0.0000	184	0.0007	172	-	152	0.0001	203
249	paravision-004	0.0000	283	0.0007	181	0.0570	25	0.0002	247
250	paravision-008	0.0000	121	0.0010	223	-	322	0.0001	199
251	pensees-001	0.0000	190	0.0000	10	-	133	0.0000	77
252	pixelall-006	0.0000	16	0.0000	36	-	184	0.0000	57
253	pixelall-007	0.0000	138	0.0000	55	-	282	0.0000	33
254	psl-008	0.0000	197	0.0003	125	-	72	0.0000	119
255	psl-009	0.0000	218	0.0004	135	-	334	0.0000	106
256	ptakuratsatu-000	0.0000	183	0.0007	179	-	147	0.0001	175
257	pxl-001	0.0000	332	0.0044	322	-	88	0.0005	304
258	pyramid-000	0.0001	340	0.0041	318	-	311	0.0005	303
259	qnap-000	0.0000	162	0.0007	180	-	241	0.0002	243
260	qnap-001	0.0000	166	0.0000	108	-	216	0.0000	156
261	quantasoft-003	0.0000	290	0.0015	265	-	303	0.0005	302
262	rankone-011	0.0000	151	0.0000	74	-	254	0.0000	40
263	rankone-012	0.0000	98	0.0000	85	-	357	0.0000	7
264	realnetworks-004	0.0000	220	0.0003	123	-	346	0.0000	107
265	realnetworks-005	0.0000	246	0.0002	121	-	243	0.0000	108
266	regula-000	0.0000	119	0.0000	93	-	327	0.0000	21
267	regula-001	0.0000	127	0.0000	63	-	292	0.0000	26
268	remarkai-001	0.0000	132	0.0000	57	-	270	0.0000	31
269	remarkai-003	0.0000	244	0.0007	168	-	237	0.0000	155
270	rendip-000	0.0000	270	0.0016	267	-	99	0.0002	246
271	revealmedia-005	0.0000	286	0.0007	175	-	246	0.0009	332
272	rokid-000	0.0000	26	0.0072	343	-	162	0.0001	201
273	rokid-001	0.0000	109	0.0013	255	-	345	0.0000	16
274	s1-003	0.0000	72	0.0002	120	-	93	0.0007	321
275	s1-004	0.0000	59	0.0000	110	-	80	0.0000	171
276	saffe-001	0.0000	141	0.0000	77	0.0000	14	0.0000	35
277	saffe-002	0.0000	37	0.0000	46	-	148	0.0000	71
278	samsungsd-000	0.0000	274	0.0055	337	-	330	0.0038	368
279	samtech-001	0.0001	339	0.0032	303	-	211	0.0004	297
280	scanovate-002	0.0000	249	0.0018	275	-	217	0.0000	169
281	scanovate-003	0.0000	253	0.0233	358	-	81	0.0006	316
282	securifai-003	0.0000	100	0.0000	81	-	363	0.0000	11
283	securifai-004	0.0000	67	0.0000	25	-	89	0.0000	94
284	sensetime-005	0.0000	90	0.0004	134	-	375	0.0000	138
285	sensetime-006	0.0000	21	0.0004	133	-	193	0.0000	140
286	sertis-000	0.0000	131	0.0007	174	-	300	0.0000	173
287	sertis-002	0.0000	149	0.0007	165	-	255	0.0000	167
288	seventhsense-000	0.0000	215	0.0006	161	-	332	0.0001	179
289	shaman-000	0.0000	10	0.0000	40	0.0000	12	0.0000	54
290	shaman-001	0.0000	92	0.0000	90	0.0000	21	0.0000	2

Table 29: FTE is the proportion of failed template generation attempts. Failures can occur because the software throws an exception, or because the software electively refuses to process the input image. This would typically occur if a face is not detected. FTE is measured as the number of function calls that give EITHER a non-zero error code OR that give a “small” template. This is defined as one whose size is less than 0.3 times the median template size for that algorithm. This second rule is needed because some algorithms incorrectly fail to return a non-zero error code when template generation fails.

<sup>1</sup> The effects of FTE are included in the accuracy results of this report by regarding any template comparison involving a failed template to produce a low similarity score. Thus higher FTE results in higher FNMR and lower FMR.

	Algorithm	Failure to Enrol Rate <sup>1</sup>						
		APPLICATION	BORDER	CHILD-EXPLOIT	MUGSHOT	VISA	WILD	
Name	SEC. 2.2	SEC. 2.3	SEC. ??	SEC. 2.4	SEC. 2.1	SEC. 2.5		
291	shu-002	0.0000	263	0.0010	228	-	293	0.0005
292	shu-003	0.0000	12	0.0007	163	-	182	0.0001
293	siat-002	0.0000	203	0.0012	249	0.0616	26	0.0000
294	siat-004	0.0000	245	0.0011	238	-	238	0.0000
295	sjtu-003	0.0000	78	0.0005	149	-	55	0.0000
296	sjtu-004	0.0000	2	0.0000	42	-	201	0.0000
297	sktelecom-000	0.0000	198	0.0008	193	-	77	0.0000
298	smartengines-000	0.0066	371	0.0150	354	-	342	0.0022
299	smilart-002	0.0000	328	0.0036	312	0.2422	39	-
300	smilart-003	0.0003	353	0.0100	348	-	126	0.0014
301	sodec-000	0.0000	71	0.0000	21	-	97	0.0000
302	sqisoft-001	0.0000	5	0.0003	130	-	204	0.0000
303	sqisoft-002	0.0000	93	0.0003	129	-	377	0.0000
304	stachu-000	0.0000	85	0.0000	16	-	66	0.0000
305	starhybrid-001	0.0001	342	0.0033	307	0.2340	38	0.0009
306	suprema-000	0.0000	252	0.0017	271	-	109	0.0002
307	suprema-001	0.0000	273	0.0027	292	-	380	0.0003
308	supremaid-001	0.0000	175	0.0020	282	-	160	0.0001
309	synesis-006	0.0000	139	0.0003	131	-	283	0.0000
310	synesis-007	0.0000	193	0.0013	254	-	103	0.0002
311	synology-000	0.0000	63	0.0000	29	-	79	0.0000
312	synology-002	0.0000	147	0.0000	76	-	248	0.0000
313	sztu-000	0.0000	53	0.0000	4	-	119	0.0000
314	sztu-001	0.0000	152	0.0000	71	-	262	0.0000
315	tech5-004	0.0000	174	0.0008	186	-	199	0.0003
316	tech5-005	0.0000	186	0.0007	182	-	150	0.0000
317	techsign-000	0.0007	361	0.0334	367	-	308	0.0020
318	tevian-007	0.0000	171	0.0015	266	-	187	0.0002
319	tevian-008	0.0000	191	0.0006	151	-	138	0.0000
320	tiger-005	0.0000	221	0.0009	215	-	340	0.0001
321	tiger-006	0.0000	248	0.0011	239	-	208	0.0001
322	tinkoff-001	0.0000	265	0.0008	192	-	277	0.0001
323	tongyi-005	0.0000	23	0.0000	31	0.0000	9	0.0000
324	toppanidgate-000	0.0000	240	0.0008	189	-	260	0.0004
325	toshiba-003	0.0000	128	0.0001	114	-	296	0.0001
326	toshiba-004	0.0000	46	0.0000	11	-	134	0.0000
327	trueface-002	0.0000	261	0.0046	329	-	335	0.0003
328	trueface-003	0.0000	258	0.0046	328	-	358	0.0003
329	tuputech-000	0.0003	355	0.0116	352	-	135	-
330	twface-000	0.0000	9	0.0000	41	-	220	0.0000
331	twface-001	0.0000	160	0.0000	67	-	240	0.0000
332	ulsee-001	0.0000	17	0.0000	38	-	186	0.0000
333	ultinous-000	-	384	-	383	0.0007	23	-
334	ultinous-001	-	382	-	381	0.0007	22	-
335	uluface-002	0.0000	28	0.0000	54	0.0000	7	0.0000
336	uluface-003	0.0000	110	0.0001	117	-	339	0.0002
337	unissey-001	0.0000	150	0.0000	73	-	256	0.0000
338	upc-001	0.0000	303	0.0003	127	0.0450	24	0.0003
339	vcog-002	-	383	-	380	0.2209	37	-
340	vd-002	0.0000	158	0.0000	70	-	228	0.0000
341	vd-003	0.0001	337	0.0041	317	-	52	0.0030
342	veridas-006	0.0000	297	0.0026	289	-	130	0.0001
343	veridas-007	0.0000	302	0.0026	290	-	232	0.0001
344	verigram-000	0.0000	277	0.0068	340	-	245	0.0003
345	verihubs-inteligensia-000	0.0000	237	0.0029	298	-	267	0.0001
346	via-000	0.0000	66	0.0000	24	0.0000	3	0.0000
347	via-001	0.0000	39	0.0000	44	-	155	0.0000
348	videmo-000	0.0000	254	0.0019	278	-	83	0.0003

Table 30: FTE is the proportion of failed template generation attempts. Failures can occur because the software throws an exception, or because the software electively refuses to process the input image. This would typically occur if a face is not detected. FTE is measured as the number of function calls that give EITHER a non-zero error code OR that give a “small” template. This is defined as one whose size is less than 0.3 times the median template size for that algorithm. This second rule is needed because some algorithms incorrectly fail to return a non-zero error code when template generation fails.

<sup>1</sup>The effects of FTE are included in the accuracy results of this report by regarding any template comparison involving a failed template to produce a low similarity score. Thus higher FTE results in higher FNMR and lower FMR.

	Algorithm	Failure to Enrol Rate <sup>1</sup>											
		Name	APPLICATION		BORDER		CHILD-EXPLOIT		MUGSHOT		VISA		
			SEC. 2.2	SEC. 2.3	SEC. ??	SEC. 2.4	SEC. 2.1	SEC. 2.5					
349	videmo-001	0.0000	293	0.0170	355	-	257	0.0010	336	0.0011	344	0.0847	357
350	videonetics-001	0.0004	356	0.0309	365	0.4799	45	0.0015	346	0.0010	335	0.0112	311
351	videonetics-002	0.0000	268	0.0459	374	0.4598	43	0.0006	317	0.0005	314	0.0013	258
352	viettelighttech-000	0.0000	309	0.0019	279	-	91	0.0007	322	0.0005	311	0.0024	276
353	vigilantsolutions-010	0.0000	288	0.0028	295	-	344	0.0001	186	0.0004	175	0.0005	207
354	vigilantsolutions-011	0.0000	291	0.0028	294	-	280	0.0001	188	0.0004	176	0.0005	206
355	vinaï-000	0.0000	65	0.0000	23	-	86	0.0000	93	0.0000	90	0.0000	18
356	vinbigdata-001	0.0000	55	0.0000	6	-	115	0.0000	83	0.0000	86	0.0000	9
357	vion-000	0.0050	369	0.0392	373	0.6388	49	0.0130	377	0.0078	377	0.1389	374
358	visage-000	0.0000	311	0.0054	336	-	325	0.0009	330	0.0006	320	0.0064	298
359	visionbox-001	0.0000	329	0.0033	306	-	51	0.0005	310	0.0011	343	0.0028	280
360	visionbox-002	0.0000	75	0.0017	269	-	98	0.0000	148	0.0004	276	0.0046	290
361	visionlabs-010	0.0000	279	0.0009	208	-	175	0.0001	224	0.0004	219	0.0006	225
362	visionlabs-011	0.0000	51	0.0006	156	-	117	0.0001	191	0.0004	184	0.0004	160
363	visteam-001	0.0000	282	0.0014	260	-	364	0.0002	241	0.0004	223	0.0011	253
364	visteam-002	0.0000	285	0.0014	261	-	276	0.0002	238	0.0004	226	0.0011	252
365	vnppt-002	0.0000	201	0.0002	119	-	95	0.0003	283	0.0003	132	0.0001	107
366	vnppt-003	0.0000	7	0.0004	132	-	214	0.0002	233	0.0004	168	0.0001	109
367	vocord-008	0.0000	210	0.0015	264	-	372	0.0003	284	0.0001	112	0.0007	231
368	vocord-009	0.0000	231	0.0006	155	-	305	0.0001	229	0.0003	129	0.0003	130
369	vts-000	0.0000	275	0.0011	235	-	307	0.0001	230	0.0004	268	0.0013	259
370	winsense-001	0.0000	136	0.0000	56	0.0000	15	0.0000	32	0.0000	36	0.0000	56
371	winsense-002	0.0000	91	0.0000	89	-	381	0.0000	3	0.0000	4	0.0000	72
372	wuhantianyu-001	0.0000	146	0.0007	166	-	252	0.0001	177	0.0004	215	0.0002	119
373	x-laboratory-000	0.0247	379	0.0000	30	0.0000	11	0.0005	309	0.0002	121	0.0000	40
374	x-laboratory-001	0.0000	181	0.0012	246	-	169	0.0001	217	0.0004	258	0.0007	228
375	xforwardai-001	0.0000	194	0.0007	176	-	116	0.0003	274	0.0004	255	0.0004	159
376	xforwardai-002	0.0000	172	0.0007	177	-	194	0.0003	273	0.0004	253	0.0004	163
377	xm-000	0.0000	8	0.0007	164	-	222	0.0001	180	0.0003	141	0.0004	197
378	yisheng-004	0.0002	350	-	384	0.4279	42	0.0013	340	0.0006	322	0.0321	337
379	yitu-003	0.0000	111	0.0000	97	-	341	0.0009	329	0.0000	19	0.0000	82
380	yoonik-002	0.0000	267	0.0010	225	-	230	0.0003	267	0.0006	318	0.0005	208
381	yoonik-003	0.0000	256	0.0009	212	-	63	0.0002	236	0.0004	237	0.0008	236
382	ytu-000	0.0000	177	0.0010	232	-	156	0.0002	261	0.0004	254	0.0011	256
383	yuan-002	0.0000	298	0.0010	230	-	379	0.0005	306	0.0005	298	0.0005	212
384	yuan-003	0.0000	300	0.0010	229	-	365	0.0005	307	0.0005	299	0.0005	213

Table 31: FTE is the proportion of failed template generation attempts. Failures can occur because the software throws an exception, or because the software electively refuses to process the input image. This would typically occur if a face is not detected. FTE is measured as the number of function calls that give EITHER a non-zero error code OR that give a “small” template. This is defined as one whose size is less than 0.3 times the median template size for that algorithm. This second rule is needed because some algorithms incorrectly fail to return a non-zero error code when template generation fails.

<sup>1</sup> The effects of FTE are included in the accuracy results of this report by regarding any template comparison involving a failed template to produce a low similarity score. Thus higher FTE results in higher FNMR and lower FMR.

### 3.4 Recognition accuracy

Core algorithm accuracy is stated via:

▷ **Cooperative subjects**

- The summary table of Figure 24;
- The visa image DETs of Figure 58;
- The mugshot DETs of Figure 77;
- The mugshot ageing profiles of Figure 277;
- The human-difficult pairs of Figure 19

▷ **Non-cooperative subjects**

- The photojournalism DET of Figure 93

Figure 221 shows dependence of false match rate on algorithm score threshold. This allows a deployer to set a threshold to target a particular false match rate appropriate to the security objectives of the application.

Figure 182 likewise shows FMR(T) but for mugshots, and specially four subsets of the population.

Note that in both the mugshot and visa sets false match rates vary with the ethnicity, age, and sex, of the enrollee and impostor. For example figure 112 summarizes FMR for impostors paired from four groups black females, black males, white females, white males.

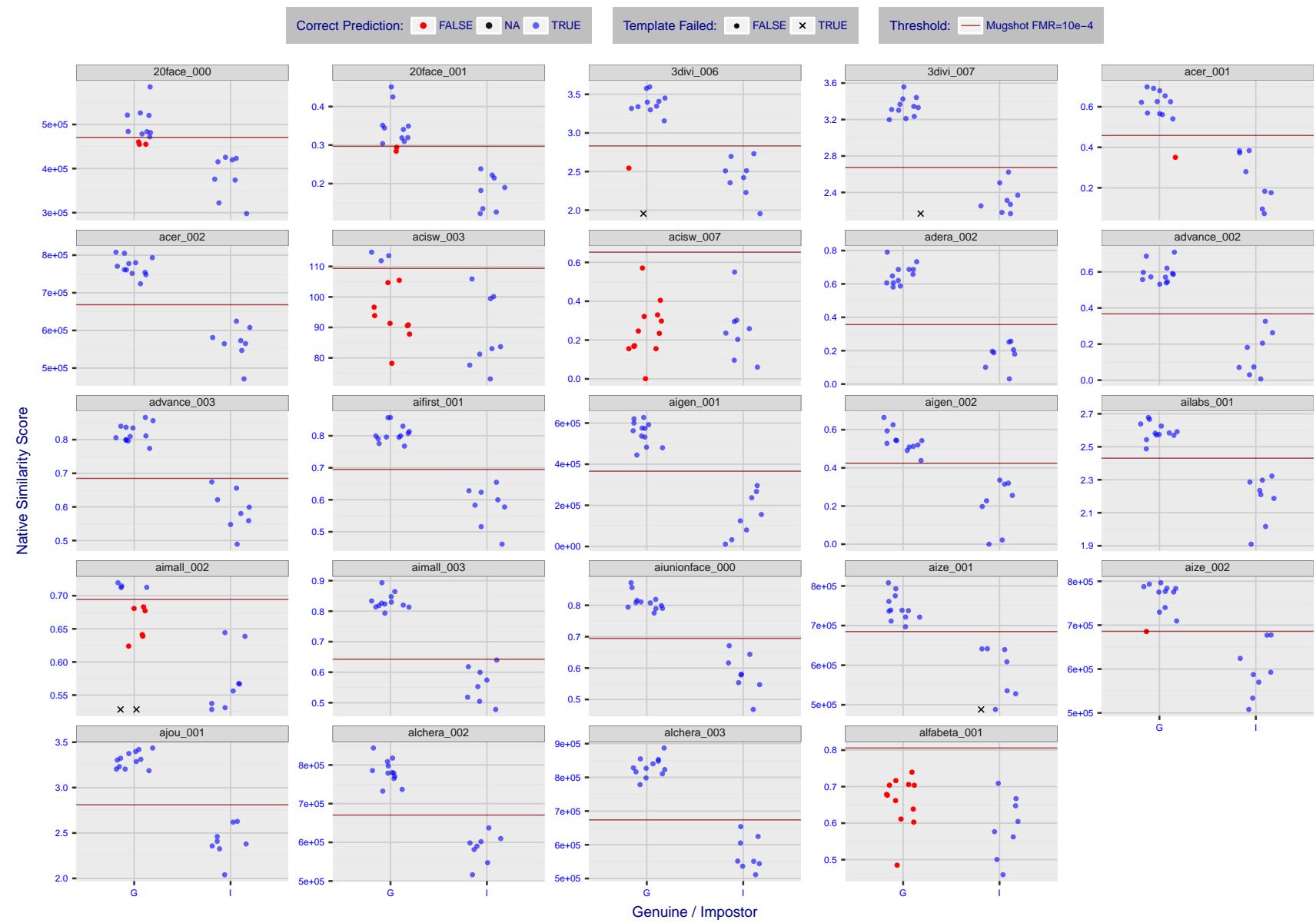


Figure 4: The figure shows algorithms' similarity scores for 12 genuine and 8 impostor image pairs used in the May 2018 paper Face recognition accuracy of forensic examiners, superrecognizers, and face recognition algorithms (Phillips et al. [1]). The threshold (red horizontal line) is a value calibrated to give  $FMR = 0.0001$  on mugshot images. Points above the threshold correspond to pairs predicted to be genuine, and points below the threshold correspond to pairs predicted to be impostors. The figure shows whether the predicted class (genuine or impostor) matches the real class. Blue denotes a correct prediction, and red denotes incorrect. An "X" represents face detection failure in either of the images in the pair. Note that the sample size ( $n=20$ ) is small, and the figure may change substantially if larger or different sets are used. The images can be downloaded from the [Supplemental Information](#) page provided with that publication.

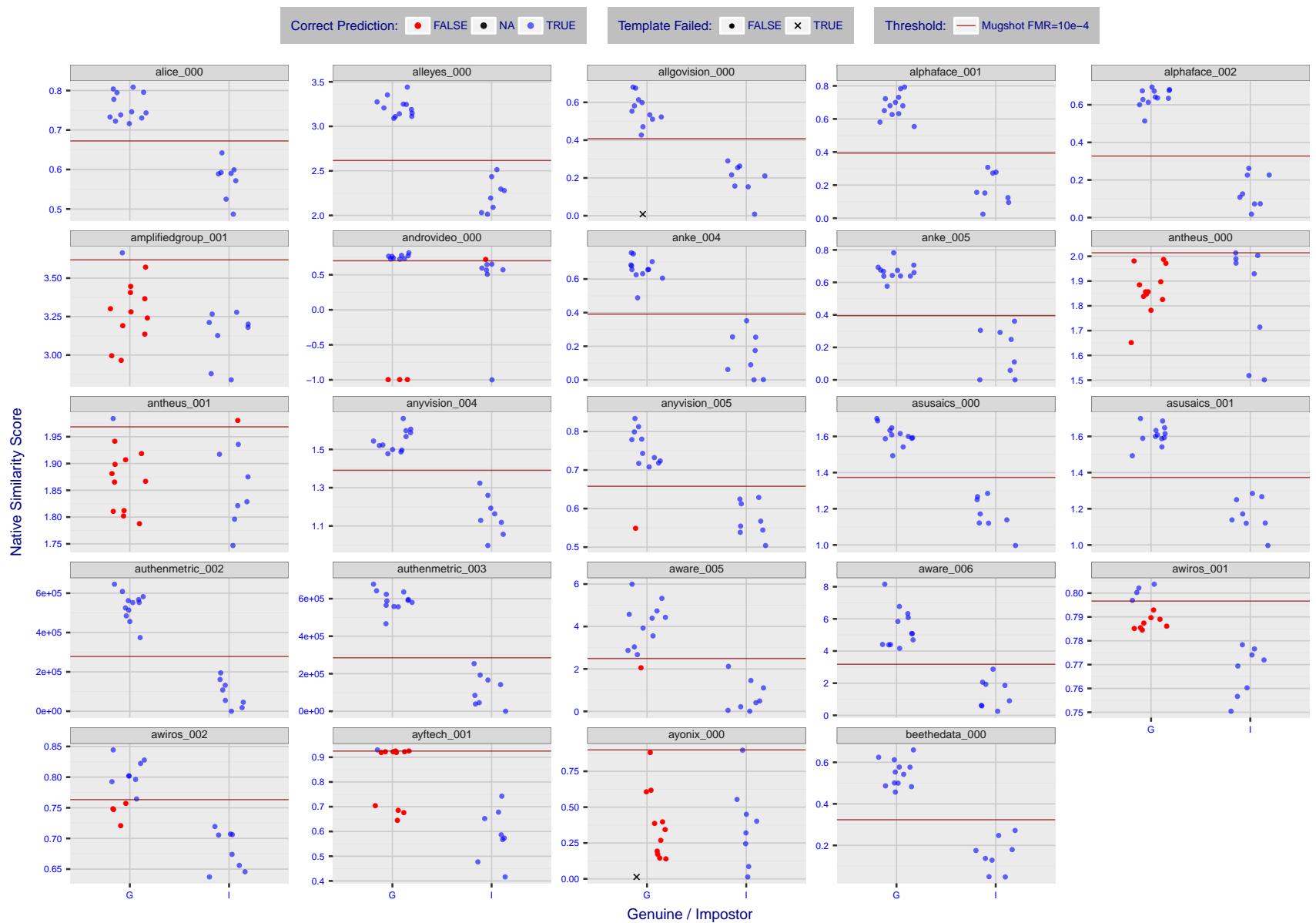


Figure 5: The figure shows algorithms' similarity scores for 12 genuine and 8 impostor image pairs used in the May 2018 paper Face recognition accuracy of forensic examiners, superrecognizers, and face recognition algorithms (Phillips et al. [1]). The threshold (red horizontal line) is a value calibrated to give  $FMR = 0.0001$  on mugshot images. Points above the threshold correspond to pairs predicted to be genuine, and points below the threshold correspond to pairs predicted to be impostors. The figure shows whether the predicted class (genuine or impostor) matches the real class. Blue denotes a correct prediction, and red denotes incorrect. An "X" represents face detection failure in either of the images in the pair. Note that the sample size ( $n=20$ ) is small, and the figure may change substantially if larger or different sets are used. The images can be downloaded from the [Supplemental Information](#) page provided with that publication.

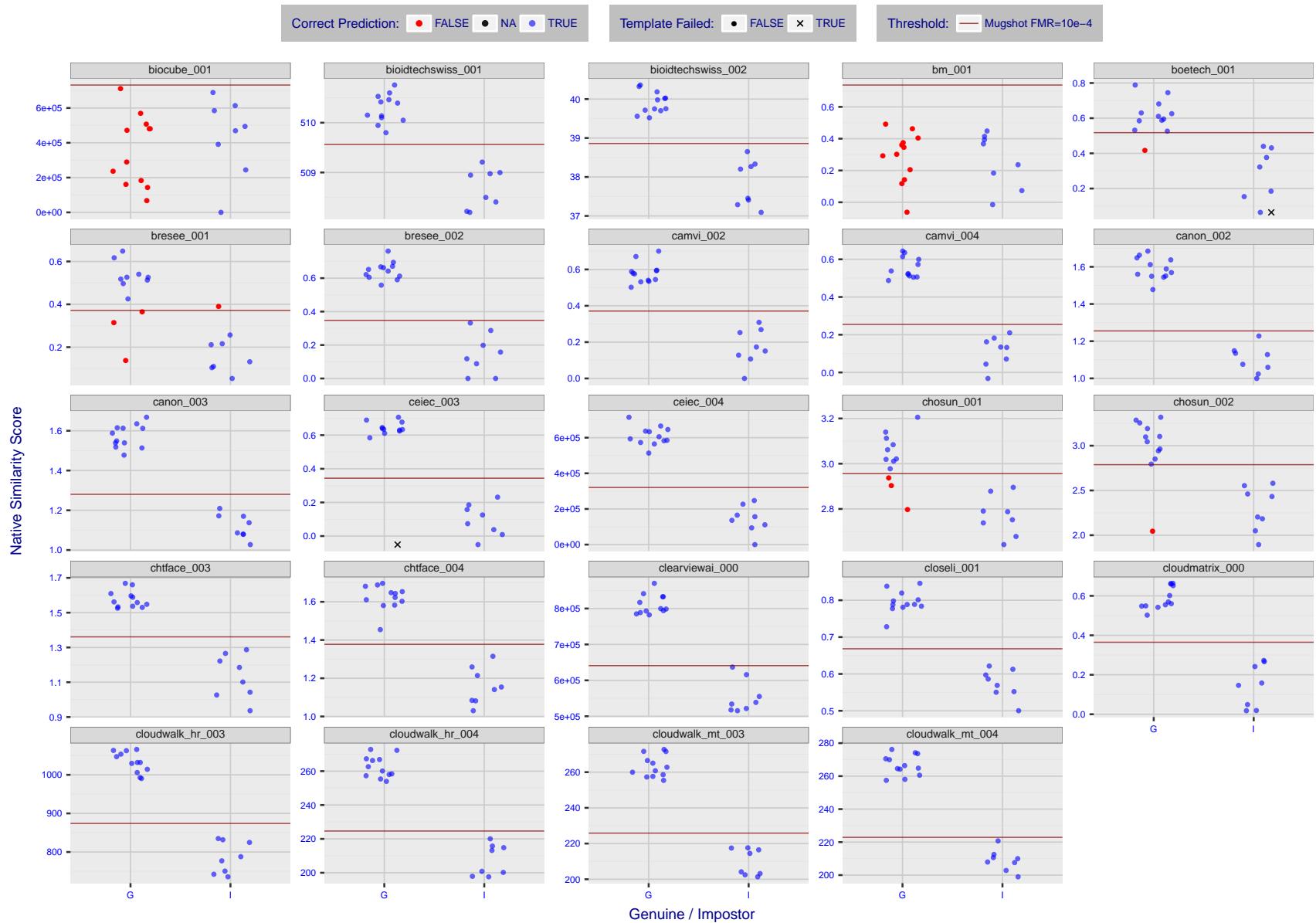


Figure 6: The figure shows algorithms' similarity scores for 12 genuine and 8 impostor image pairs used in the May 2018 paper Face recognition accuracy of forensic examiners, superrecognizers, and face recognition algorithms (Phillips et al. [1]). The threshold (red horizontal line) is a value calibrated to give  $FMR = 0.0001$  on mugshot images. Points above the threshold correspond to pairs predicted to be genuine, and points below the threshold correspond to pairs predicted to be impostors. The figure shows whether the predicted class (genuine or impostor) matches the real class. Blue denotes a correct prediction, and red denotes incorrect. An "X" represents face detection failure in either of the images in the pair. Note that the sample size ( $n=20$ ) is small, and the figure may change substantially if larger or different sets are used. The images can be downloaded from the [Supplemental Information](#) page provided with that publication.

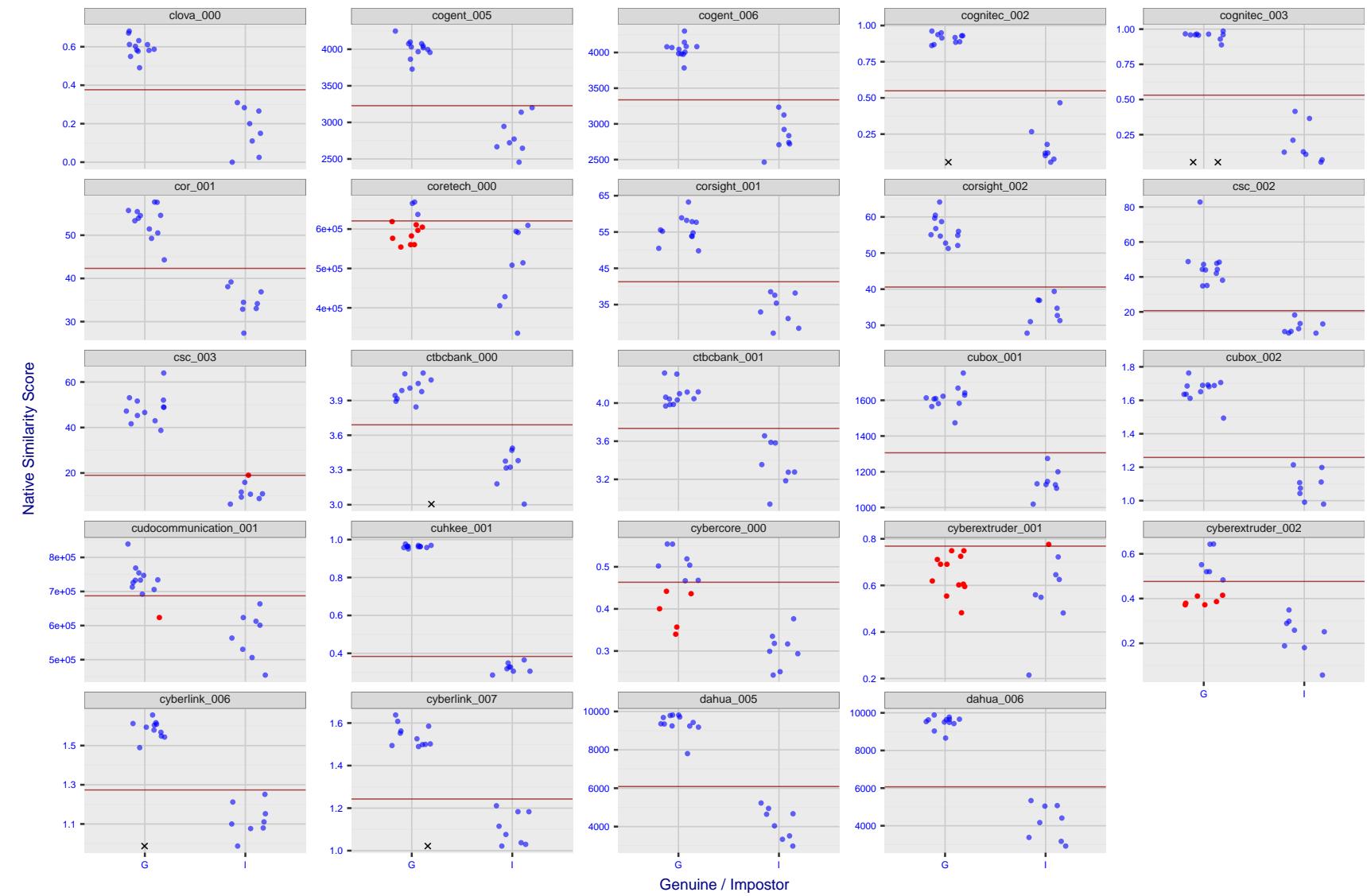


Figure 7: The figure shows algorithms' similarity scores for 12 genuine and 8 impostor image pairs used in the May 2018 paper Face recognition accuracy of forensic examiners, superrecognizers, and face recognition algorithms (Phillips et al. [1]). The threshold (red horizontal line) is a value calibrated to give  $FMR = 0.0001$  on mugshot images. Points above the threshold correspond to pairs predicted to be genuine, and points below the threshold correspond to pairs predicted to be impostors. The figure shows whether the predicted class (genuine or impostor) matches the real class. Blue denotes a correct prediction, and red denotes incorrect. An "X" represents face detection failure in either of the images in the pair. Note that the sample size ( $n=20$ ) is small, and the figure may change substantially if larger or different sets are used. The images can be downloaded from the [Supplemental Information](#) page provided with that publication.

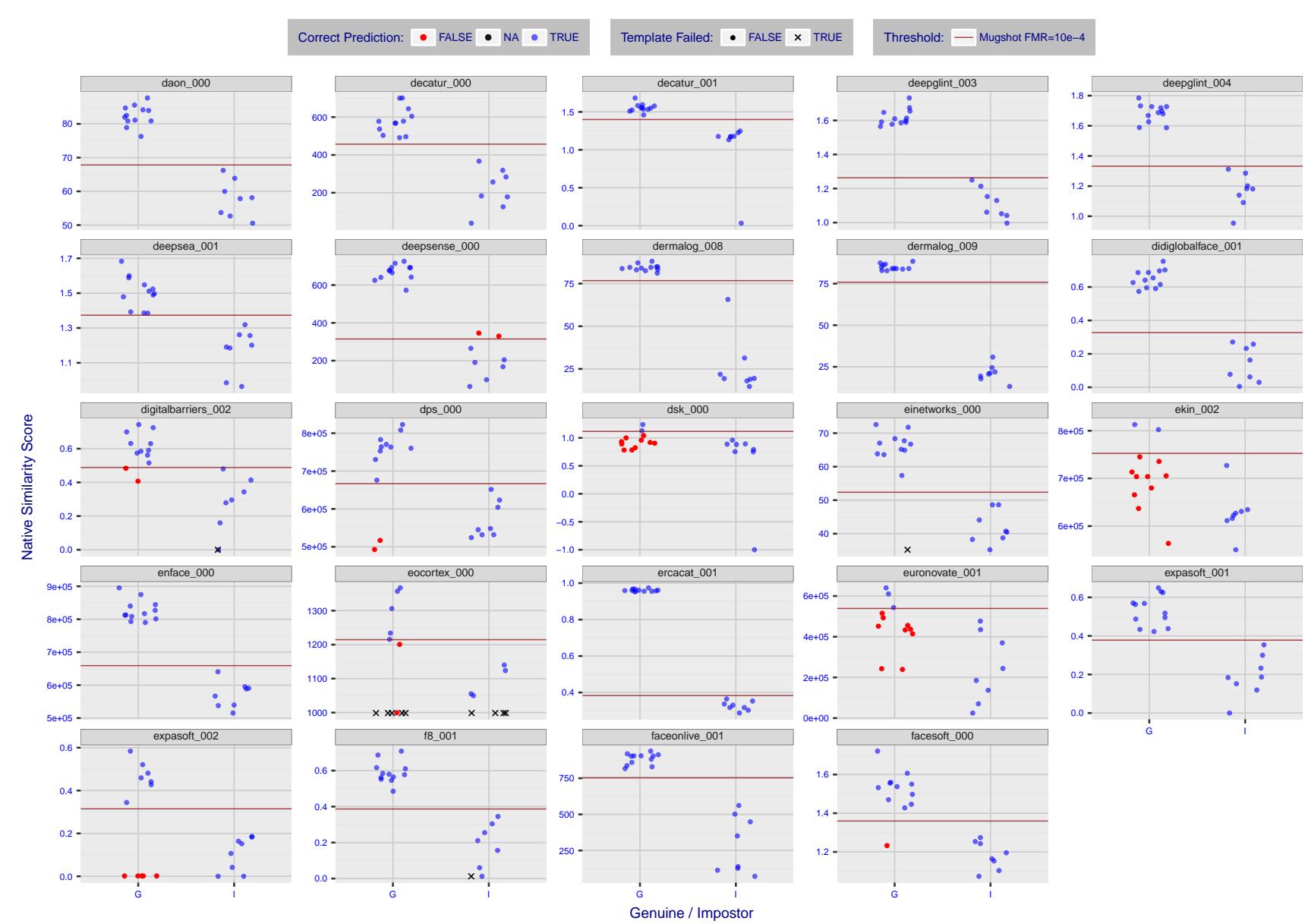


Figure 8: The figure shows algorithms' similarity scores for 12 genuine and 8 impostor image pairs used in the May 2018 paper Face recognition accuracy of forensic examiners, superrecognizers, and face recognition algorithms (Phillips et al. [1]). The threshold (red horizontal line) is a value calibrated to give FMR = 0.0001 on mugshot images. Points above the threshold correspond to pairs predicted to be genuine, and points below the threshold correspond to pairs predicted to be impostors. The figure shows whether the predicted class (genuine or impostor) matches the real class. Blue denotes a correct prediction, and red denotes incorrect. An "X" represents face detection failure in either of the images in the pair. Note that the sample size ( $n=20$ ) is small, and the figure may change substantially if larger or different sets are used. The images can be downloaded from the [Supplemental Information](#) page provided with that publication.

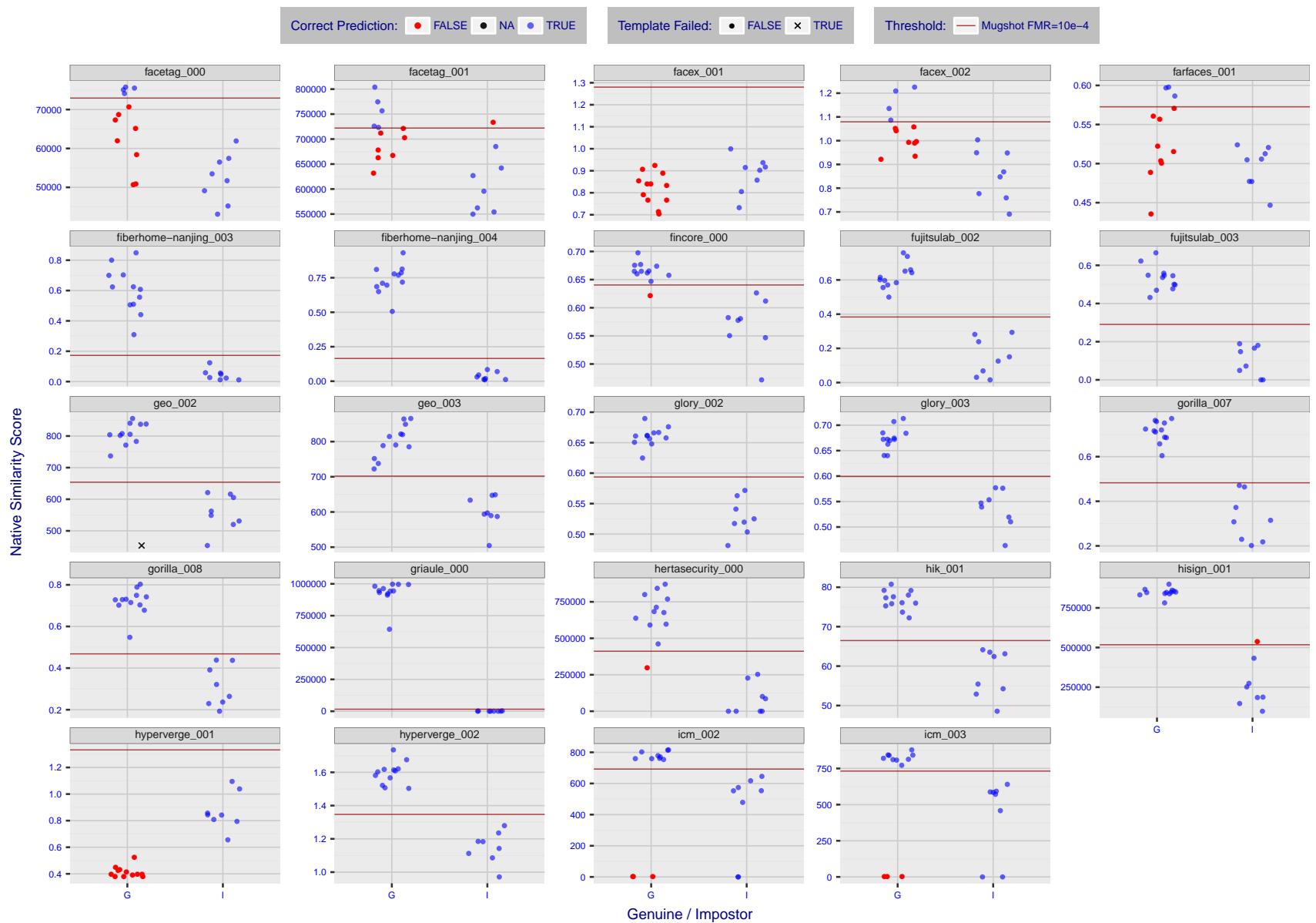


Figure 9: The figure shows algorithms' similarity scores for 12 genuine and 8 impostor image pairs used in the May 2018 paper Face recognition accuracy of forensic examiners, superrecognizers, and face recognition algorithms (Phillips et al. [1]). The threshold (red horizontal line) is a value calibrated to give  $FMR = 0.0001$  on mugshot images. Points above the threshold correspond to pairs predicted to be genuine, and points below the threshold correspond to pairs predicted to be impostors. The figure shows whether the predicted class (genuine or impostor) matches the real class. Blue denotes a correct prediction, and red denotes incorrect. An "X" represents face detection failure in either of the images in the pair. Note that the sample size ( $n=20$ ) is small, and the figure may change substantially if larger or different sets are used. The images can be downloaded from the [Supplemental Information](#) page provided with that publication.

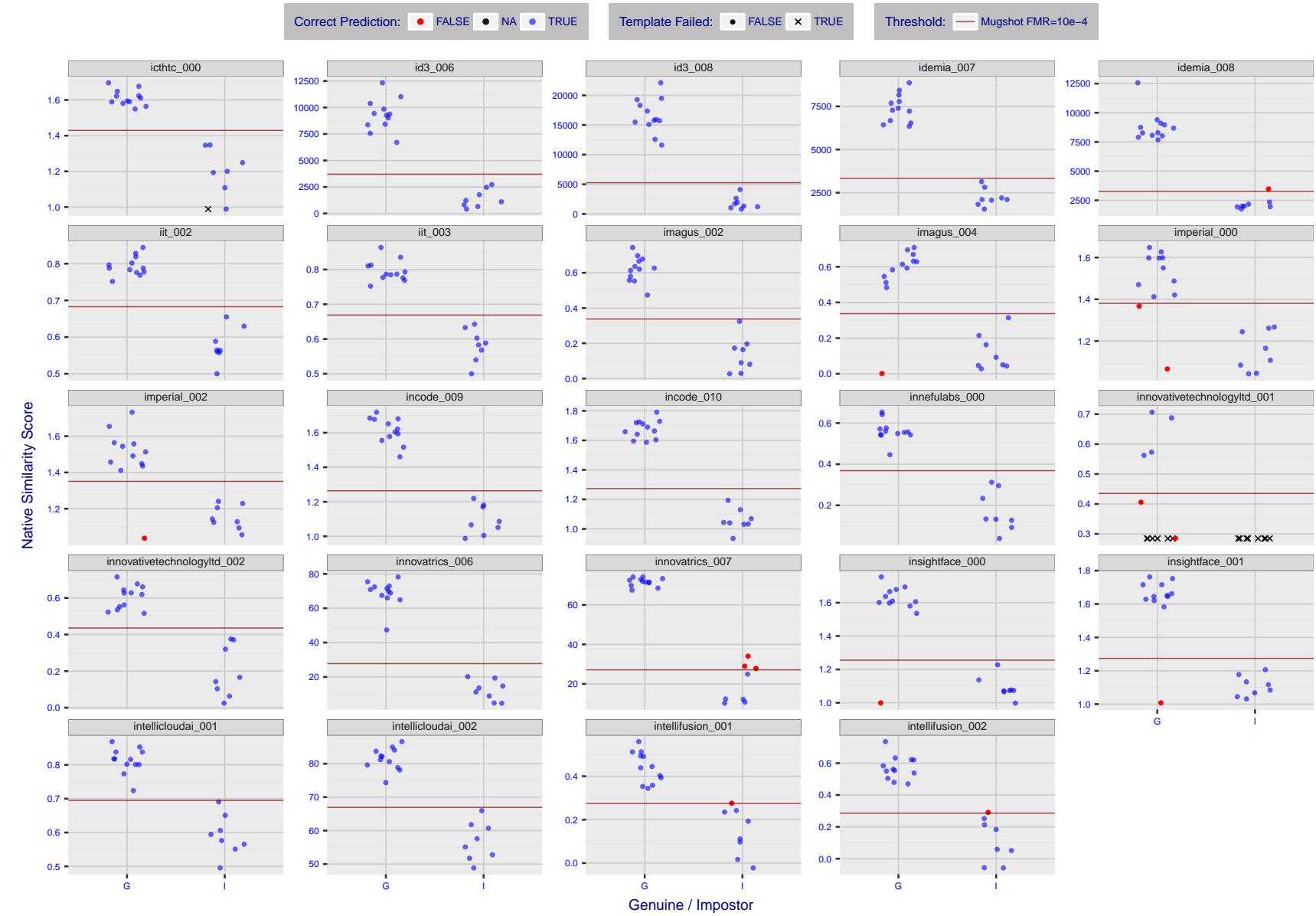


Figure 10: The figure shows algorithms' similarity scores for 12 genuine and 8 impostor image pairs used in the May 2018 paper Face recognition accuracy of forensic examiners, superrecognizers, and face recognition algorithms (Phillips et al. [1]). The threshold (red horizontal line) is a value calibrated to give  $FMR = 0.0001$  on mugshot images. Points above the threshold correspond to pairs predicted to be genuine, and points below the threshold correspond to pairs predicted to be impostors. The figure shows whether the predicted class (genuine or impostor) matches the real class. Blue denotes a correct prediction, and red denotes incorrect. An "X" represents face detection failure in either of the images in the pair. Note that the sample size ( $n=20$ ) is small, and the figure may change substantially if larger or different sets are used. The images can be downloaded from the [Supplemental Information](#) page provided with that publication.

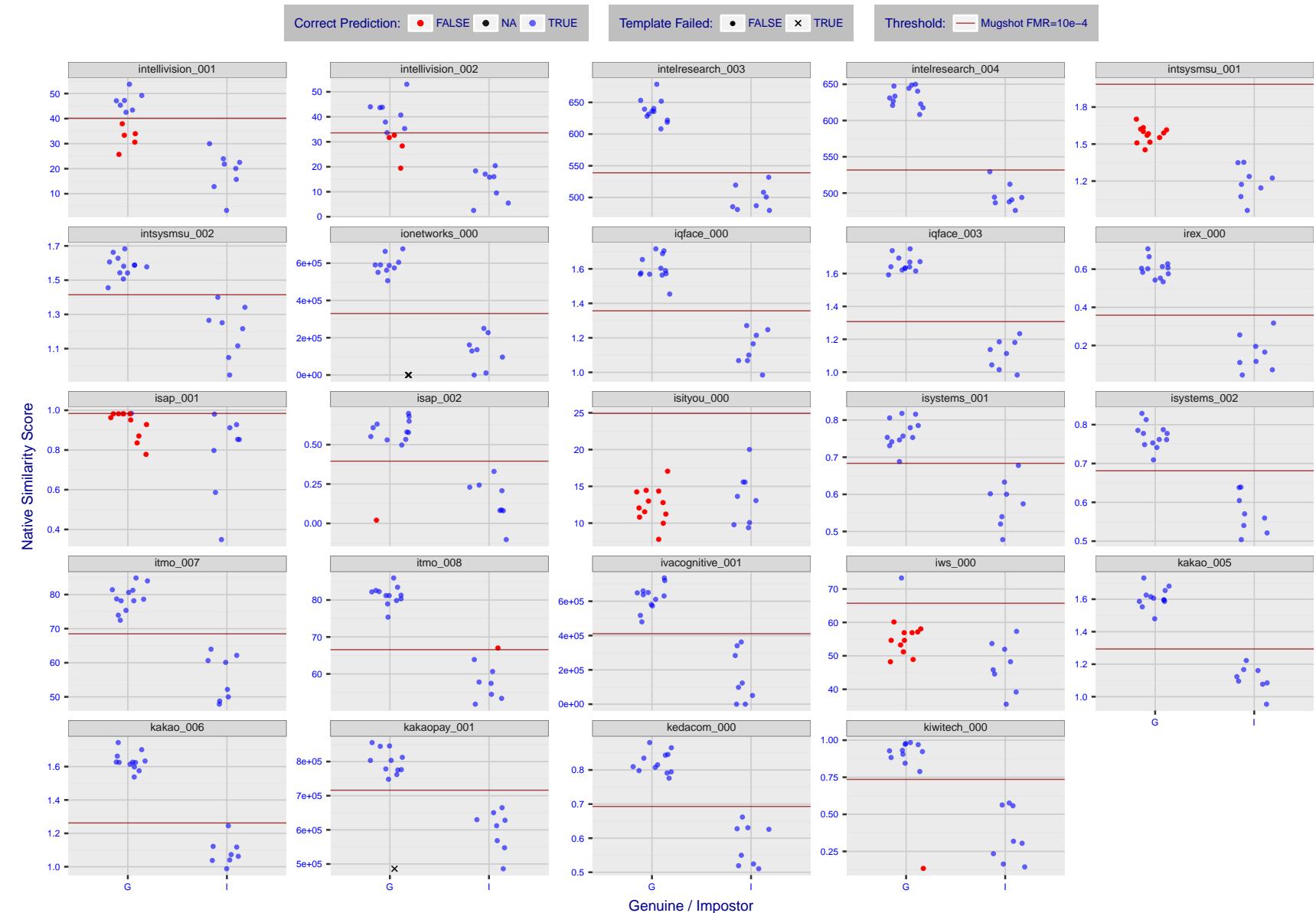


Figure 11: The figure shows algorithms' similarity scores for 12 genuine and 8 impostor image pairs used in the May 2018 paper Face recognition accuracy of forensic examiners, superrecognizers, and face recognition algorithms (Phillips et al. [1]). The threshold (red horizontal line) is a value calibrated to give  $FMR = 0.0001$  on mugshot images. Points above the threshold correspond to pairs predicted to be genuine, and points below the threshold correspond to pairs predicted to be impostors. The figure shows whether the predicted class (genuine or impostor) matches the real class. Blue denotes a correct prediction, and red denotes incorrect. An "X" represents face detection failure in either of the images in the pair. Note that the sample size ( $n=20$ ) is small, and the figure may change substantially if larger or different sets are used. The images can be downloaded from the [Supplemental Information](#) page provided with that publication.

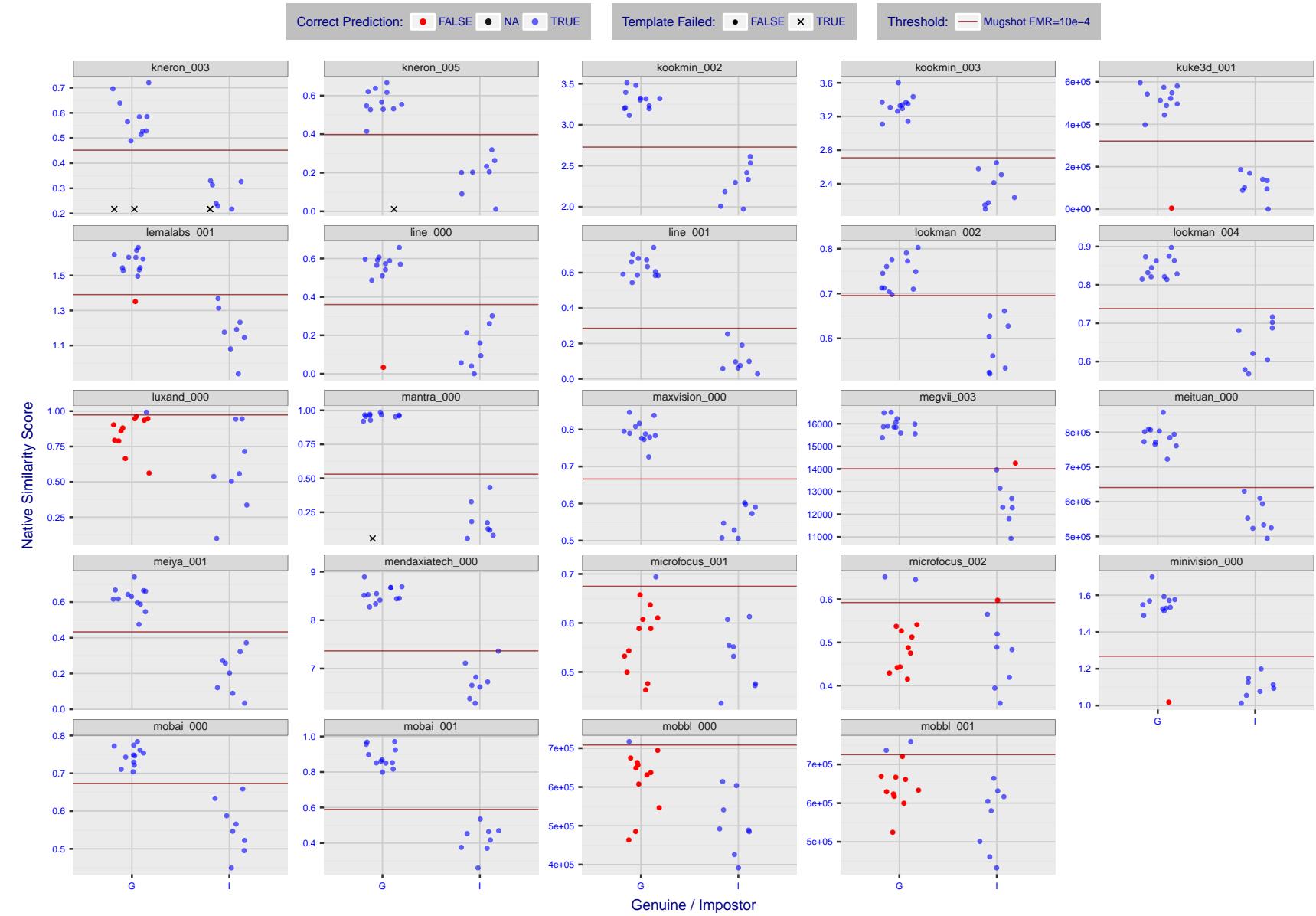


Figure 12: The figure shows algorithms' similarity scores for 12 genuine and 8 impostor image pairs used in the May 2018 paper Face recognition accuracy of forensic examiners, superrecognizers, and face recognition algorithms (Phillips et al. [1]). The threshold (red horizontal line) is a value calibrated to give  $FMR = 0.0001$  on mugshot images. Points above the threshold correspond to pairs predicted to be genuine, and points below the threshold correspond to pairs predicted to be impostors. The figure shows whether the predicted class (genuine or impostor) matches the real class. Blue denotes a correct prediction, and red denotes incorrect. An "X" represents face detection failure in either of the images in the pair. Note that the sample size ( $n=20$ ) is small, and the figure may change substantially if larger or different sets are used. The images can be downloaded from the [Supplemental Information](#) page provided with that publication.

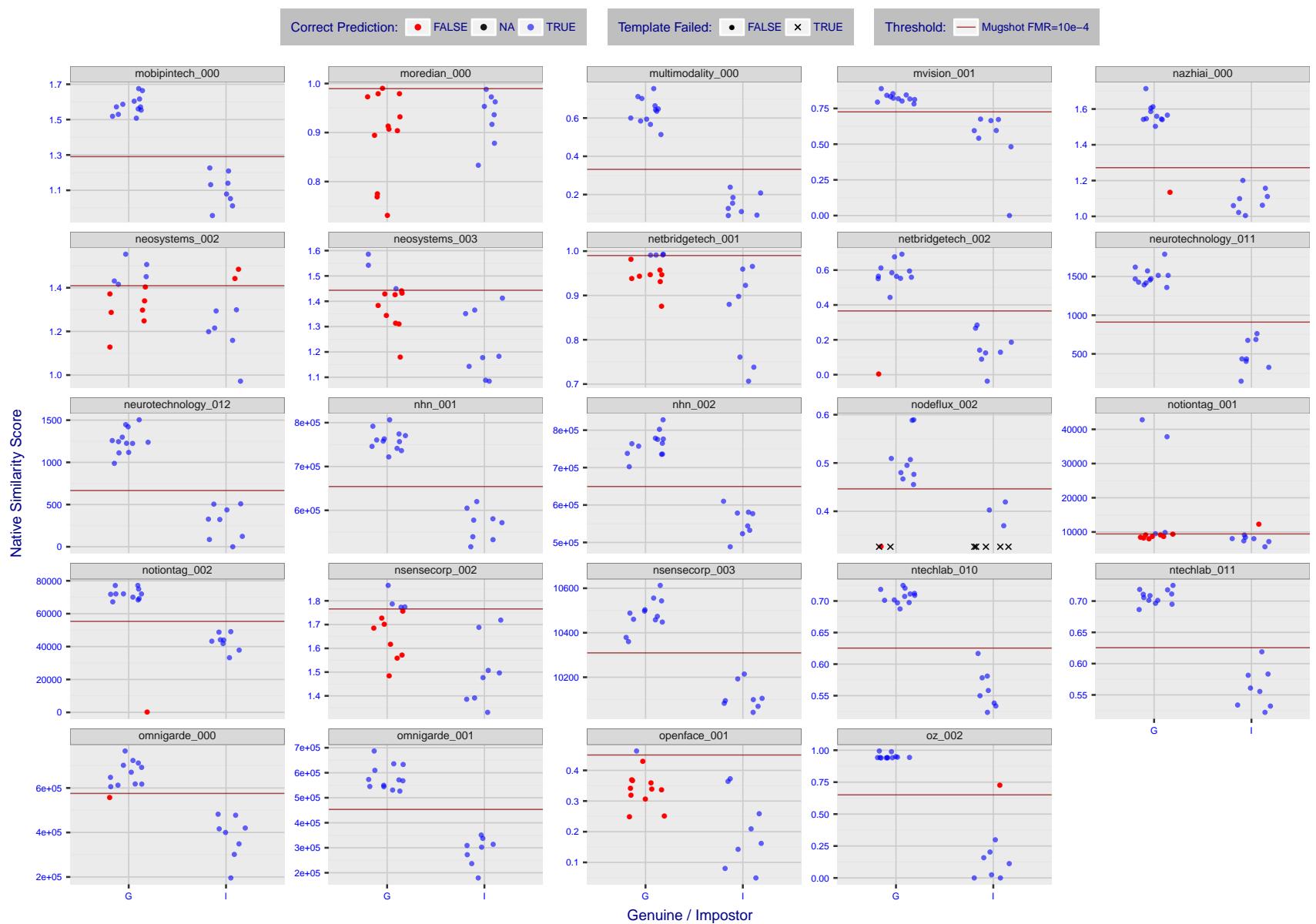


Figure 13: The figure shows algorithms' similarity scores for 12 genuine and 8 impostor image pairs used in the May 2018 paper Face recognition accuracy of forensic examiners, superrecognizers, and face recognition algorithms (Phillips et al. [1]). The threshold (red horizontal line) is a value calibrated to give  $FMR = 0.0001$  on mugshot images. Points above the threshold correspond to pairs predicted to be genuine, and points below the threshold correspond to pairs predicted to be impostors. The figure shows whether the predicted class (genuine or impostor) matches the real class. Blue denotes a correct prediction, and red denotes incorrect. An "X" represents face detection failure in either of the images in the pair. Note that the sample size ( $n=20$ ) is small, and the figure may change substantially if larger or different sets are used. The images can be downloaded from the [Supplemental Information](#) page provided with that publication.

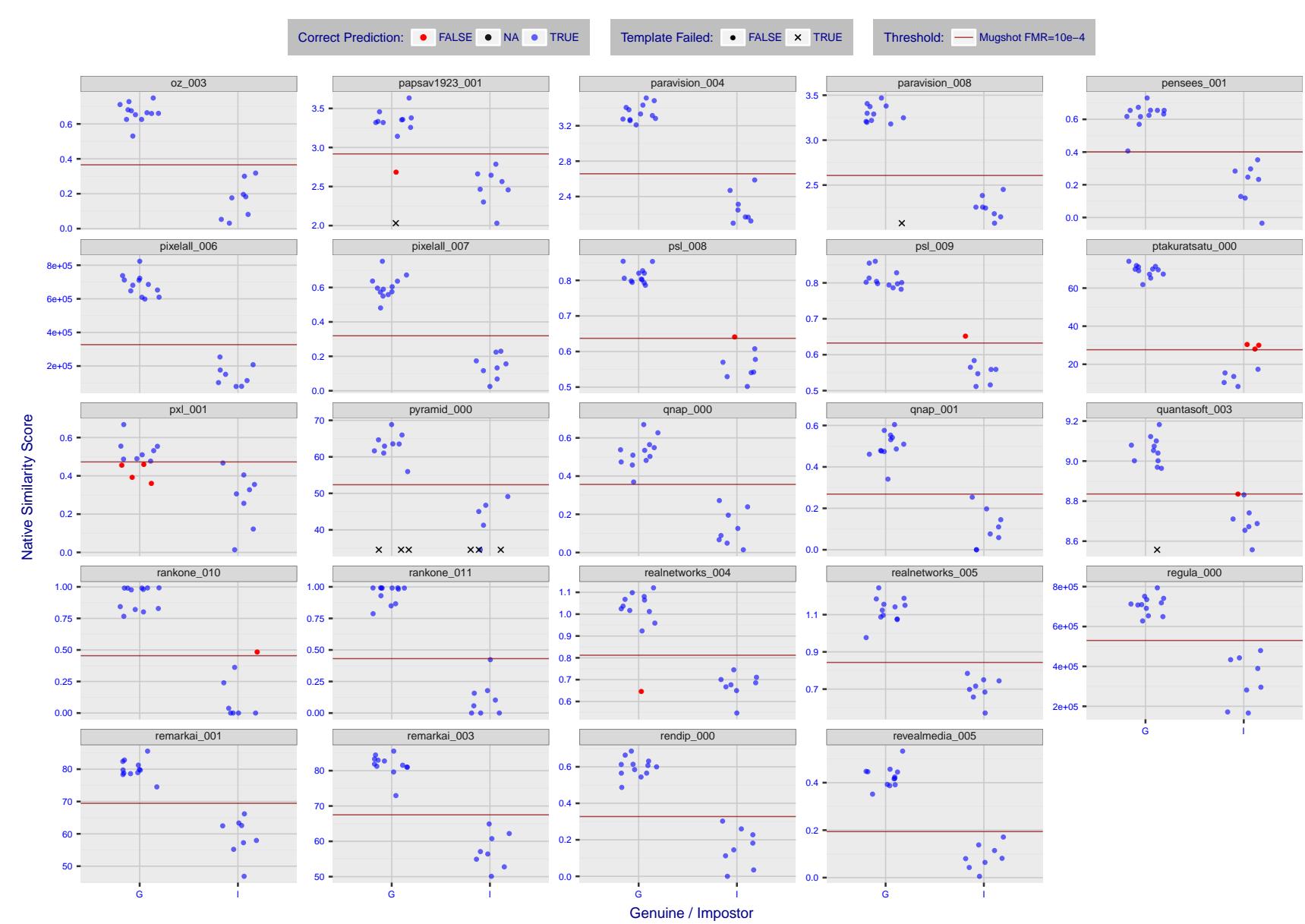


Figure 14: The figure shows algorithms' similarity scores for 12 genuine and 8 impostor image pairs used in the May 2018 paper Face recognition accuracy of forensic examiners, superrecognizers, and face recognition algorithms (Phillips et al. [1]). The threshold (red horizontal line) is a value calibrated to give  $FMR = 0.0001$  on mugshot images. Points above the threshold correspond to pairs predicted to be genuine, and points below the threshold correspond to pairs predicted to be impostors. The figure shows whether the predicted class (genuine or impostor) matches the real class. Blue denotes a correct prediction, and red denotes incorrect. An "X" represents face detection failure in either of the images in the pair. Note that the sample size ( $n=20$ ) is small, and the figure may change substantially if larger or different sets are used. The images can be downloaded from the [Supplemental Information](#) page provided with that publication.

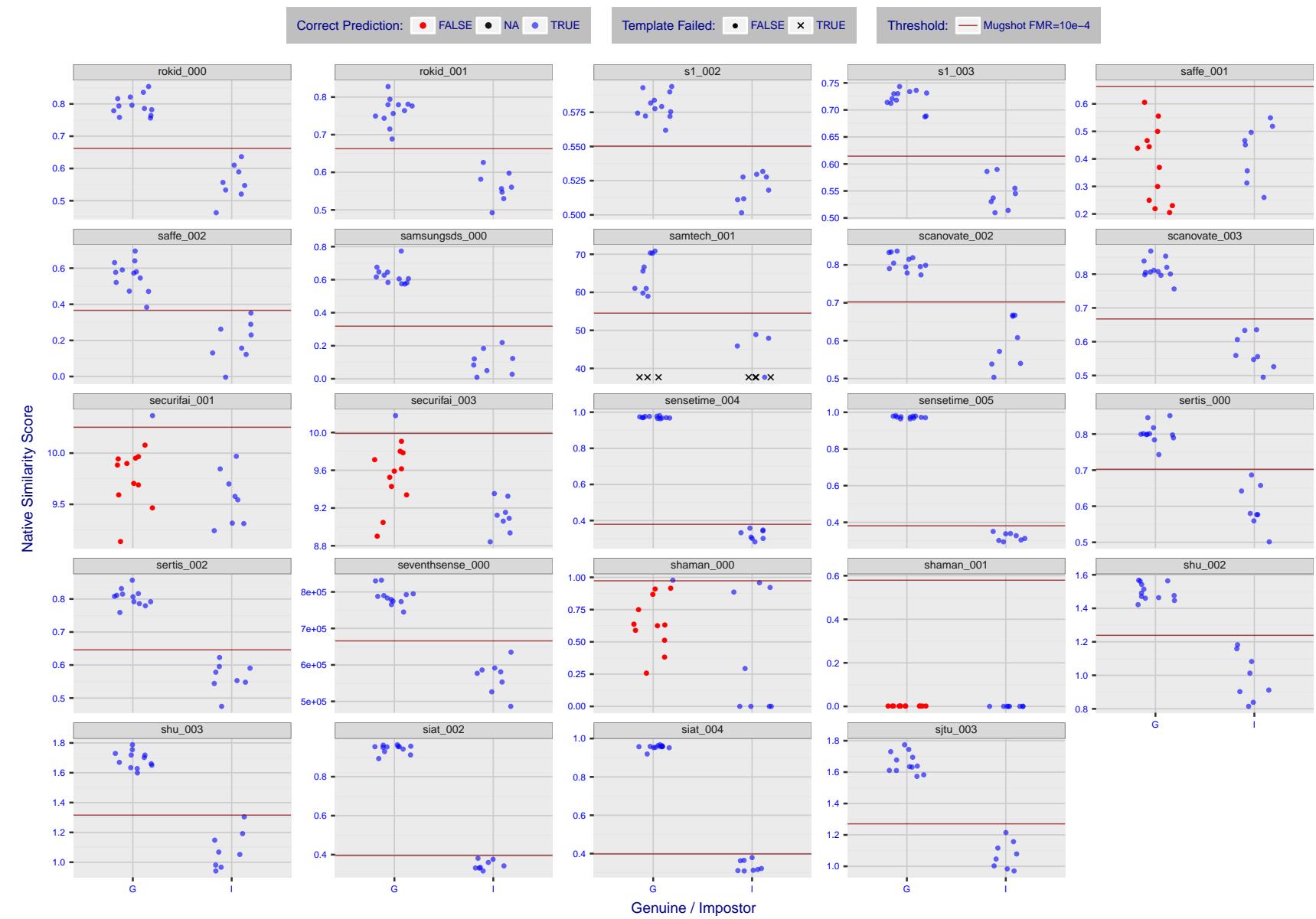


Figure 15: The figure shows algorithms' similarity scores for 12 genuine and 8 impostor image pairs used in the May 2018 paper Face recognition accuracy of forensic examiners, superrecognizers, and face recognition algorithms (Phillips et al. [1]). The threshold (red horizontal line) is a value calibrated to give  $FMR = 0.0001$  on mugshot images. Points above the threshold correspond to pairs predicted to be genuine, and points below the threshold correspond to pairs predicted to be impostors. The figure shows whether the predicted class (genuine or impostor) matches the real class. Blue denotes a correct prediction, and red denotes incorrect. An "X" represents face detection failure in either of the images in the pair. Note that the sample size ( $n=20$ ) is small, and the figure may change substantially if larger or different sets are used. The images can be downloaded from the [Supplemental Information](#) page provided with that publication.

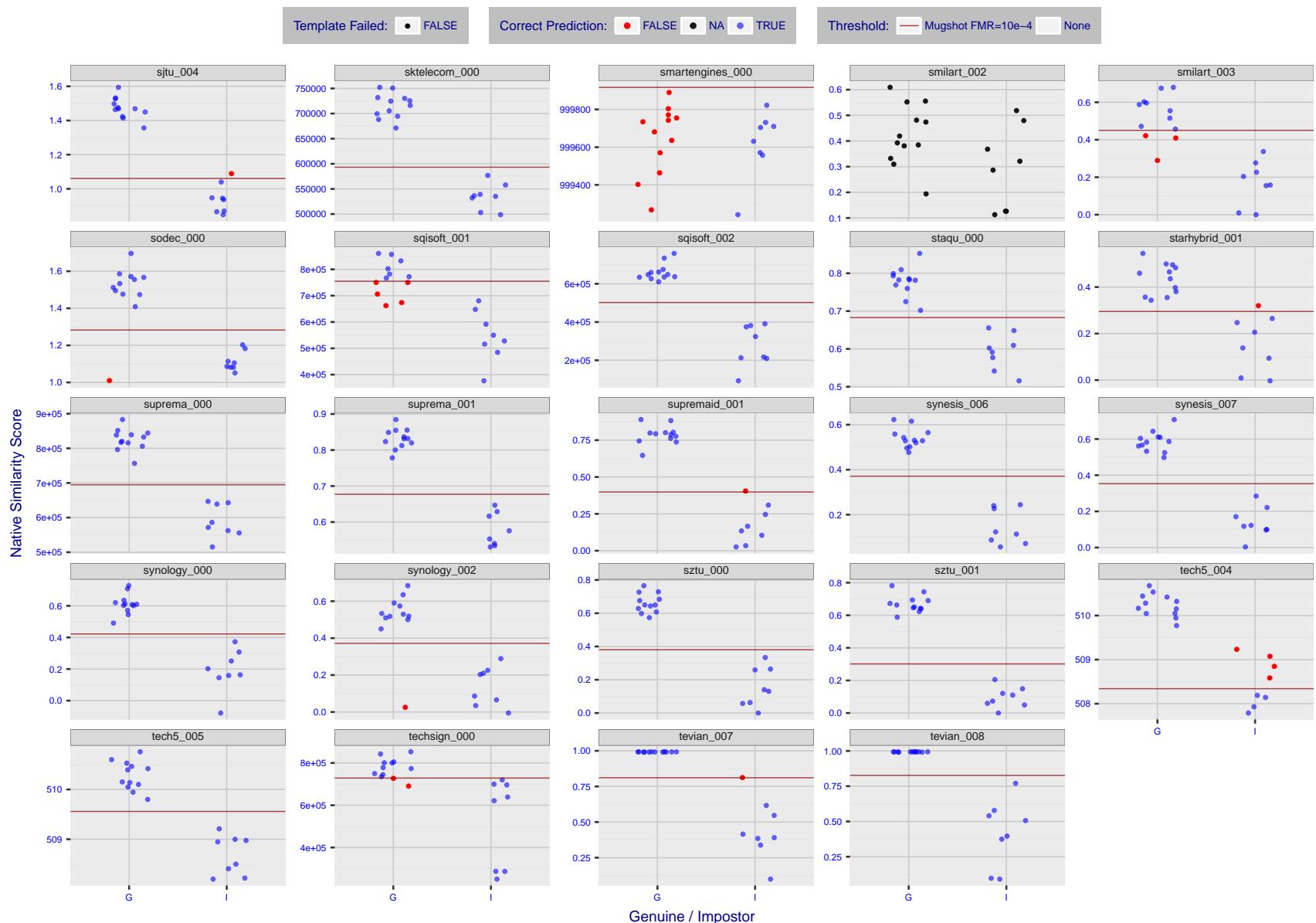


Figure 16: The figure shows algorithms' similarity scores for 12 genuine and 8 impostor image pairs used in the May 2018 paper Face recognition accuracy of forensic examiners, superrecognizers, and face recognition algorithms (Phillips et al. [1]). The threshold (red horizontal line) is a value calibrated to give  $FMR = 0.0001$  on mugshot images. Points above the threshold correspond to pairs predicted to be genuine, and points below the threshold correspond to pairs predicted to be impostors. The figure shows whether the predicted class (genuine or impostor) matches the real class. Blue denotes a correct prediction, and red denotes incorrect. An "X" represents face detection failure in either of the images in the pair. Note that the sample size ( $n=20$ ) is small, and the figure may change substantially if larger or different sets are used. The images can be downloaded from the [Supplemental Information](#) page provided with that publication.

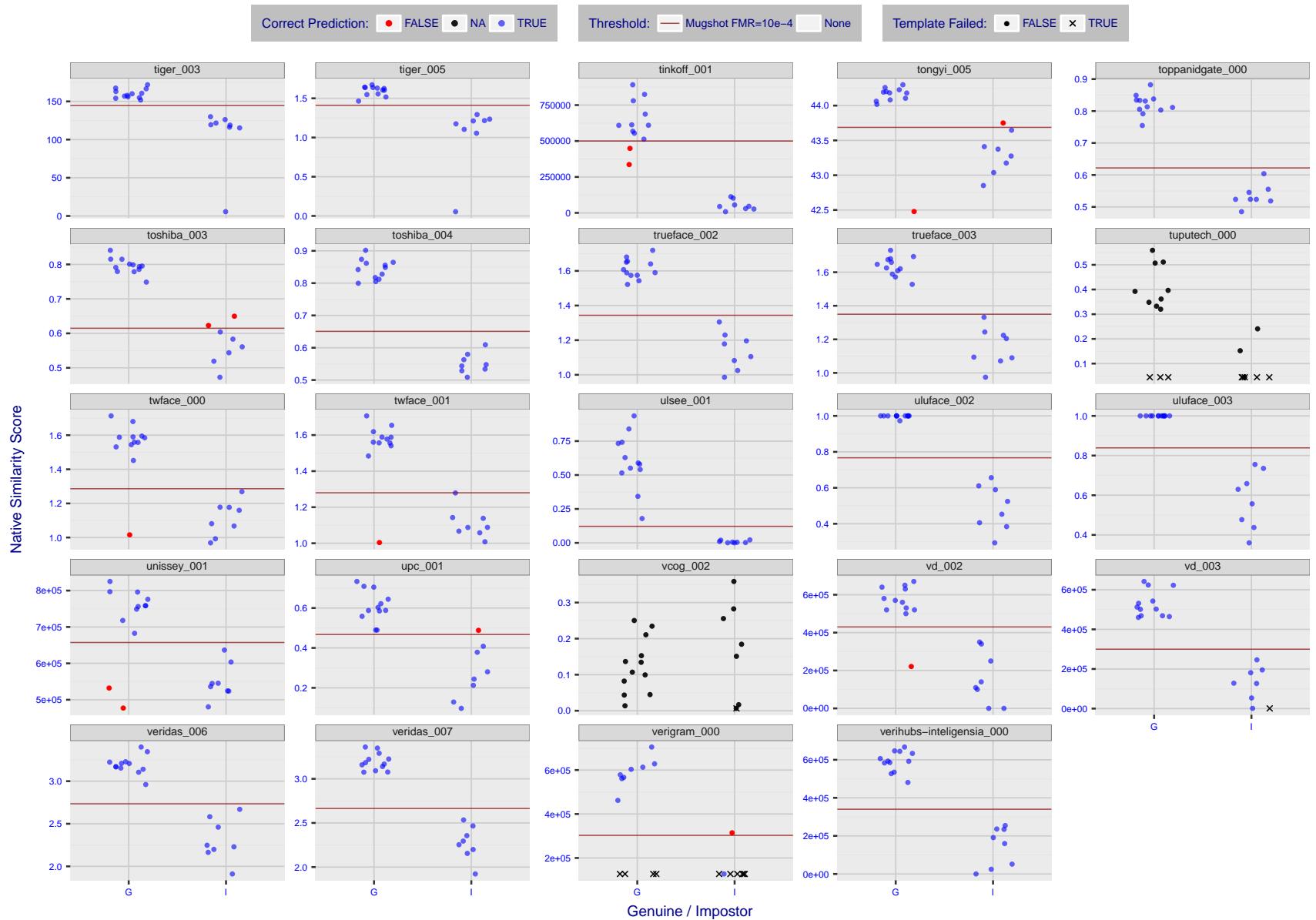


Figure 17: The figure shows algorithms' similarity scores for 12 genuine and 8 impostor image pairs used in the May 2018 paper Face recognition accuracy of forensic examiners, superrecognizers, and face recognition algorithms (Phillips et al. [1]). The threshold (red horizontal line) is a value calibrated to give  $FMR = 0.0001$  on mugshot images. Points above the threshold correspond to pairs predicted to be genuine, and points below the threshold correspond to pairs predicted to be impostors. The figure shows whether the predicted class (genuine or impostor) matches the real class. Blue denotes a correct prediction, and red denotes incorrect. An "X" represents face detection failure in either of the images in the pair. Note that the sample size ( $n=20$ ) is small, and the figure may change substantially if larger or different sets are used. The images can be downloaded from the [Supplemental Information](#) page provided with that publication.

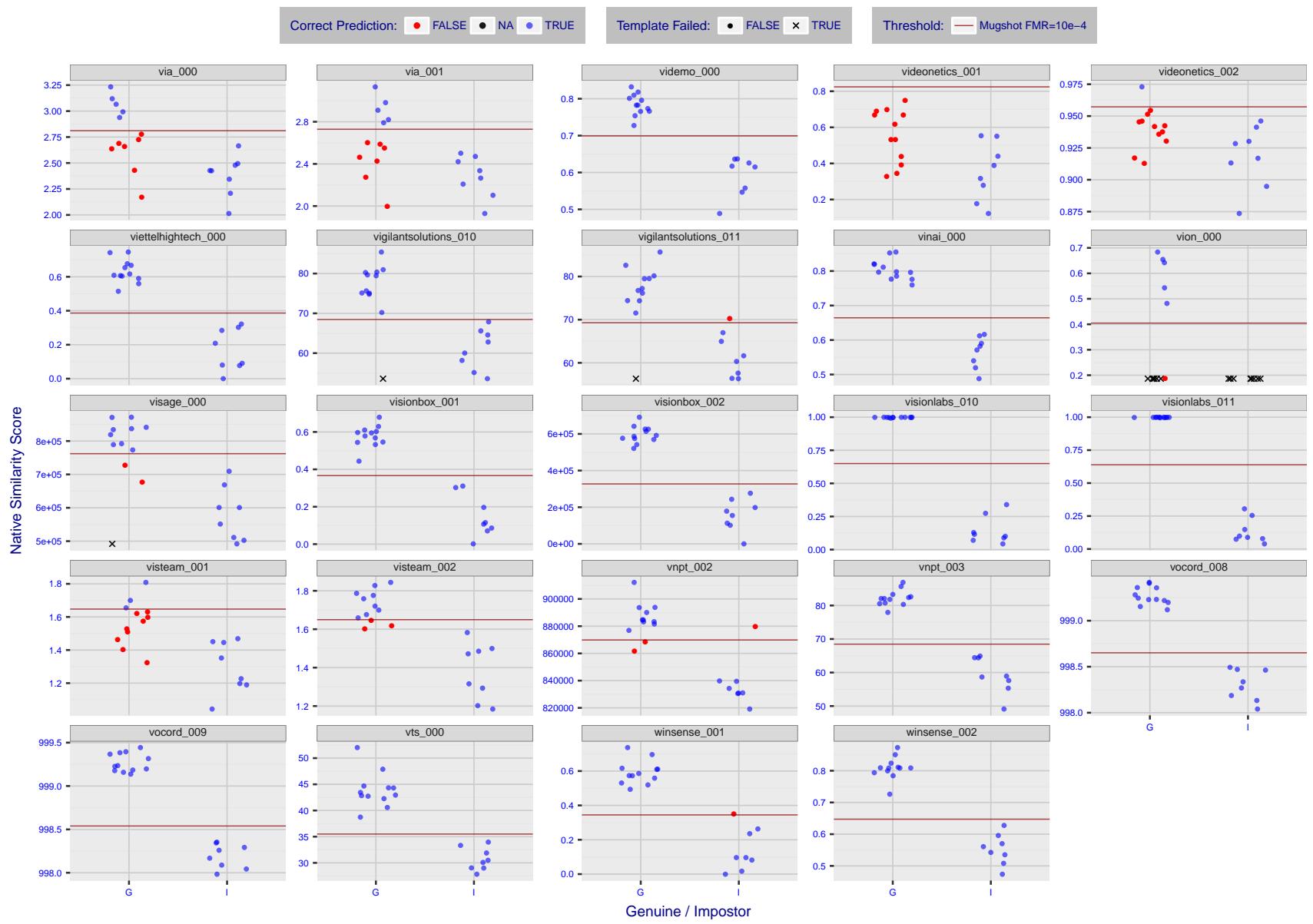


Figure 18: The figure shows algorithms' similarity scores for 12 genuine and 8 impostor image pairs used in the May 2018 paper Face recognition accuracy of forensic examiners, superrecognizers, and face recognition algorithms (Phillips et al. [1]). The threshold (red horizontal line) is a value calibrated to give  $FMR = 0.0001$  on mugshot images. Points above the threshold correspond to pairs predicted to be genuine, and points below the threshold correspond to pairs predicted to be impostors. The figure shows whether the predicted class (genuine or impostor) matches the real class. Blue denotes a correct prediction, and red denotes incorrect. An "X" represents face detection failure in either of the images in the pair. Note that the sample size ( $n=20$ ) is small, and the figure may change substantially if larger or different sets are used. The images can be downloaded from the [Supplemental Information](#) page provided with that publication.

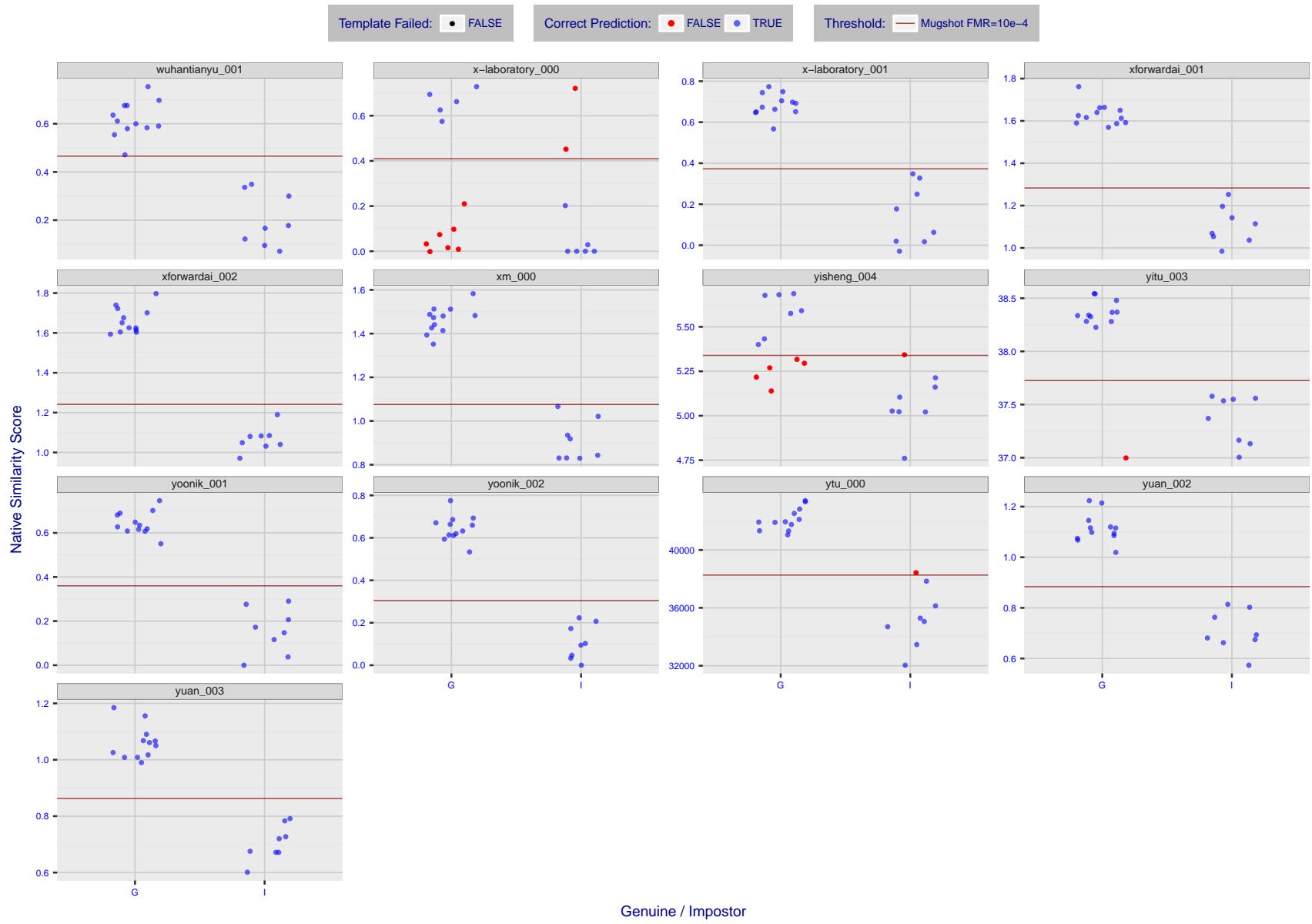


Figure 19: The figure shows algorithms' similarity scores for 12 genuine and 8 impostor image pairs used in the May 2018 paper Face recognition accuracy of forensic examiners, superrecognizers, and face recognition algorithms (Phillips et al. [1]). The threshold (red horizontal line) is a value calibrated to give  $FMR = 0.0001$  on mugshot images. Points above the threshold correspond to pairs predicted to be genuine, and points below the threshold correspond to pairs predicted to be impostors. The figure shows whether the predicted class (genuine or impostor) matches the real class. Blue denotes a correct prediction, and red denotes incorrect. An "X" represents face detection failure in either of the images in the pair. Note that the sample size ( $n=20$ ) is small, and the figure may change substantially if larger or different sets are used. The images can be downloaded from the [Supplemental Information](#) page provided with that publication.

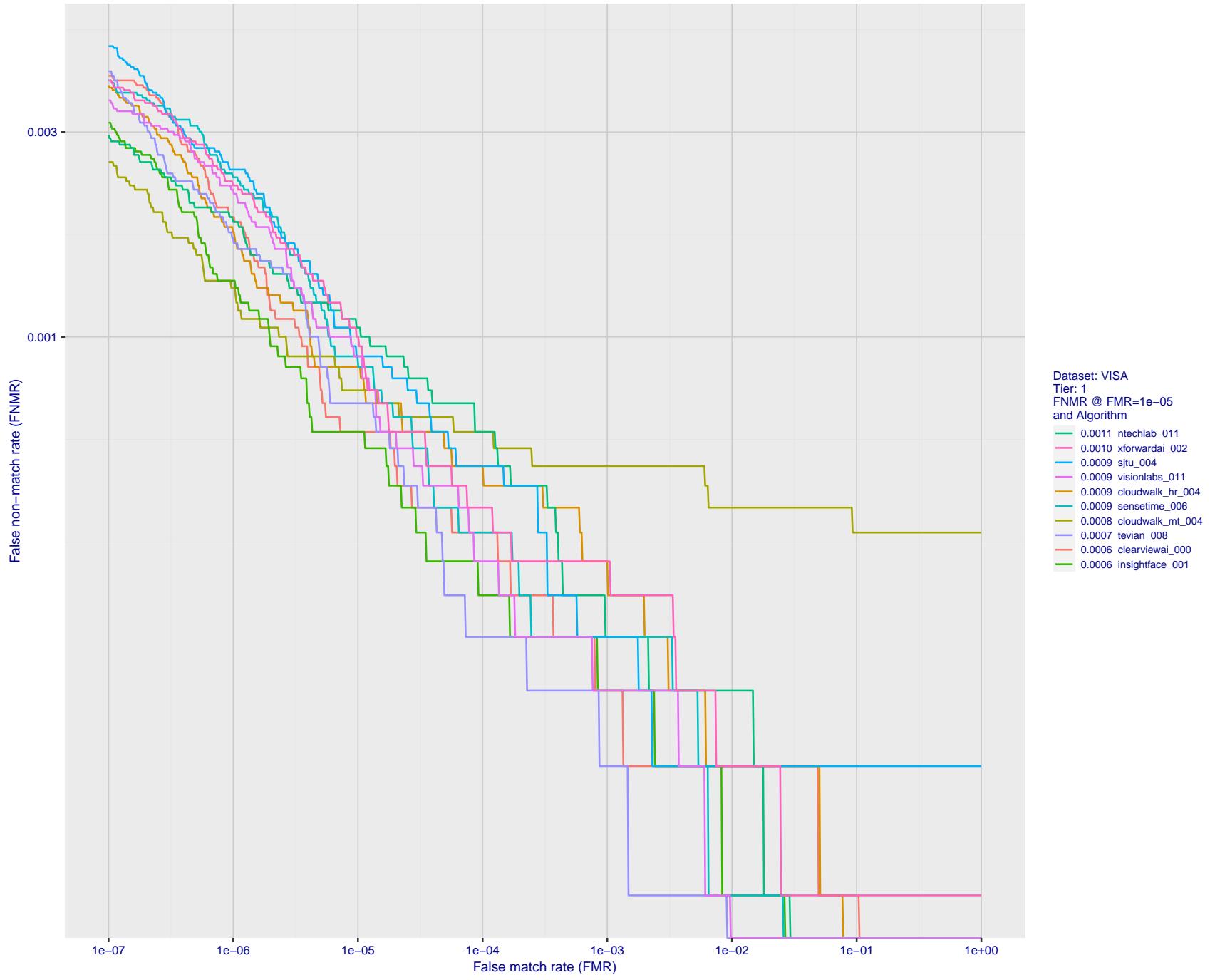


Figure 20: For the visa images, detection error tradeoff (DET) characteristics showing false non-match rate vs. false match rate plotted parametrically on threshold,  $T$ . The scales are logarithmic in order to show many decades of FMR.

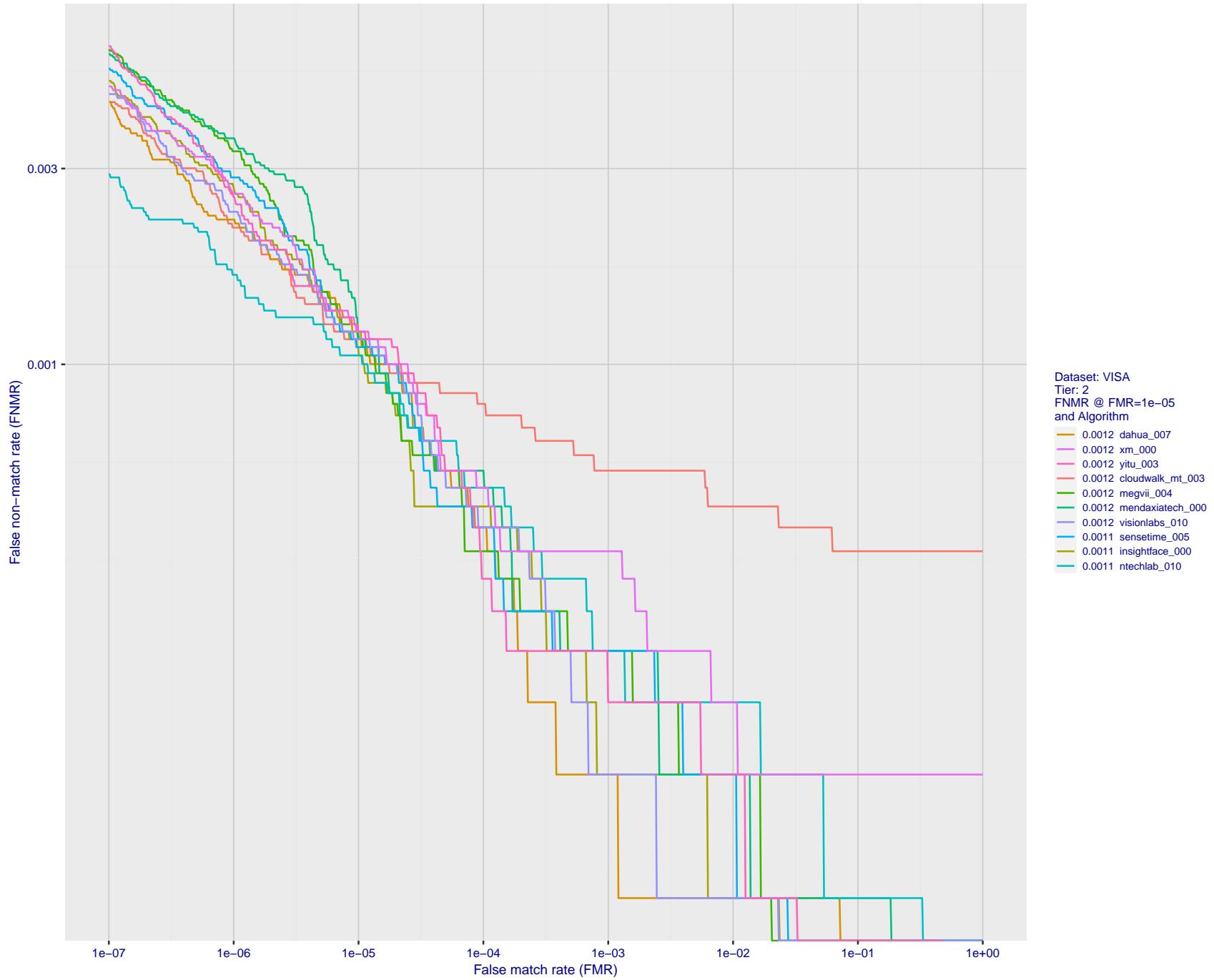


Figure 21: For the visa images, detection error tradeoff (DET) characteristics showing false non-match rate vs. false match rate plotted parametrically on threshold,  $T$ . The scales are logarithmic in order to show many decades of FMR.

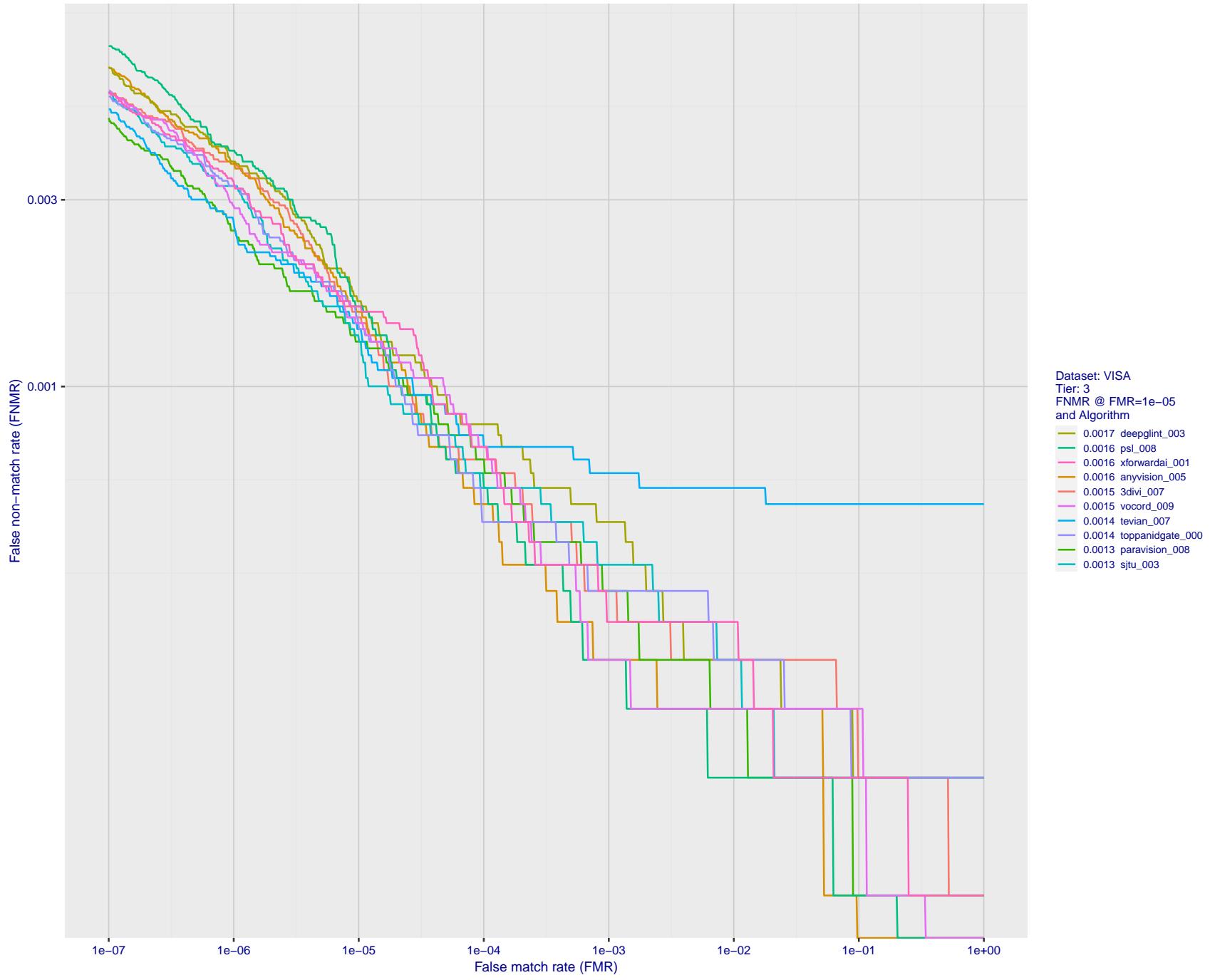


Figure 22: For the visa images, detection error tradeoff (DET) characteristics showing false non-match rate vs. false match rate plotted parametrically on threshold,  $T$ . The scales are logarithmic in order to show many decades of FMR.

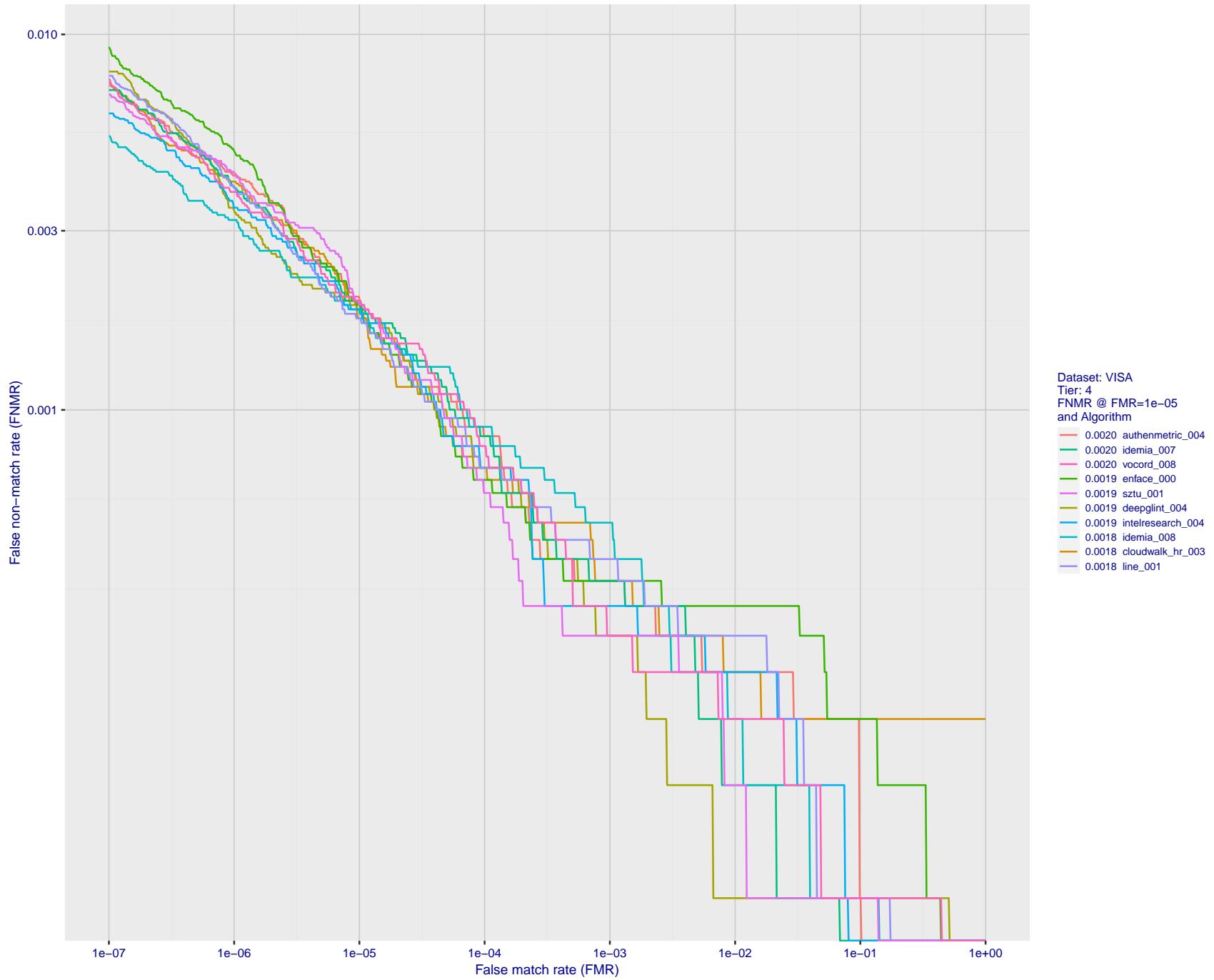


Figure 23: For the visa images, detection error tradeoff (DET) characteristics showing false non-match rate vs. false match rate plotted parametrically on threshold,  $T$ . The scales are logarithmic in order to show many decades of FMR.

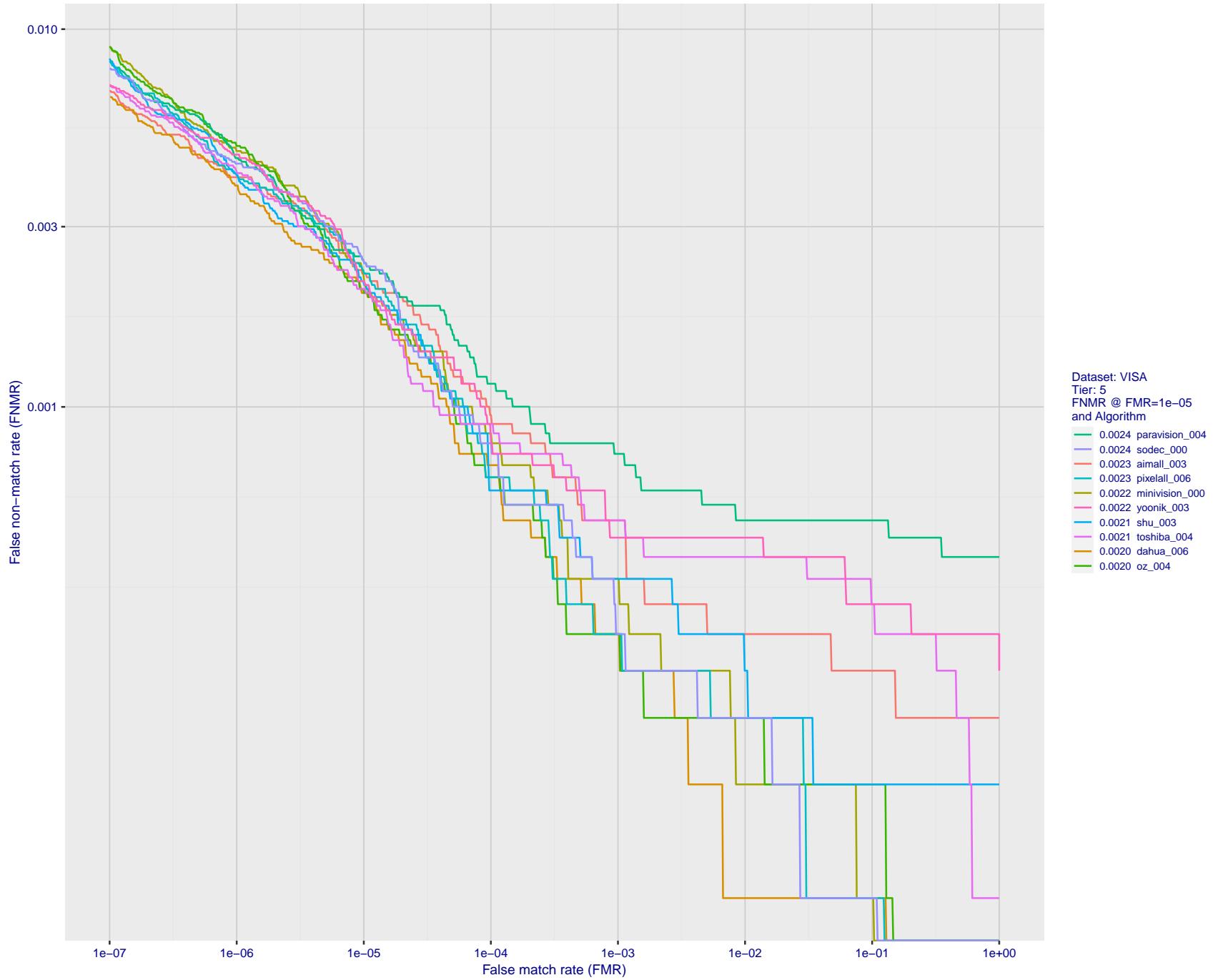


Figure 24: For the visa images, detection error tradeoff (DET) characteristics showing false non-match rate vs. false match rate plotted parametrically on threshold,  $T$ . The scales are logarithmic in order to show many decades of FMR.

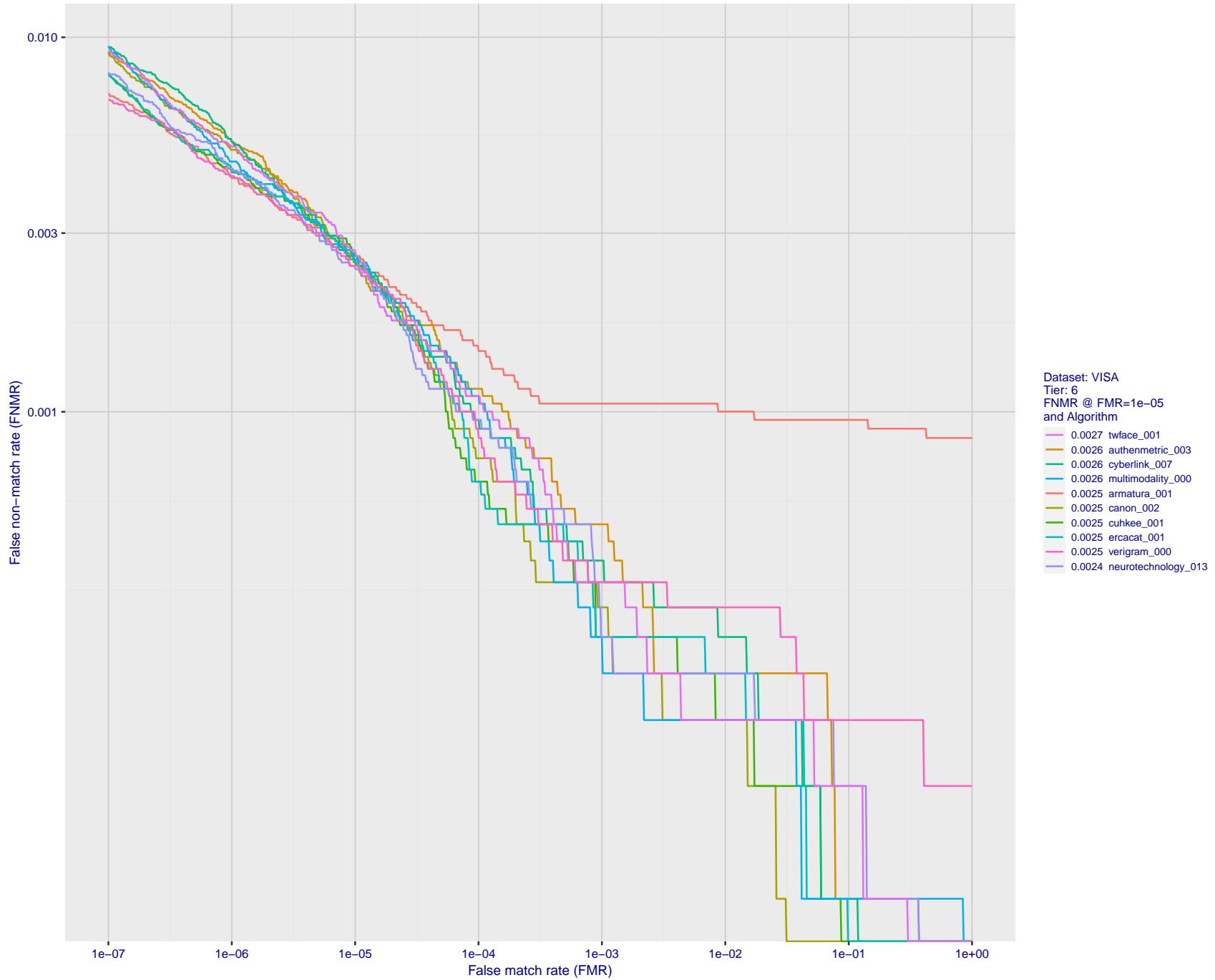


Figure 25: For the visa images, detection error tradeoff (DET) characteristics showing false non-match rate vs. false match rate plotted parametrically on threshold,  $T$ . The scales are logarithmic in order to show many decades of FMR.

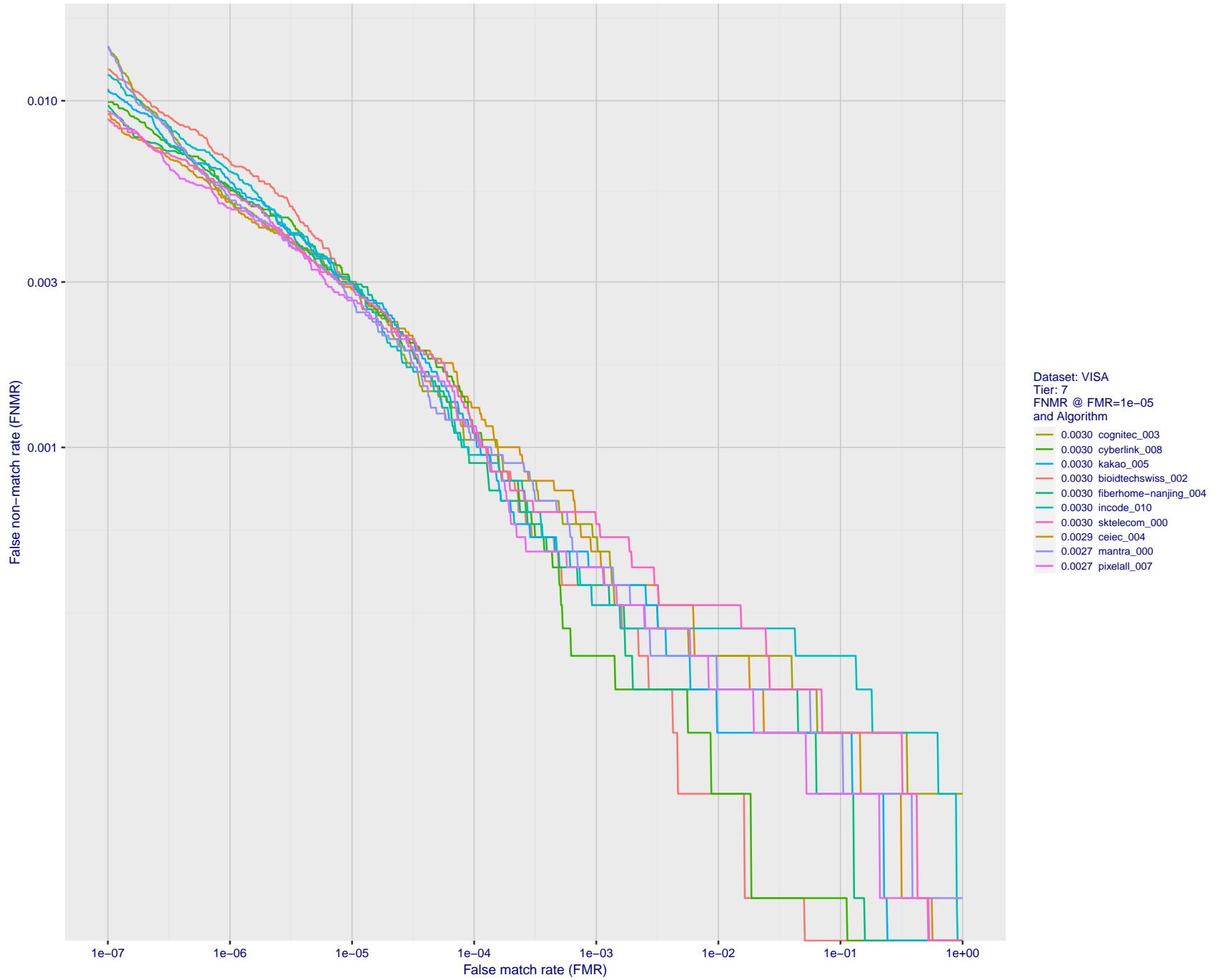


Figure 26: For the visa images, detection error tradeoff (DET) characteristics showing false non-match rate vs. false match rate plotted parametrically on threshold,  $T$ . The scales are logarithmic in order to show many decades of FMR.

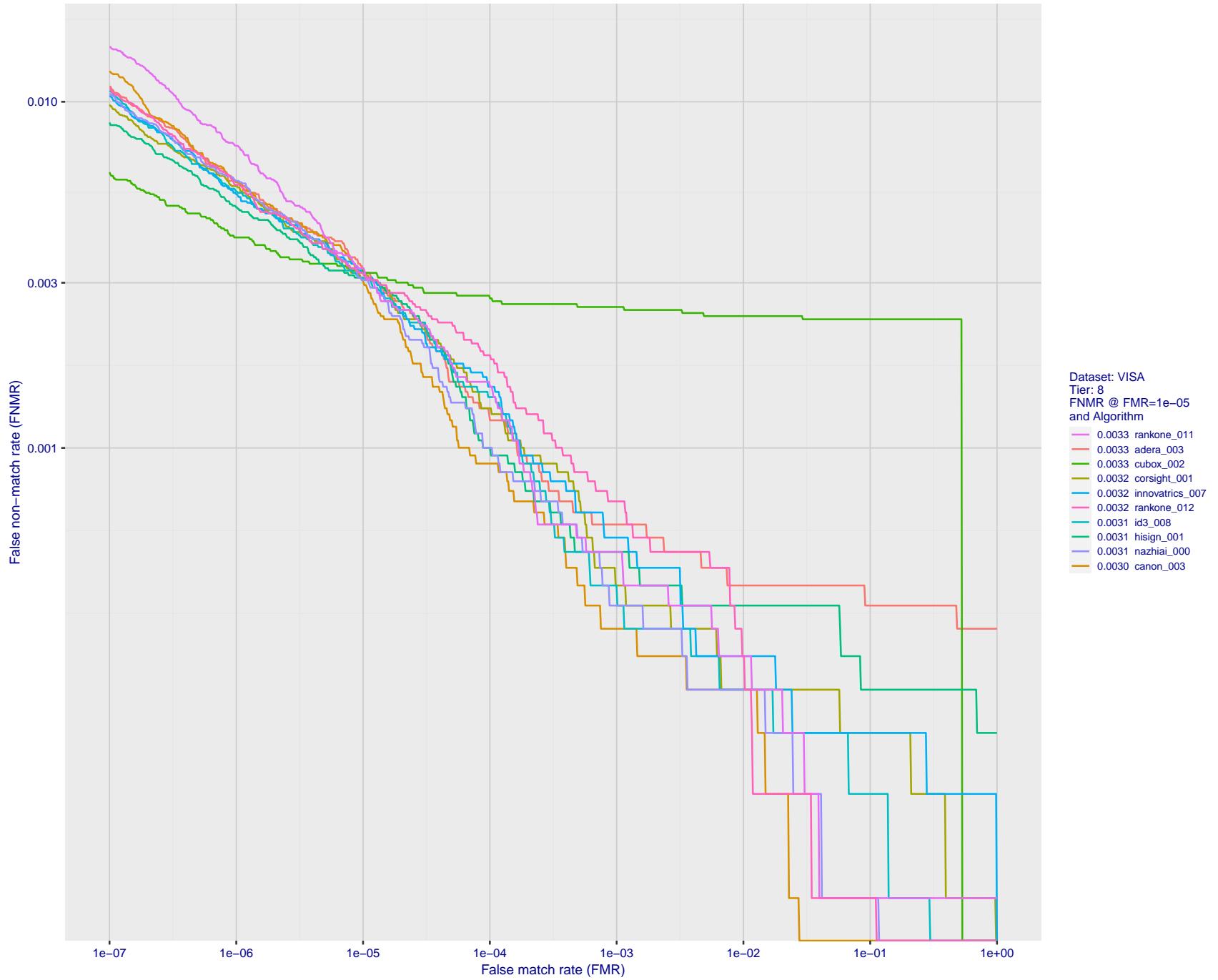


Figure 27: For the visa images, detection error tradeoff (DET) characteristics showing false non-match rate vs. false match rate plotted parametrically on threshold,  $T$ . The scales are logarithmic in order to show many decades of FMR.

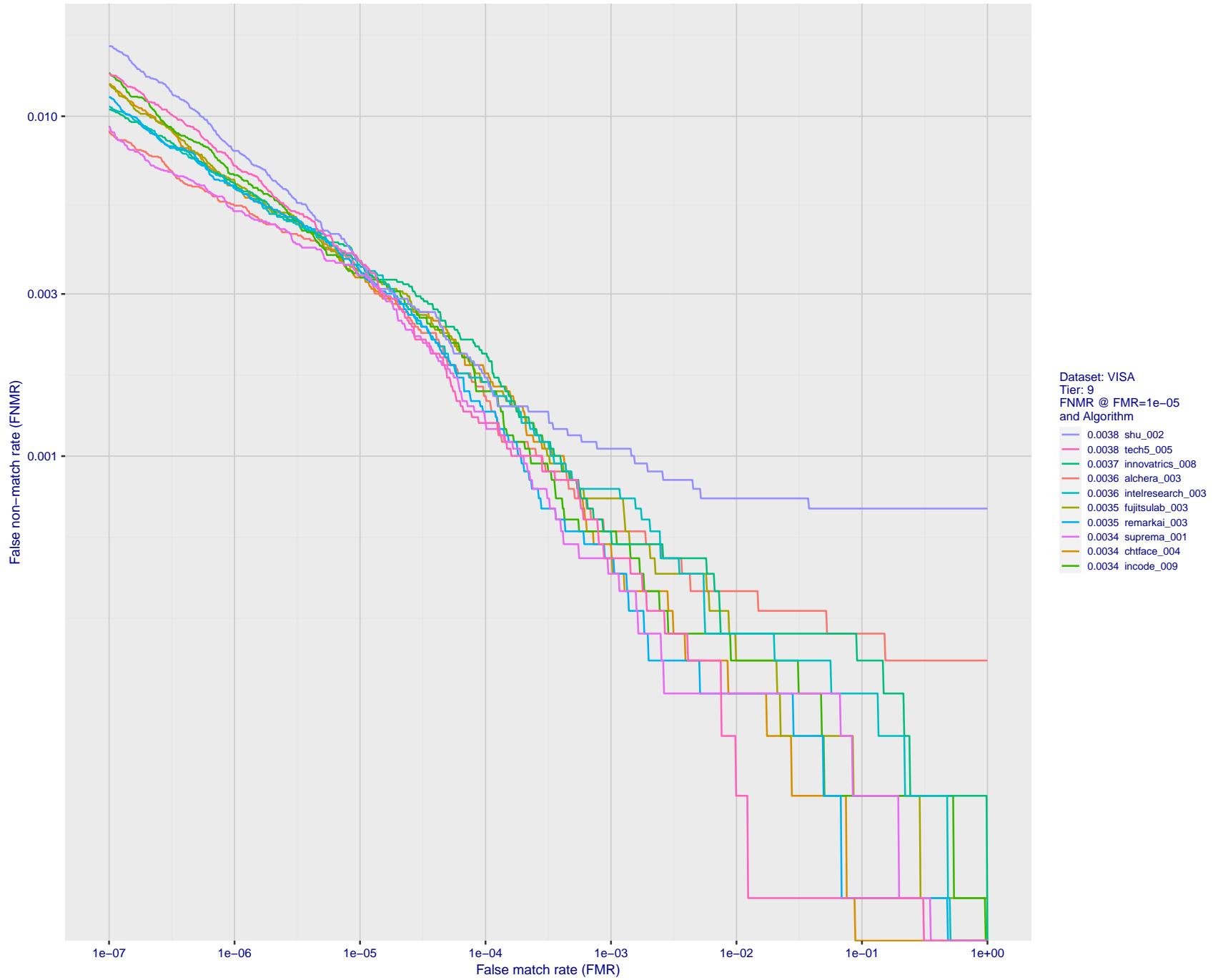


Figure 28: For the visa images, detection error tradeoff (DET) characteristics showing false non-match rate vs. false match rate plotted parametrically on threshold,  $T$ . The scales are logarithmic in order to show many decades of FMR.

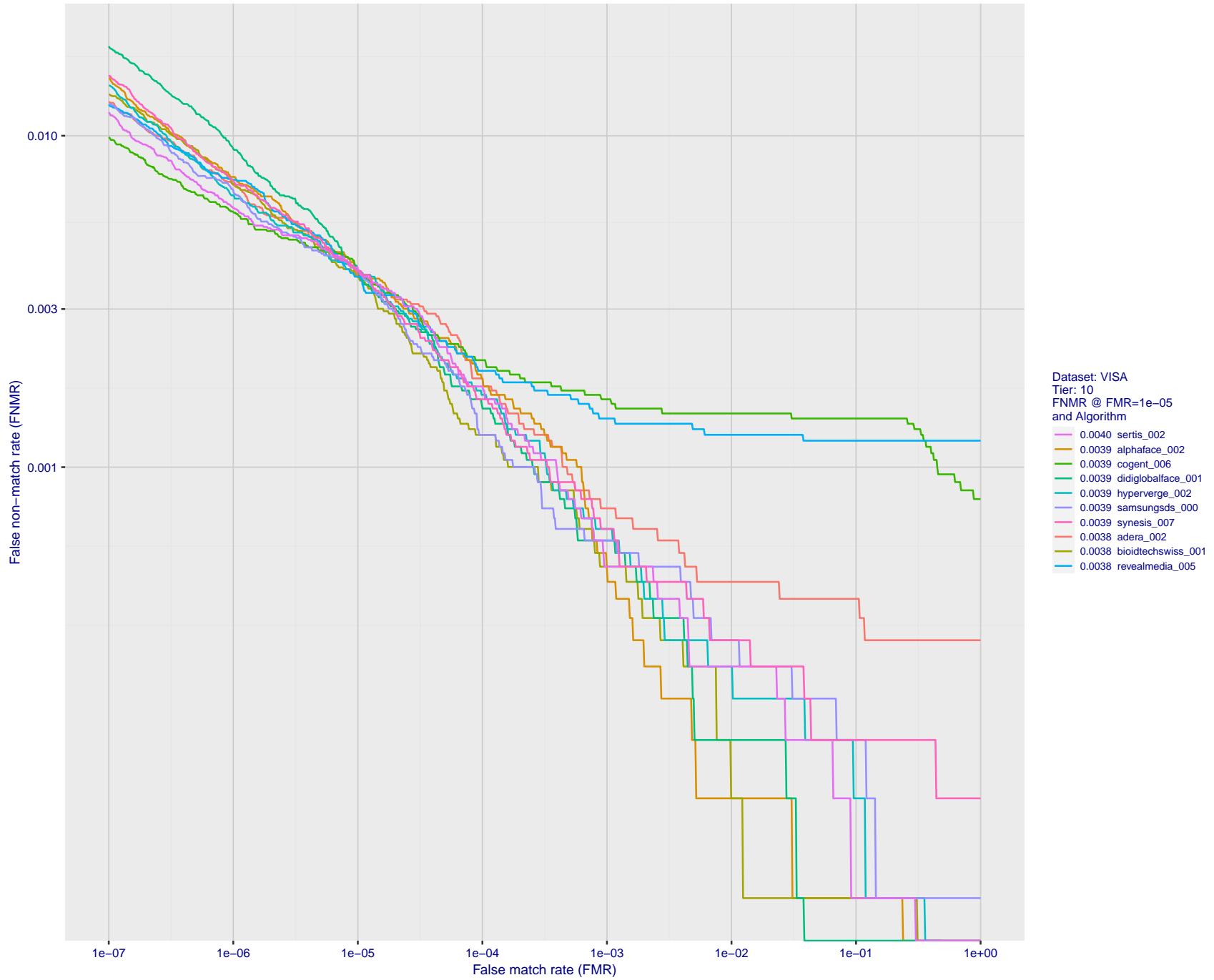


Figure 29: For the visa images, detection error tradeoff (DET) characteristics showing false non-match rate vs. false match rate plotted parametrically on threshold,  $T$ . The scales are logarithmic in order to show many decades of FMR.

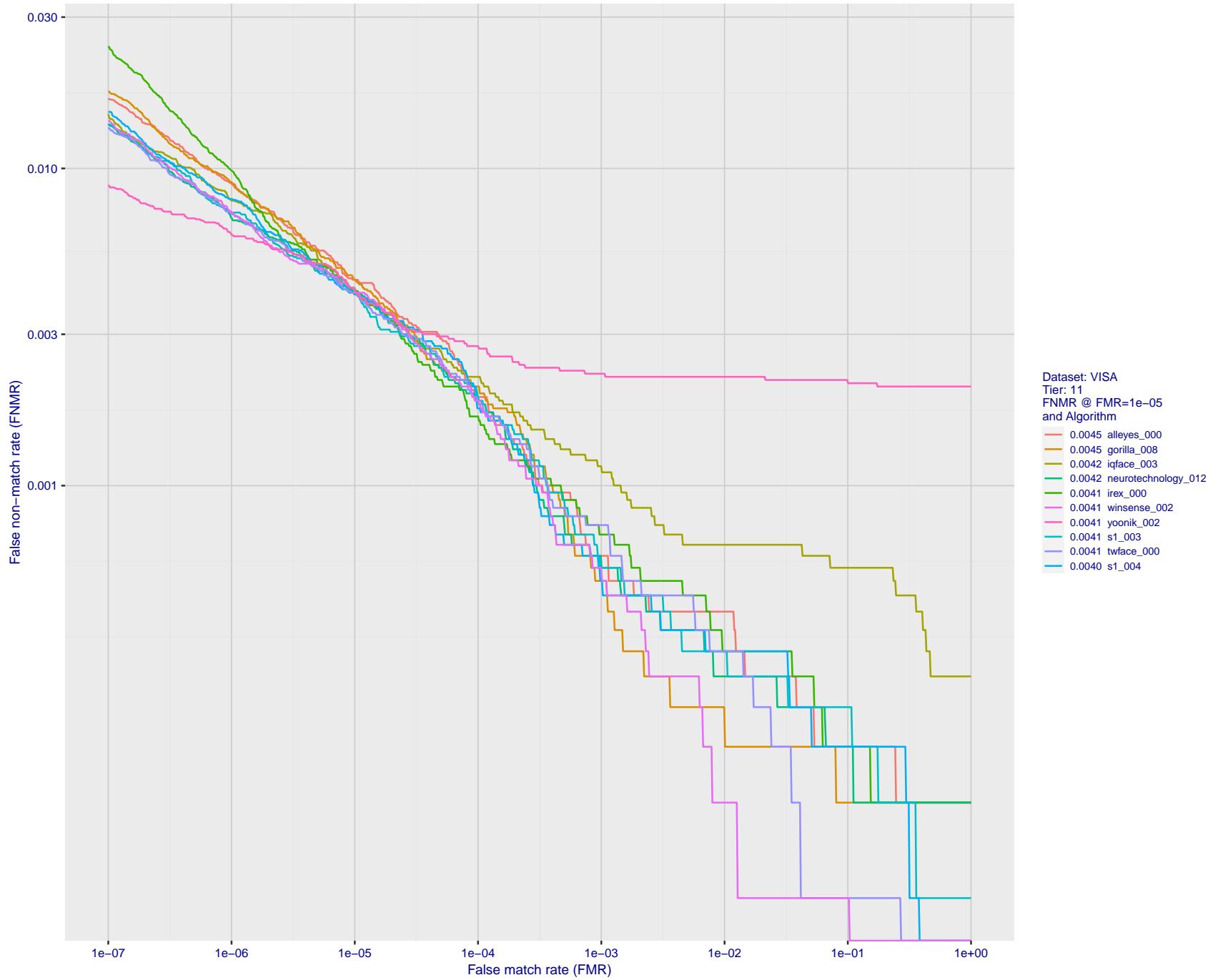


Figure 30: For the visa images, detection error tradeoff (DET) characteristics showing false non-match rate vs. false match rate plotted parametrically on threshold,  $T$ . The scales are logarithmic in order to show many decades of FMR.

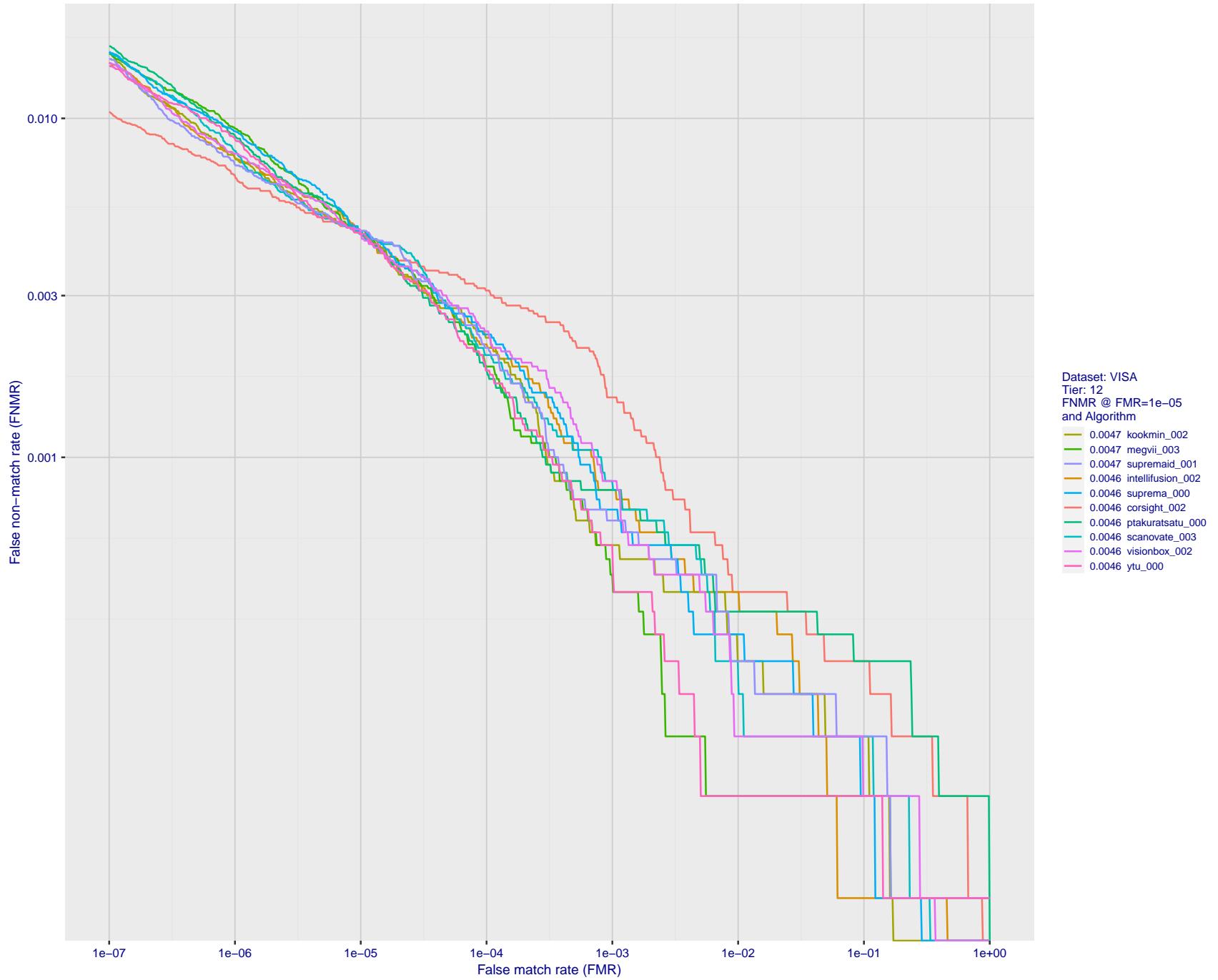


Figure 31: For the visa images, detection error tradeoff (DET) characteristics showing false non-match rate vs. false match rate plotted parametrically on threshold,  $T$ . The scales are logarithmic in order to show many decades of FMR.

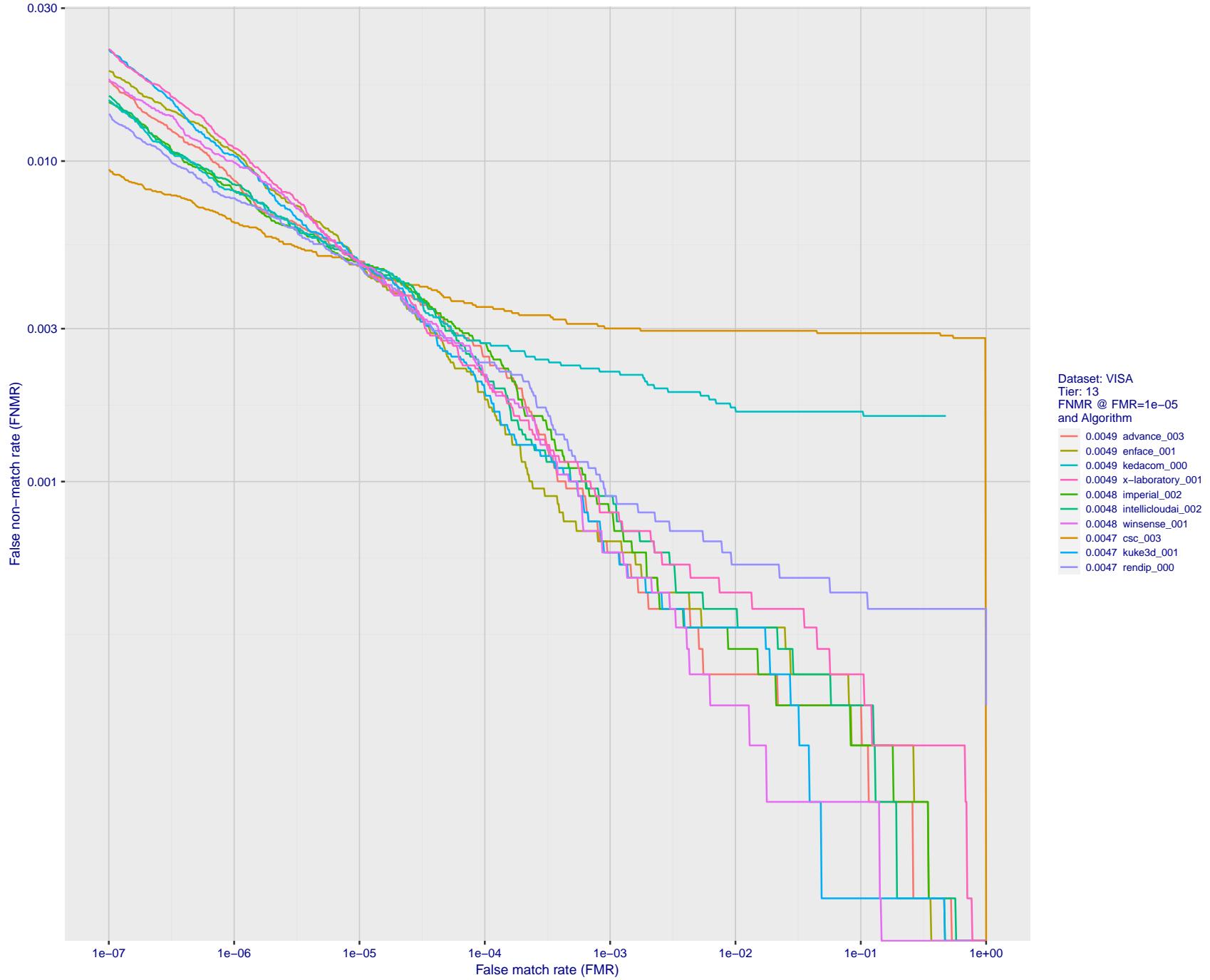


Figure 32: For the visa images, detection error tradeoff (DET) characteristics showing false non-match rate vs. false match rate plotted parametrically on threshold,  $T$ . The scales are logarithmic in order to show many decades of FMR.

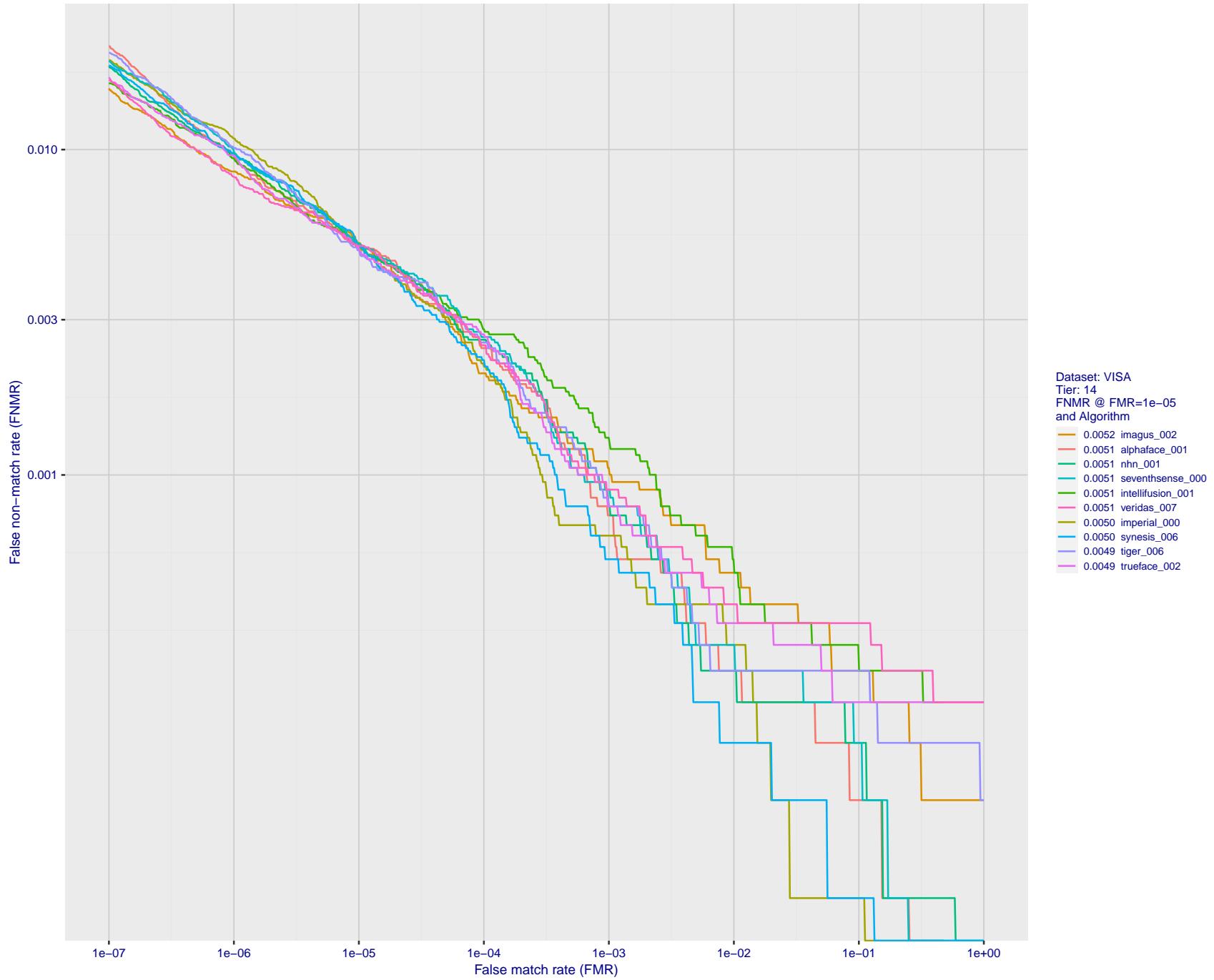


Figure 33: For the visa images, detection error tradeoff (DET) characteristics showing false non-match rate vs. false match rate plotted parametrically on threshold,  $T$ . The scales are logarithmic in order to show many decades of FMR.

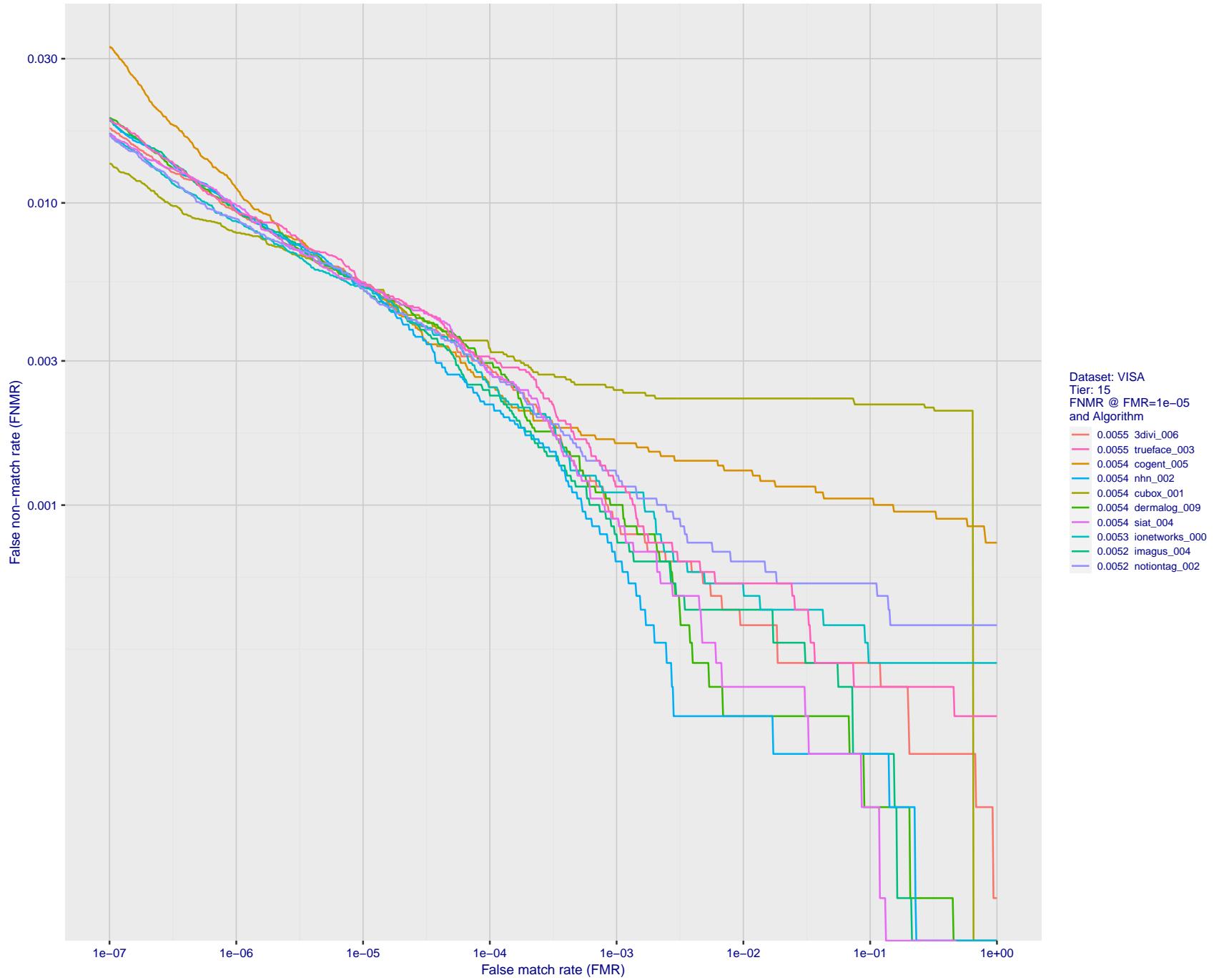


Figure 34: For the visa images, detection error tradeoff (DET) characteristics showing false non-match rate vs. false match rate plotted parametrically on threshold,  $T$ . The scales are logarithmic in order to show many decades of FMR.

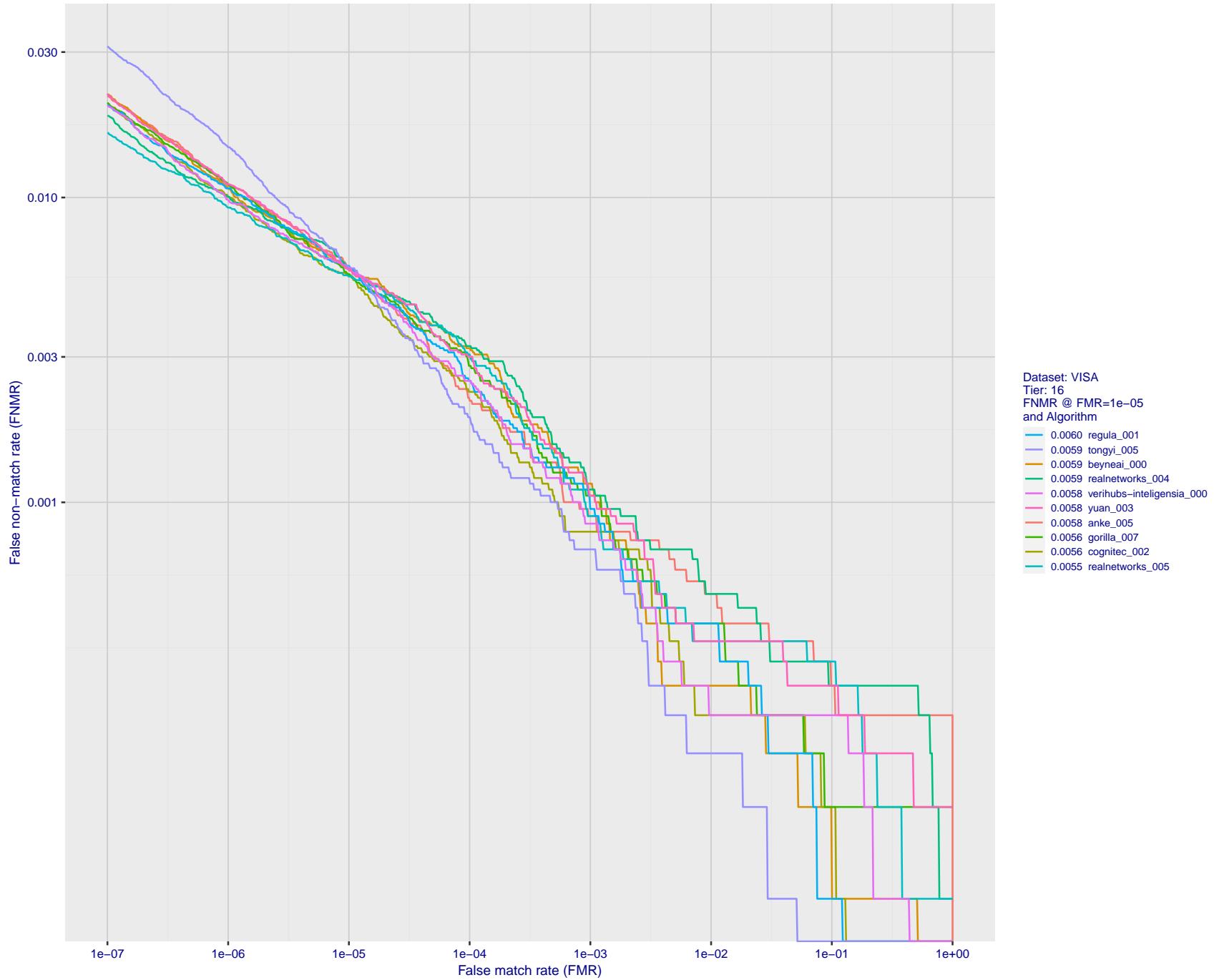


Figure 35: For the visa images, detection error tradeoff (DET) characteristics showing false non-match rate vs. false match rate plotted parametrically on threshold,  $T$ . The scales are logarithmic in order to show many decades of FMR.

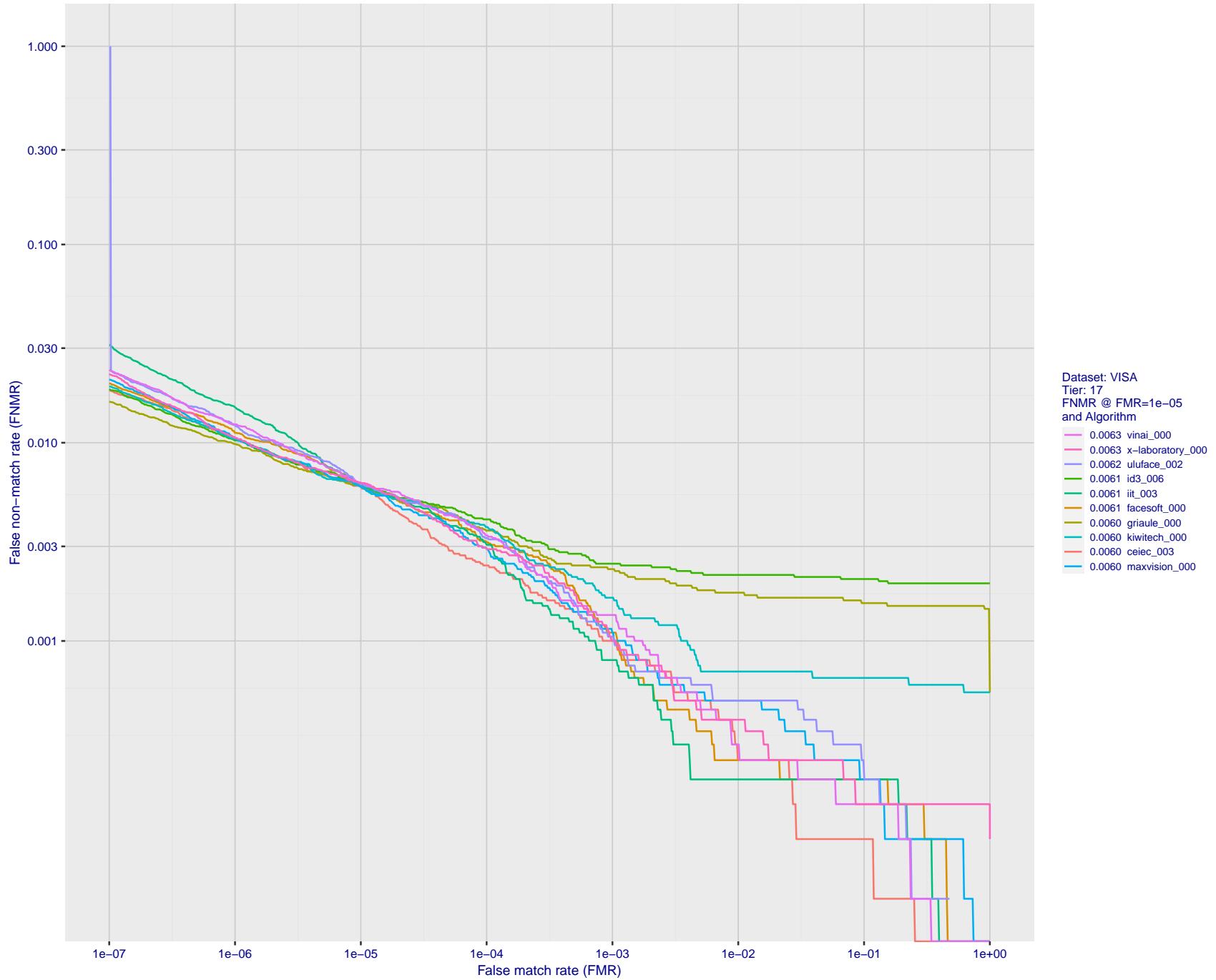


Figure 36: For the visa images, detection error tradeoff (DET) characteristics showing false non-match rate vs. false match rate plotted parametrically on threshold,  $T$ . The scales are logarithmic in order to show many decades of FMR.

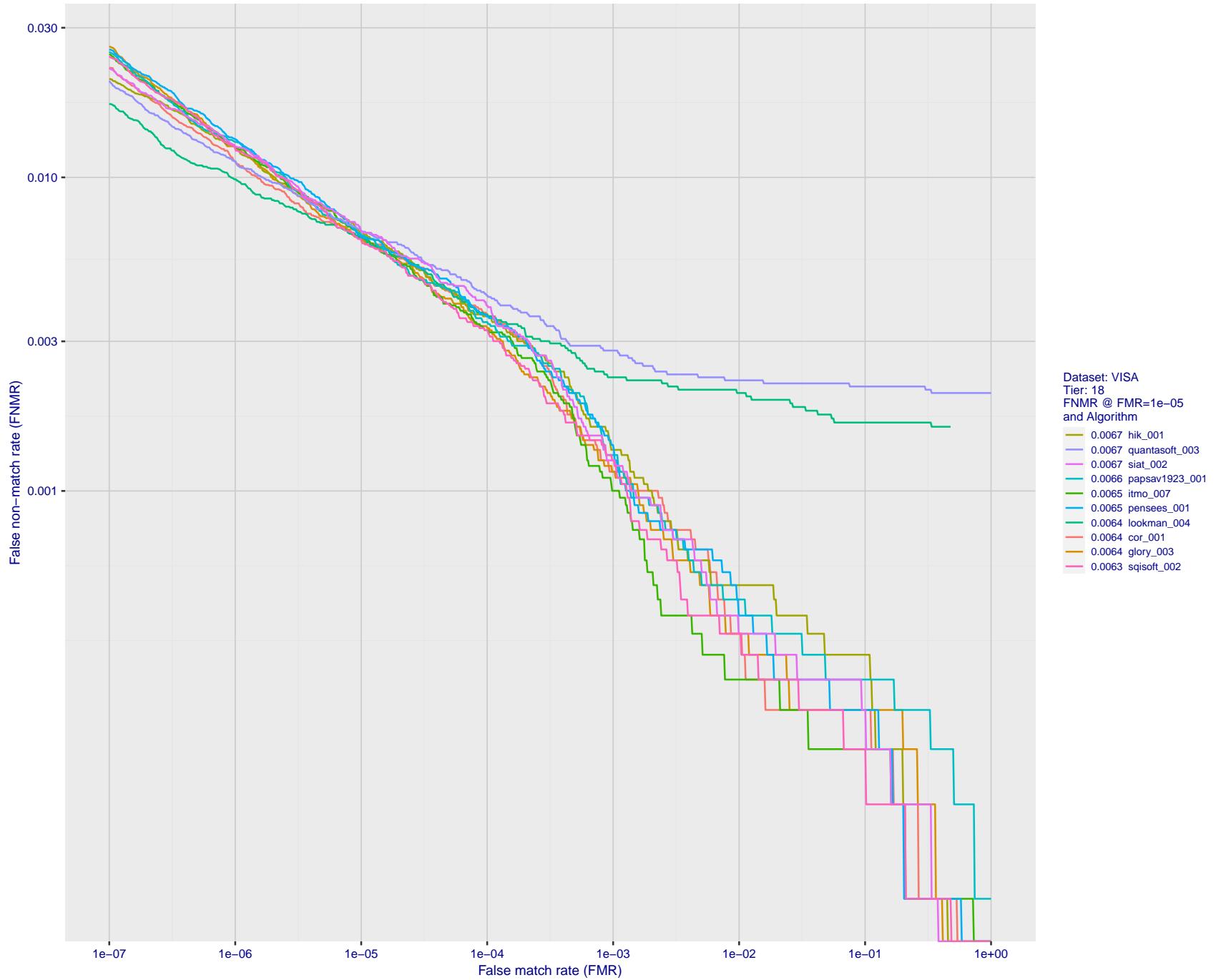


Figure 37: For the visa images, detection error tradeoff (DET) characteristics showing false non-match rate vs. false match rate plotted parametrically on threshold,  $T$ . The scales are logarithmic in order to show many decades of FMR.

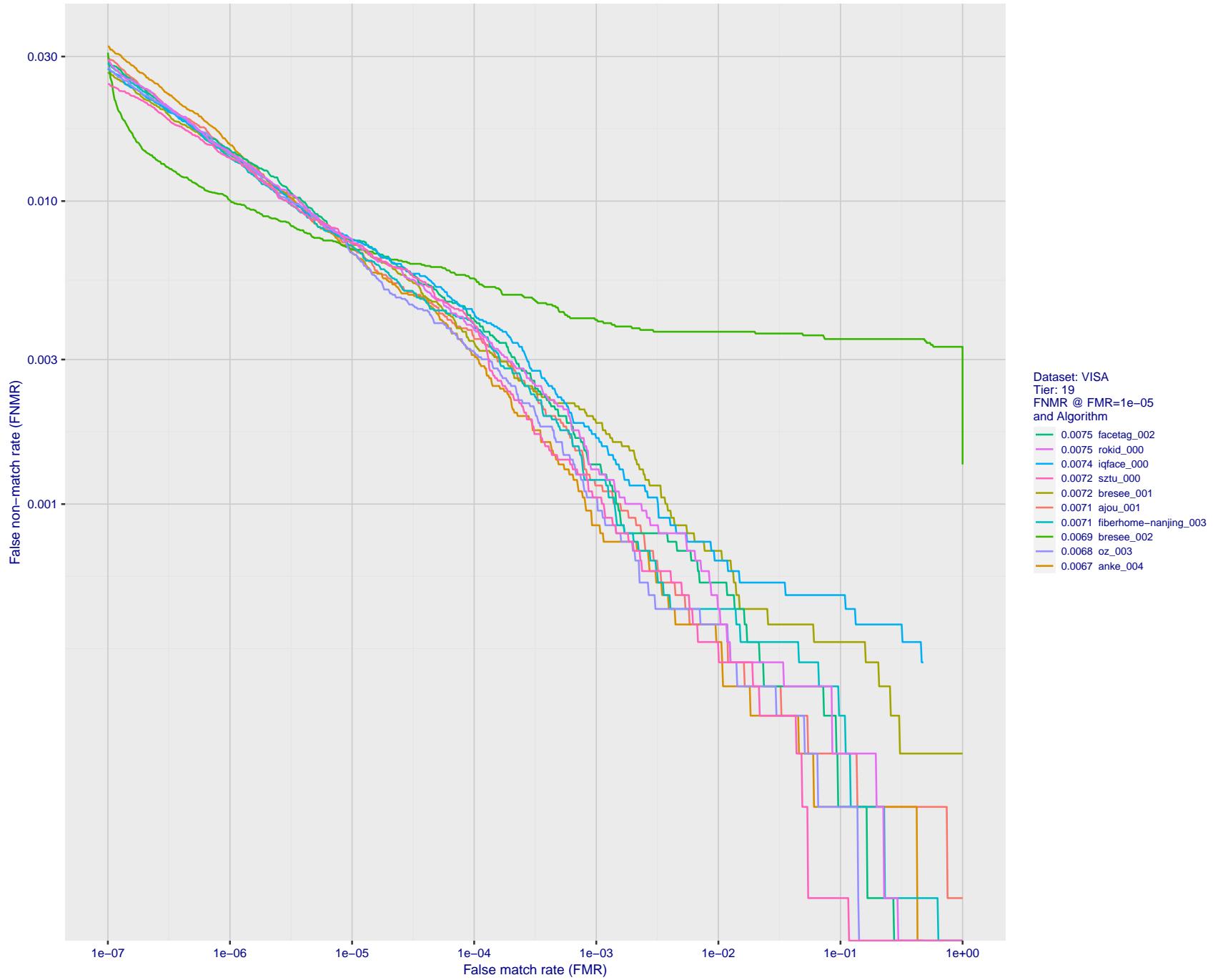


Figure 38: For the visa images, detection error tradeoff (DET) characteristics showing false non-match rate vs. false match rate plotted parametrically on threshold,  $T$ . The scales are logarithmic in order to show many decades of FMR.

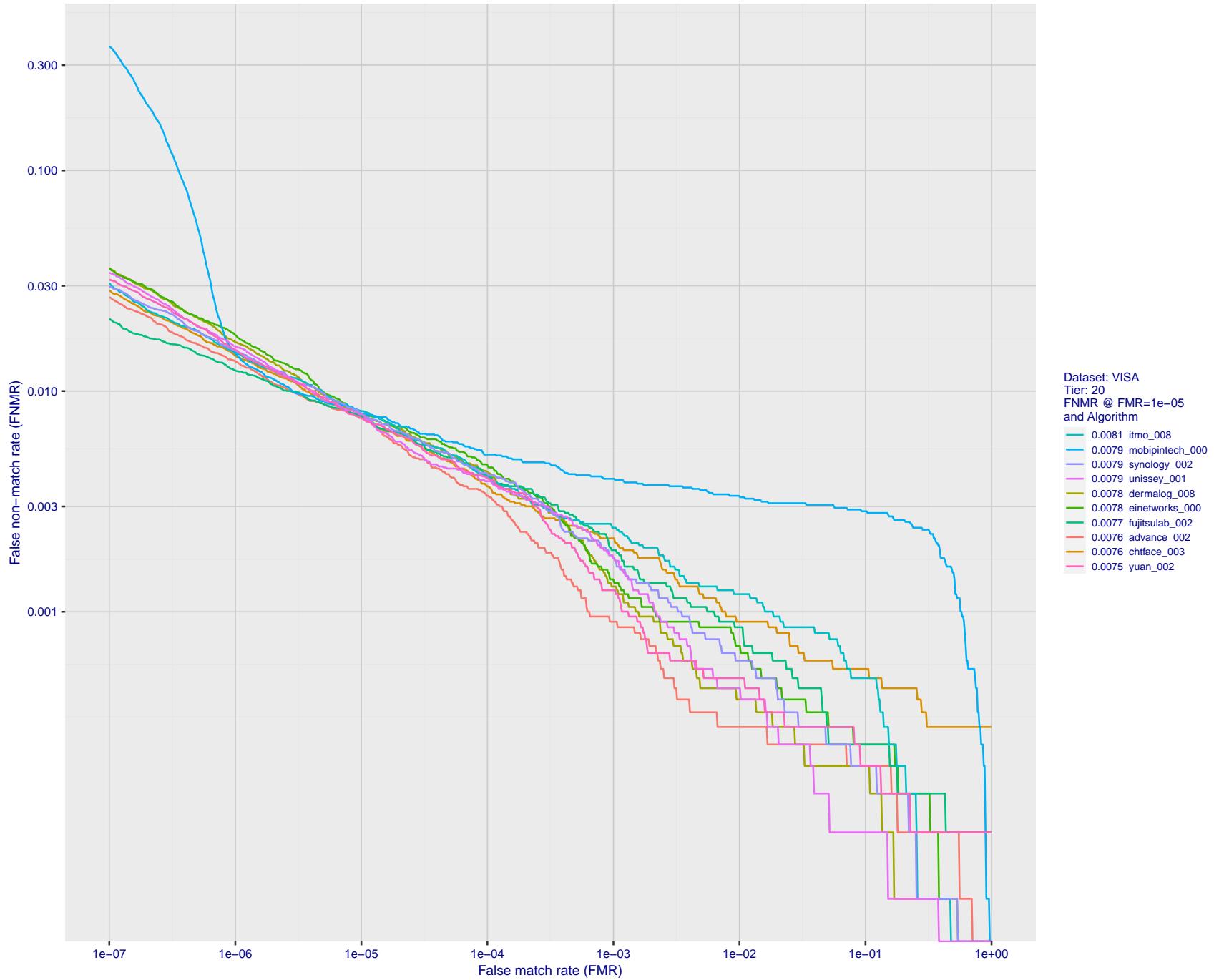


Figure 39: For the visa images, detection error tradeoff (DET) characteristics showing false non-match rate vs. false match rate plotted parametrically on threshold,  $T$ . The scales are logarithmic in order to show many decades of FMR.

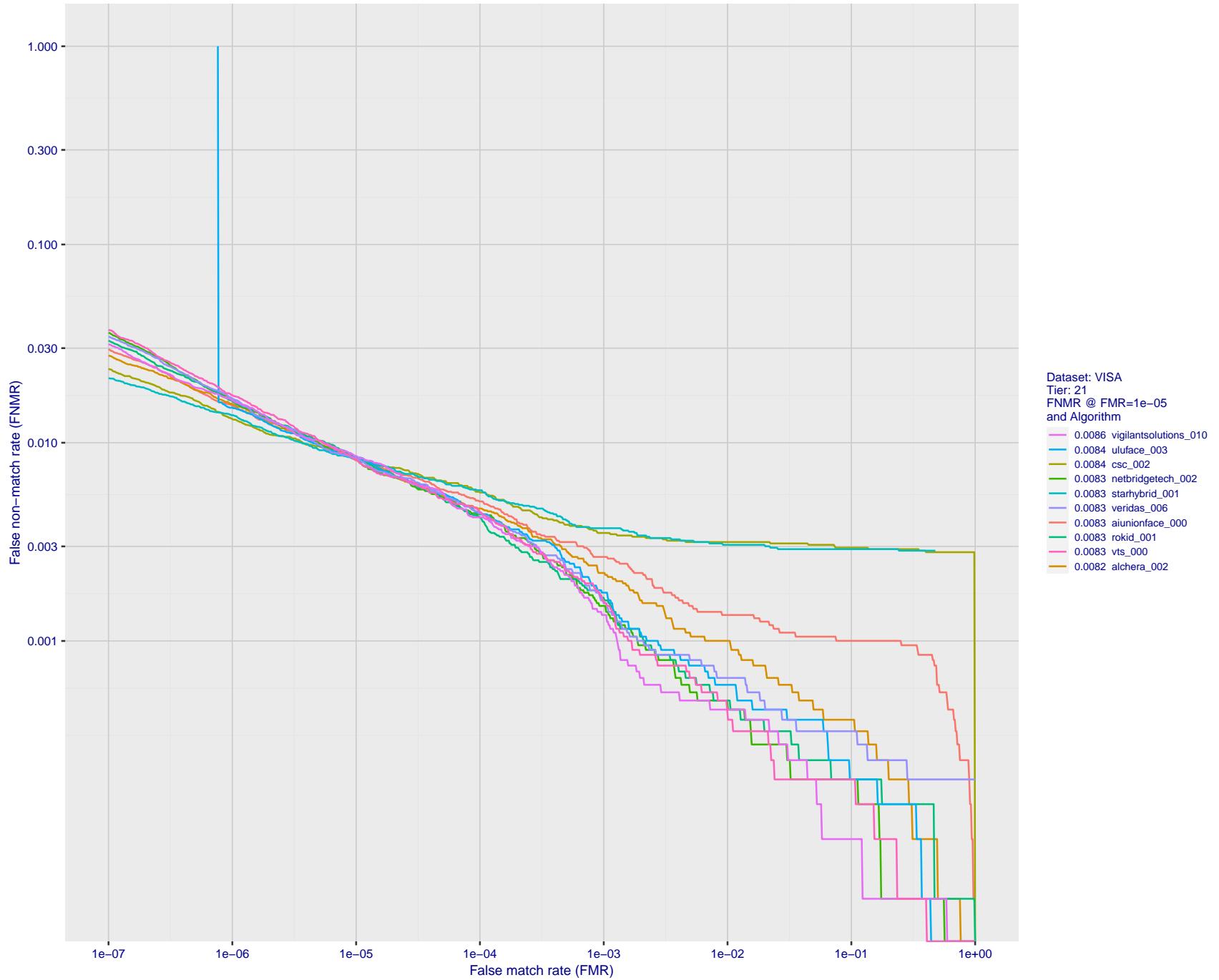


Figure 40: For the visa images, detection error tradeoff (DET) characteristics showing false non-match rate vs. false match rate plotted parametrically on threshold,  $T$ . The scales are logarithmic in order to show many decades of FMR.

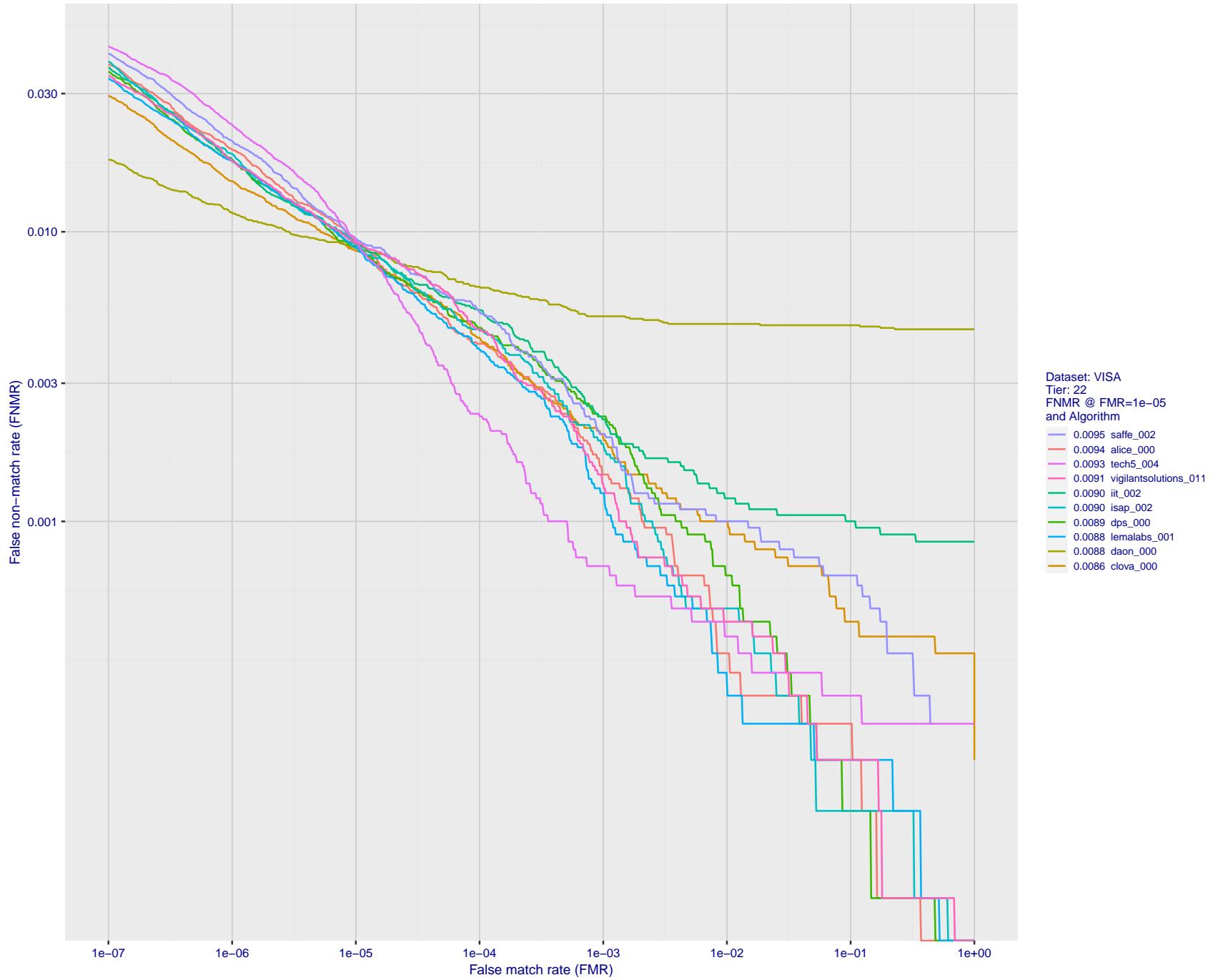


Figure 41: For the visa images, detection error tradeoff (DET) characteristics showing false non-match rate vs. false match rate plotted parametrically on threshold,  $T$ . The scales are logarithmic in order to show many decades of FMR.

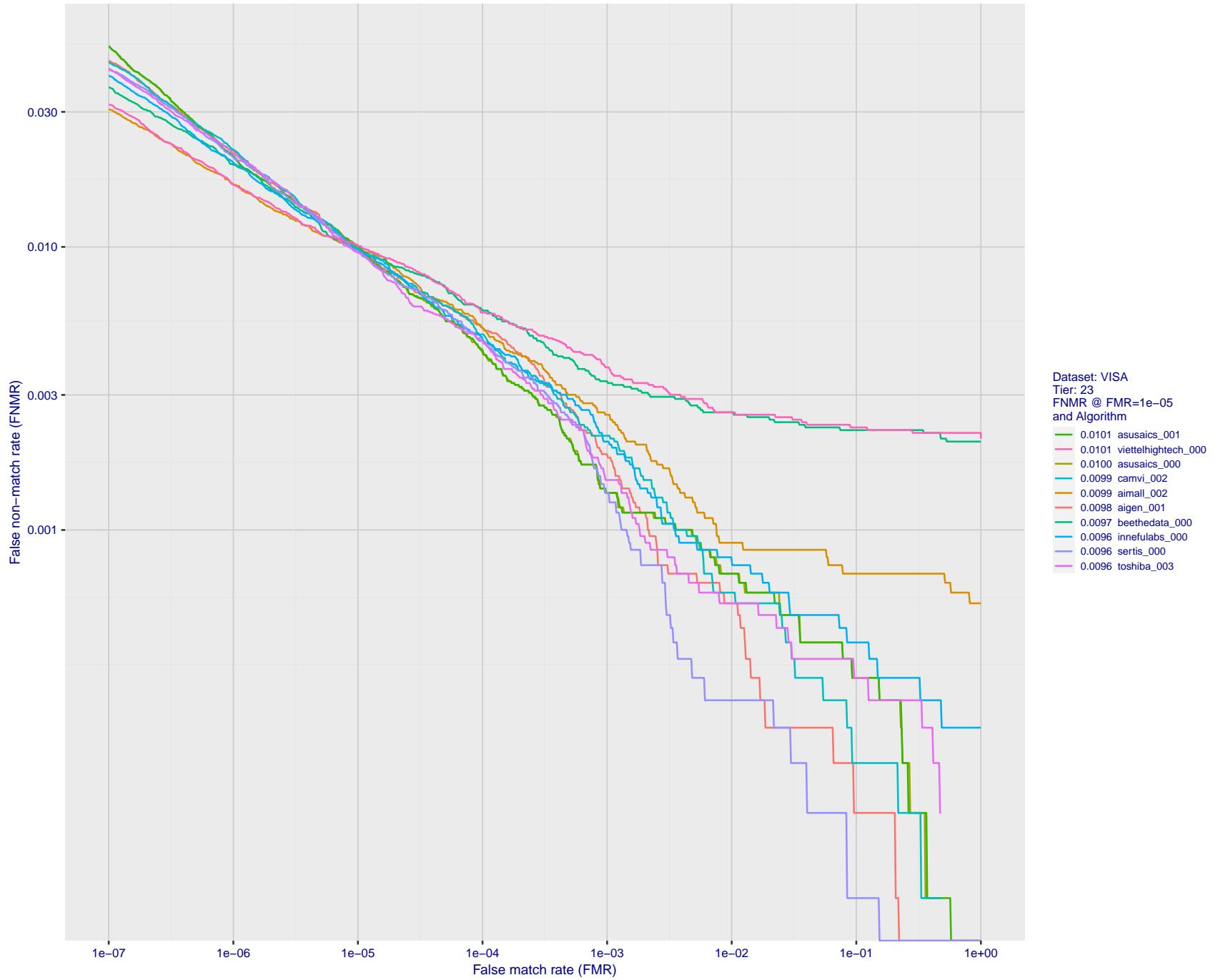


Figure 42: For the visa images, detection error tradeoff (DET) characteristics showing false non-match rate vs. false match rate plotted parametrically on threshold,  $T$ . The scales are logarithmic in order to show many decades of FMR.

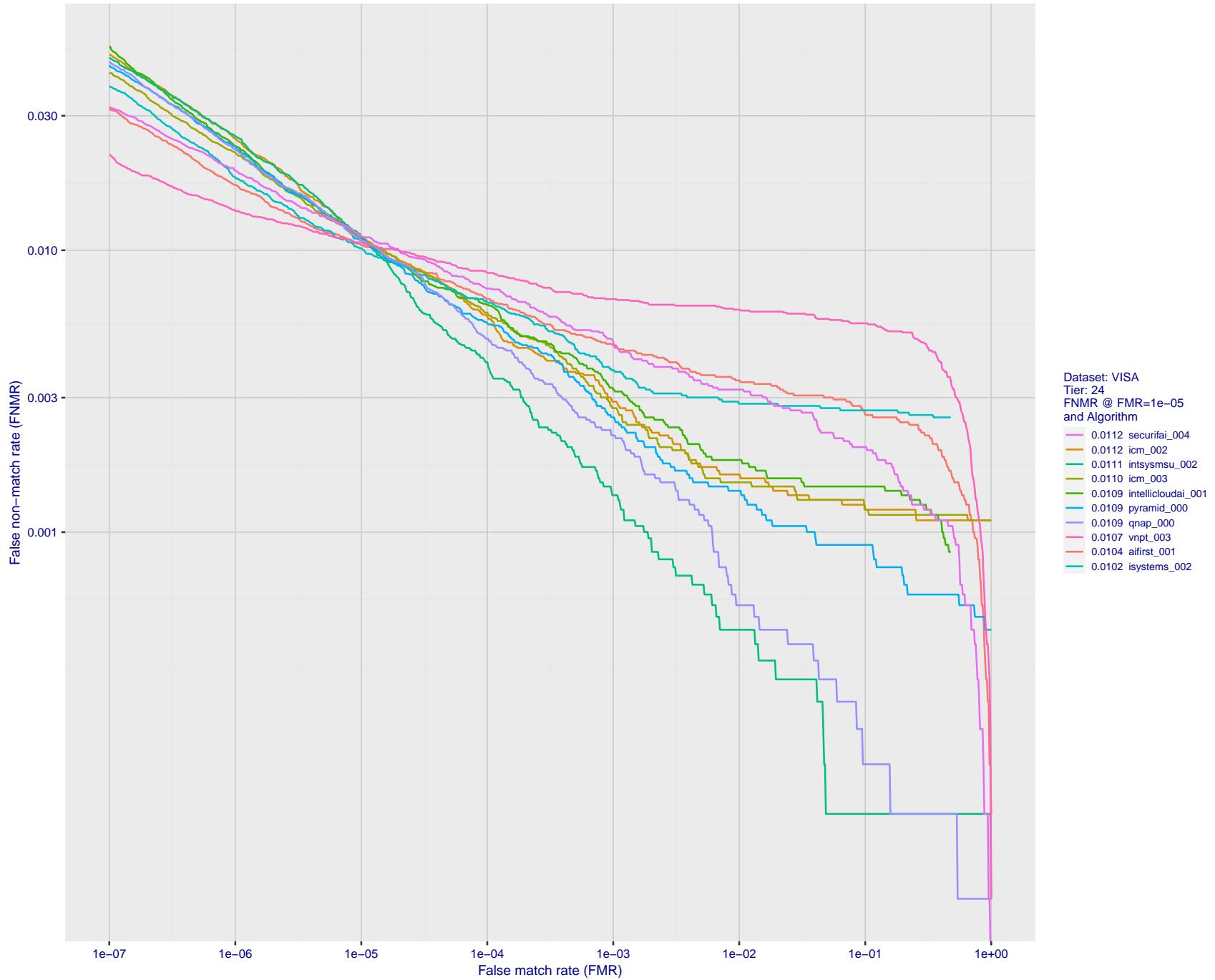


Figure 43: For the visa images, detection error tradeoff (DET) characteristics showing false non-match rate vs. false match rate plotted parametrically on threshold,  $T$ . The scales are logarithmic in order to show many decades of FMR.

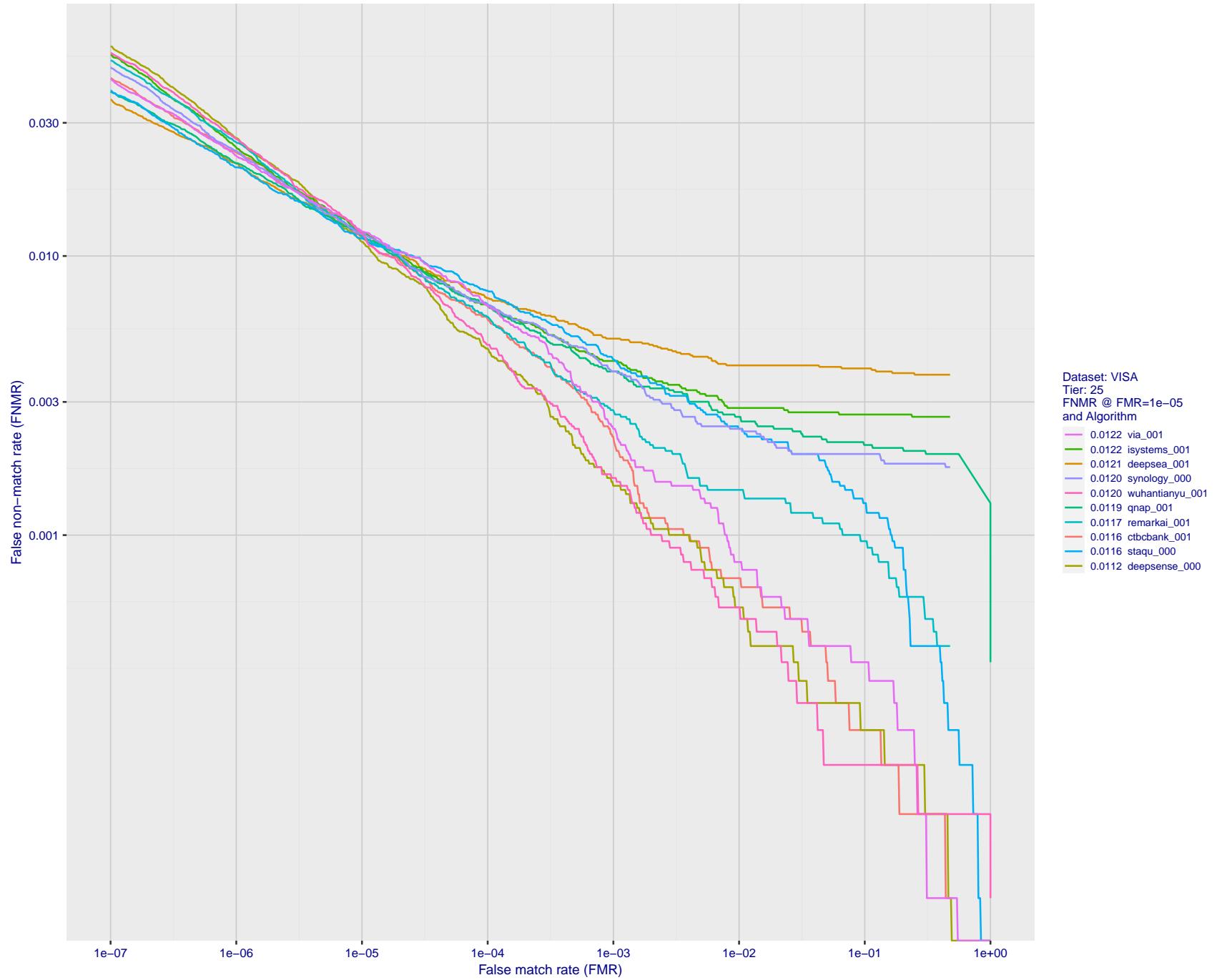


Figure 44: For the visa images, detection error tradeoff (DET) characteristics showing false non-match rate vs. false match rate plotted parametrically on threshold,  $T$ . The scales are logarithmic in order to show many decades of FMR.

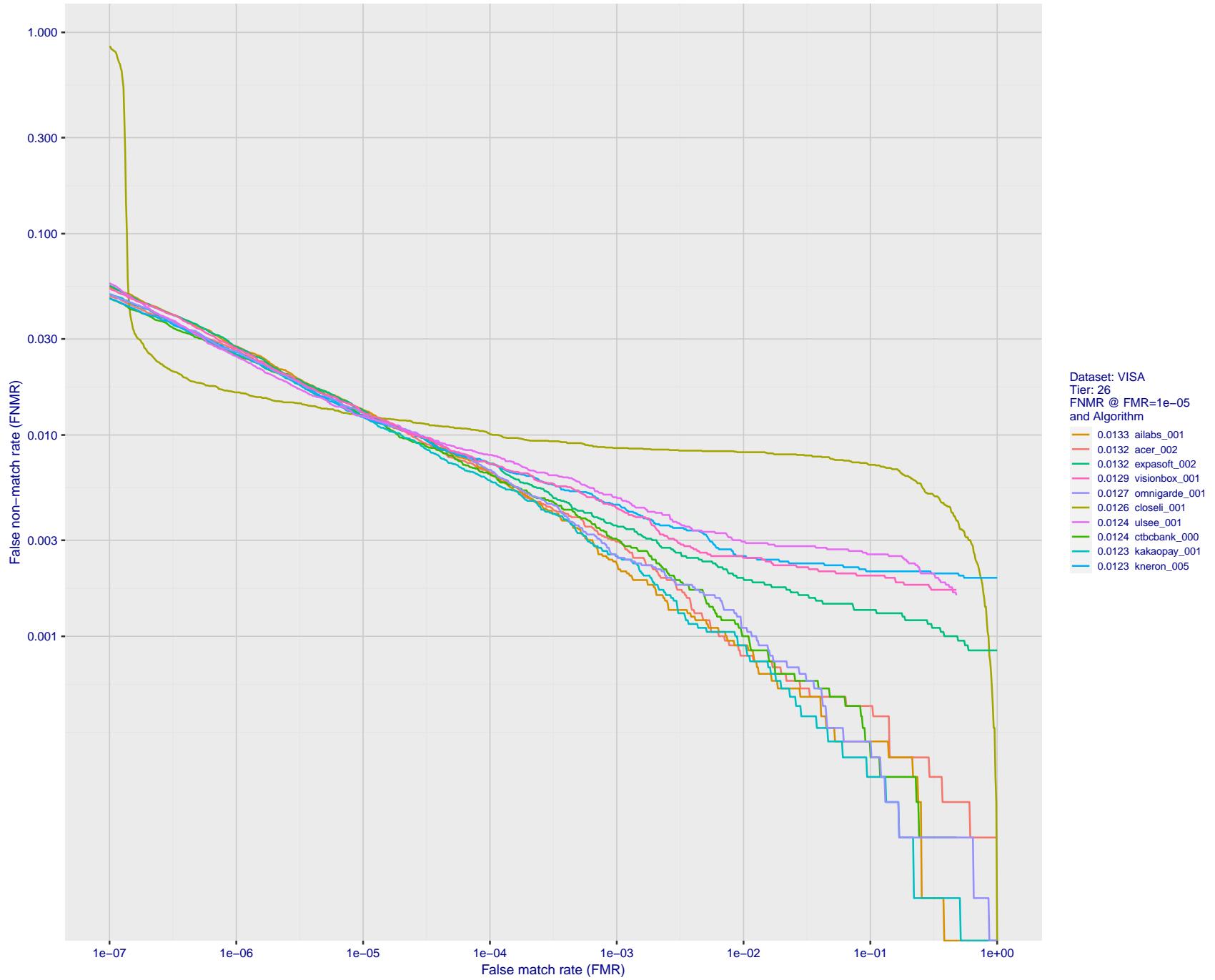


Figure 45: For the visa images, detection error tradeoff (DET) characteristics showing false non-match rate vs. false match rate plotted parametrically on threshold,  $T$ . The scales are logarithmic in order to show many decades of FMR.

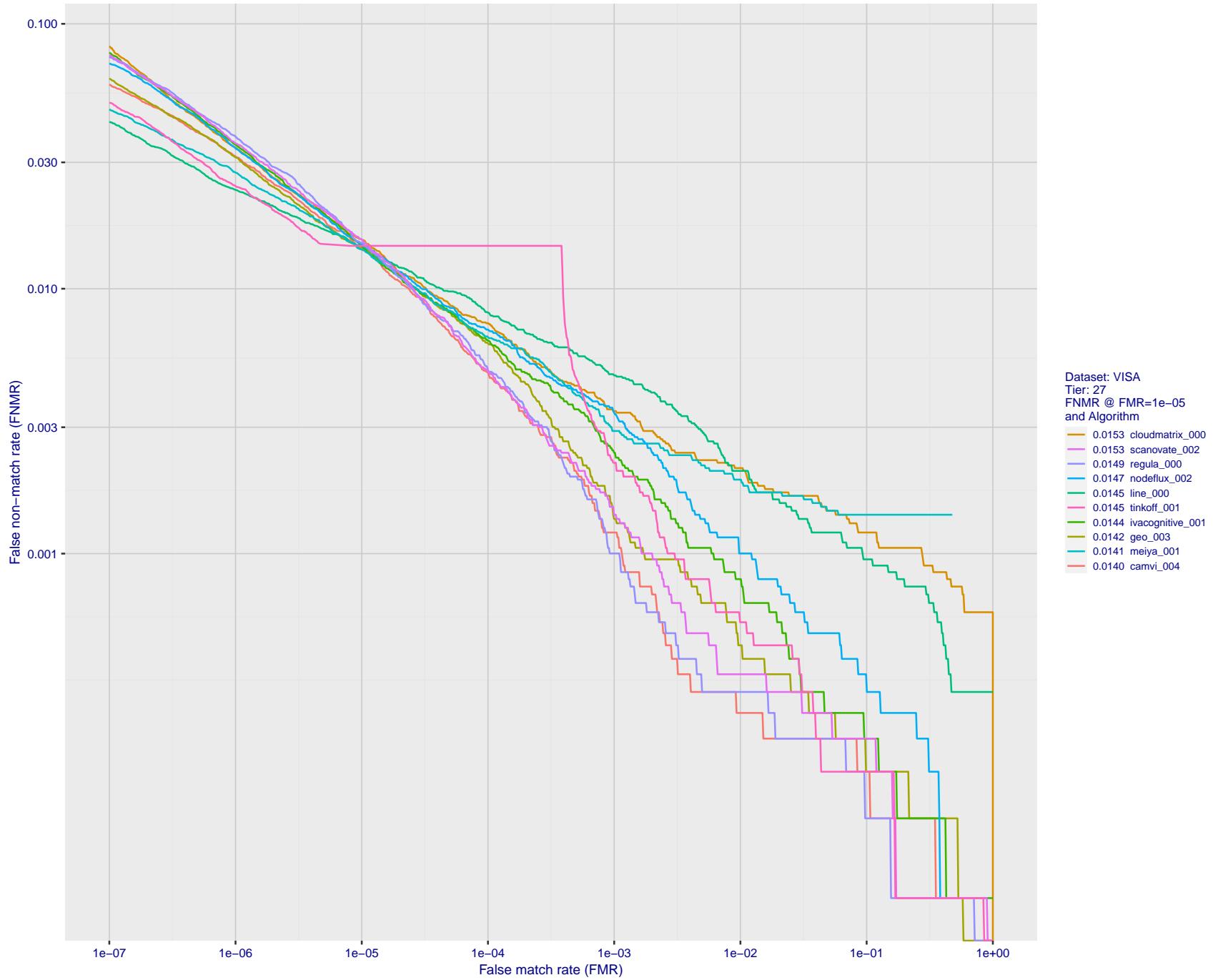


Figure 46: For the visa images, detection error tradeoff (DET) characteristics showing false non-match rate vs. false match rate plotted parametrically on threshold,  $T$ . The scales are logarithmic in order to show many decades of FMR.

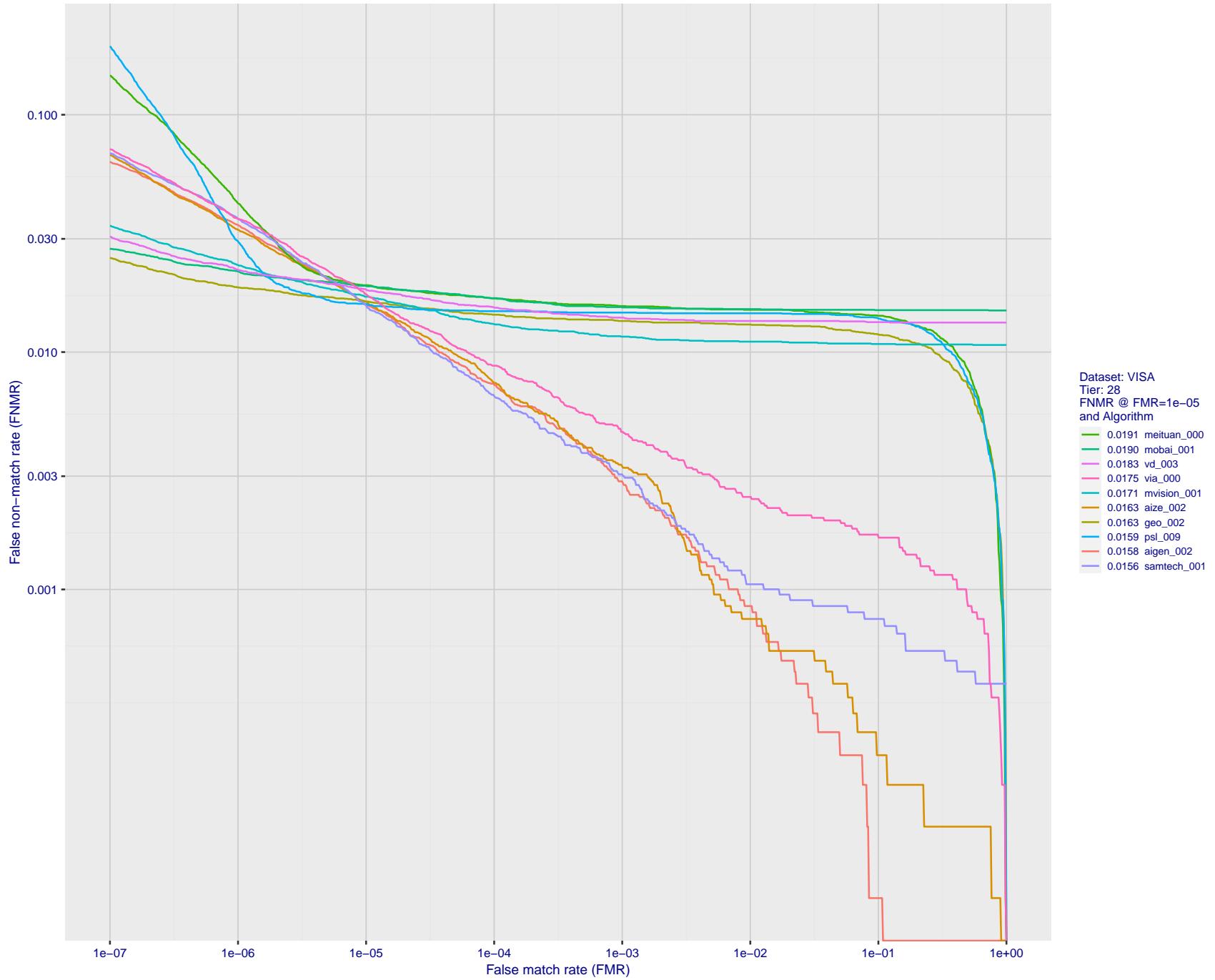


Figure 47: For the visa images, detection error tradeoff (DET) characteristics showing false non-match rate vs. false match rate plotted parametrically on threshold,  $T$ . The scales are logarithmic in order to show many decades of FMR.

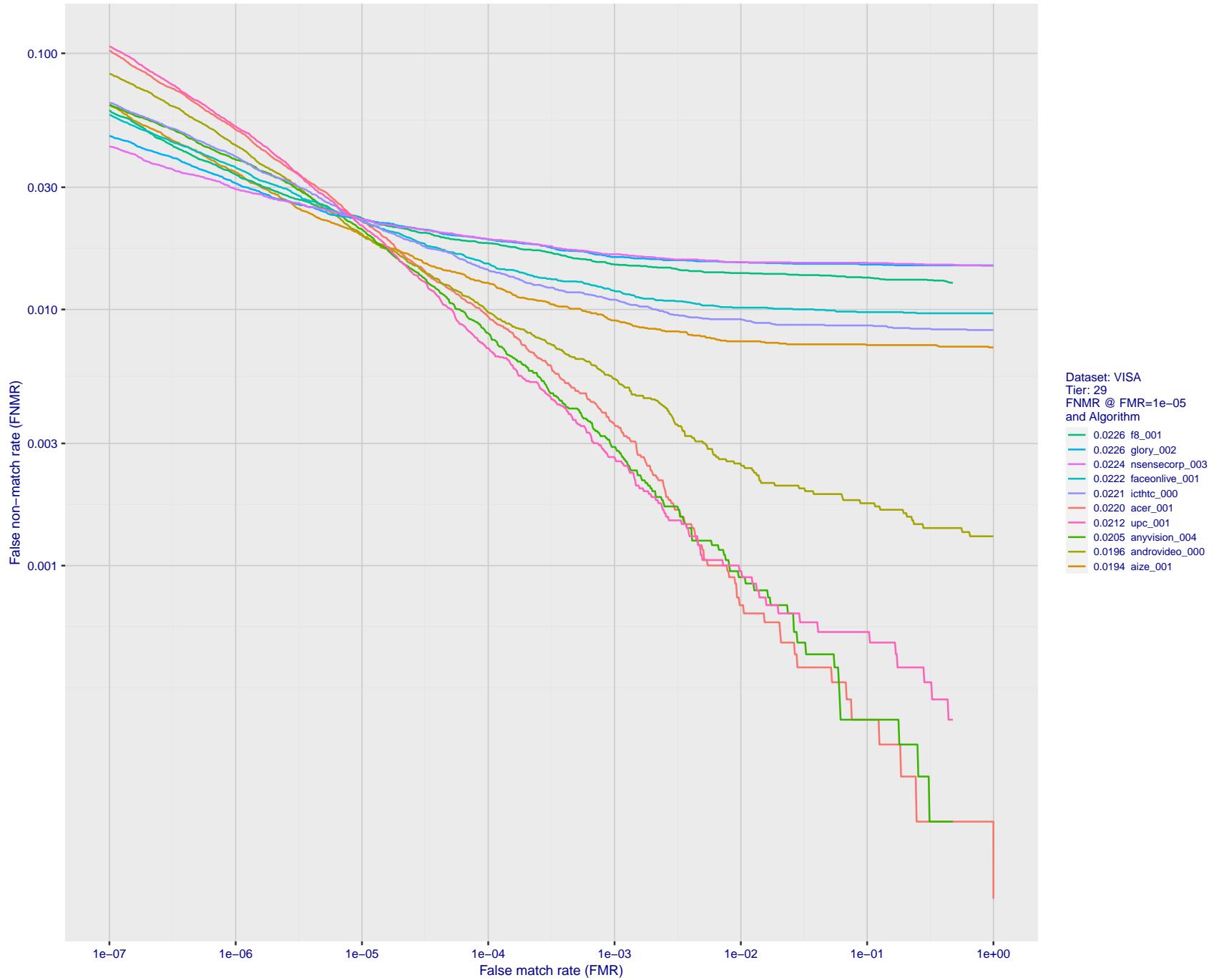


Figure 48: For the visa images, detection error tradeoff (DET) characteristics showing false non-match rate vs. false match rate plotted parametrically on threshold,  $T$ . The scales are logarithmic in order to show many decades of FMR.

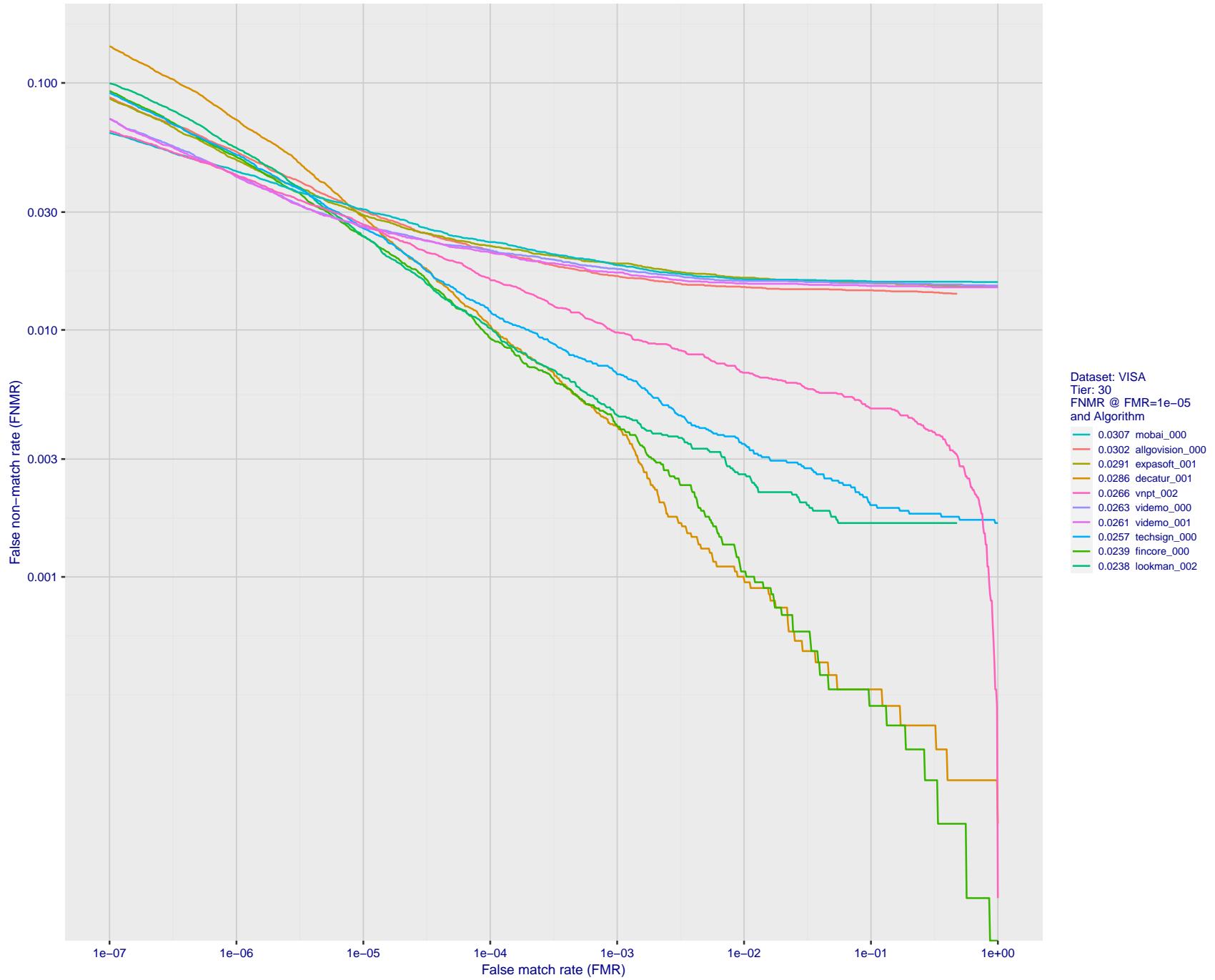


Figure 49: For the visa images, detection error tradeoff (DET) characteristics showing false non-match rate vs. false match rate plotted parametrically on threshold,  $T$ . The scales are logarithmic in order to show many decades of FMR.

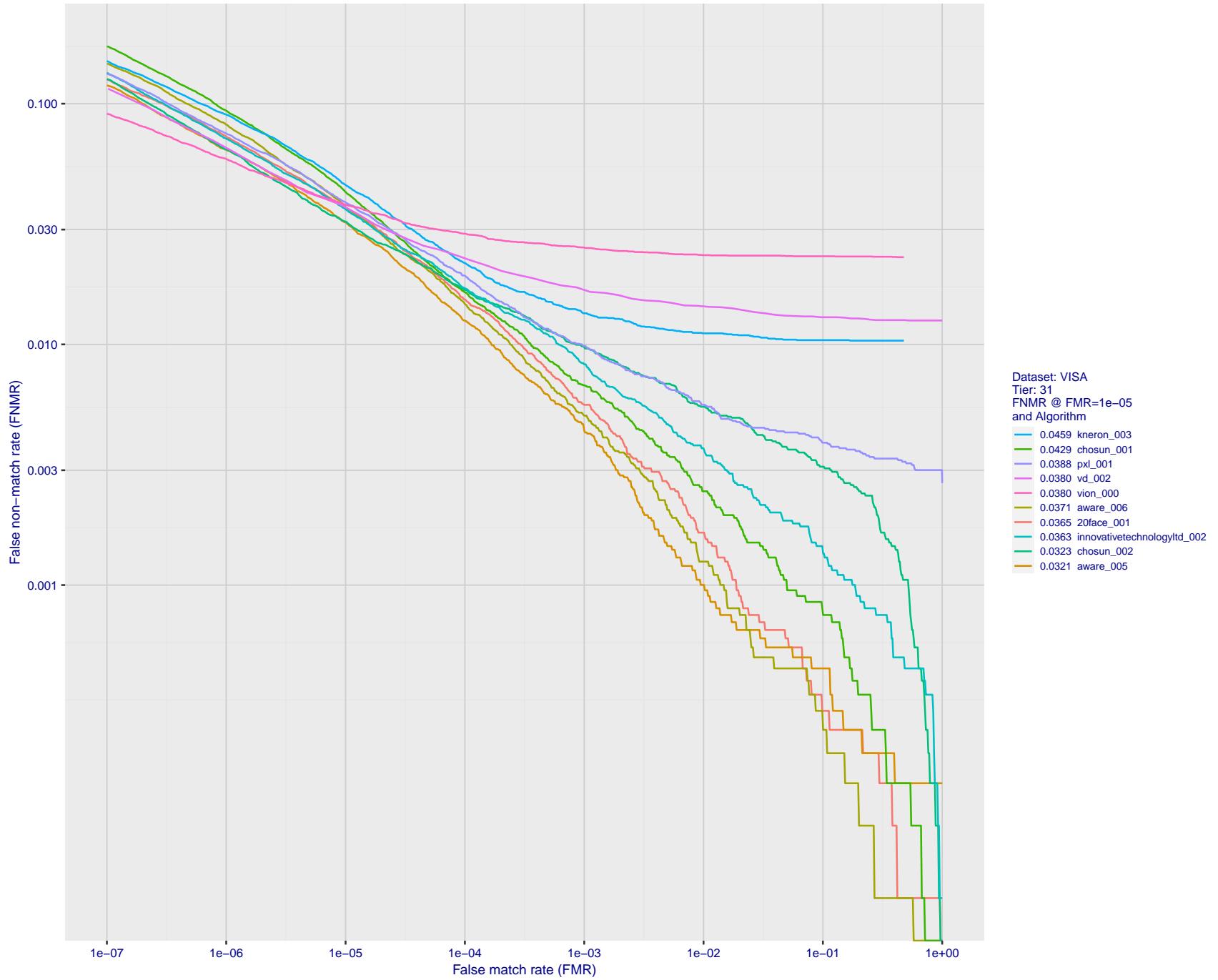


Figure 50: For the visa images, detection error tradeoff (DET) characteristics showing false non-match rate vs. false match rate plotted parametrically on threshold,  $T$ . The scales are logarithmic in order to show many decades of FMR.

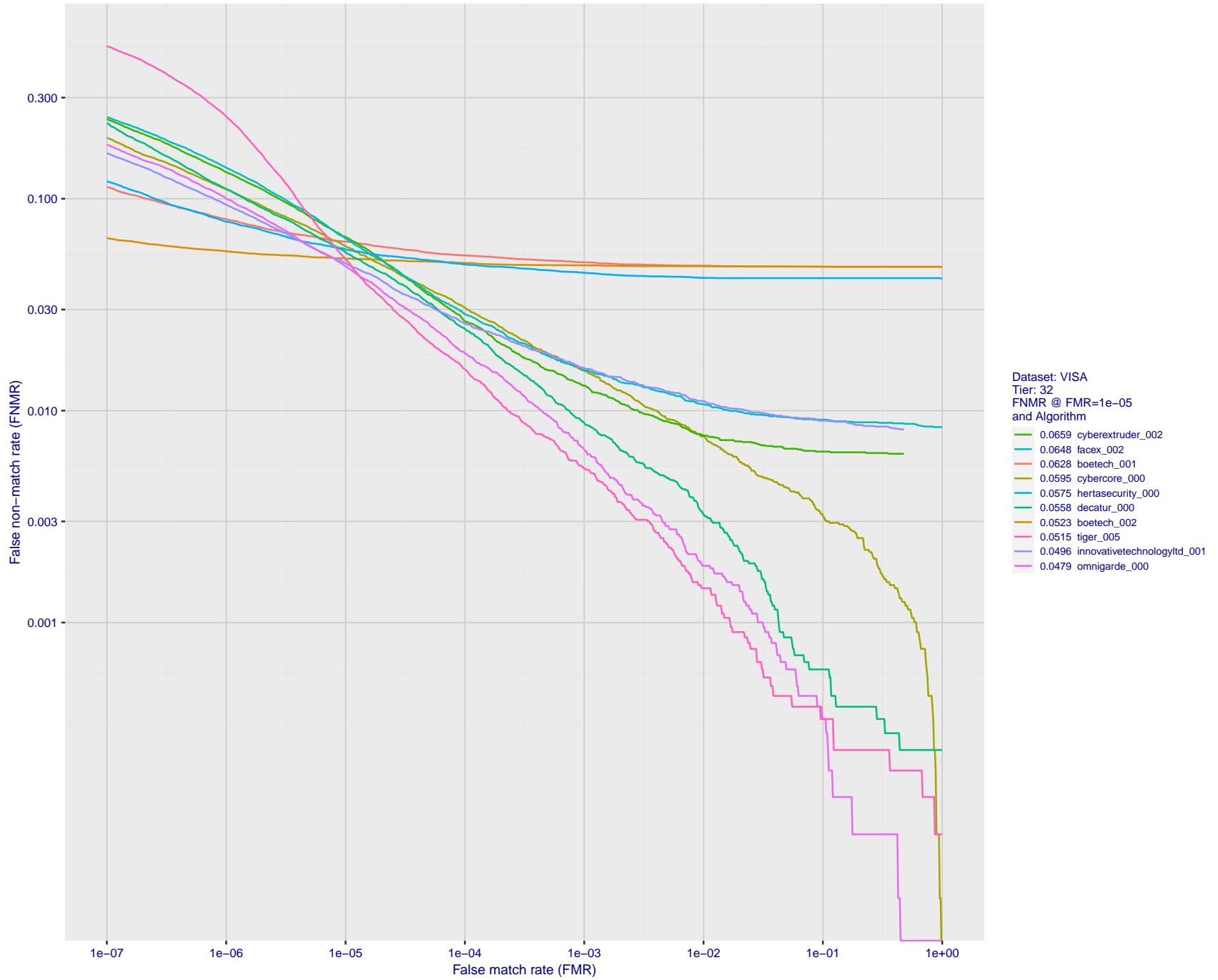


Figure 51: For the visa images, detection error tradeoff (DET) characteristics showing false non-match rate vs. false match rate plotted parametrically on threshold,  $T$ . The scales are logarithmic in order to show many decades of FMR.

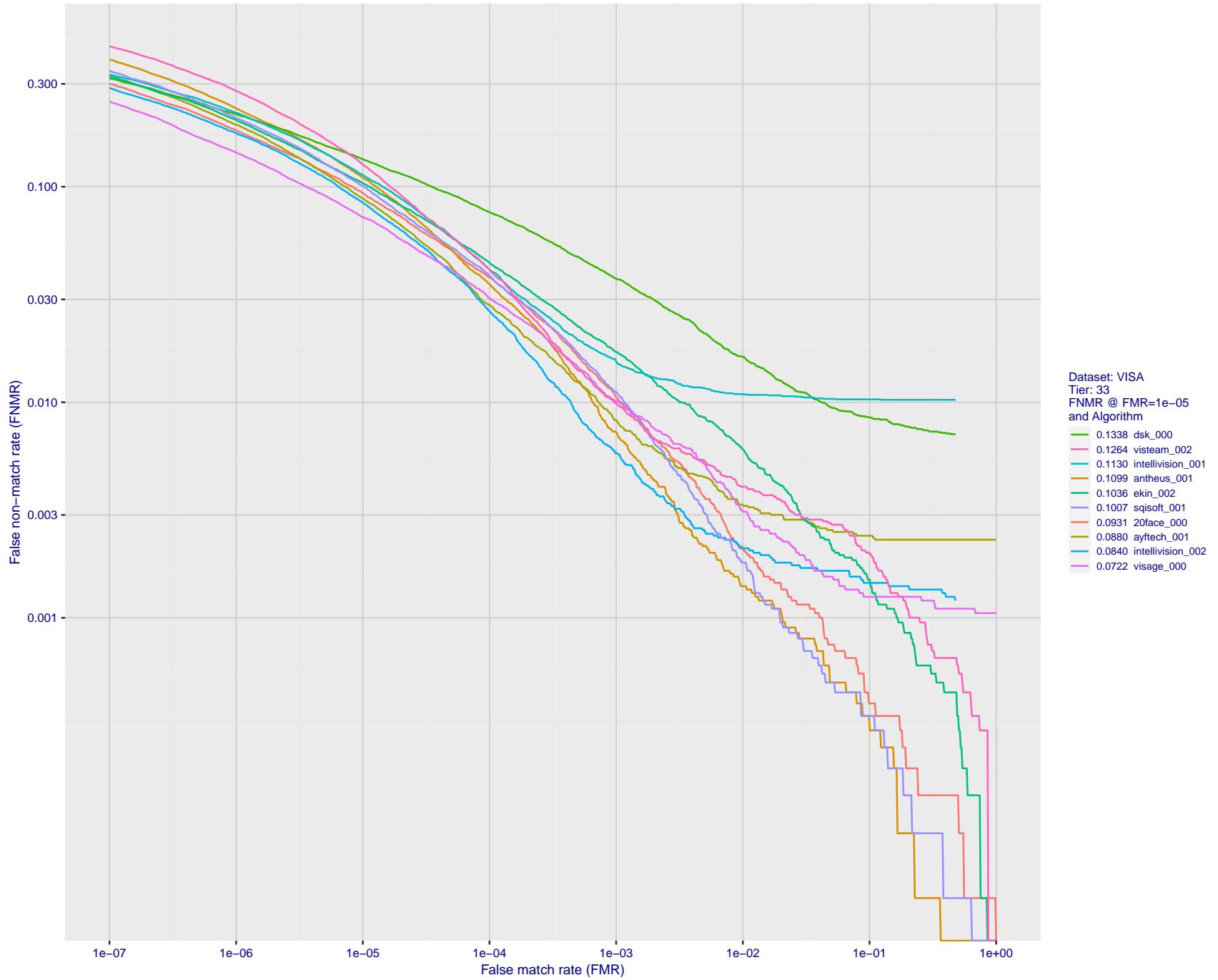


Figure 52: For the visa images, detection error tradeoff (DET) characteristics showing false non-match rate vs. false match rate plotted parametrically on threshold,  $T$ . The scales are logarithmic in order to show many decades of FMR.

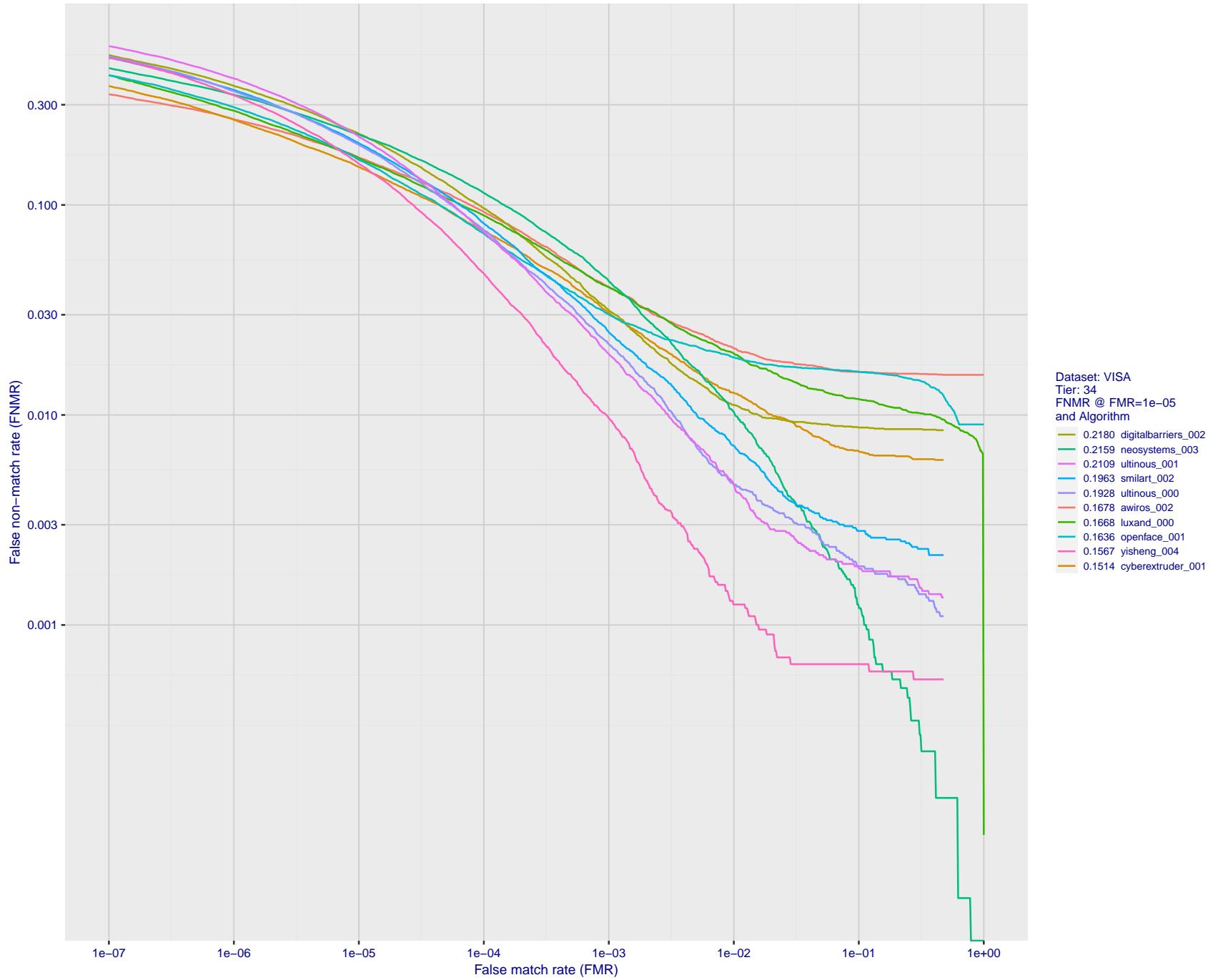


Figure 53: For the visa images, detection error tradeoff (DET) characteristics showing false non-match rate vs. false match rate plotted parametrically on threshold,  $T$ . The scales are logarithmic in order to show many decades of FMR.

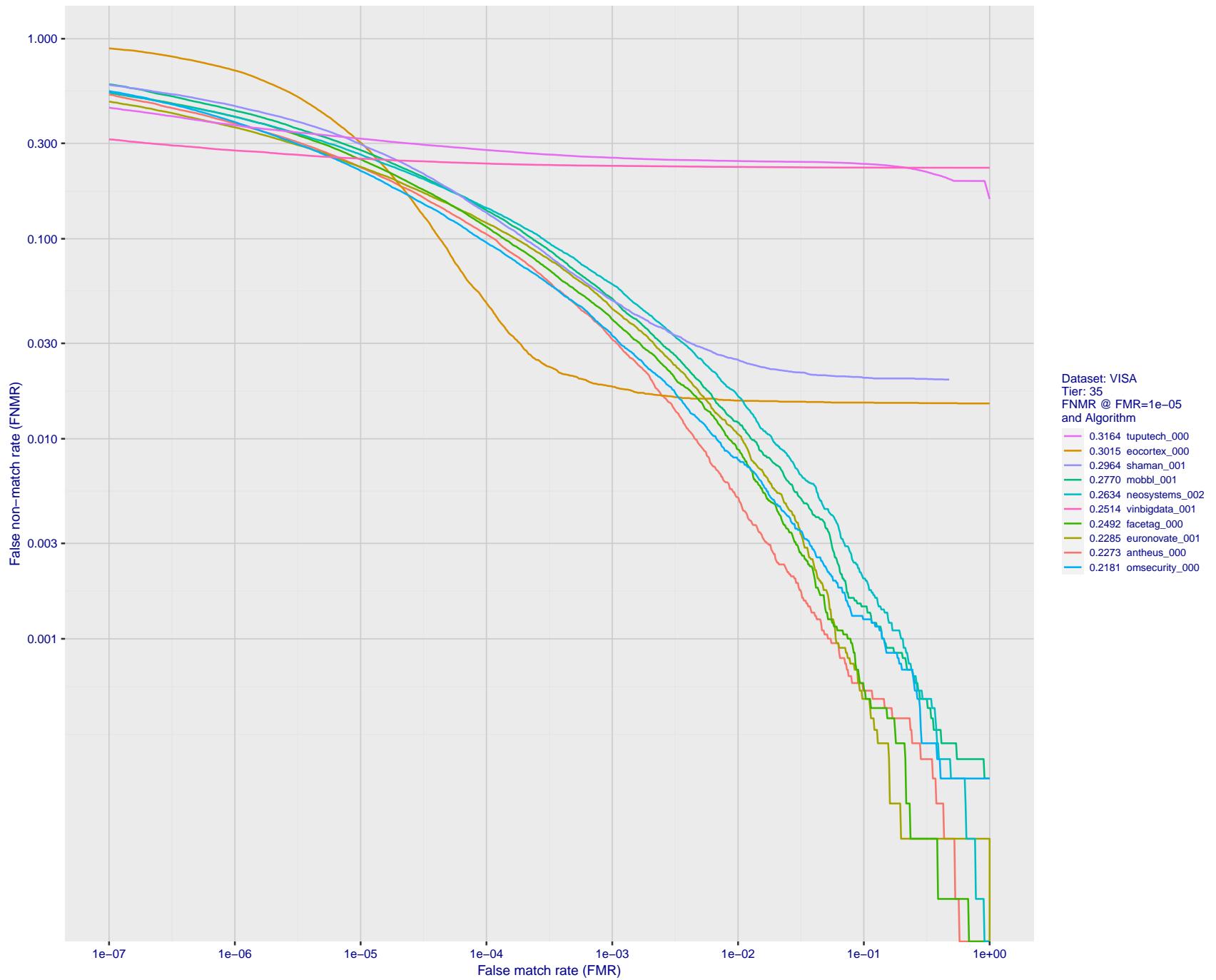


Figure 54: For the visa images, detection error tradeoff (DET) characteristics showing false non-match rate vs. false match rate plotted parametrically on threshold,  $T$ . The scales are logarithmic in order to show many decades of FMR.

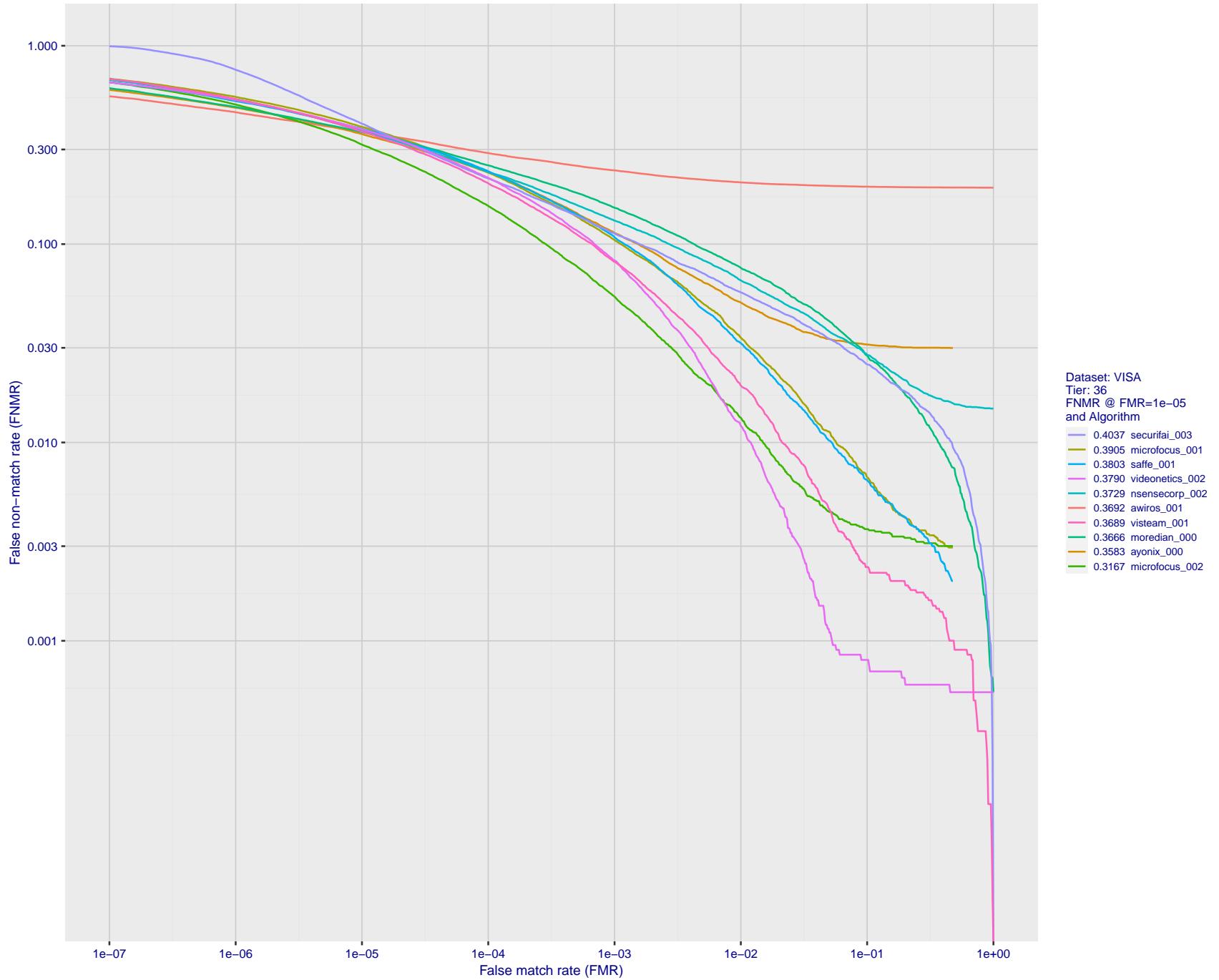


Figure 55: For the visa images, detection error tradeoff (DET) characteristics showing false non-match rate vs. false match rate plotted parametrically on threshold,  $T$ . The scales are logarithmic in order to show many decades of FMR.

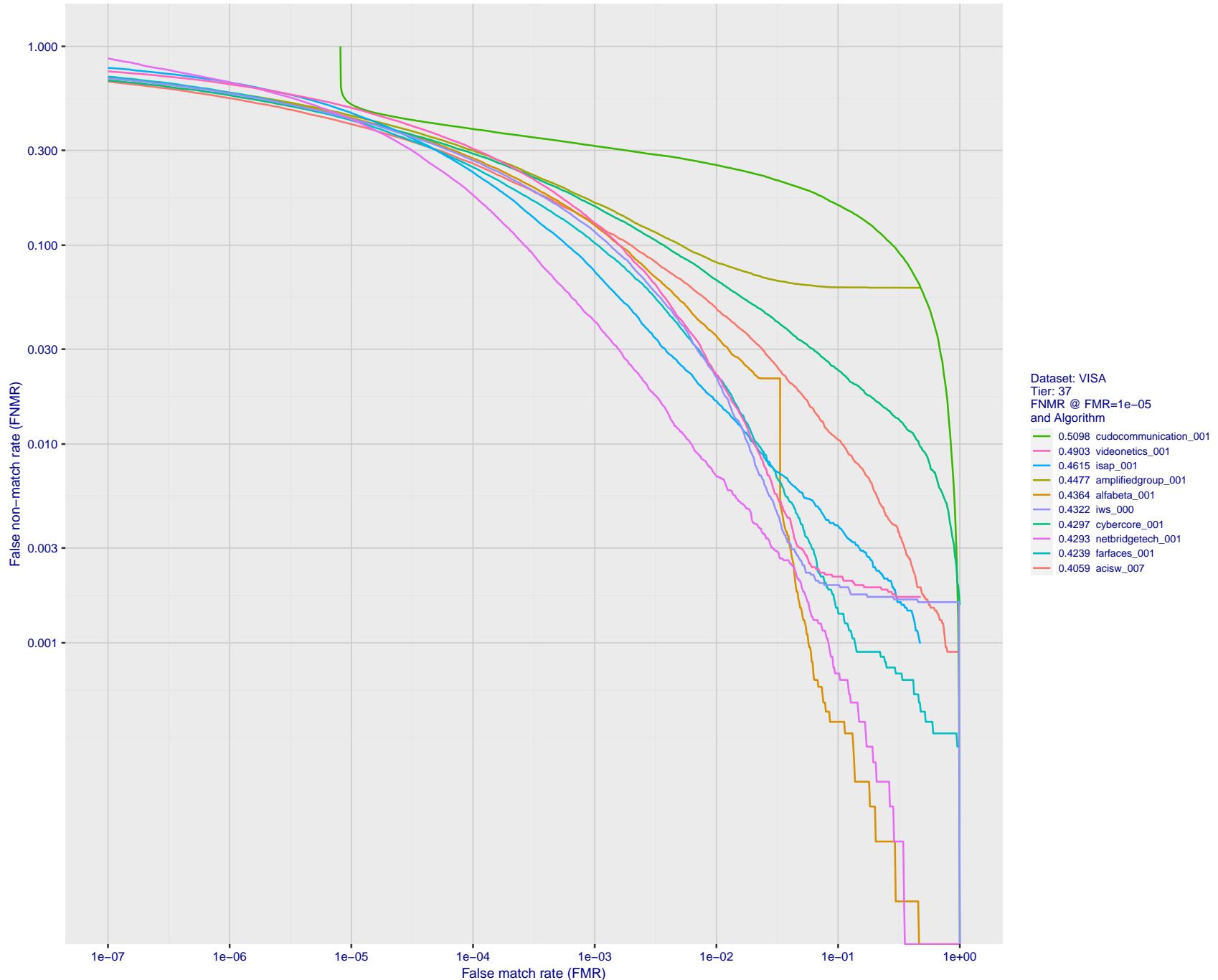


Figure 56: For the visa images, detection error tradeoff (DET) characteristics showing false non-match rate vs. false match rate plotted parametrically on threshold,  $T$ . The scales are logarithmic in order to show many decades of FMR.

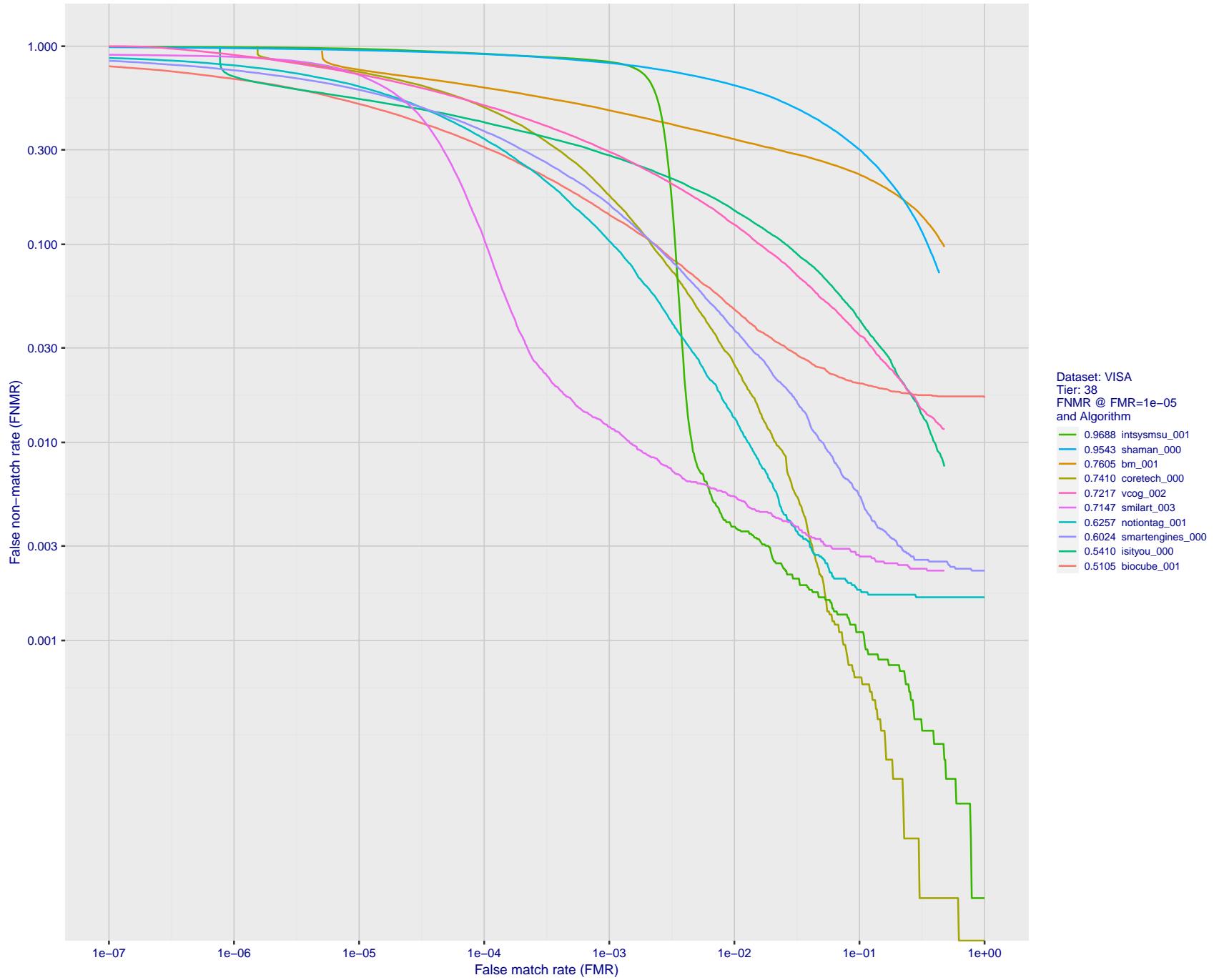


Figure 57: For the visa images, detection error tradeoff (DET) characteristics showing false non-match rate vs. false match rate plotted parametrically on threshold,  $T$ . The scales are logarithmic in order to show many decades of FMR.

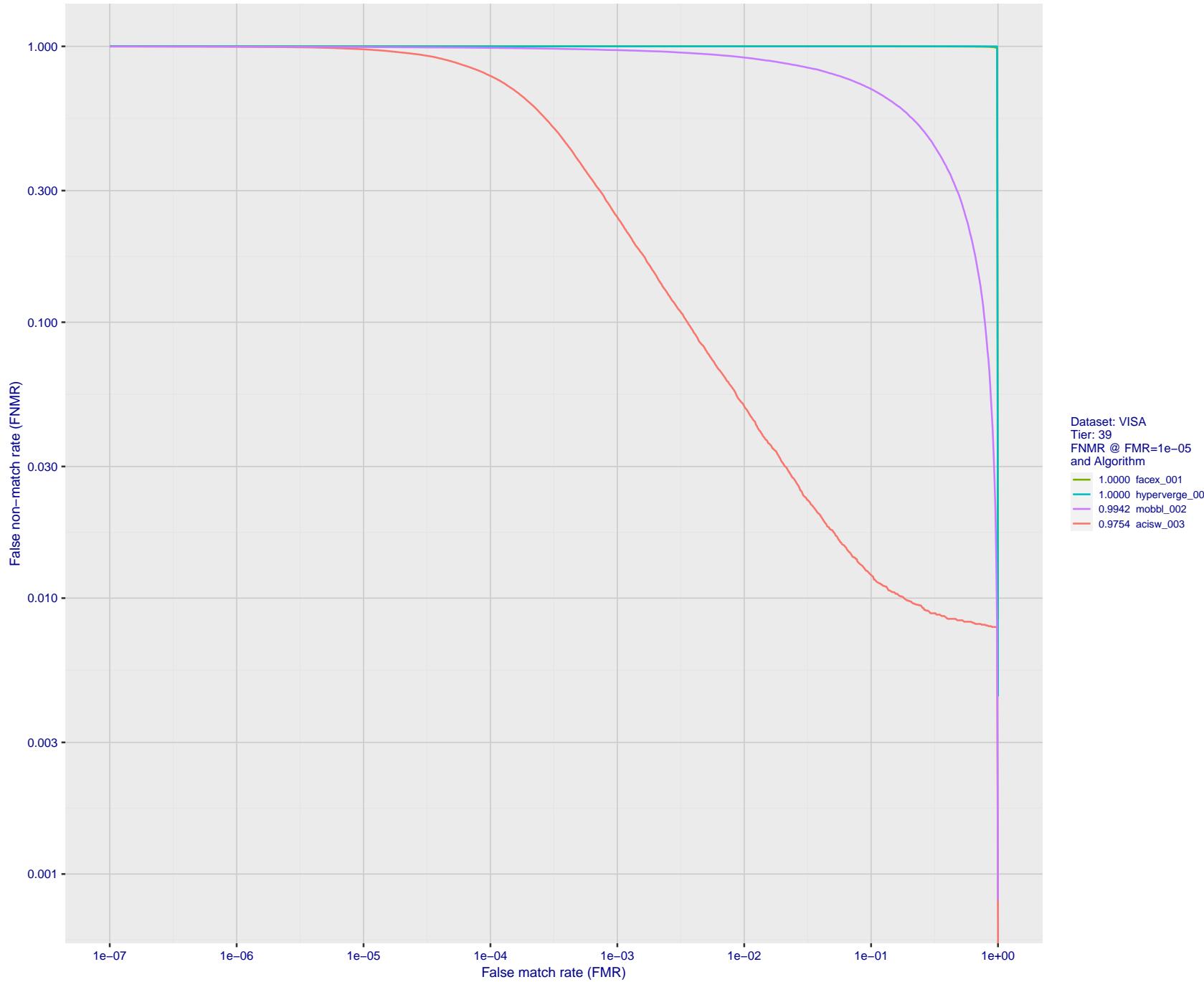


Figure 58: For the visa images, detection error tradeoff (DET) characteristics showing false non-match rate vs. false match rate plotted parametrically on threshold,  $T$ . The scales are logarithmic in order to show many decades of FMR.

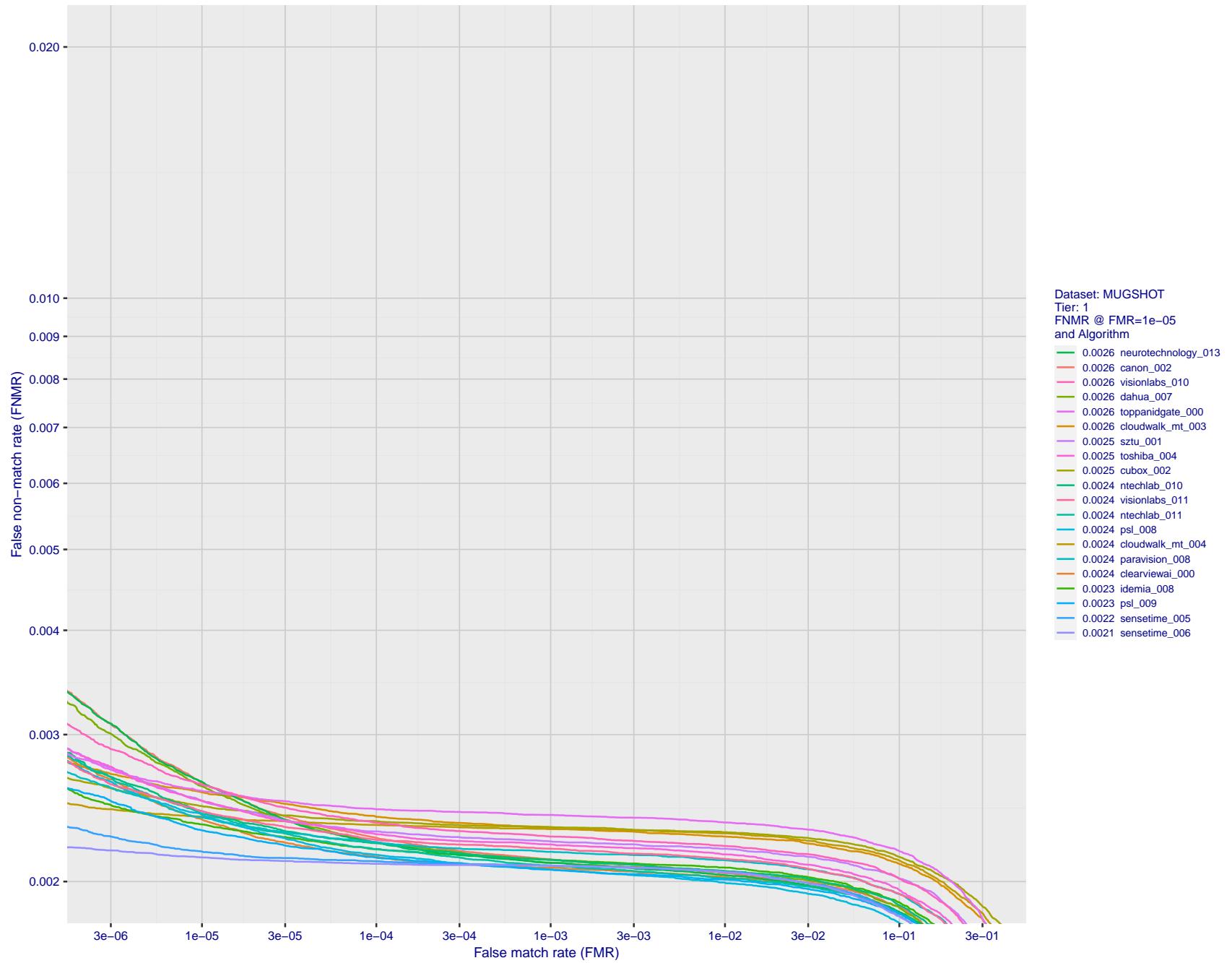


Figure 59: For the mugshot images, detection error tradeoff (DET) characteristics showing false non-match rate vs. false match rate plotted parametrically on threshold,  $T$ . The scales are logarithmic in order to show decades of FMR.

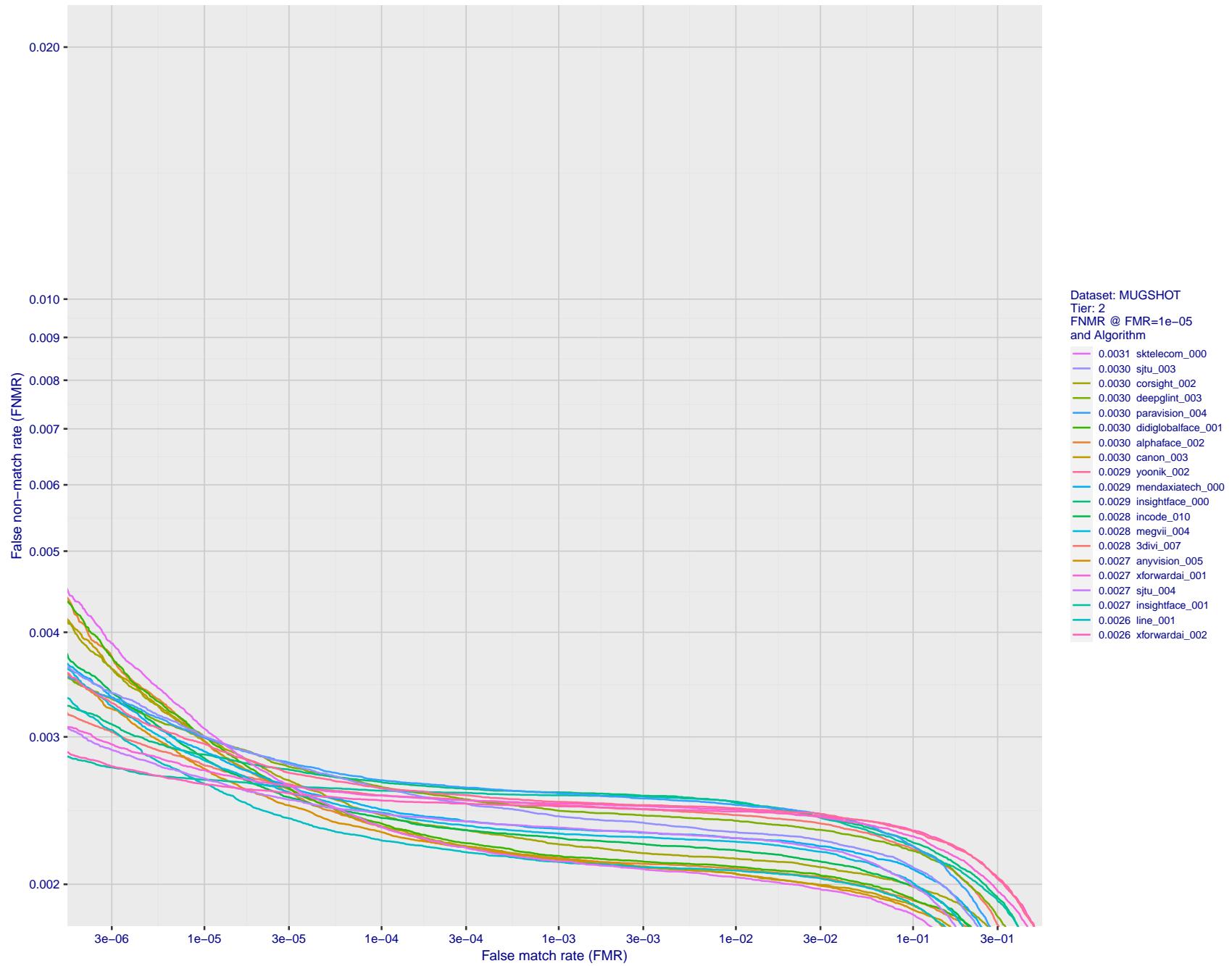


Figure 60: For the mugshot images, detection error tradeoff (DET) characteristics showing false non-match rate vs. false match rate plotted parametrically on threshold,  $T$ . The scales are logarithmic in order to show decades of FMR.

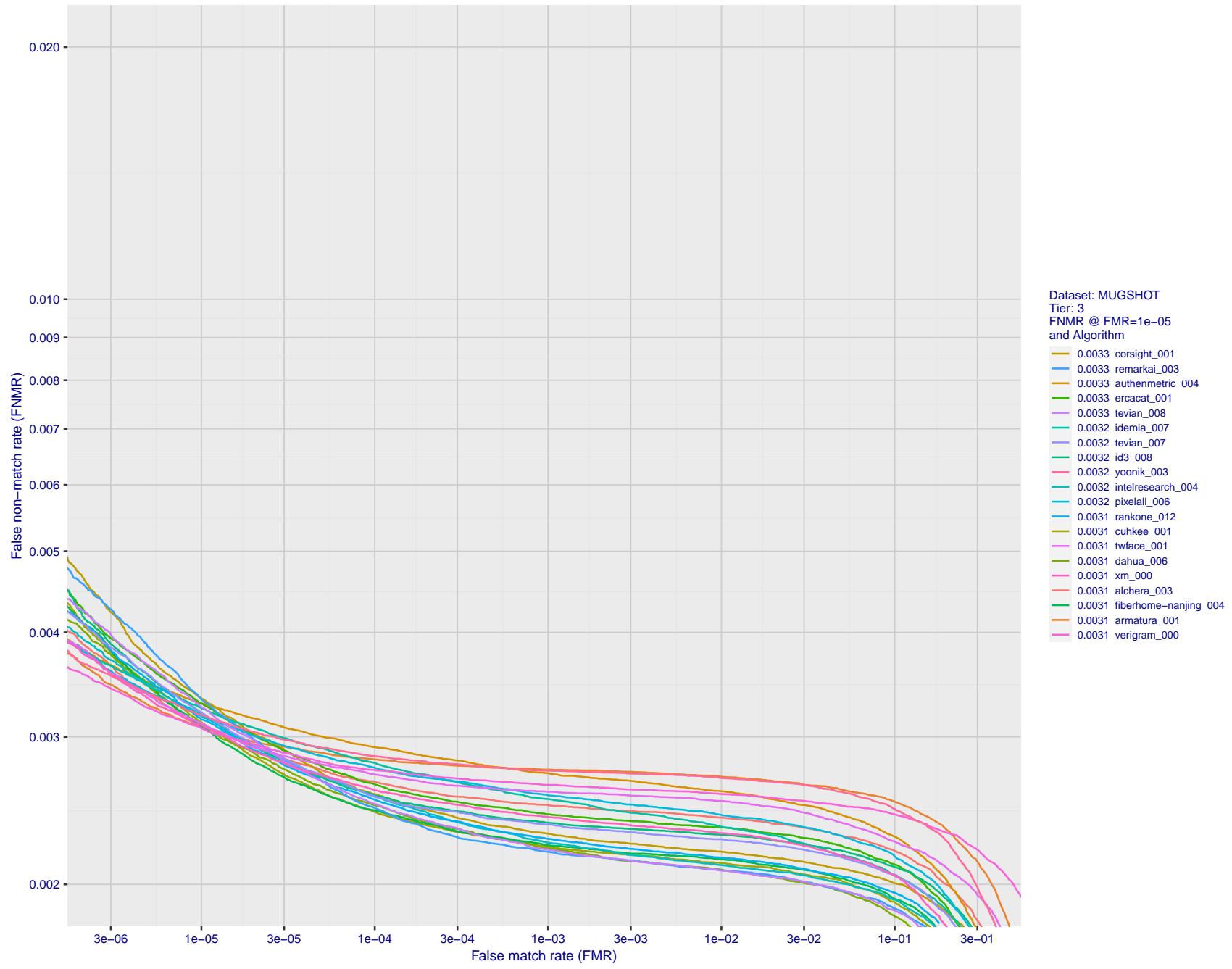


Figure 61: For the mugshot images, detection error tradeoff (DET) characteristics showing false non-match rate vs. false match rate plotted parametrically on threshold,  $T$ . The scales are logarithmic in order to show decades of FMR.

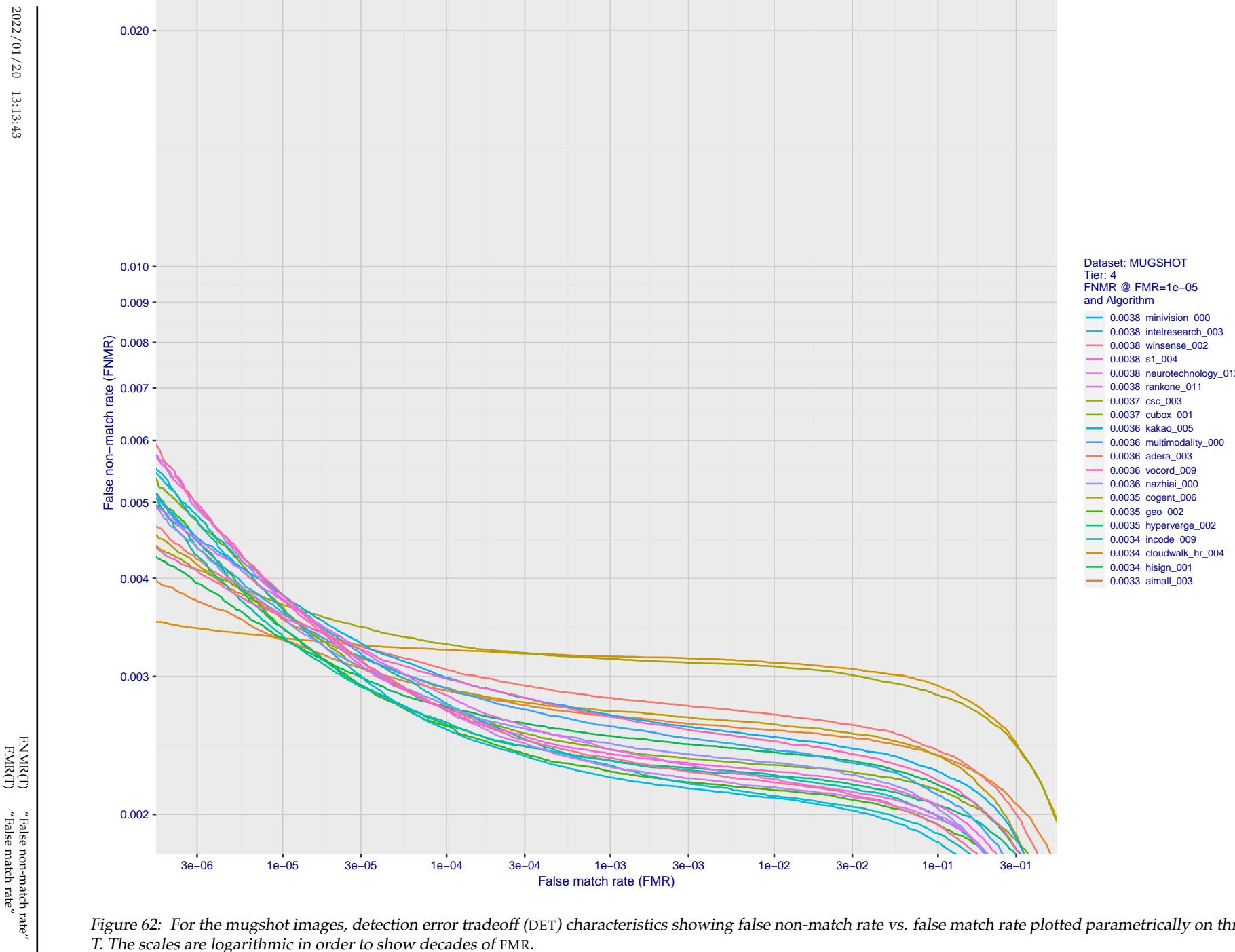


Figure 62: For the mugshot images, detection error tradeoff (DET) characteristics showing false non-match rate vs. false match rate plotted parametrically on threshold,  $T$ . The scales are logarithmic in order to show decades of FMR.

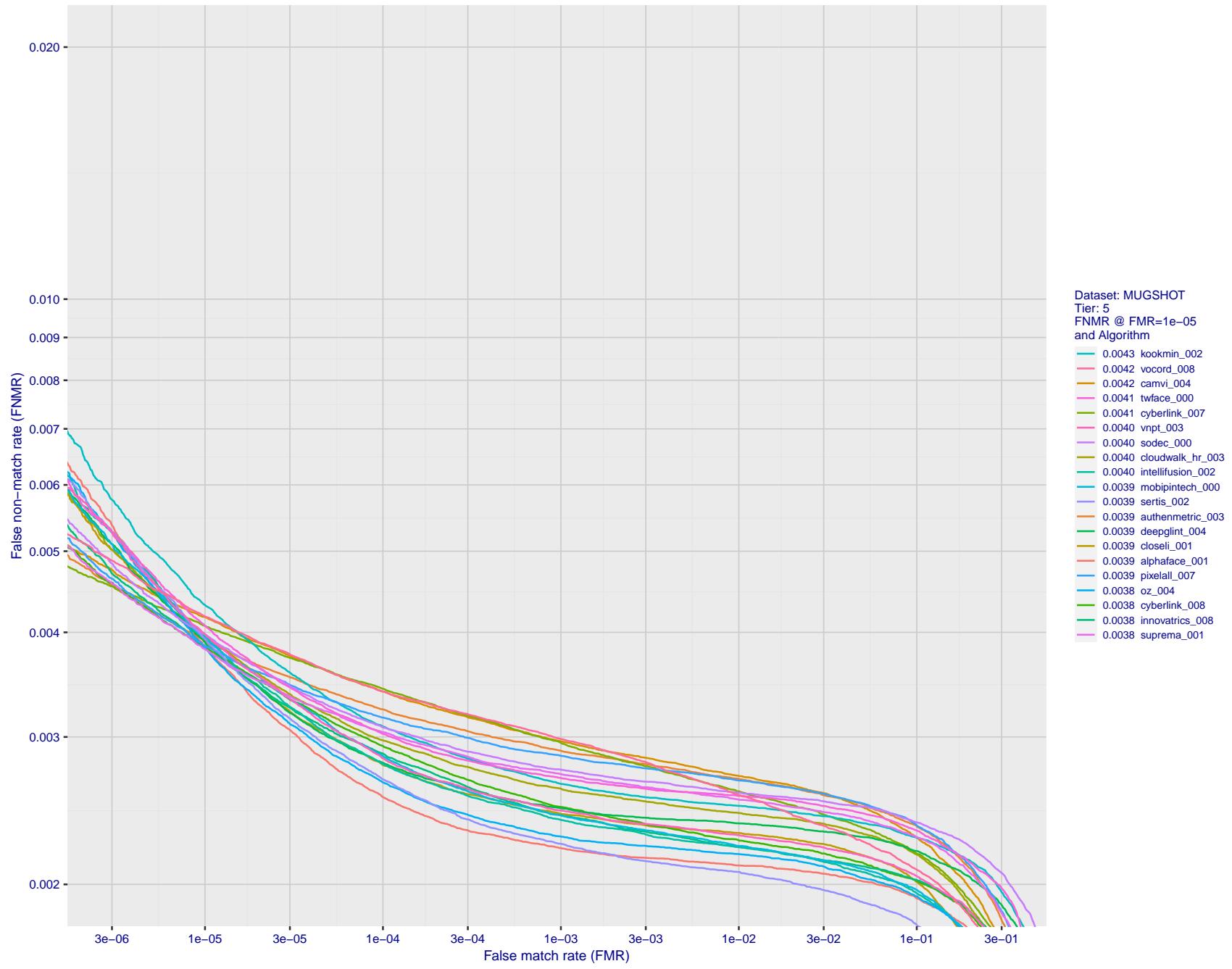


Figure 63: For the mugshot images, detection error tradeoff (DET) characteristics showing false non-match rate vs. false match rate plotted parametrically on threshold,  $T$ . The scales are logarithmic in order to show decades of FMR.

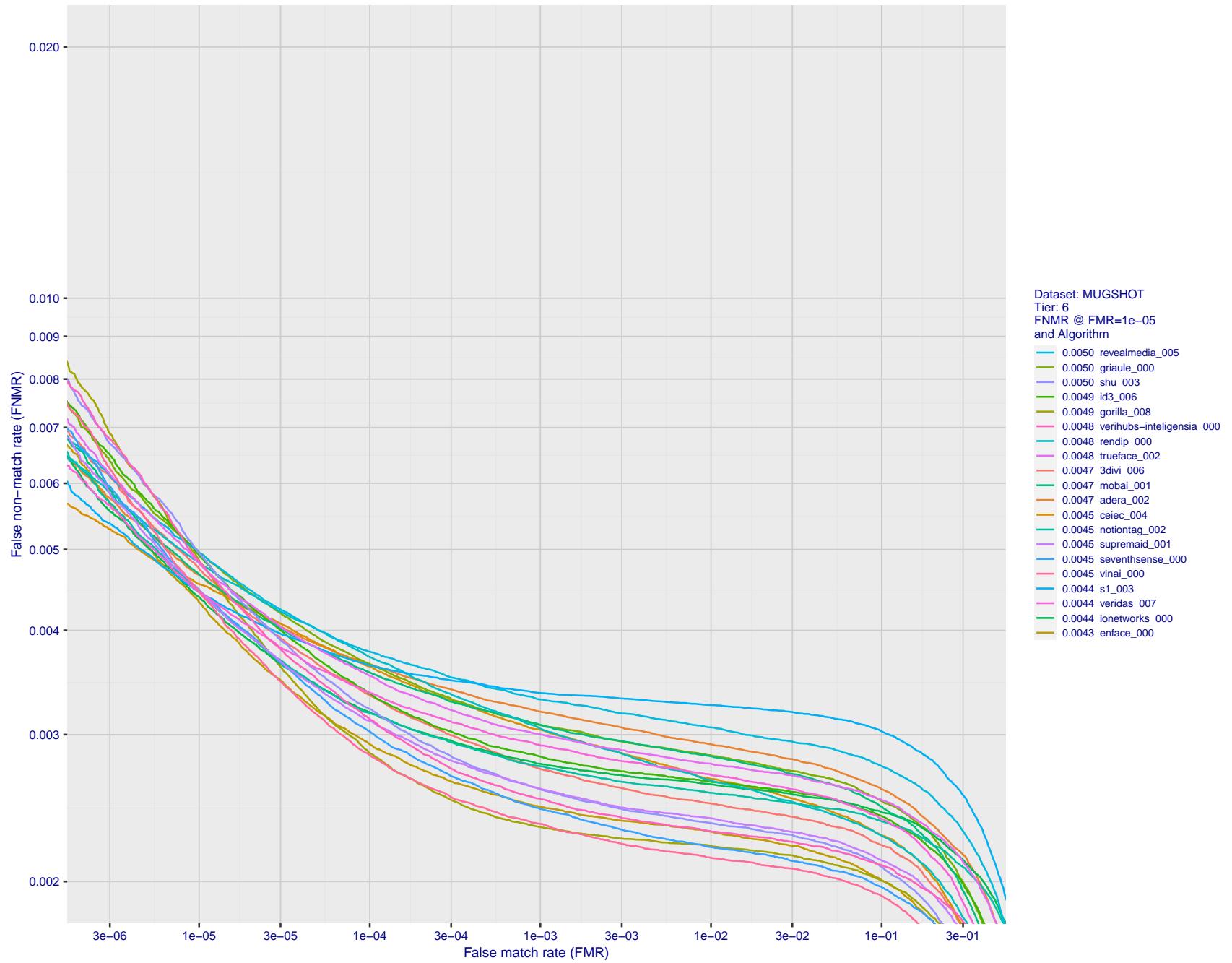


Figure 64: For the mugshot images, detection error tradeoff (DET) characteristics showing false non-match rate vs. false match rate plotted parametrically on threshold,  $T$ . The scales are logarithmic in order to show decades of FMR.

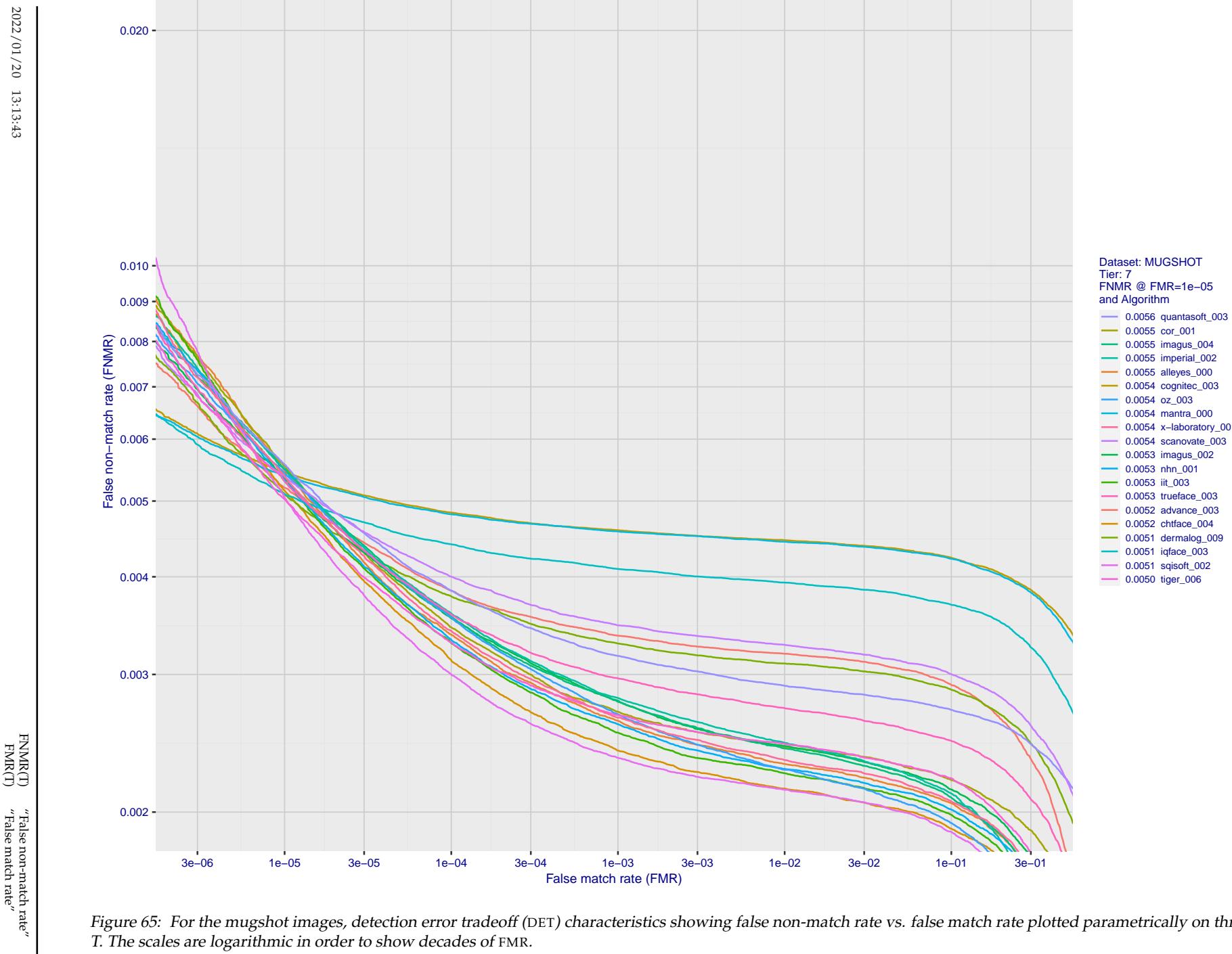


Figure 65: For the mugshot images, detection error tradeoff (DET) characteristics showing false non-match rate vs. false match rate plotted parametrically on threshold,  $T$ . The scales are logarithmic in order to show decades of FMR.

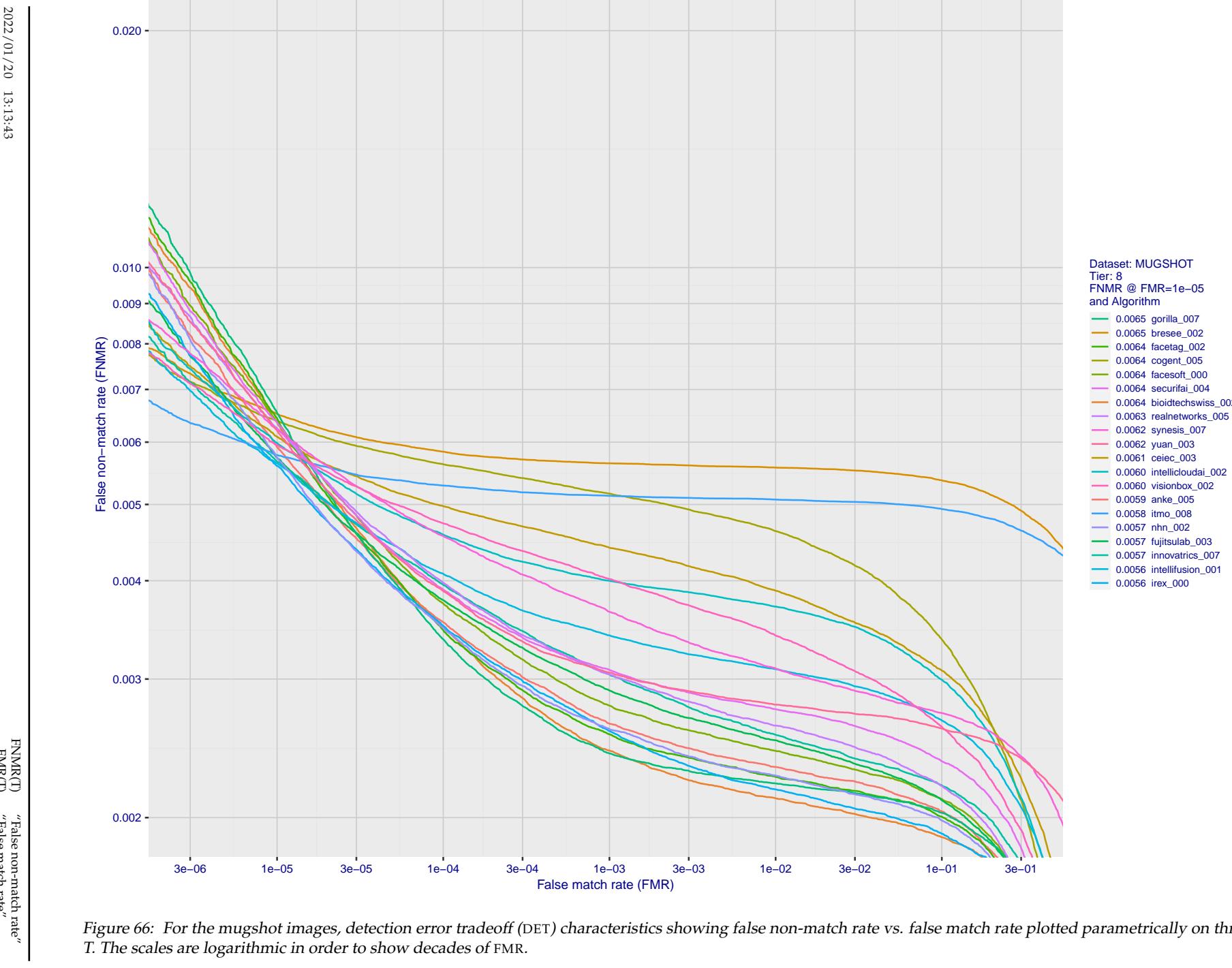


Figure 66: For the mugshot images, detection error tradeoff (DET) characteristics showing false non-match rate vs. false match rate plotted parametrically on threshold,  $T$ . The scales are logarithmic in order to show decades of FMR.

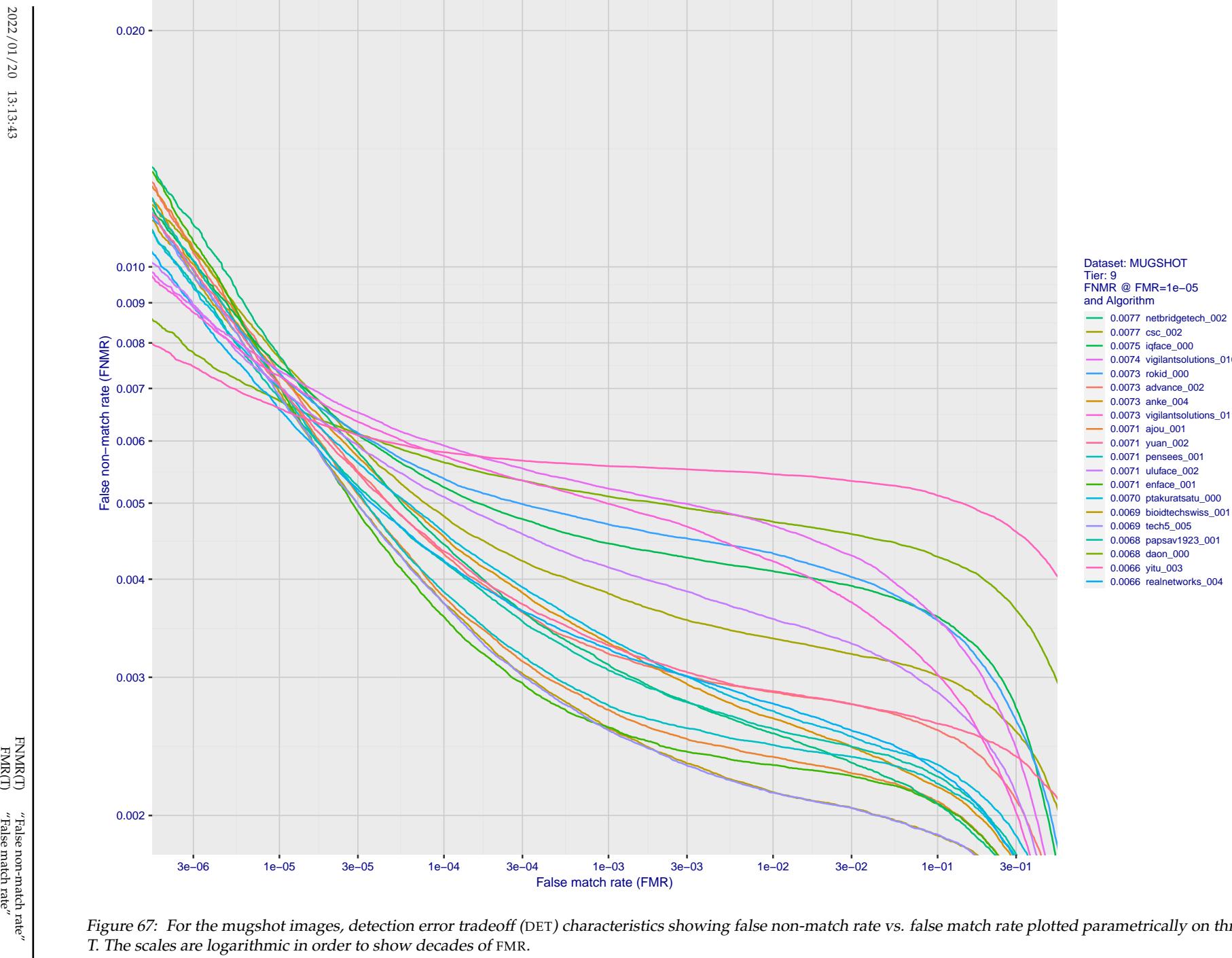


Figure 67: For the mugshot images, detection error tradeoff (DET) characteristics showing false non-match rate vs. false match rate plotted parametrically on threshold,  $T$ . The scales are logarithmic in order to show decades of FMR.

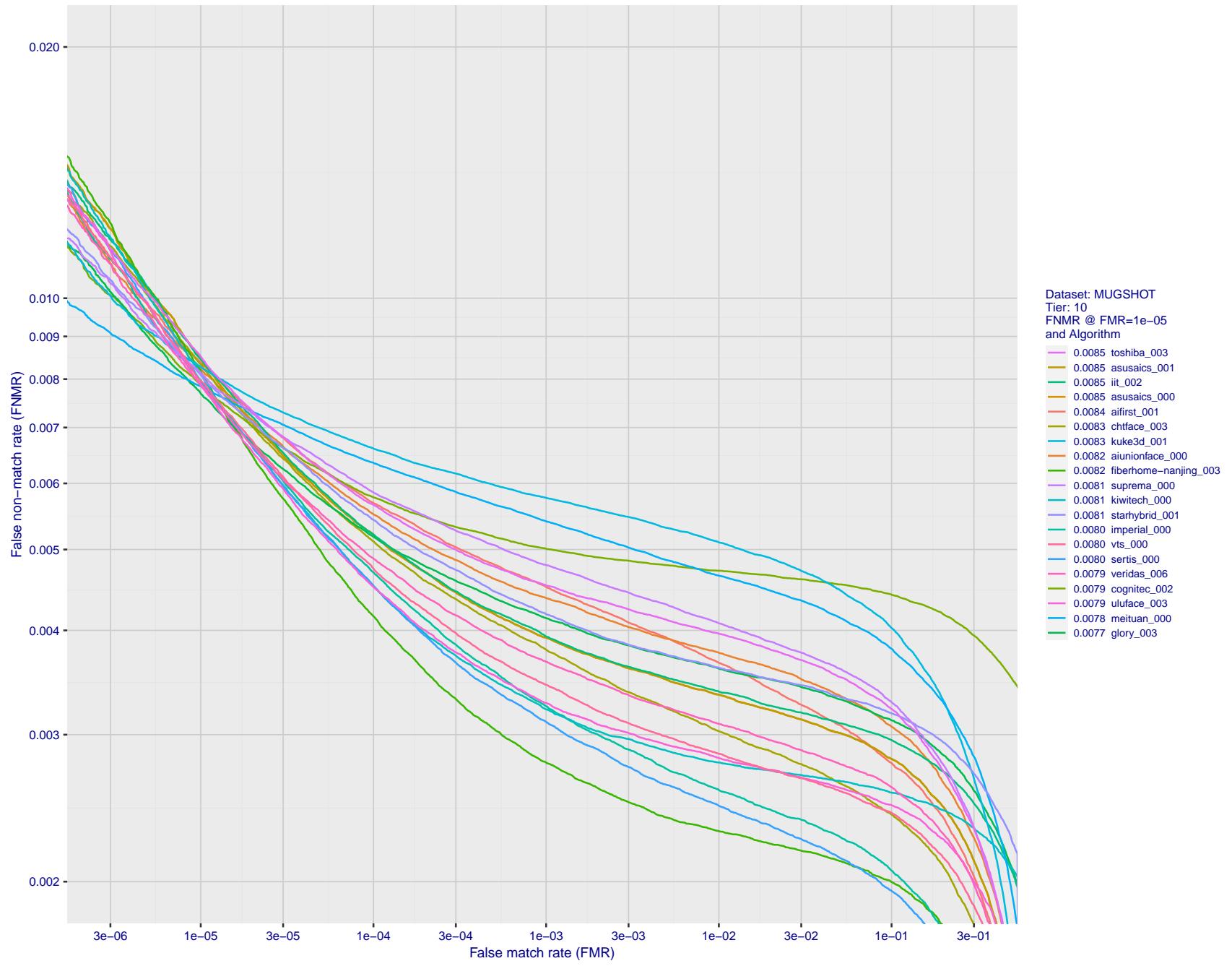


Figure 68: For the mugshot images, detection error tradeoff (DET) characteristics showing false non-match rate vs. false match rate plotted parametrically on threshold, T. The scales are logarithmic in order to show decades of FMR.

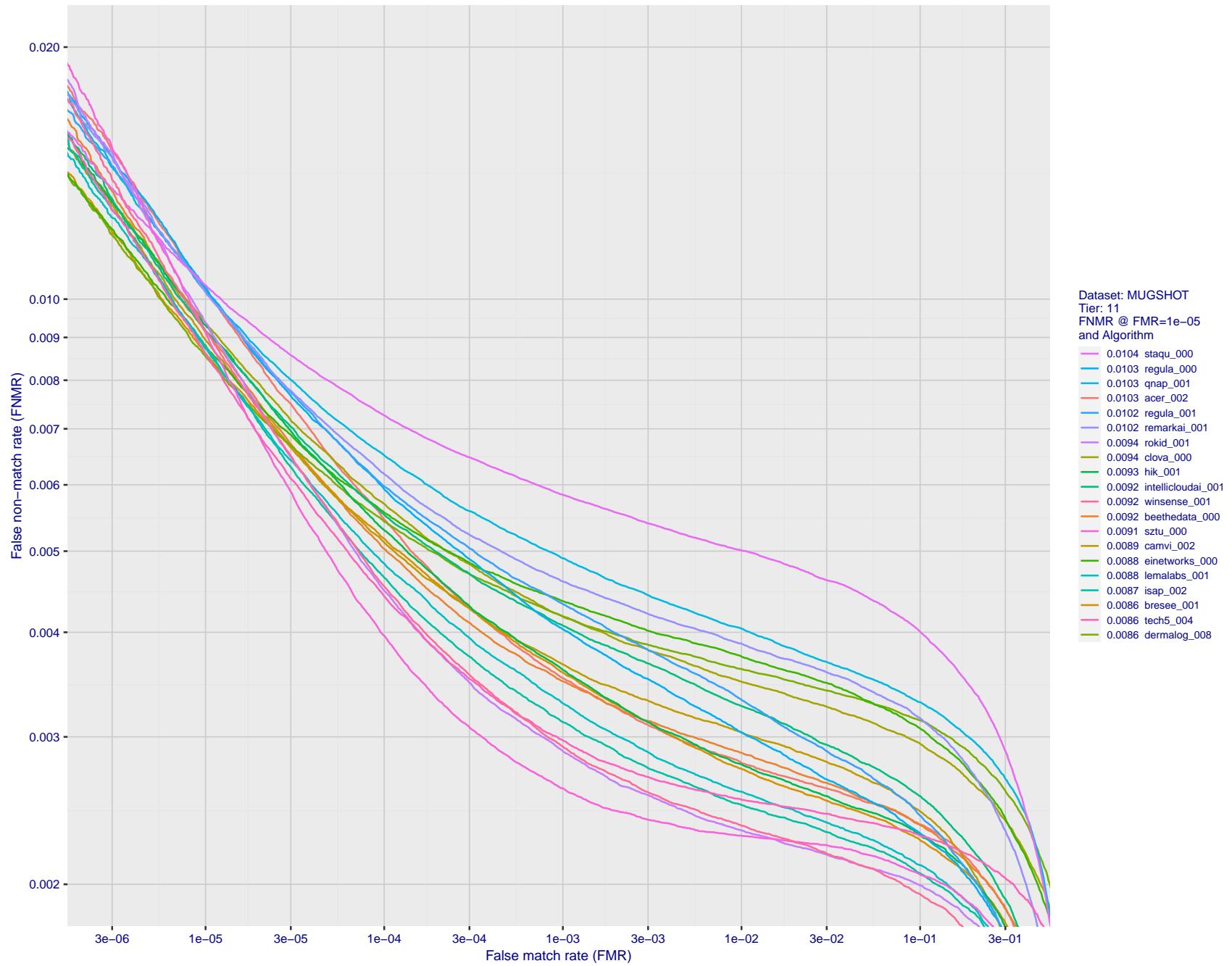
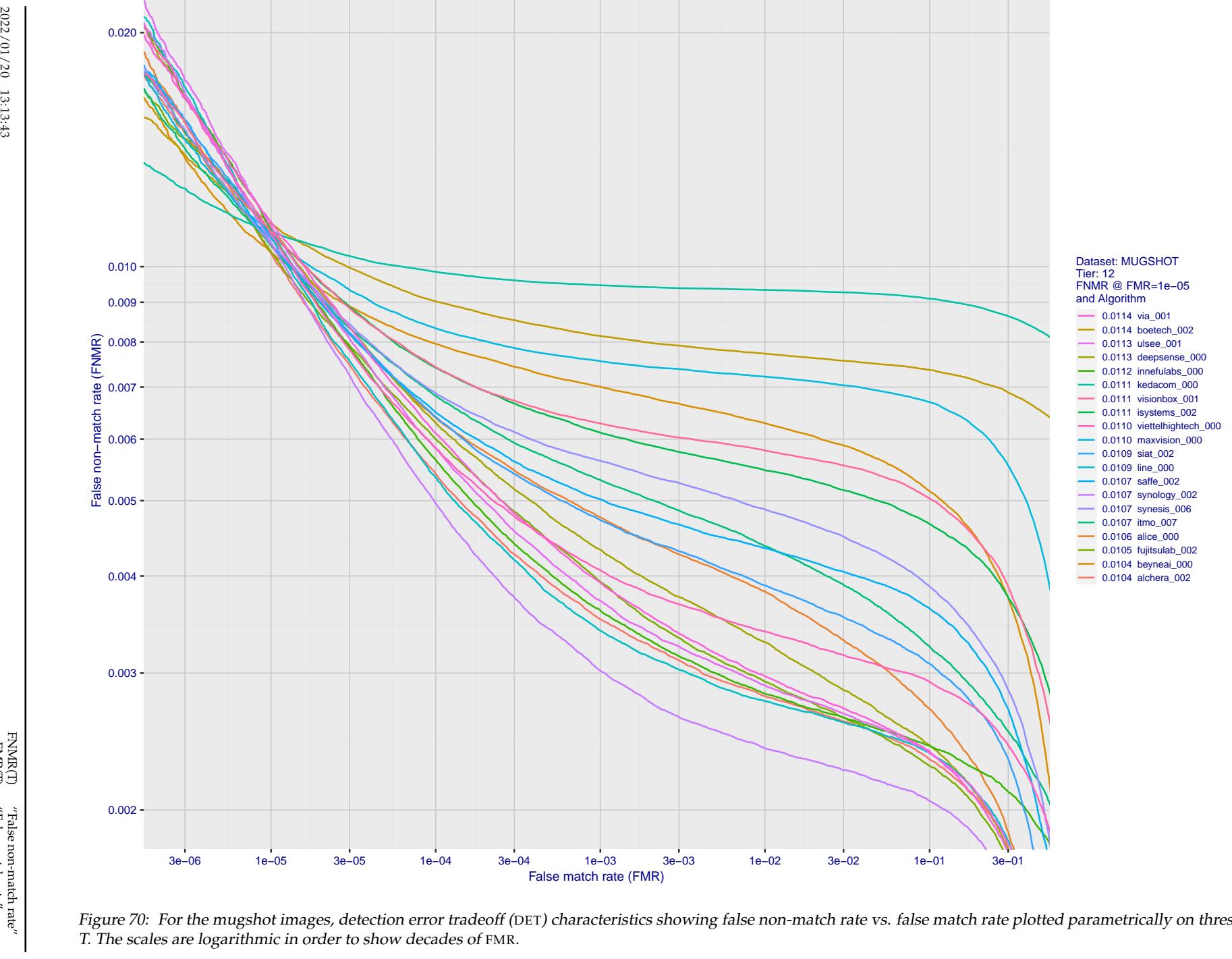


Figure 69: For the mugshot images, detection error tradeoff (DET) characteristics showing false non-match rate vs. false match rate plotted parametrically on threshold,  $T$ . The scales are logarithmic in order to show decades of FMR.



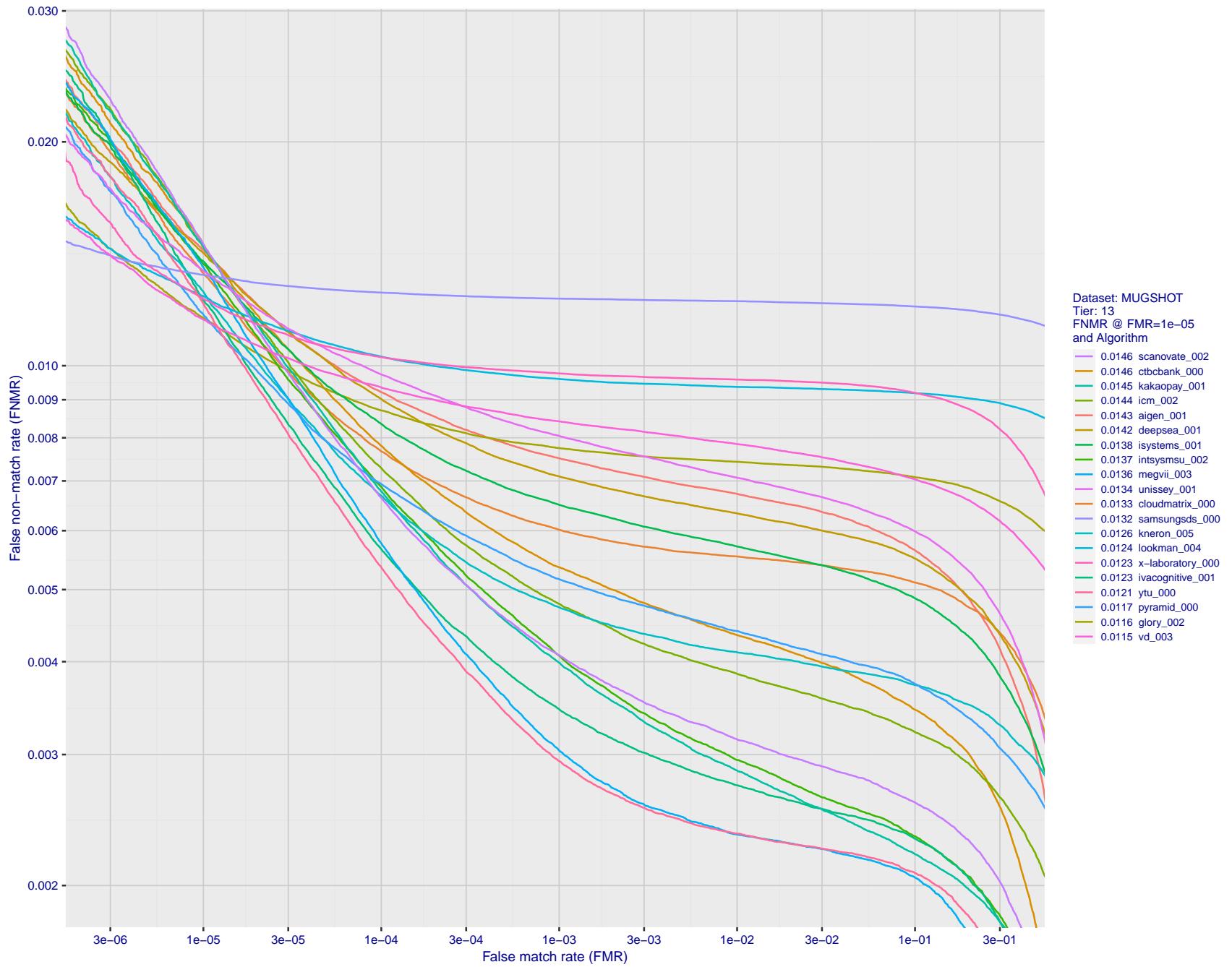


Figure 71: For the mugshot images, detection error tradeoff (DET) characteristics showing false non-match rate vs. false match rate plotted parametrically on threshold,  $T$ . The scales are logarithmic in order to show decades of FMR.

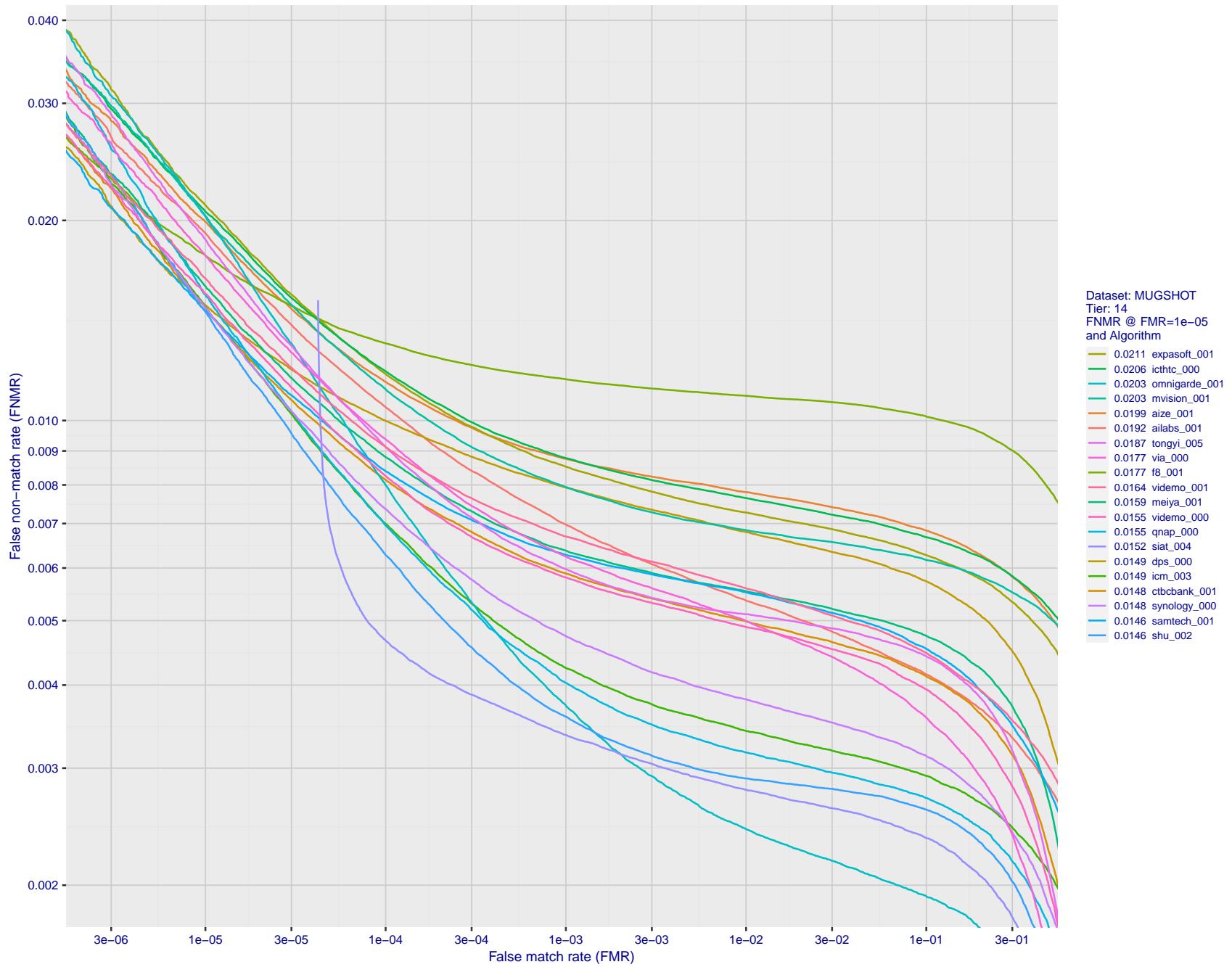


Figure 72: For the mugshot images, detection error tradeoff (DET) characteristics showing false non-match rate vs. false match rate plotted parametrically on threshold,  $T$ . The scales are logarithmic in order to show decades of FMR.

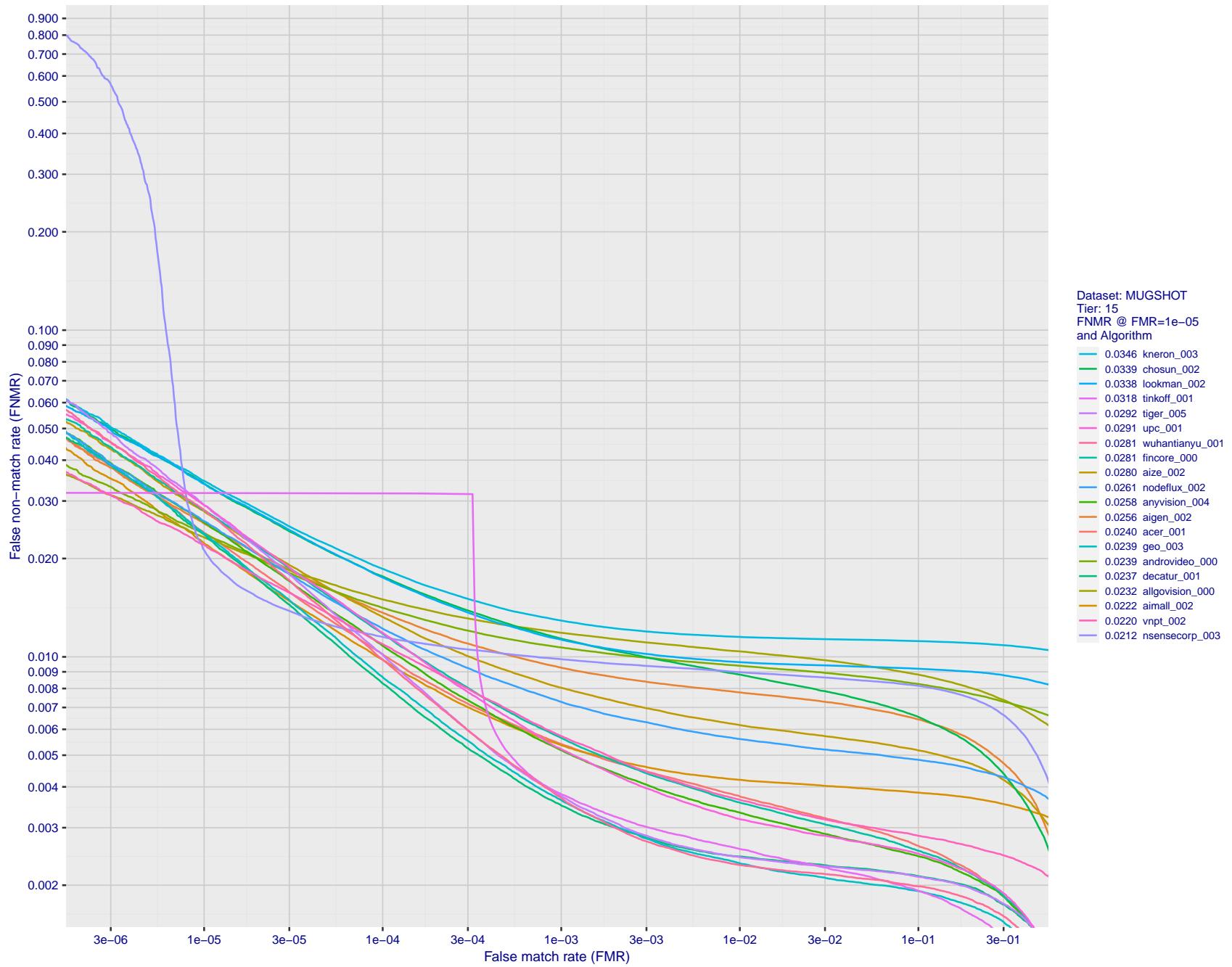


Figure 73: For the mugshot images, detection error tradeoff (DET) characteristics showing false non-match rate vs. false match rate plotted parametrically on threshold, T. The scales are logarithmic in order to show decades of FMR.

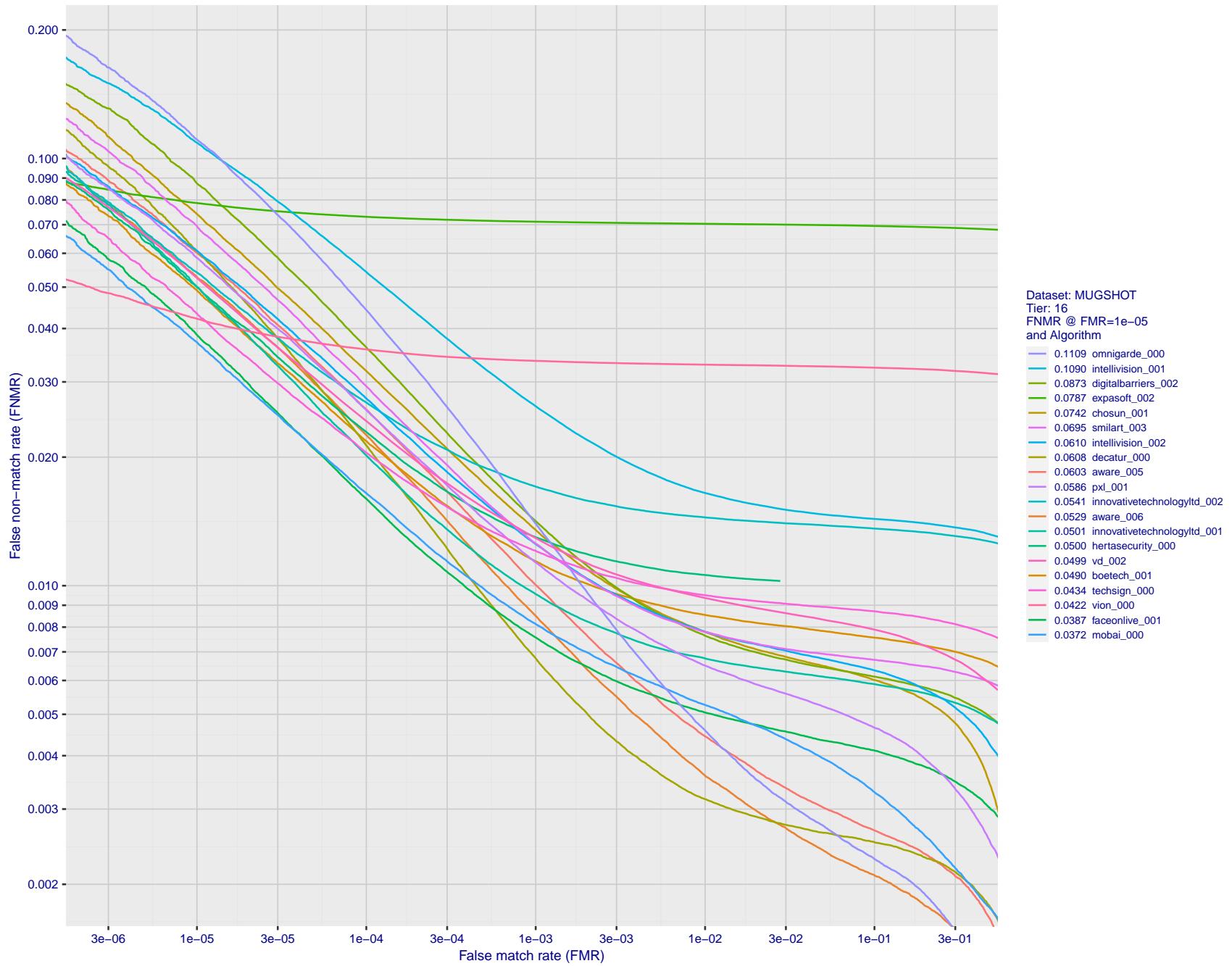


Figure 74: For the mugshot images, detection error tradeoff (DET) characteristics showing false non-match rate vs. false match rate plotted parametrically on threshold,  $T$ . The scales are logarithmic in order to show decades of FMR.

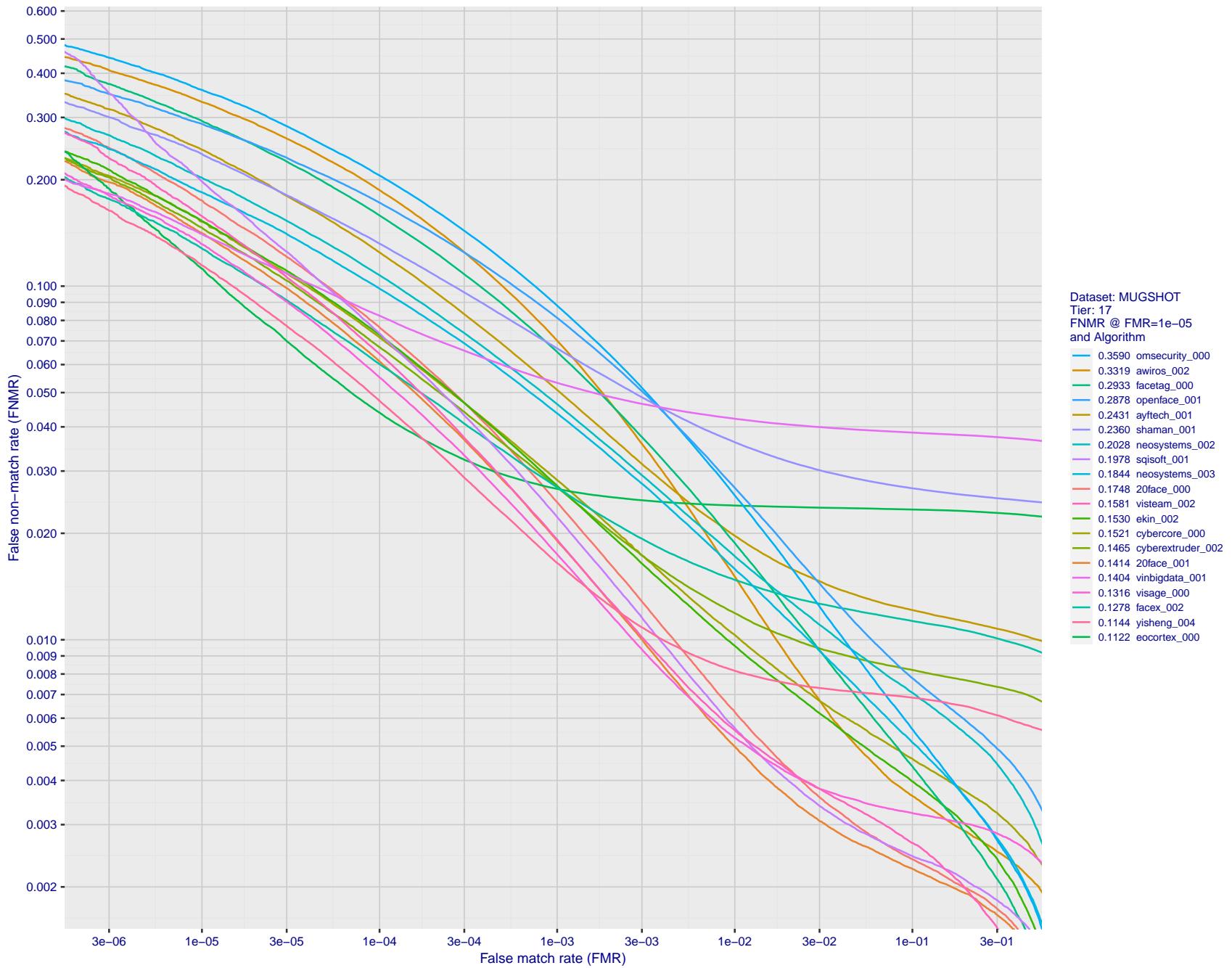


Figure 75: For the mugshot images, detection error tradeoff (DET) characteristics showing false non-match rate vs. false match rate plotted parametrically on threshold,  $T$ . The scales are logarithmic in order to show decades of FMR.

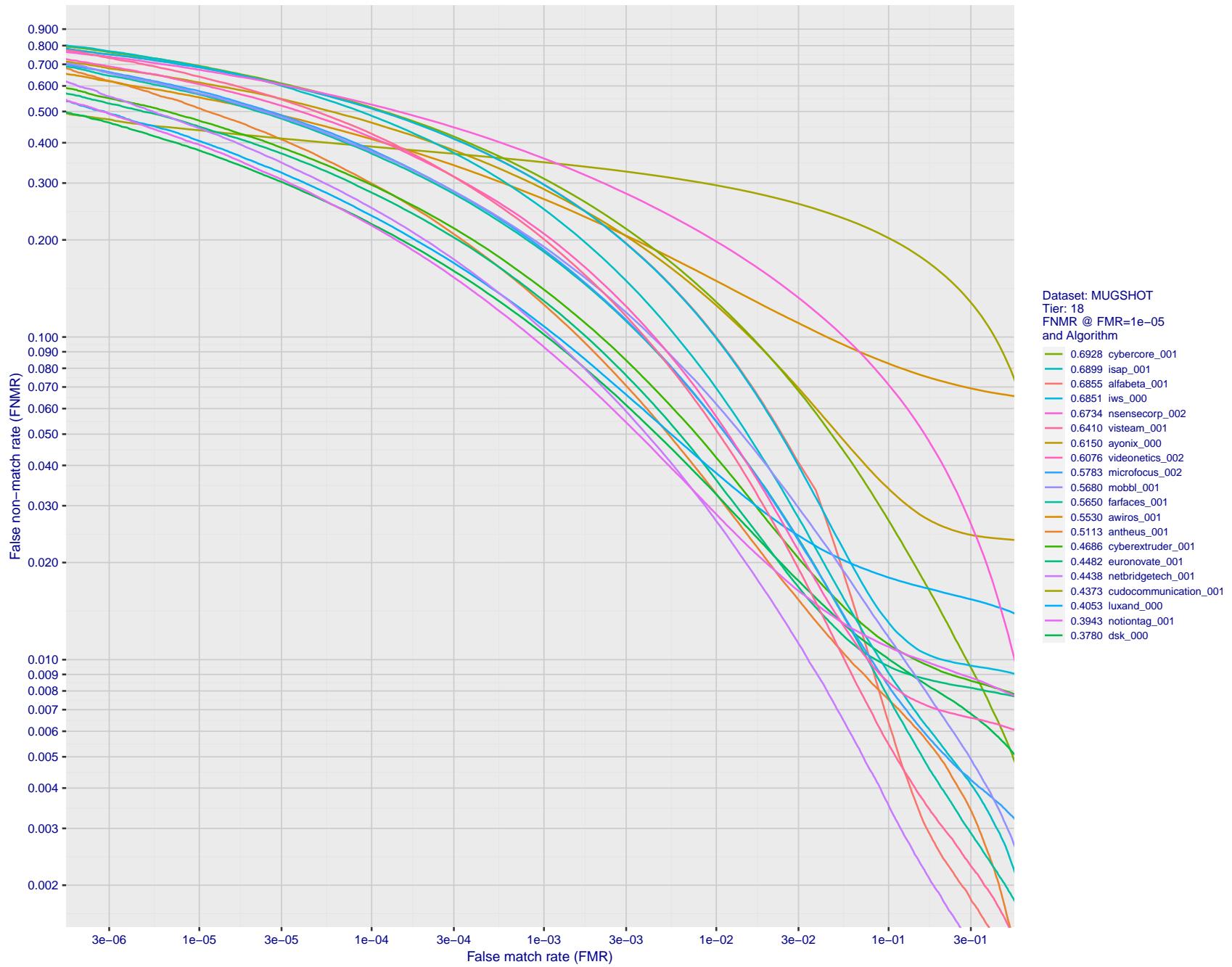


Figure 76: For the mugshot images, detection error tradeoff (DET) characteristics showing false non-match rate vs. false match rate plotted parametrically on threshold, T. The scales are logarithmic in order to show decades of FMR.

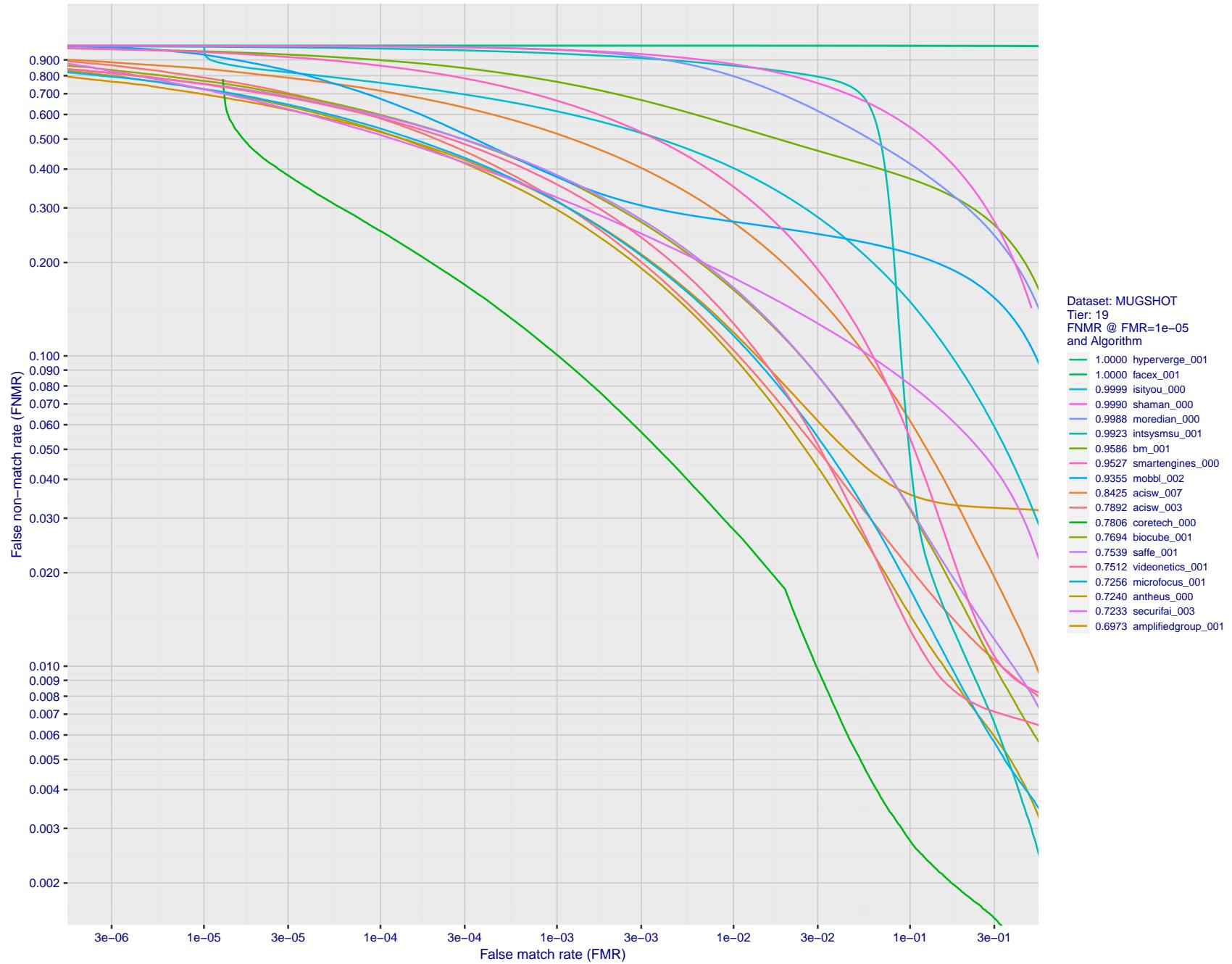


Figure 77: For the mugshot images, detection error tradeoff (DET) characteristics showing false non-match rate vs. false match rate plotted parametrically on threshold,  $T$ . The scales are logarithmic in order to show decades of FMR.

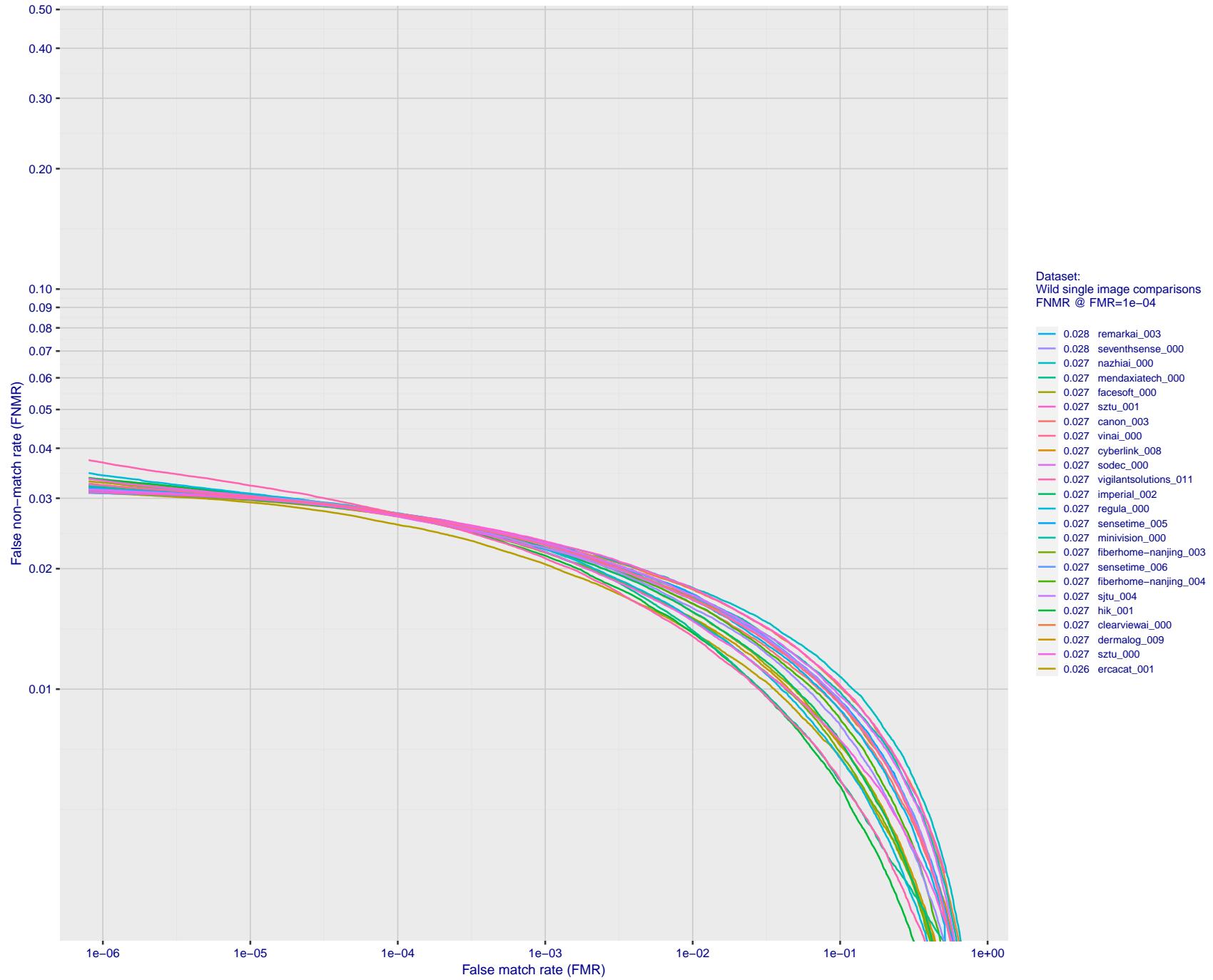


Figure 78: For the 2018 wild image comparisons, detection error tradeoff (DET) characteristics showing false non-match rate vs. false match rate plotted parametrically on threshold,  $T$ . The scales are logarithmic in order to show several decades of FMR.

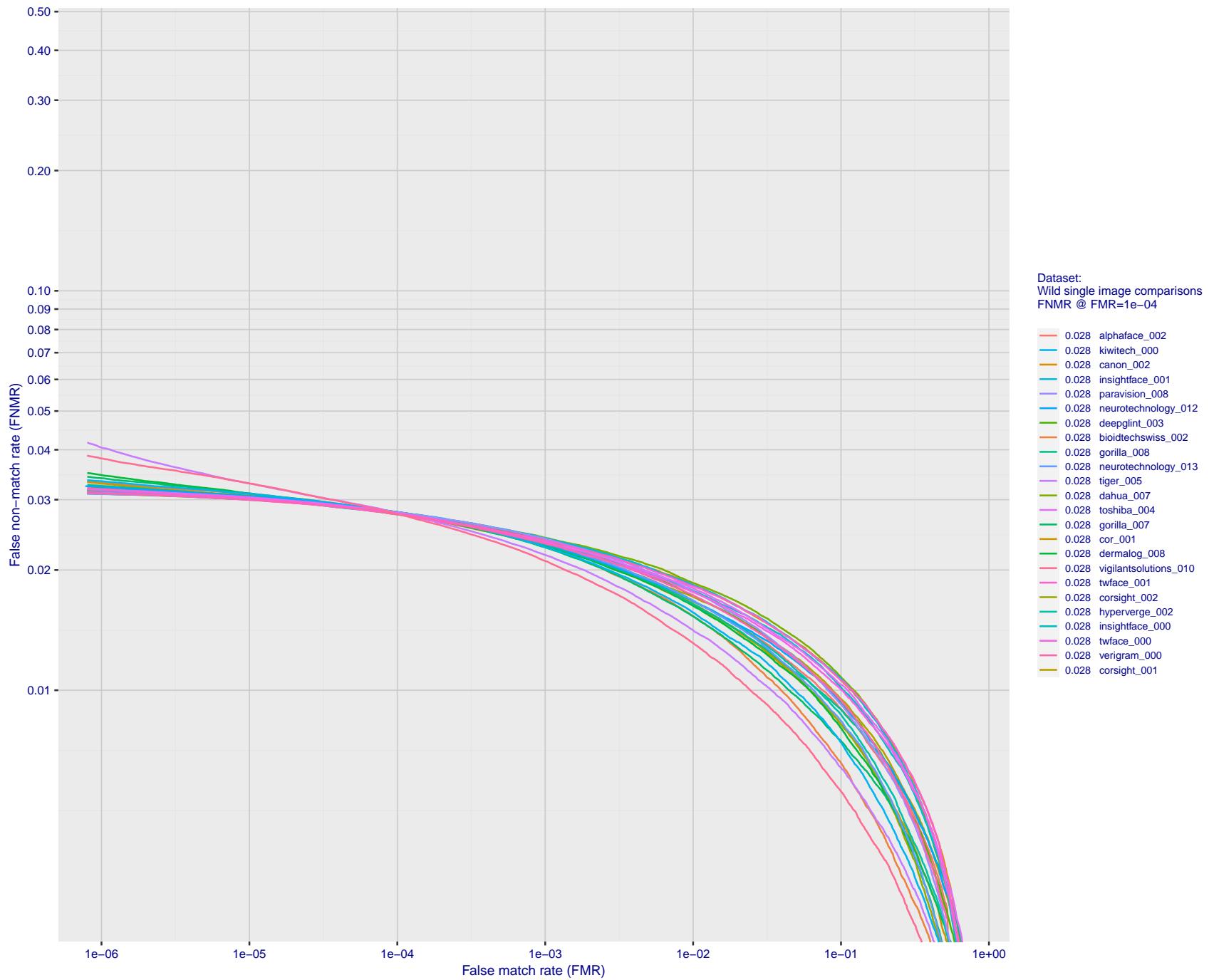


Figure 79: For the 2018 wild image comparisons, detection error tradeoff (DET) characteristics showing false non-match rate vs. false match rate plotted parametrically on threshold,  $T$ . The scales are logarithmic in order to show several decades of FMR.

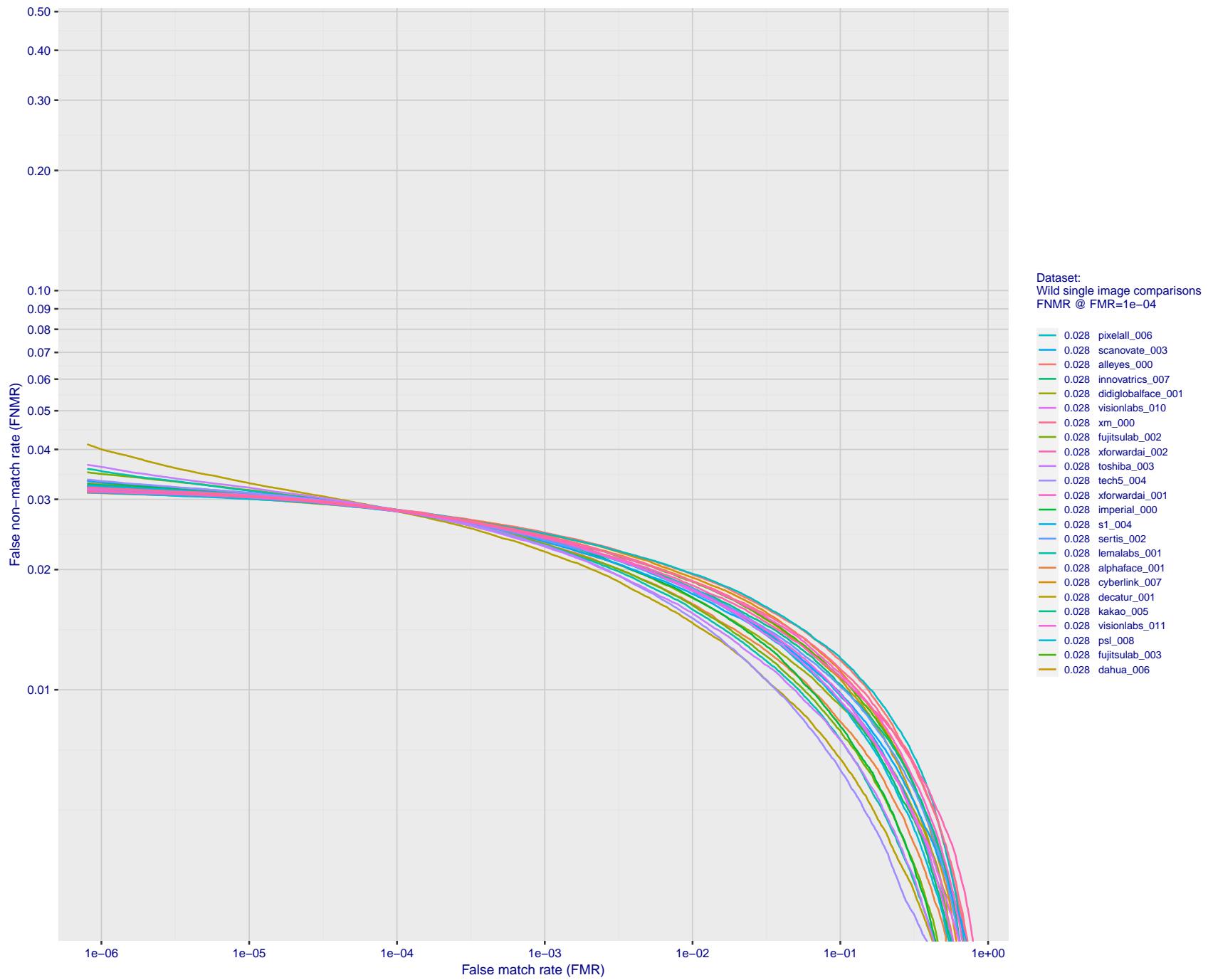


Figure 80: For the 2018 wild image comparisons, detection error tradeoff (DET) characteristics showing false non-match rate vs. false match rate plotted parametrically on threshold,  $T$ . The scales are logarithmic in order to show several decades of FMR.

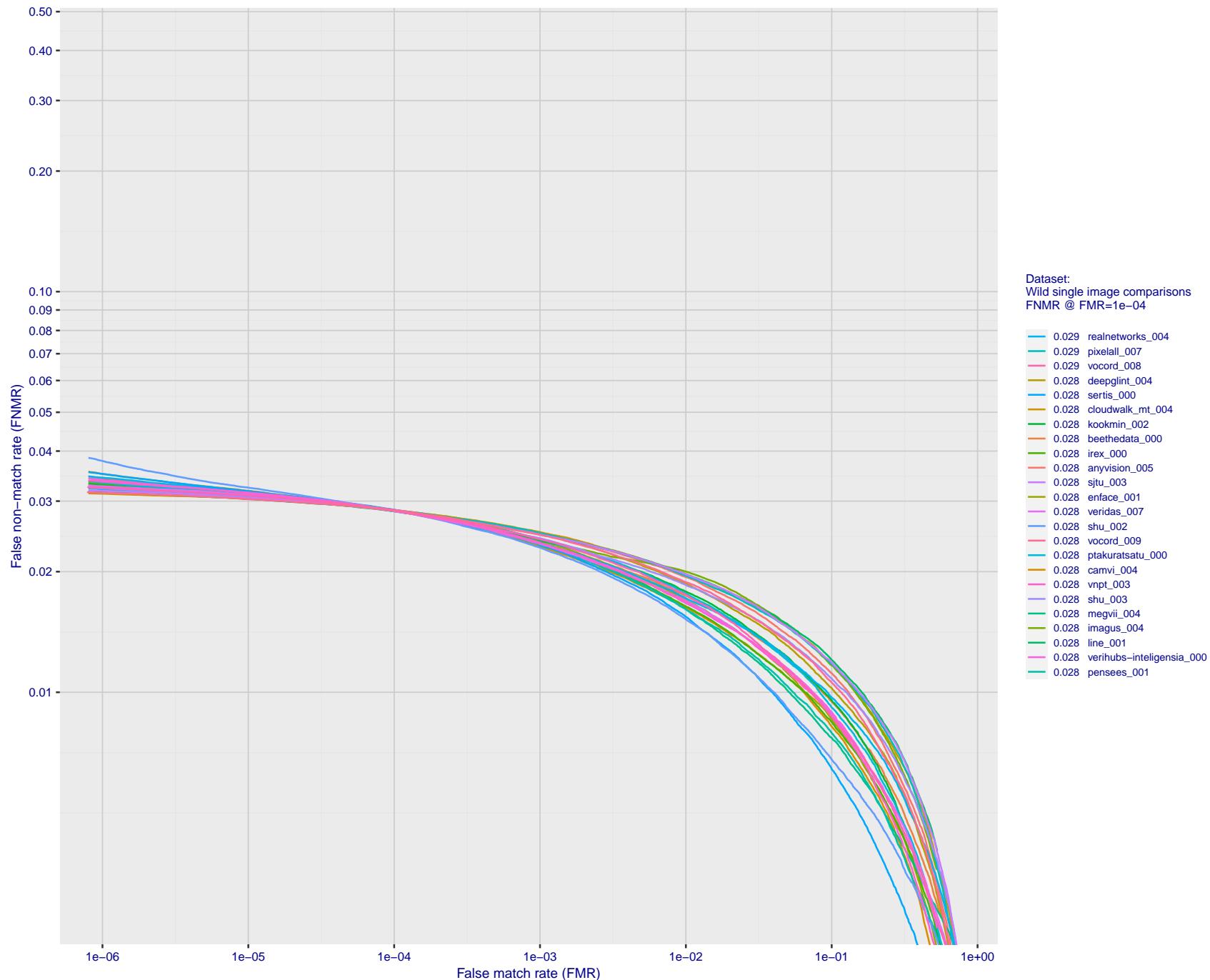


Figure 81: For the 2018 wild image comparisons, detection error tradeoff (DET) characteristics showing false non-match rate vs. false match rate plotted parametrically on threshold, T. The scales are logarithmic in order to show several decades of FMR.

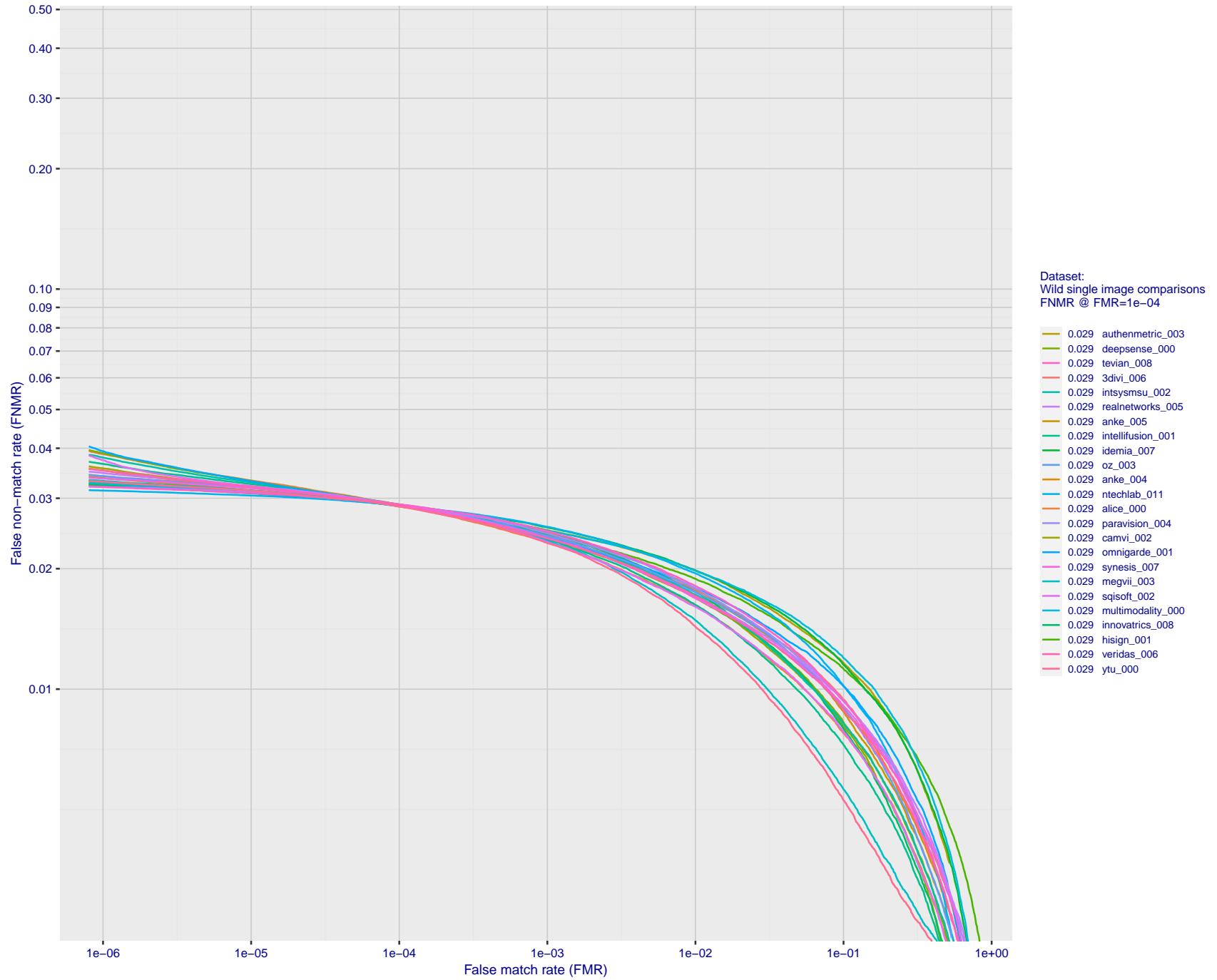


Figure 82: For the 2018 wild image comparisons, detection error tradeoff (DET) characteristics showing false non-match rate vs. false match rate plotted parametrically on threshold,  $T$ . The scales are logarithmic in order to show several decades of FMR.

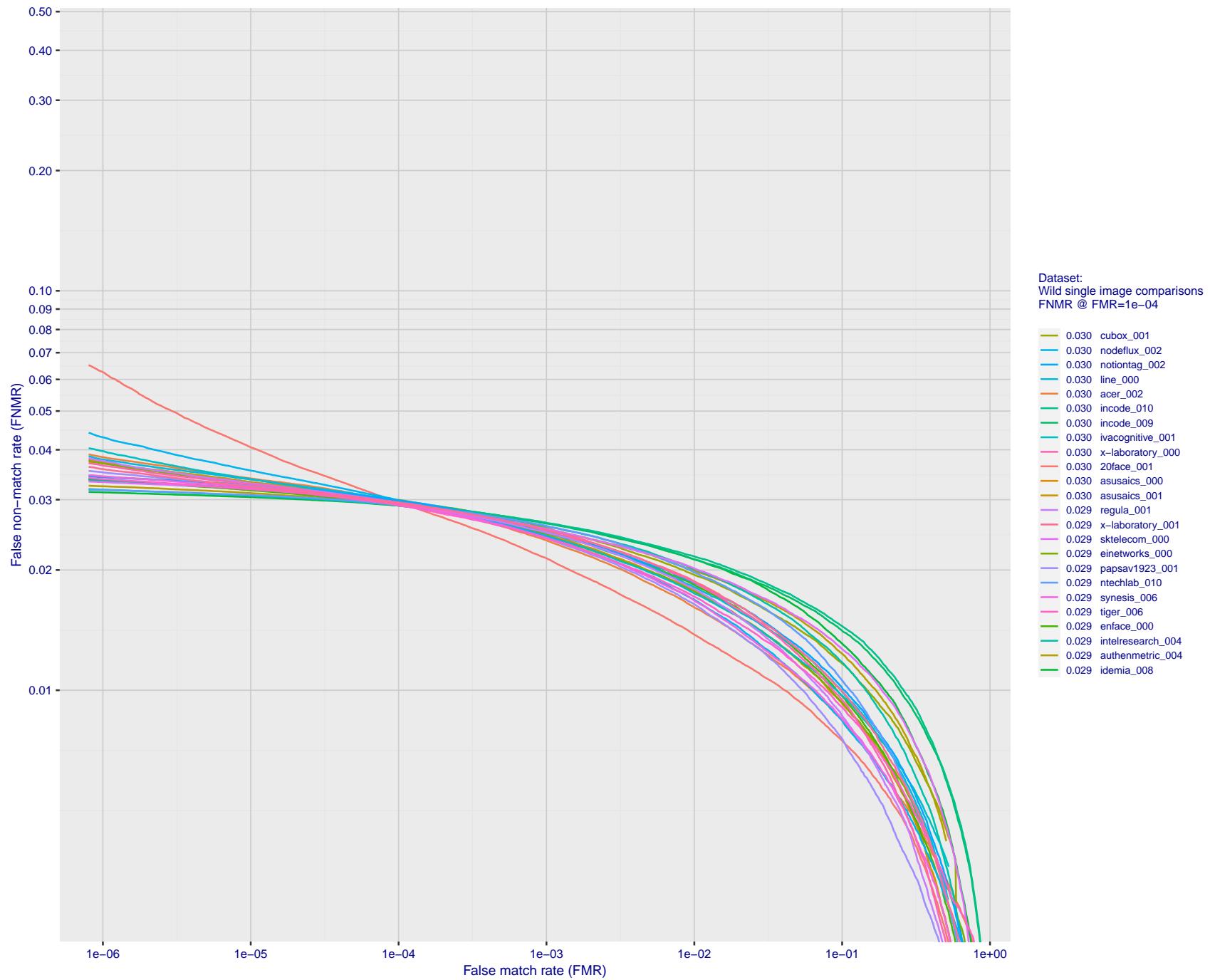


Figure 83: For the 2018 wild image comparisons, detection error tradeoff (DET) characteristics showing false non-match rate vs. false match rate plotted parametrically on threshold,  $T$ . The scales are logarithmic in order to show several decades of FMR.

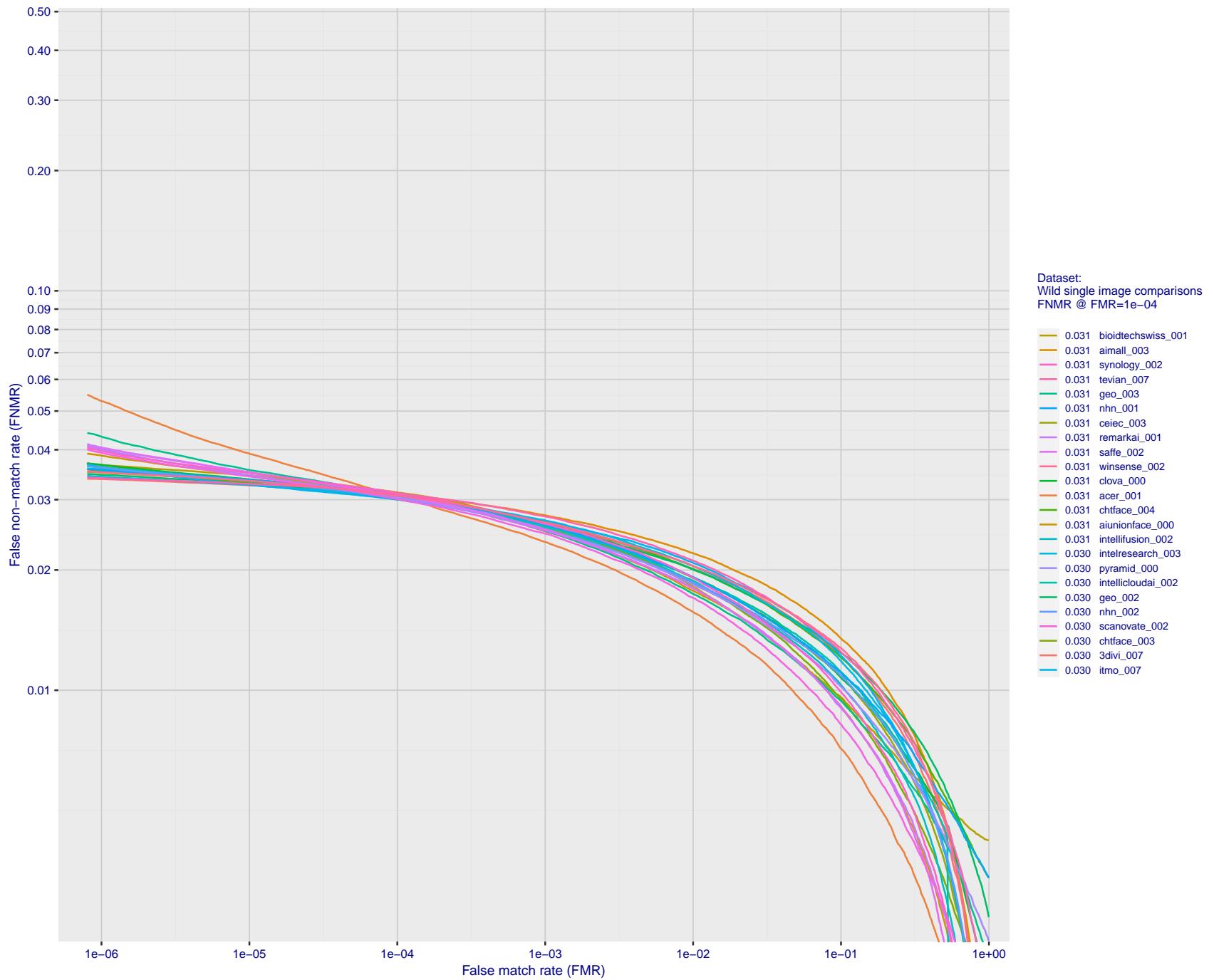


Figure 84: For the 2018 wild image comparisons, detection error tradeoff (DET) characteristics showing false non-match rate vs. false match rate plotted parametrically on threshold, T. The scales are logarithmic in order to show several decades of FMR.

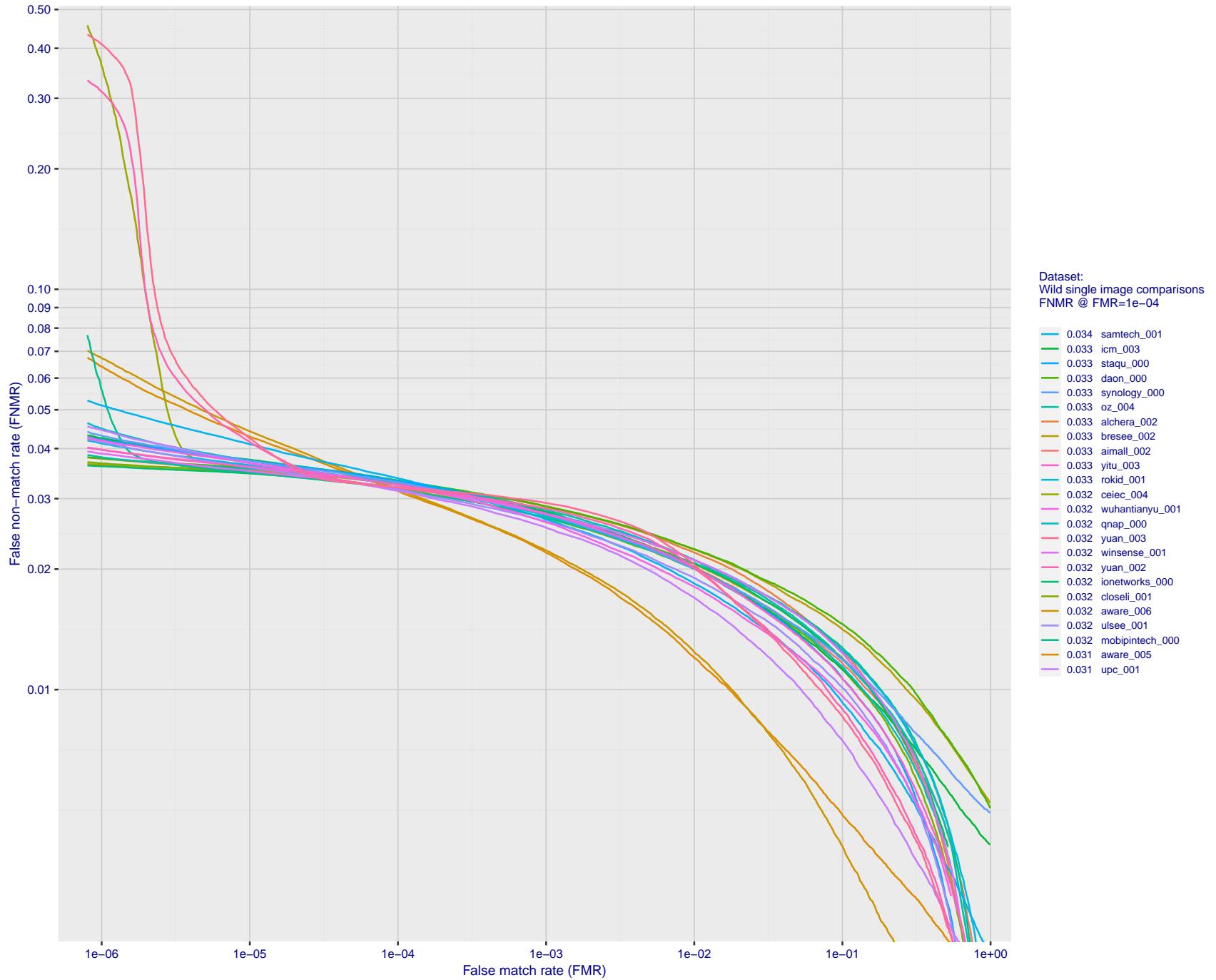


Figure 85: For the 2018 wild image comparisons, detection error tradeoff (DET) characteristics showing false non-match rate vs. false match rate plotted parametrically on threshold,  $T$ . The scales are logarithmic in order to show several decades of FMR.

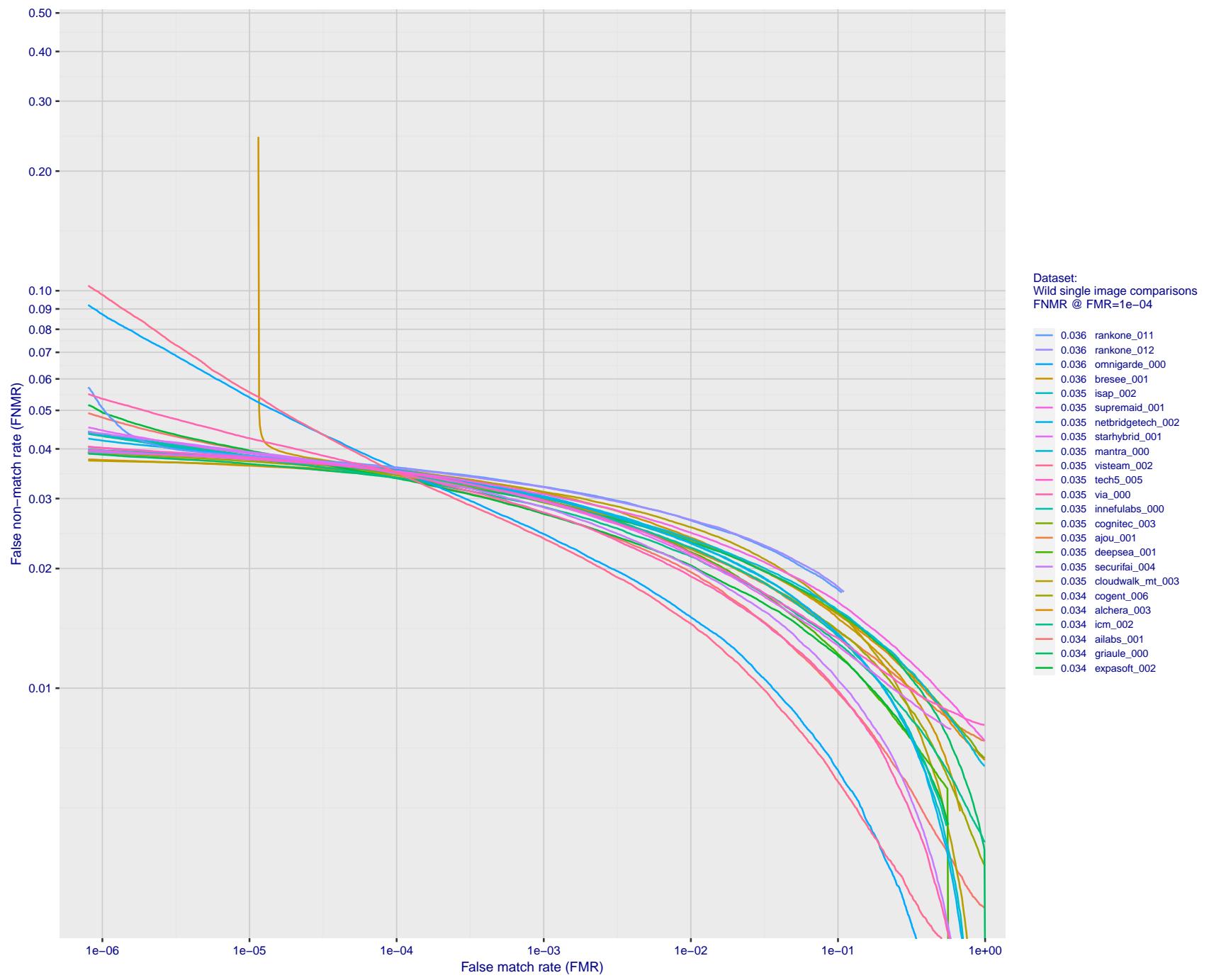


Figure 86: For the 2018 wild image comparisons, detection error tradeoff (DET) characteristics showing false non-match rate vs. false match rate plotted parametrically on threshold,  $T$ . The scales are logarithmic in order to show several decades of FMR.

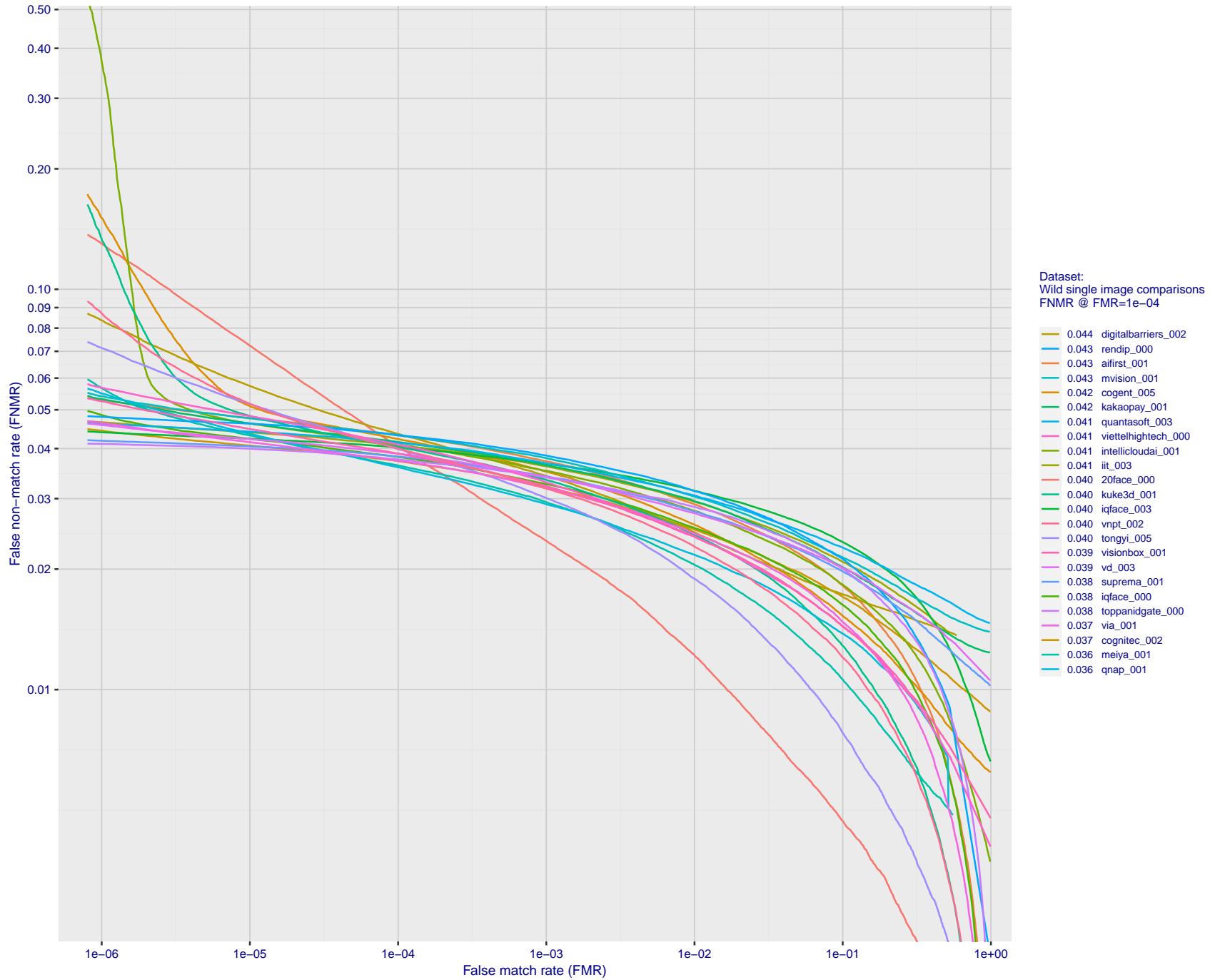


Figure 87: For the 2018 wild image comparisons, detection error tradeoff (DET) characteristics showing false non-match rate vs. false match rate plotted parametrically on threshold,  $T$ . The scales are logarithmic in order to show several decades of FMR.

2022/01/20 13:13:43

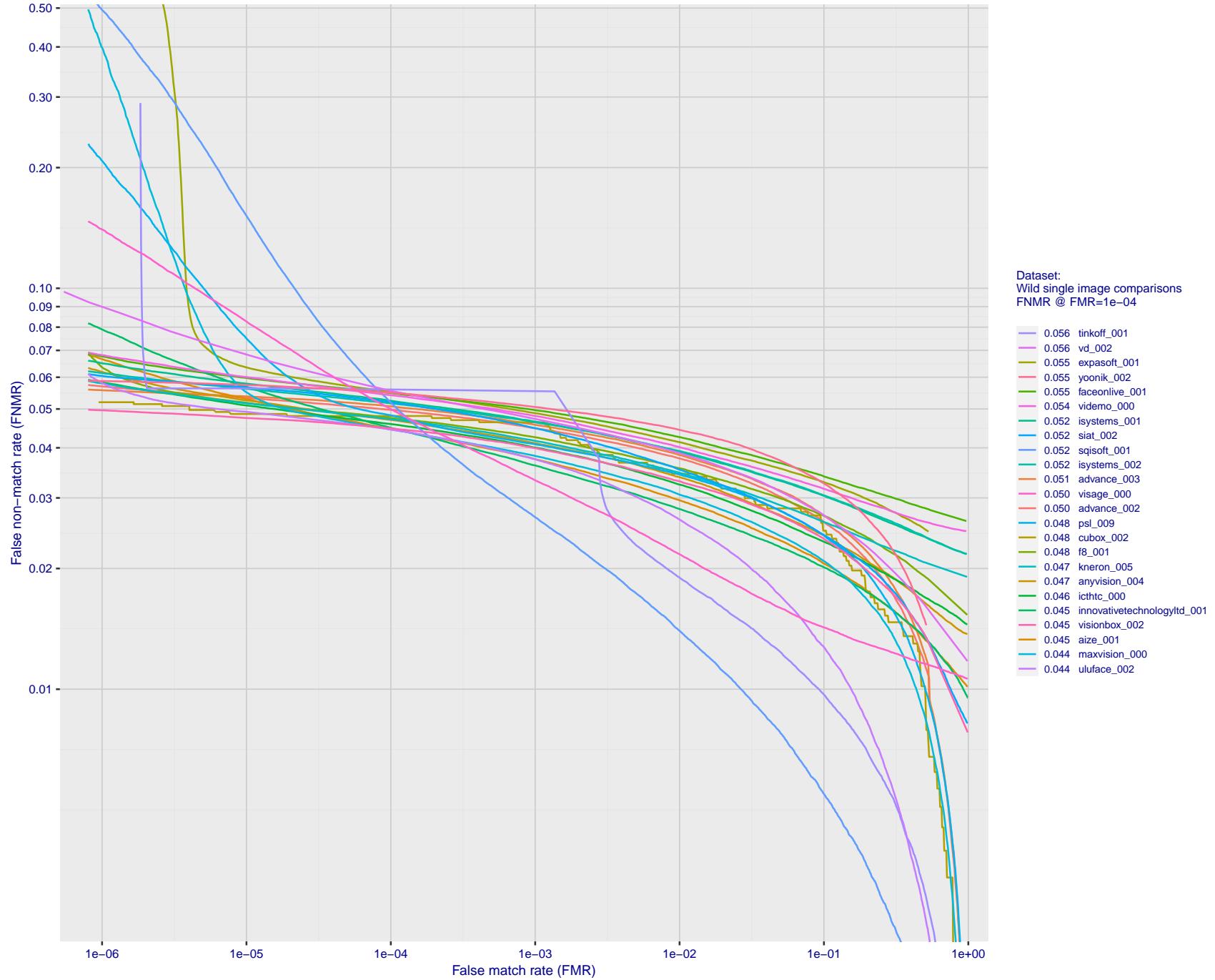


Figure 88: For the 2018 wild image comparisons, detection error tradeoff (DET) characteristics showing false non-match rate vs. false match rate plotted parametrically on threshold,  $T$ . The scales are logarithmic in order to show several decades of FMR.

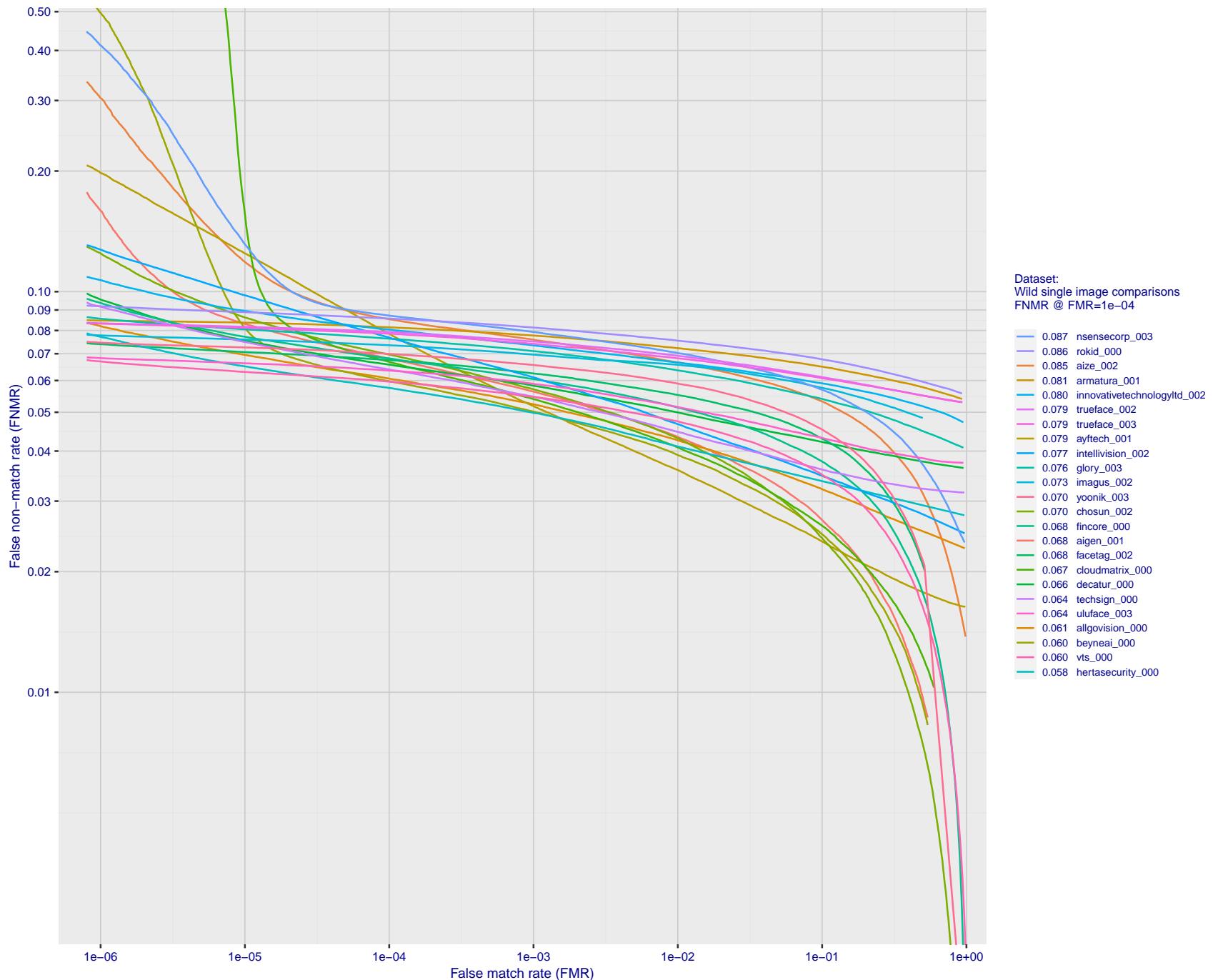


Figure 89: For the 2018 wild image comparisons, detection error tradeoff (DET) characteristics showing false non-match rate vs. false match rate plotted parametrically on threshold,  $T$ . The scales are logarithmic in order to show several decades of FMR.

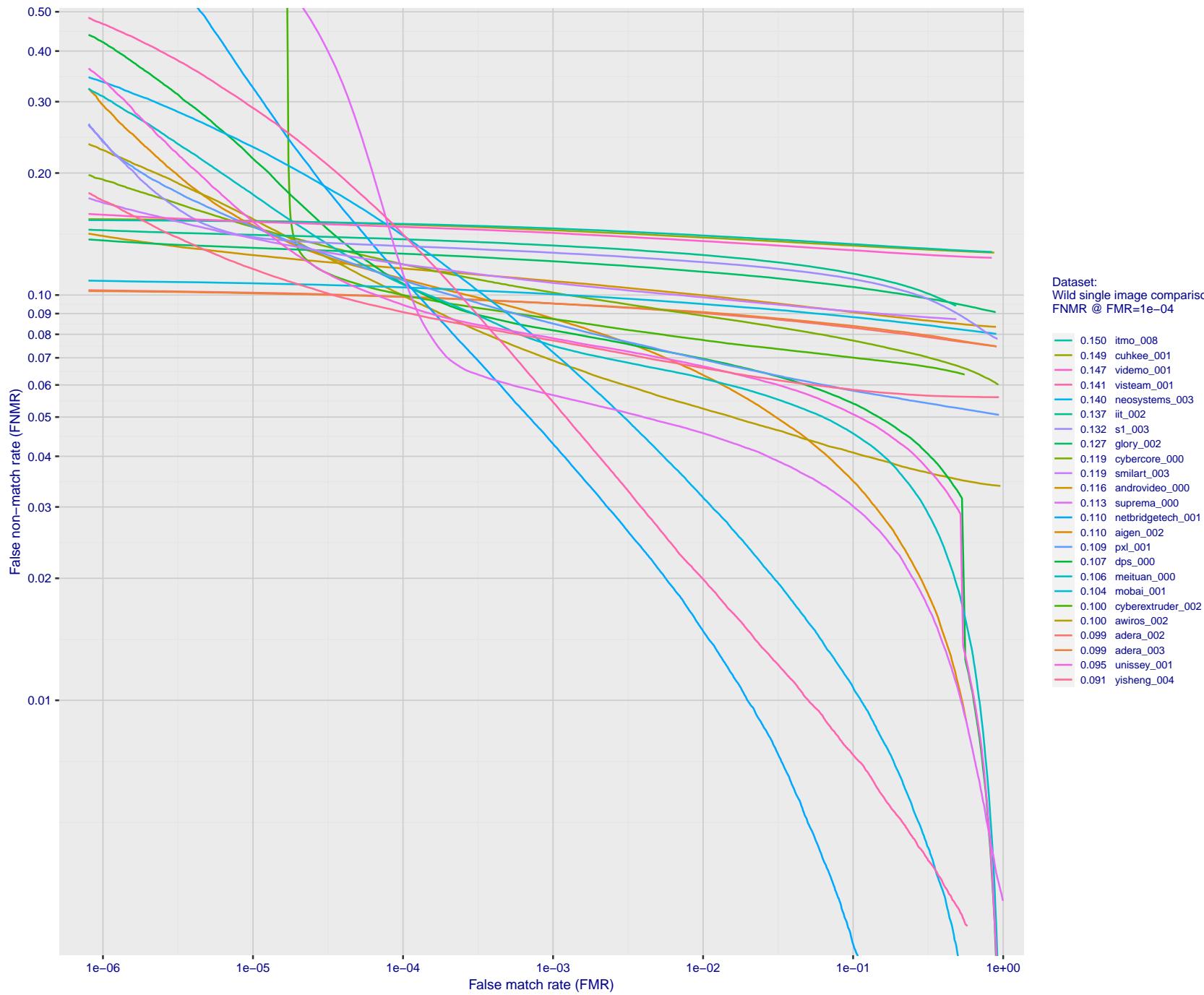


Figure 90: For the 2018 wild image comparisons, detection error tradeoff (DET) characteristics showing false non-match rate vs. false match rate plotted parametrically on threshold,  $T$ . The scales are logarithmic in order to show several decades of FMR.

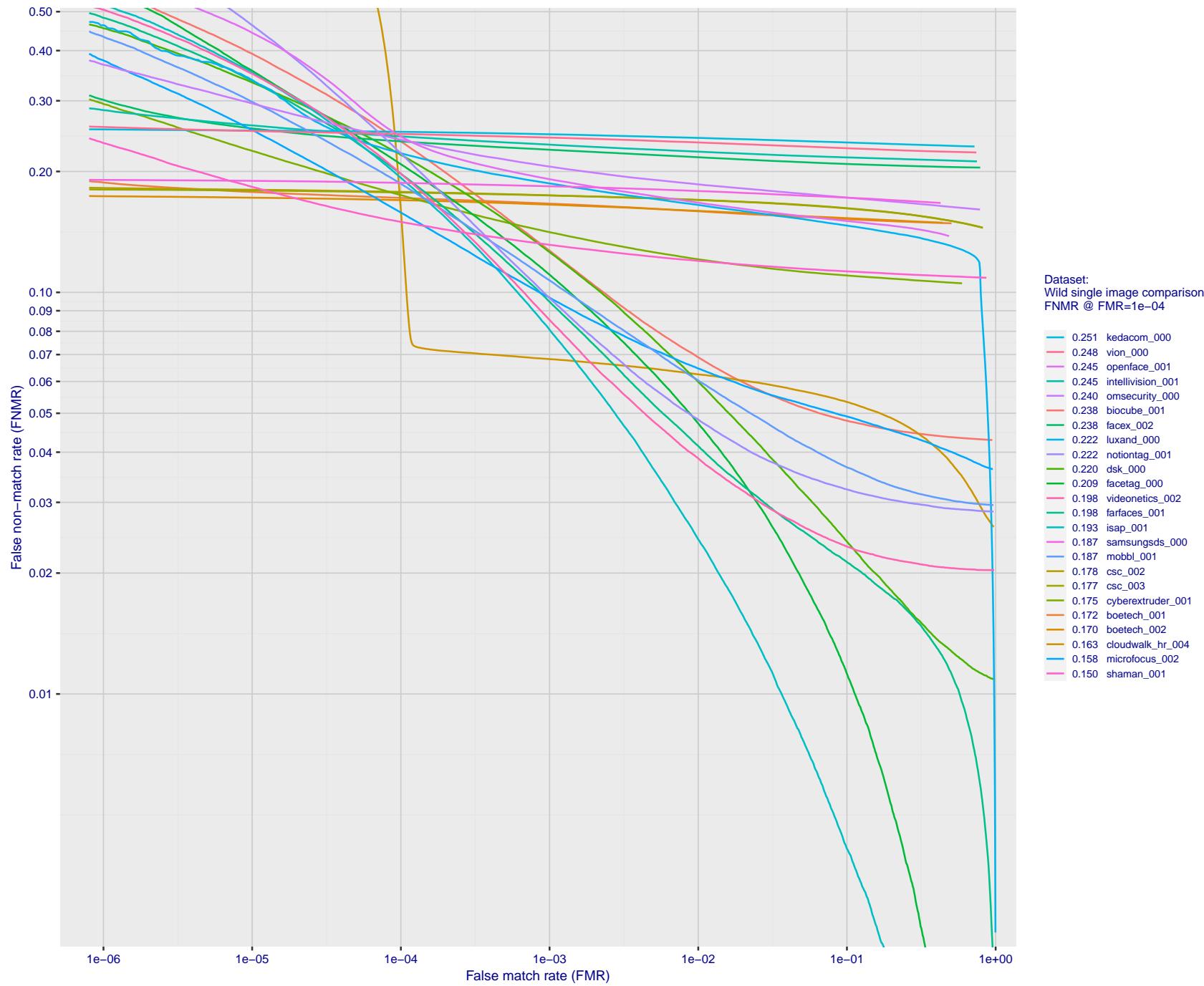


Figure 91: For the 2018 wild image comparisons, detection error tradeoff (DET) characteristics showing false non-match rate vs. false match rate plotted parametrically on threshold,  $T$ . The scales are logarithmic in order to show several decades of FMR.

2022/01/20 13:13:43

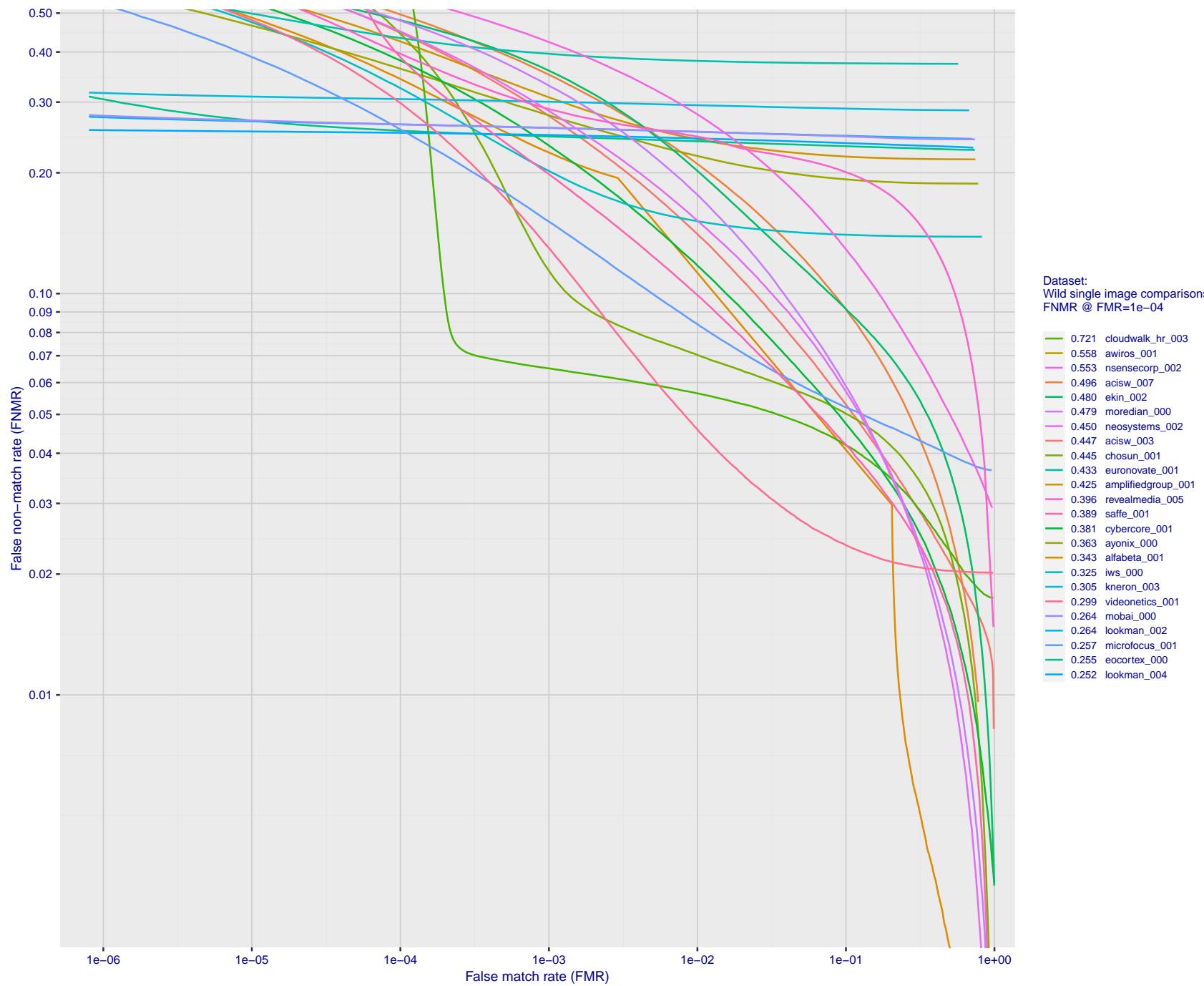


Figure 92: For the 2018 wild image comparisons, detection error tradeoff (DET) characteristics showing false non-match rate vs. false match rate plotted parametrically on threshold,  $T$ . The scales are logarithmic in order to show several decades of FMR.

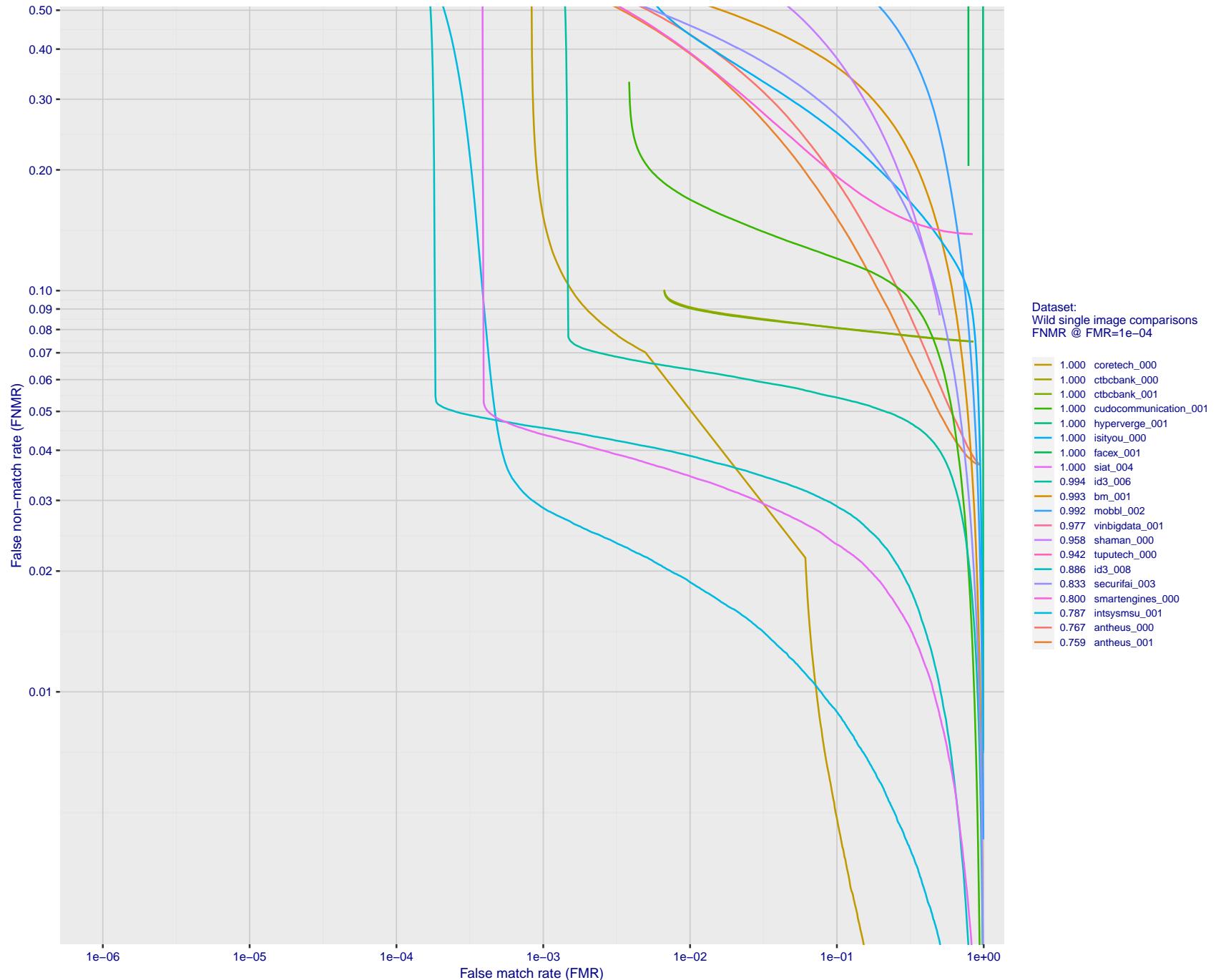


Figure 93: For the 2018 wild image comparisons, detection error tradeoff (DET) characteristics showing false non-match rate vs. false match rate plotted parametrically on threshold,  $T$ . The scales are logarithmic in order to show several decades of FMR.

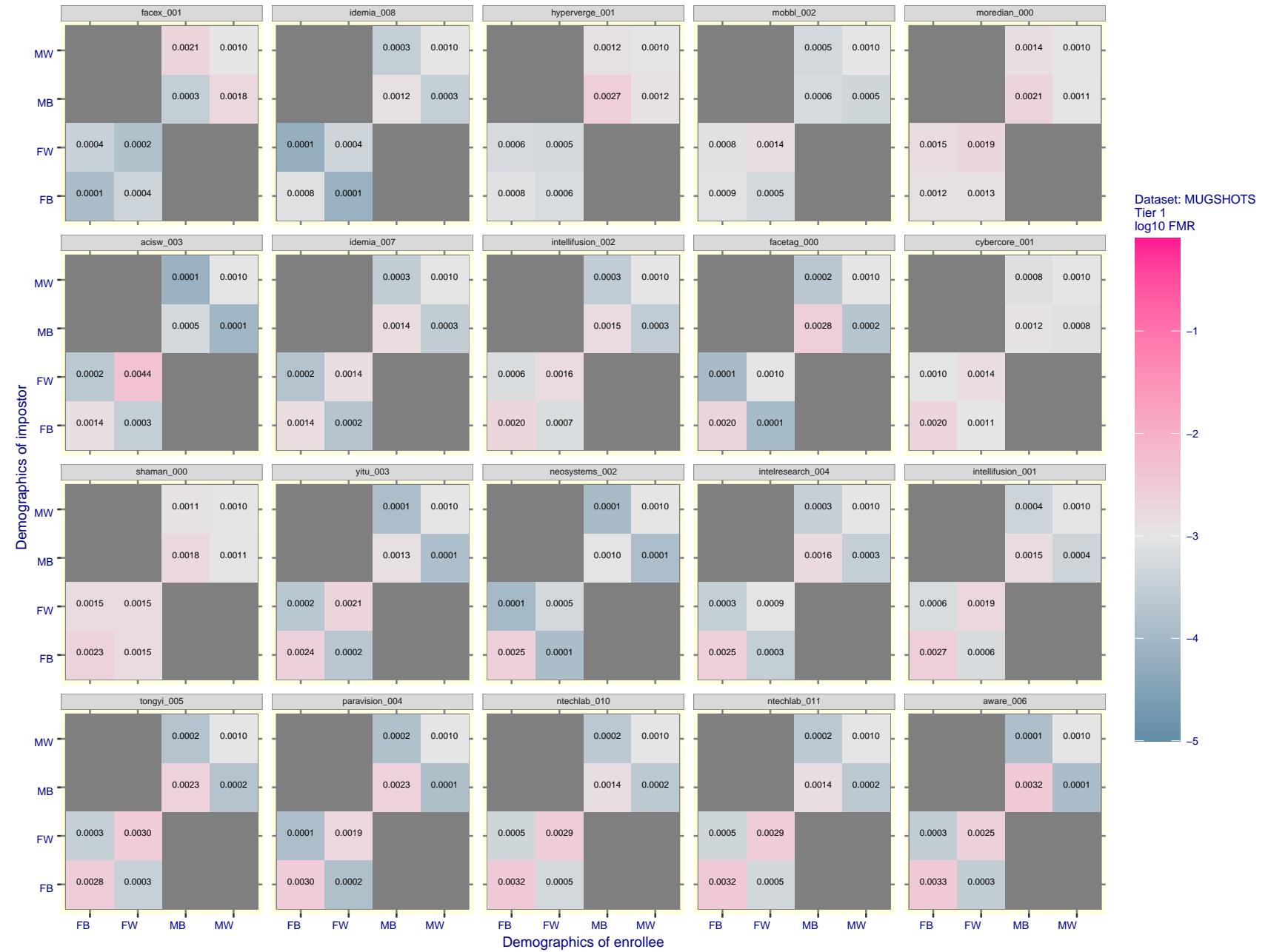


Figure 94: For the mugshot images, FMR for same-sex impostor pairs of images annotated with codes for black female, black male, white female, white male. The threshold is set for each algorithm to give FMR = 0.001 for white males which is the demographic that usually gives the lowest FMR. This means the top right box is the same color in all panels. The panels are sorted over multiple pages in order of FMR on black females, which is the demographic that usually gives the highest FMR.

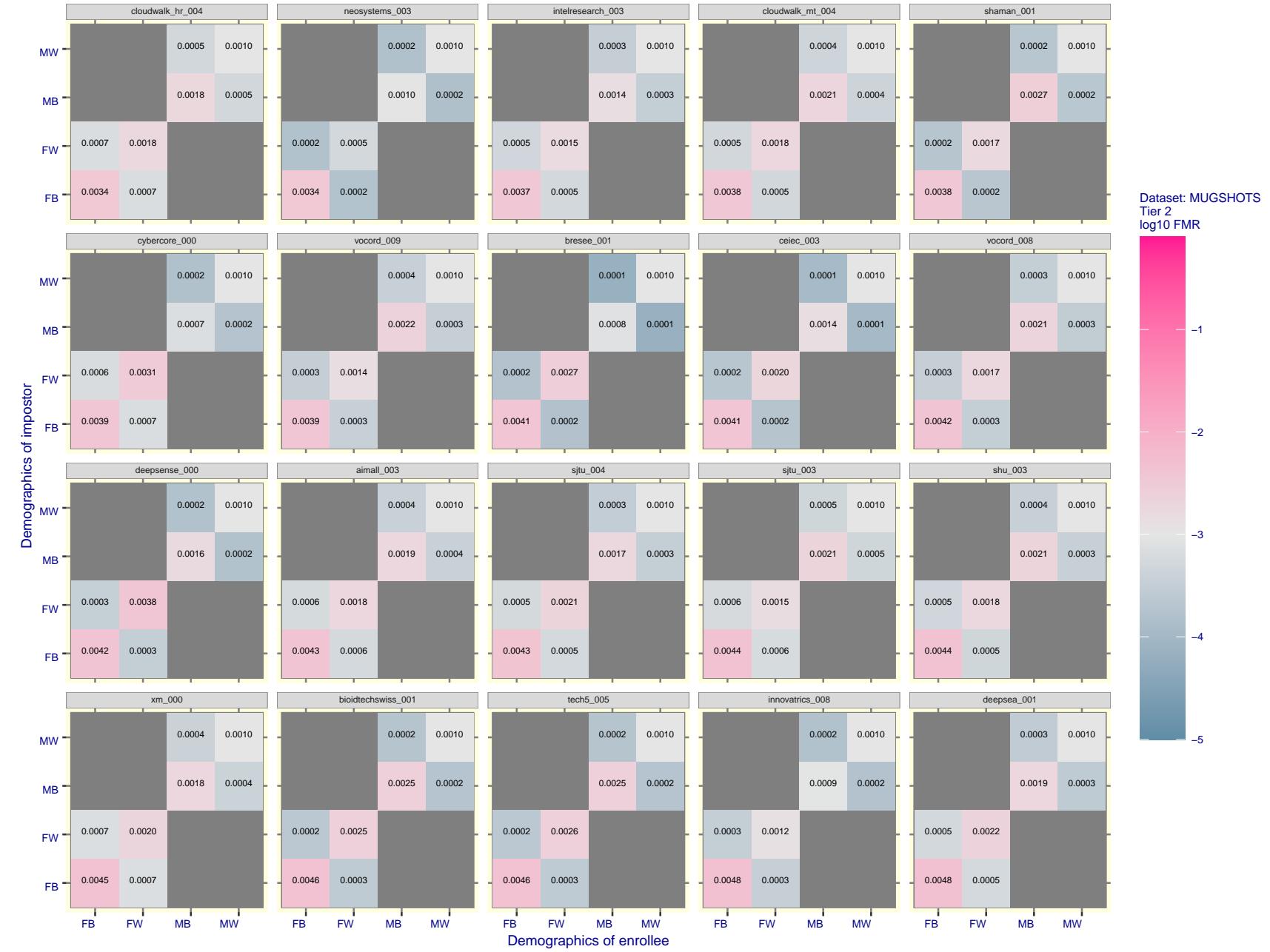


Figure 95: For the mugshot images, FMR for same-sex impostor pairs of images annotated with codes for black female, black male, white female, white male. The threshold is set for each algorithm to give FMR = 0.001 for white males which is the demographic that usually gives the lowest FMR. This means the top right box is the same color in all panels. The panels are sorted over multiple pages in order of FMR on black females, which is the demographic that usually gives the highest FMR.

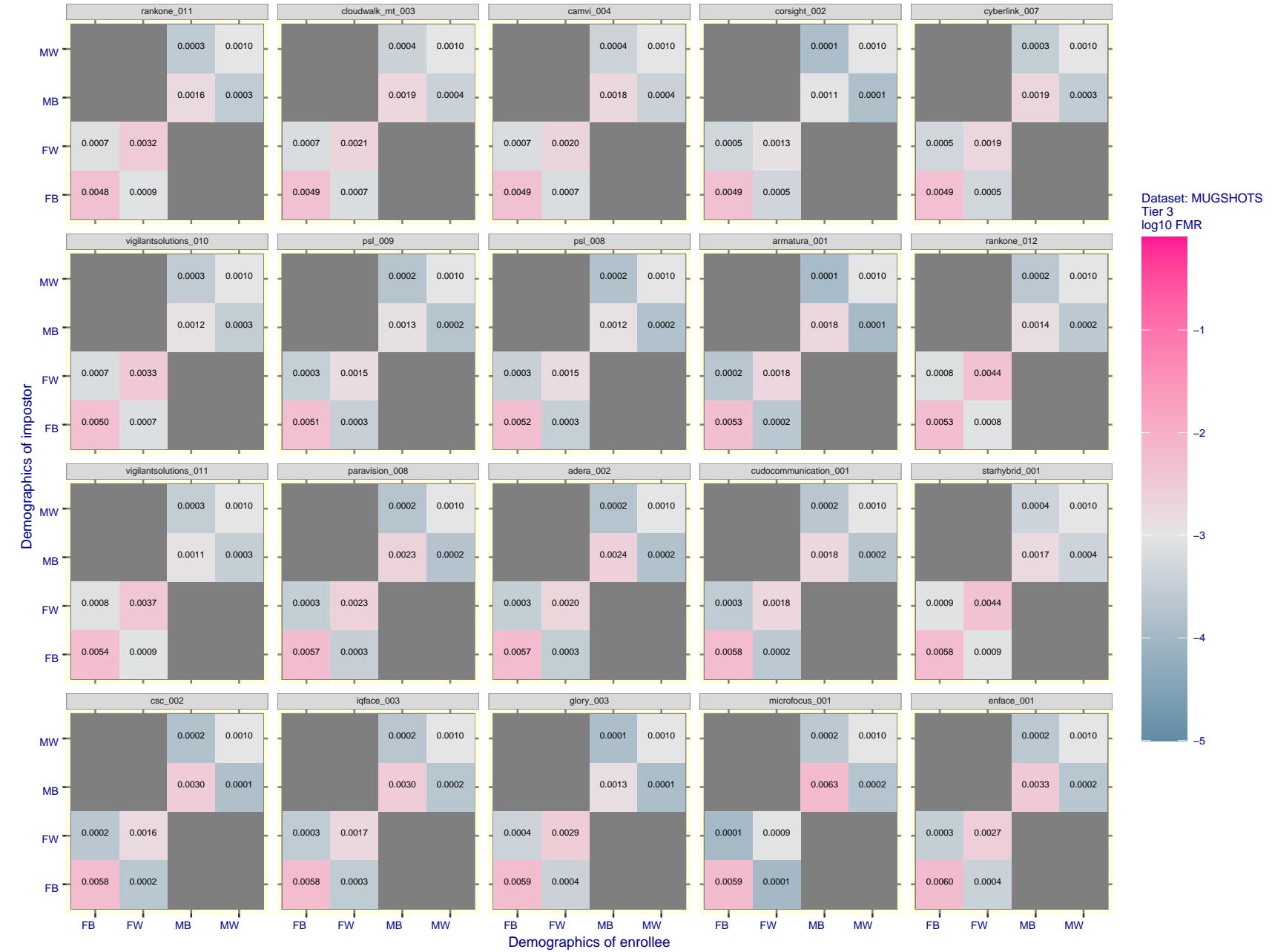


Figure 96: For the mugshot images, FMR for same-sex impostor pairs of images annotated with codes for black female, black male, white female, white male. The threshold is set for each algorithm to give FMR = 0.001 for white males which is the demographic that usually gives the lowest FMR. This means the top right box is the same color in all panels. The panels are sorted over multiple pages in order of FMR on black females, which is the demographic that usually gives the highest FMR.

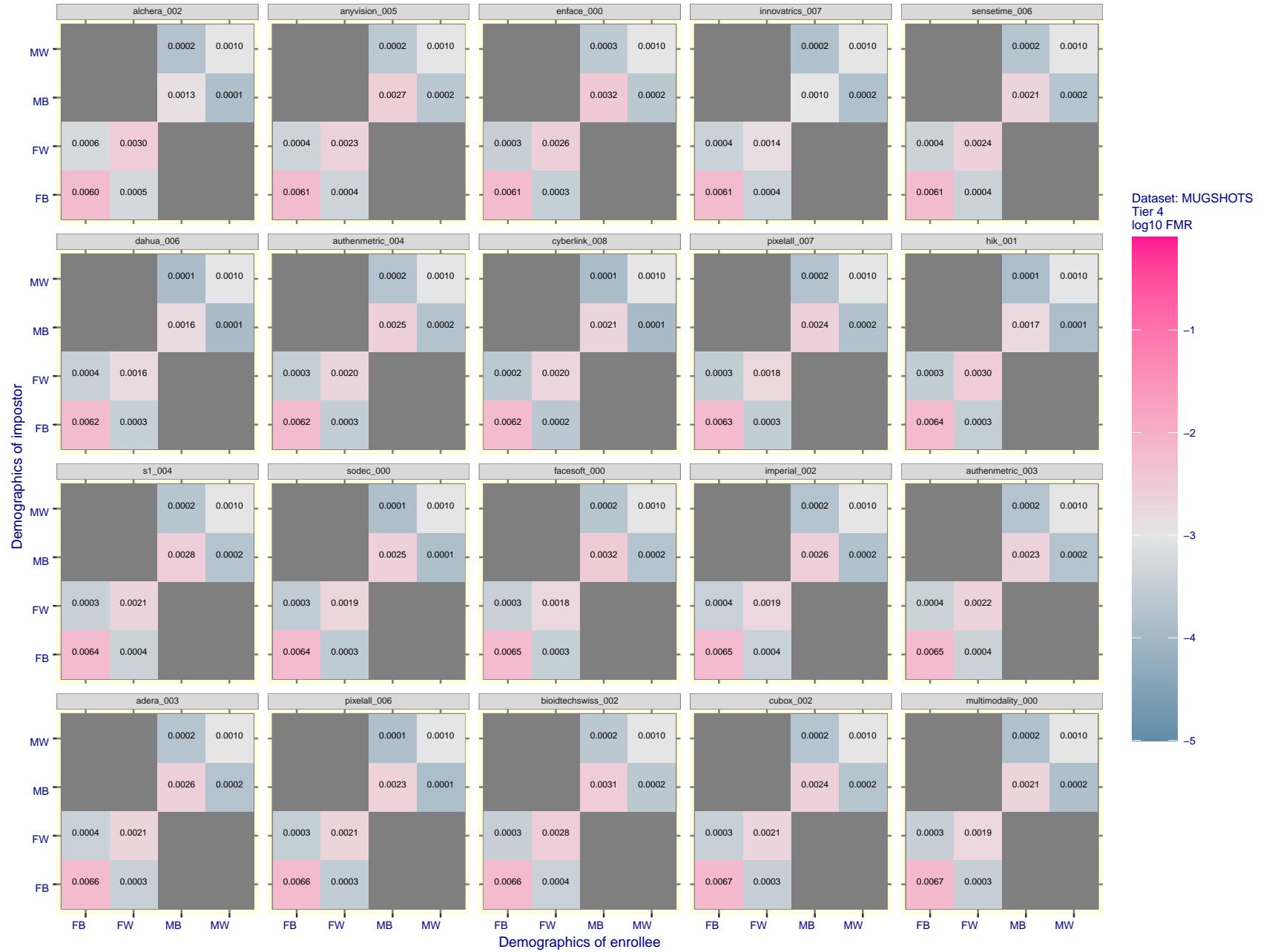


Figure 97: For the mugshot images, FMR for same-sex impostor pairs of images annotated with codes for black female, black male, white female, white male. The threshold is set for each algorithm to give FMR = 0.001 for white males which is the demographic that usually gives the lowest FMR. This means the top right box is the same color in all panels. The panels are sorted over multiple pages in order of FMR on black females, which is the demographic that usually gives the highest FMR.

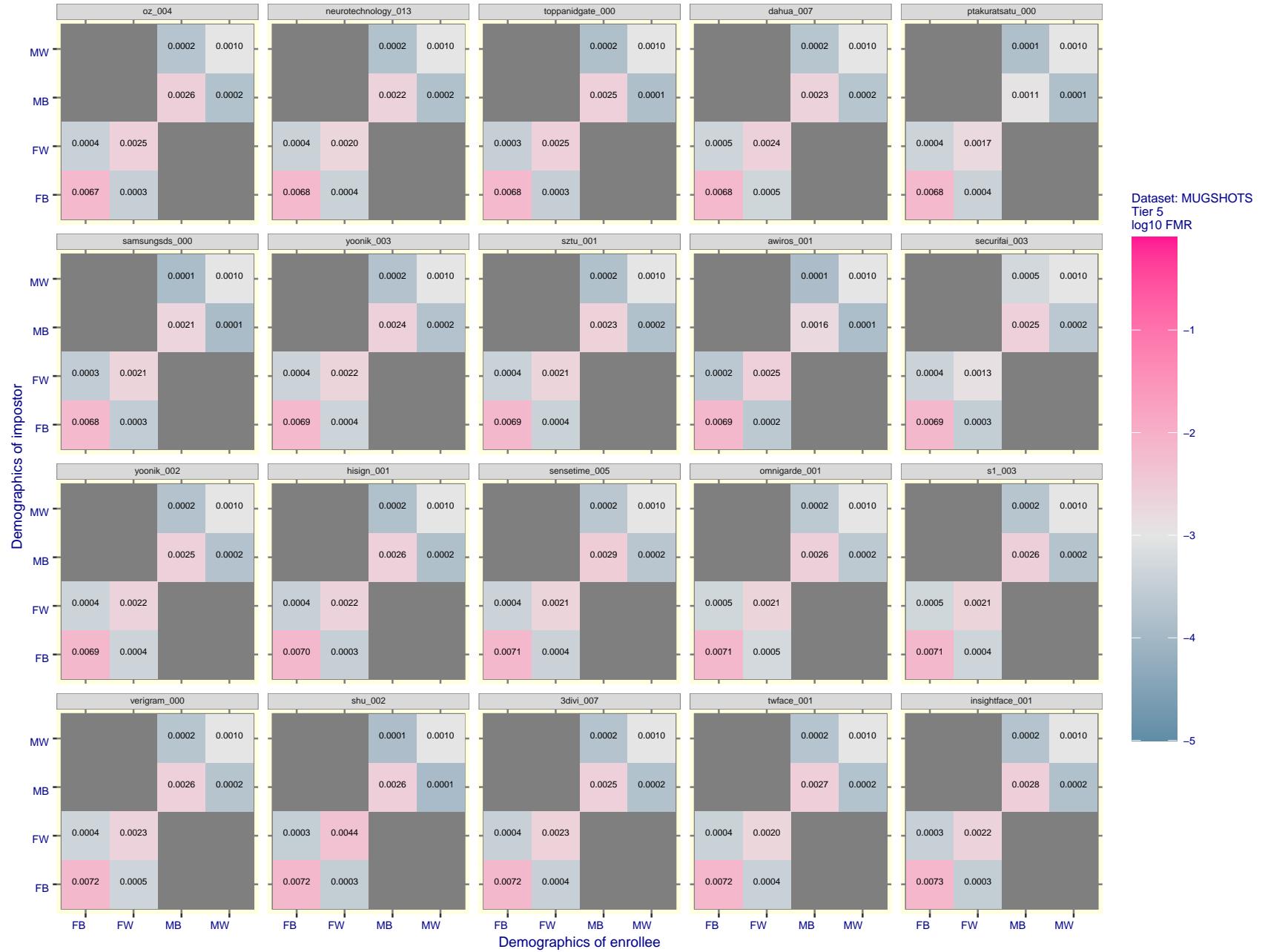


Figure 98: For the mugshot images, FMR for same-sex impostor pairs of images annotated with codes for black female, black male, white female, white male. The threshold is set for each algorithm to give FMR = 0.001 for white males which is the demographic that usually gives the lowest FMR. This means the top right box is the same color in all panels. The panels are sorted over multiple pages in order of FMR on black females, which is the demographic that usually gives the highest FMR.

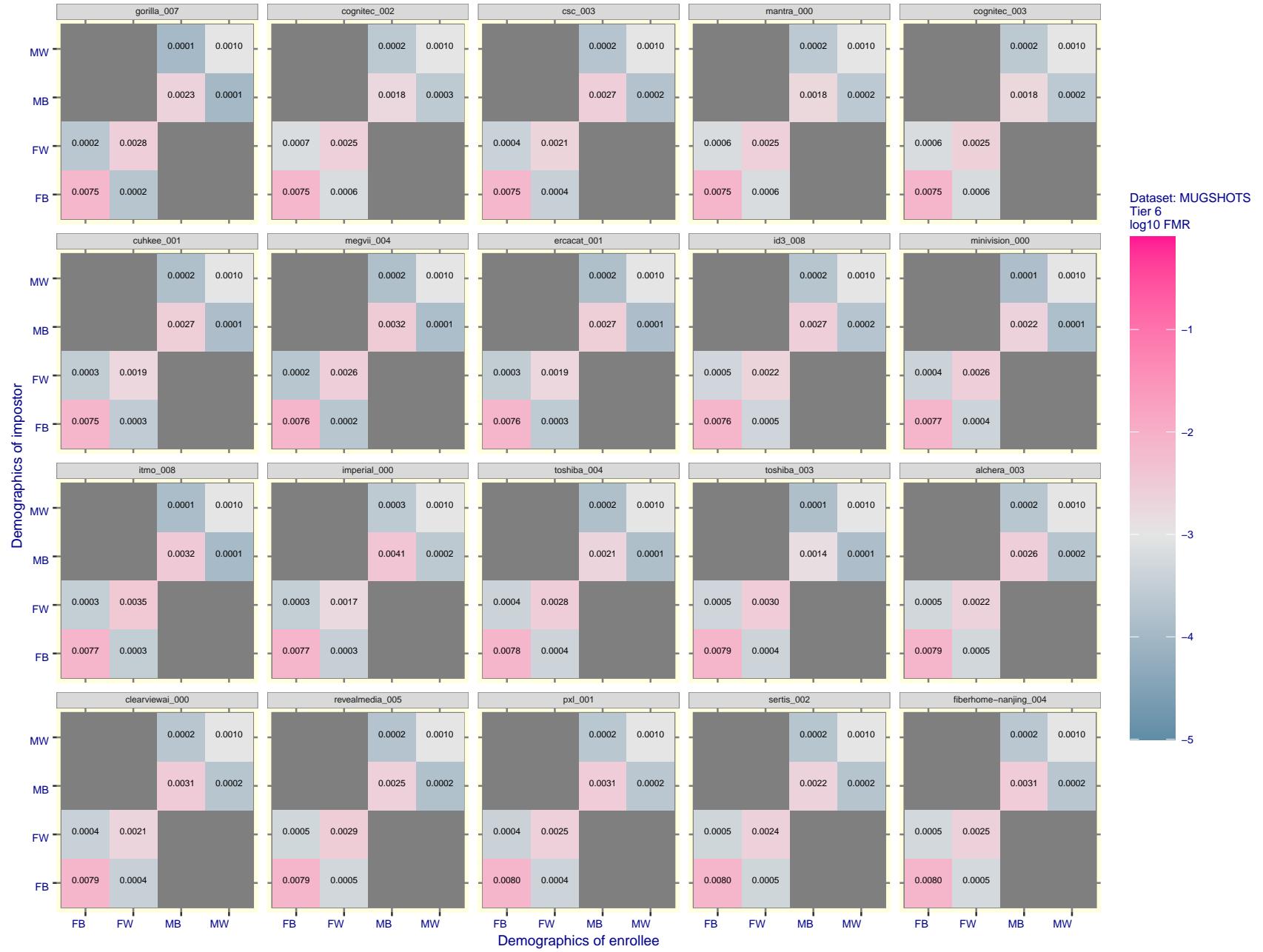


Figure 99: For the mugshot images, FMR for same-sex impostor pairs of images annotated with codes for black female, black male, white female, white male. The threshold is set for each algorithm to give FMR = 0.001 for white males which is the demographic that usually gives the lowest FMR. This means the top right box is the same color in all panels. The panels are sorted over multiple pages in order of FMR on black females, which is the demographic that usually gives the highest FMR.

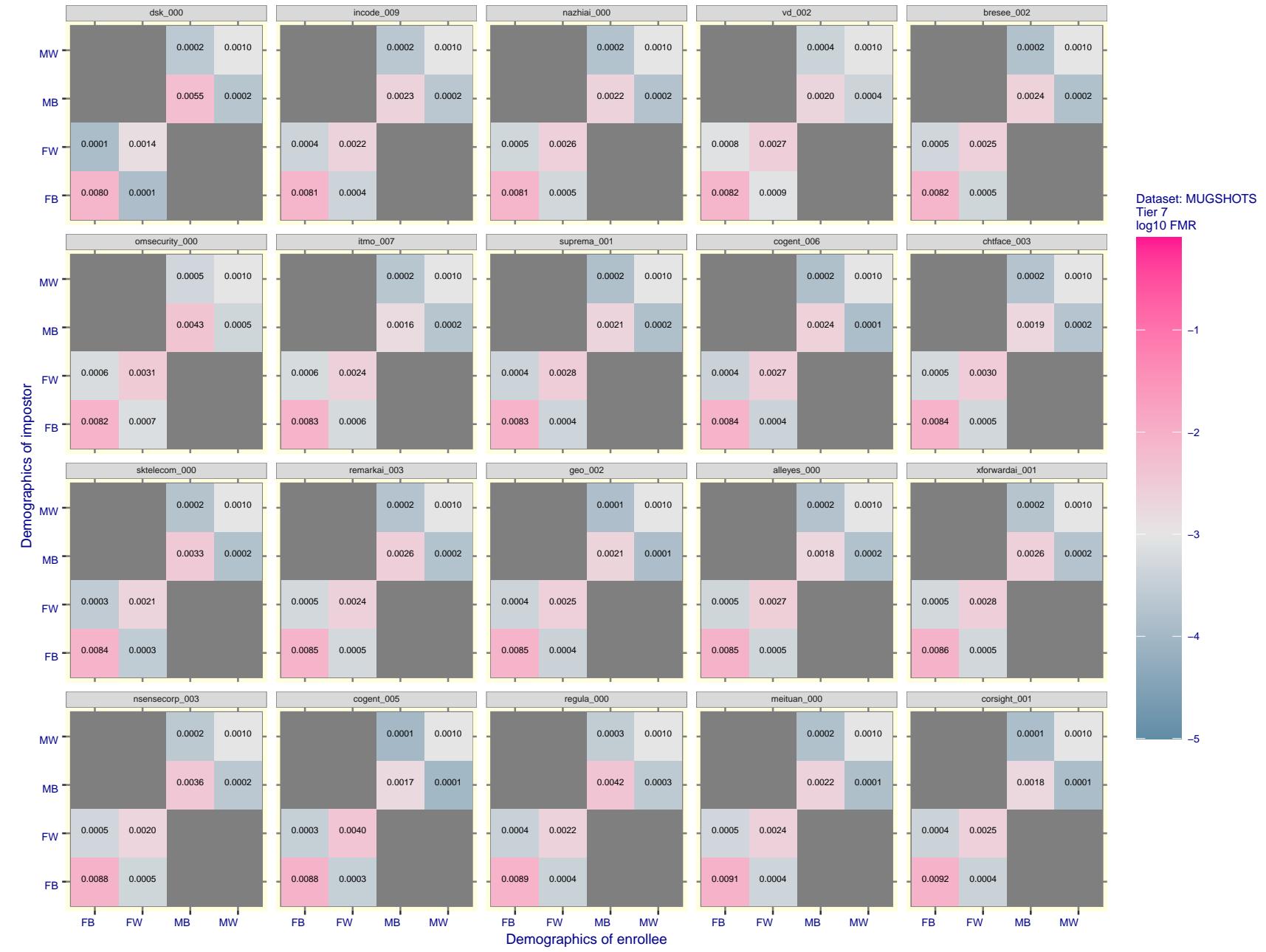


Figure 100: For the mugshot images, FMR for same-sex impostor pairs of images annotated with codes for black female, black male, white female, white male. The threshold is set for each algorithm to give FMR = 0.001 for white males which is the demographic that usually gives the lowest FMR. This means the top right box is the same color in all panels. The panels are sorted over multiple pages in order of FMR on black females, which is the demographic that usually gives the highest FMR.

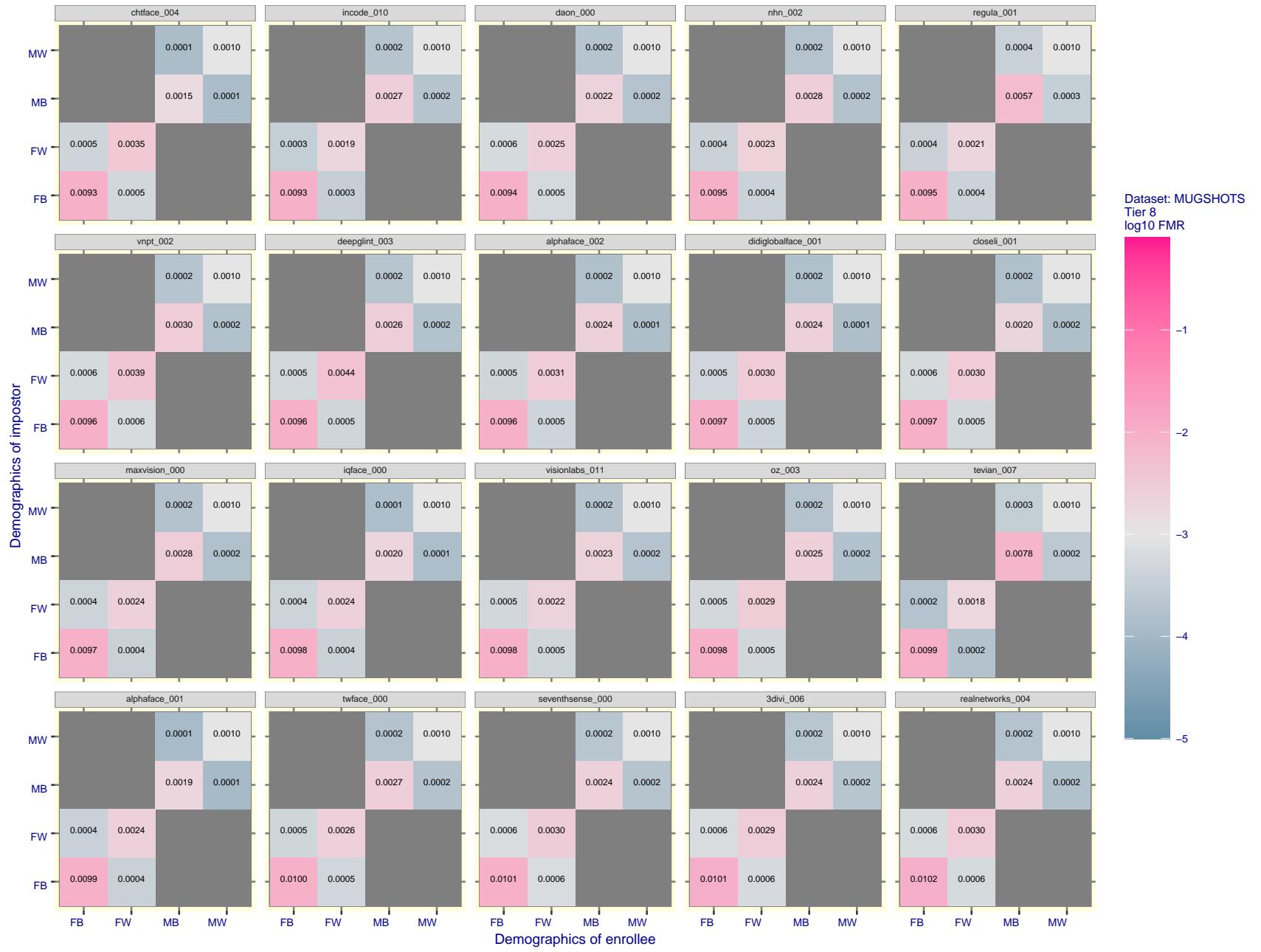


Figure 101: For the mugshot images, FMR for same-sex impostor pairs of images annotated with codes for black female, black male, white female, white male. The threshold is set for each algorithm to give FMR = 0.001 for white males which is the demographic that usually gives the lowest FMR. This means the top right box is the same color in all panels. The panels are sorted over multiple pages in order of FMR on black females, which is the demographic that usually gives the highest FMR.

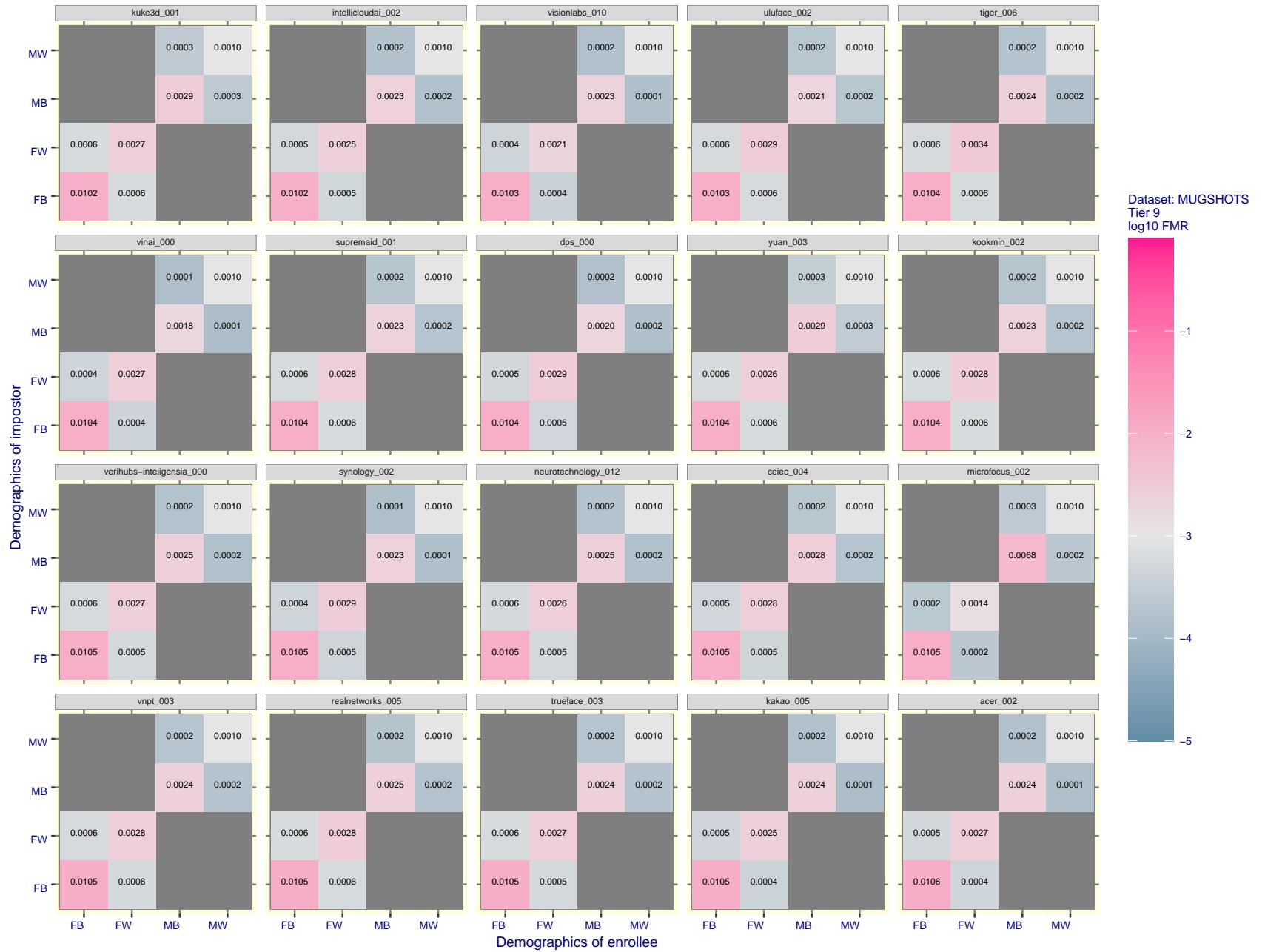


Figure 102: For the mugshot images, FMR for same-sex impostor pairs of images annotated with codes for black female, black male, white female, white male. The threshold is set for each algorithm to give FMR = 0.001 for white males which is the demographic that usually gives the lowest FMR. This means the top right box is the same color in all panels. The panels are sorted over multiple pages in order of FMR on black females, which is the demographic that usually gives the highest FMR.

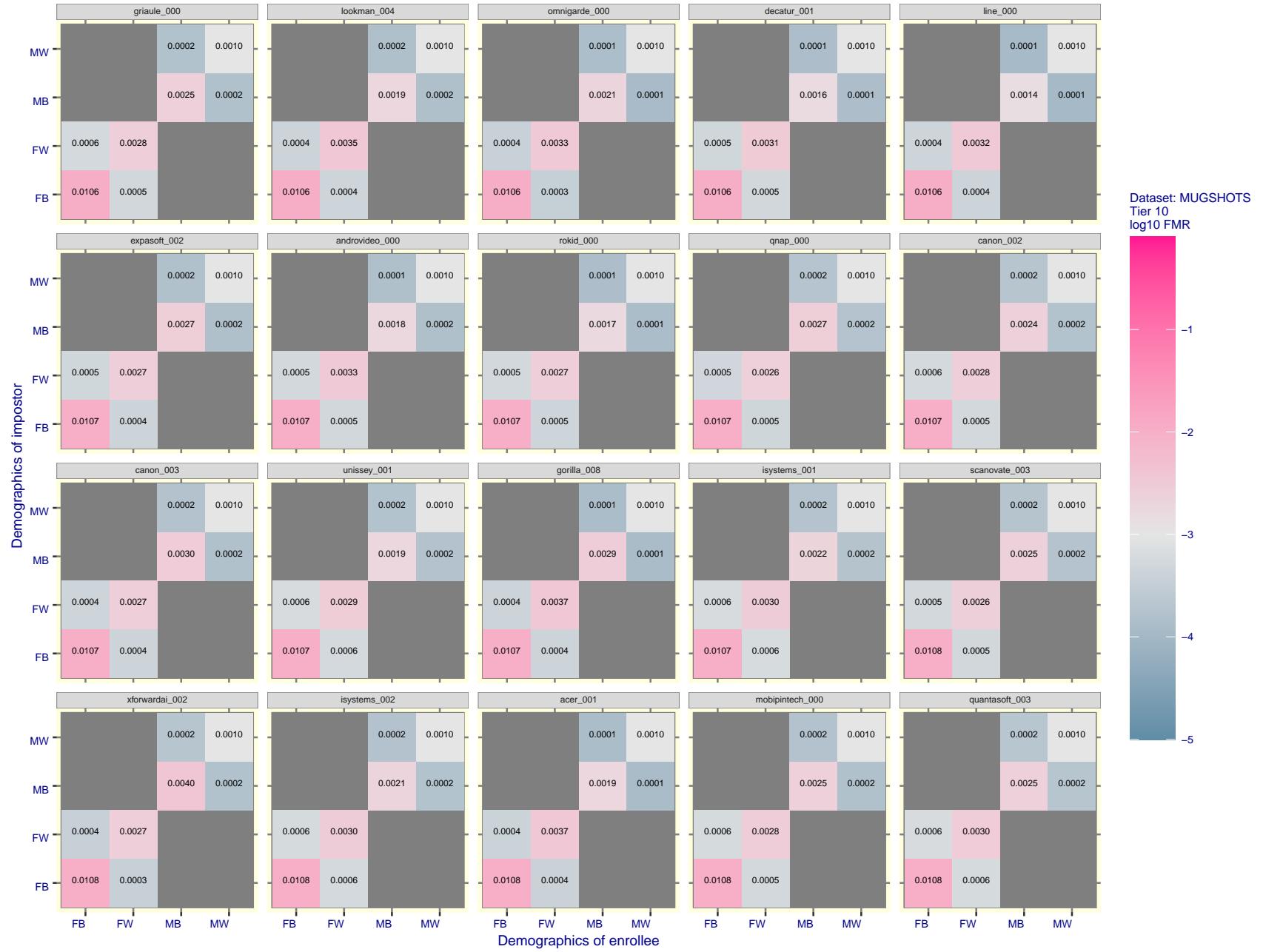


Figure 103: For the mugshot images, FMR for same-sex impostor pairs of images annotated with codes for black female, black male, white female, white male. The threshold is set for each algorithm to give FMR = 0.001 for white males which is the demographic that usually gives the lowest FMR. This means the top right box is the same color in all panels. The panels are sorted over multiple pages in order of FMR on black females, which is the demographic that usually gives the highest FMR.

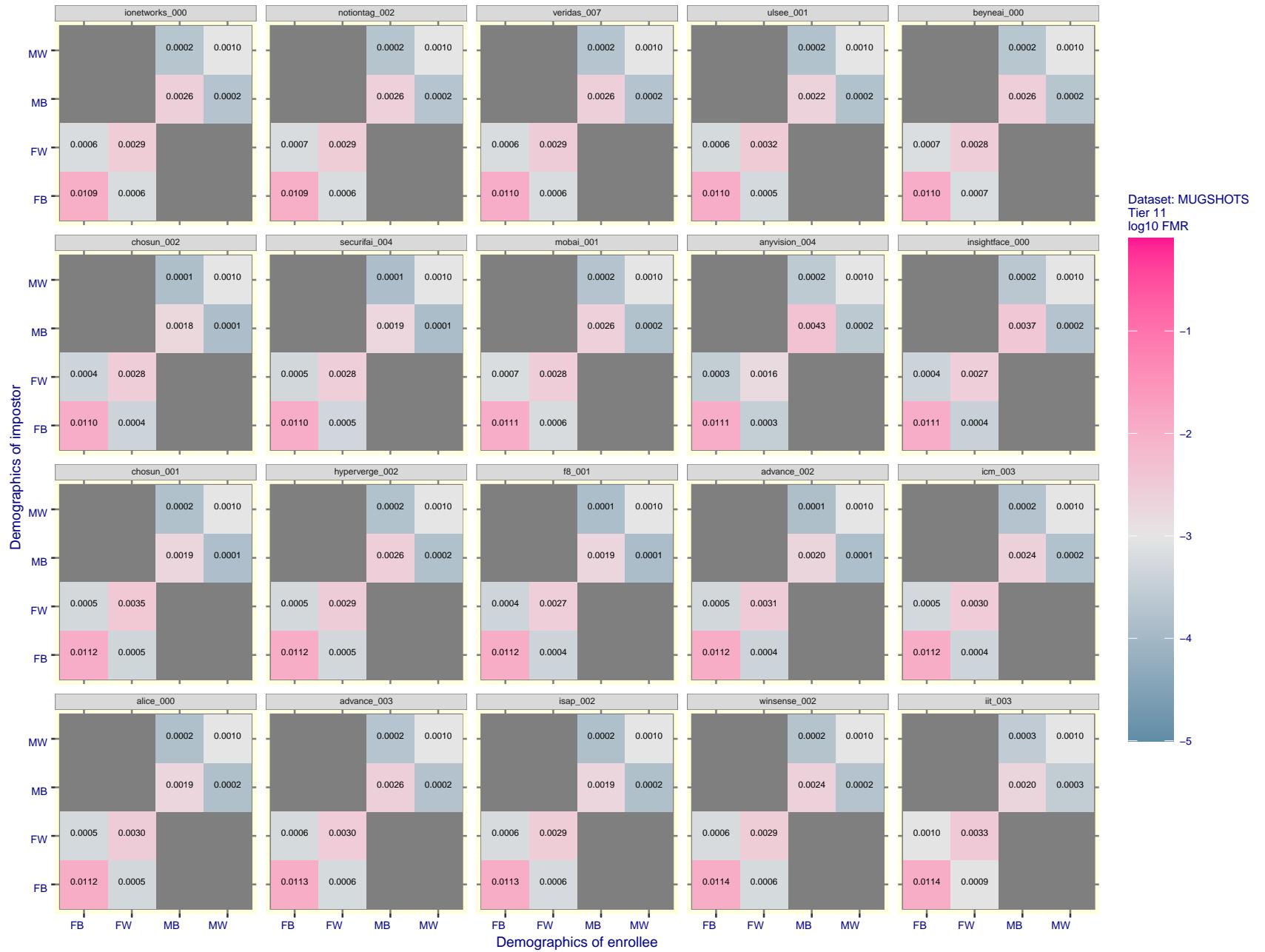


Figure 104: For the mugshot images, FMR for same-sex impostor pairs of images annotated with codes for black female, black male, white female, white male. The threshold is set for each algorithm to give FMR = 0.001 for white males which is the demographic that usually gives the lowest FMR. This means the top right box is the same color in all panels. The panels are sorted over multiple pages in order of FMR on black females, which is the demographic that usually gives the highest FMR.

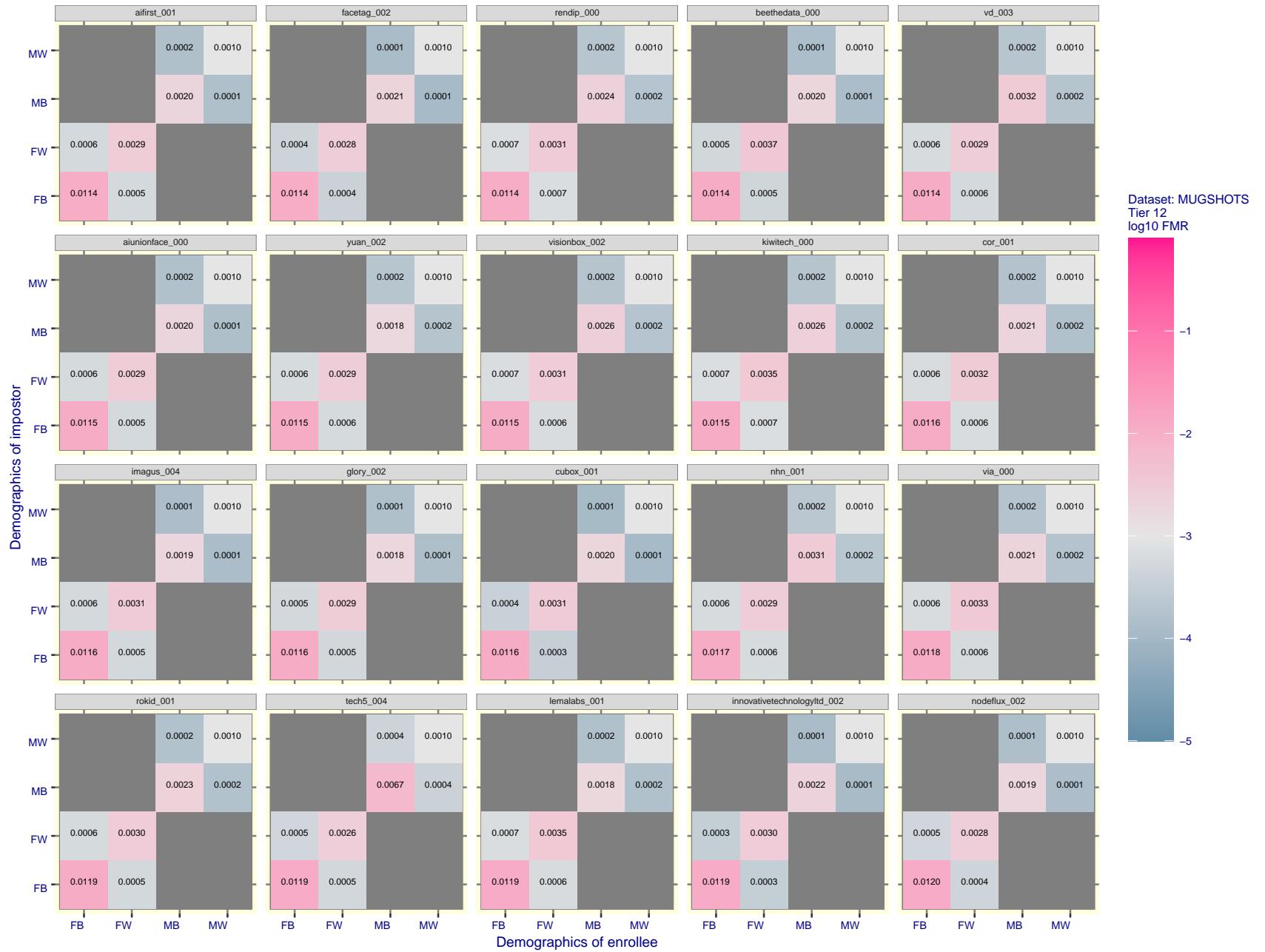


Figure 105: For the mugshot images, FMR for same-sex impostor pairs of images annotated with codes for black female, black male, white female, white male. The threshold is set for each algorithm to give FMR = 0.001 for white males which is the demographic that usually gives the lowest FMR. This means the top right box is the same color in all panels. The panels are sorted over multiple pages in order of FMR on black females, which is the demographic that usually gives the highest FMR.

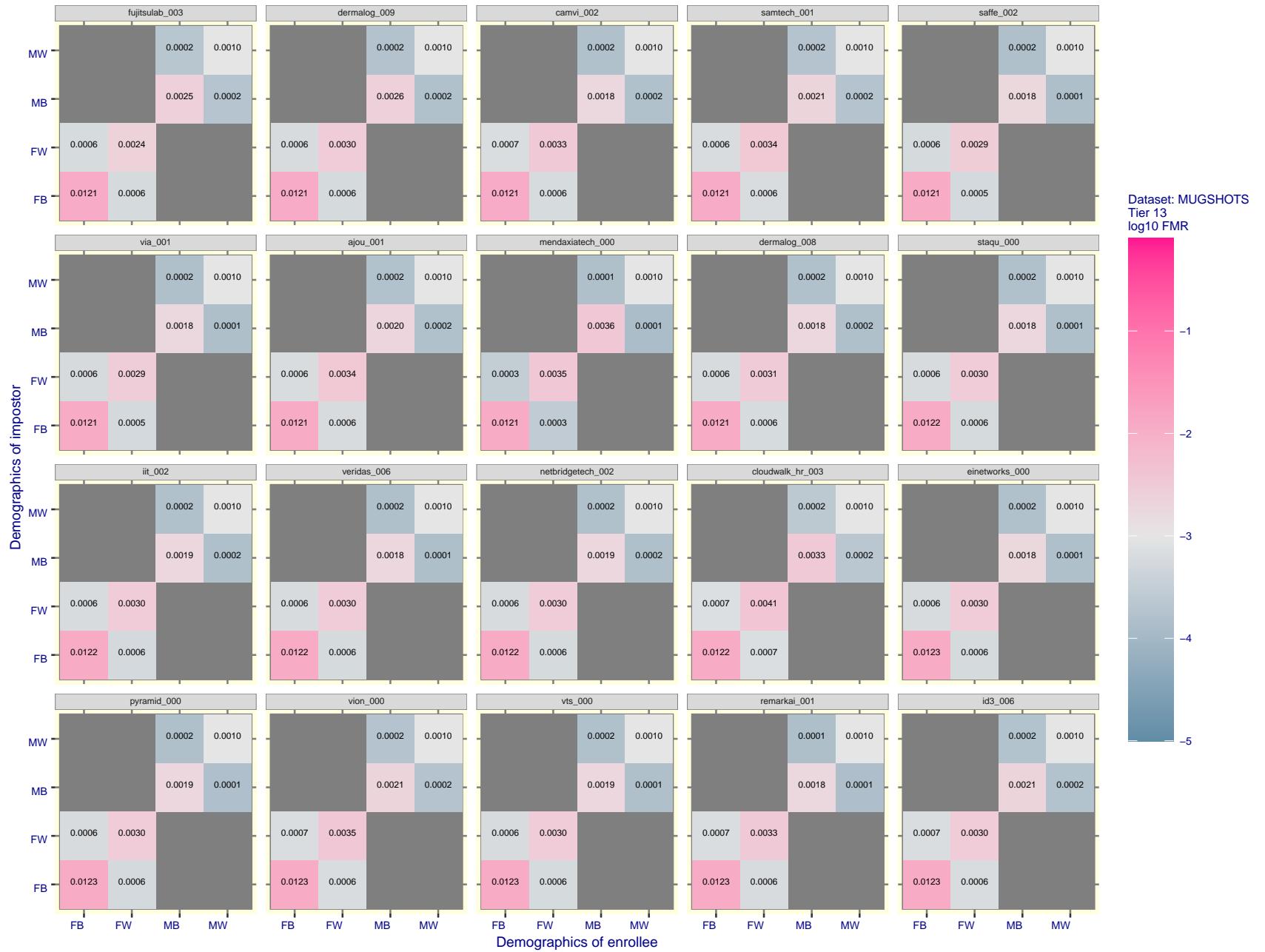


Figure 106: For the mugshot images, FMR for same-sex impostor pairs of images annotated with codes for black female, black male, white female, white male. The threshold is set for each algorithm to give  $FMR = 0.001$  for white males which is the demographic that usually gives the lowest FMR. This means the top right box is the same color in all panels. The panels are sorted over multiple pages in order of FMR on black females, which is the demographic that usually gives the highest FMR.

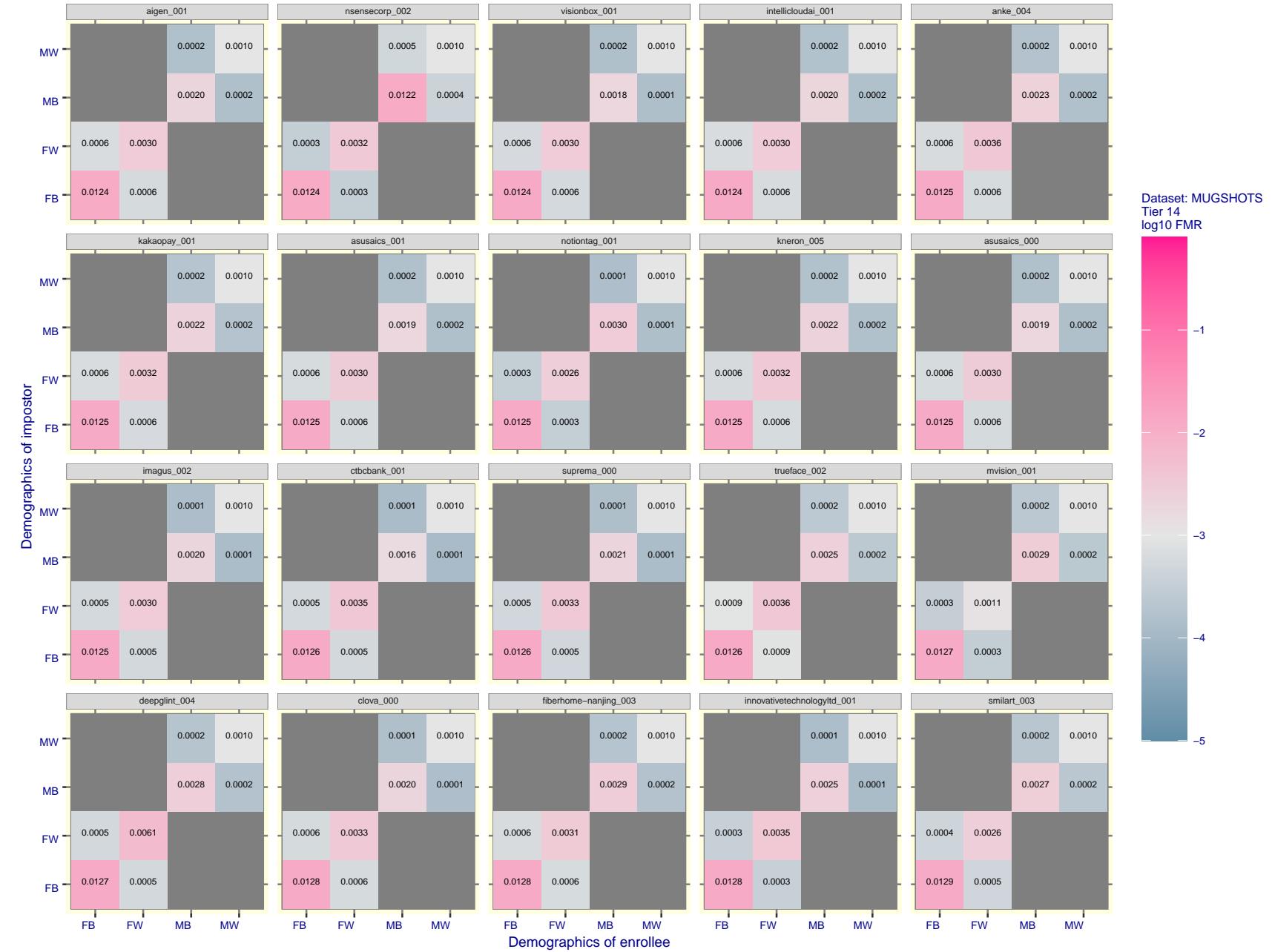


Figure 107: For the mugshot images, FMR for same-sex impostor pairs of images annotated with codes for black female, black male, white female, white male. The threshold is set for each algorithm to give FMR = 0.001 for white males which is the demographic that usually gives the lowest FMR. This means the top right box is the same color in all panels. The panels are sorted over multiple pages in order of FMR on black females, which is the demographic that usually gives the highest FMR.

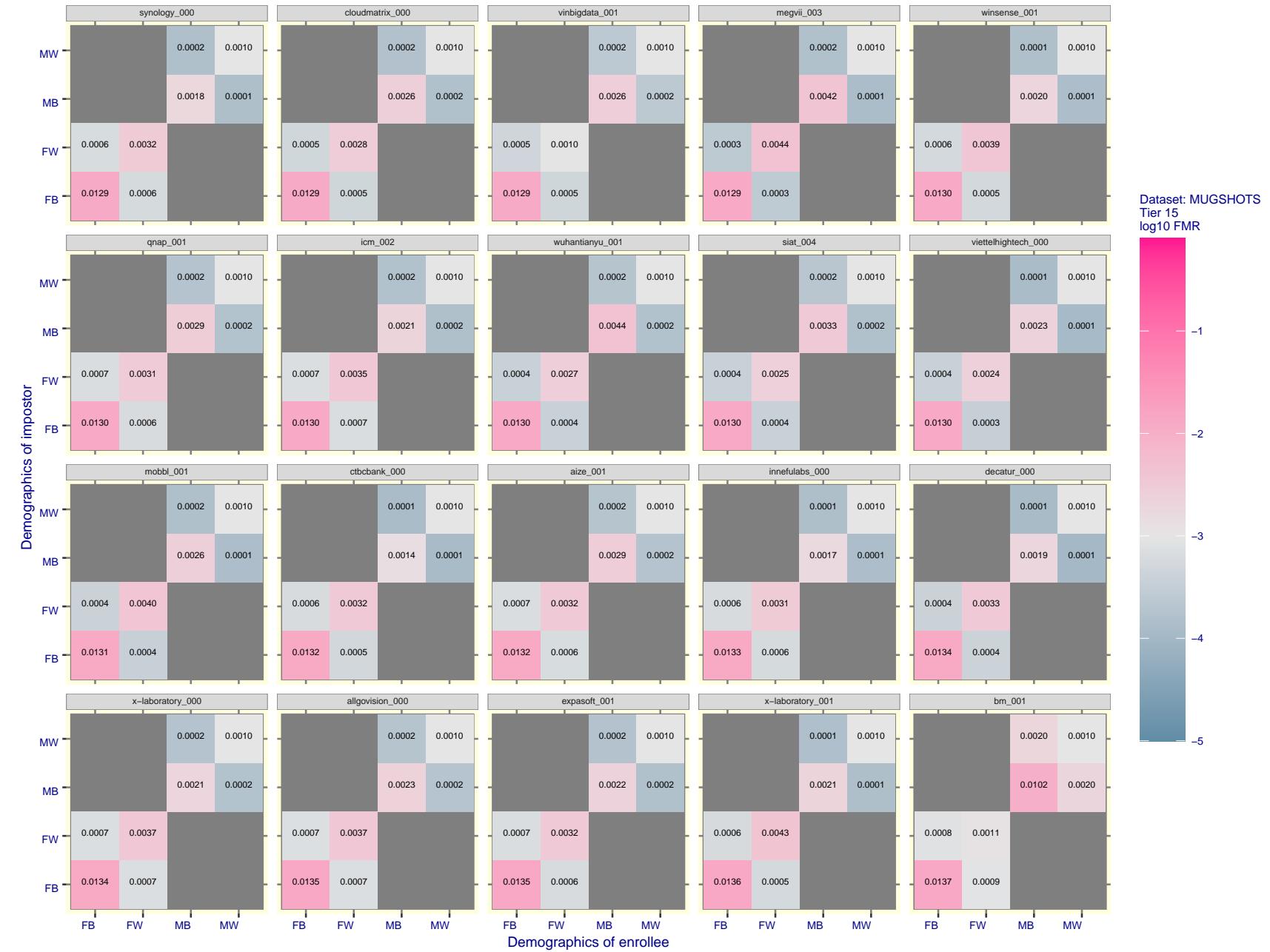


Figure 108: For the mugshot images, FMR for same-sex impostor pairs of images annotated with codes for black female, black male, white female, white male. The threshold is set for each algorithm to give  $FMR = 0.001$  for white males which is the demographic that usually gives the lowest FMR. This means the top right box is the same color in all panels. The panels are sorted over multiple pages in order of FMR on black females, which is the demographic that usually gives the highest FMR.

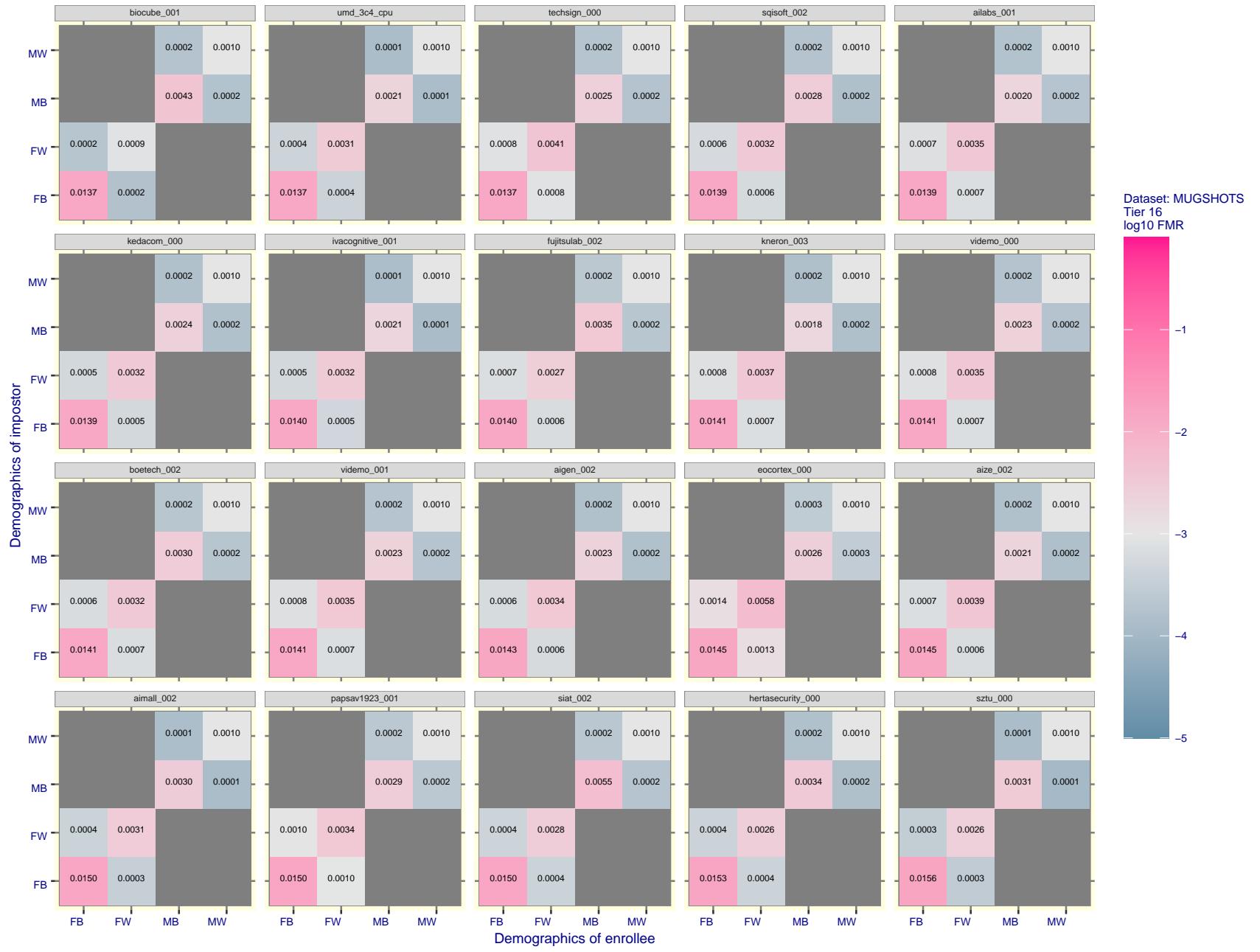


Figure 109: For the mugshot images, FMR for same-sex impostor pairs of images annotated with codes for black female, black male, white female, white male. The threshold is set for each algorithm to give  $\text{FMR} = 0.001$  for white males which is the demographic that usually gives the lowest FMR. This means the top right box is the same color in all panels. The panels are sorted over multiple pages in order of FMR on black females, which is the demographic that usually gives the highest FMR.

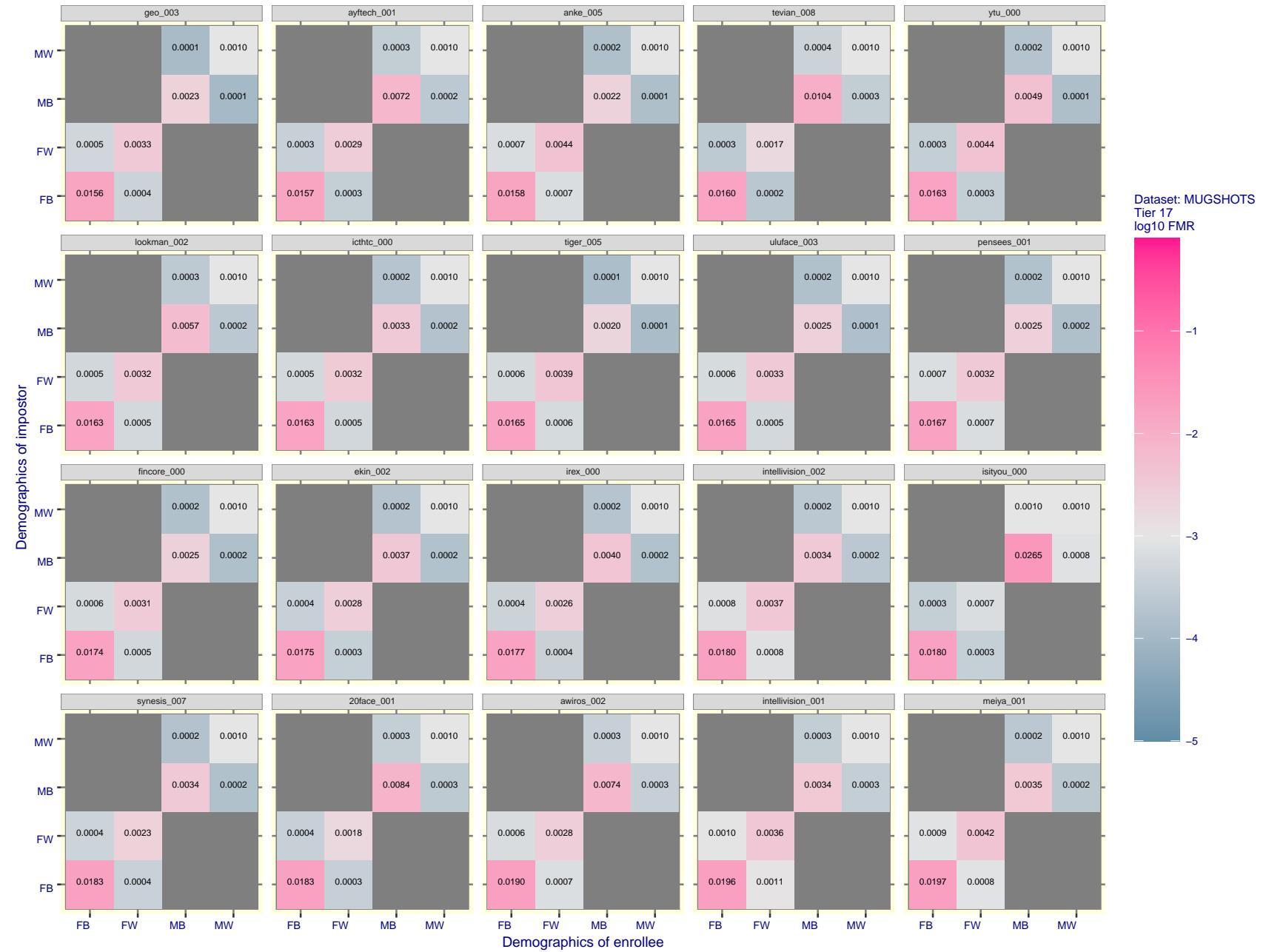


Figure 110: For the mugshot images, FMR for same-sex impostor pairs of images annotated with codes for black female, black male, white female, white male. The threshold is set for each algorithm to give FMR = 0.001 for white males which is the demographic that usually gives the lowest FMR. This means the top right box is the same color in all panels. The panels are sorted over multiple pages in order of FMR on black females, which is the demographic that usually gives the highest FMR.

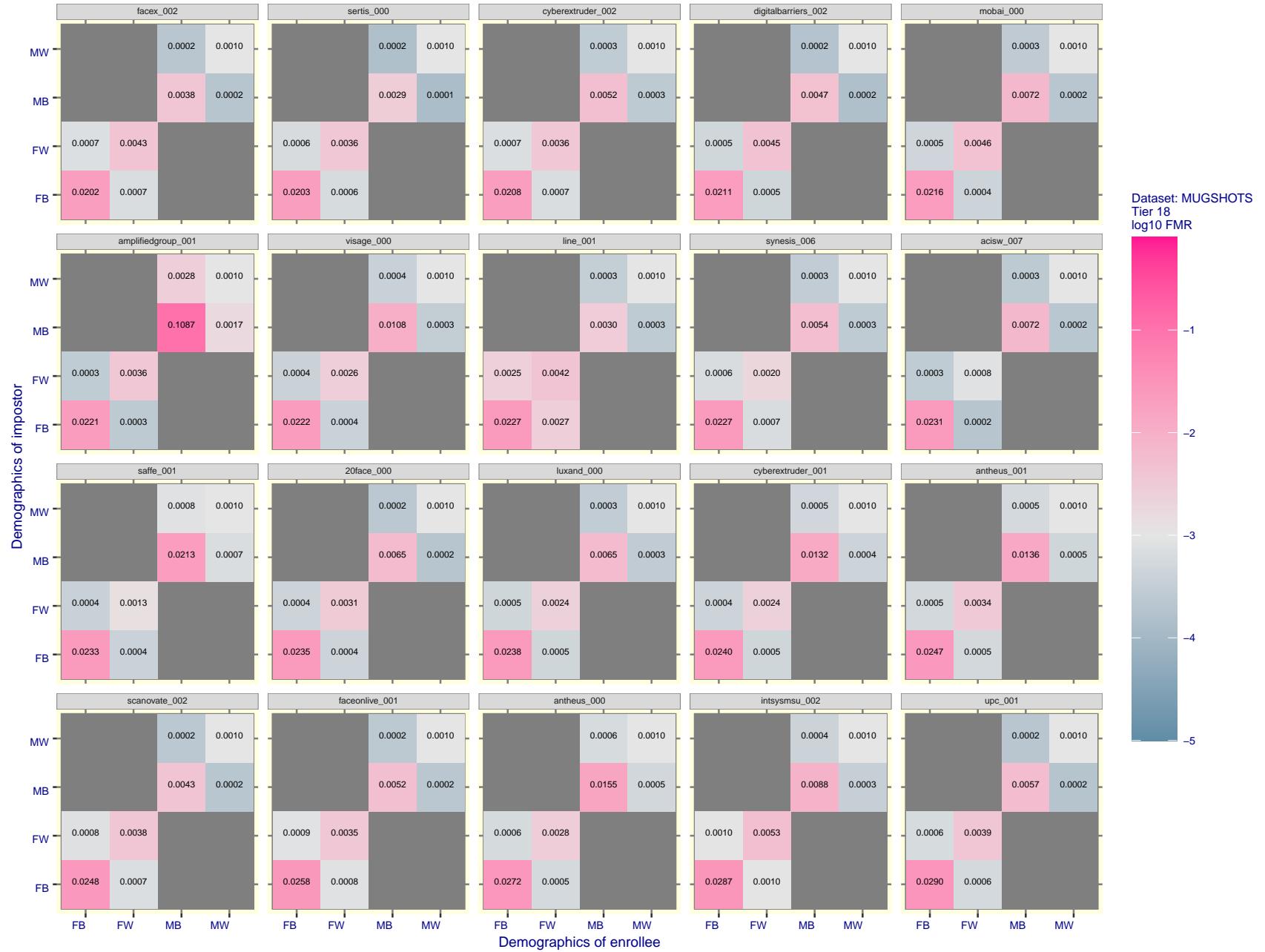


Figure 111: For the mugshot images, FMR for same-sex impostor pairs of images annotated with codes for black female, black male, white female, white male. The threshold is set for each algorithm to give FMR = 0.001 for white males which is the demographic that usually gives the lowest FMR. This means the top right box is the same color in all panels. The panels are sorted over multiple pages in order of FMR on black females, which is the demographic that usually gives the highest FMR.



Figure 112: For the mugshot images, FMR for same-sex impostor pairs of images annotated with codes for black female, black male, white female, white male. The threshold is set for each algorithm to give FMR = 0.001 for white males which is the demographic that usually gives the lowest FMR. This means the top right box is the same color in all panels. The panels are sorted over multiple pages in order of FMR on black females, which is the demographic that usually gives the highest FMR.

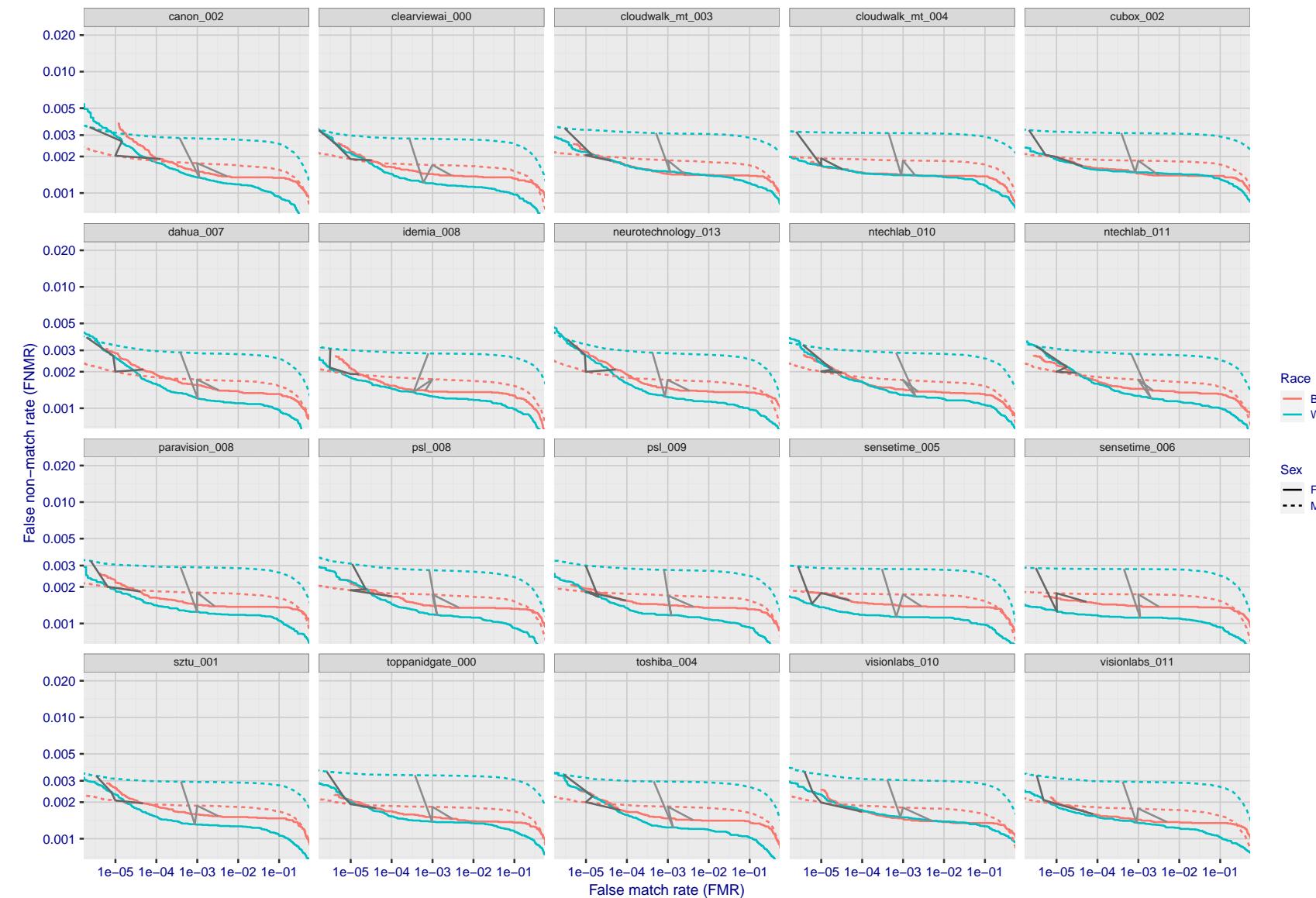


Figure 113: For the mugshot images, error tradeoff characteristics for white females, black females, black males and white males. The Z-shaped grey lines correspond to fixed thresholds, showing both FNMR and FMR vary at one  $T$  value. Note: Many of the plots will naively be read as saying women gives worse error rates than men because the solid traces lie above the dotted ones. However, this is misleading and incomplete: The grey lines show the traces reveal horizontal shifts. Thus for the cogent-003 algorithm FNMR for men is higher than for women at a fixed threshold but, at the same time, FMR is higher for women - see Figure 182. As access control systems almost always operate at a fixed threshold, the naive interpretation is incorrect.

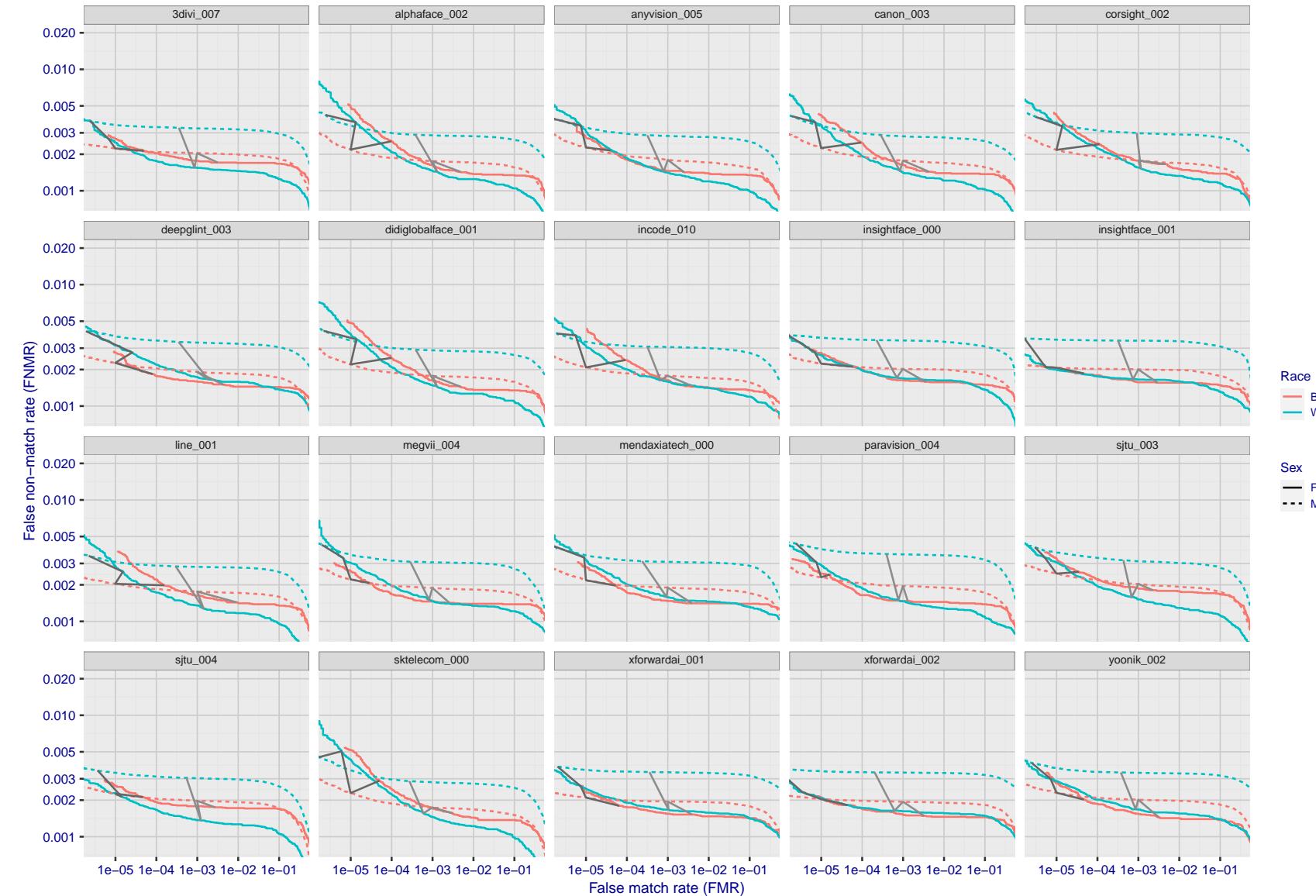


Figure 114: For the mugshot images, error tradeoff characteristics for white females, black females, black males and white males. The Z-shaped grey lines correspond to fixed thresholds, showing both FNMR and FMR vary at one  $T$  value. Note: Many of the plots will naively be read as saying women gives worse error rates than men because the solid traces lie above the dotted ones. However, this is misleading and incomplete: The grey lines show the traces reveal horizontal shifts. Thus for the cogent-003 algorithm FNMR for men is higher than for women at a fixed threshold but, at the same time, FMR is higher for women - see Figure 182. As access control systems almost always operate at a fixed threshold, the naive interpretation is incorrect.

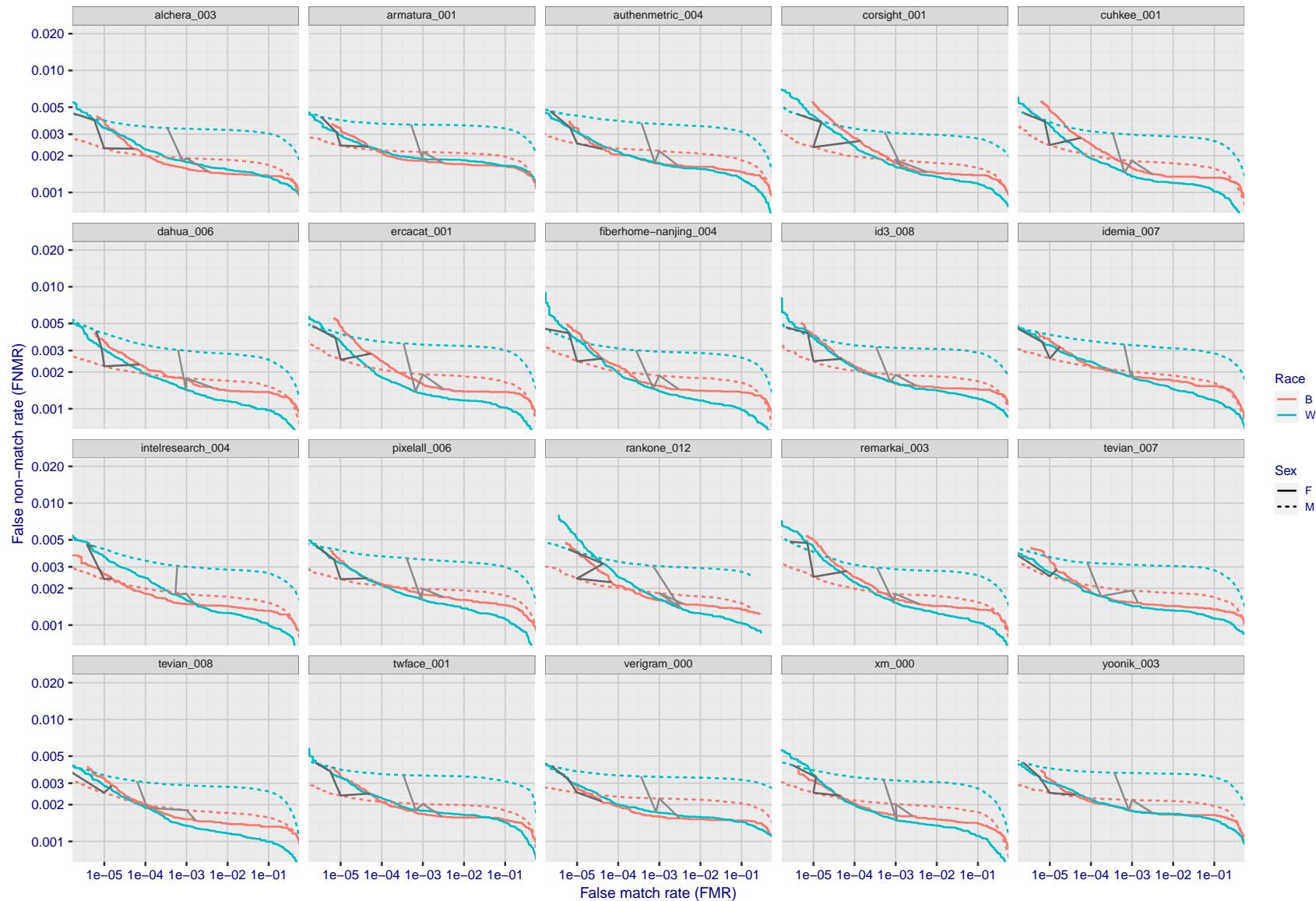


Figure 115: For the mugshot images, error tradeoff characteristics for white females, black females, black males and white males. The Z-shaped grey lines correspond to fixed thresholds, showing both FNMR and FMR vary at one T value. Note: Many of the plots will naively be read as saying women gives worse error rates than men because the solid traces lie above the dotted ones. However, this is misleading and incomplete: The grey lines show the traces reveal horizontal shifts. Thus for the cogent-003 algorithm FNMR for men is higher than for women at a fixed threshold but, at the same time, FMR is higher for women - see Figure 182. As access control systems almost always operate at a fixed threshold, the naive interpretation is incorrect.

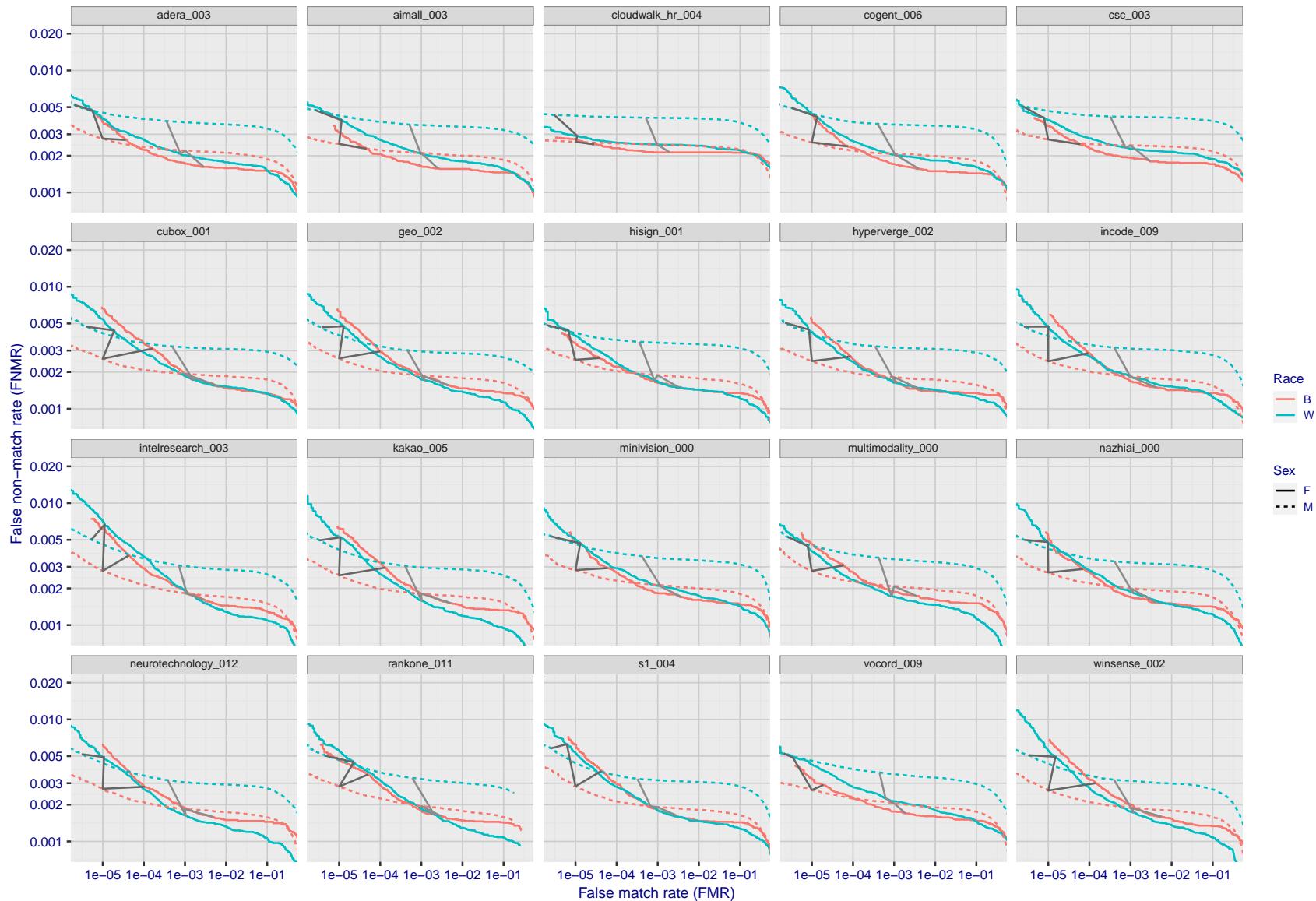


Figure 116: For the mugshot images, error tradeoff characteristics for white females, black females, black males and white males. The Z-shaped grey lines correspond to fixed thresholds, showing both FNMR and FMR vary at one T value. Note: Many of the plots will naively be read as saying women gives worse error rates than men because the solid traces lie above the dotted ones. However, this is misleading and incomplete: The grey lines show the traces reveal horizontal shifts. Thus for the cogent-003 algorithm FNMR for men is higher than for women at a fixed threshold but, at the same time, FMR is higher for women - see Figure 182. As access control systems almost always operate at a fixed threshold, the naive interpretation is incorrect.

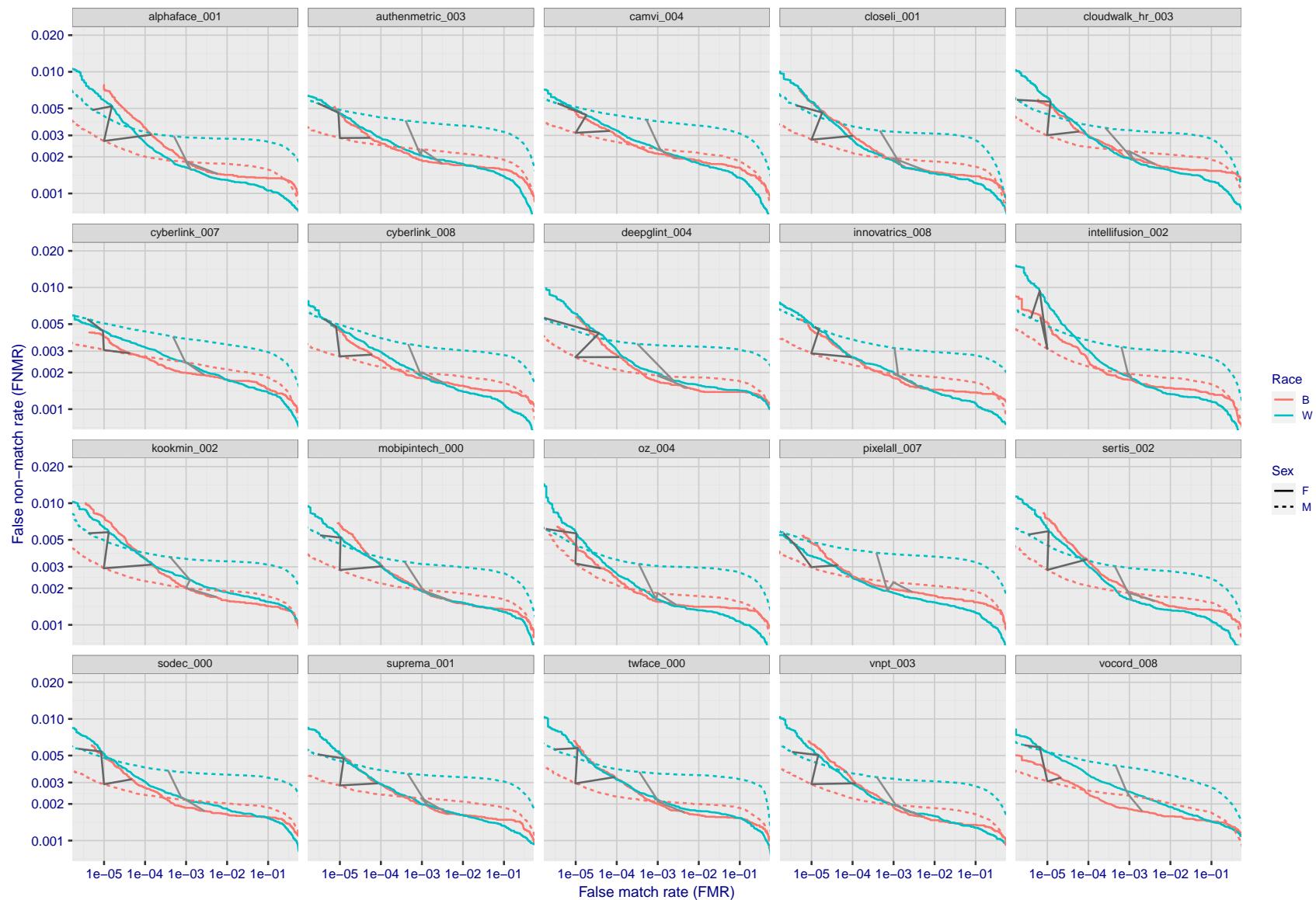


Figure 117: For the mugshot images, error tradeoff characteristics for white females, black females, black males and white males. The Z-shaped grey lines correspond to fixed thresholds, showing both FNMR and FMR vary at one T value. Note: Many of the plots will naively be read as saying women gives worse error rates than men because the solid traces lie above the dotted ones. However, this is misleading and incomplete: The grey lines show the traces reveal horizontal shifts. Thus for the cogent-003 algorithm FNMR for men is higher than for women at a fixed threshold but, at the same time, FMR is higher for women - see Figure 182. As access control systems almost always operate at a fixed threshold, the naive interpretation is incorrect.

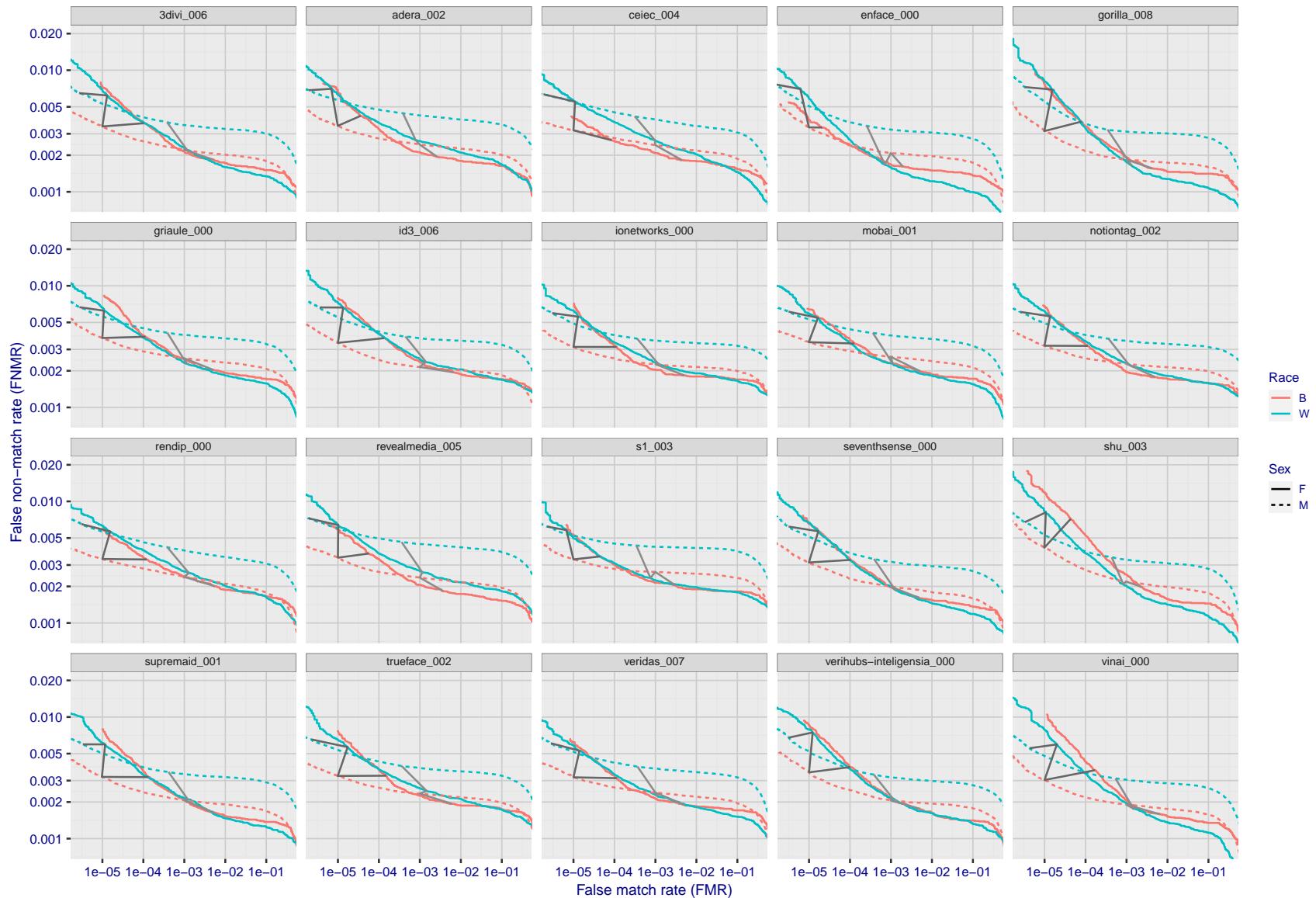


Figure 118: For the mugshot images, error tradeoff characteristics for white females, black females, black males and white males. The Z-shaped grey lines correspond to fixed thresholds, showing both FNMR and FMR vary at one T value. Note: Many of the plots will naively be read as saying women gives worse error rates than men because the solid traces lie above the dotted ones. However, this is misleading and incomplete: The grey lines show the traces reveal horizontal shifts. Thus for the cogent-003 algorithm FNMR for men is higher than for women at a fixed threshold but, at the same time, FMR is higher for women - see Figure 182. As access control systems almost always operate at a fixed threshold, the naive interpretation is incorrect.

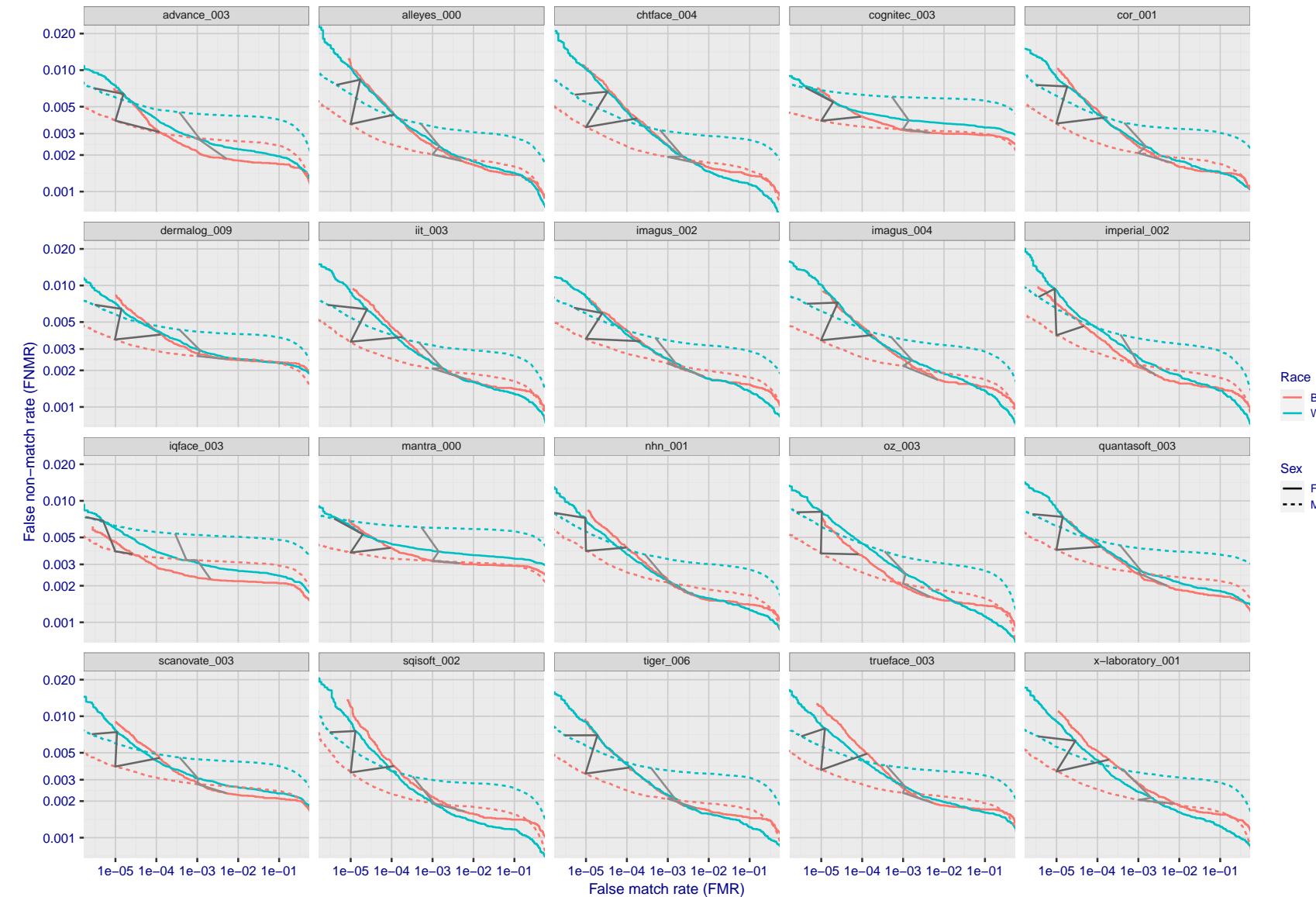


Figure 119: For the mugshot images, error tradeoff characteristics for white females, black females, black males and white males. The Z-shaped grey lines correspond to fixed thresholds, showing both FNMR and FMR vary at one  $T$  value. Note: Many of the plots will naively be read as saying women gives worse error rates than men because the solid traces lie above the dotted ones. However, this is misleading and incomplete: The grey lines show the traces reveal horizontal shifts. Thus for the cogent-003 algorithm FNMR for men is higher than for women at a fixed threshold but, at the same time, FMR is higher for women - see Figure 182. As access control systems almost always operate at a fixed threshold, the naive interpretation is incorrect.

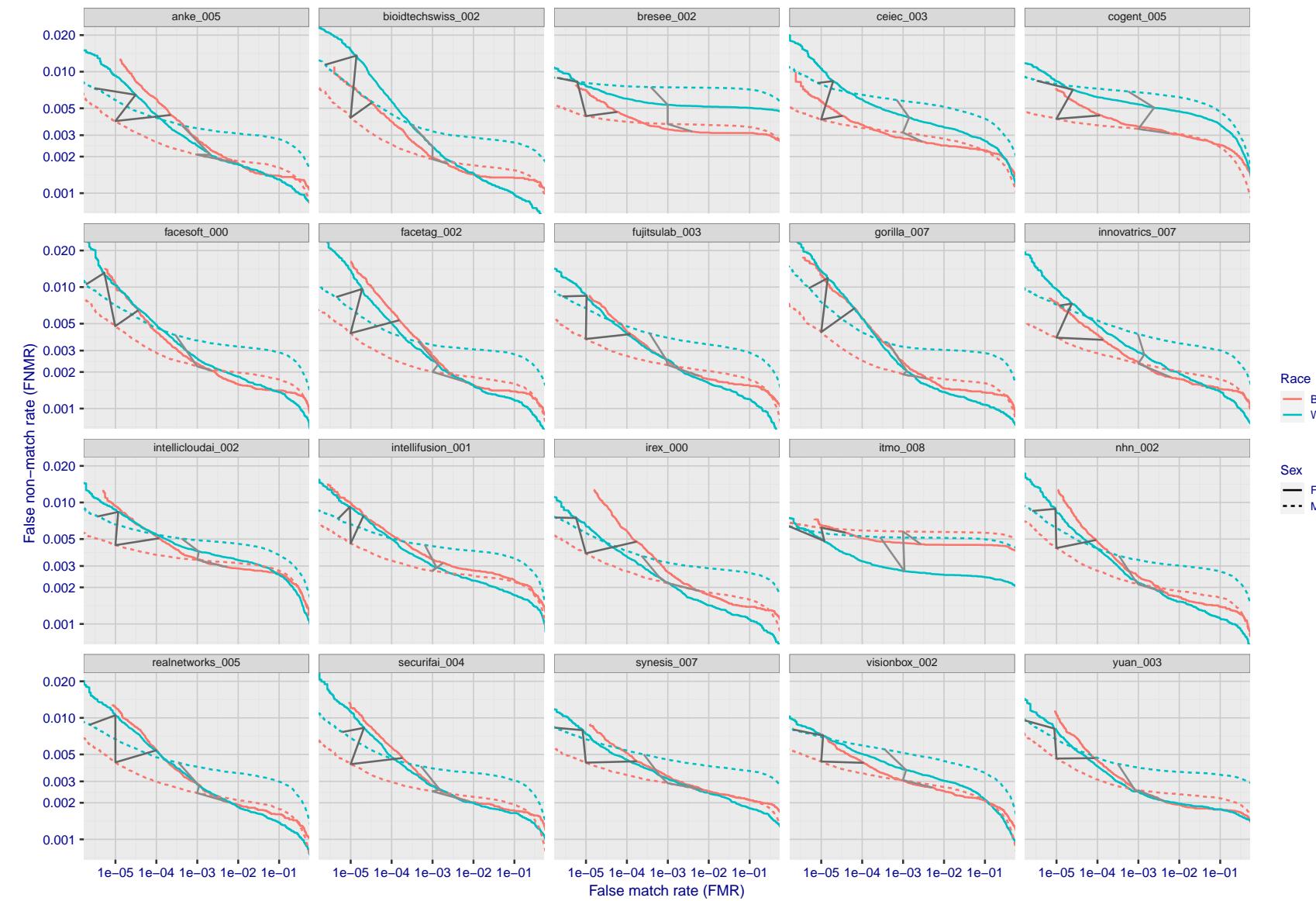


Figure 120: For the mugshot images, error tradeoff characteristics for white females, black females, black males and white males. The Z-shaped grey lines correspond to fixed thresholds, showing both FNMR and FMR vary at one  $T$  value. Note: Many of the plots will naively be read as saying women gives worse error rates than men because the solid traces lie above the dotted ones. However, this is misleading and incomplete: The grey lines show the traces reveal horizontal shifts. Thus for the cogent-003 algorithm FNMR for men is higher than for women at a fixed threshold but, at the same time, FMR is higher for women - see Figure 182. As access control systems almost always operate at a fixed threshold, the naive interpretation is incorrect.

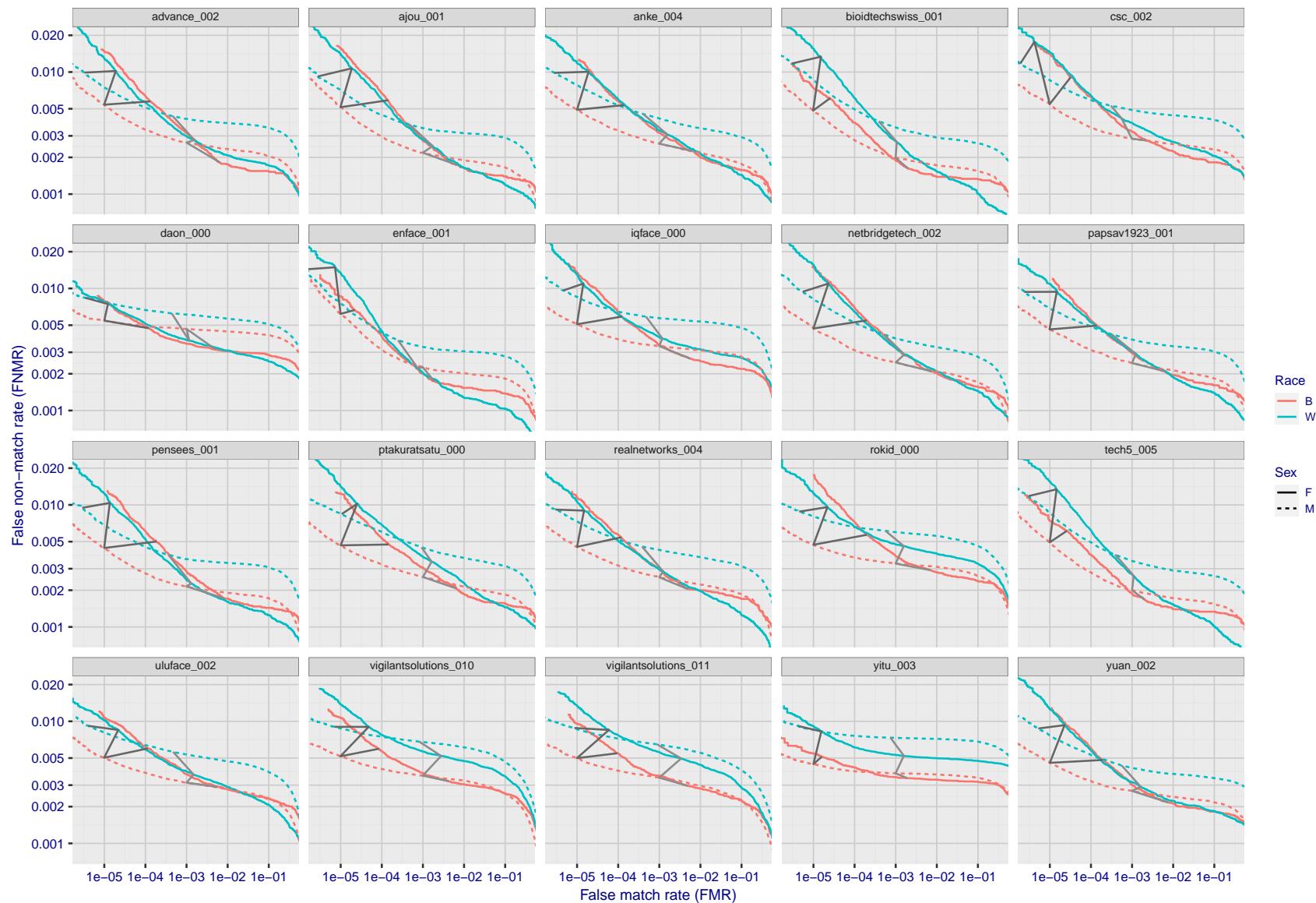


Figure 121: For the mugshot images, error tradeoff characteristics for white females, black females, black males and white males. The Z-shaped grey lines correspond to fixed thresholds, showing both FNMR and FMR vary at one T value. Note: Many of the plots will naively be read as saying women gives worse error rates than men because the solid traces lie above the dotted ones. However, this is misleading and incomplete: The grey lines show the traces reveal horizontal shifts. Thus for the cogent-003 algorithm FNMR for men is higher than for women at a fixed threshold but, at the same time, FMR is higher for women - see Figure 182. As access control systems almost always operate at a fixed threshold, the naive interpretation is incorrect.

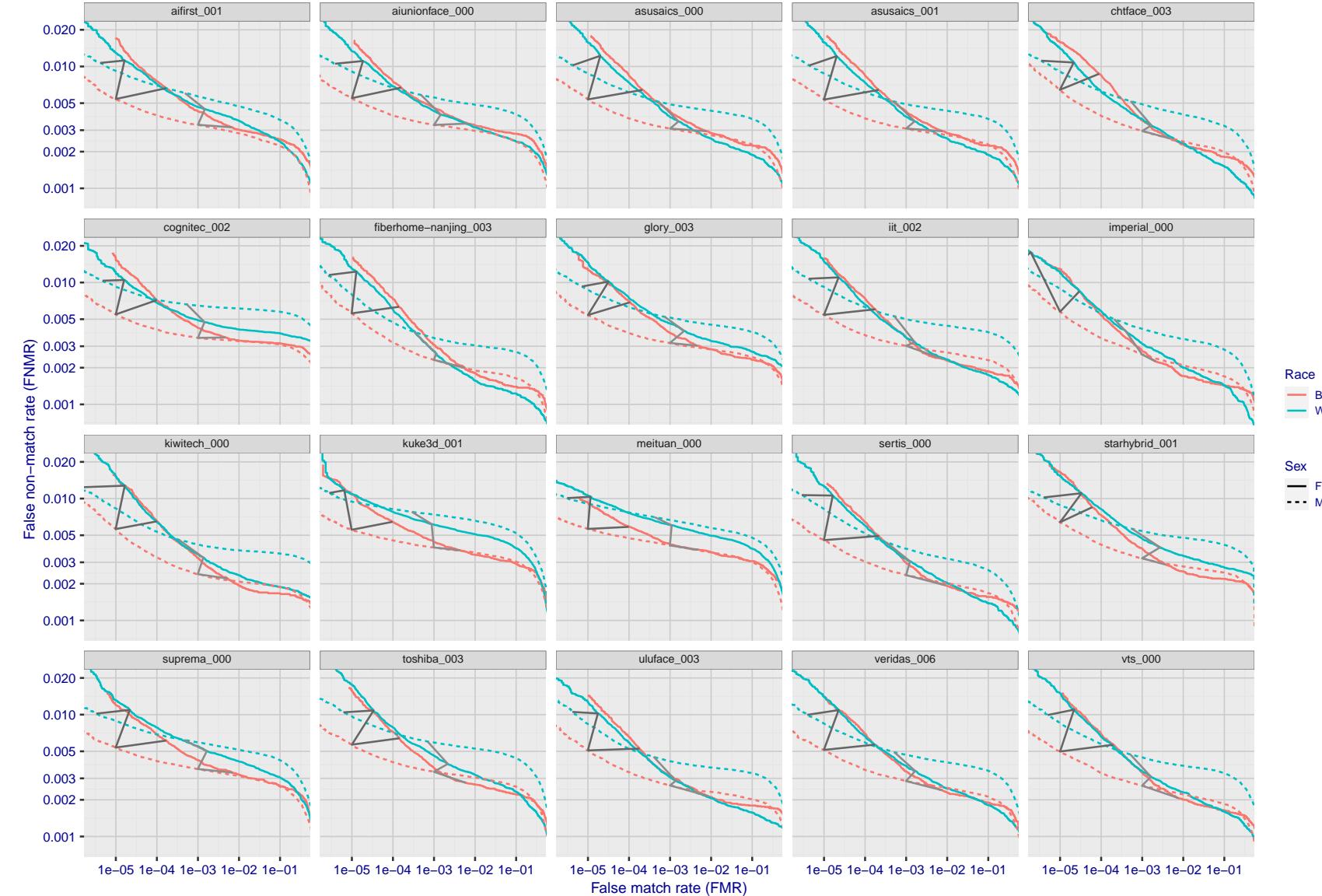


Figure 122: For the mugshot images, error tradeoff characteristics for white females, black females, black males and white males. The Z-shaped grey lines correspond to fixed thresholds, showing both FNMR and FMR vary at one  $T$  value. Note: Many of the plots will naively be read as saying women gives worse error rates than men because the solid traces lie above the dotted ones. However, this is misleading and incomplete: The grey lines show the traces reveal horizontal shifts. Thus for the cogent-003 algorithm FNMR for men is higher than for women at a fixed threshold but, at the same time, FMR is higher for women - see Figure 182. As access control systems almost always operate at a fixed threshold, the naive interpretation is incorrect.

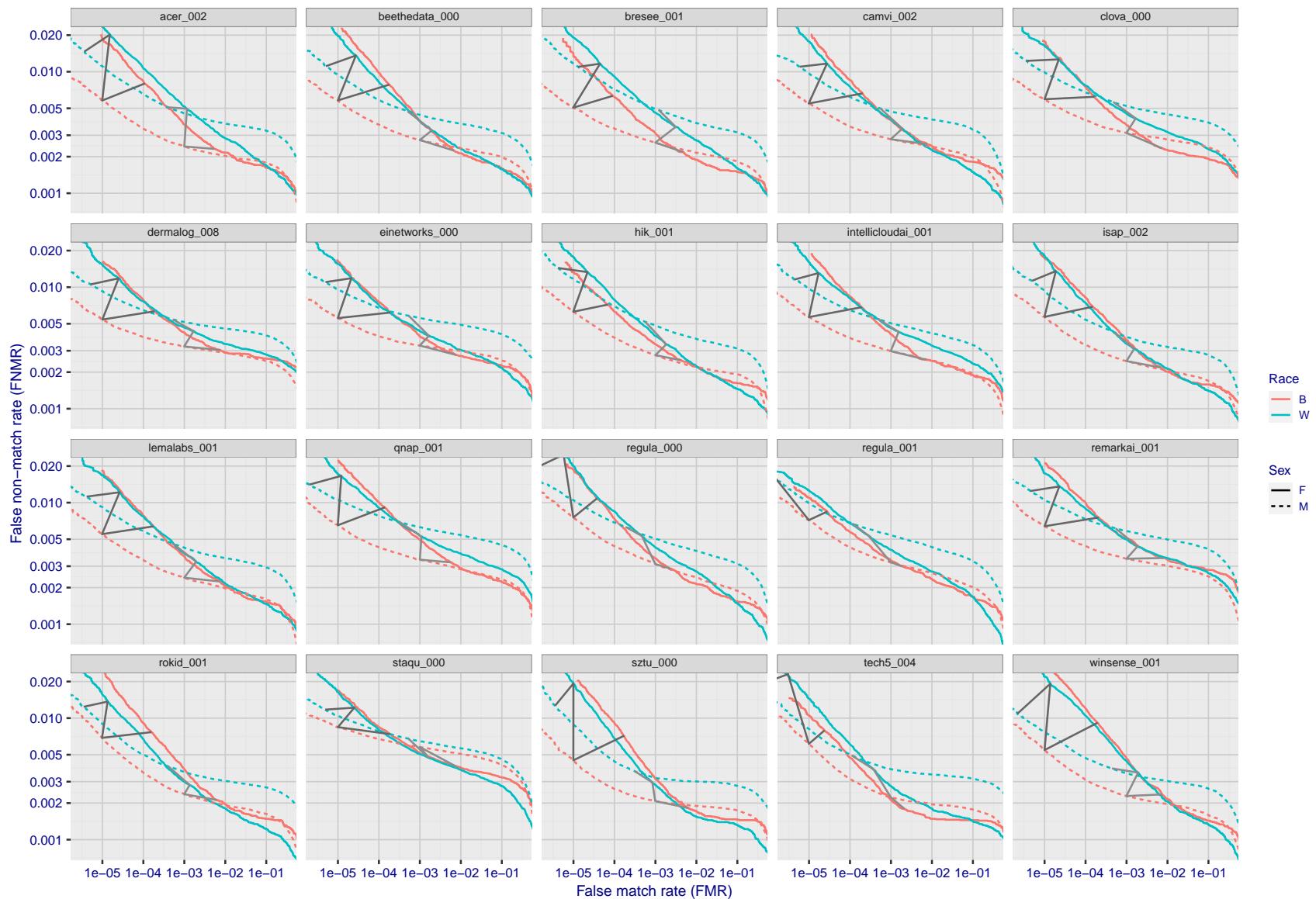


Figure 123: For the mugshot images, error tradeoff characteristics for white females, black females, black males and white males. The Z-shaped grey lines correspond to fixed thresholds, showing both FNMR and FMR vary at one  $T$  value. Note: Many of the plots will naively be read as saying women gives worse error rates than men because the solid traces lie above the dotted ones. However, this is misleading and incomplete: The grey lines show the traces reveal horizontal shifts. Thus for the cogent-003 algorithm FNMR for men is higher than for women at a fixed threshold but, at the same time, FMR is higher for women - see Figure 182. As access control systems almost always operate at a fixed threshold, the naive interpretation is incorrect.

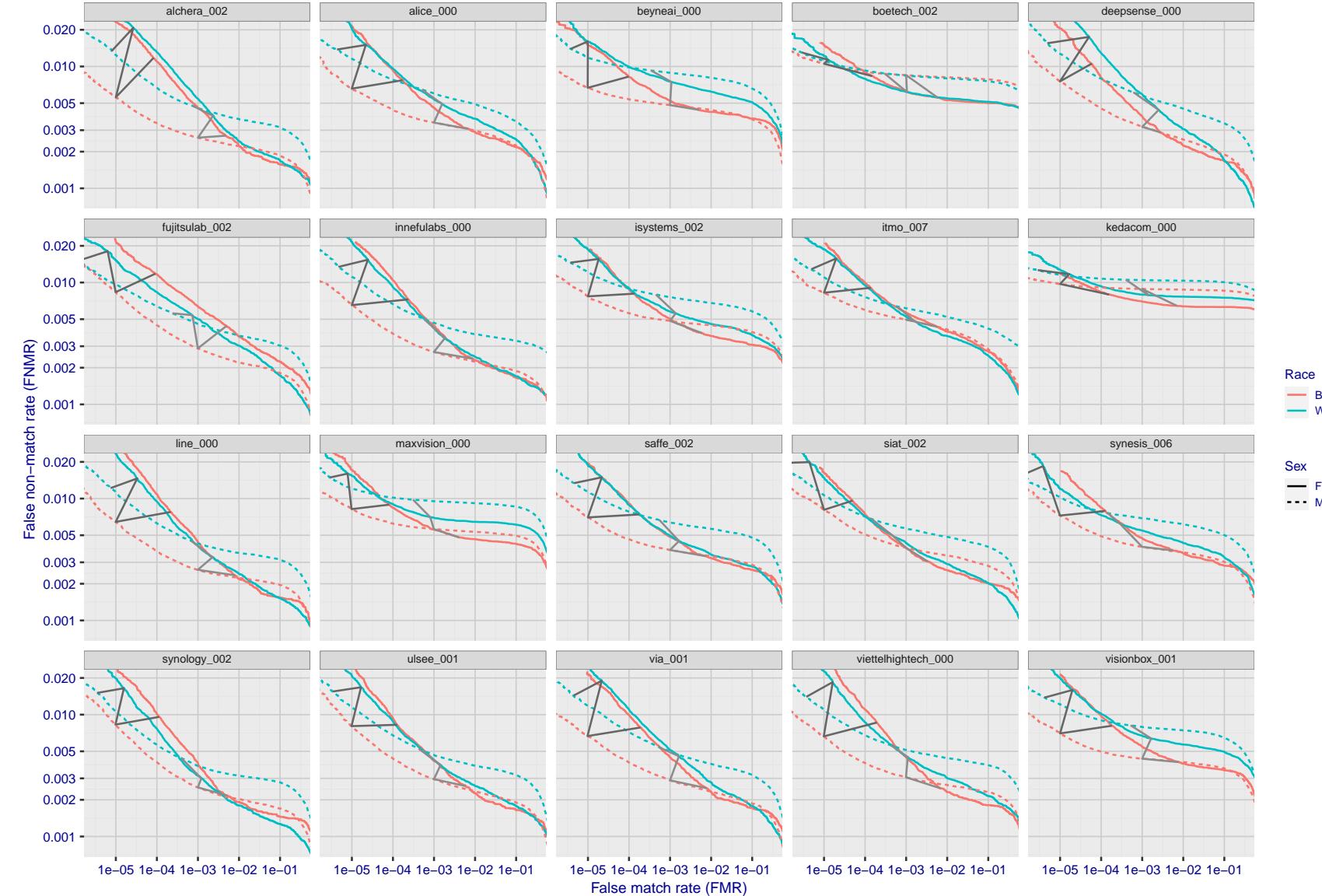


Figure 124: For the mugshot images, error tradeoff characteristics for white females, black females, black males and white males. The Z-shaped grey lines correspond to fixed thresholds, showing both FNMR and FMR vary at one  $T$  value. Note: Many of the plots will naively be read as saying women gives worse error rates than men because the solid traces lie above the dotted ones. However, this is misleading and incomplete: The grey lines show the traces reveal horizontal shifts. Thus for the cogent-003 algorithm FNMR for men is higher than for women at a fixed threshold but, at the same time, FMR is higher for women - see Figure 182. As access control systems almost always operate at a fixed threshold, the naive interpretation is incorrect.

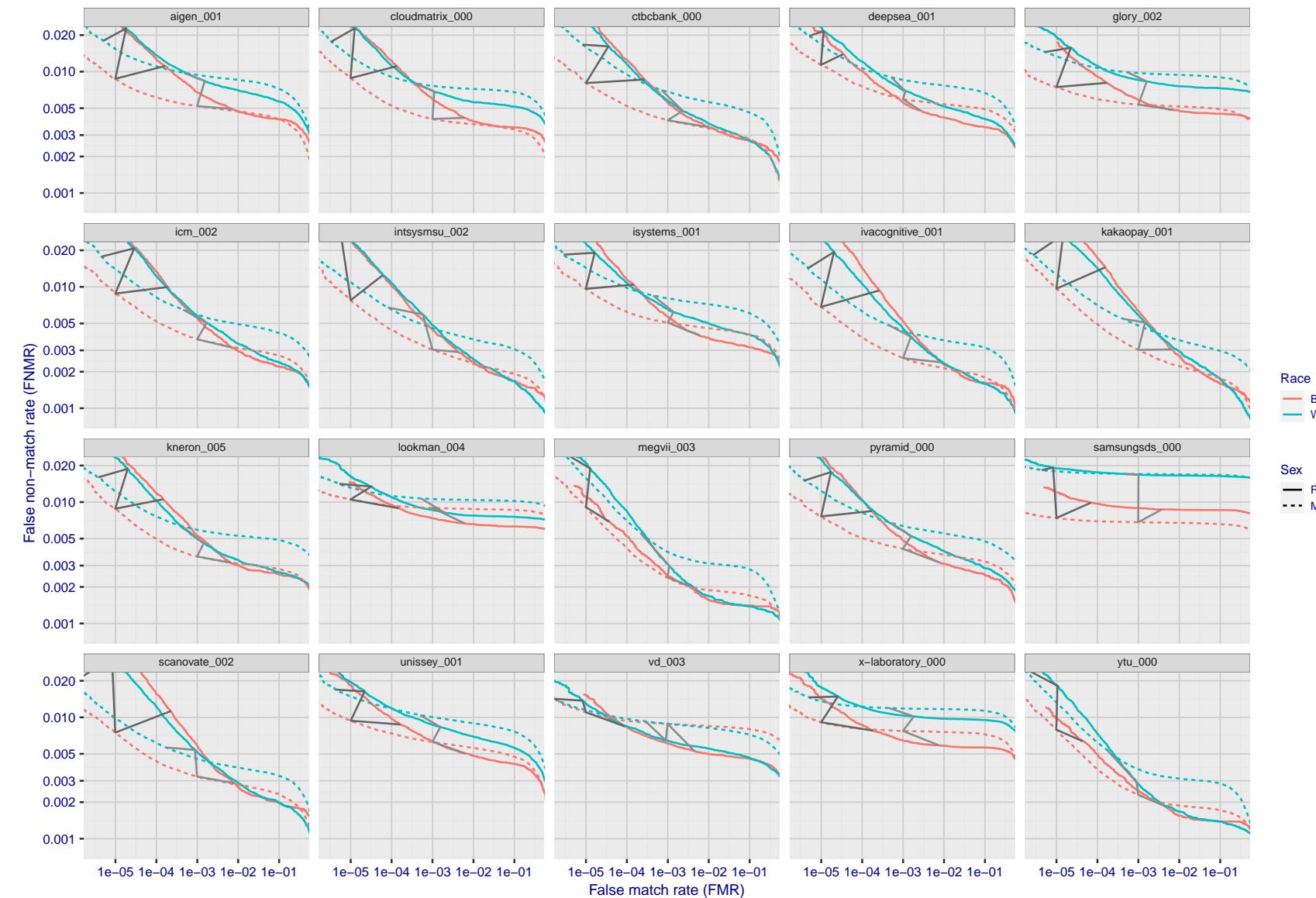


Figure 125: For the mugshot images, error tradeoff characteristics for white females, black females, black males and white males. The Z-shaped grey lines correspond to fixed thresholds, showing both FNMR and FMR vary at one  $T$  value. Note: Many of the plots will naively be read as saying women gives worse error rates than men because the solid traces lie above the dotted ones. However, this is misleading and incomplete: The grey lines show the traces reveal horizontal shifts. Thus for the cogent-003 algorithm FNMR for men is higher than for women at a fixed threshold but, at the same time, FMR is higher for women - see Figure 182. As access control systems almost always operate at a fixed threshold, the naive interpretation is incorrect.

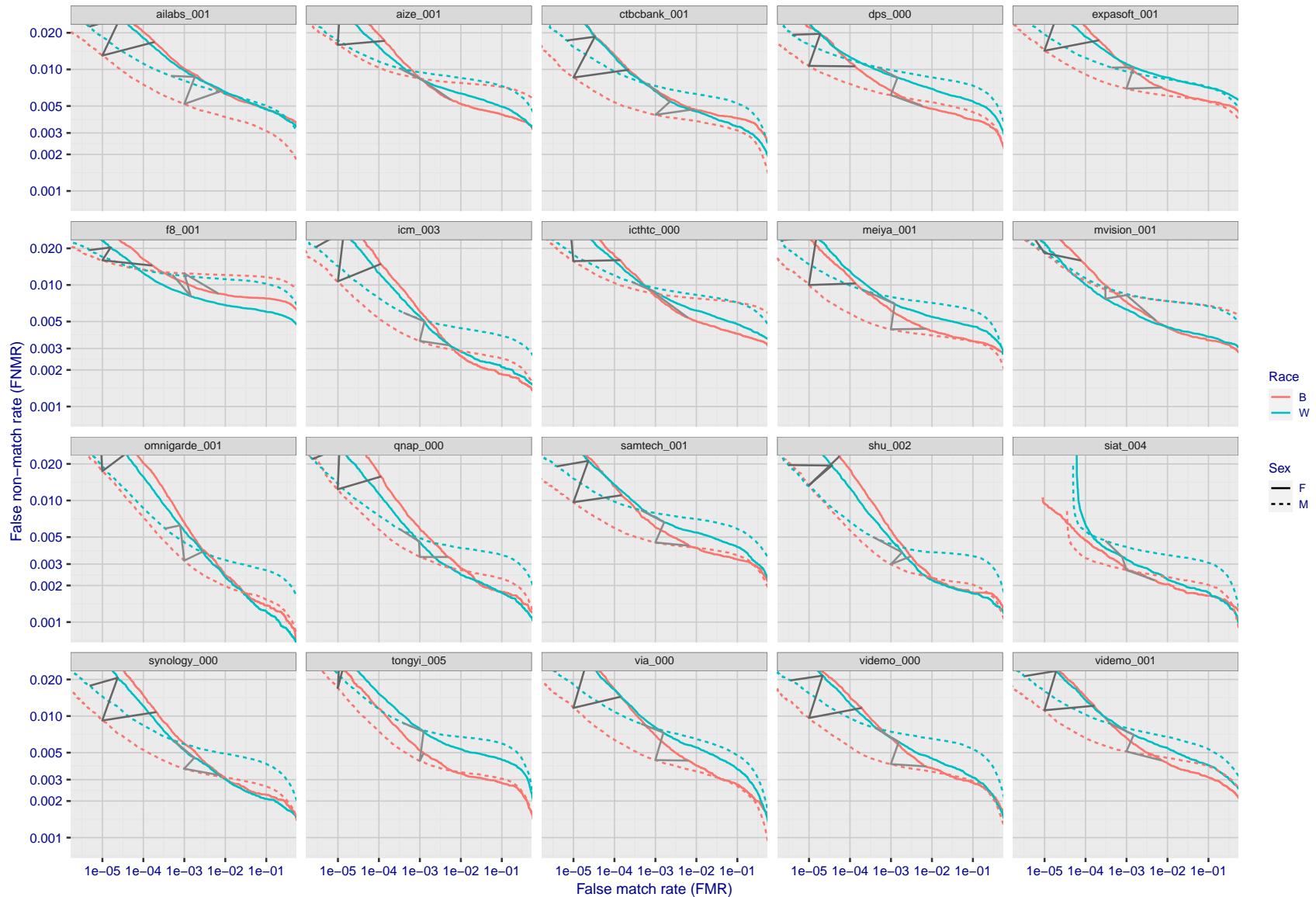


Figure 126: For the mugshot images, error tradeoff characteristics for white females, black females, black males and white males. The Z-shaped grey lines correspond to fixed thresholds, showing both FNMR and FMR vary at one T value. Note: Many of the plots will naively be read as saying women gives worse error rates than men because the solid traces lie above the dotted ones. However, this is misleading and incomplete: The grey lines show the traces reveal horizontal shifts. Thus for the cogent-003 algorithm FNMR for men is higher than for women at a fixed threshold but, at the same time, FMR is higher for women - see Figure 182. As access control systems almost always operate at a fixed threshold, the naive interpretation is incorrect.

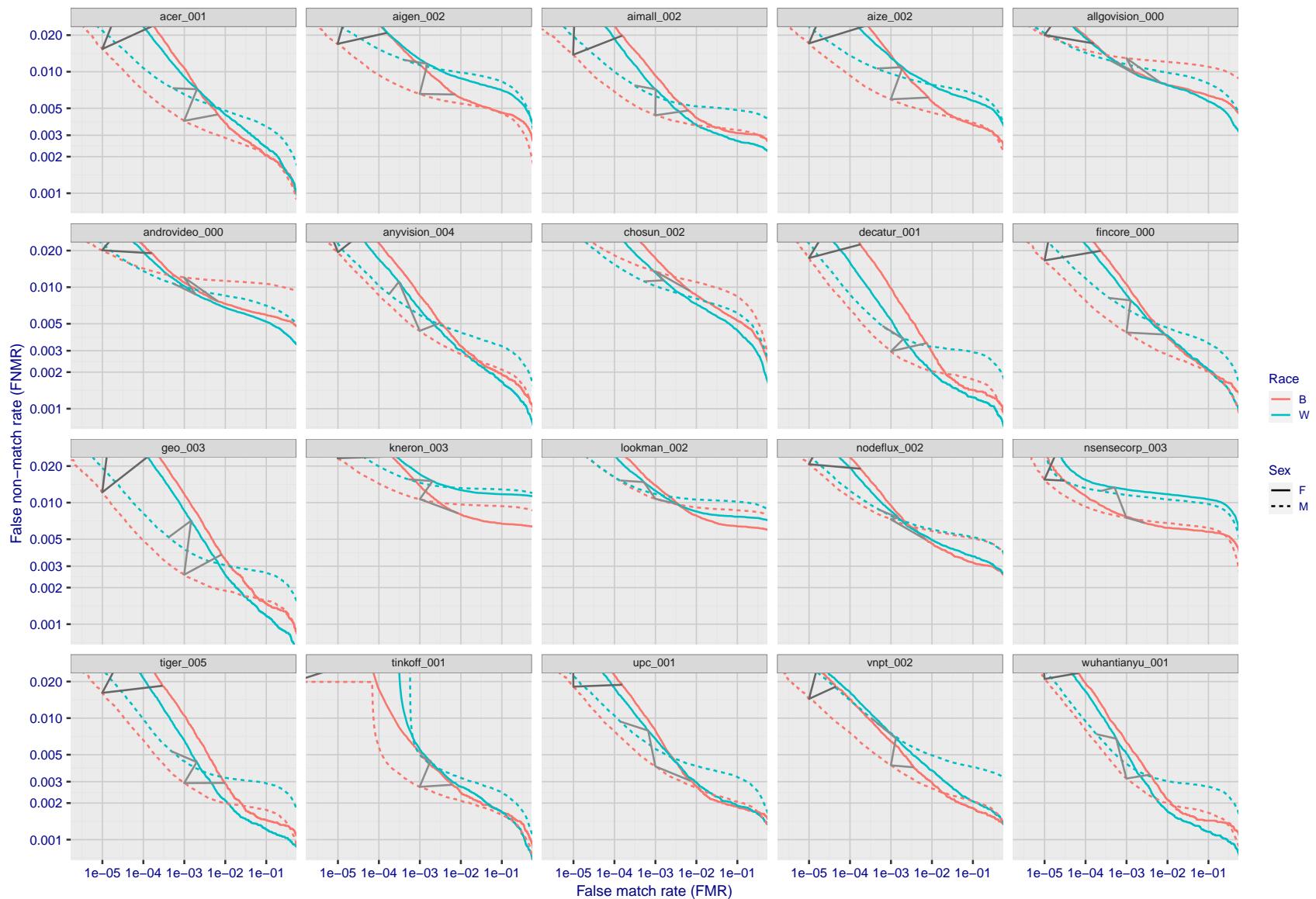


Figure 127: For the mugshot images, error tradeoff characteristics for white females, black females, black males and white males. The Z-shaped grey lines correspond to fixed thresholds, showing both FNMR and FMR vary at one  $T$  value. Note: Many of the plots will naively be read as saying women gives worse error rates than men because the solid traces lie above the dotted ones. However, this is misleading and incomplete: The grey lines show the traces reveal horizontal shifts. Thus for the cogent-003 algorithm FNMR for men is higher than for women at a fixed threshold but, at the same time, FMR is higher for women - see Figure 182. As access control systems almost always operate at a fixed threshold, the naive interpretation is incorrect.

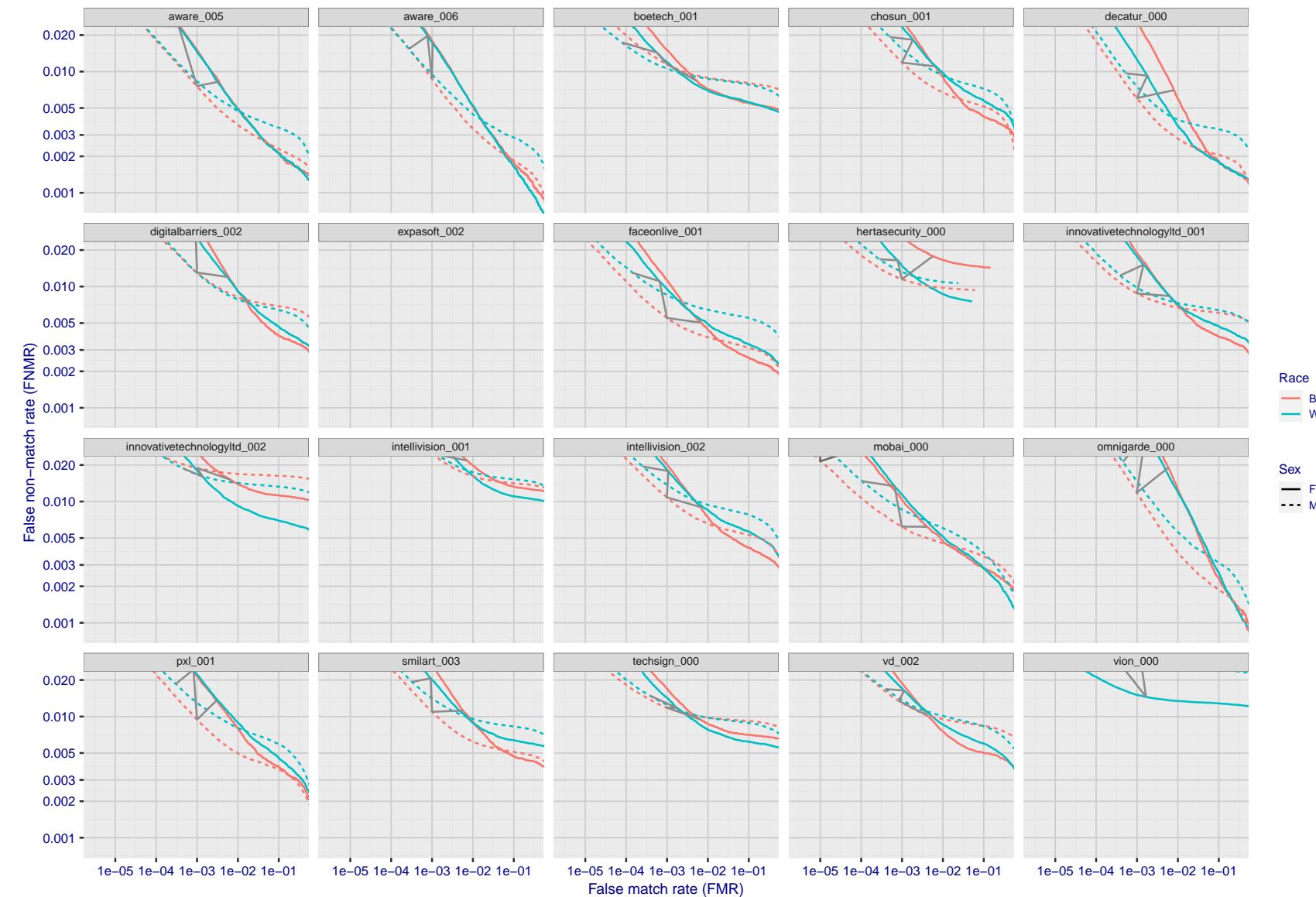


Figure 128: For the mugshot images, error tradeoff characteristics for white females, black females, black males and white males. The Z-shaped grey lines correspond to fixed thresholds, showing both FNMR and FMR vary at one T value. Note: Many of the plots will naively be read as saying women gives worse error rates than men because the solid traces lie above the dotted ones. However, this is misleading and incomplete: The grey lines show the traces reveal horizontal shifts. Thus for the cogent-003 algorithm FNMR for men is higher than for women at a fixed threshold but, at the same time, FMR is higher for women - see Figure 182. As access control systems almost always operate at a fixed threshold, the naive interpretation is incorrect.

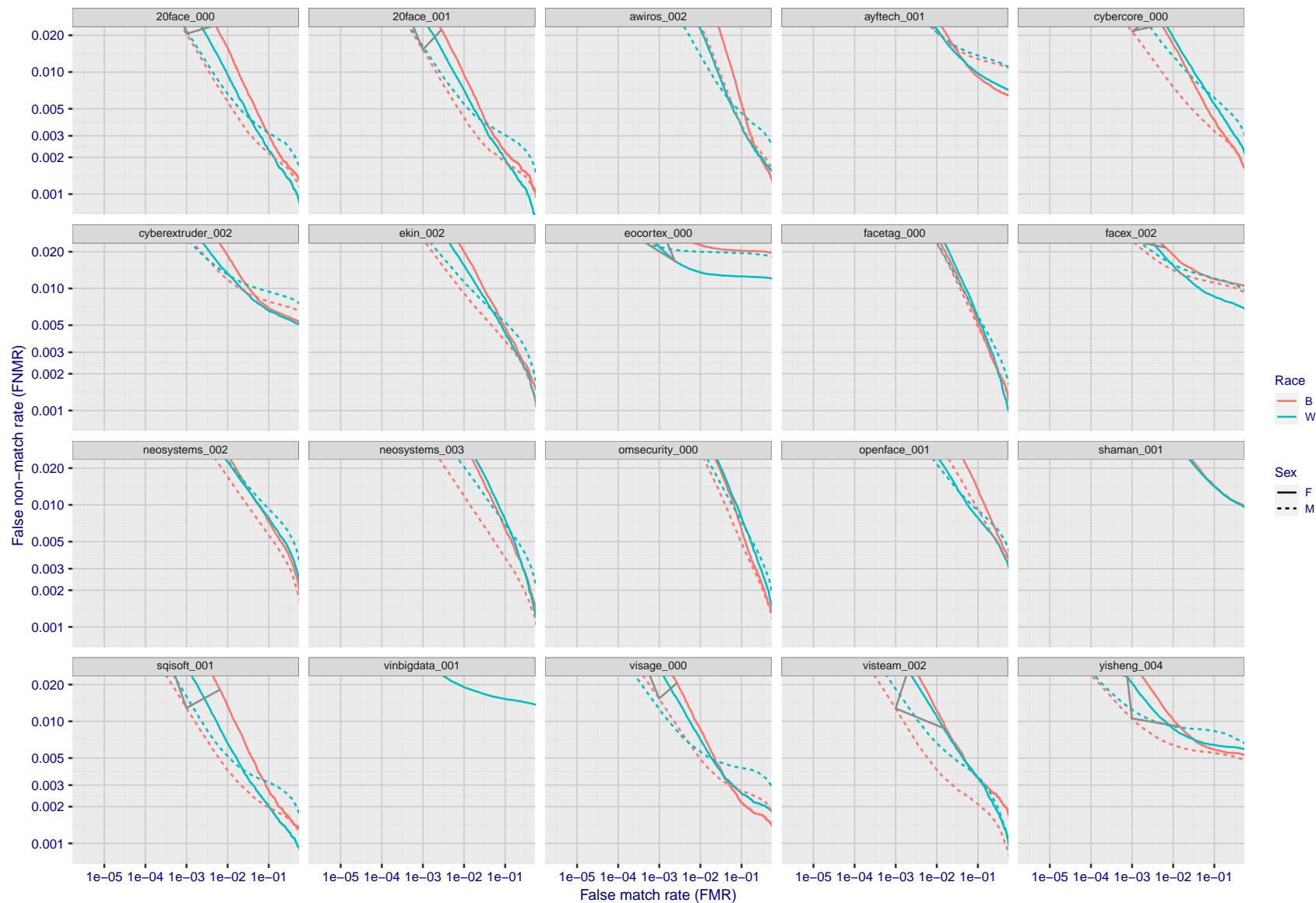


Figure 129: For the mugshot images, error tradeoff characteristics for white females, black females, black males and white males. The Z-shaped grey lines correspond to fixed thresholds, showing both FNMR and FMR vary at one  $T$  value. Note: Many of the plots will naively be read as saying women gives worse error rates than men because the solid traces lie above the dotted ones. However, this is misleading and incomplete: The grey lines show the traces reveal horizontal shifts. Thus for the cogent-003 algorithm FNMR for men is higher than for women at a fixed threshold but, at the same time, FMR is higher for women - see Figure 182. As access control systems almost always operate at a fixed threshold, the naive interpretation is incorrect.

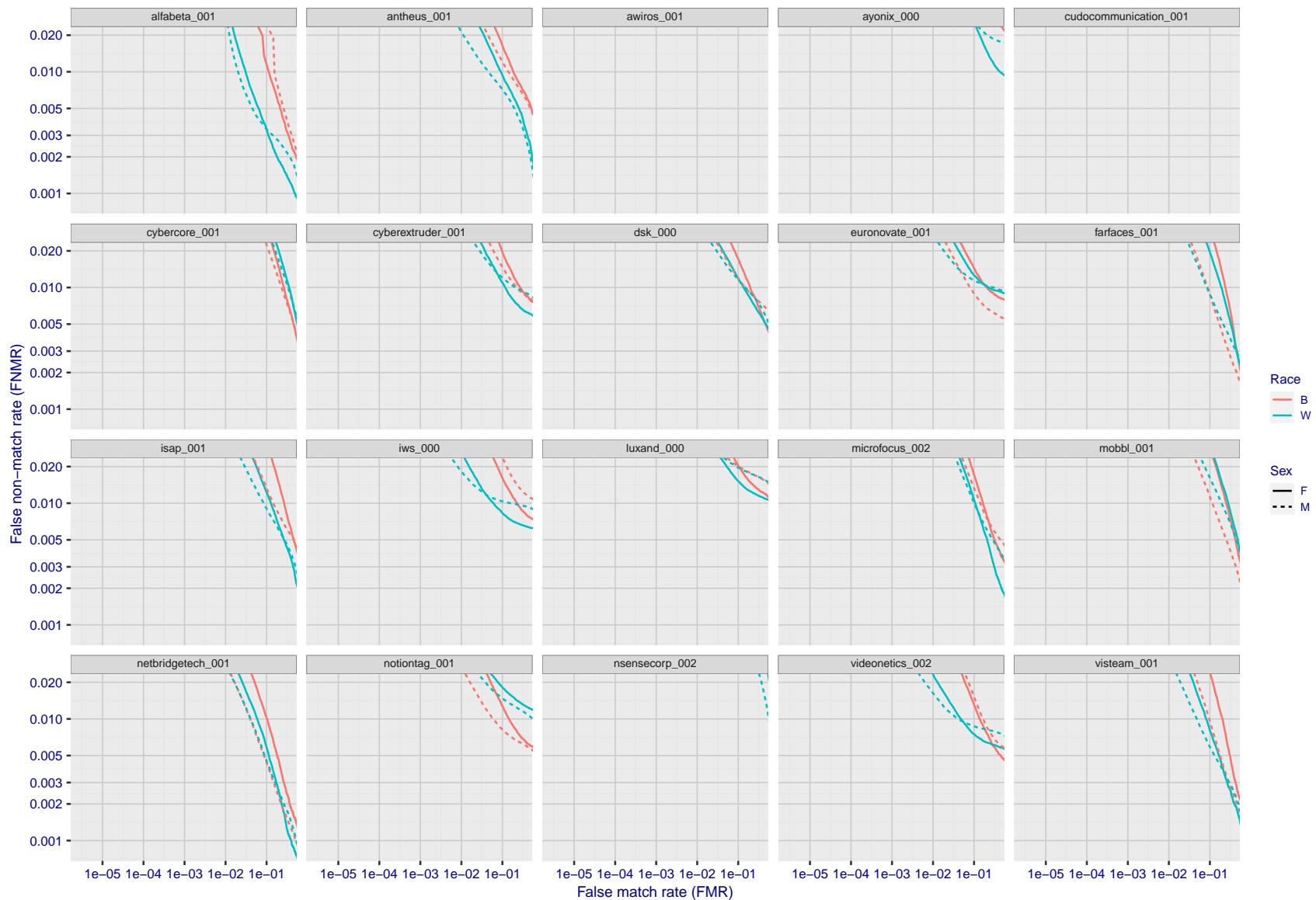


Figure 130: For the mugshot images, error tradeoff characteristics for white females, black females, black males and white males. The Z-shaped grey lines correspond to fixed thresholds, showing both FNMR and FMR vary at one  $T$  value. Note: Many of the plots will naively be read as saying women gives worse error rates than men because the solid traces lie above the dotted ones. However, this is misleading and incomplete: The grey lines show the traces reveal horizontal shifts. Thus for the cogent-003 algorithm FNMR for men is higher than for women at a fixed threshold but, at the same time, FMR is higher for women - see Figure 182. As access control systems almost always operate at a fixed threshold, the naive interpretation is incorrect.

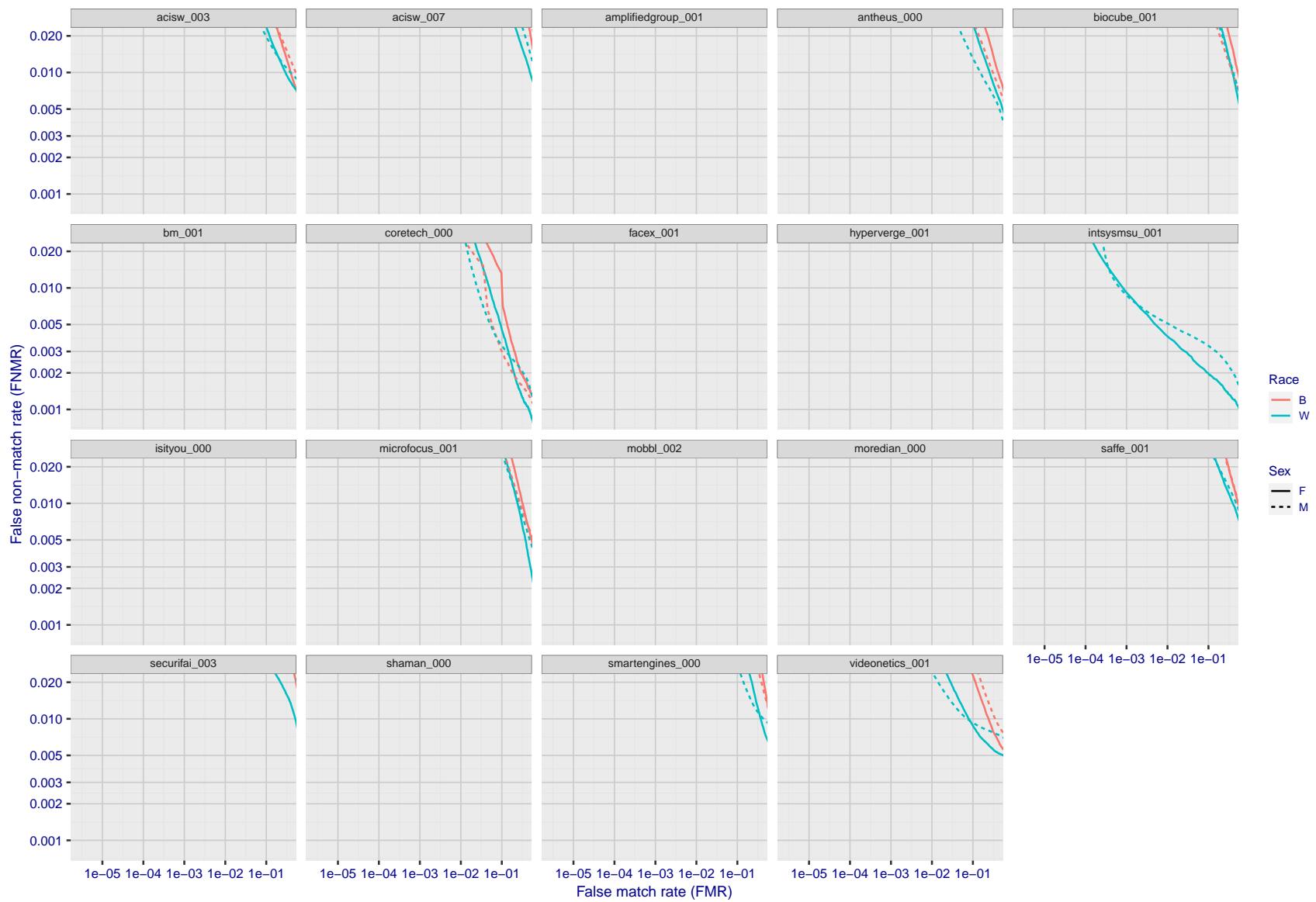


Figure 131: For the mugshot images, error tradeoff characteristics for white females, black females, black males and white males. The Z-shaped grey lines correspond to fixed thresholds, showing both FNMR and FMR vary at one T value. Note: Many of the plots will naively be read as saying women gives worse error rates than men because the solid traces lie above the dotted ones. However, this is misleading and incomplete: The grey lines show the traces reveal horizontal shifts. Thus for the cogent-003 algorithm FNMR for men is higher than for women at a fixed threshold but, at the same time, FMR is higher for women - see Figure 182. As access control systems almost always operate at a fixed threshold, the naive interpretation is incorrect.

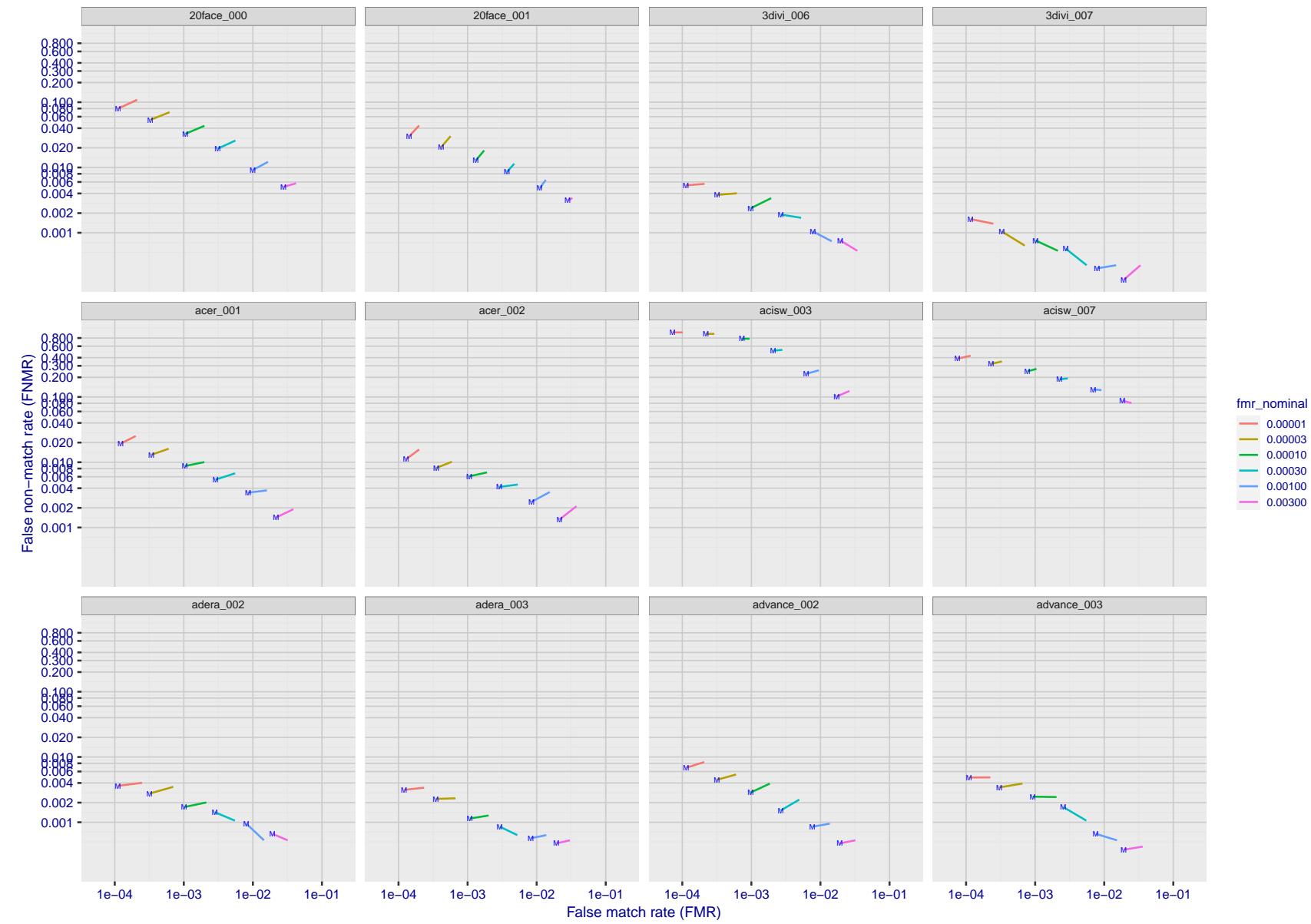


Figure 132: For the visa images, FNMR and FMR at six operating points along the DET characteristic. At each point a line is drawn between  $(FMR, FNMR)_{MALE}$  and  $(FMR, FNMR)_{FEMALE}$  showing how which sex has lower FMR and/or FNMR. The "M" label denotes male, the other end of the line corresponds to female. The six operating thresholds are selected to give the nominal false match rates given in the legend, and are computed over all impostor pairs regardless of age, sex, and place of birth. The plotted FMR values are broadly an order of magnitude larger than the nominal rates because FMR is computed over demographically-matched impostor pairs i.e individuals of the same sex, from the same geographic region (see section 3.6.1), and the same age group (see section 3.6.2).

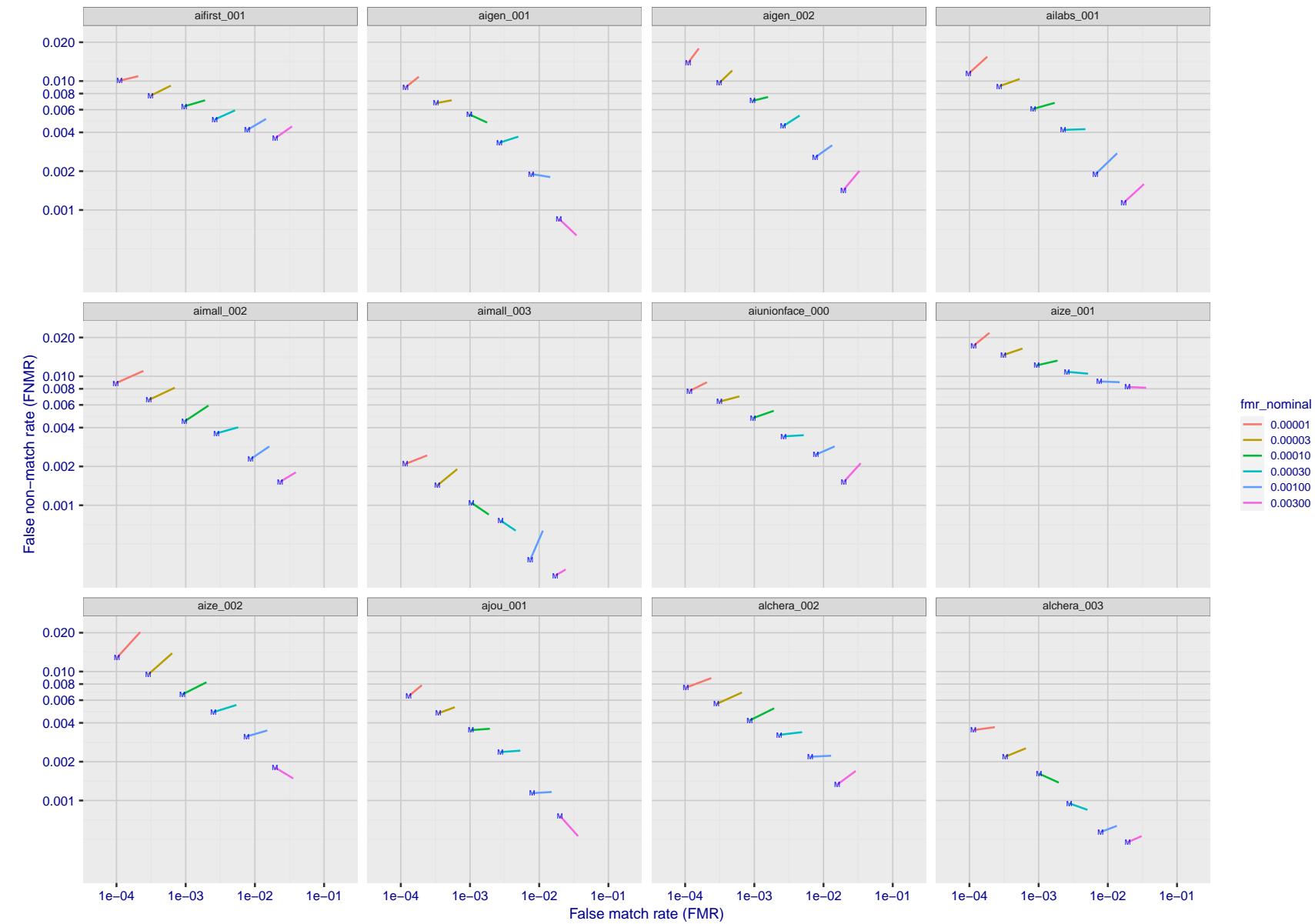


Figure 133: For the visa images, FNMR and FMR at six operating points along the DET characteristic. At each point a line is drawn between  $(FMR, FNMR)_{MALE}$  and  $(FMR, FNMR)_{FEMALE}$  showing how which sex has lower FMR and/or FNMR. The "M" label denotes male, the other end of the line corresponds to female. The six operating thresholds are selected to give the nominal false match rates given in the legend, and are computed over all impostor pairs regardless of age, sex, and place of birth. The plotted FMR values are broadly an order of magnitude larger than the nominal rates because FMR is computed over demographically-matched impostor pairs i.e individuals of the same sex, from the same geographic region (see section 3.6.1), and the same age group (see section 3.6.2).

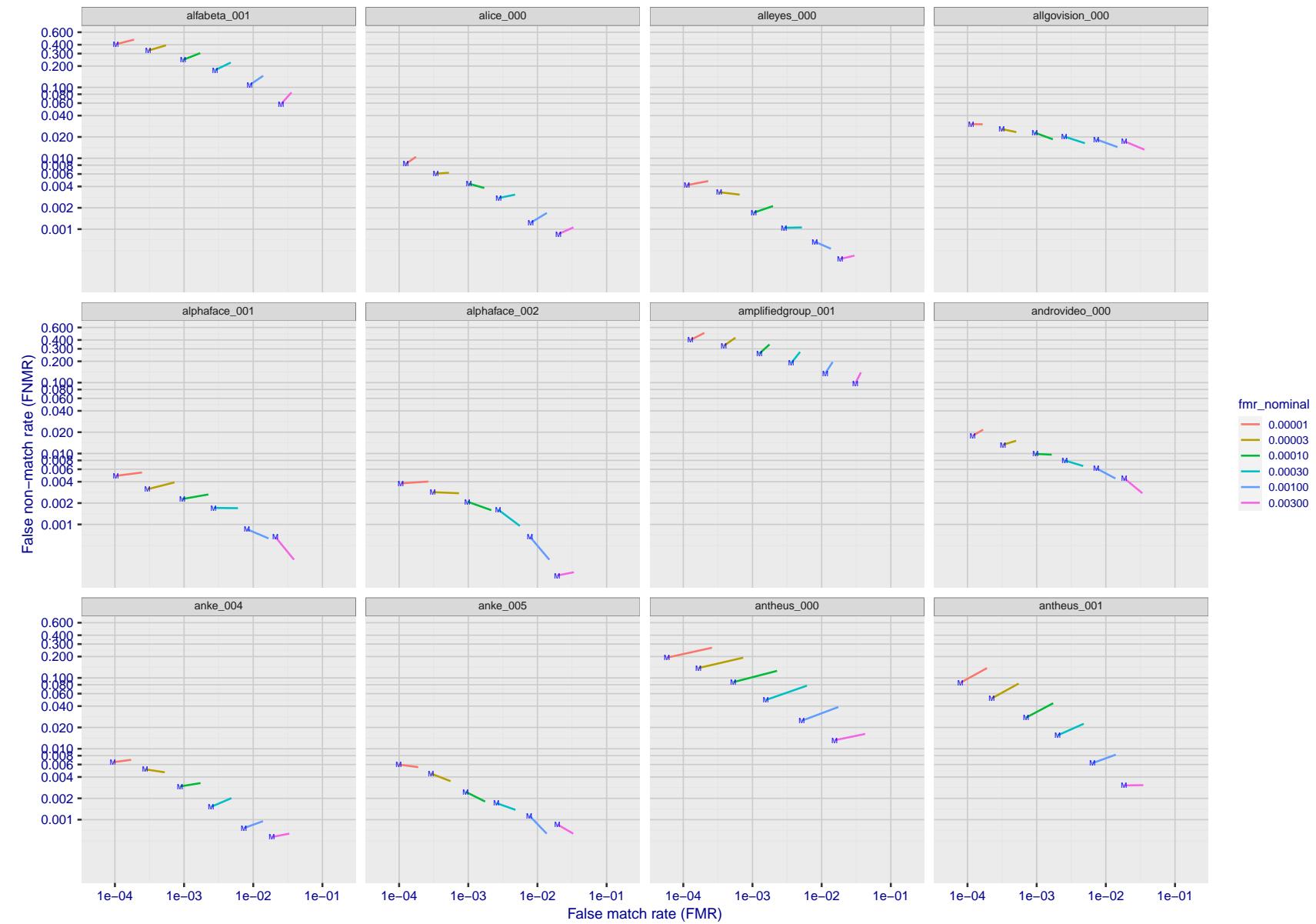


Figure 134: For the visa images, FNMR and FMR at six operating points along the DET characteristic. At each point a line is drawn between  $(FMR, FNMR)_{MALE}$  and  $(FMR, FNMR)_{FEMALE}$  showing how which sex has lower FMR and/or FNMR. The "M" label denotes male, the other end of the line corresponds to female. The six operating thresholds are selected to give the nominal false match rates given in the legend, and are computed over all impostor pairs regardless of age, sex, and place of birth. The plotted FMR values are broadly an order of magnitude larger than the nominal rates because FMR is computed over demographically-matched impostor pairs i.e individuals of the same sex, from the same geographic region (see section 3.6.1), and the same age group (see section 3.6.2).

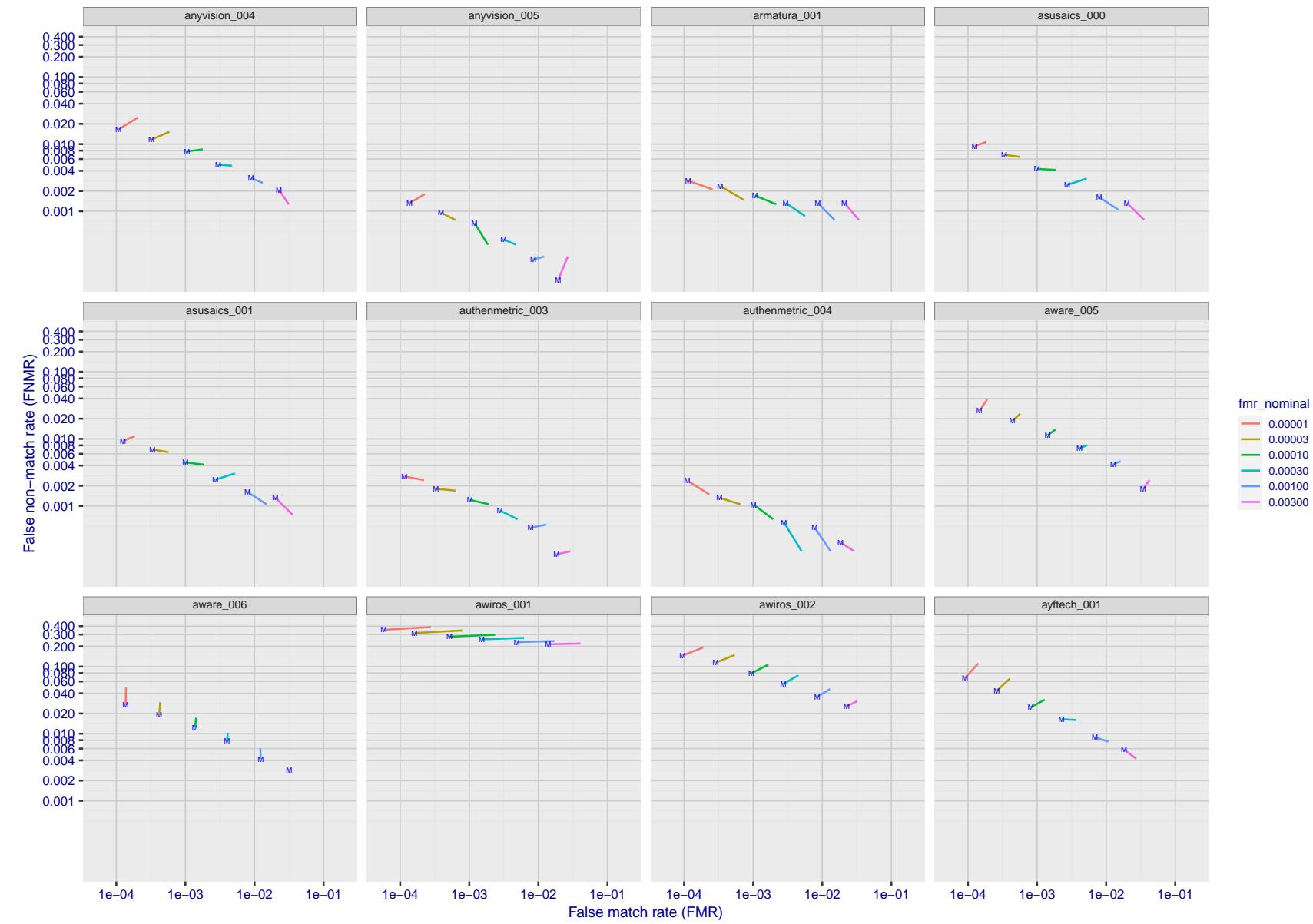


Figure 135: For the visa images, FNMR and FMR at six operating points along the DET characteristic. At each point a line is drawn between  $(FMR, FNMR)_{MALE}$  and  $(FMR, FNMR)_{FEMALE}$  showing how which sex has lower FMR and/or FNMR. The "M" label denotes male, the other end of the line corresponds to female. The six operating thresholds are selected to give the nominal false match rates given in the legend, and are computed over all impostor pairs regardless of age, sex, and place of birth. The plotted FMR values are broadly an order of magnitude larger than the nominal rates because FMR is computed over demographically-matched impostor pairs i.e individuals of the same sex, from the same geographic region (see section 3.6.1), and the same age group (see section 3.6.2).

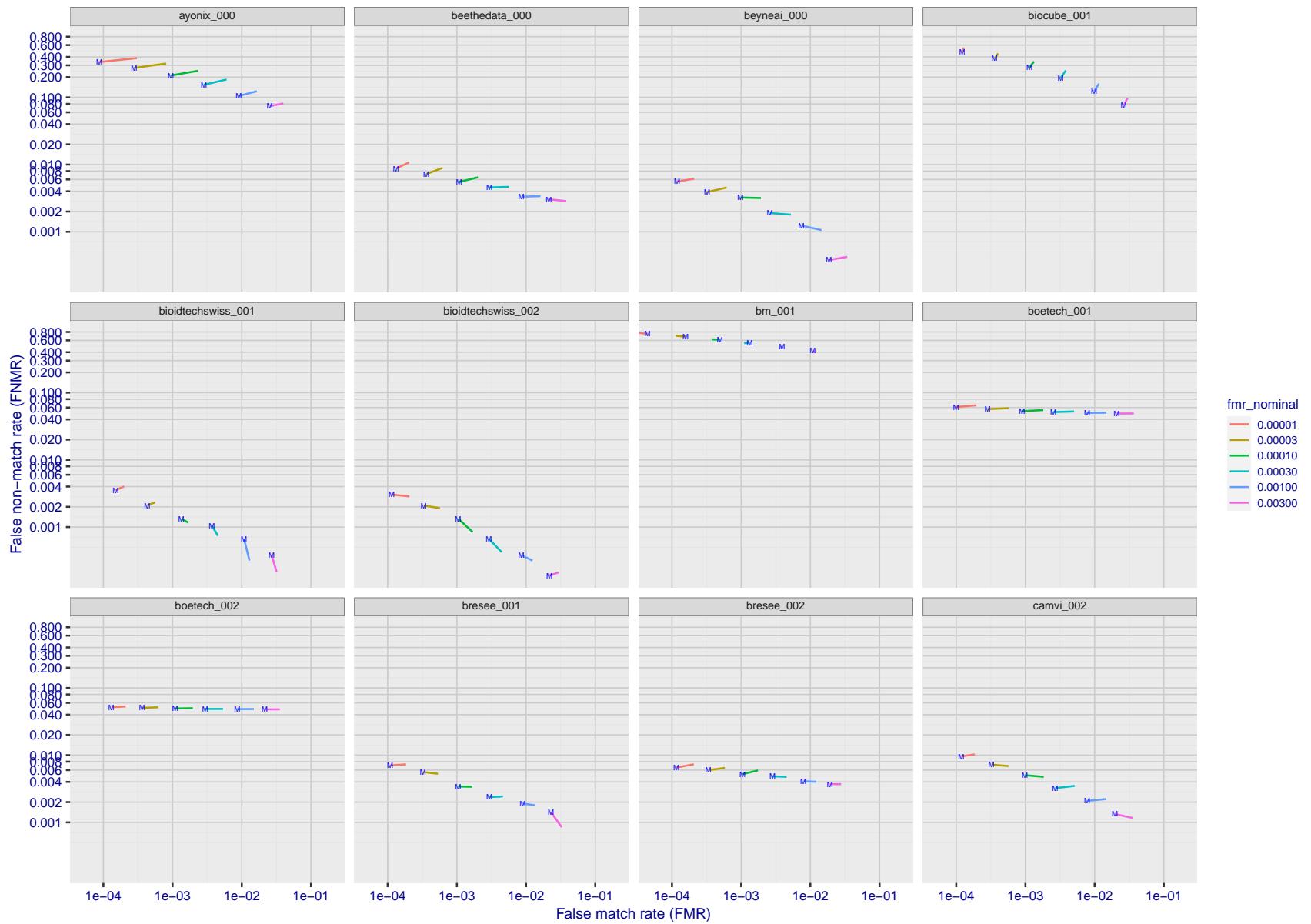


Figure 136: For the visa images, FNMR and FMR at six operating points along the DET characteristic. At each point a line is drawn between  $(FMR, FNMR)_{MALE}$  and  $(FMR, FNMR)_{FEMALE}$  showing how which sex has lower FMR and/or FNMR. The "M" label denotes male, the other end of the line corresponds to female. The six operating thresholds are selected to give the nominal false match rates given in the legend, and are computed over all impostor pairs regardless of age, sex, and place of birth. The plotted FMR values are broadly an order of magnitude larger than the nominal rates because FMR is computed over demographically-matched impostor pairs i.e individuals of the same sex, from the same geographic region (see section 3.6.1), and the same age group (see section 3.6.2).

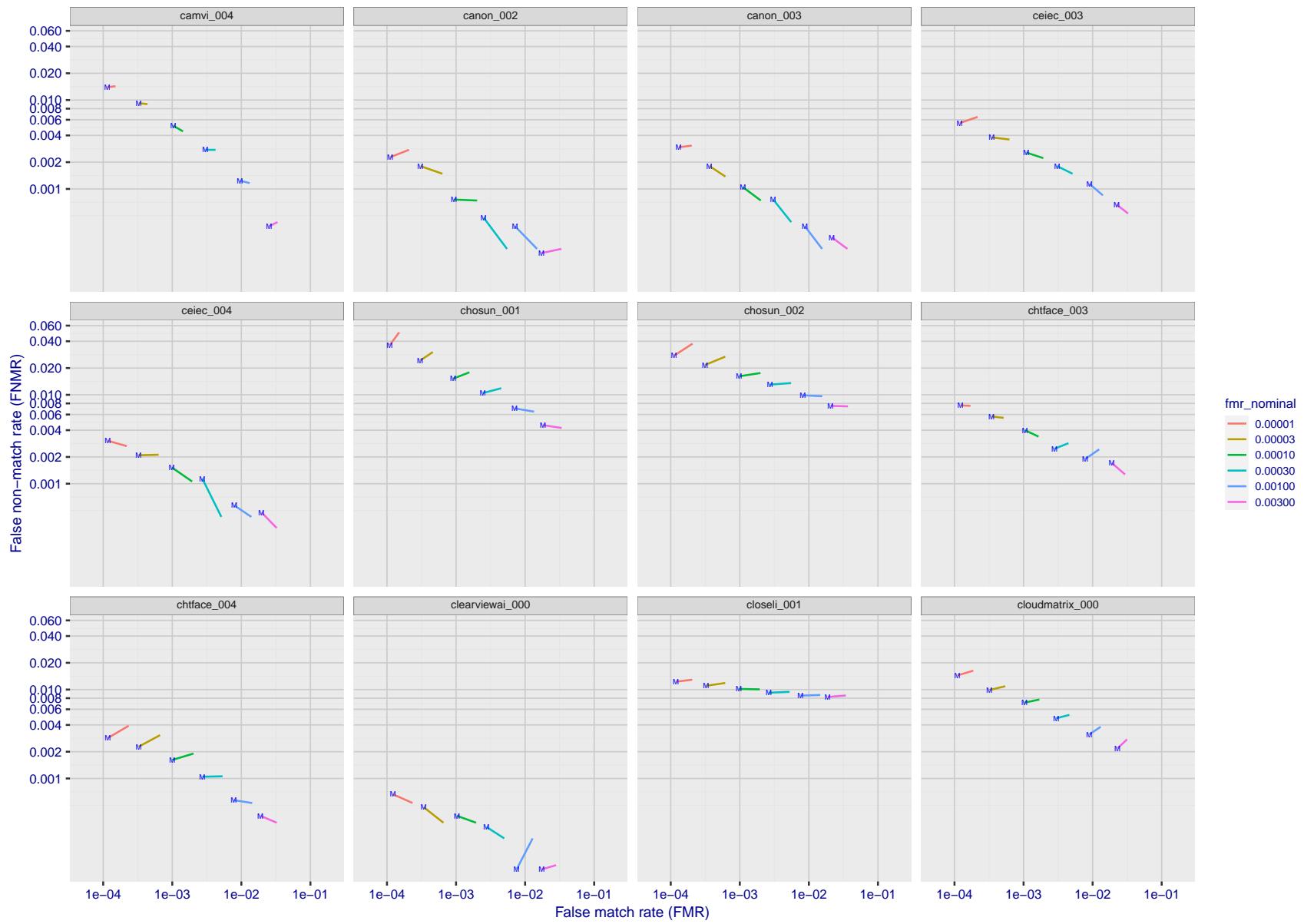


Figure 137: For the visa images, FNMR and FMR at six operating points along the DET characteristic. At each point a line is drawn between  $(FMR, FNMR)_{MALE}$  and  $(FMR, FNMR)_{FEMALE}$  showing how which sex has lower FMR and/or FNMR. The "M" label denotes male, the other end of the line corresponds to female. The six operating thresholds are selected to give the nominal false match rates given in the legend, and are computed over all impostor pairs regardless of age, sex, and place of birth. The plotted FMR values are broadly an order of magnitude larger than the nominal rates because FMR is computed over demographically-matched impostor pairs i.e individuals of the same sex, from the same geographic region (see section 3.6.1), and the same age group (see section 3.6.2).

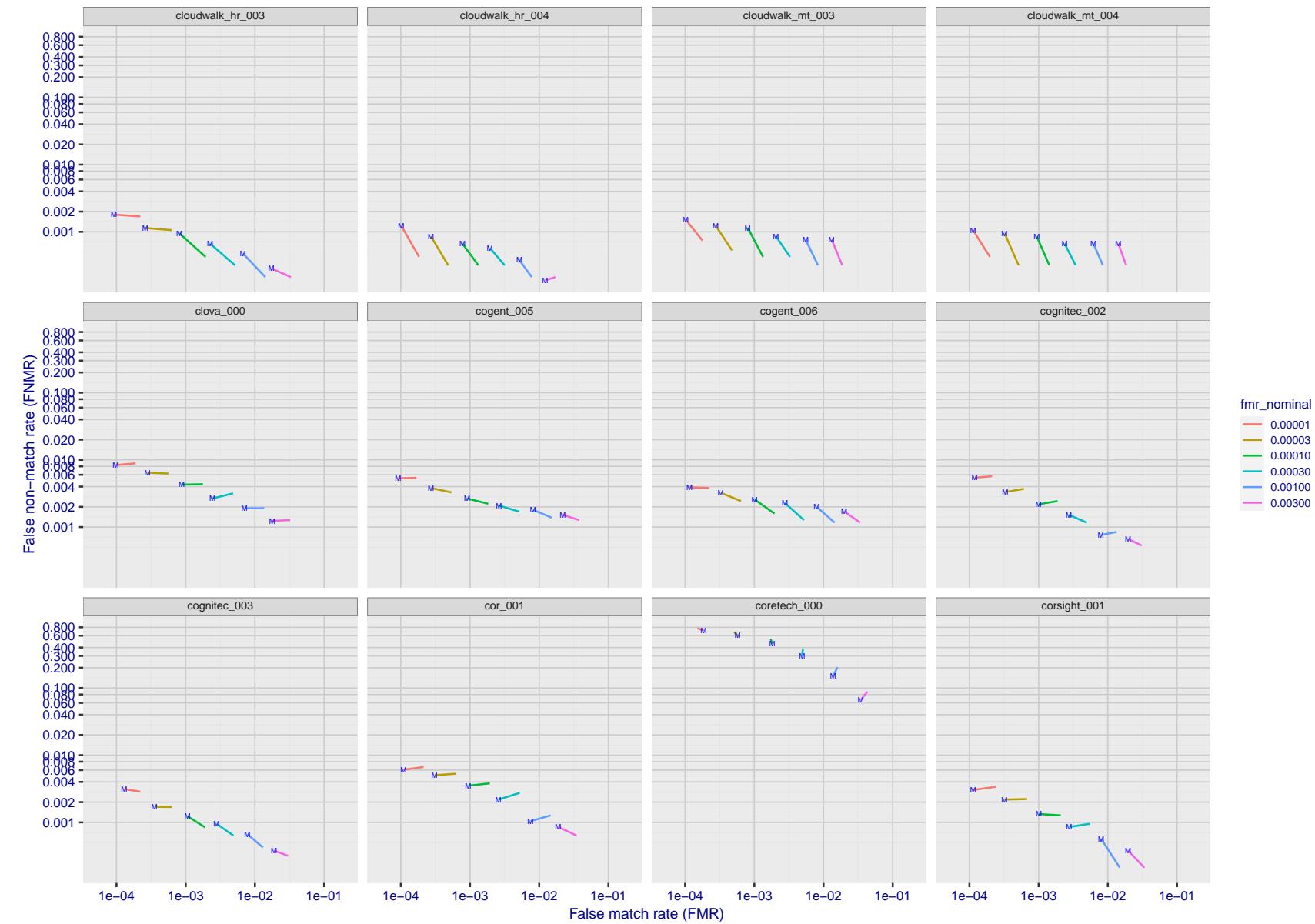


Figure 138: For the visa images, FNMR and FMR at six operating points along the DET characteristic. At each point a line is drawn between  $(FMR, FNMR)_{MALE}$  and  $(FMR, FNMR)_{FEMALE}$  showing how which sex has lower FMR and/or FNMR. The "M" label denotes male, the other end of the line corresponds to female. The six operating thresholds are selected to give the nominal false match rates given in the legend, and are computed over all impostor pairs regardless of age, sex, and place of birth. The plotted FMR values are broadly an order of magnitude larger than the nominal rates because FMR is computed over demographically-matched impostor pairs i.e individuals of the same sex, from the same geographic region (see section 3.6.1), and the same age group (see section 3.6.2).

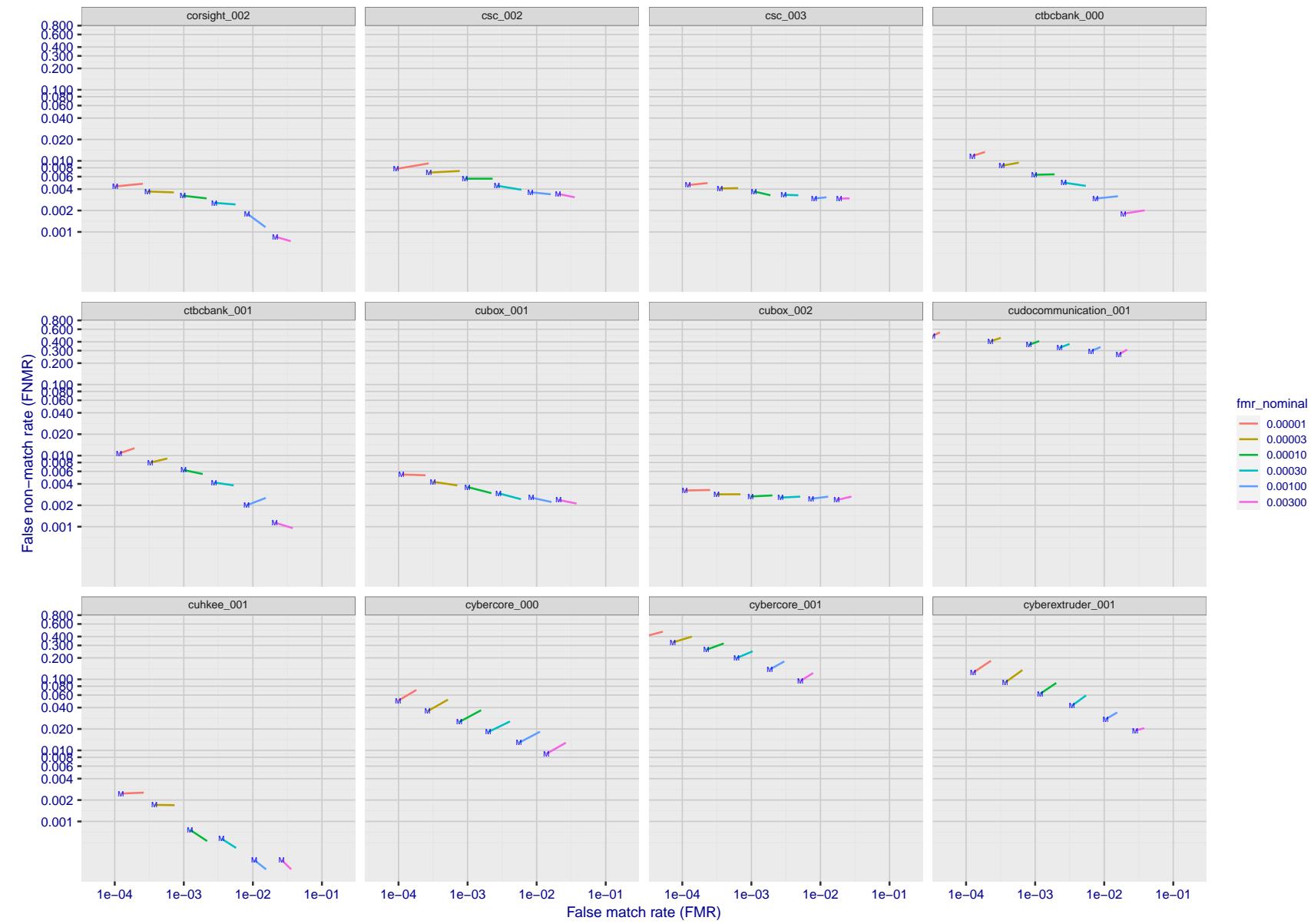


Figure 139: For the visa images, FNMR and FMR at six operating points along the DET characteristic. At each point a line is drawn between  $(FMR, FNMR)_{MALE}$  and  $(FMR, FNMR)_{FEMALE}$  showing how which sex has lower FMR and/or FNMR. The "M" label denotes male, the other end of the line corresponds to female. The six operating thresholds are selected to give the nominal false match rates given in the legend, and are computed over all impostor pairs regardless of age, sex, and place of birth. The plotted FMR values are broadly an order of magnitude larger than the nominal rates because FMR is computed over demographically-matched impostor pairs i.e individuals of the same sex, from the same geographic region (see section 3.6.1), and the same age group (see section 3.6.2).

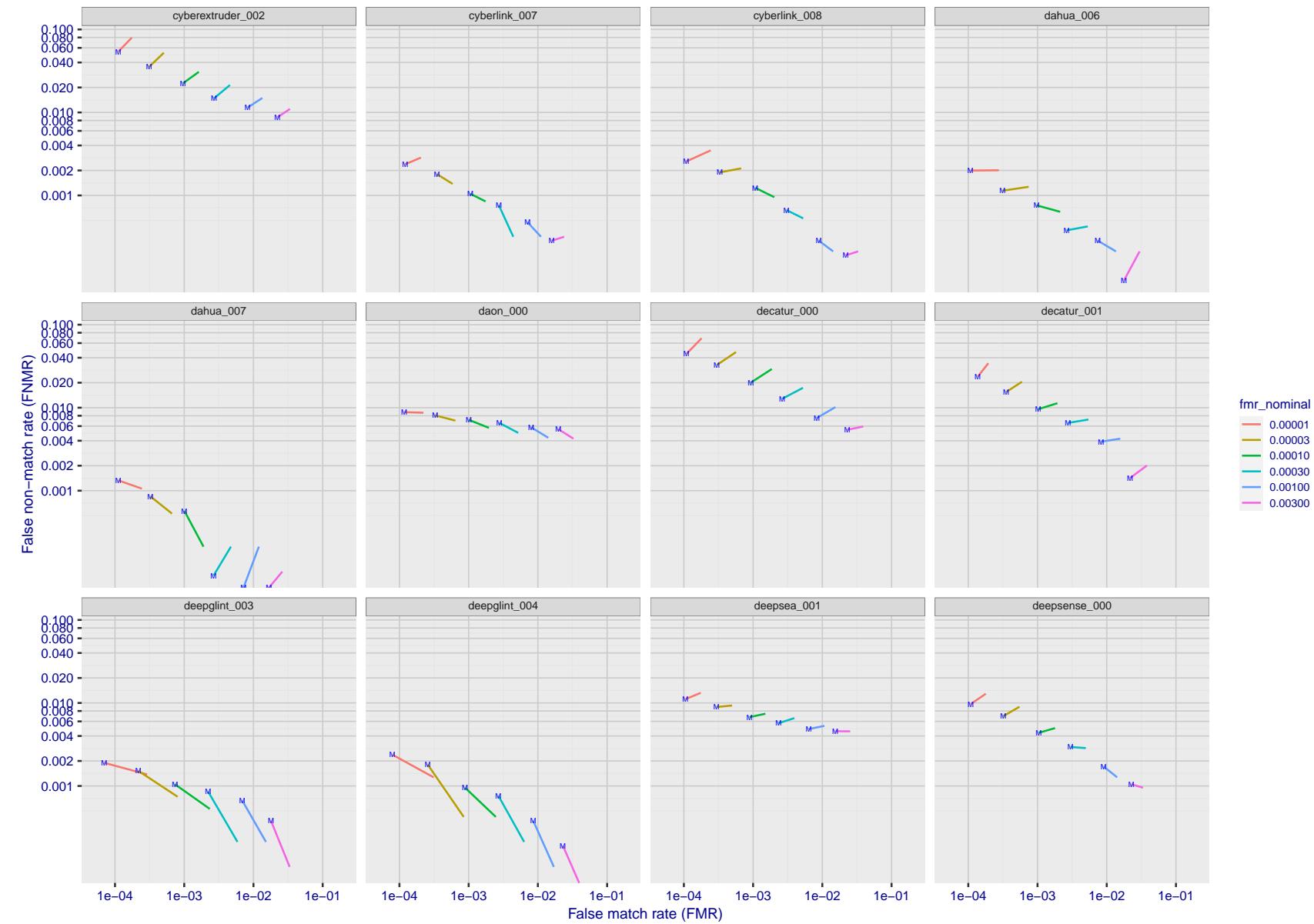


Figure 140: For the visa images, FNMR and FMR at six operating points along the DET characteristic. At each point a line is drawn between  $(FMR, FNMR)_{MALE}$  and  $(FMR, FNMR)_{FEMALE}$  showing how which sex has lower FMR and/or FNMR. The "M" label denotes male, the other end of the line corresponds to female. The six operating thresholds are selected to give the nominal false match rates given in the legend, and are computed over all impostor pairs regardless of age, sex, and place of birth. The plotted FMR values are broadly an order of magnitude larger than the nominal rates because FMR is computed over demographically-matched impostor pairs i.e individuals of the same sex, from the same geographic region (see section 3.6.1), and the same age group (see section 3.6.2).

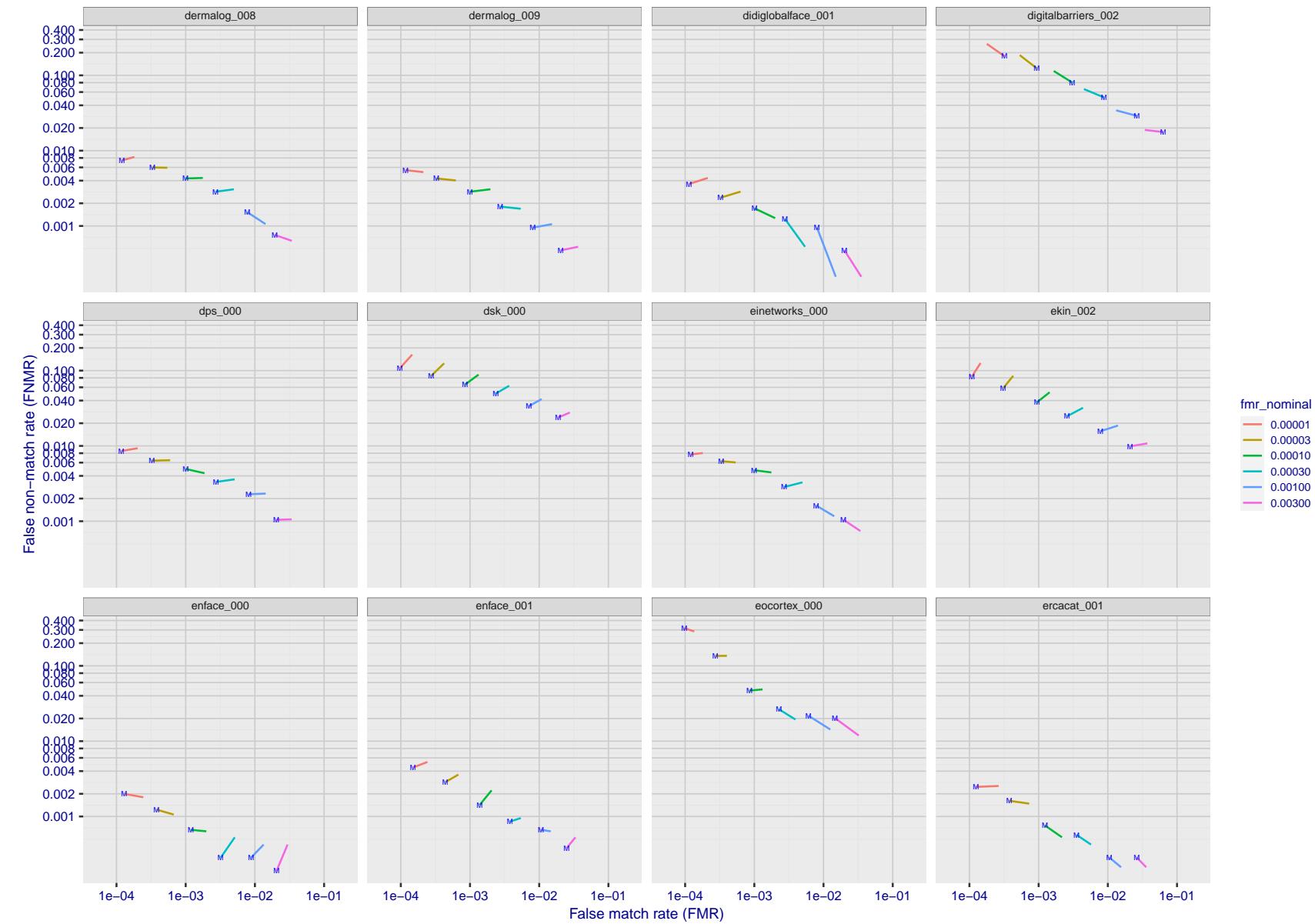


Figure 141: For the visa images, FNMR and FMR at six operating points along the DET characteristic. At each point a line is drawn between  $(FMR, FNMR)_{MALE}$  and  $(FMR, FNMR)_{FEMALE}$  showing how which sex has lower FMR and/or FNMR. The "M" label denotes male, the other end of the line corresponds to female. The six operating thresholds are selected to give the nominal false match rates given in the legend, and are computed over all impostor pairs regardless of age, sex, and place of birth. The plotted FMR values are broadly an order of magnitude larger than the nominal rates because FMR is computed over demographically-matched impostor pairs i.e individuals of the same sex, from the same geographic region (see section 3.6.1), and the same age group (see section 3.6.2).

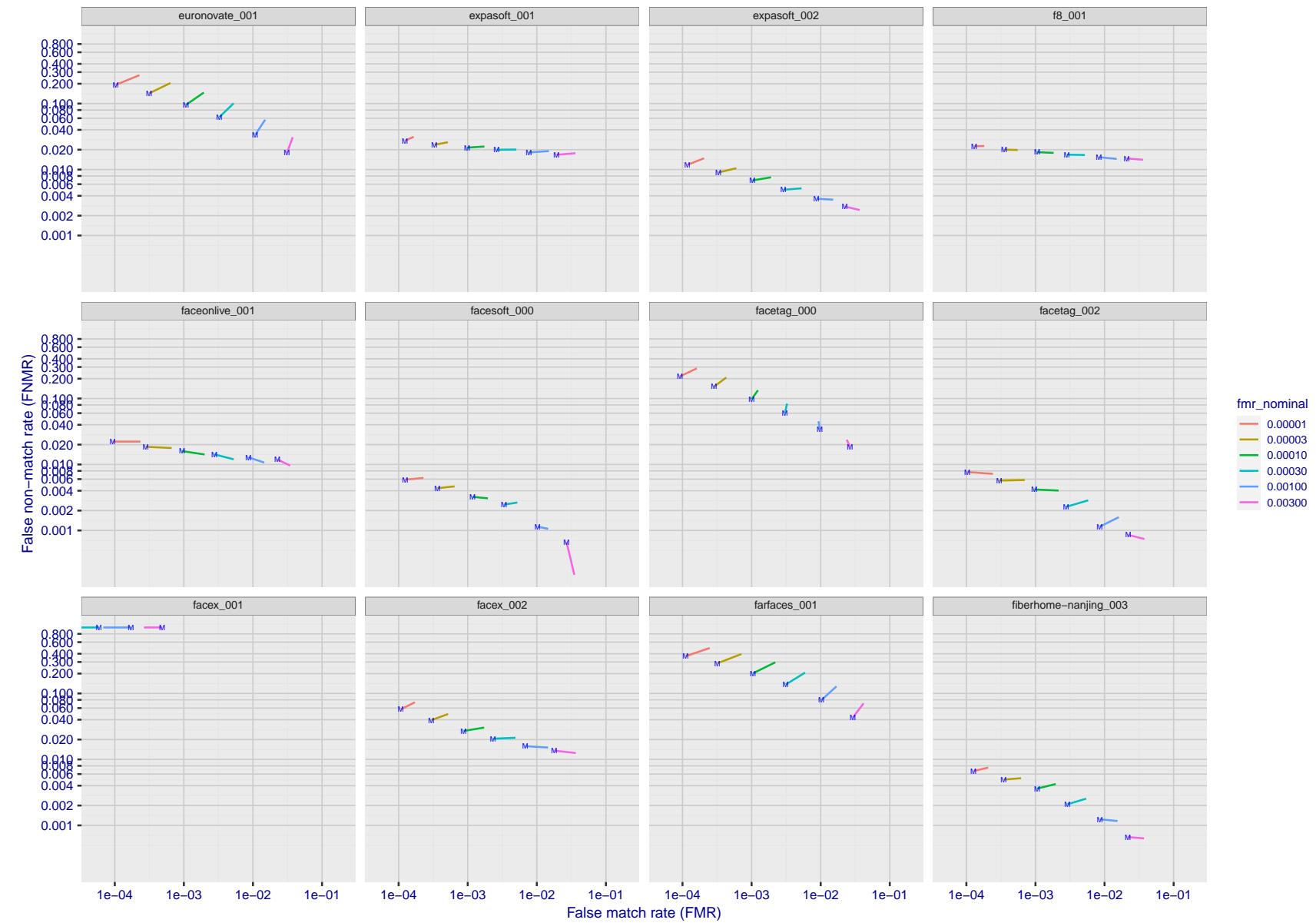


Figure 142: For the visa images, FNMR and FMR at six operating points along the DET characteristic. At each point a line is drawn between  $(FMR, FNMR)_{MALE}$  and  $(FMR, FNMR)_{FEMALE}$  showing how which sex has lower FMR and/or FNMR. The "M" label denotes male, the other end of the line corresponds to female. The six operating thresholds are selected to give the nominal false match rates given in the legend, and are computed over all impostor pairs regardless of age, sex, and place of birth. The plotted FMR values are broadly an order of magnitude larger than the nominal rates because FMR is computed over demographically-matched impostor pairs i.e individuals of the same sex, from the same geographic region (see section 3.6.1), and the same age group (see section 3.6.2).

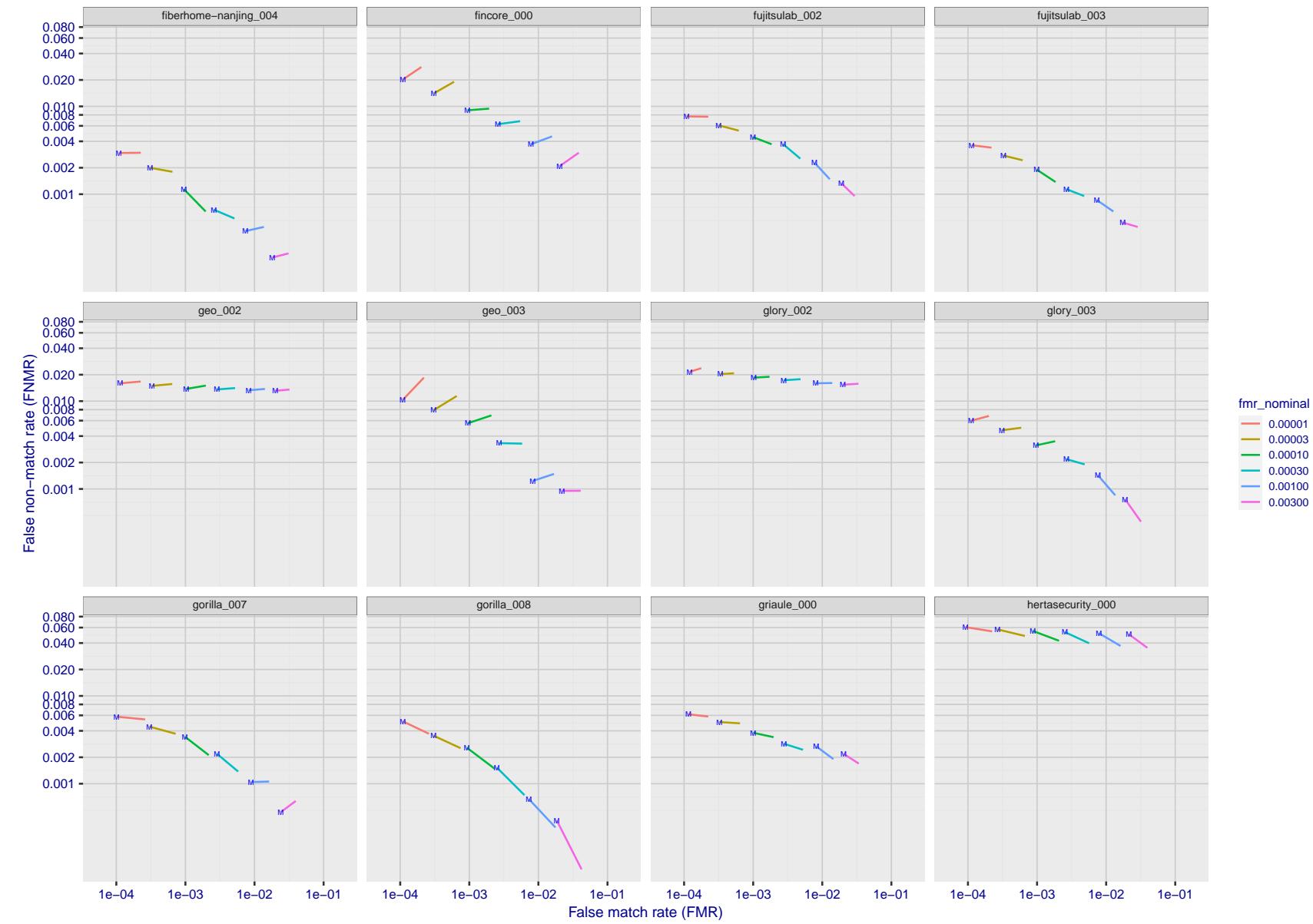


Figure 143: For the visa images, FNMR and FMR at six operating points along the DET characteristic. At each point a line is drawn between  $(FMR, FNMR)_{MALE}$  and  $(FMR, FNMR)_{FEMALE}$  showing how which sex has lower FMR and/or FNMR. The "M" label denotes male, the other end of the line corresponds to female. The six operating thresholds are selected to give the nominal false match rates given in the legend, and are computed over all impostor pairs regardless of age, sex, and place of birth. The plotted FMR values are broadly an order of magnitude larger than the nominal rates because FMR is computed over demographically-matched impostor pairs i.e individuals of the same sex, from the same geographic region (see section 3.6.1), and the same age group (see section 3.6.2).

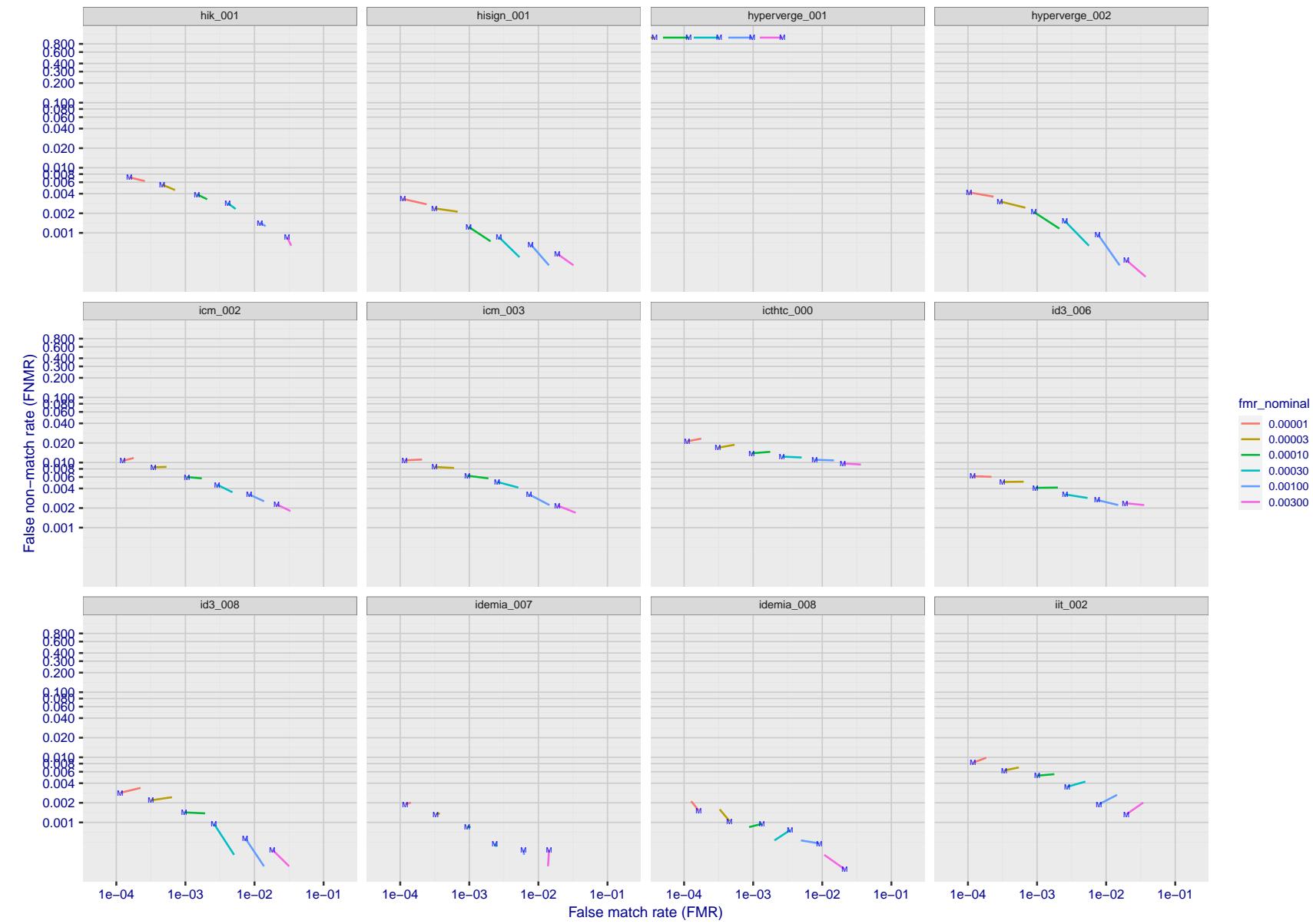


Figure 144: For the visa images, FNMR and FMR at six operating points along the DET characteristic. At each point a line is drawn between  $(FMR, FNMR)_{MALE}$  and  $(FMR, FNMR)_{FEMALE}$  showing how which sex has lower FMR and/or FNMR. The "M" label denotes male, the other end of the line corresponds to female. The six operating thresholds are selected to give the nominal false match rates given in the legend, and are computed over all impostor pairs regardless of age, sex, and place of birth. The plotted FMR values are broadly an order of magnitude larger than the nominal rates because FMR is computed over demographically-matched impostor pairs i.e individuals of the same sex, from the same geographic region (see section 3.6.1), and the same age group (see section 3.6.2).

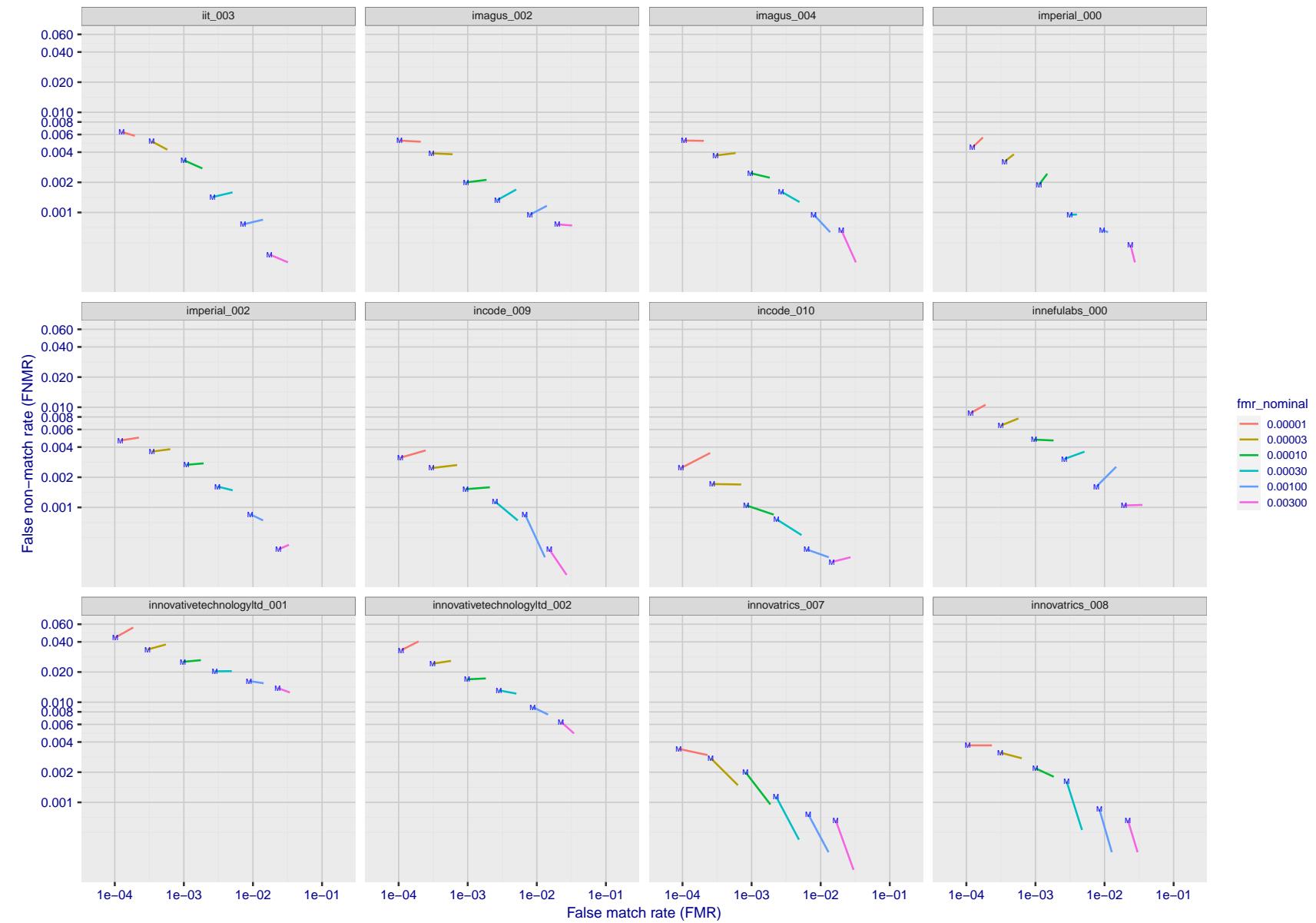


Figure 145: For the visa images, FNMR and FMR at six operating points along the DET characteristic. At each point a line is drawn between  $(FMR, FNMR)_{MALE}$  and  $(FMR, FNMR)_{FEMALE}$  showing how which sex has lower FMR and/or FNMR. The "M" label denotes male, the other end of the line corresponds to female. The six operating thresholds are selected to give the nominal false match rates given in the legend, and are computed over all impostor pairs regardless of age, sex, and place of birth. The plotted FMR values are broadly an order of magnitude larger than the nominal rates because FMR is computed over demographically-matched impostor pairs i.e individuals of the same sex, from the same geographic region (see section 3.6.1), and the same age group (see section 3.6.2).

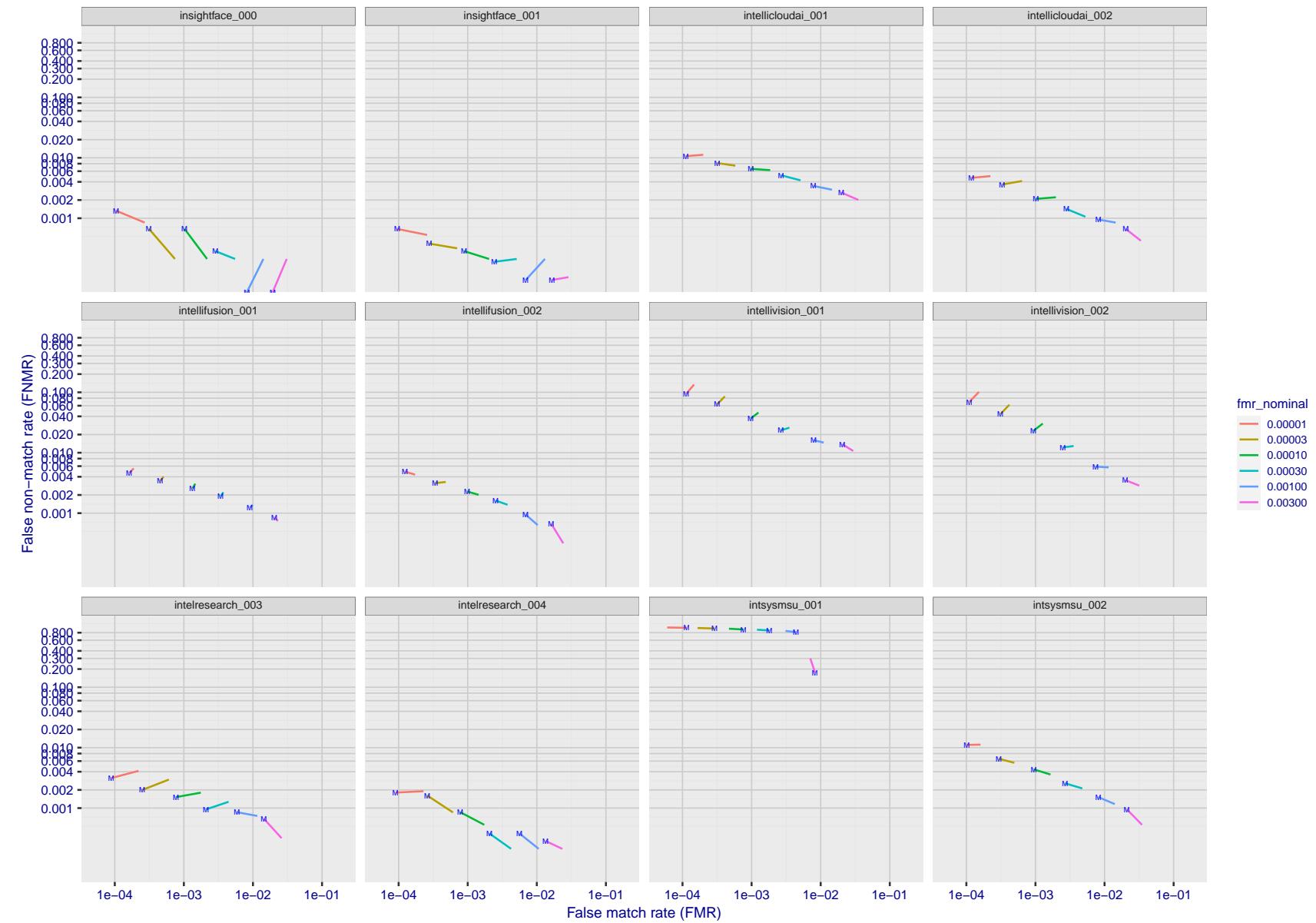


Figure 146: For the visa images, FNMR and FMR at six operating points along the DET characteristic. At each point a line is drawn between  $(FMR, FNMR)_{MALE}$  and  $(FMR, FNMR)_{FEMALE}$  showing how which sex has lower FMR and/or FNMR. The "M" label denotes male, the other end of the line corresponds to female. The six operating thresholds are selected to give the nominal false match rates given in the legend, and are computed over all impostor pairs regardless of age, sex, and place of birth. The plotted FMR values are broadly an order of magnitude larger than the nominal rates because FMR is computed over demographically-matched impostor pairs i.e individuals of the same sex, from the same geographic region (see section 3.6.1), and the same age group (see section 3.6.2).

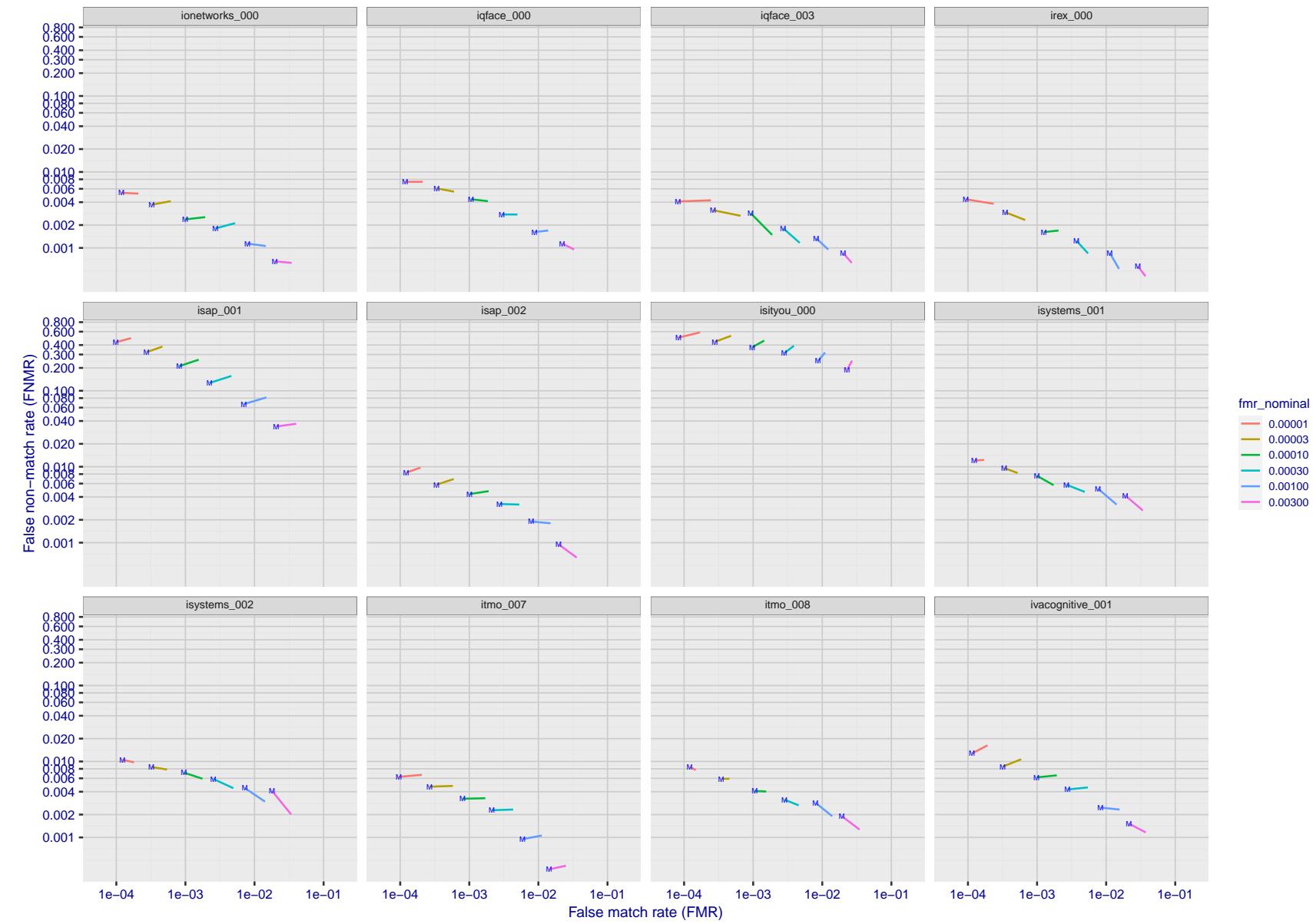


Figure 147: For the visa images, FNMR and FMR at six operating points along the DET characteristic. At each point a line is drawn between  $(FMR, FNMR)_{MALE}$  and  $(FMR, FNMR)_{FEMALE}$  showing how which sex has lower FMR and/or FNMR. The "M" label denotes male, the other end of the line corresponds to female. The six operating thresholds are selected to give the nominal false match rates given in the legend, and are computed over all impostor pairs regardless of age, sex, and place of birth. The plotted FMR values are broadly an order of magnitude larger than the nominal rates because FMR is computed over demographically-matched impostor pairs i.e individuals of the same sex, from the same geographic region (see section 3.6.1), and the same age group (see section 3.6.2).

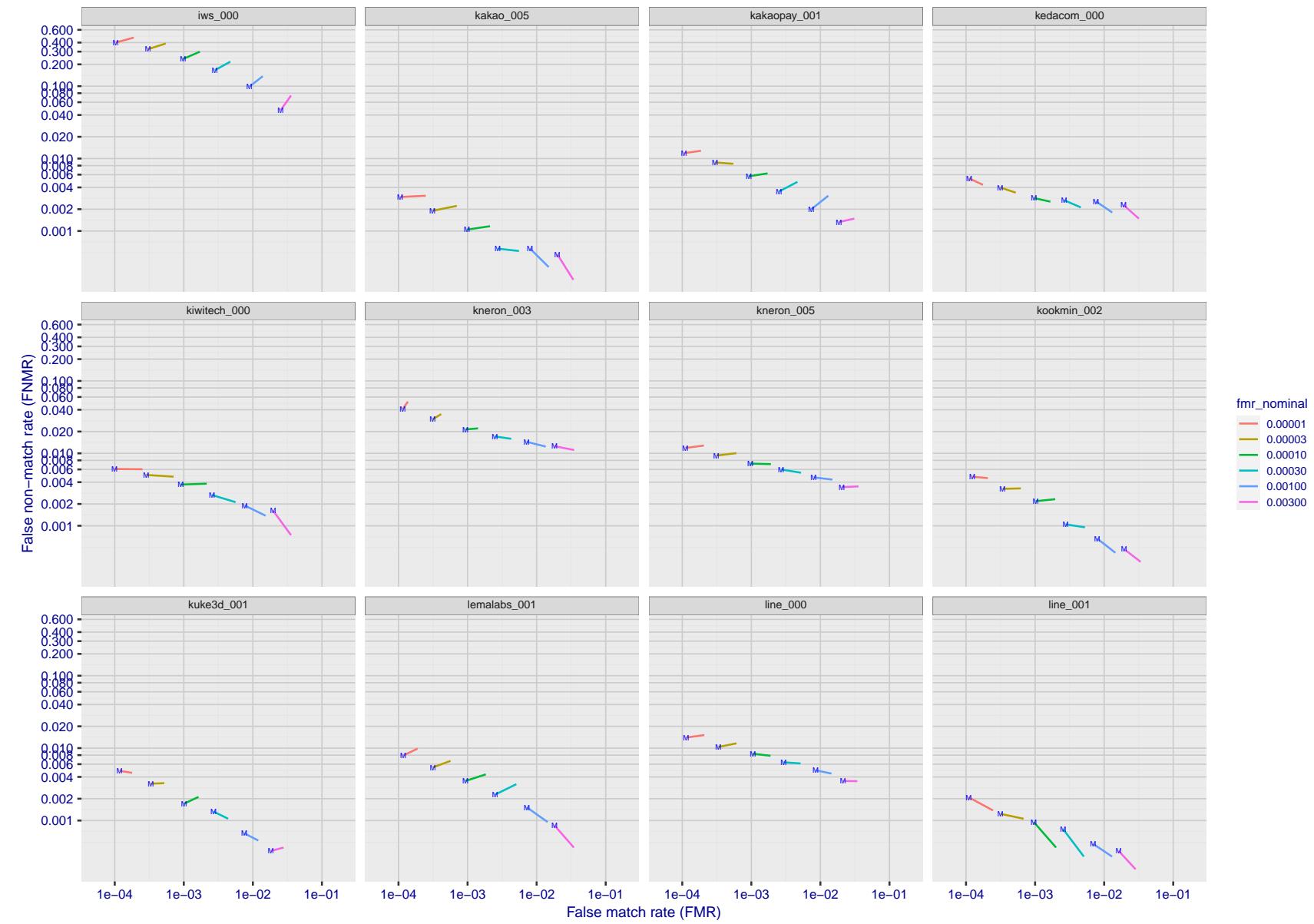


Figure 148: For the visa images, FNMR and FMR at six operating points along the DET characteristic. At each point a line is drawn between  $(FMR, FNMR)_{MALE}$  and  $(FMR, FNMR)_{FEMALE}$  showing how which sex has lower FMR and/or FNMR. The "M" label denotes male, the other end of the line corresponds to female. The six operating thresholds are selected to give the nominal false match rates given in the legend, and are computed over all impostor pairs regardless of age, sex, and place of birth. The plotted FMR values are broadly an order of magnitude larger than the nominal rates because FMR is computed over demographically-matched impostor pairs i.e individuals of the same sex, from the same geographic region (see section 3.6.1), and the same age group (see section 3.6.2).

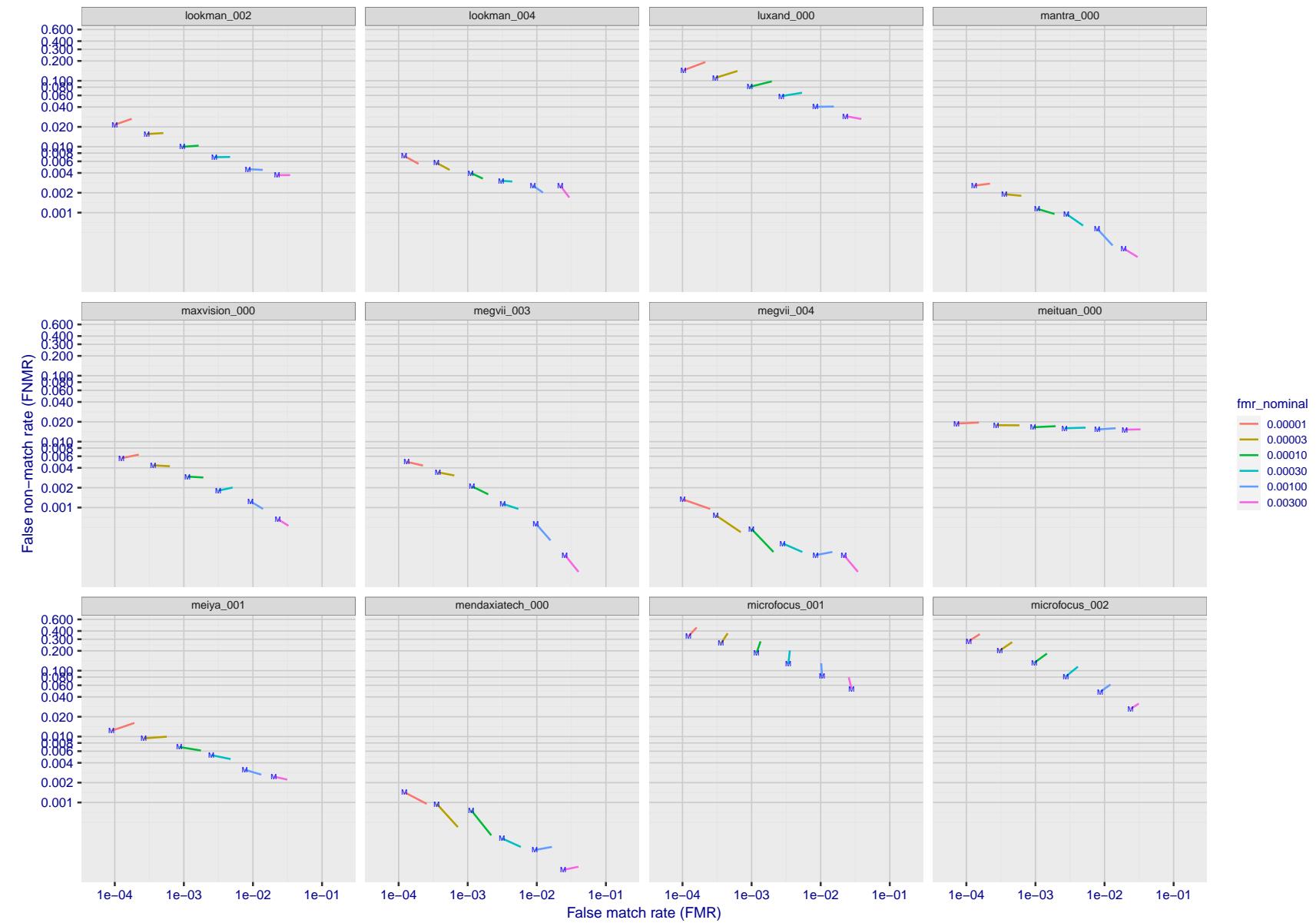


Figure 149: For the visa images, FNMR and FMR at six operating points along the DET characteristic. At each point a line is drawn between  $(FMR, FNMR)_{MALE}$  and  $(FMR, FNMR)_{FEMALE}$  showing how which sex has lower FMR and/or FNMR. The "M" label denotes male, the other end of the line corresponds to female. The six operating thresholds are selected to give the nominal false match rates given in the legend, and are computed over all impostor pairs regardless of age, sex, and place of birth. The plotted FMR values are broadly an order of magnitude larger than the nominal rates because FMR is computed over demographically-matched impostor pairs i.e individuals of the same sex, from the same geographic region (see section 3.6.1), and the same age group (see section 3.6.2).

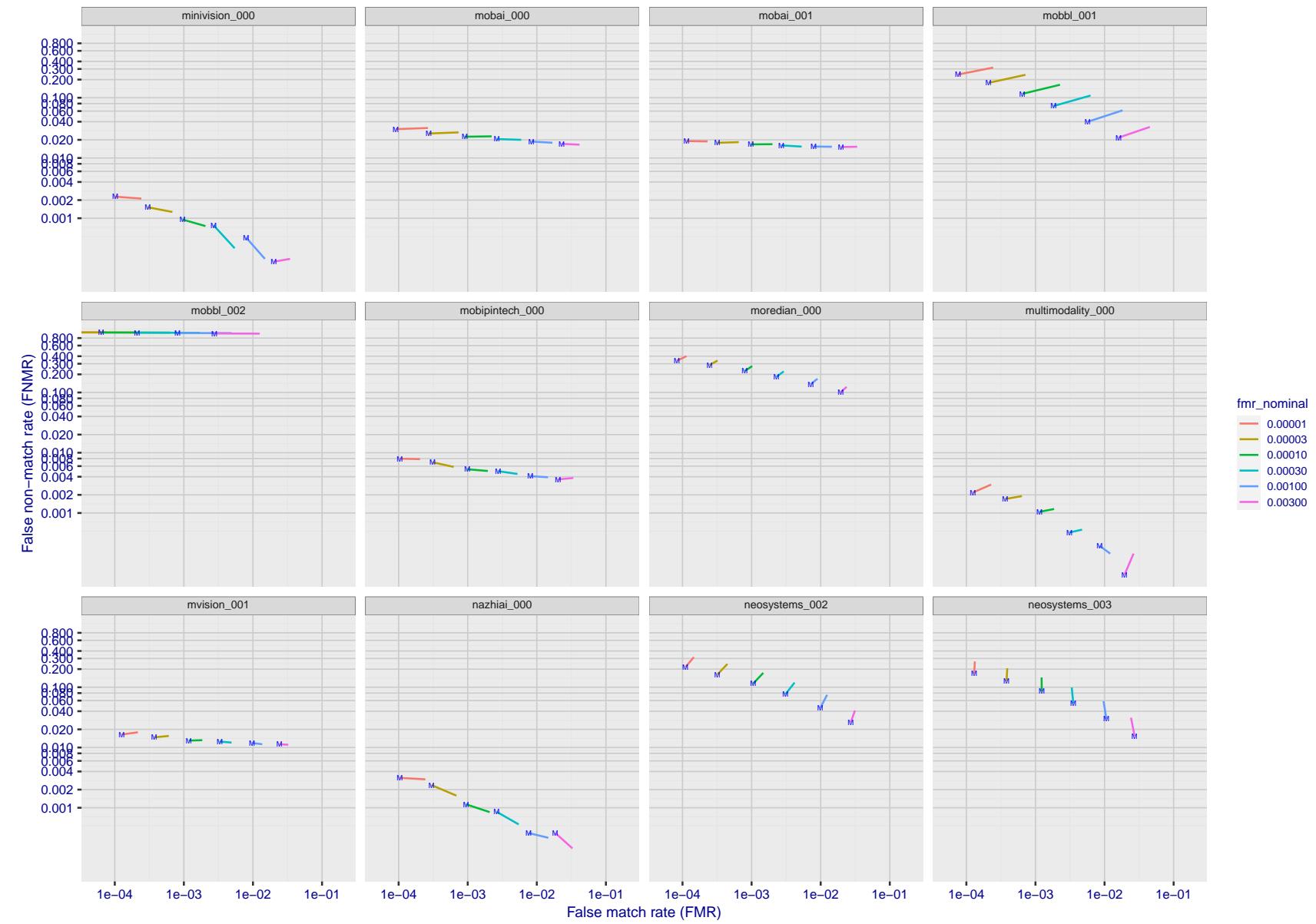


Figure 150: For the visa images, FNMR and FMR at six operating points along the DET characteristic. At each point a line is drawn between  $(FMR, FNMR)_{MALE}$  and  $(FMR, FNMR)_{FEMALE}$  showing how which sex has lower FMR and/or FNMR. The "M" label denotes male, the other end of the line corresponds to female. The six operating thresholds are selected to give the nominal false match rates given in the legend, and are computed over all impostor pairs regardless of age, sex, and place of birth. The plotted FMR values are broadly an order of magnitude larger than the nominal rates because FMR is computed over demographically-matched impostor pairs i.e individuals of the same sex, from the same geographic region (see section 3.6.1), and the same age group (see section 3.6.2).

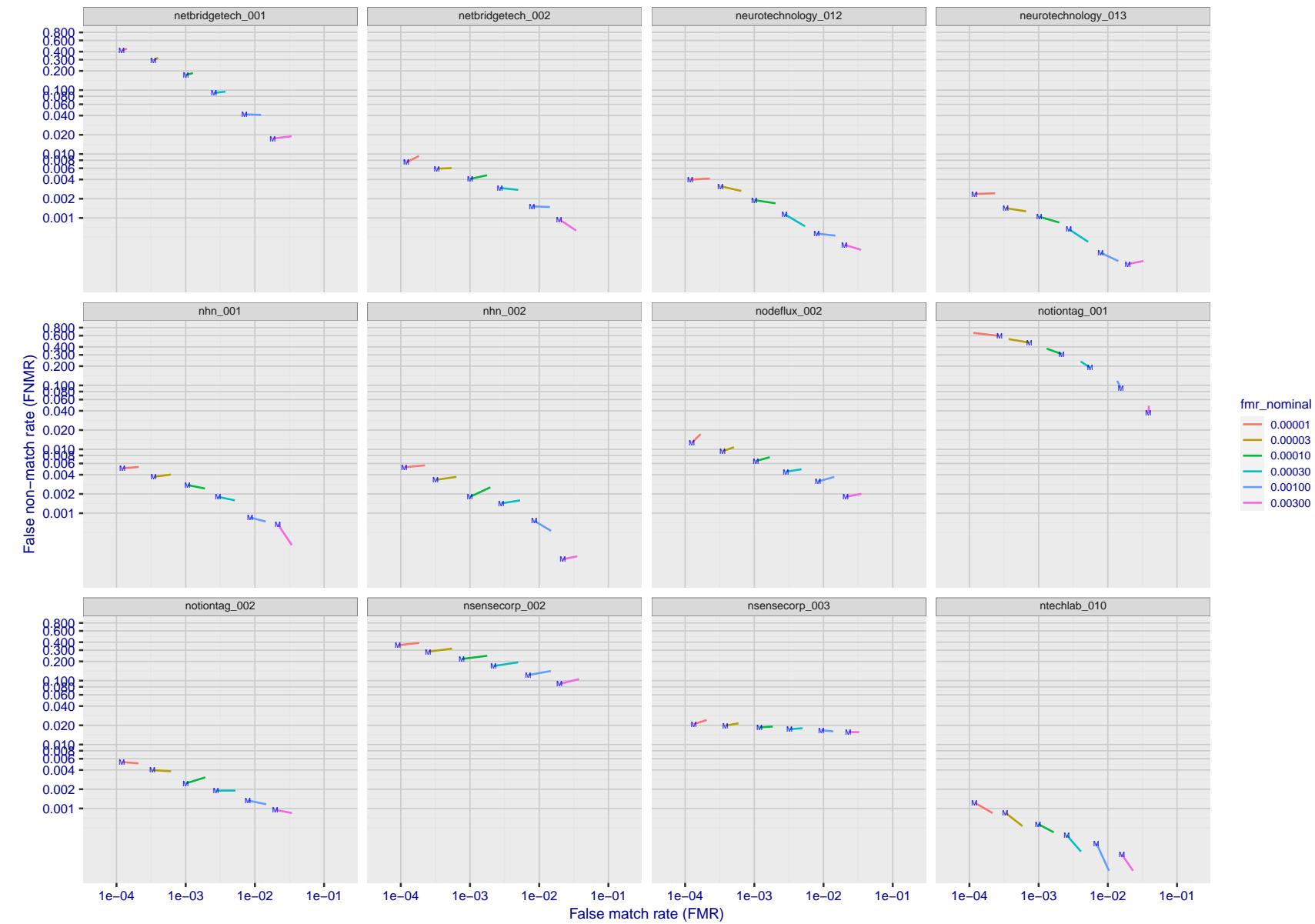


Figure 151: For the visa images, FNMR and FMR at six operating points along the DET characteristic. At each point a line is drawn between  $(FMR, FNMR)_{MALE}$  and  $(FMR, FNMR)_{FEMALE}$  showing how which sex has lower FMR and/or FNMR. The "M" label denotes male, the other end of the line corresponds to female. The six operating thresholds are selected to give the nominal false match rates given in the legend, and are computed over all impostor pairs regardless of age, sex, and place of birth. The plotted FMR values are broadly an order of magnitude larger than the nominal rates because FMR is computed over demographically-matched impostor pairs i.e individuals of the same sex, from the same geographic region (see section 3.6.1), and the same age group (see section 3.6.2).

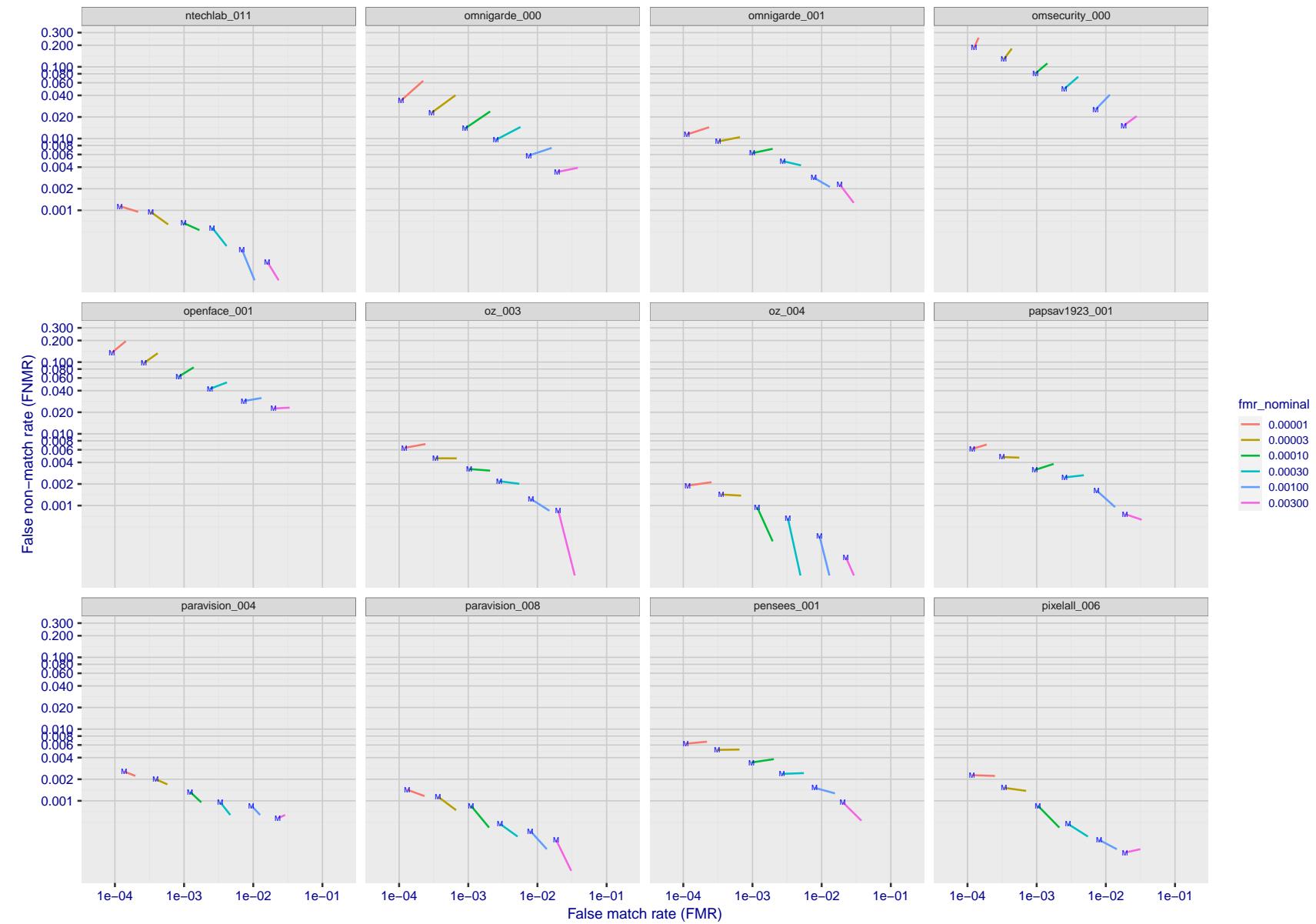


Figure 152: For the visa images, FNMR and FMR at six operating points along the DET characteristic. At each point a line is drawn between  $(FMR, FNMR)_{MALE}$  and  $(FMR, FNMR)_{FEMALE}$  showing how which sex has lower FMR and/or FNMR. The "M" label denotes male, the other end of the line corresponds to female. The six operating thresholds are selected to give the nominal false match rates given in the legend, and are computed over all impostor pairs regardless of age, sex, and place of birth. The plotted FMR values are broadly an order of magnitude larger than the nominal rates because FMR is computed over demographically-matched impostor pairs i.e individuals of the same sex, from the same geographic region (see section 3.6.1), and the same age group (see section 3.6.2).

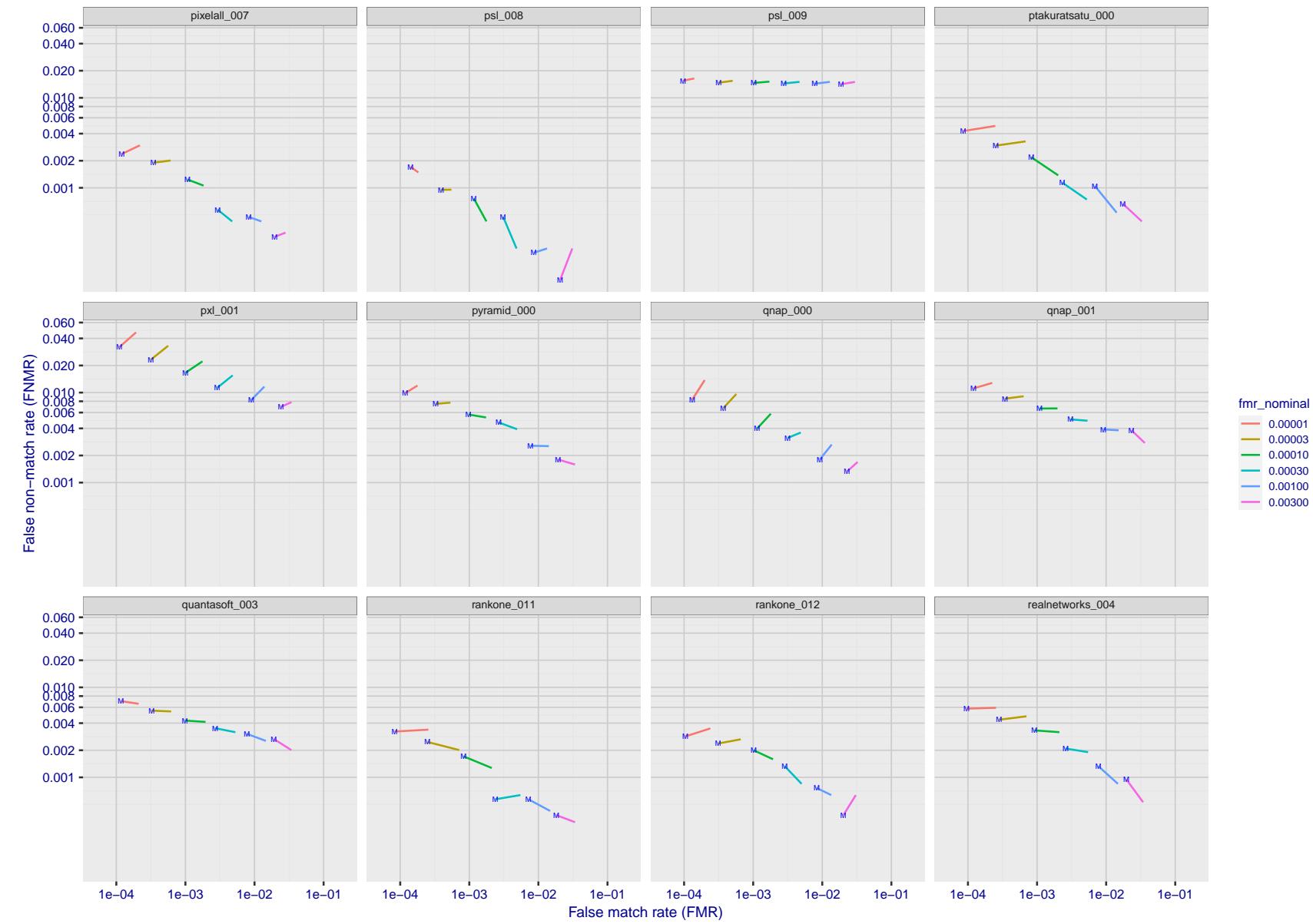


Figure 153: For the visa images, FNMR and FMR at six operating points along the DET characteristic. At each point a line is drawn between  $(FMR, FNMR)_{MALE}$  and  $(FMR, FNMR)_{FEMALE}$  showing how which sex has lower FMR and/or FNMR. The "M" label denotes male, the other end of the line corresponds to female. The six operating thresholds are selected to give the nominal false match rates given in the legend, and are computed over all impostor pairs regardless of age, sex, and place of birth. The plotted FMR values are broadly an order of magnitude larger than the nominal rates because FMR is computed over demographically-matched impostor pairs i.e individuals of the same sex, from the same geographic region (see section 3.6.1), and the same age group (see section 3.6.2).

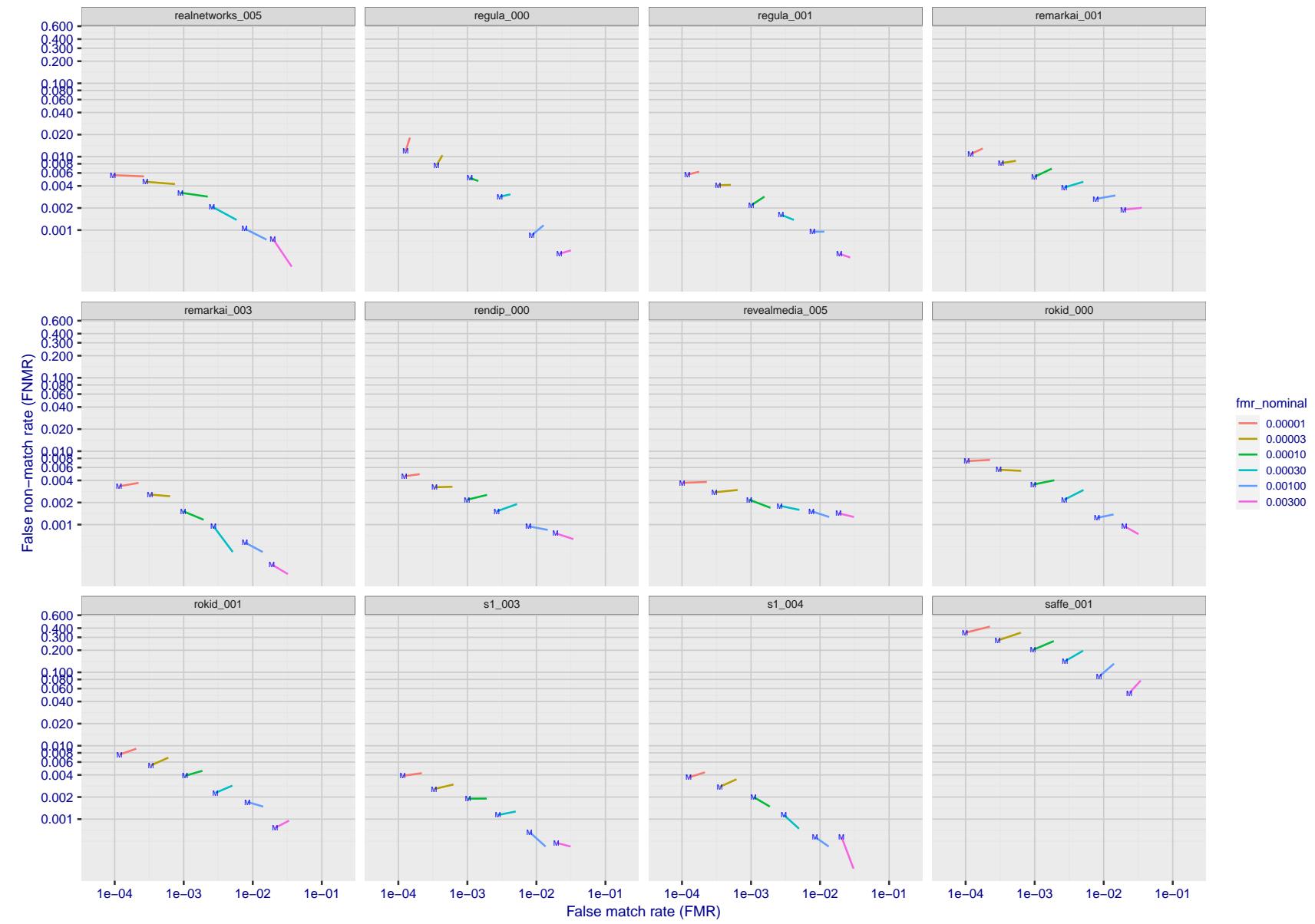


Figure 154: For the visa images, FNMR and FMR at six operating points along the DET characteristic. At each point a line is drawn between  $(FMR, FNMR)_{MALE}$  and  $(FMR, FNMR)_{FEMALE}$  showing how which sex has lower FMR and/or FNMR. The "M" label denotes male, the other end of the line corresponds to female. The six operating thresholds are selected to give the nominal false match rates given in the legend, and are computed over all impostor pairs regardless of age, sex, and place of birth. The plotted FMR values are broadly an order of magnitude larger than the nominal rates because FMR is computed over demographically-matched impostor pairs i.e individuals of the same sex, from the same geographic region (see section 3.6.1), and the same age group (see section 3.6.2).

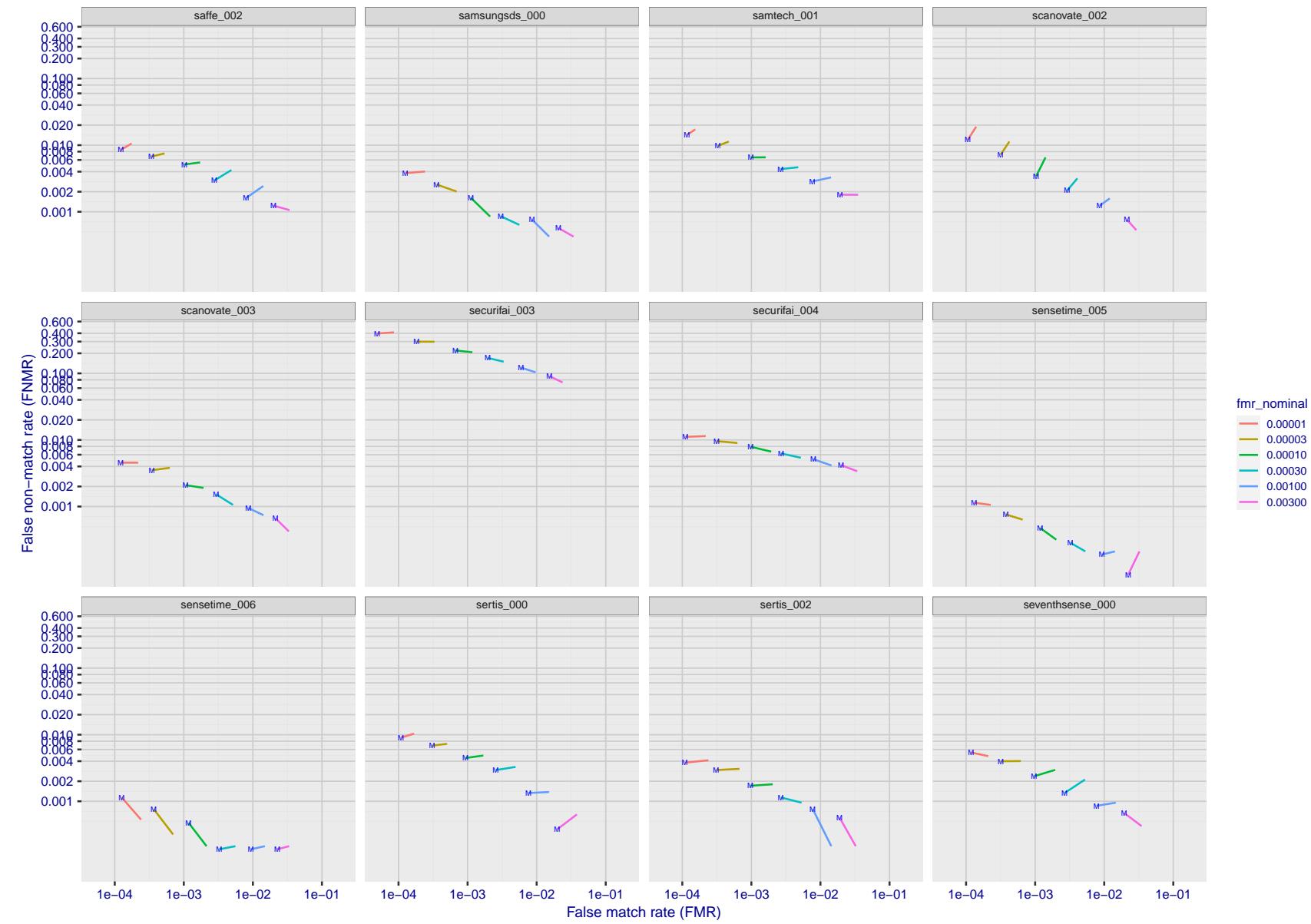


Figure 155: For the visa images, FNMR and FMR at six operating points along the DET characteristic. At each point a line is drawn between  $(FMR, FNMR)_{MALE}$  and  $(FMR, FNMR)_{FEMALE}$  showing how which sex has lower FMR and/or FNMR. The "M" label denotes male, the other end of the line corresponds to female. The six operating thresholds are selected to give the nominal false match rates given in the legend, and are computed over all impostor pairs regardless of age, sex, and place of birth. The plotted FMR values are broadly an order of magnitude larger than the nominal rates because FMR is computed over demographically-matched impostor pairs i.e individuals of the same sex, from the same geographic region (see section 3.6.1), and the same age group (see section 3.6.2).

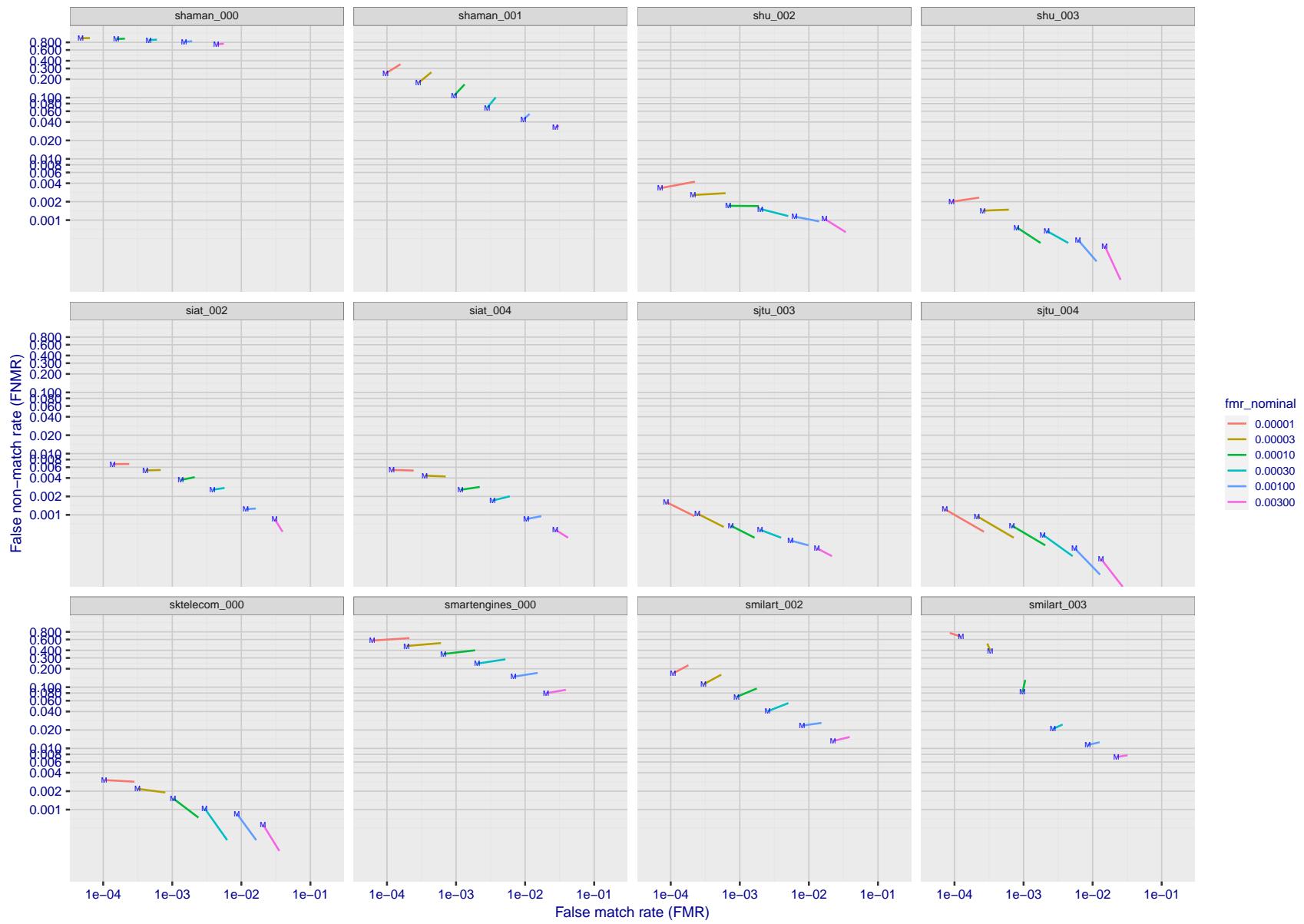


Figure 156: For the visa images, FNMR and FMR at six operating points along the DET characteristic. At each point a line is drawn between  $(FMR, FNMR)_{MALE}$  and  $(FMR, FNMR)_{FEMALE}$  showing how which sex has lower FMR and/or FNMR. The "M" label denotes male, the other end of the line corresponds to female. The six operating thresholds are selected to give the nominal false match rates given in the legend, and are computed over all impostor pairs regardless of age, sex, and place of birth. The plotted FMR values are broadly an order of magnitude larger than the nominal rates because FMR is computed over demographically-matched impostor pairs i.e individuals of the same sex, from the same geographic region (see section 3.6.1), and the same age group (see section 3.6.2).

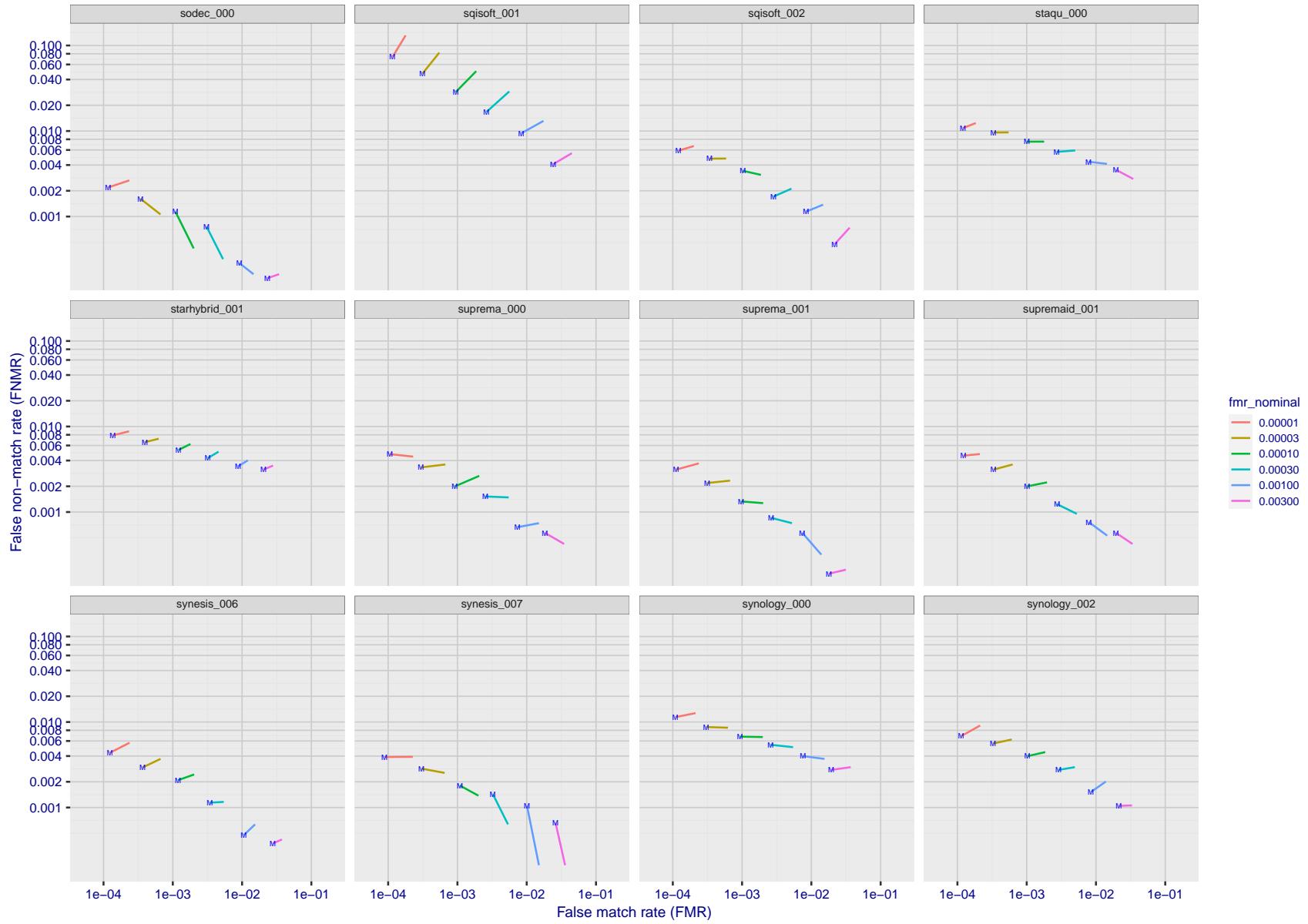


Figure 157: For the visa images, FNMR and FMR at six operating points along the DET characteristic. At each point a line is drawn between  $(FMR, FNMR)_{MALE}$  and  $(FMR, FNMR)_{FEMALE}$  showing how which sex has lower FMR and/or FNMR. The "M" label denotes male, the other end of the line corresponds to female. The six operating thresholds are selected to give the nominal false match rates given in the legend, and are computed over all impostor pairs regardless of age, sex, and place of birth. The plotted FMR values are broadly an order of magnitude larger than the nominal rates because FMR is computed over demographically-matched impostor pairs i.e individuals of the same sex, from the same geographic region (see section 3.6.1), and the same age group (see section 3.6.2).

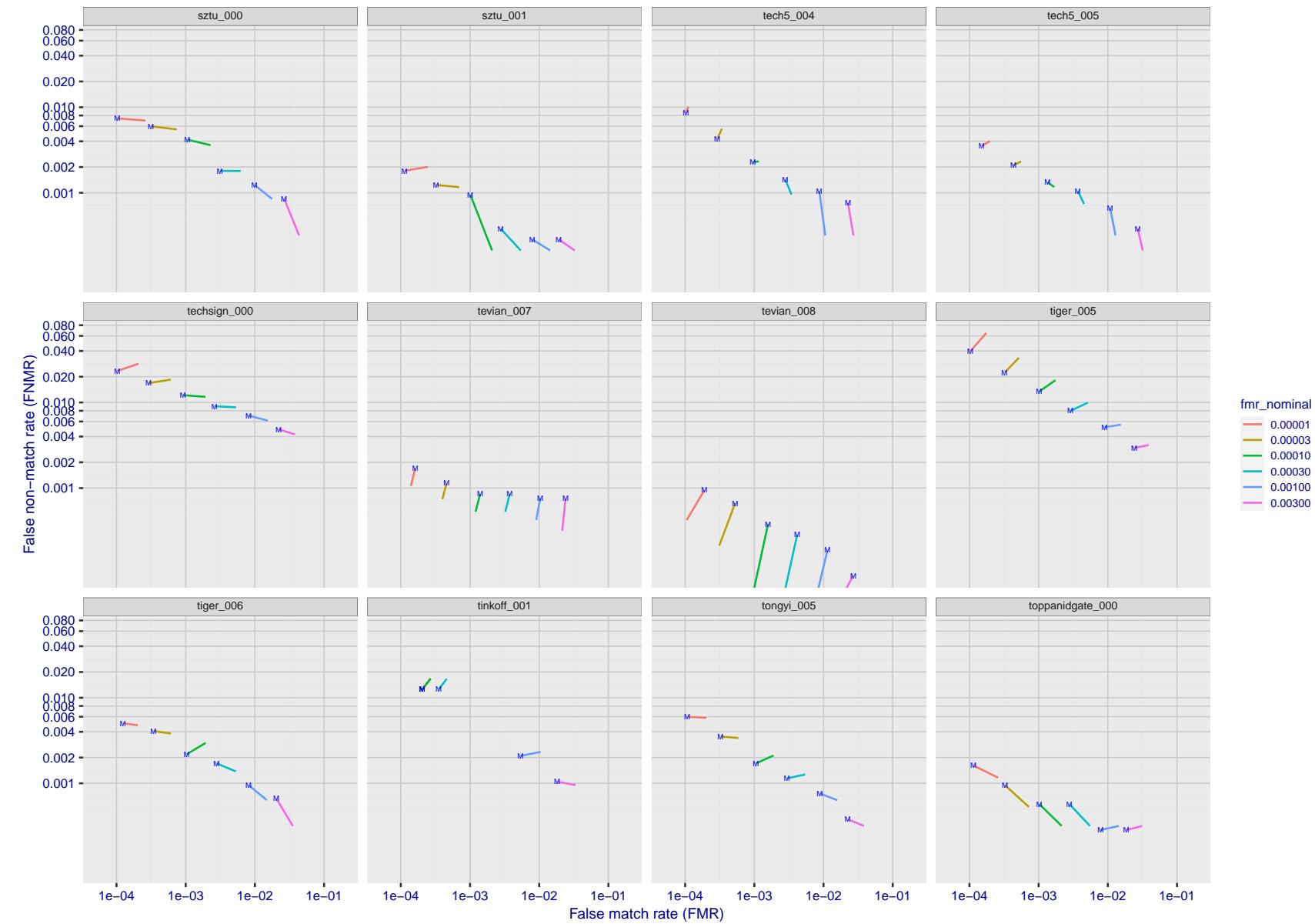


Figure 158: For the visa images, FNMR and FMR at six operating points along the DET characteristic. At each point a line is drawn between  $(FMR, FNMR)_{MALE}$  and  $(FMR, FNMR)_{FEMALE}$  showing how which sex has lower FMR and/or FNMR. The "M" label denotes male, the other end of the line corresponds to female. The six operating thresholds are selected to give the nominal false match rates given in the legend, and are computed over all impostor pairs regardless of age, sex, and place of birth. The plotted FMR values are broadly an order of magnitude larger than the nominal rates because FMR is computed over demographically-matched impostor pairs i.e individuals of the same sex, from the same geographic region (see section 3.6.1), and the same age group (see section 3.6.2).

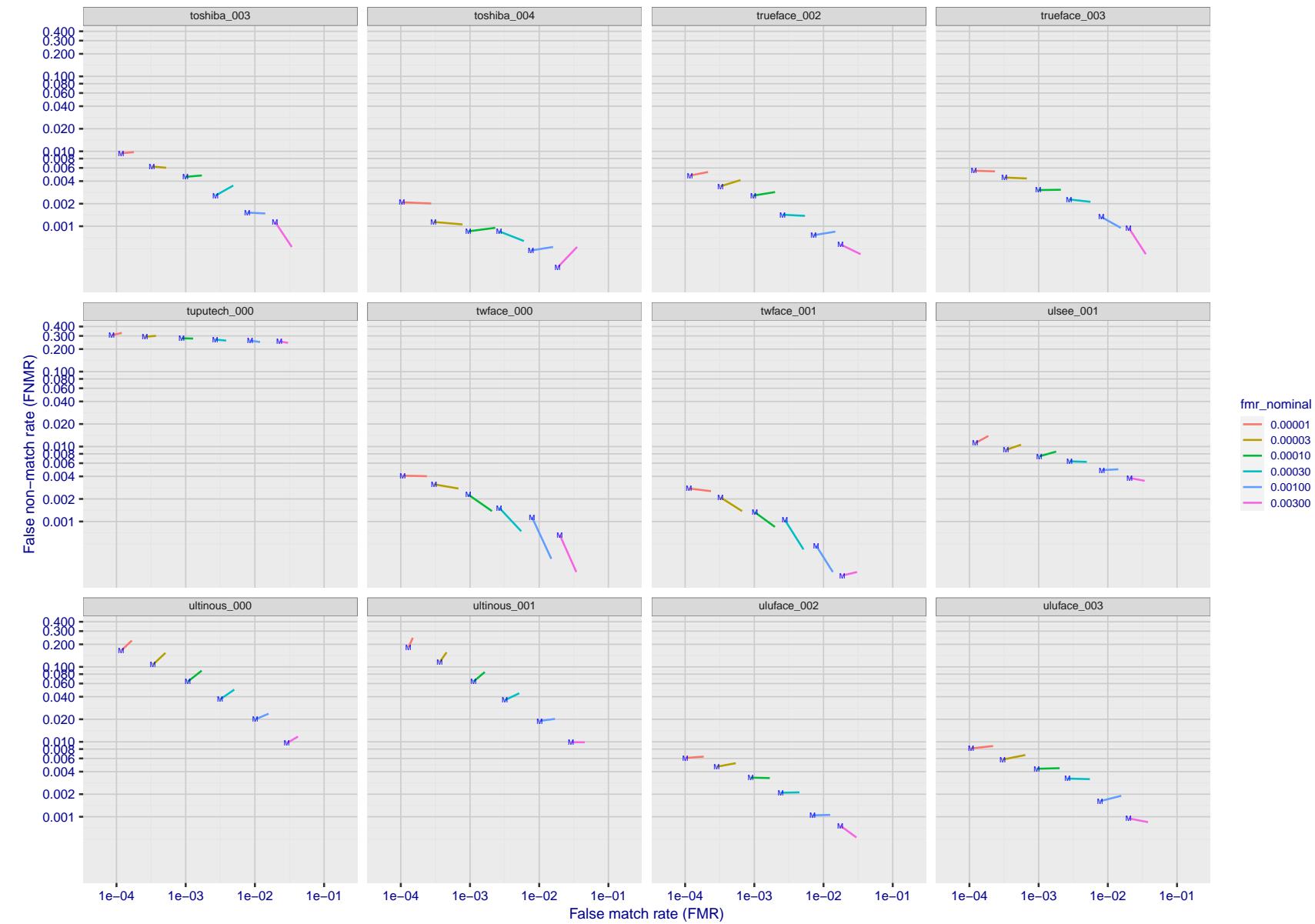


Figure 159: For the visa images, FNMR and FMR at six operating points along the DET characteristic. At each point a line is drawn between  $(FMR, FNMR)_{MALE}$  and  $(FMR, FNMR)_{FEMALE}$  showing how which sex has lower FMR and/or FNMR. The "M" label denotes male, the other end of the line corresponds to female. The six operating thresholds are selected to give the nominal false match rates given in the legend, and are computed over all impostor pairs regardless of age, sex, and place of birth. The plotted FMR values are broadly an order of magnitude larger than the nominal rates because FMR is computed over demographically-matched impostor pairs i.e individuals of the same sex, from the same geographic region (see section 3.6.1), and the same age group (see section 3.6.2).

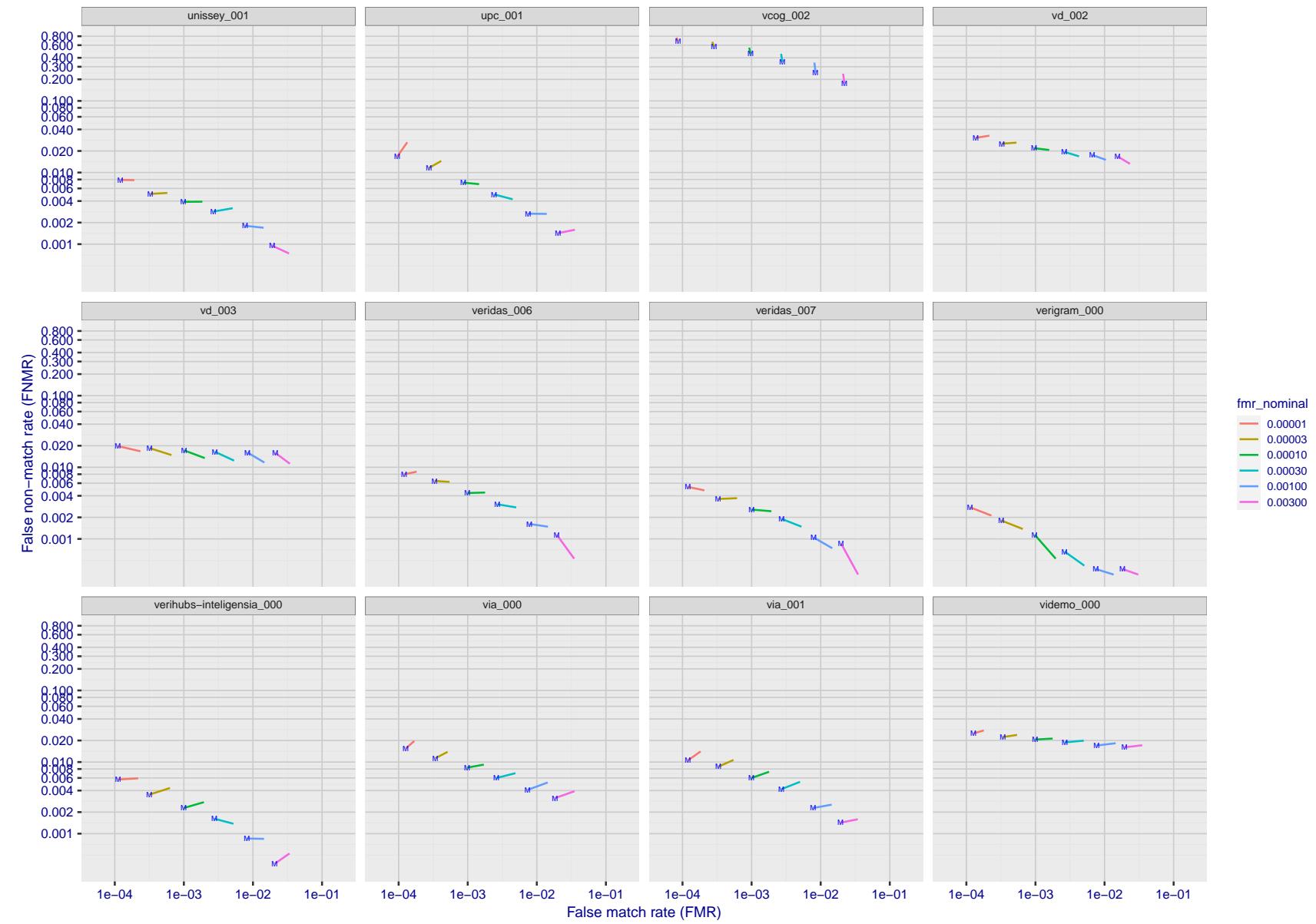


Figure 160: For the visa images, FNMR and FMR at six operating points along the DET characteristic. At each point a line is drawn between  $(FMR, FNMR)_{MALE}$  and  $(FMR, FNMR)_{FEMALE}$  showing how which sex has lower FMR and/or FNMR. The "M" label denotes male, the other end of the line corresponds to female. The six operating thresholds are selected to give the nominal false match rates given in the legend, and are computed over all impostor pairs regardless of age, sex, and place of birth. The plotted FMR values are broadly an order of magnitude larger than the nominal rates because FMR is computed over demographically-matched impostor pairs i.e individuals of the same sex, from the same geographic region (see section 3.6.1), and the same age group (see section 3.6.2).

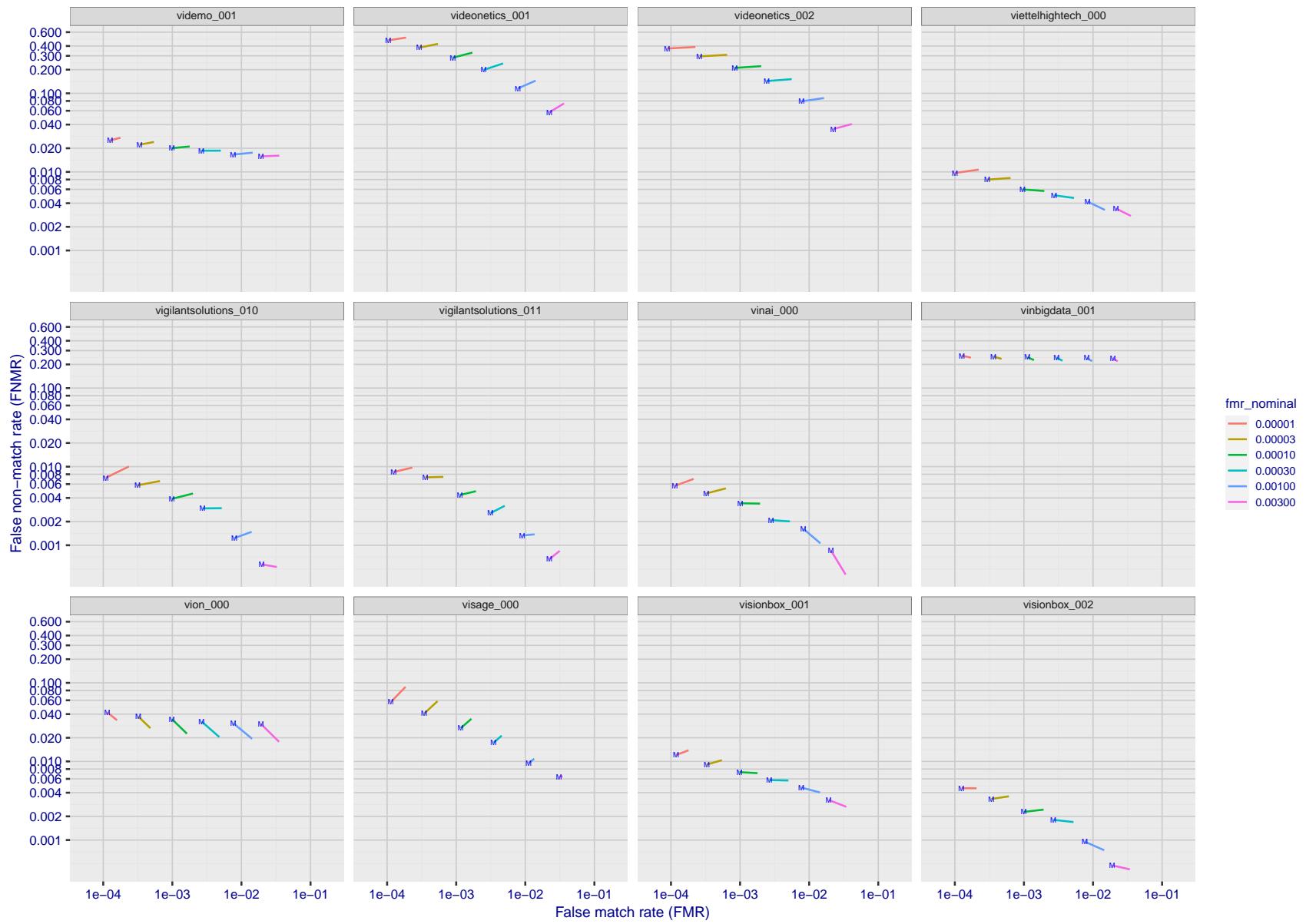


Figure 161: For the visa images, FNMR and FMR at six operating points along the DET characteristic. At each point a line is drawn between  $(FMR, FNMR)_{MALE}$  and  $(FMR, FNMR)_{FEMALE}$  showing how which sex has lower FMR and/or FNMR. The "M" label denotes male, the other end of the line corresponds to female. The six operating thresholds are selected to give the nominal false match rates given in the legend, and are computed over all impostor pairs regardless of age, sex, and place of birth. The plotted FMR values are broadly an order of magnitude larger than the nominal rates because FMR is computed over demographically-matched impostor pairs i.e individuals of the same sex, from the same geographic region (see section 3.6.1), and the same age group (see section 3.6.2).

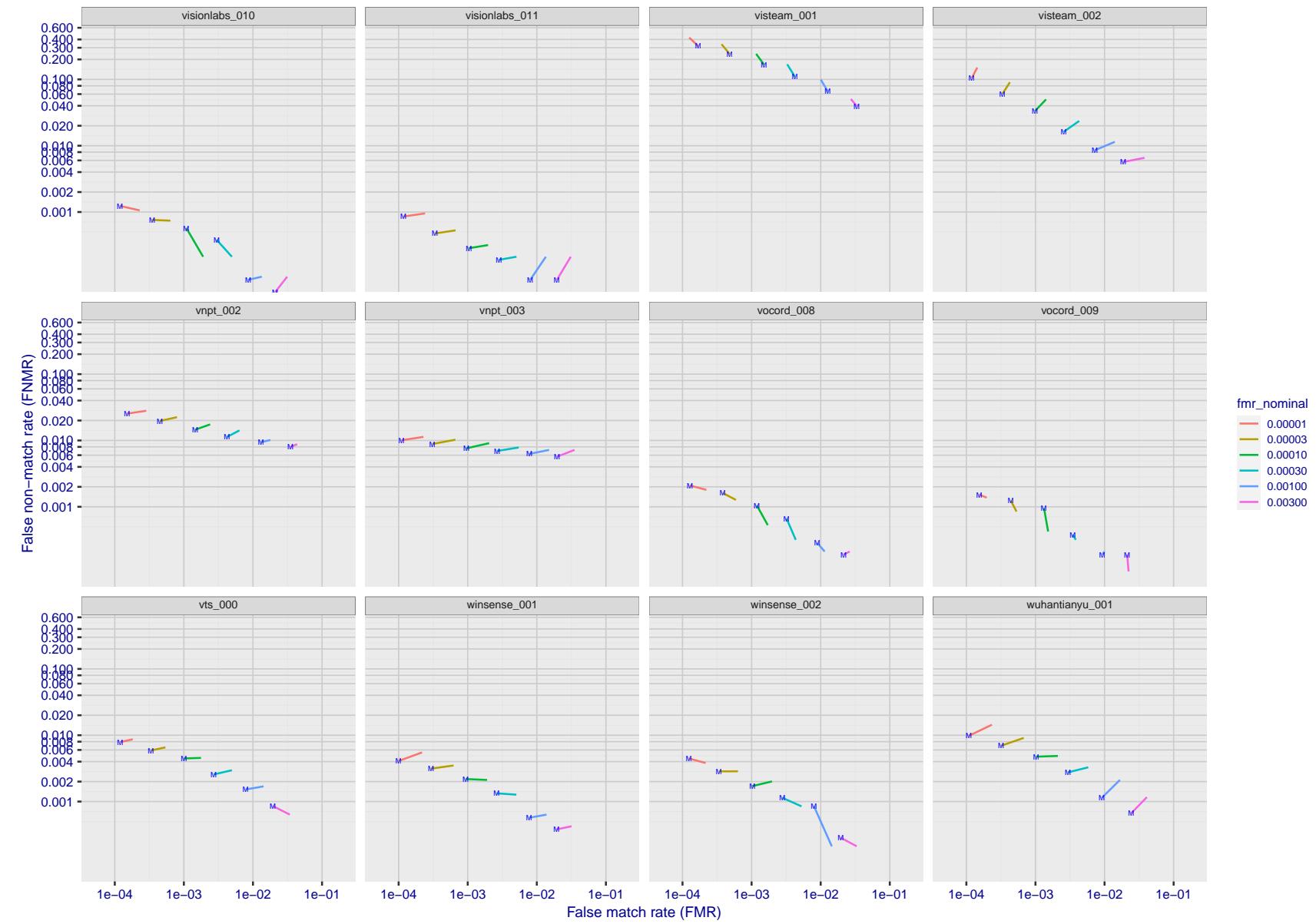


Figure 162: For the visa images, FNMR and FMR at six operating points along the DET characteristic. At each point a line is drawn between  $(FMR, FNMR)_{MALE}$  and  $(FMR, FNMR)_{FEMALE}$  showing how which sex has lower FMR and/or FNMR. The "M" label denotes male, the other end of the line corresponds to female. The six operating thresholds are selected to give the nominal false match rates given in the legend, and are computed over all impostor pairs regardless of age, sex, and place of birth. The plotted FMR values are broadly an order of magnitude larger than the nominal rates because FMR is computed over demographically-matched impostor pairs i.e individuals of the same sex, from the same geographic region (see section 3.6.1), and the same age group (see section 3.6.2).

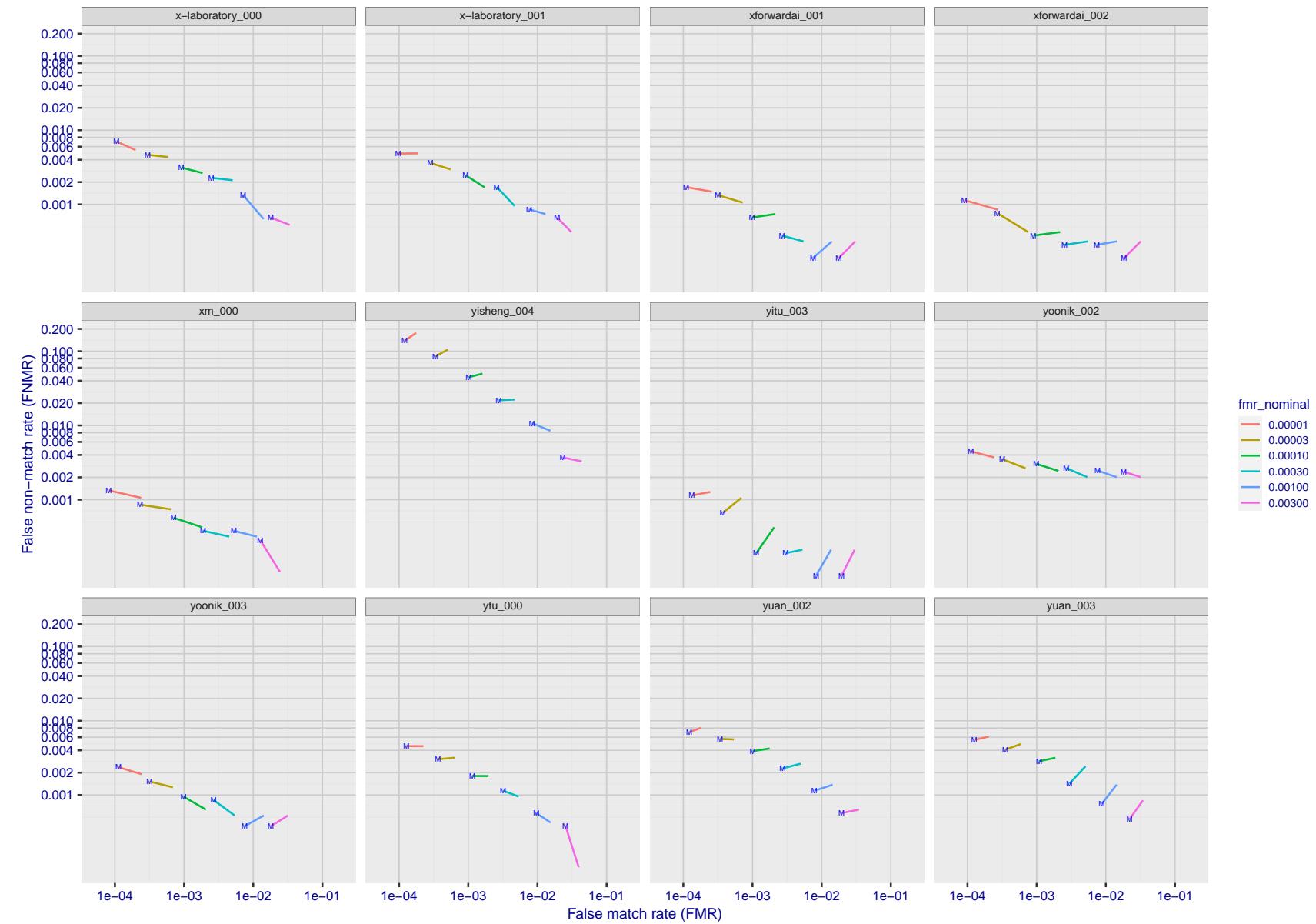


Figure 163: For the visa images, FNMR and FMR at six operating points along the DET characteristic. At each point a line is drawn between  $(FMR, FNMR)_{MALE}$  and  $(FMR, FNMR)_{FEMALE}$  showing how which sex has lower FMR and/or FNMR. The "M" label denotes male, the other end of the line corresponds to female. The six operating thresholds are selected to give the nominal false match rates given in the legend, and are computed over all impostor pairs regardless of age, sex, and place of birth. The plotted FMR values are broadly an order of magnitude larger than the nominal rates because FMR is computed over demographically-matched impostor pairs i.e individuals of the same sex, from the same geographic region (see section 3.6.1), and the same age group (see section 3.6.2).

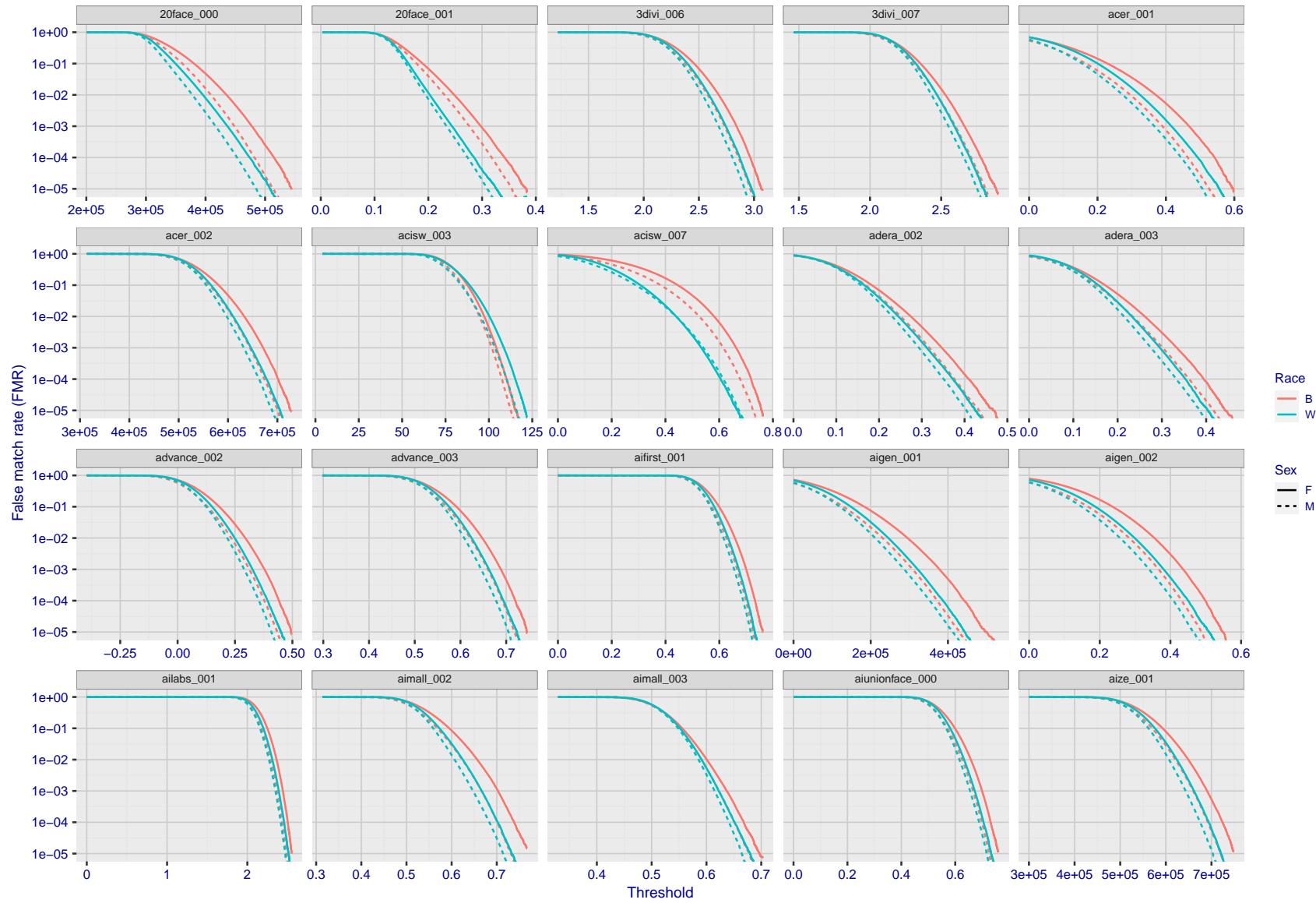


Figure 164: For the mugshot images, the false match calibration curves show false match rate vs. threshold. Separate curves appear for white females, black females, black males and white males.

2022/01/20 13:13:43

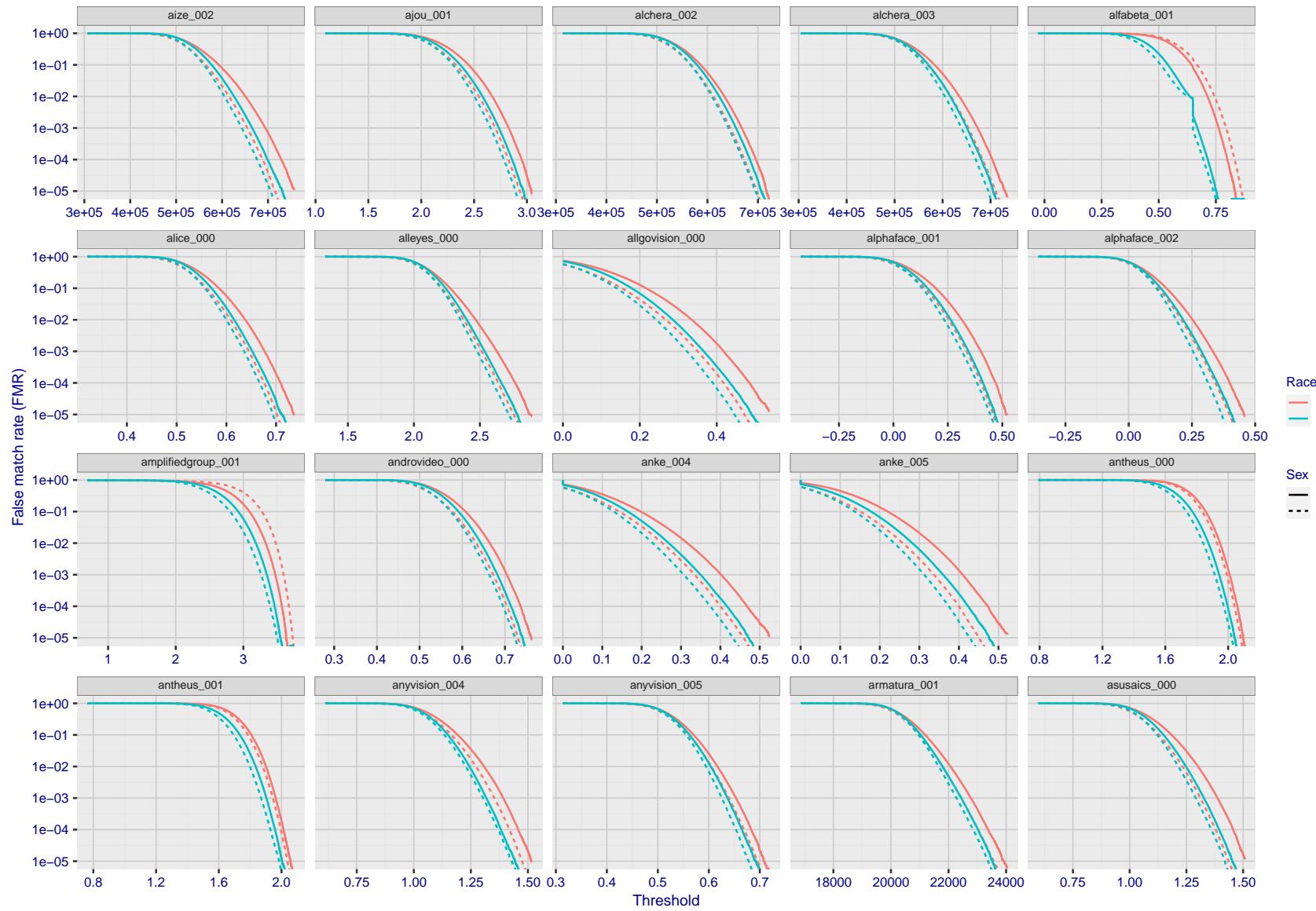


Figure 165: For the mugshot images, the false match calibration curves show false match rate vs. threshold. Separate curves appear for white females, black females, black males and white males.

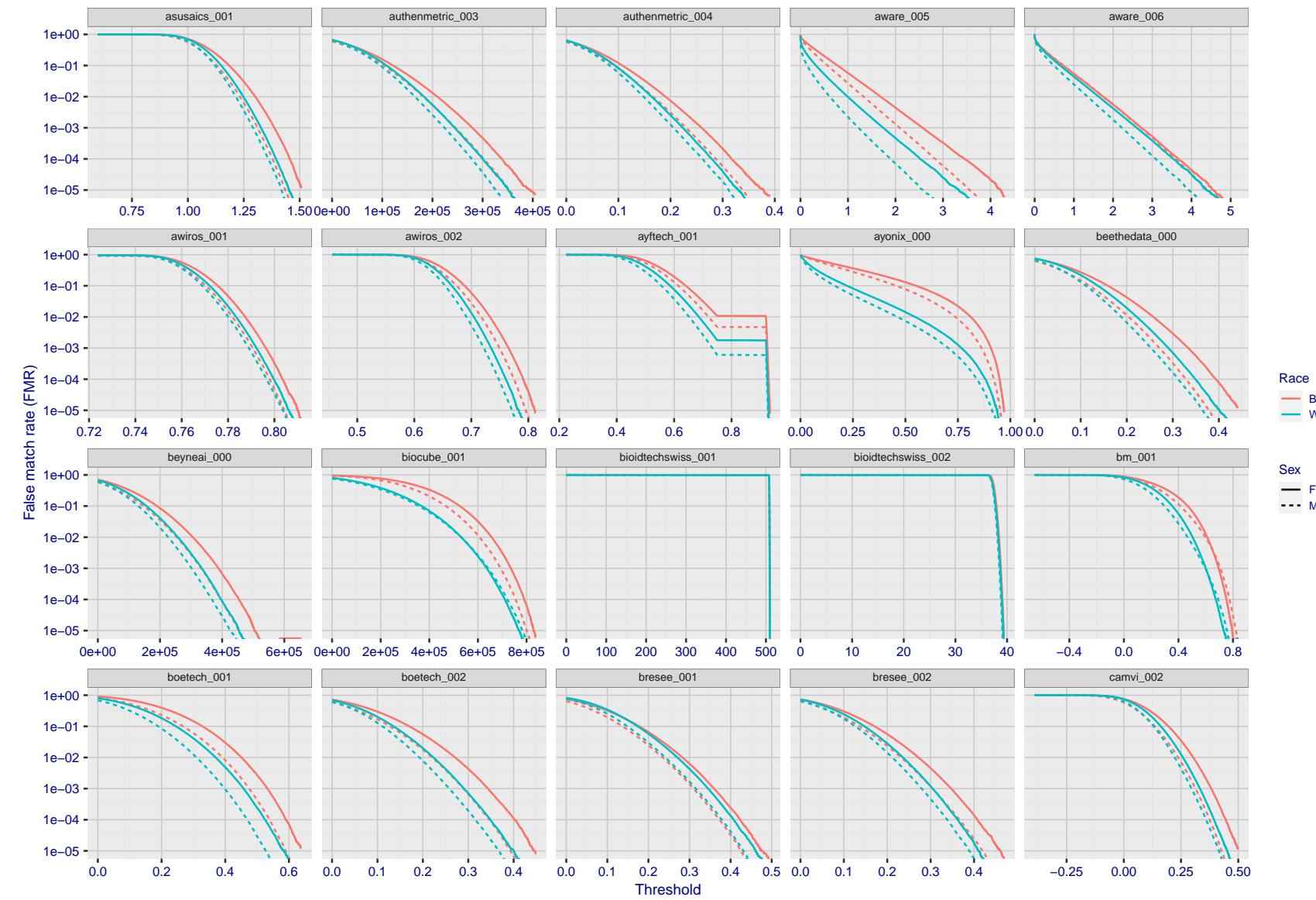


Figure 166: For the mugshot images, the false match calibration curves show false match rate vs. threshold. Separate curves appear for white females, black females, black males and white males.

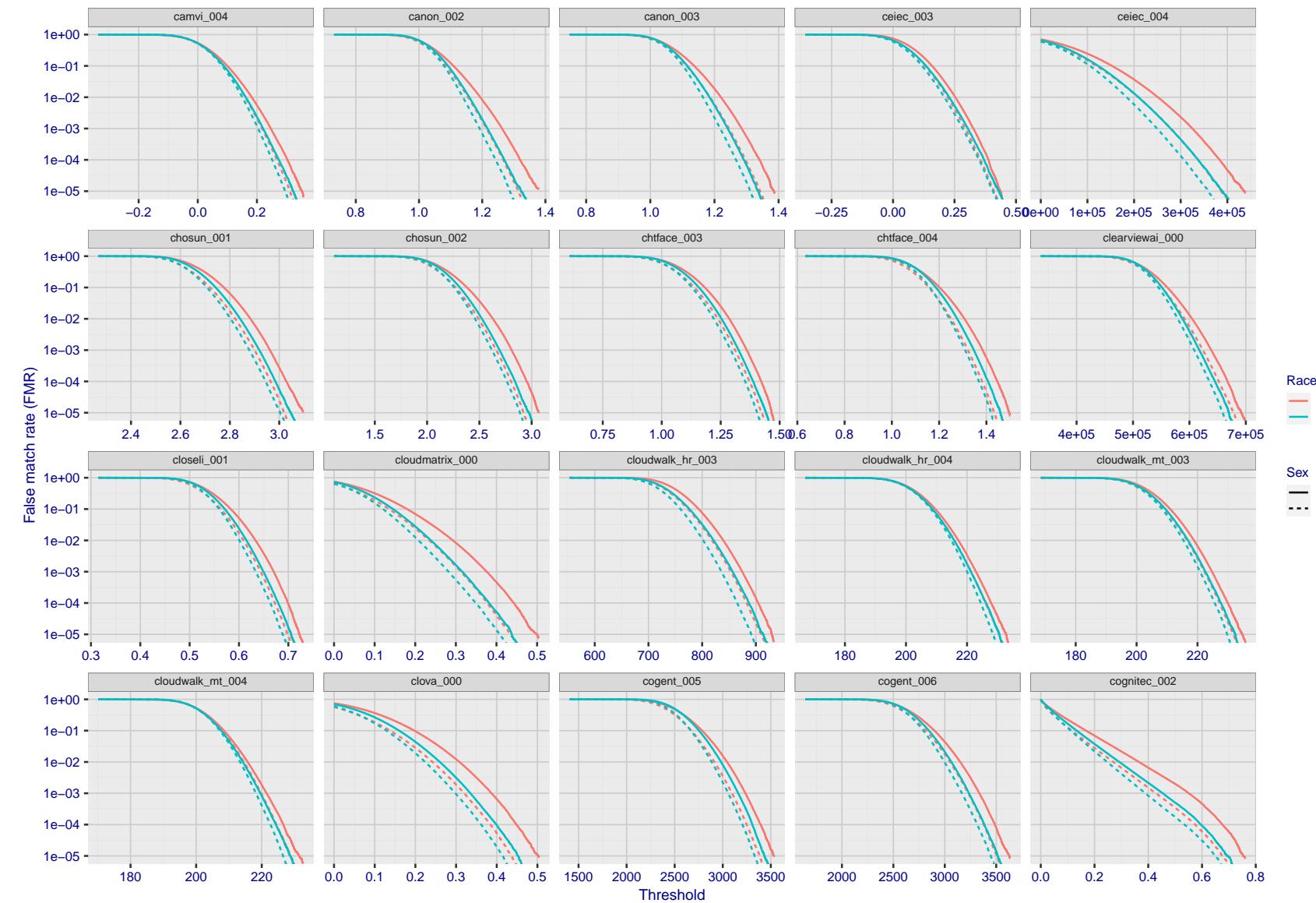


Figure 167: For the mugshot images, the false match calibration curves show false match rate vs. threshold. Separate curves appear for white females, black females, black males and white males.

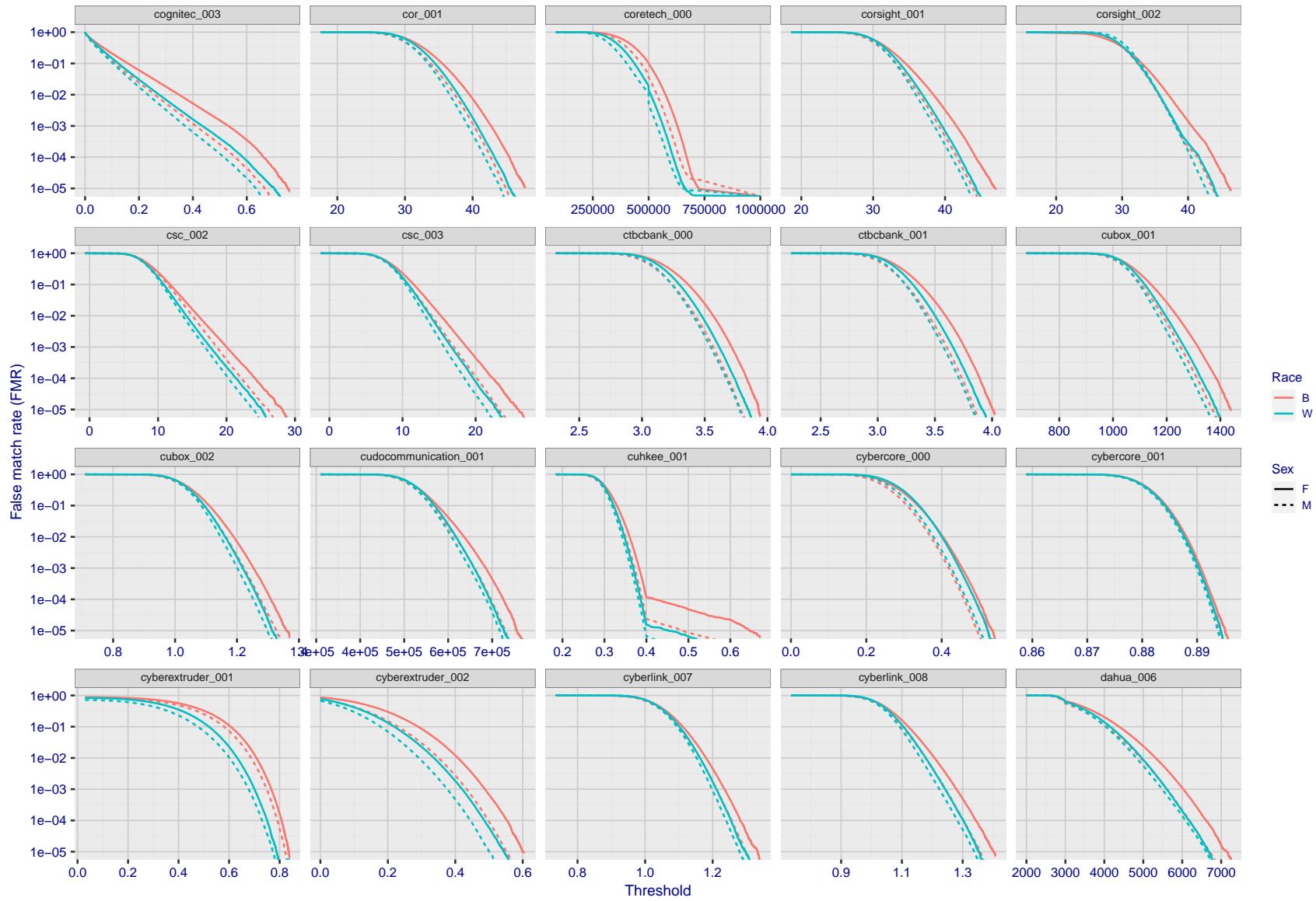


Figure 168: For the mugshot images, the false match calibration curves show false match rate vs. threshold. Separate curves appear for white females, black females, black males and white males.

2022/01/20 13:13:43

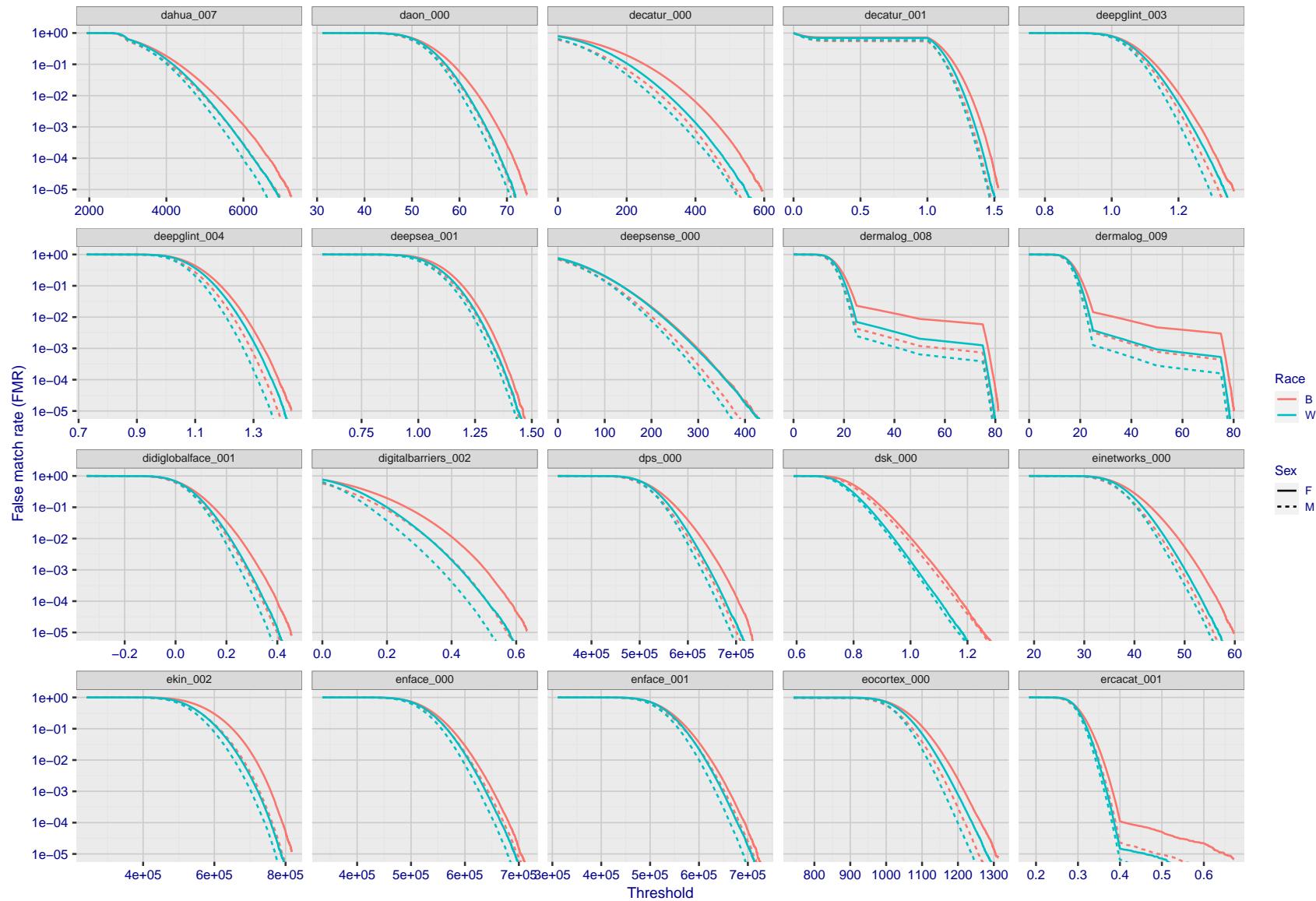


Figure 169: For the mugshot images, the false match calibration curves show false match rate vs. threshold. Separate curves appear for white females, black females, black males and white males.

FNMR(T)  
"False non-match rate"  
"False match rate"

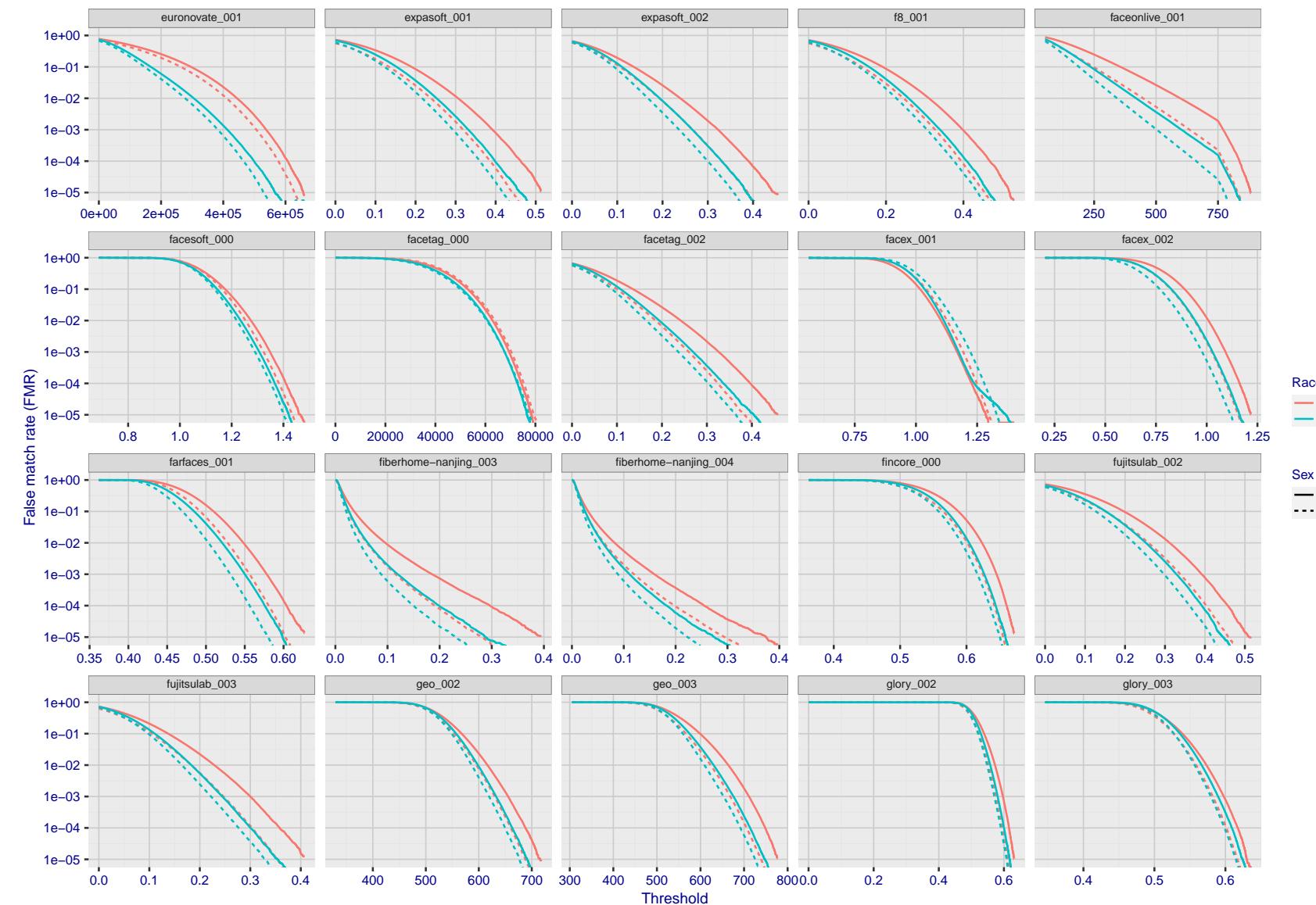


Figure 170: For the mugshot images, the false match calibration curves show false match rate vs. threshold. Separate curves appear for white females, black females, black males and white males.

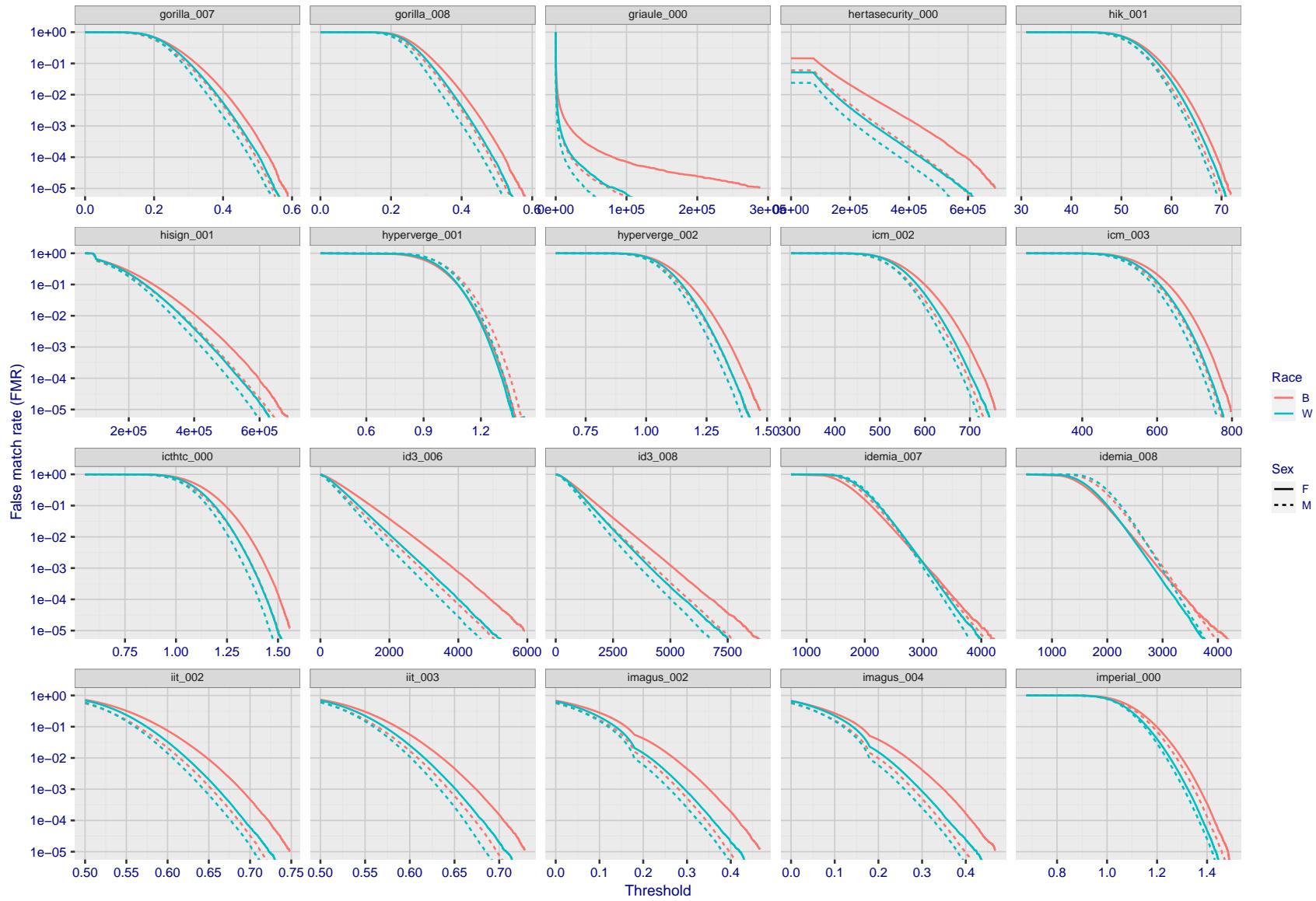


Figure 171: For the mugshot images, the false match calibration curves show false match rate vs. threshold. Separate curves appear for white females, black females, black males and white males.

2022/01/20 13:13:43

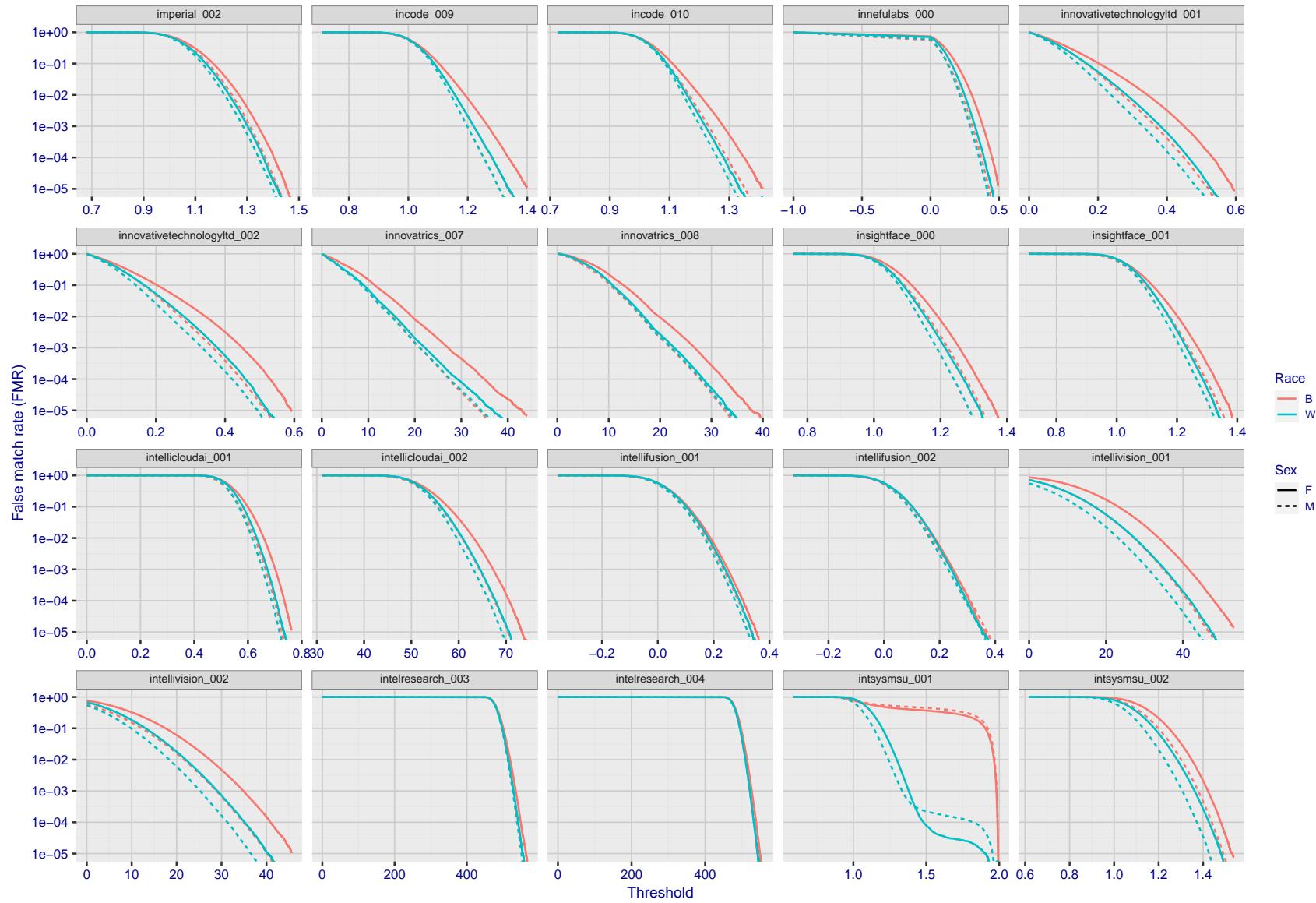


Figure 172: For the mugshot images, the false match calibration curves show false match rate vs. threshold. Separate curves appear for white females, black females, black males and white males.

2022/01/20 13:13:43

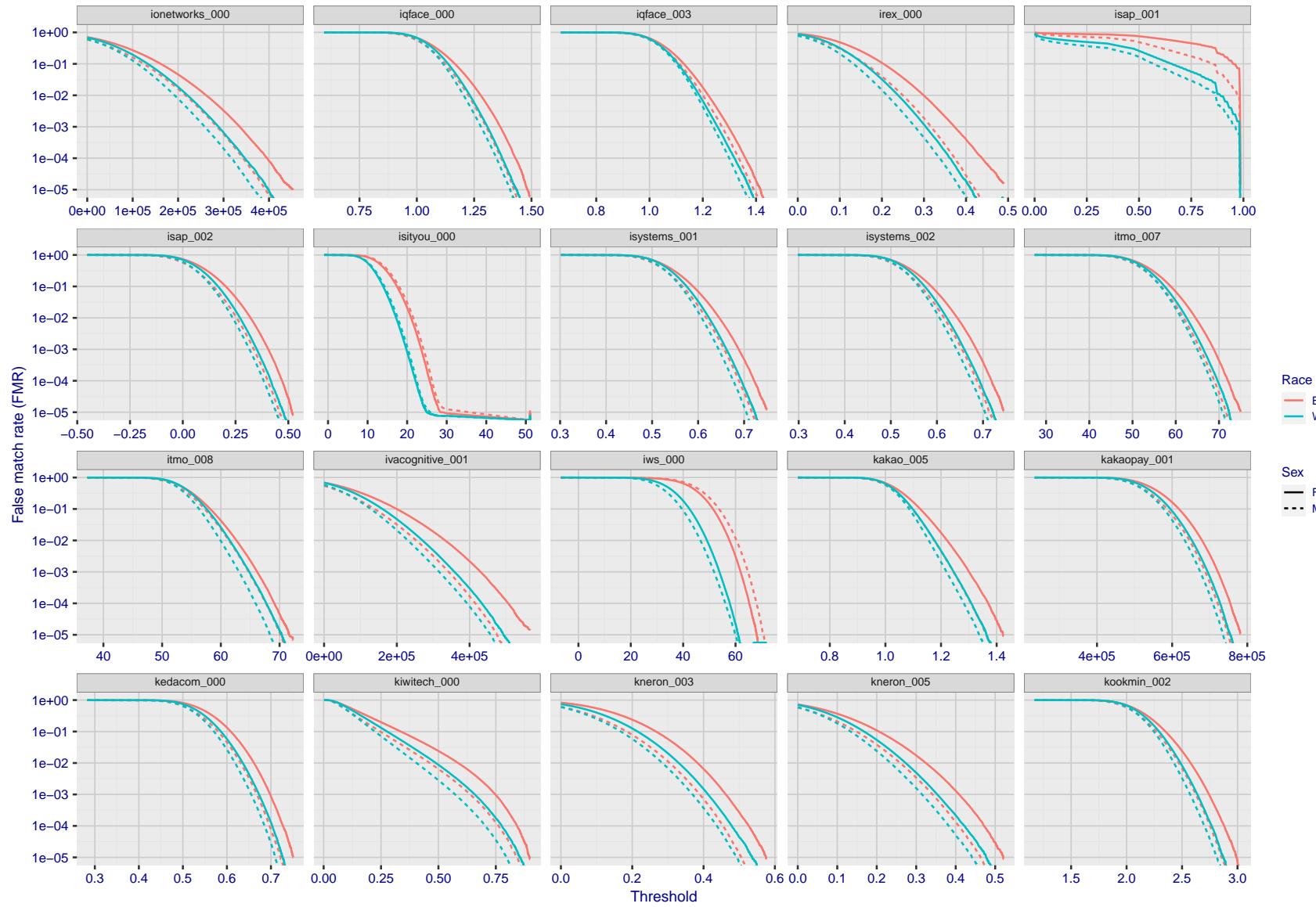


Figure 173: For the mugshot images, the false match calibration curves show false match rate vs. threshold. Separate curves appear for white females, black females, black males and white males.

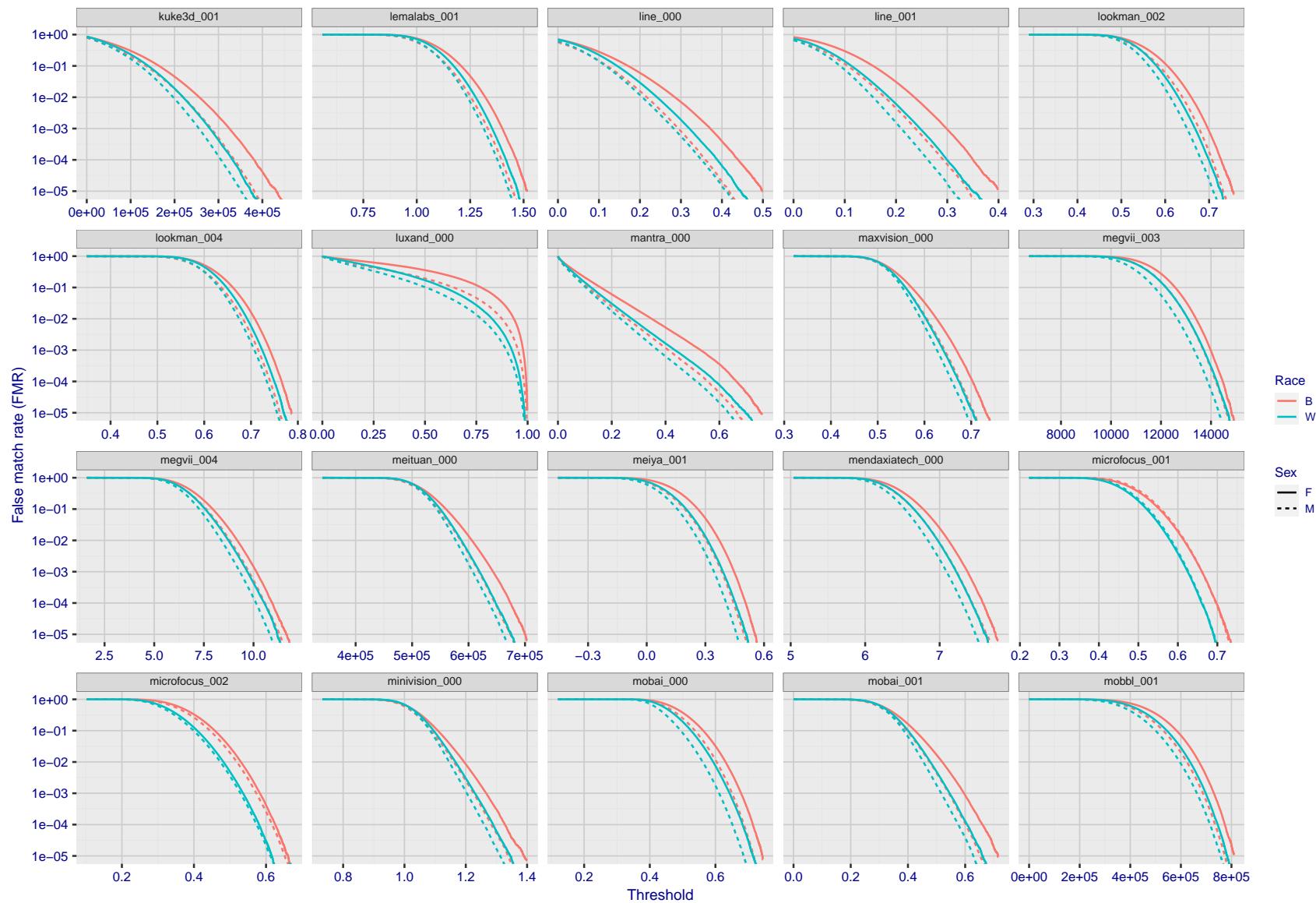


Figure 174: For the mugshot images, the false match calibration curves show false match rate vs. threshold. Separate curves appear for white females, black females, black males and white males.

2022/01/20 13:13:43

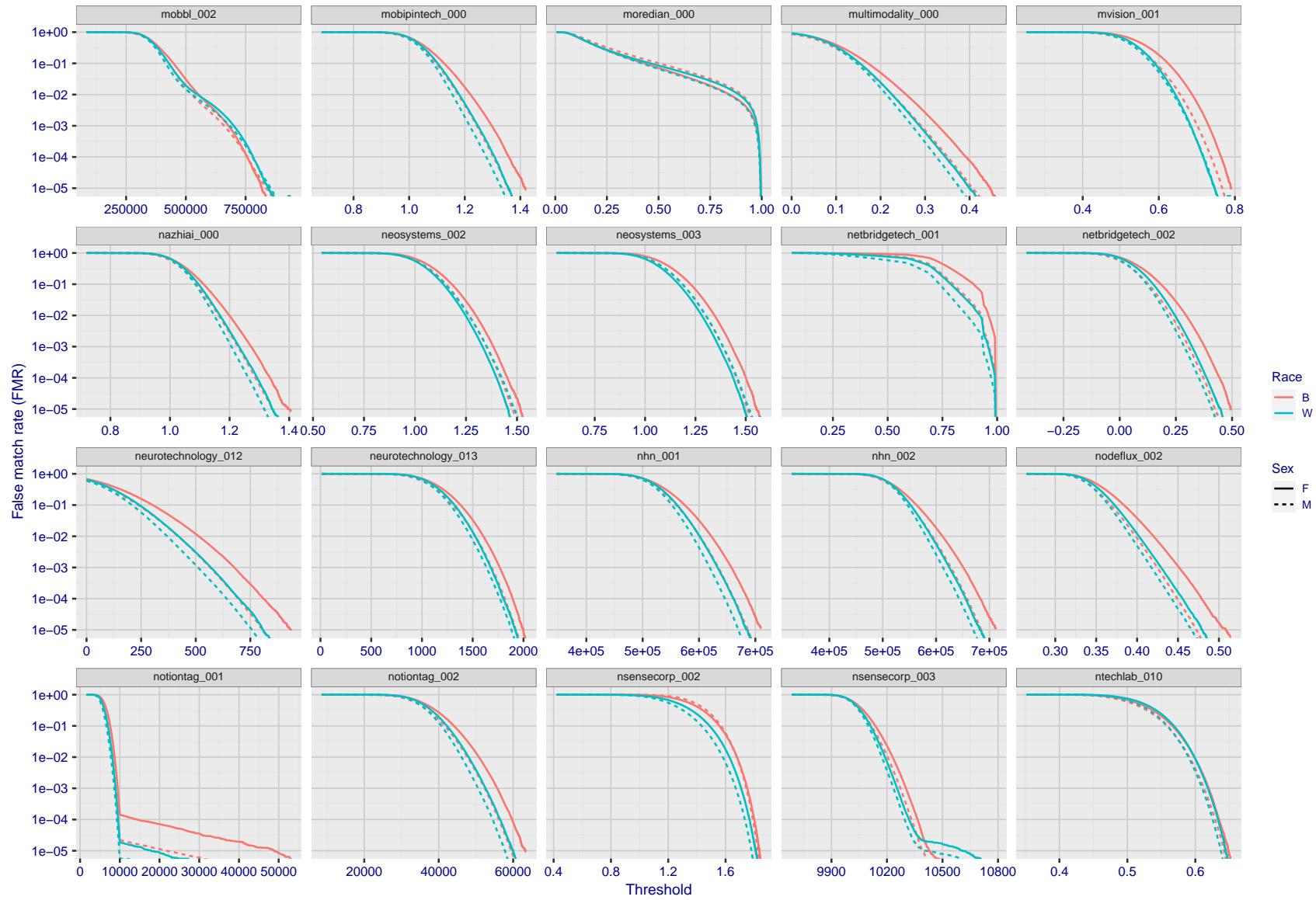


Figure 175: For the mugshot images, the false match calibration curves show false match rate vs. threshold. Separate curves appear for white females, black females, black males and white males.

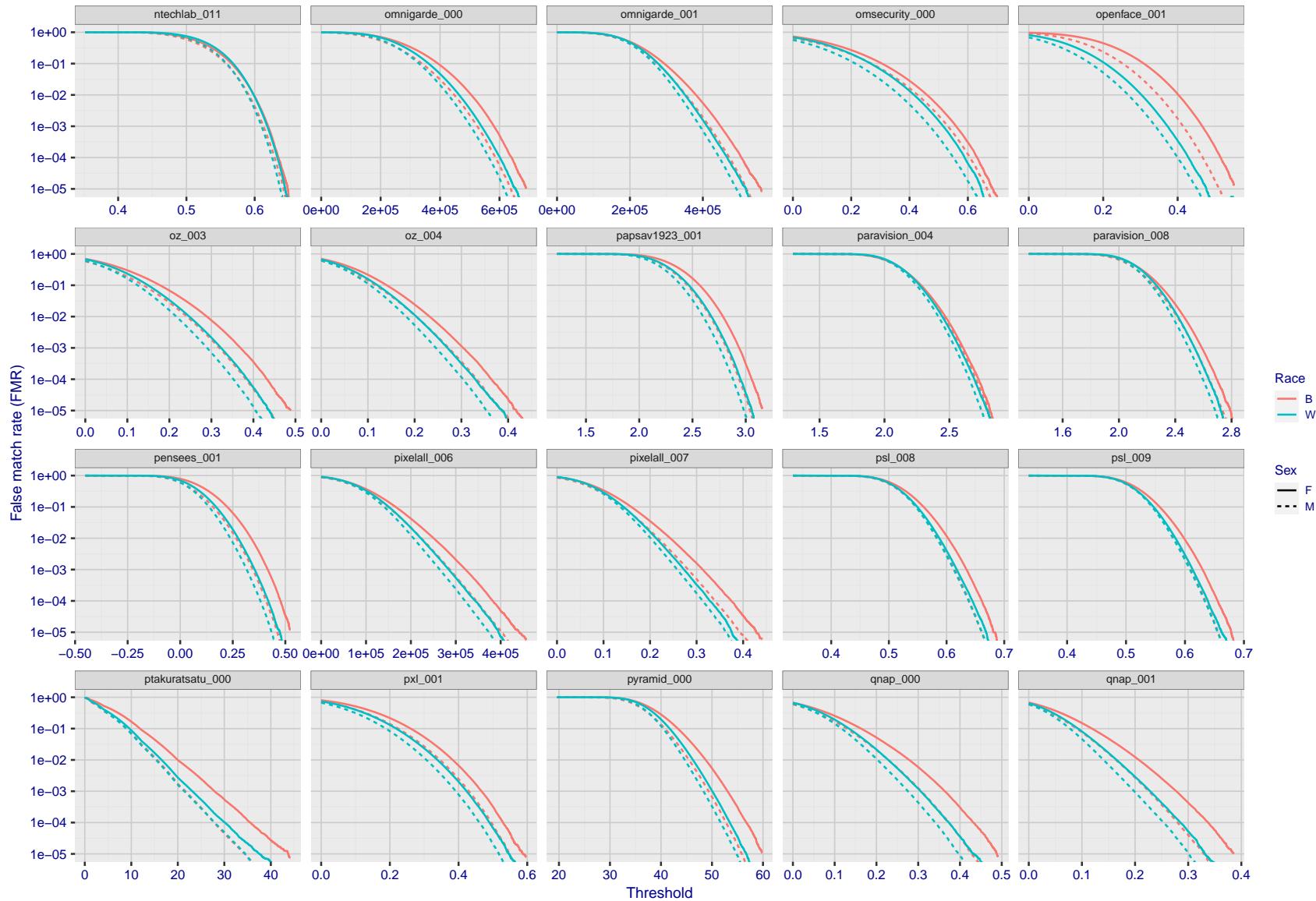


Figure 176: For the mugshot images, the false match calibration curves show false match rate vs. threshold. Separate curves appear for white females, black females, black males and white males.

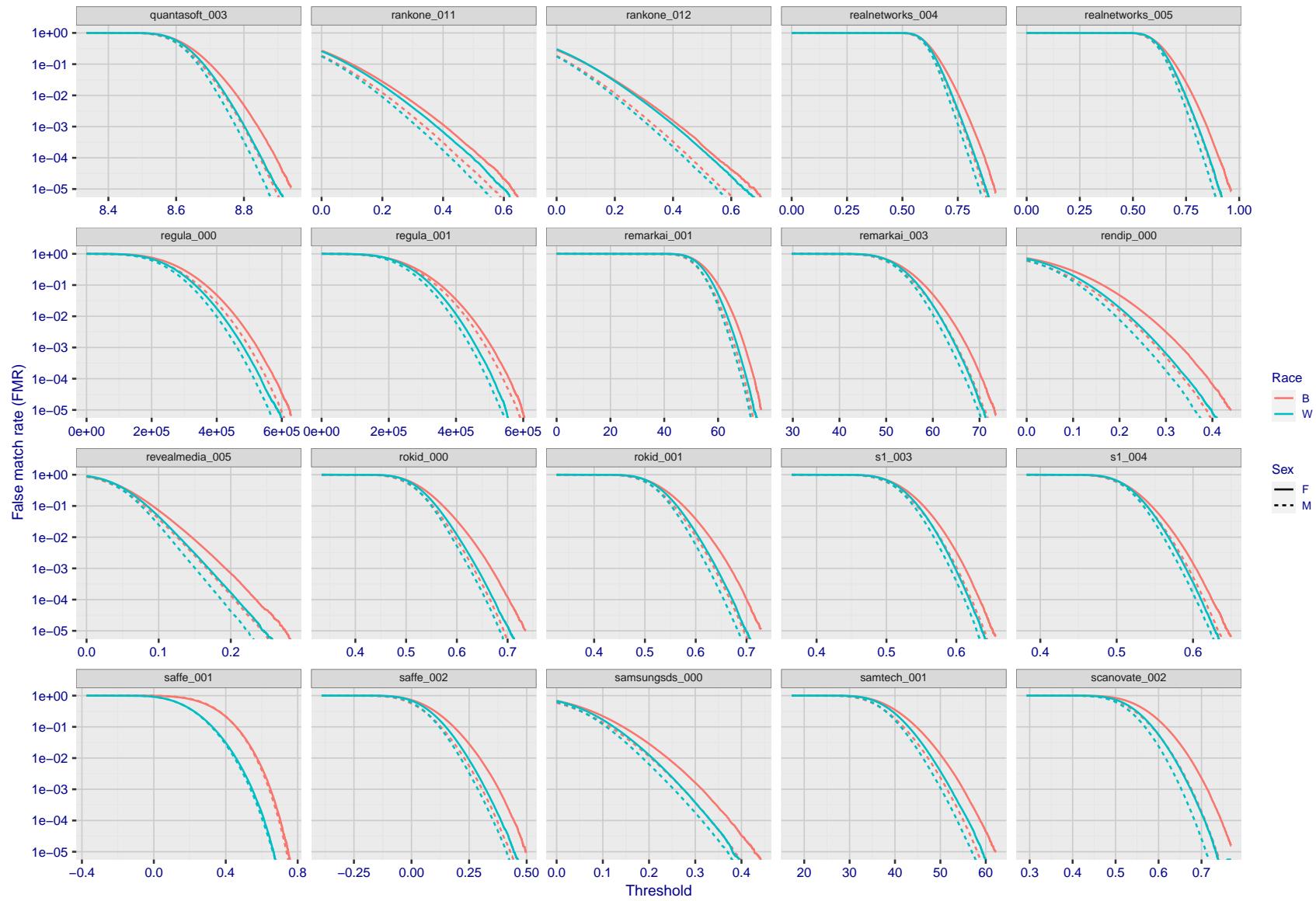


Figure 177: For the mugshot images, the false match calibration curves show false match rate vs. threshold. Separate curves appear for white females, black females, black males and white males.

2022/01/20 13:13:43

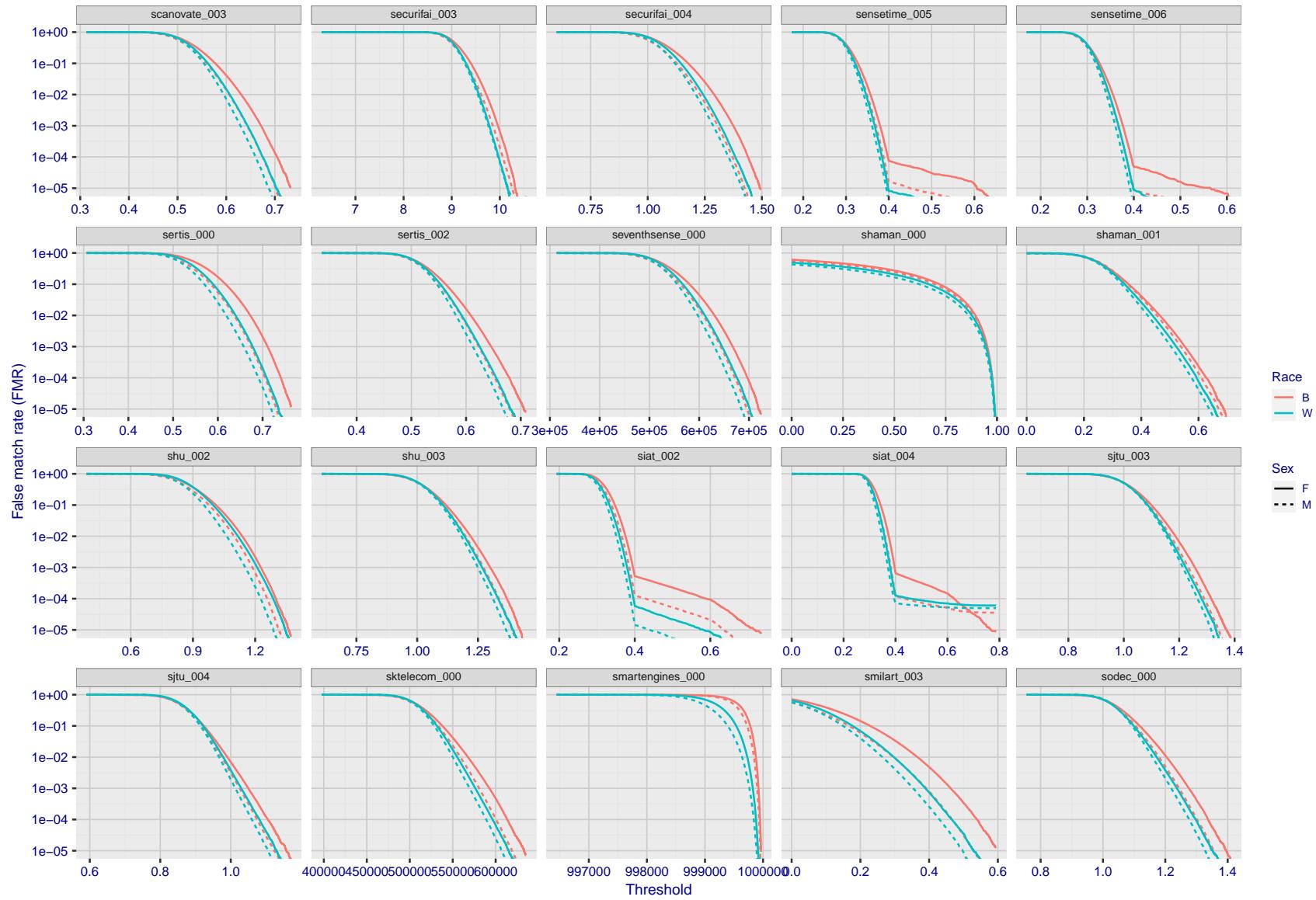


Figure 178: For the mugshot images, the false match calibration curves show false match rate vs. threshold. Separate curves appear for white females, black females, black males and white males.

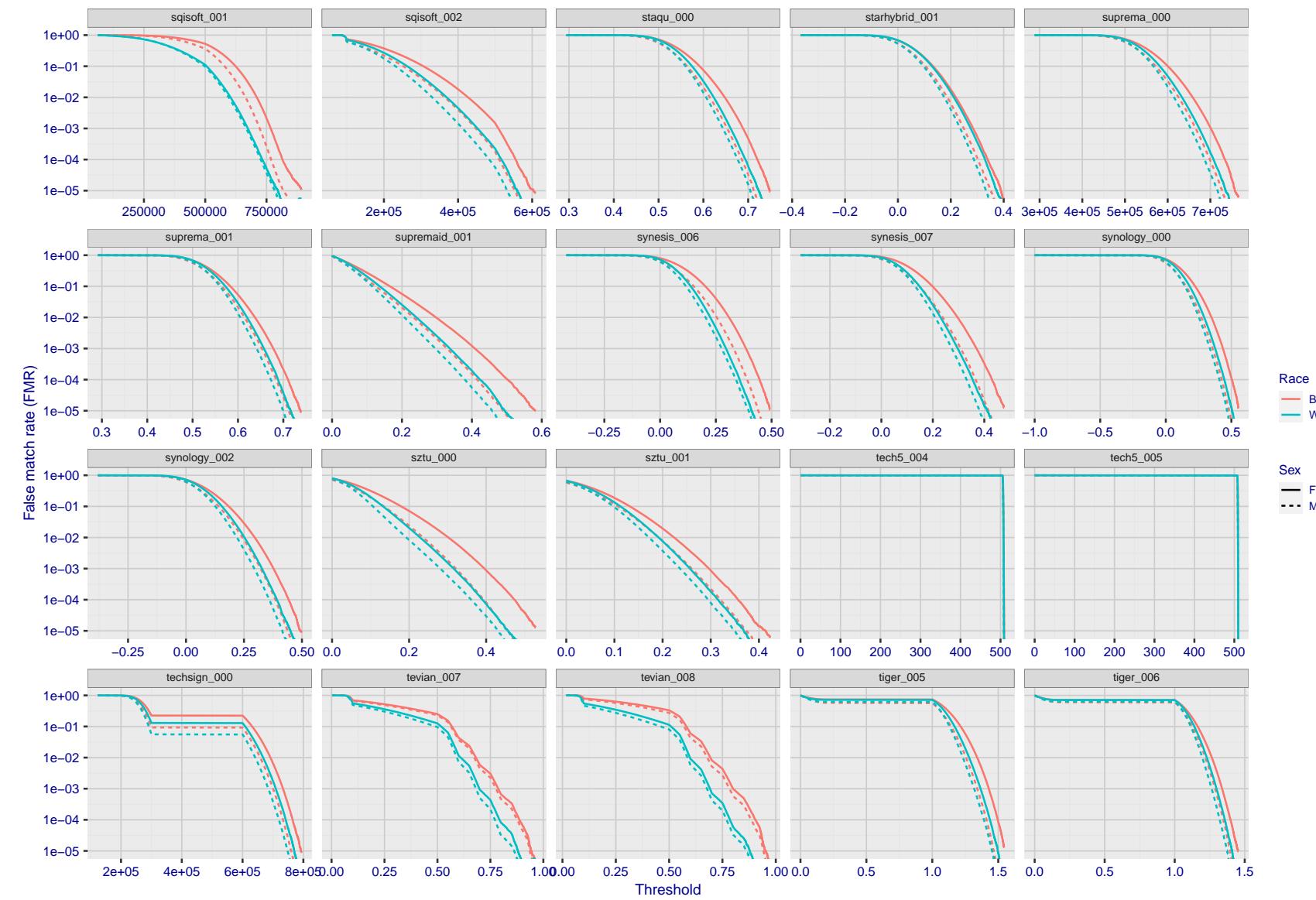


Figure 179: For the mugshot images, the false match calibration curves show false match rate vs. threshold. Separate curves appear for white females, black females, black males and white males.

2022/01/20 13:13:43

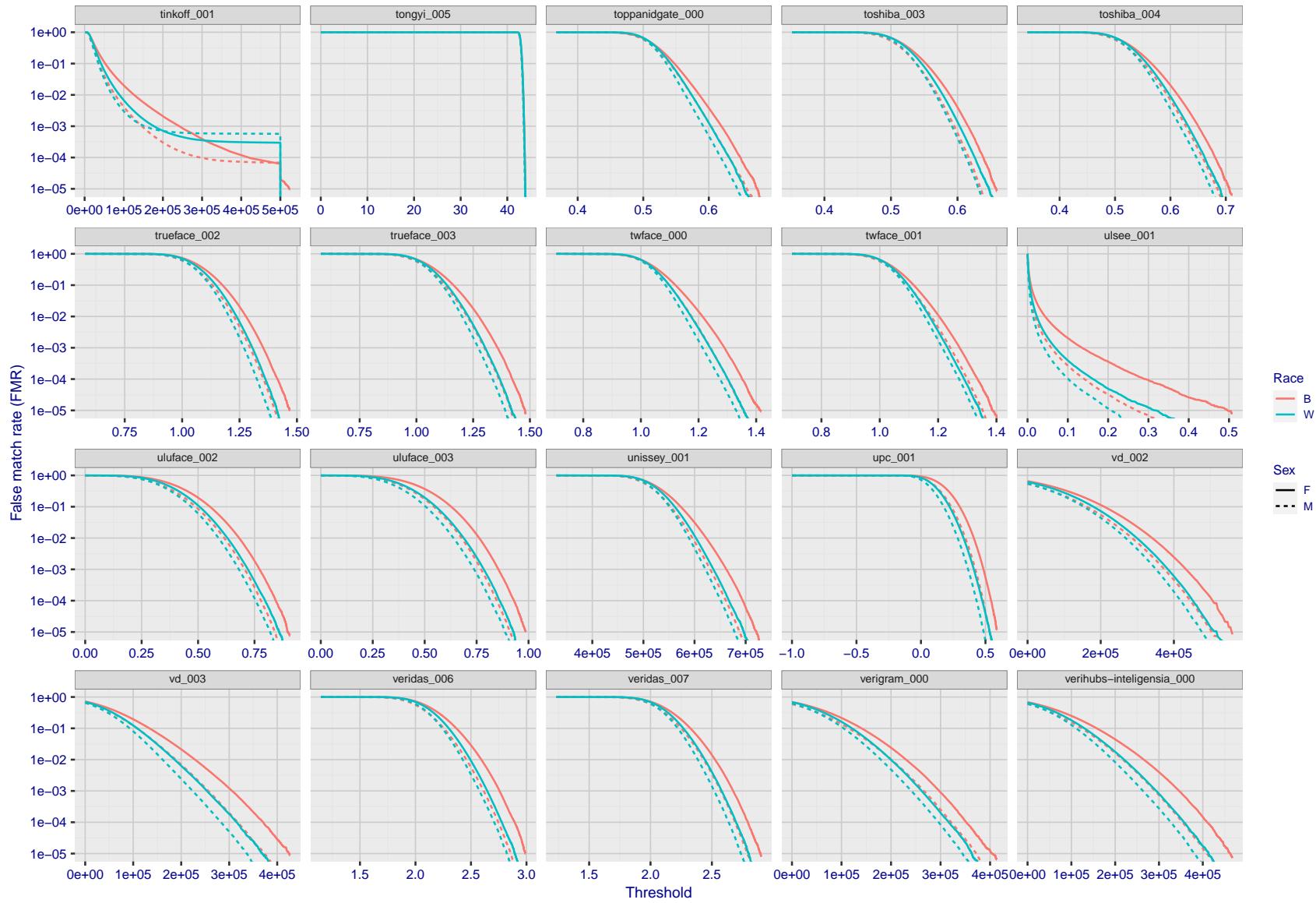


Figure 180: For the mugshot images, the false match calibration curves show false match rate vs. threshold. Separate curves appear for white females, black females, black males and white males.

FNMR(T)  
"False non-match rate"  
"False match rate"

2022/01/20 13:13:43

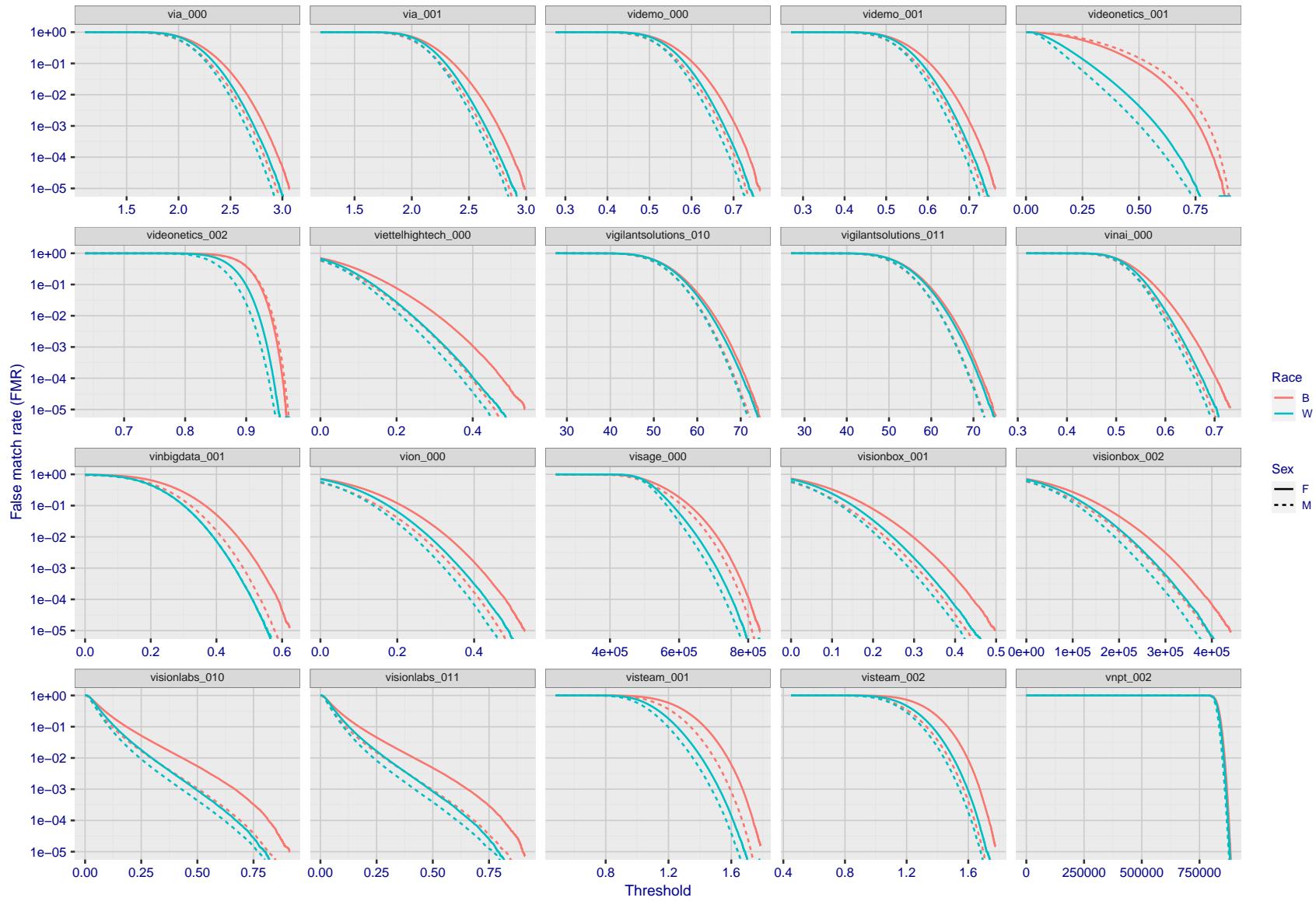


Figure 181: For the mugshot images, the false match calibration curves show false match rate vs. threshold. Separate curves appear for white females, black females, black males and white males.

2022/01/20 13:13:43

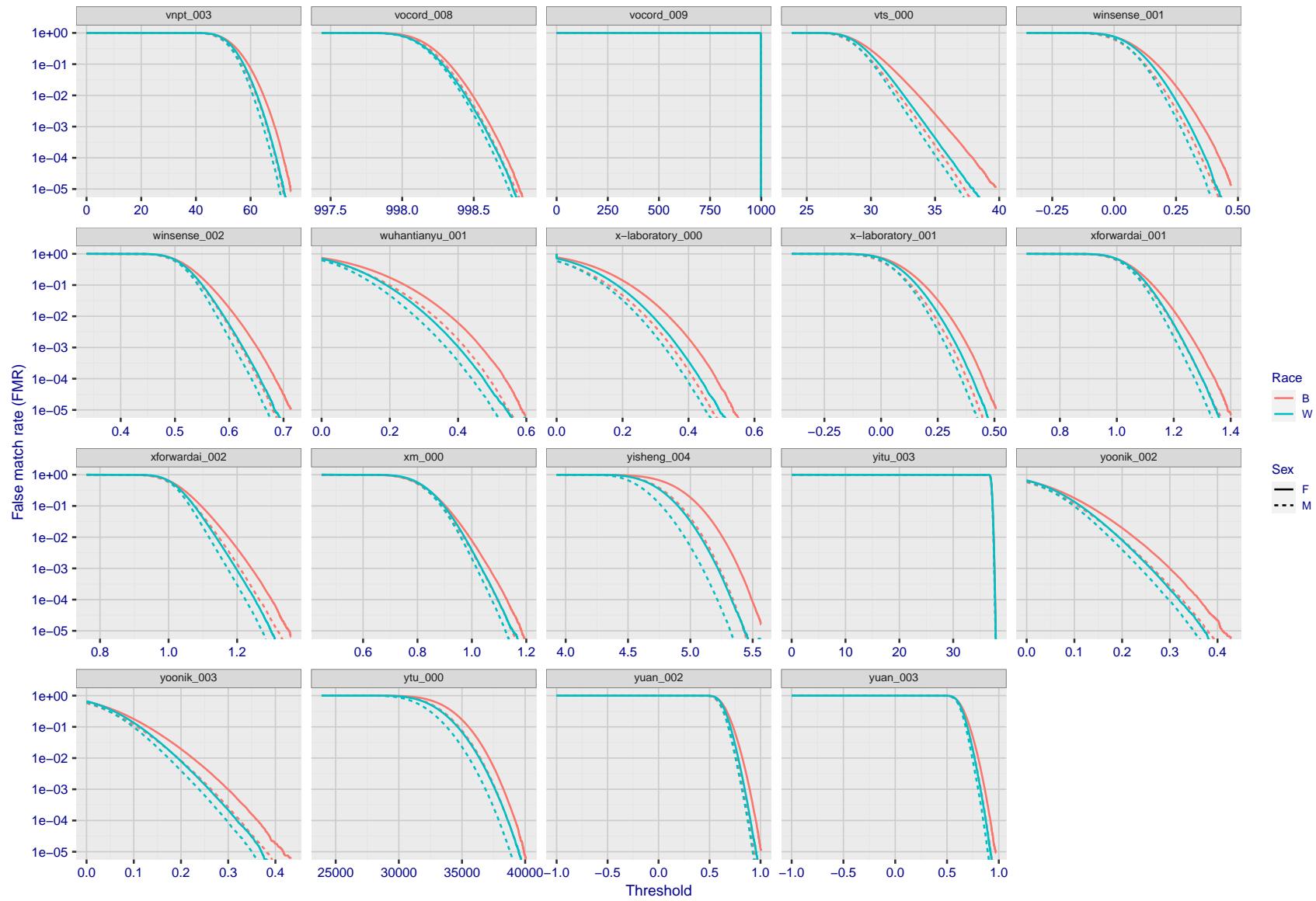


Figure 182: For the mugshot images, the false match calibration curves show false match rate vs. threshold. Separate curves appear for white females, black females, black males and white males.

FNMR(T)  
"False non-match rate"  
"False match rate"

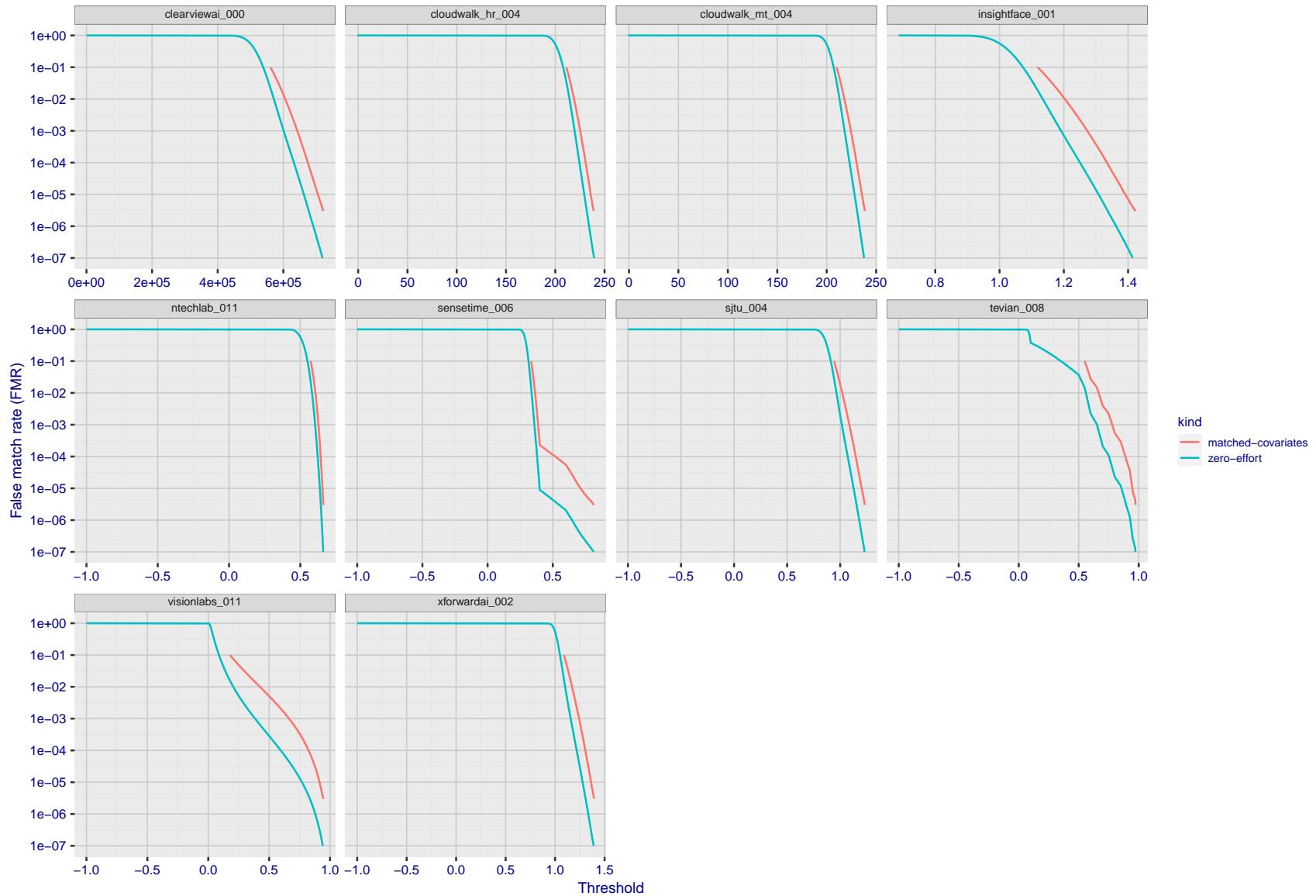


Figure 183: For the visa images, the false match calibration curves show FMR vs. threshold,  $T$ . The blue (lower) curves are for zero-effort impostors (i.e. comparing all images against all). The red (upper) curves are for persons of the same-sex, same-age, and same national-origin. This shows that FMR is underestimated (by a factor of 10 or more) by using a zero-effort impostor calculation to calibrate  $T$ . As shown later (sec. 3.6), FMR is higher for demographic-matched impostors.

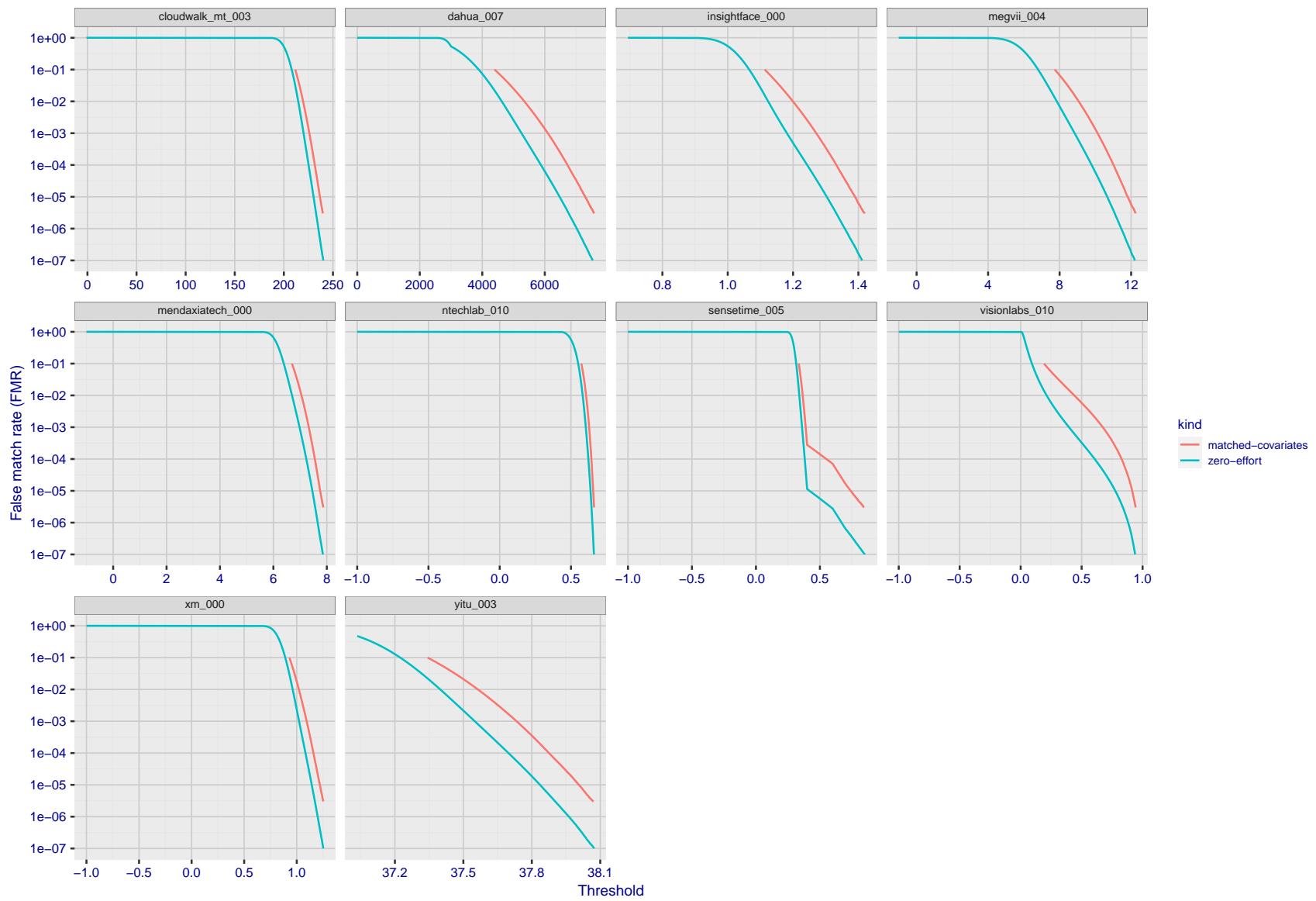


Figure 184: For the visa images, the false match calibration curves show FMR vs. threshold,  $T$ . The blue (lower) curves are for zero-effort impostors (i.e. comparing all images against all). The red (upper) curves are for persons of the same-sex, same-age, and same national-origin. This shows that FMR is underestimated (by a factor of 10 or more) by using a zero-effort impostor calculation to calibrate  $T$ . As shown later (sec. 3.6), FMR is higher for demographic-matched impostors.

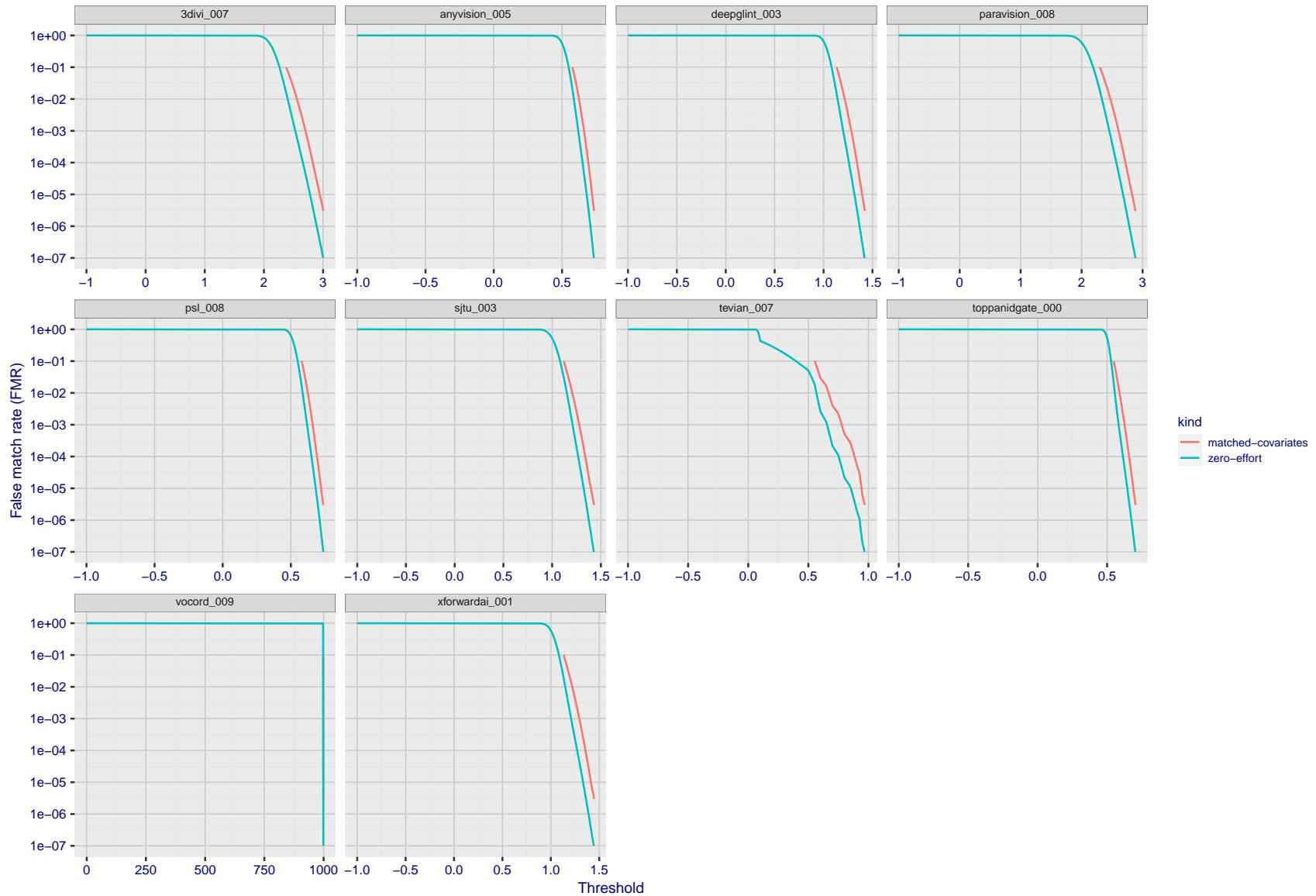


Figure 185: For the visa images, the false match calibration curves show FMR vs. threshold,  $T$ . The blue (lower) curves are for zero-effort impostors (i.e. comparing all images against all). The red (upper) curves are for persons of the same-sex, same-age, and same national-origin. This shows that FMR is underestimated (by a factor of 10 or more) by using a zero-effort impostor calculation to calibrate  $T$ . As shown later (sec. 3.6), FMR is higher for demographic-matched impostors.

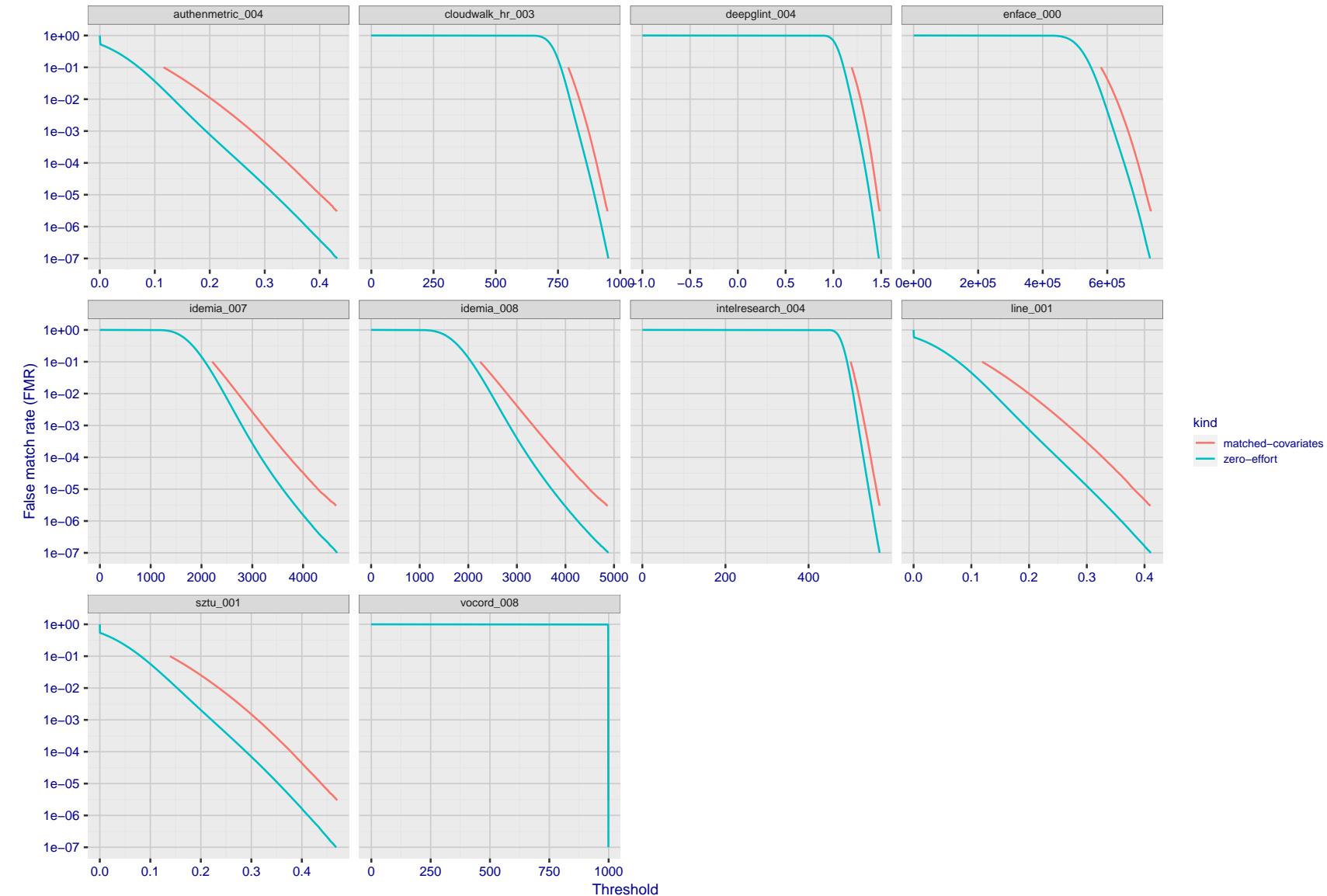


Figure 186: For the visa images, the false match calibration curves show FMR vs. threshold,  $T$ . The blue (lower) curves are for zero-effort impostors (i.e. comparing all images against all). The red (upper) curves are for persons of the same-sex, same-age, and same national-origin. This shows that FMR is underestimated (by a factor of 10 or more) by using a zero-effort impostor calculation to calibrate  $T$ . As shown later (sec. 3.6), FMR is higher for demographic-matched impostors.

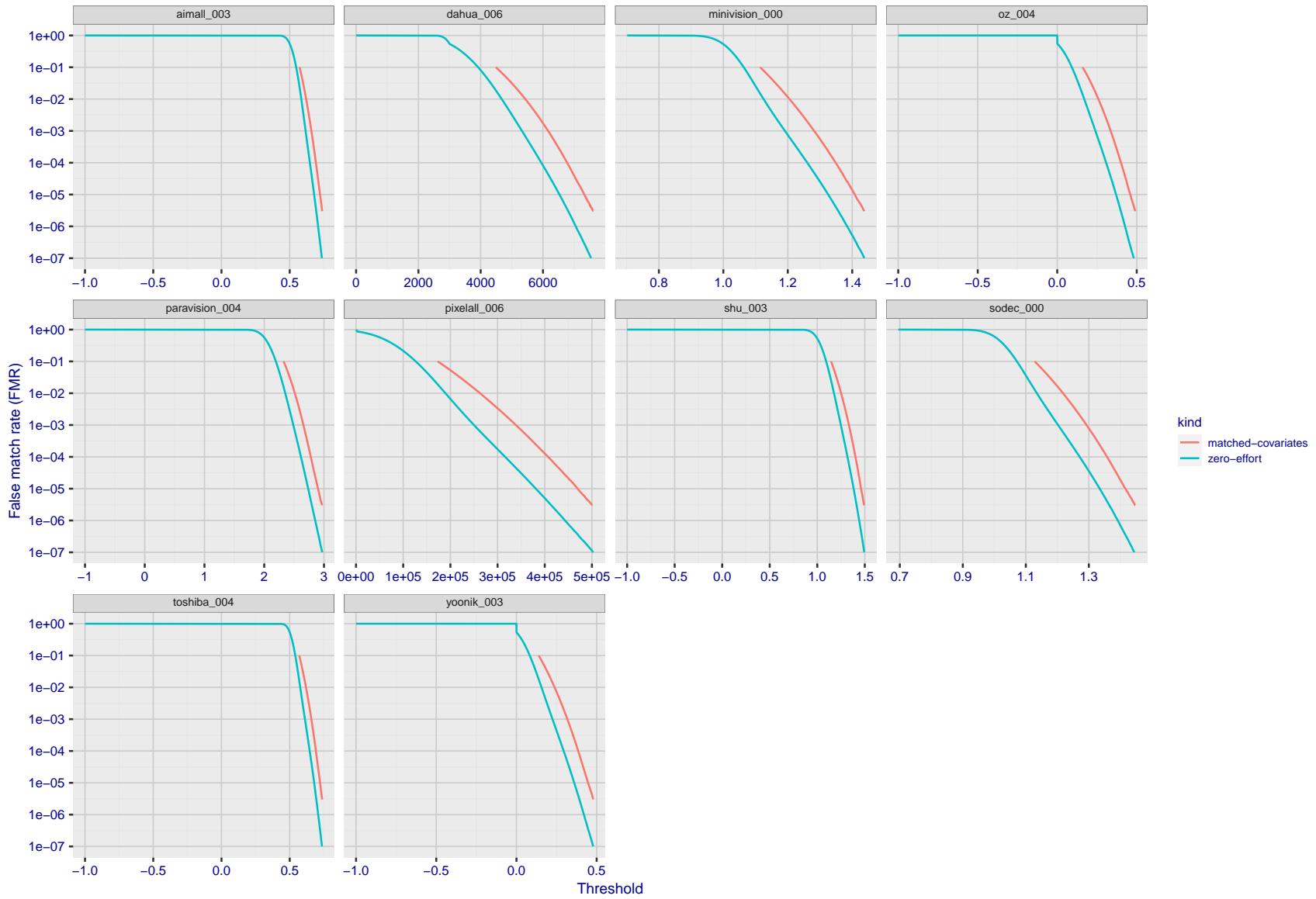


Figure 187: For the visa images, the false match calibration curves show FMR vs. threshold,  $T$ . The blue (lower) curves are for zero-effort impostors (i.e. comparing all images against all). The red (upper) curves are for persons of the same-sex, same-age, and same national-origin. This shows that FMR is underestimated (by a factor of 10 or more) by using a zero-effort impostor calculation to calibrate  $T$ . As shown later (sec. 3.6), FMR is higher for demographic-matched impostors.

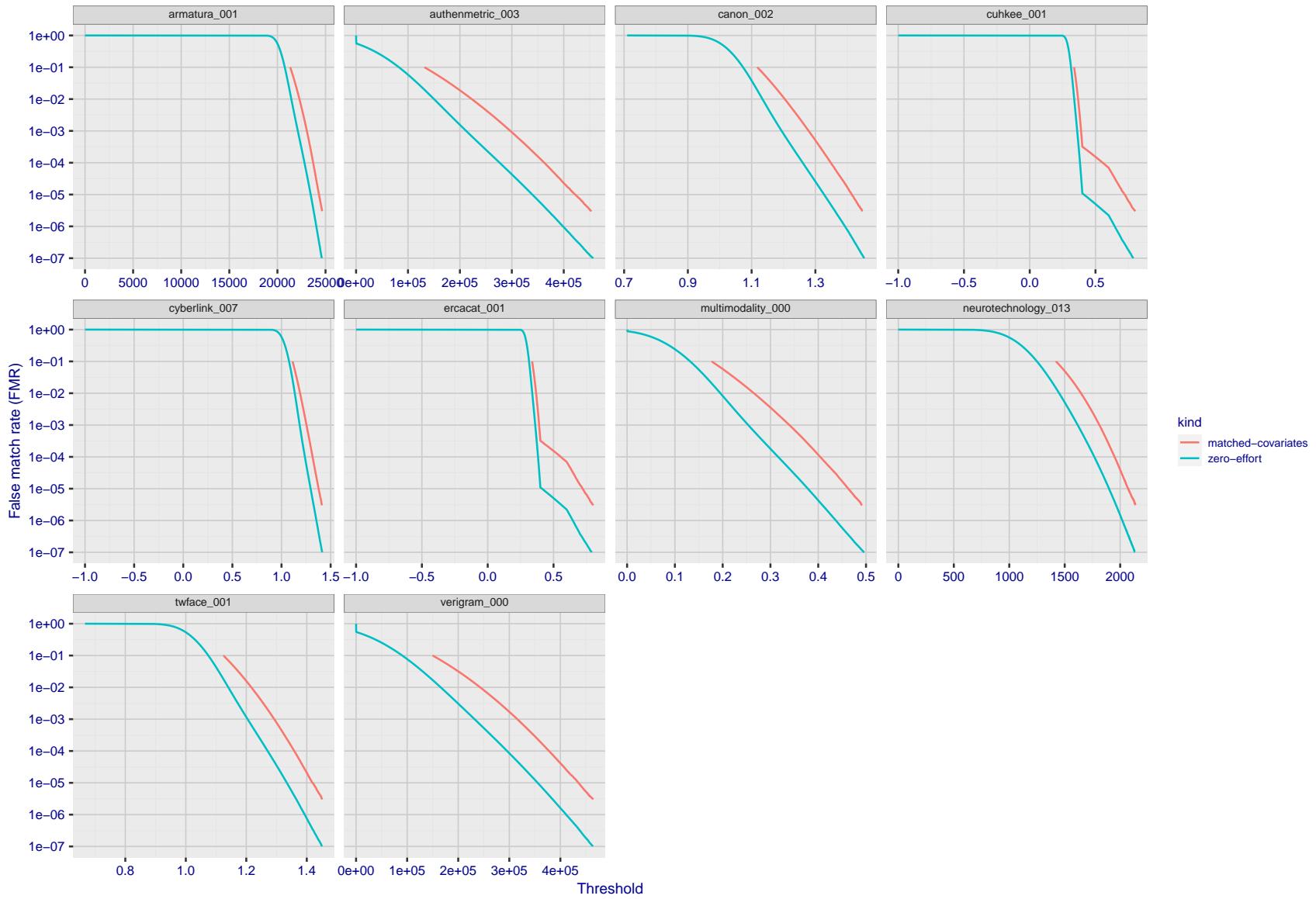


Figure 188: For the visa images, the false match calibration curves show FMR vs. threshold,  $T$ . The blue (lower) curves are for zero-effort impostors (i.e. comparing all images against all). The red (upper) curves are for persons of the same-sex, same-age, and same national-origin. This shows that FMR is underestimated (by a factor of 10 or more) by using a zero-effort impostor calculation to calibrate  $T$ . As shown later (sec. 3.6), FMR is higher for demographic-matched impostors.

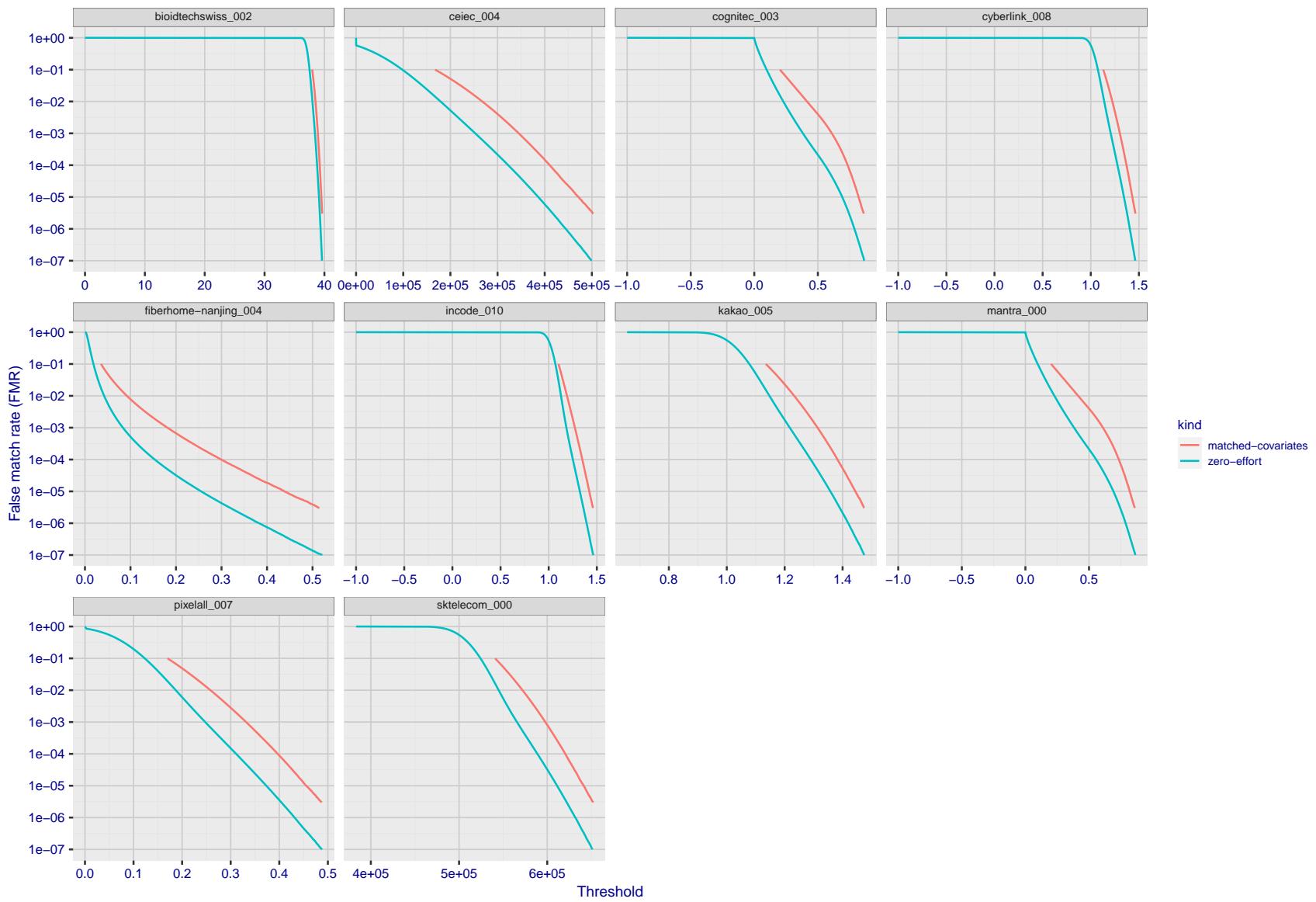


Figure 189: For the visa images, the false match calibration curves show FMR vs. threshold,  $T$ . The blue (lower) curves are for zero-effort impostors (i.e. comparing all images against all). The red (upper) curves are for persons of the same-sex, same-age, and same national-origin. This shows that FMR is underestimated (by a factor of 10 or more) by using a zero-effort impostor calculation to calibrate  $T$ . As shown later (sec. 3.6), FMR is higher for demographic-matched impostors.

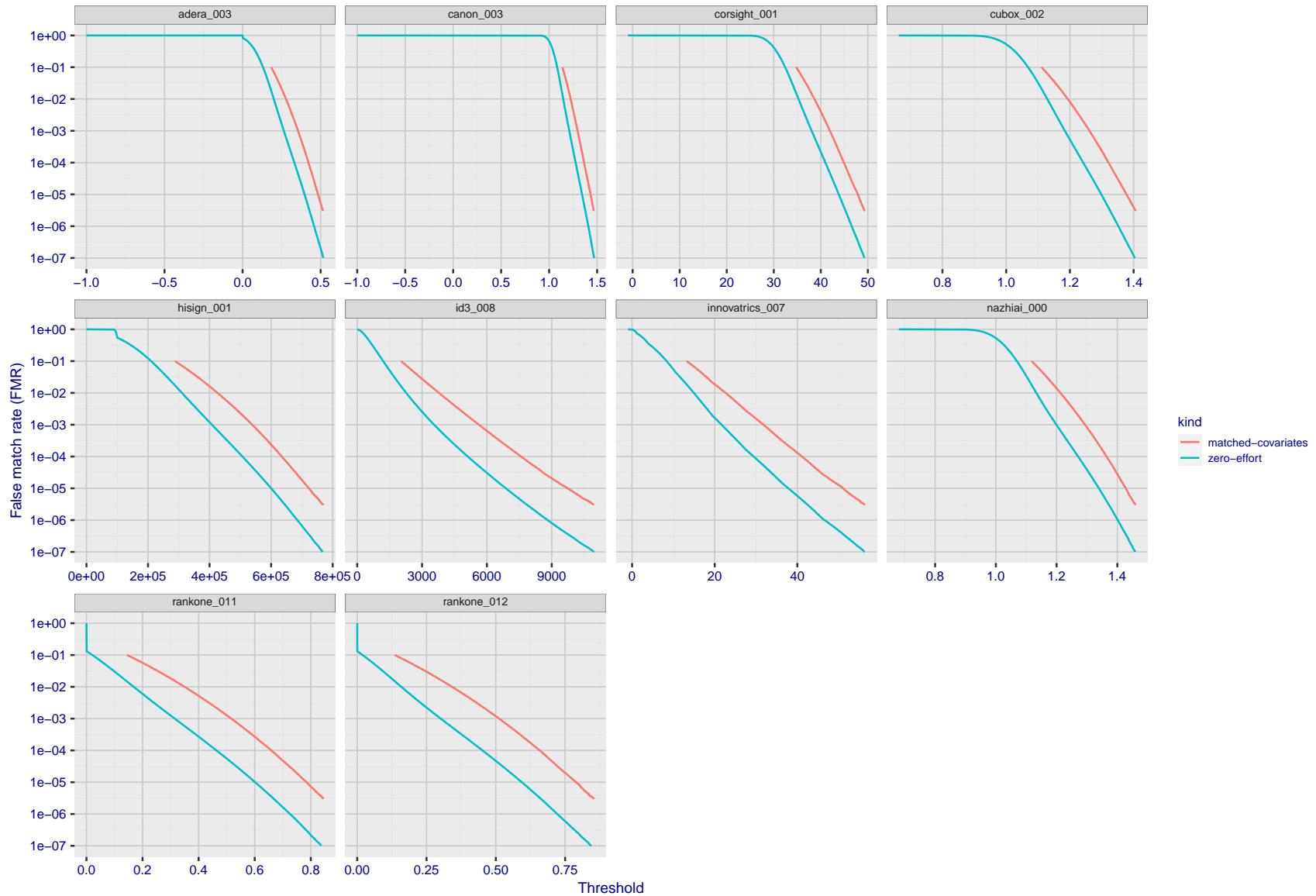


Figure 190: For the visa images, the false match calibration curves show FMR vs. threshold,  $T$ . The blue (lower) curves are for zero-effort impostors (i.e. comparing all images against all). The red (upper) curves are for persons of the same-sex, same-age, and same national-origin. This shows that FMR is underestimated (by a factor of 10 or more) by using a zero-effort impostor calculation to calibrate  $T$ . As shown later (sec. 3.6), FMR is higher for demographic-matched impostors.

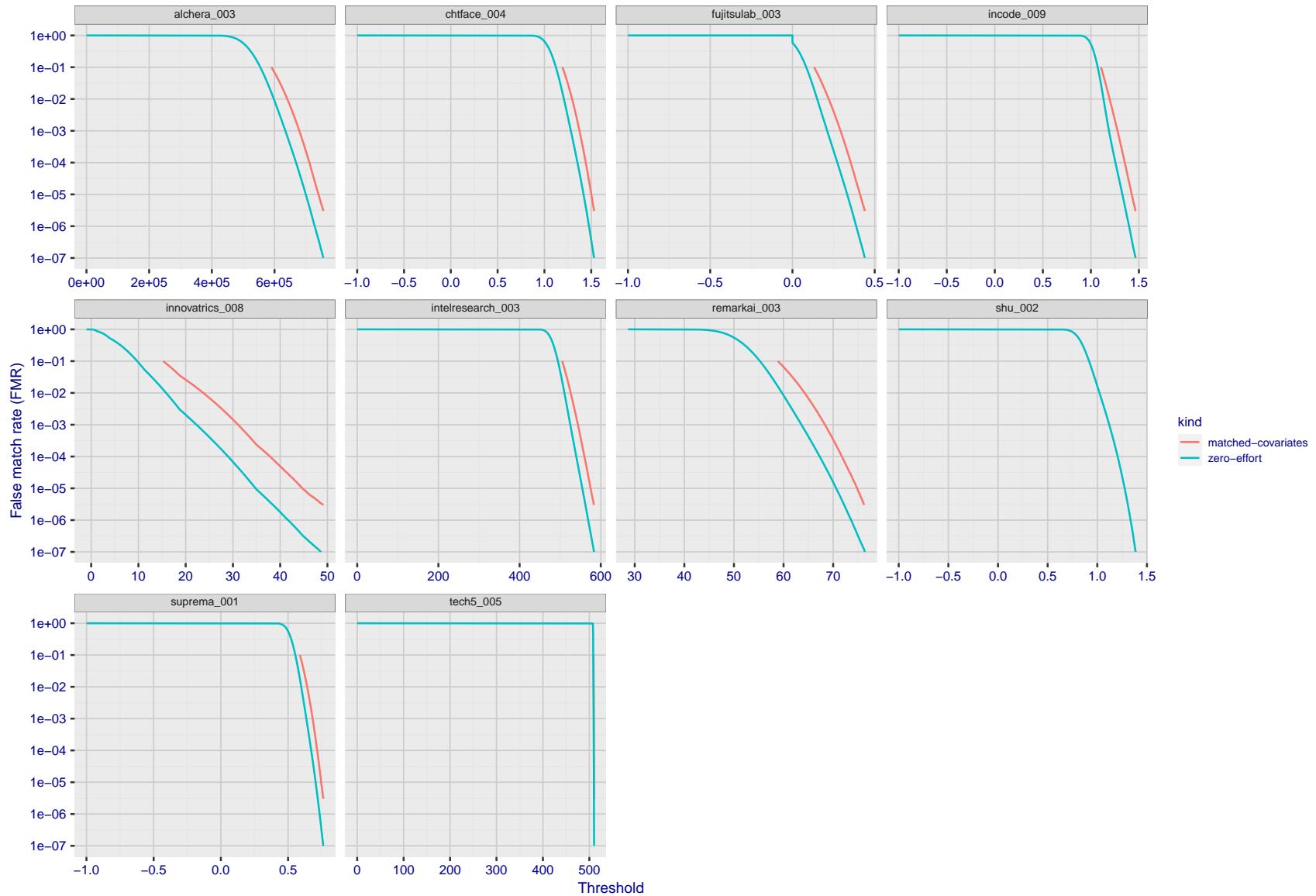


Figure 191: For the visa images, the false match calibration curves show FMR vs. threshold,  $T$ . The blue (lower) curves are for zero-effort impostors (i.e. comparing all images against all). The red (upper) curves are for persons of the same-sex, same-age, and same national-origin. This shows that FMR is underestimated (by a factor of 10 or more) by using a zero-effort impostor calculation to calibrate  $T$ . As shown later (sec. 3.6), FMR is higher for demographic-matched impostors.

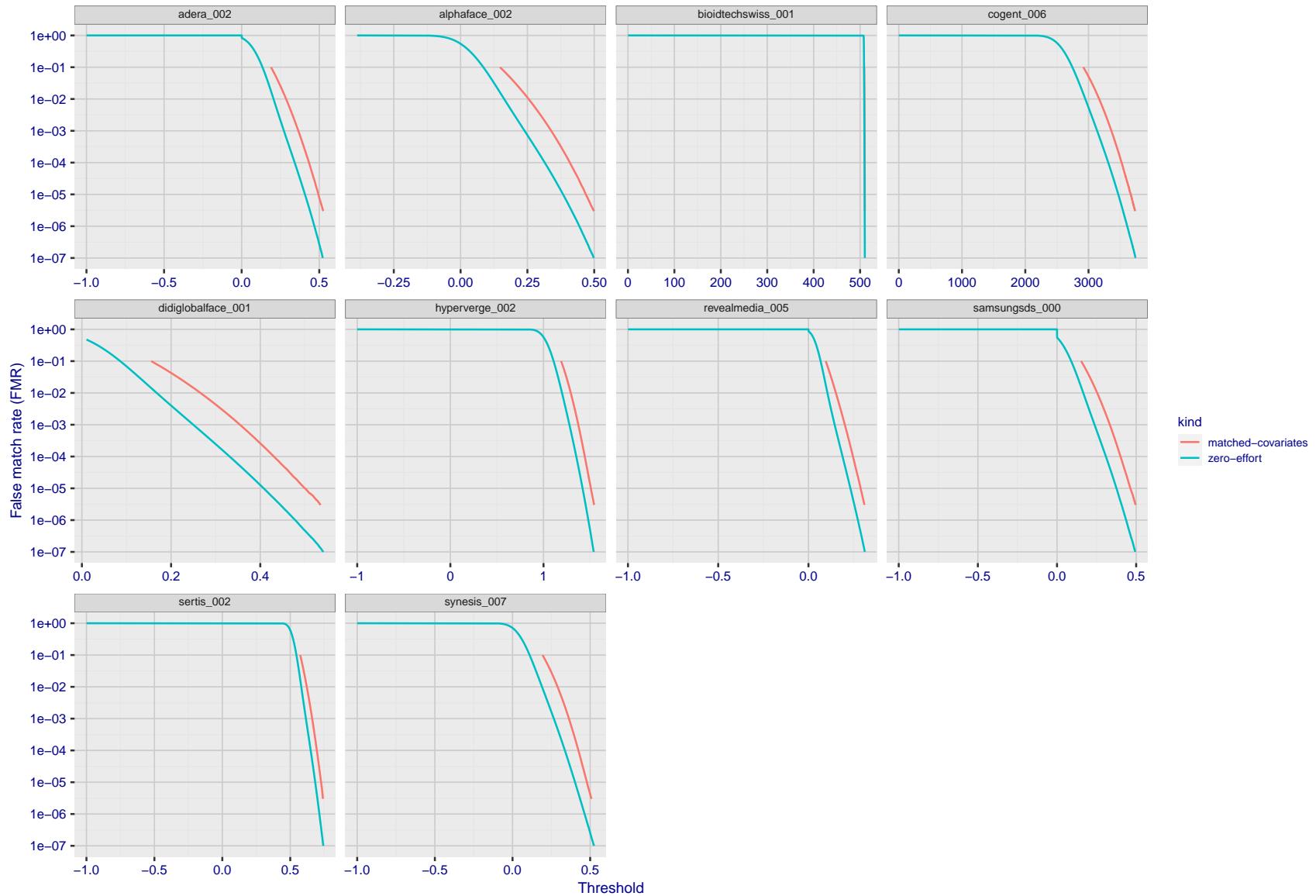


Figure 192: For the visa images, the false match calibration curves show FMR vs. threshold,  $T$ . The blue (lower) curves are for zero-effort impostors (i.e. comparing all images against all). The red (upper) curves are for persons of the same-sex, same-age, and same national-origin. This shows that FMR is underestimated (by a factor of 10 or more) by using a zero-effort impostor calculation to calibrate  $T$ . As shown later (sec. 3.6), FMR is higher for demographic-matched impostors.

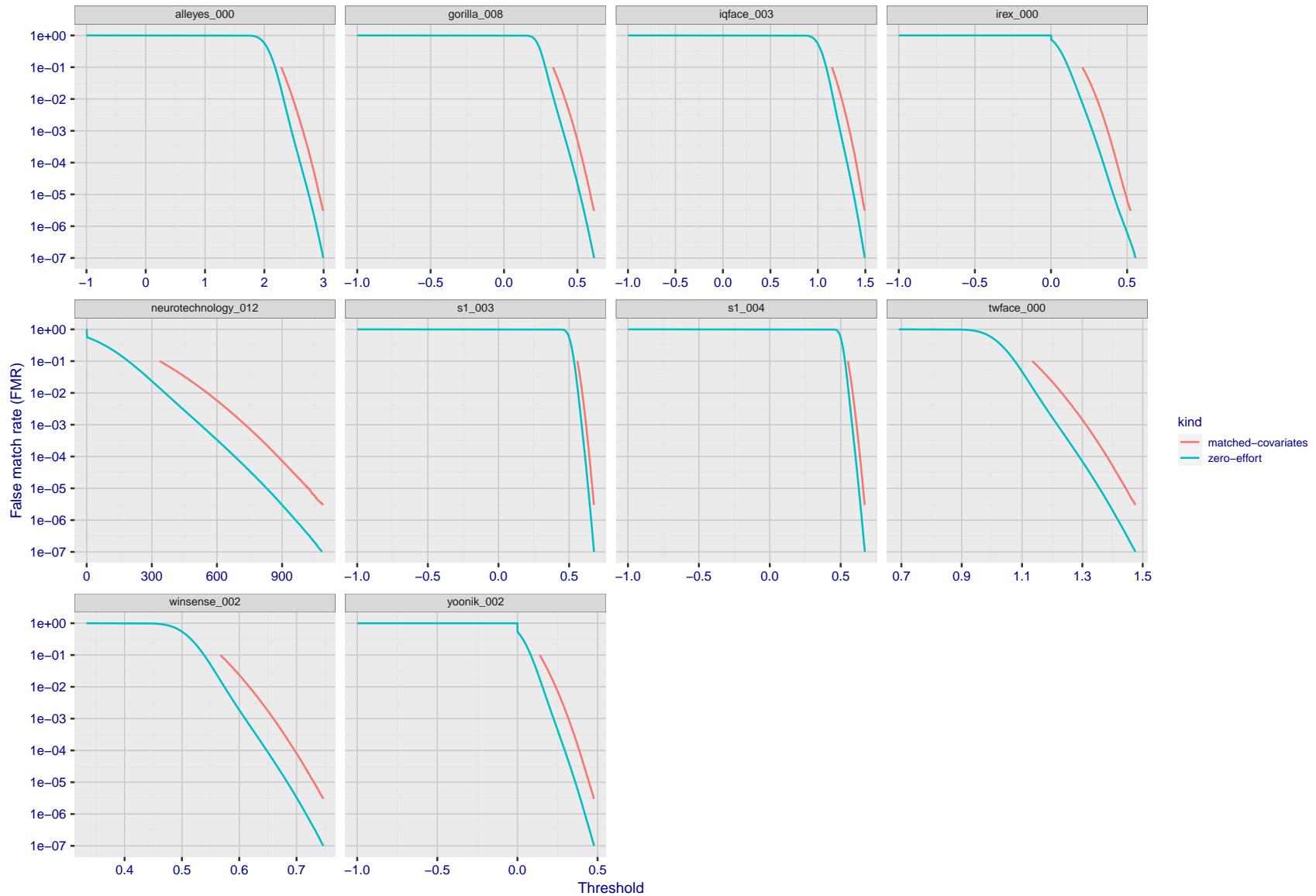


Figure 193: For the visa images, the false match calibration curves show FMR vs. threshold,  $T$ . The blue (lower) curves are for zero-effort impostors (i.e. comparing all images against all). The red (upper) curves are for persons of the same-sex, same-age, and same national-origin. This shows that FMR is underestimated (by a factor of 10 or more) by using a zero-effort impostor calculation to calibrate  $T$ . As shown later (sec. 3.6), FMR is higher for demographic-matched impostors.

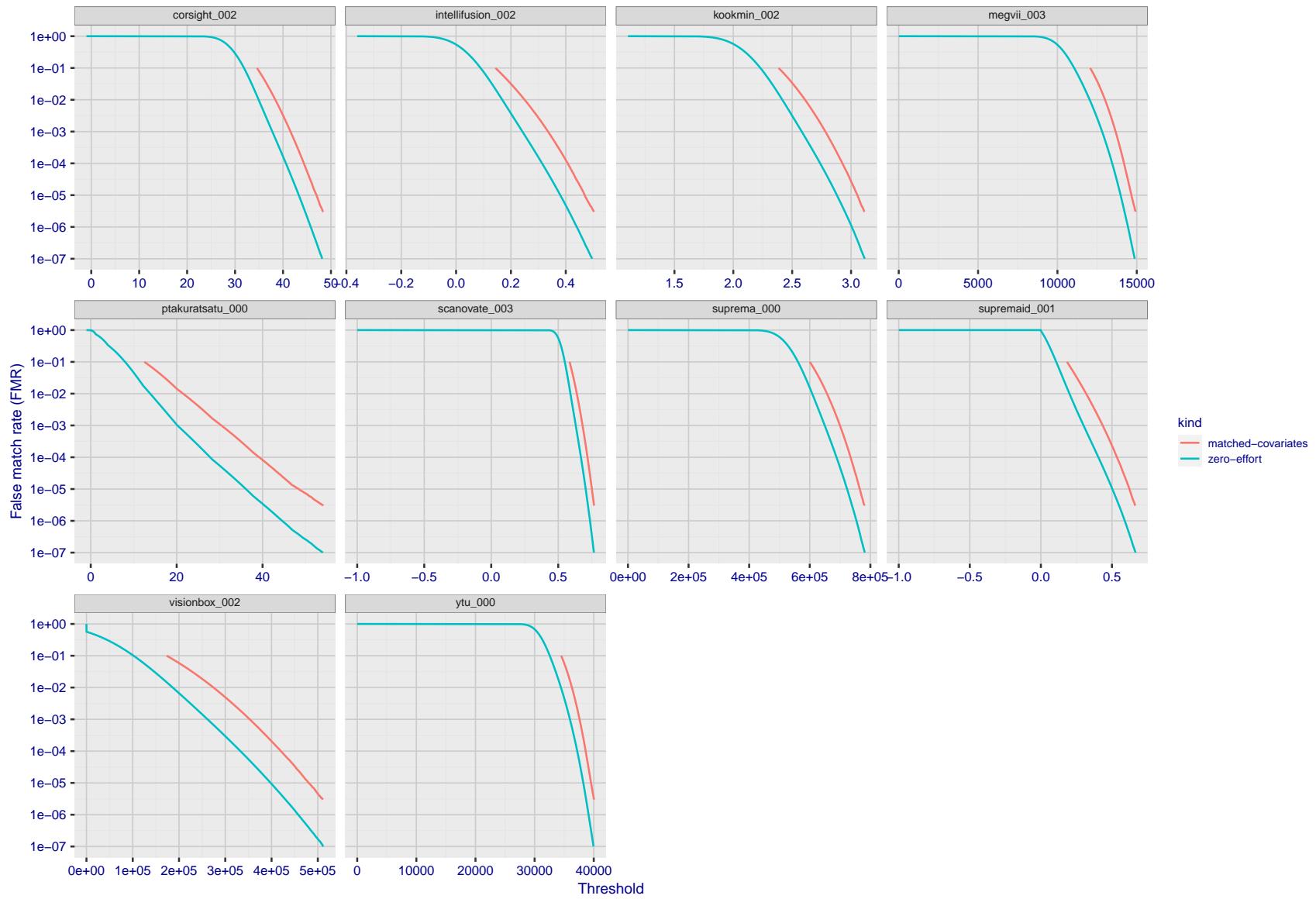


Figure 194: For the visa images, the false match calibration curves show FMR vs. threshold,  $T$ . The blue (lower) curves are for zero-effort impostors (i.e. comparing all images against all). The red (upper) curves are for persons of the same-sex, same-age, and same national-origin. This shows that FMR is underestimated (by a factor of 10 or more) by using a zero-effort impostor calculation to calibrate  $T$ . As shown later (sec. 3.6), FMR is higher for demographic-matched impostors.

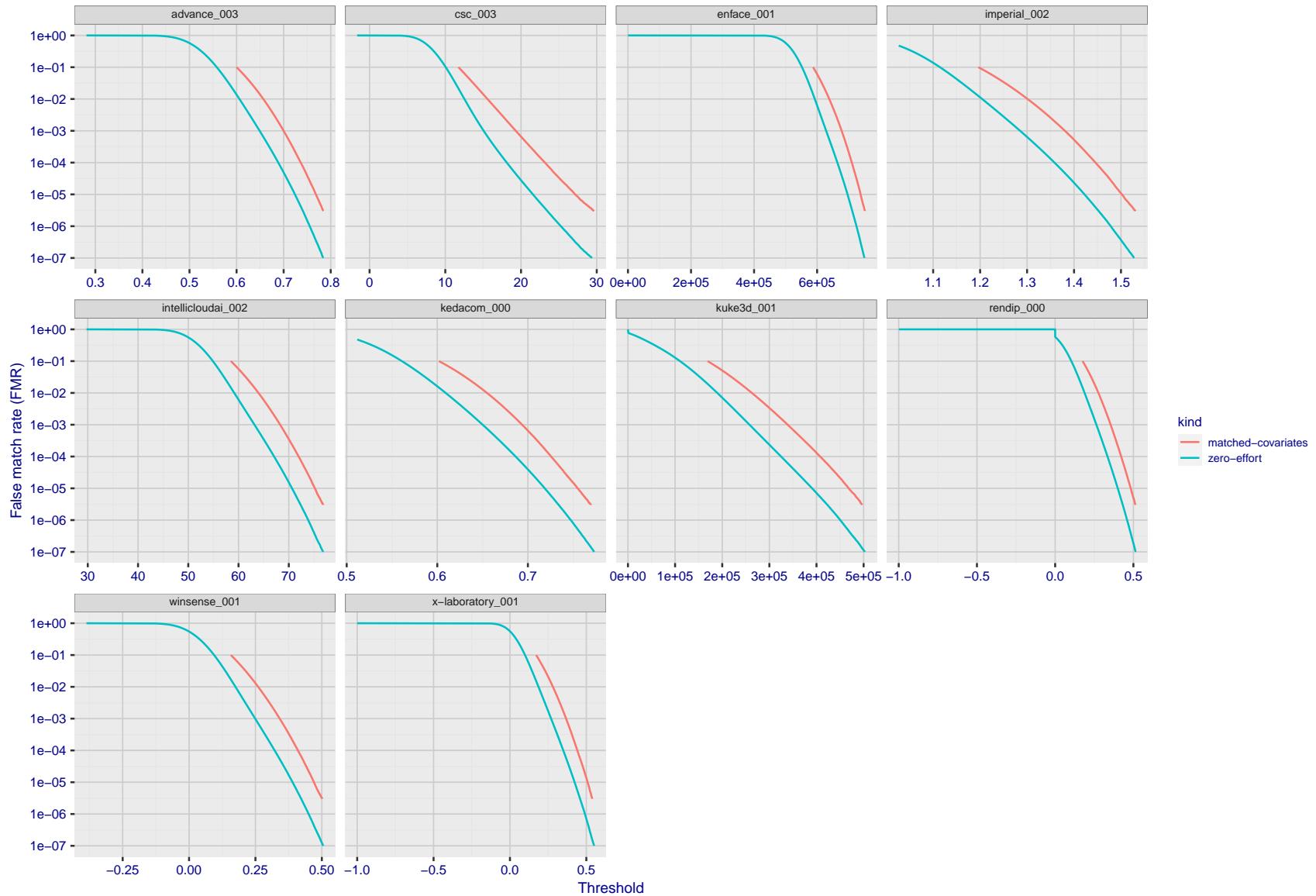


Figure 195: For the visa images, the false match calibration curves show FMR vs. threshold,  $T$ . The blue (lower) curves are for zero-effort impostors (i.e. comparing all images against all). The red (upper) curves are for persons of the same-sex, same-age, and same national-origin. This shows that FMR is underestimated (by a factor of 10 or more) by using a zero-effort impostor calculation to calibrate  $T$ . As shown later (sec. 3.6), FMR is higher for demographic-matched impostors.

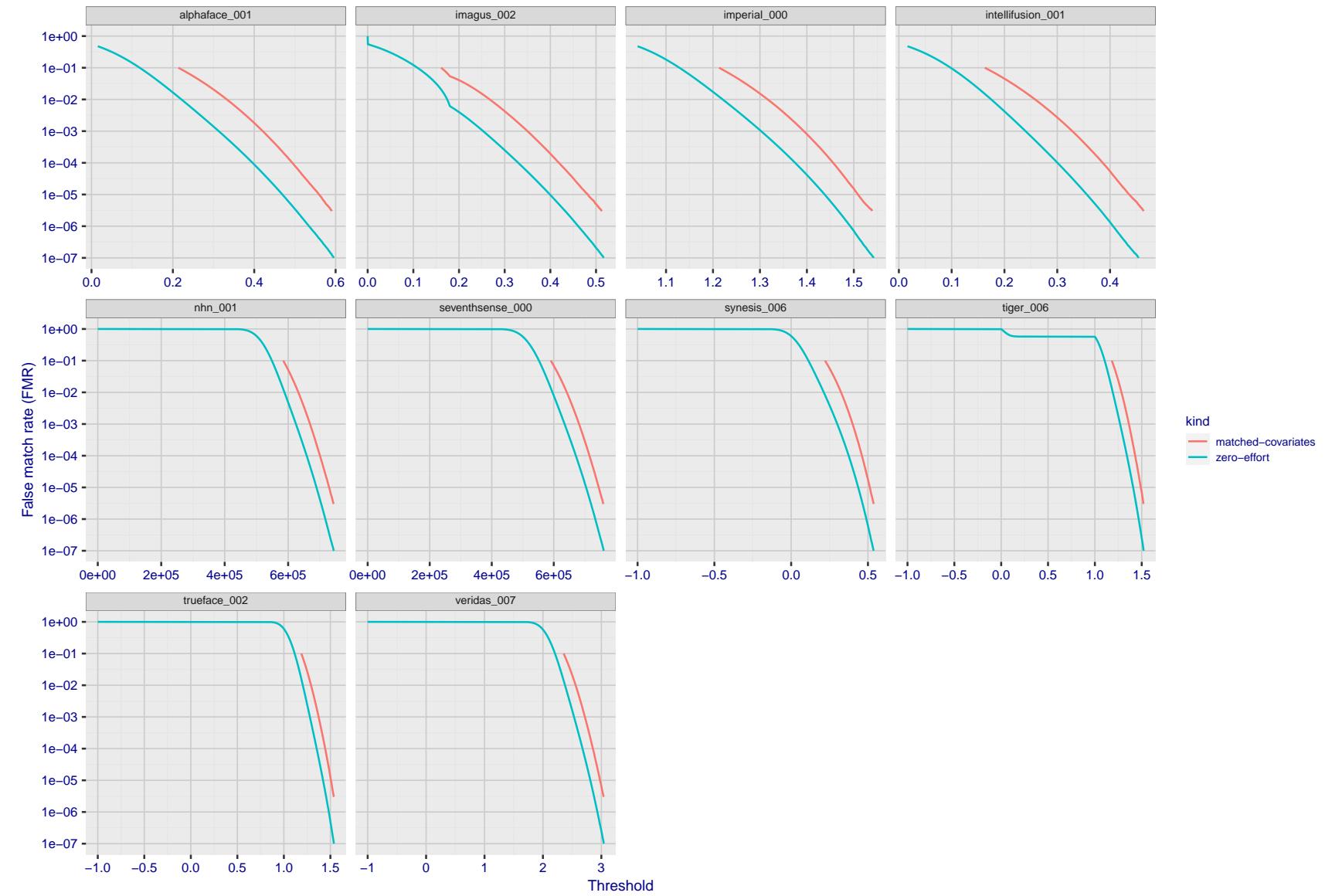


Figure 196: For the visa images, the false match calibration curves show FMR vs. threshold,  $T$ . The blue (lower) curves are for zero-effort impostors (i.e. comparing all images against all). The red (upper) curves are for persons of the same-sex, same-age, and same national-origin. This shows that FMR is underestimated (by a factor of 10 or more) by using a zero-effort impostor calculation to calibrate  $T$ . As shown later (sec. 3.6), FMR is higher for demographic-matched impostors.

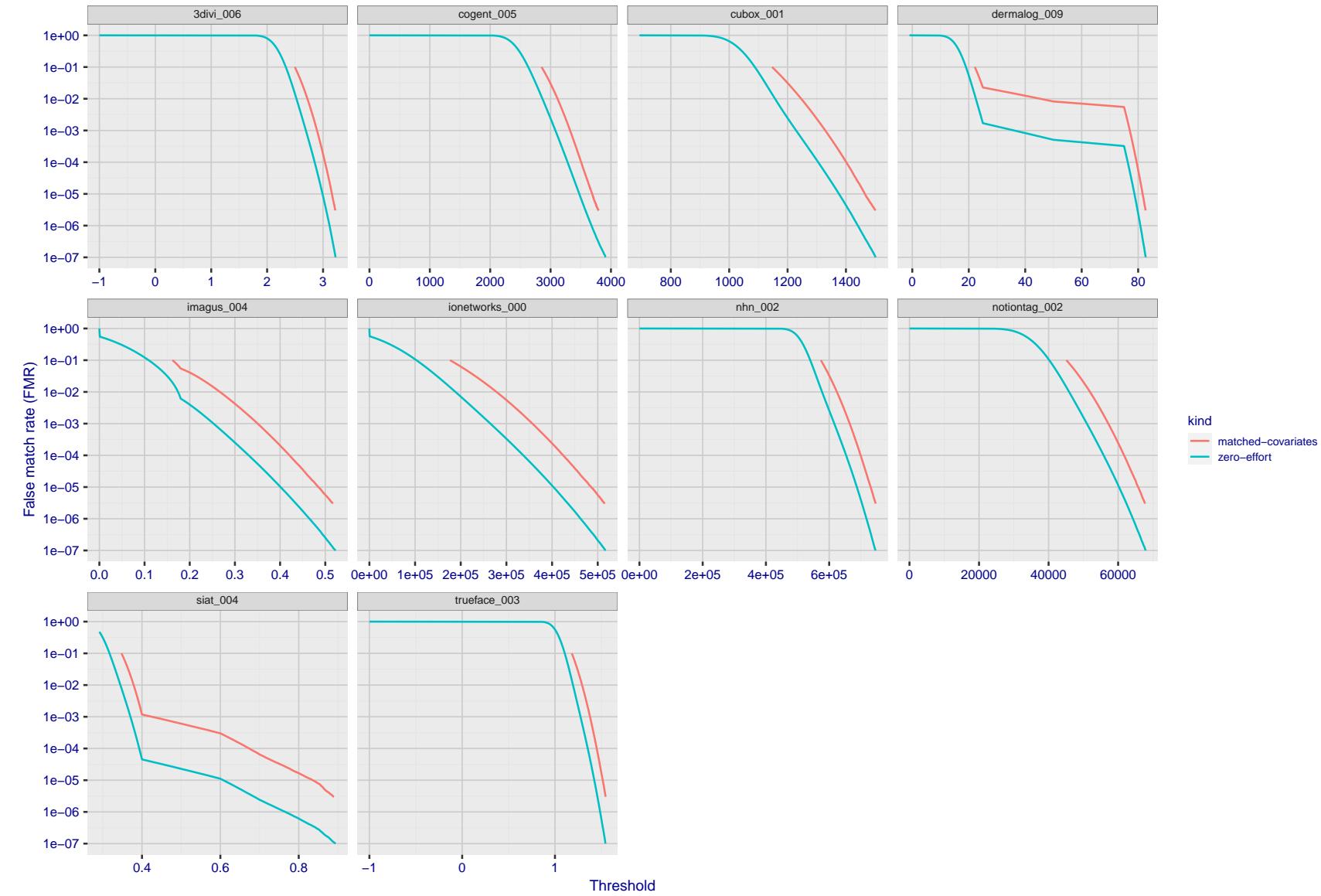


Figure 197: For the visa images, the false match calibration curves show FMR vs. threshold,  $T$ . The blue (lower) curves are for zero-effort impostors (i.e. comparing all images against all). The red (upper) curves are for persons of the same-sex, same-age, and same national-origin. This shows that FMR is underestimated (by a factor of 10 or more) by using a zero-effort impostor calculation to calibrate  $T$ . As shown later (sec. 3.6), FMR is higher for demographic-matched impostors.

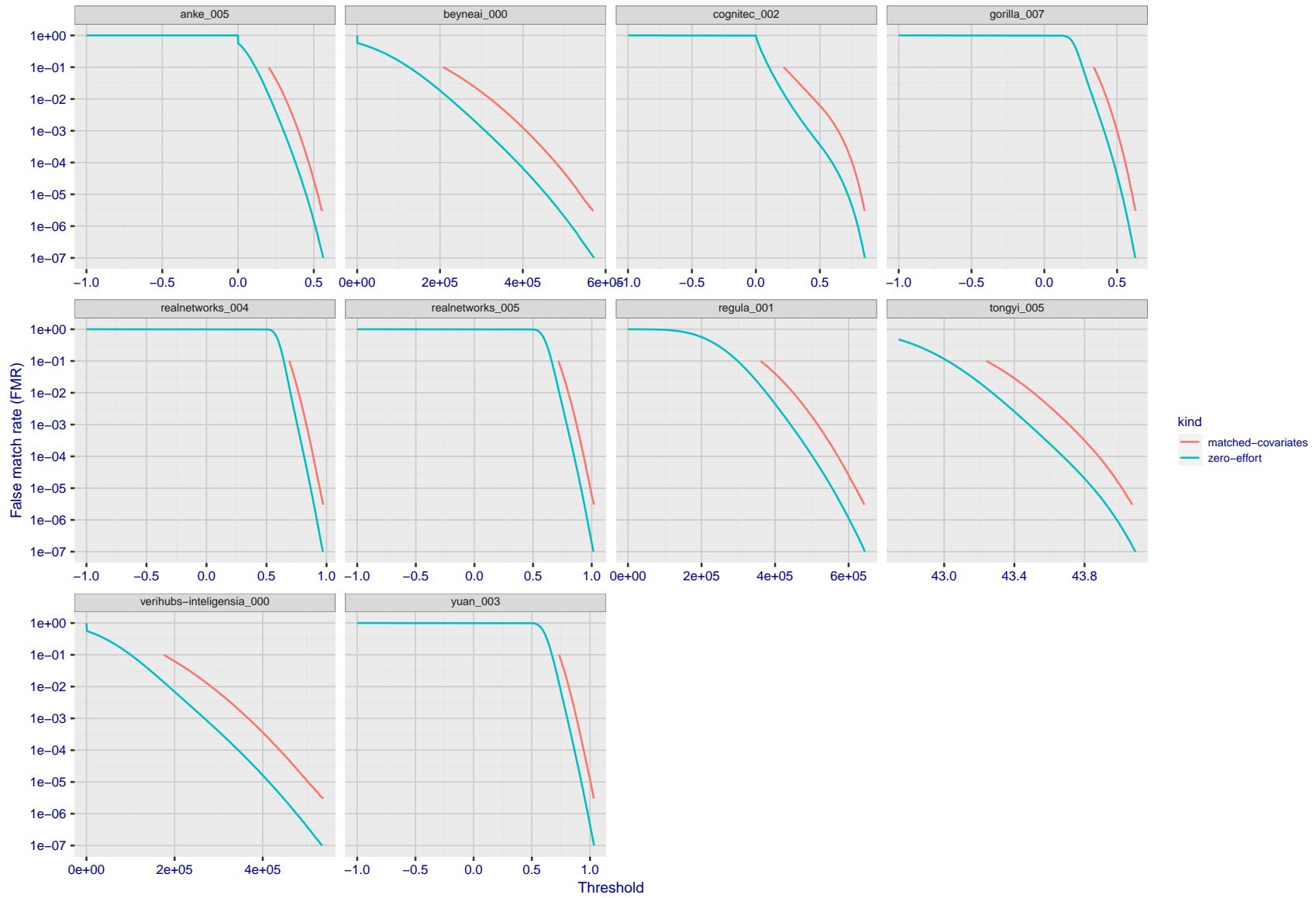


Figure 198: For the visa images, the false match calibration curves show FMR vs. threshold,  $T$ . The blue (lower) curves are for zero-effort impostors (i.e. comparing all images against all). The red (upper) curves are for persons of the same-sex, same-age, and same national-origin. This shows that FMR is underestimated (by a factor of 10 or more) by using a zero-effort impostor calculation to calibrate  $T$ . As shown later (sec. 3.6), FMR is higher for demographic-matched impostors.

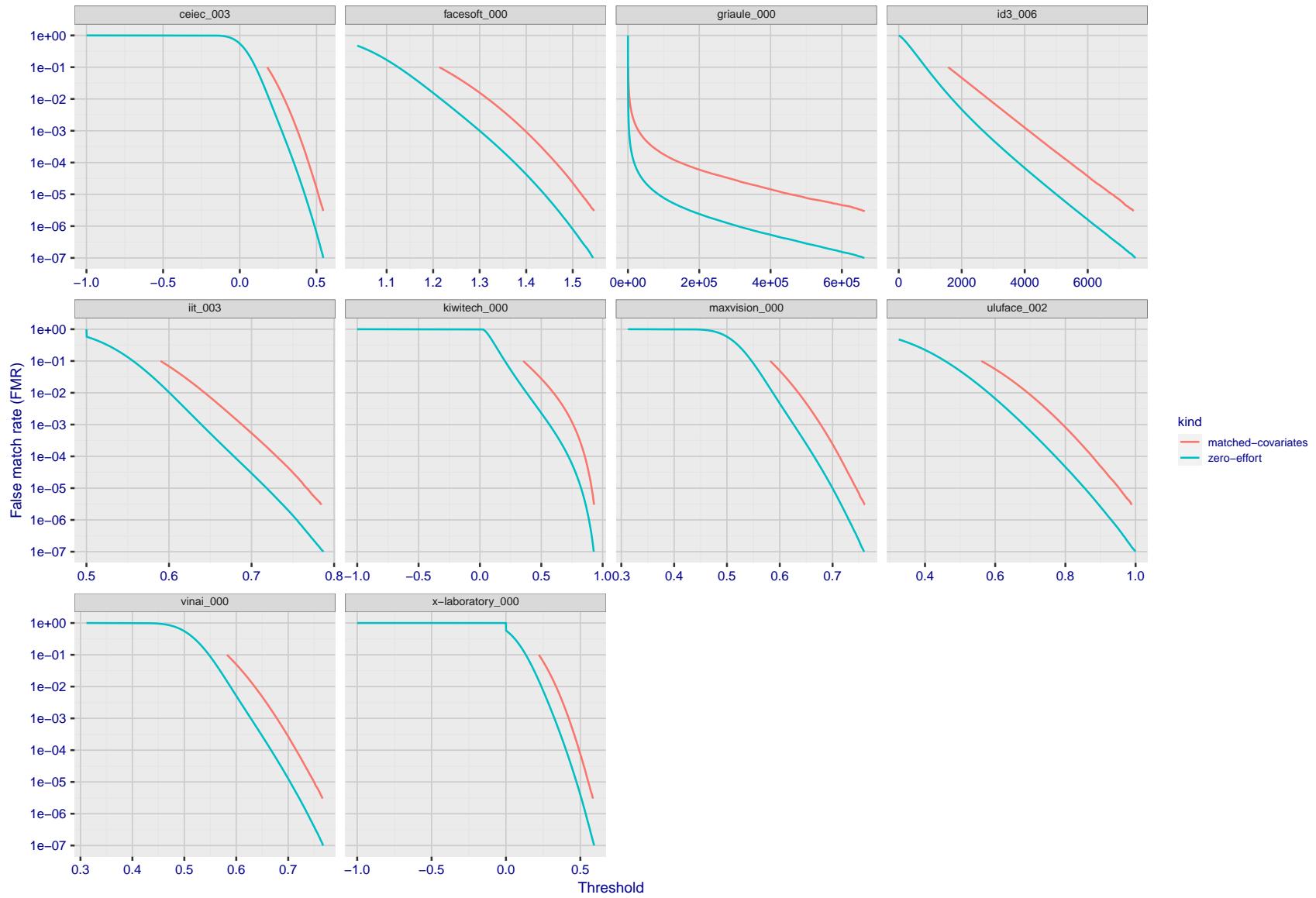


Figure 199: For the visa images, the false match calibration curves show FMR vs. threshold,  $T$ . The blue (lower) curves are for zero-effort impostors (i.e. comparing all images against all). The red (upper) curves are for persons of the same-sex, same-age, and same national-origin. This shows that FMR is underestimated (by a factor of 10 or more) by using a zero-effort impostor calculation to calibrate  $T$ . As shown later (sec. 3.6), FMR is higher for demographic-matched impostors.

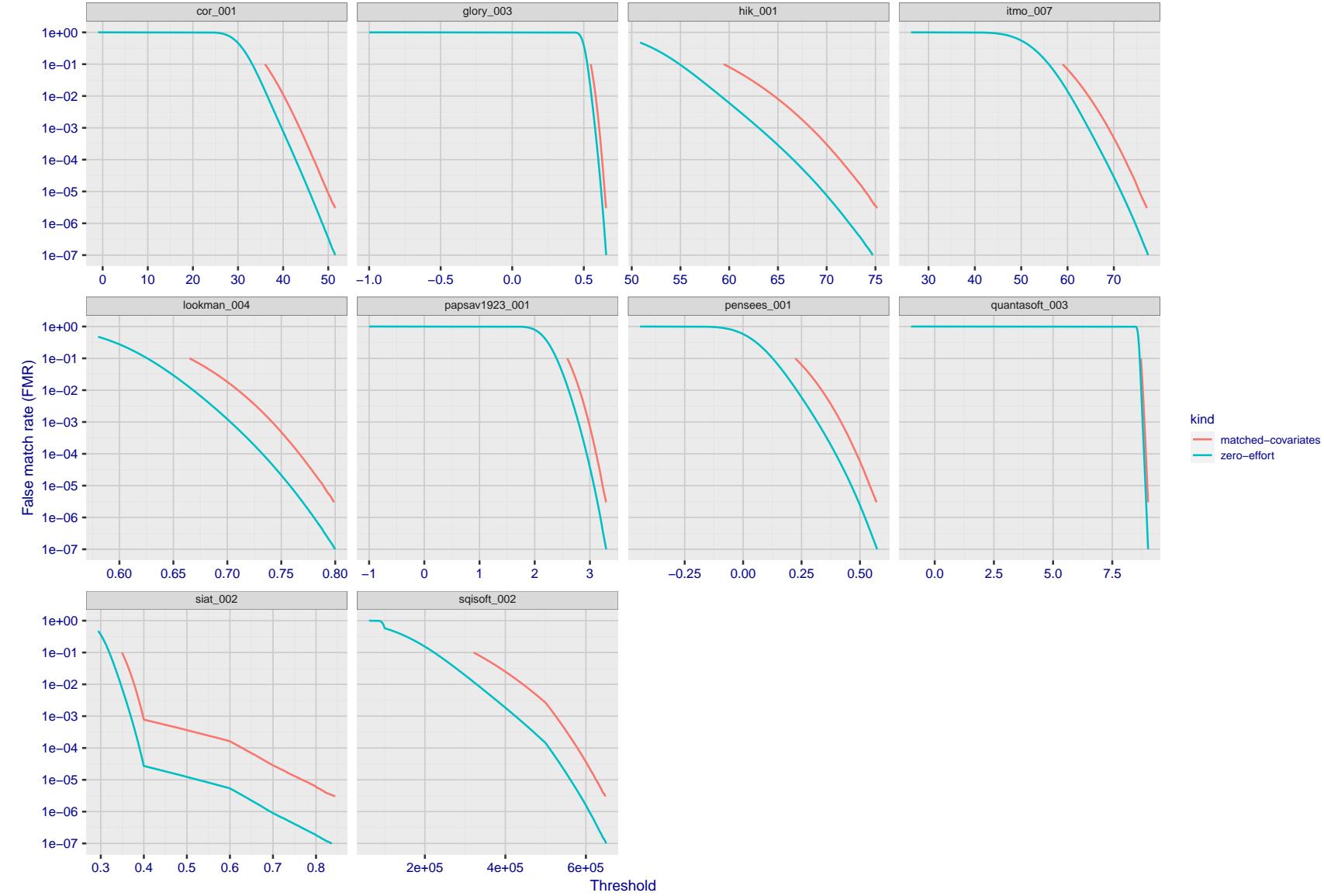


Figure 200: For the visa images, the false match calibration curves show FMR vs. threshold,  $T$ . The blue (lower) curves are for zero-effort impostors (i.e. comparing all images against all). The red (upper) curves are for persons of the same-sex, same-age, and same national-origin. This shows that FMR is underestimated (by a factor of 10 or more) by using a zero-effort impostor calculation to calibrate  $T$ . As shown later (sec. 3.6), FMR is higher for demographic-matched impostors.

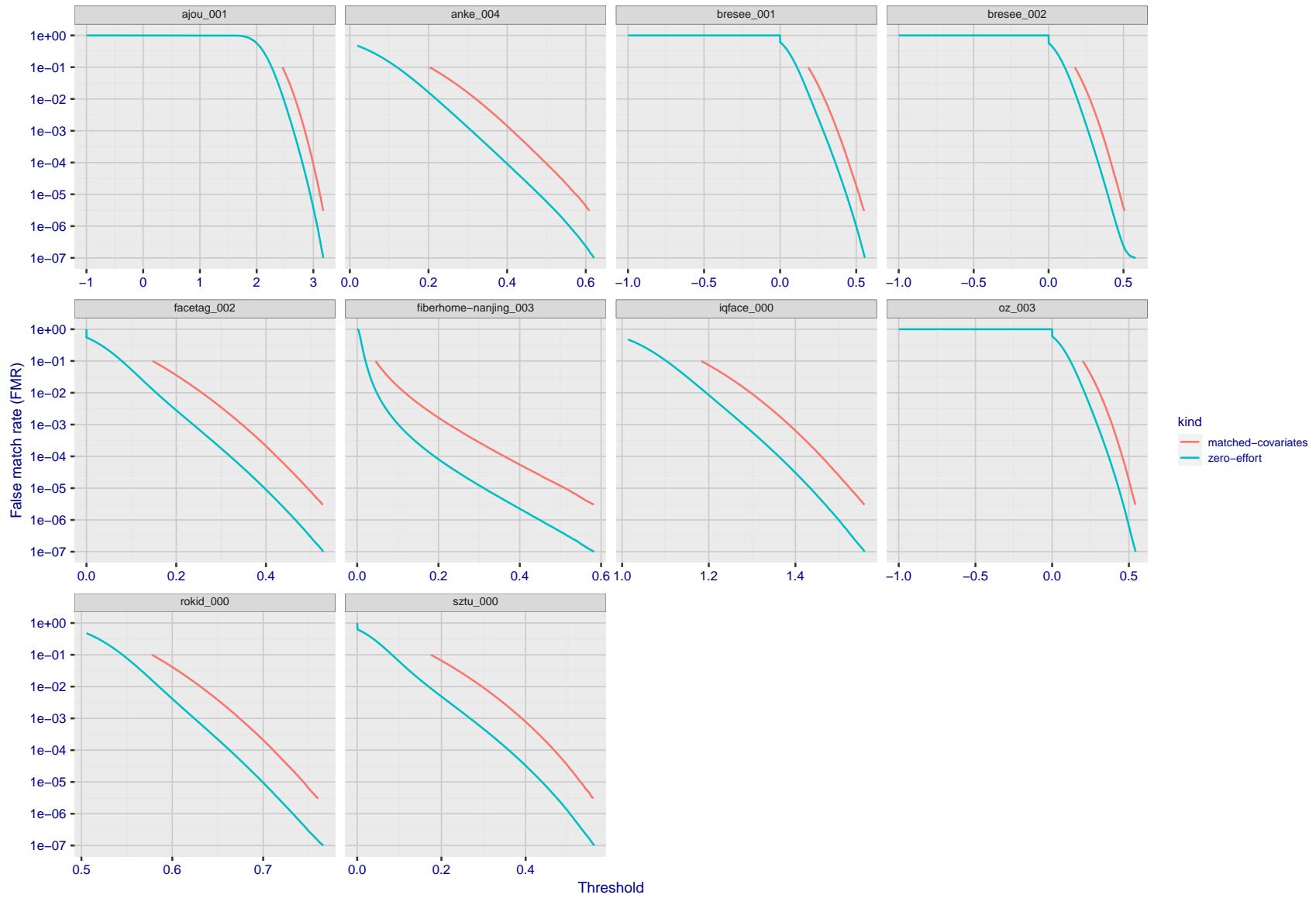


Figure 201: For the visa images, the false match calibration curves show FMR vs. threshold,  $T$ . The blue (lower) curves are for zero-effort impostors (i.e. comparing all images against all). The red (upper) curves are for persons of the same-sex, same-age, and same national-origin. This shows that FMR is underestimated (by a factor of 10 or more) by using a zero-effort impostor calculation to calibrate  $T$ . As shown later (sec. 3.6), FMR is higher for demographic-matched impostors.

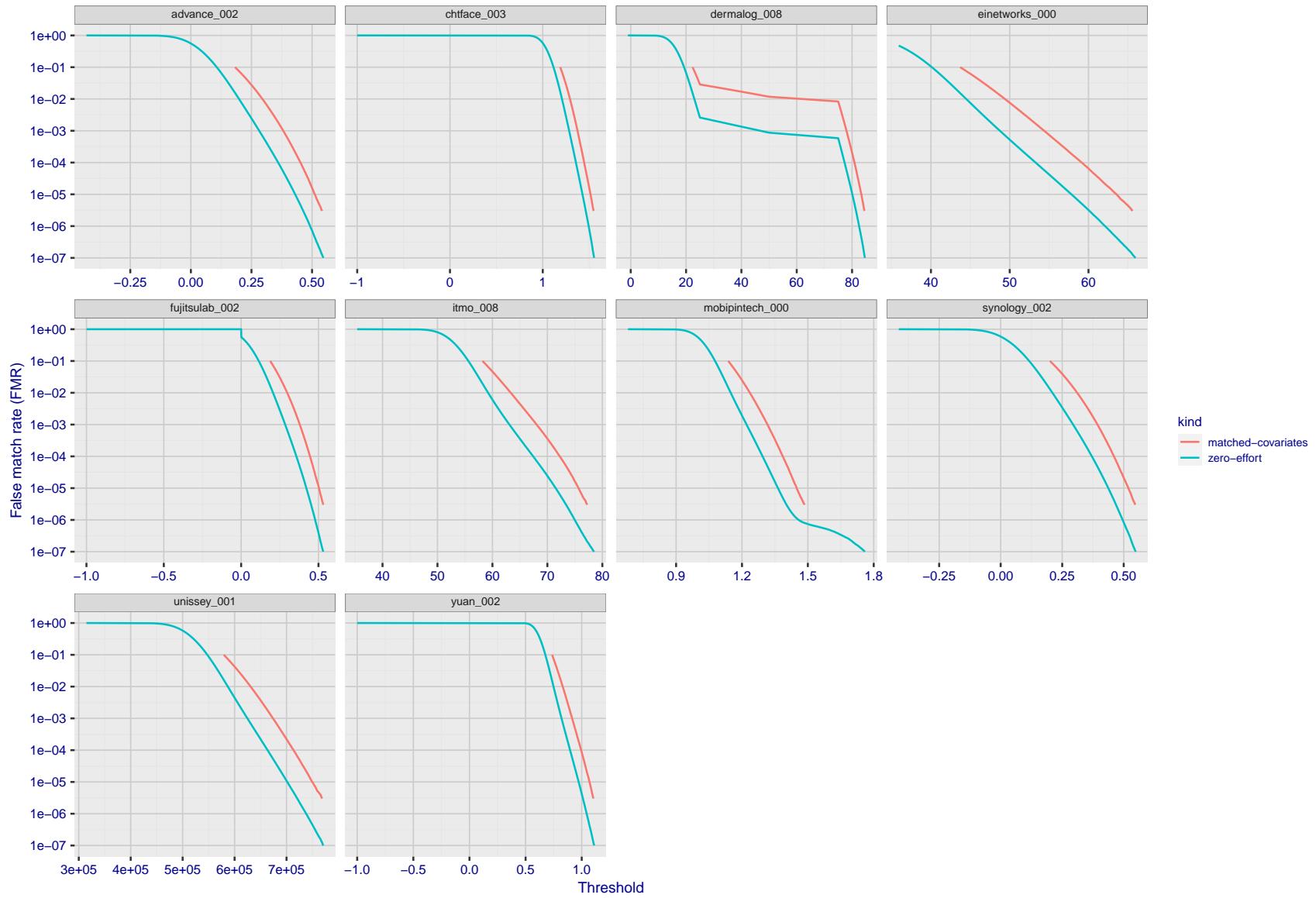


Figure 202: For the visa images, the false match calibration curves show FMR vs. threshold,  $T$ . The blue (lower) curves are for zero-effort impostors (i.e. comparing all images against all). The red (upper) curves are for persons of the same-sex, same-age, and same national-origin. This shows that FMR is underestimated (by a factor of 10 or more) by using a zero-effort impostor calculation to calibrate  $T$ . As shown later (sec. 3.6), FMR is higher for demographic-matched impostors.

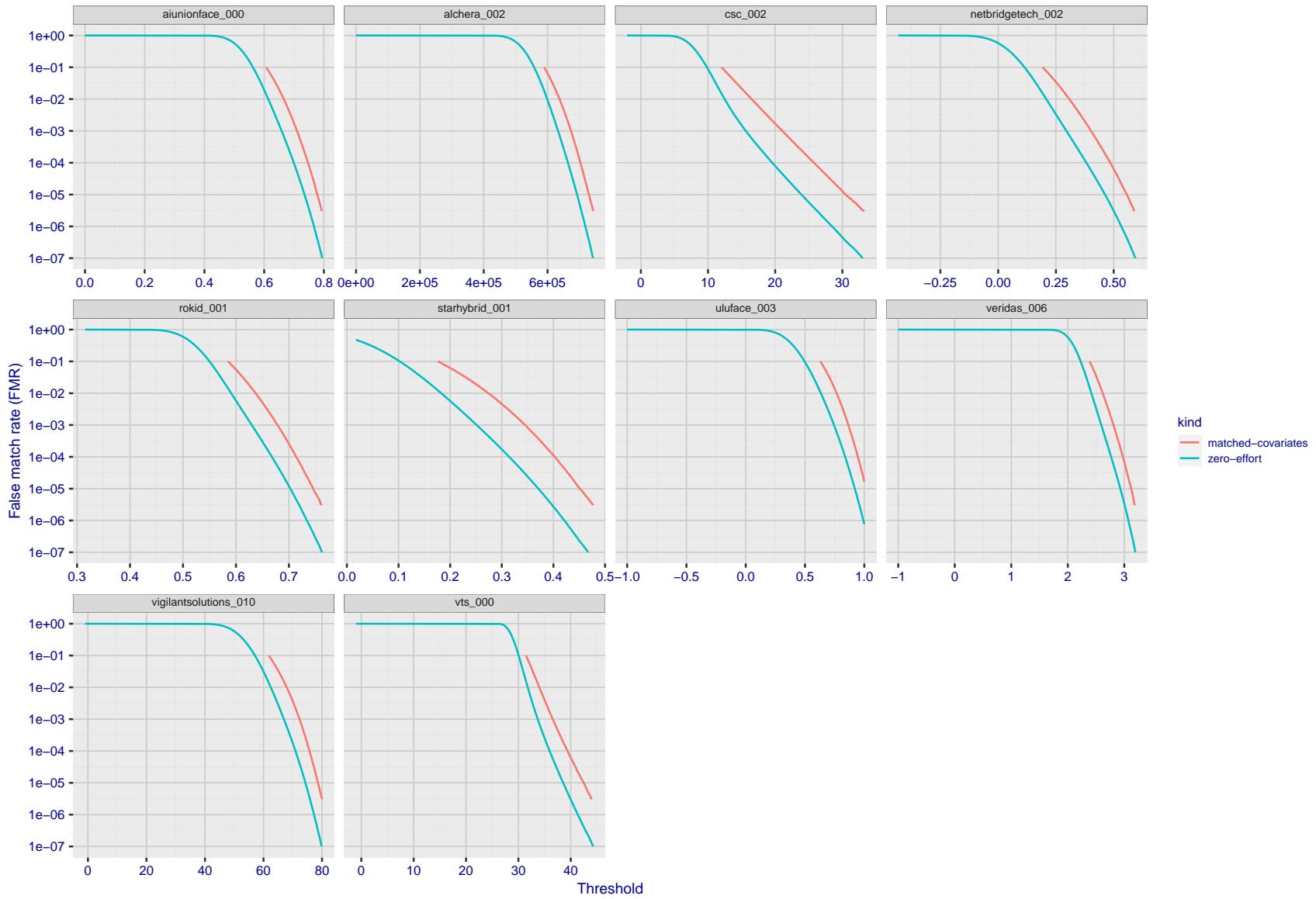


Figure 203: For the visa images, the false match calibration curves show FMR vs. threshold,  $T$ . The blue (lower) curves are for zero-effort impostors (i.e. comparing all images against all). The red (upper) curves are for persons of the same-sex, same-age, and same national-origin. This shows that FMR is underestimated (by a factor of 10 or more) by using a zero-effort impostor calculation to calibrate  $T$ . As shown later (sec. 3.6), FMR is higher for demographic-matched impostors.

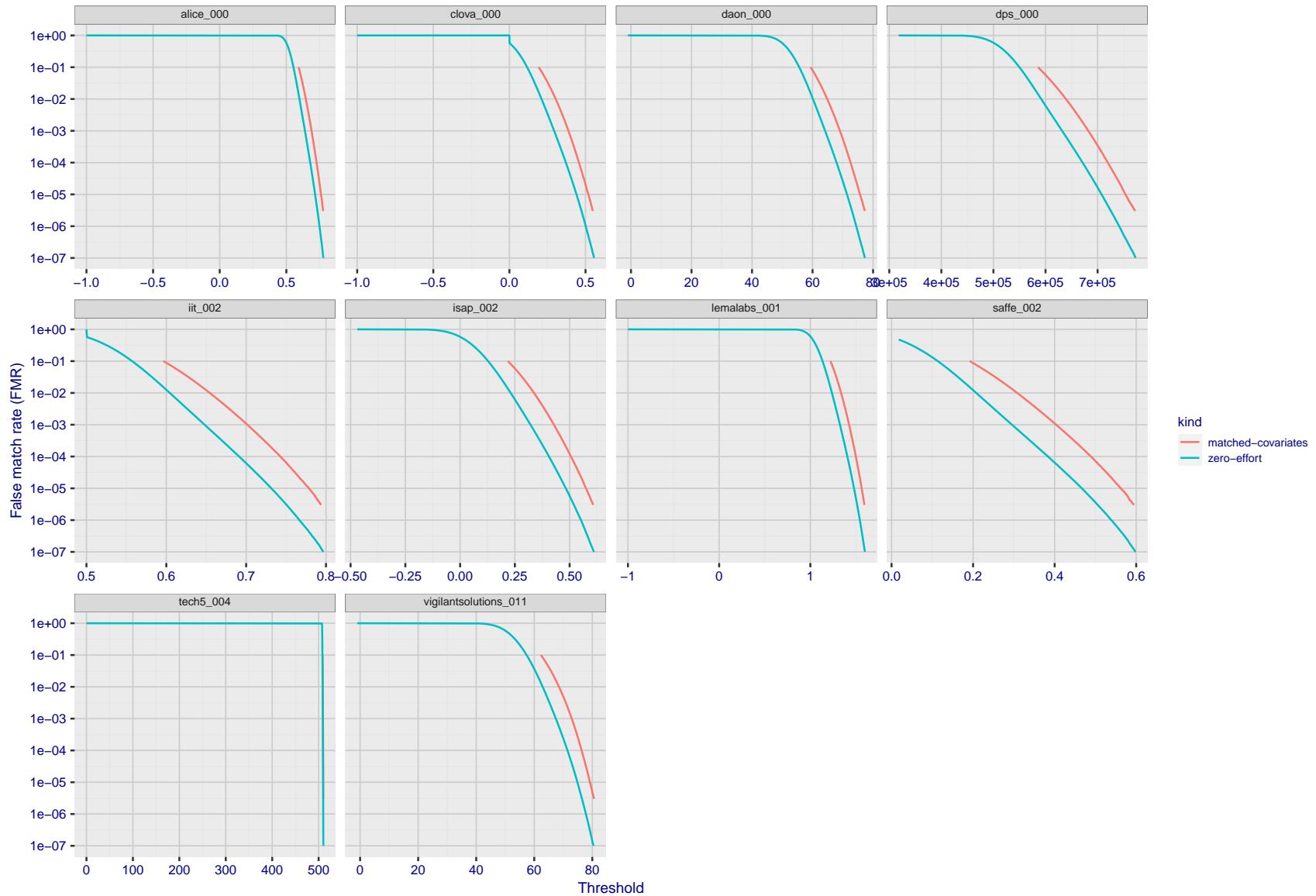


Figure 204: For the visa images, the false match calibration curves show FMR vs. threshold,  $T$ . The blue (lower) curves are for zero-effort impostors (i.e. comparing all images against all). The red (upper) curves are for persons of the same-sex, same-age, and same national-origin. This shows that FMR is underestimated (by a factor of 10 or more) by using a zero-effort impostor calculation to calibrate  $T$ . As shown later (sec. 3.6), FMR is higher for demographic-matched impostors.

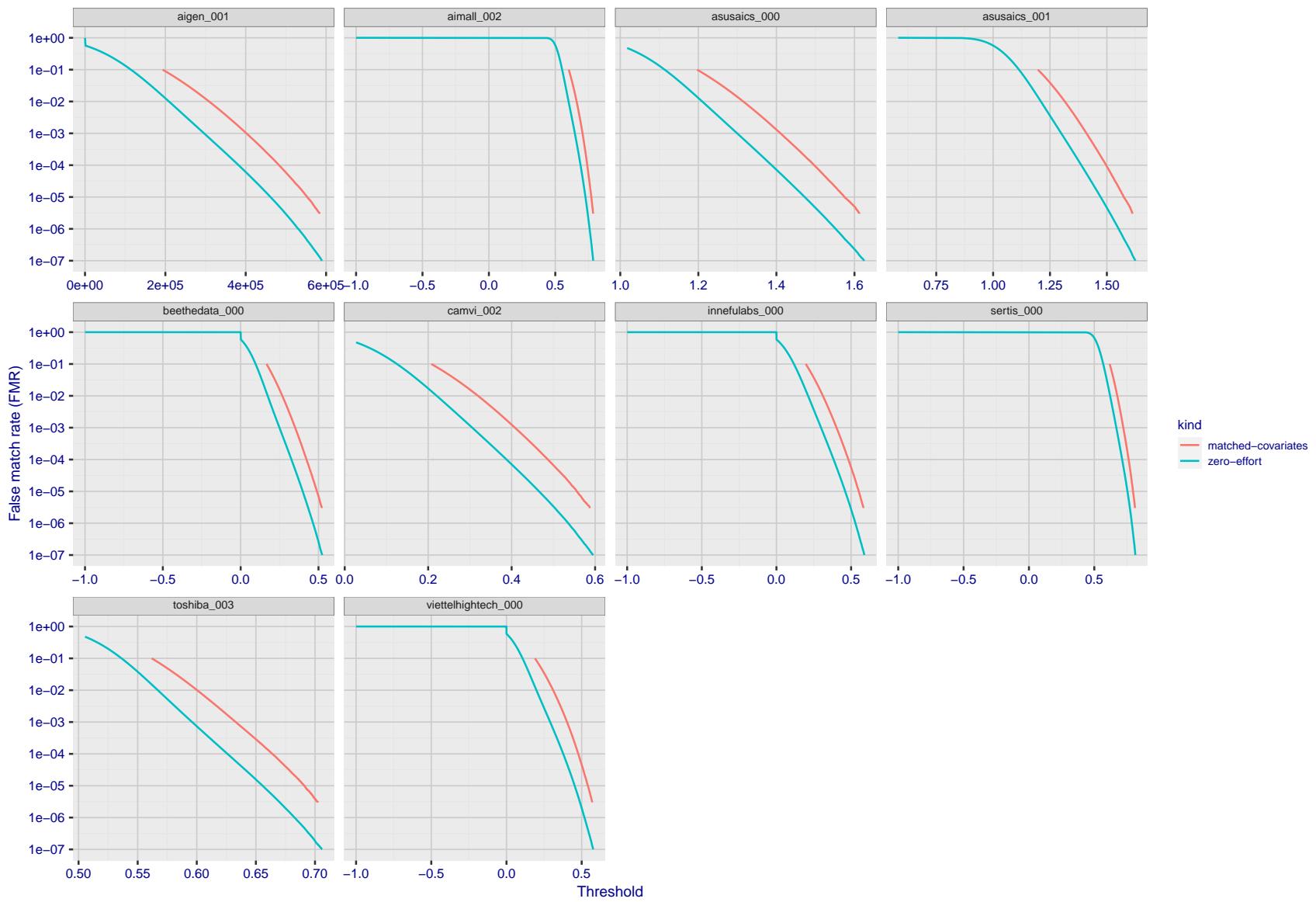


Figure 205: For the visa images, the false match calibration curves show FMR vs. threshold,  $T$ . The blue (lower) curves are for zero-effort impostors (i.e. comparing all images against all). The red (upper) curves are for persons of the same-sex, same-age, and same national-origin. This shows that FMR is underestimated (by a factor of 10 or more) by using a zero-effort impostor calculation to calibrate  $T$ . As shown later (sec. 3.6), FMR is higher for demographic-matched impostors.

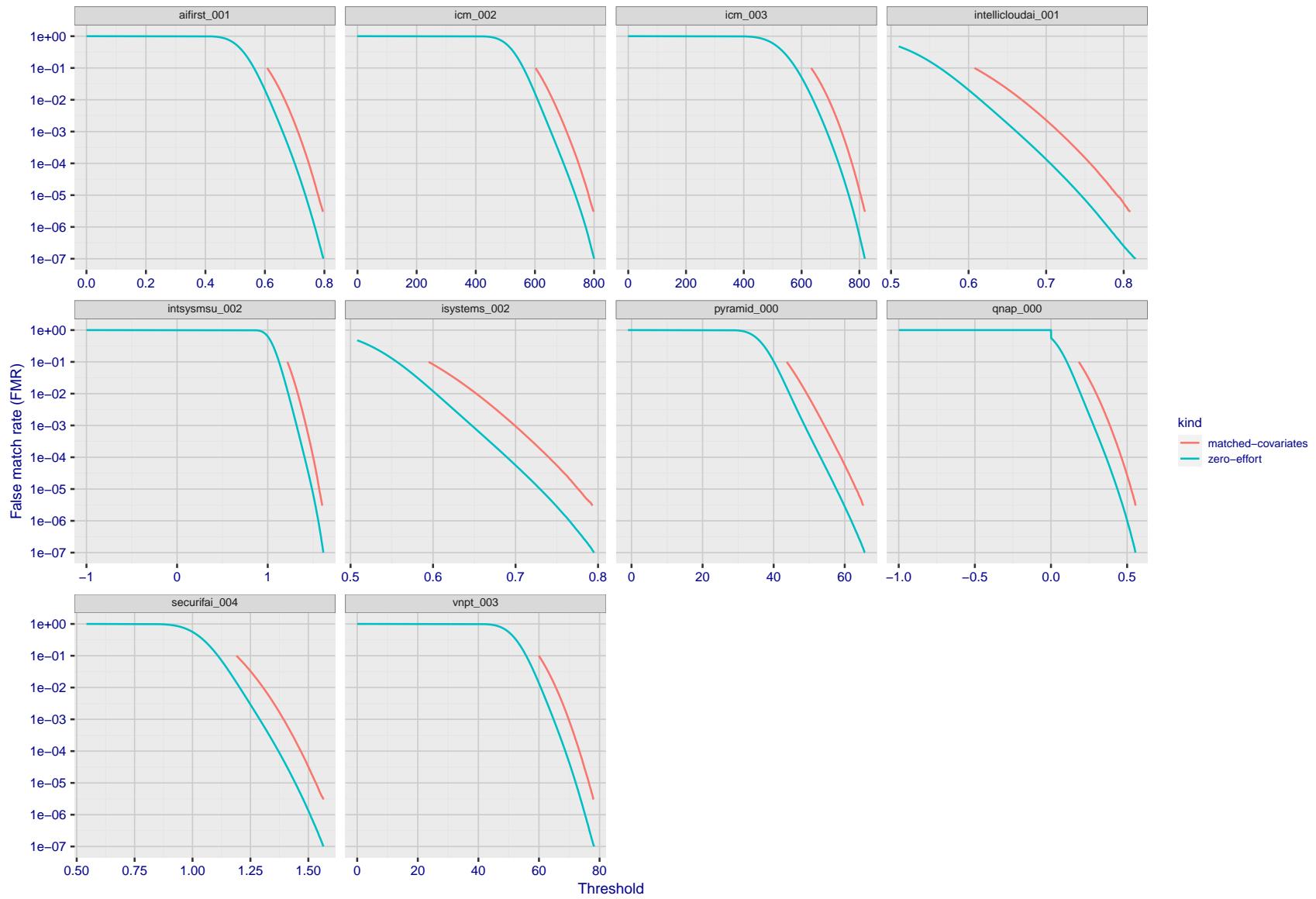


Figure 206: For the visa images, the false match calibration curves show FMR vs. threshold,  $T$ . The blue (lower) curves are for zero-effort impostors (i.e. comparing all images against all). The red (upper) curves are for persons of the same-sex, same-age, and same national-origin. This shows that FMR is underestimated (by a factor of 10 or more) by using a zero-effort impostor calculation to calibrate  $T$ . As shown later (sec. 3.6), FMR is higher for demographic-matched impostors.

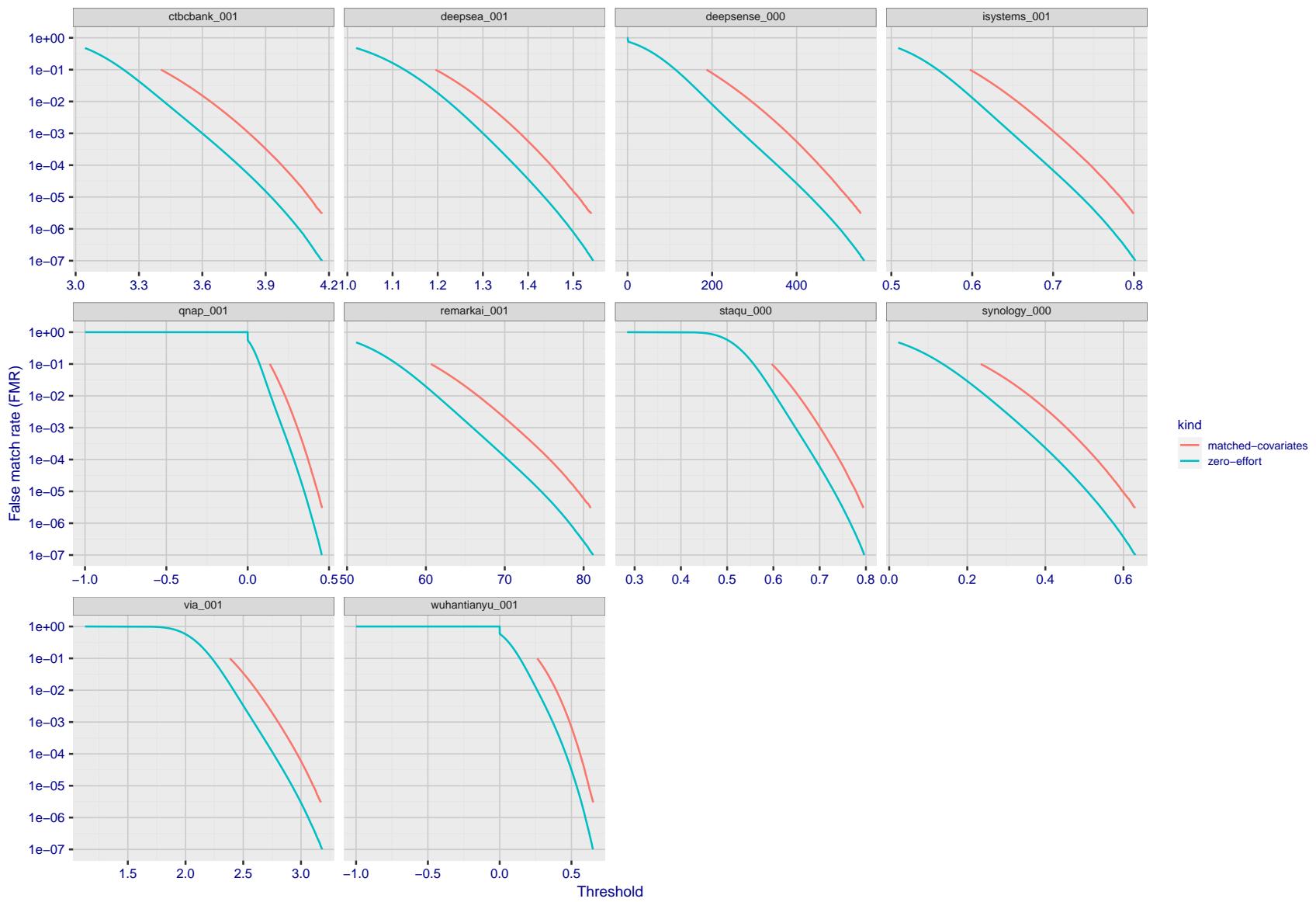


Figure 207: For the visa images, the false match calibration curves show FMR vs. threshold,  $T$ . The blue (lower) curves are for zero-effort impostors (i.e. comparing all images against all). The red (upper) curves are for persons of the same-sex, same-age, and same national-origin. This shows that FMR is underestimated (by a factor of 10 or more) by using a zero-effort impostor calculation to calibrate  $T$ . As shown later (sec. 3.6), FMR is higher for demographic-matched impostors.

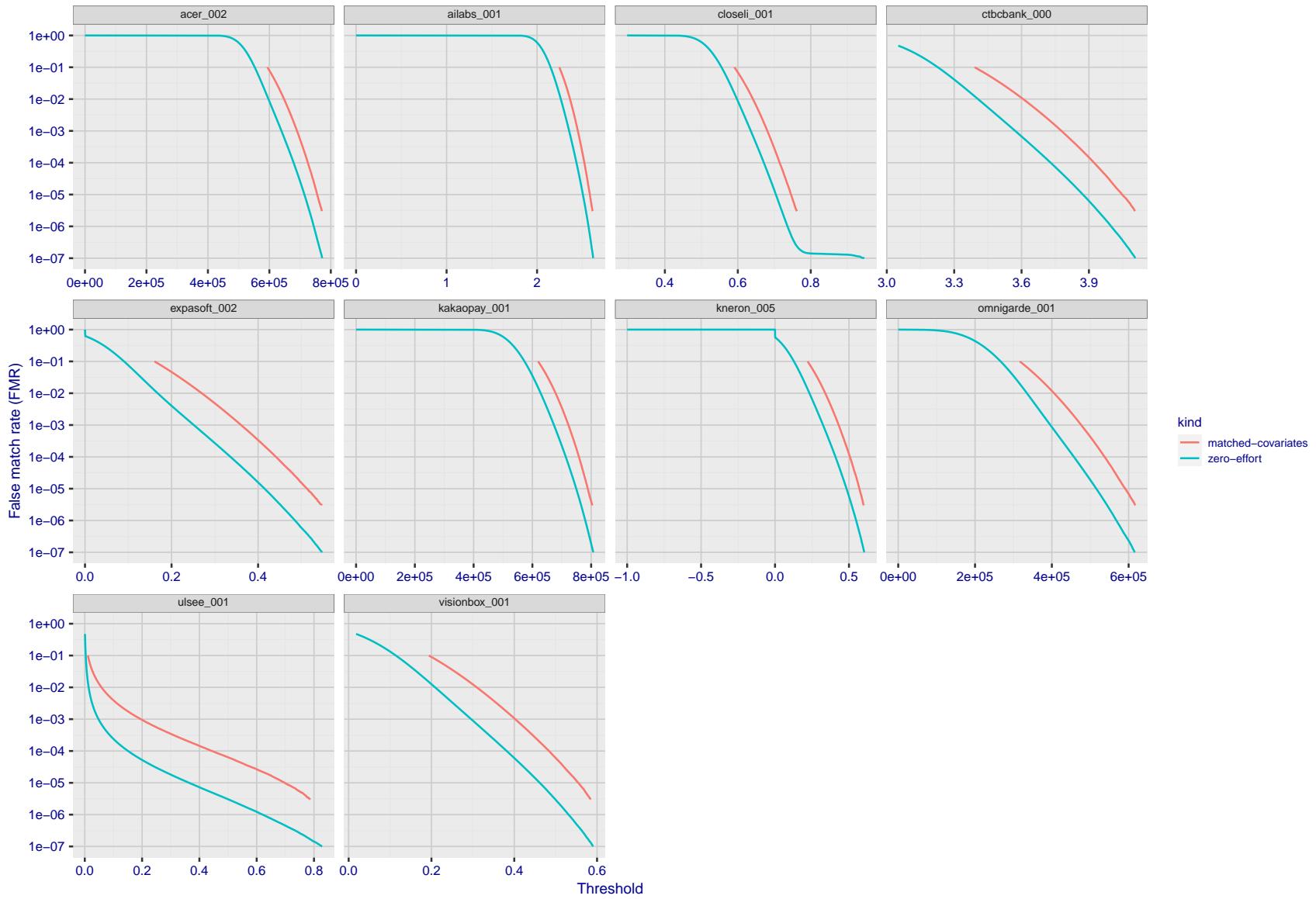


Figure 208: For the visa images, the false match calibration curves show FMR vs. threshold,  $T$ . The blue (lower) curves are for zero-effort impostors (i.e. comparing all images against all). The red (upper) curves are for persons of the same-sex, same-age, and same national-origin. This shows that FMR is underestimated (by a factor of 10 or more) by using a zero-effort impostor calculation to calibrate  $T$ . As shown later (sec. 3.6), FMR is higher for demographic-matched impostors.

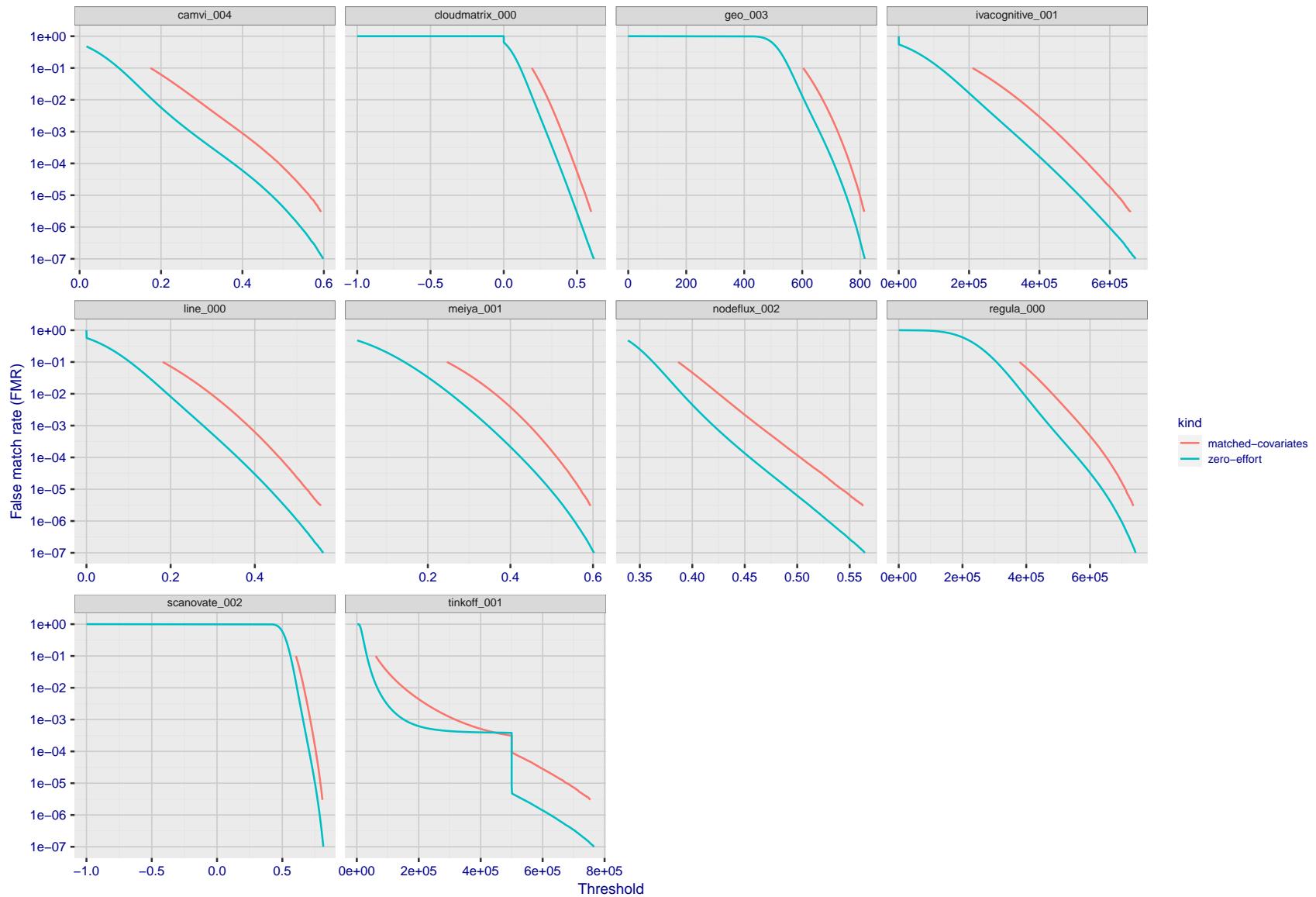


Figure 209: For the visa images, the false match calibration curves show FMR vs. threshold,  $T$ . The blue (lower) curves are for zero-effort impostors (i.e. comparing all images against all). The red (upper) curves are for persons of the same-sex, same-age, and same national-origin. This shows that FMR is underestimated (by a factor of 10 or more) by using a zero-effort impostor calculation to calibrate  $T$ . As shown later (sec. 3.6), FMR is higher for demographic-matched impostors.

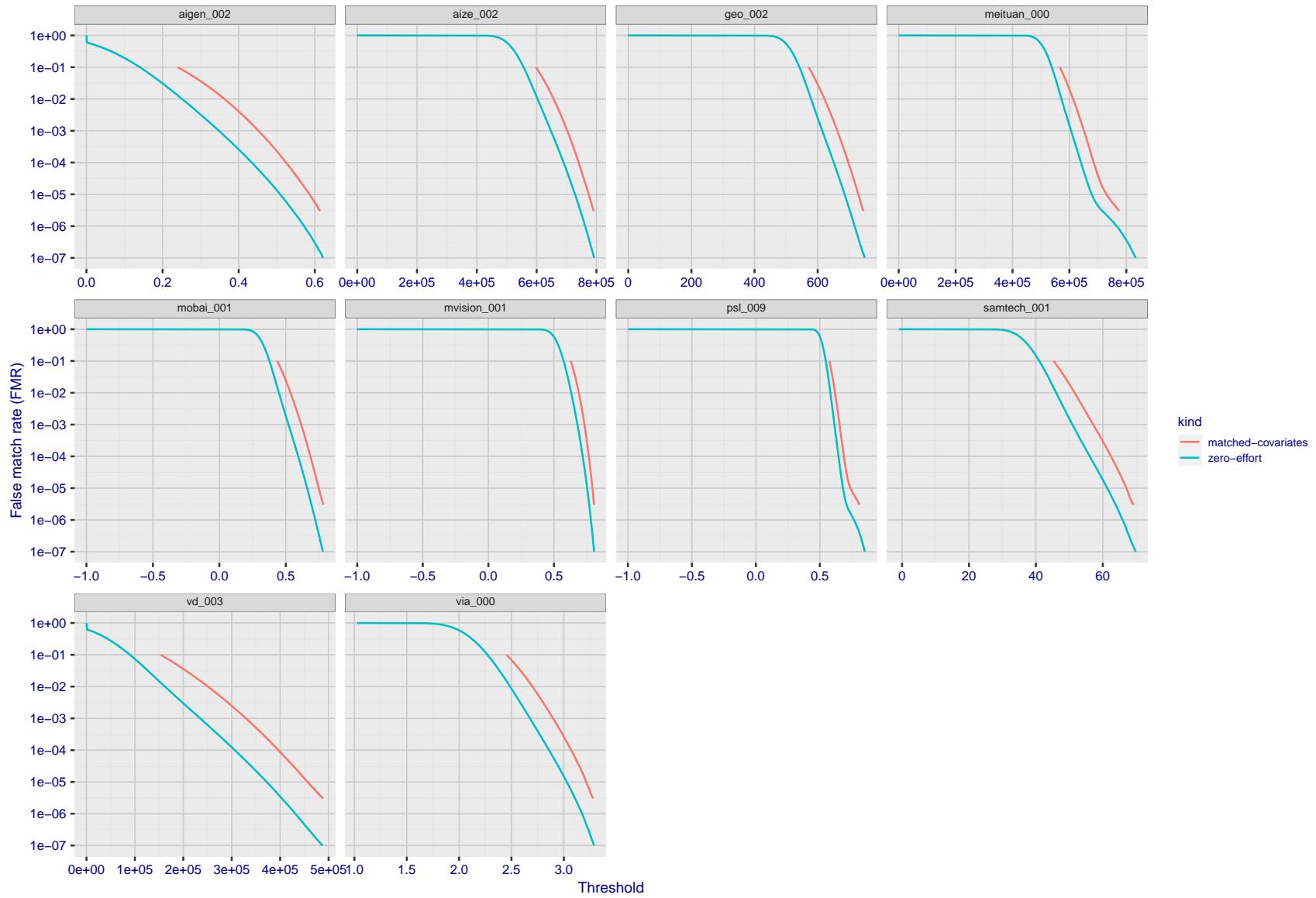


Figure 210: For the visa images, the false match calibration curves show FMR vs. threshold,  $T$ . The blue (lower) curves are for zero-effort impostors (i.e. comparing all images against all). The red (upper) curves are for persons of the same-sex, same-age, and same national-origin. This shows that FMR is underestimated (by a factor of 10 or more) by using a zero-effort impostor calculation to calibrate  $T$ . As shown later (sec. 3.6), FMR is higher for demographic-matched impostors.

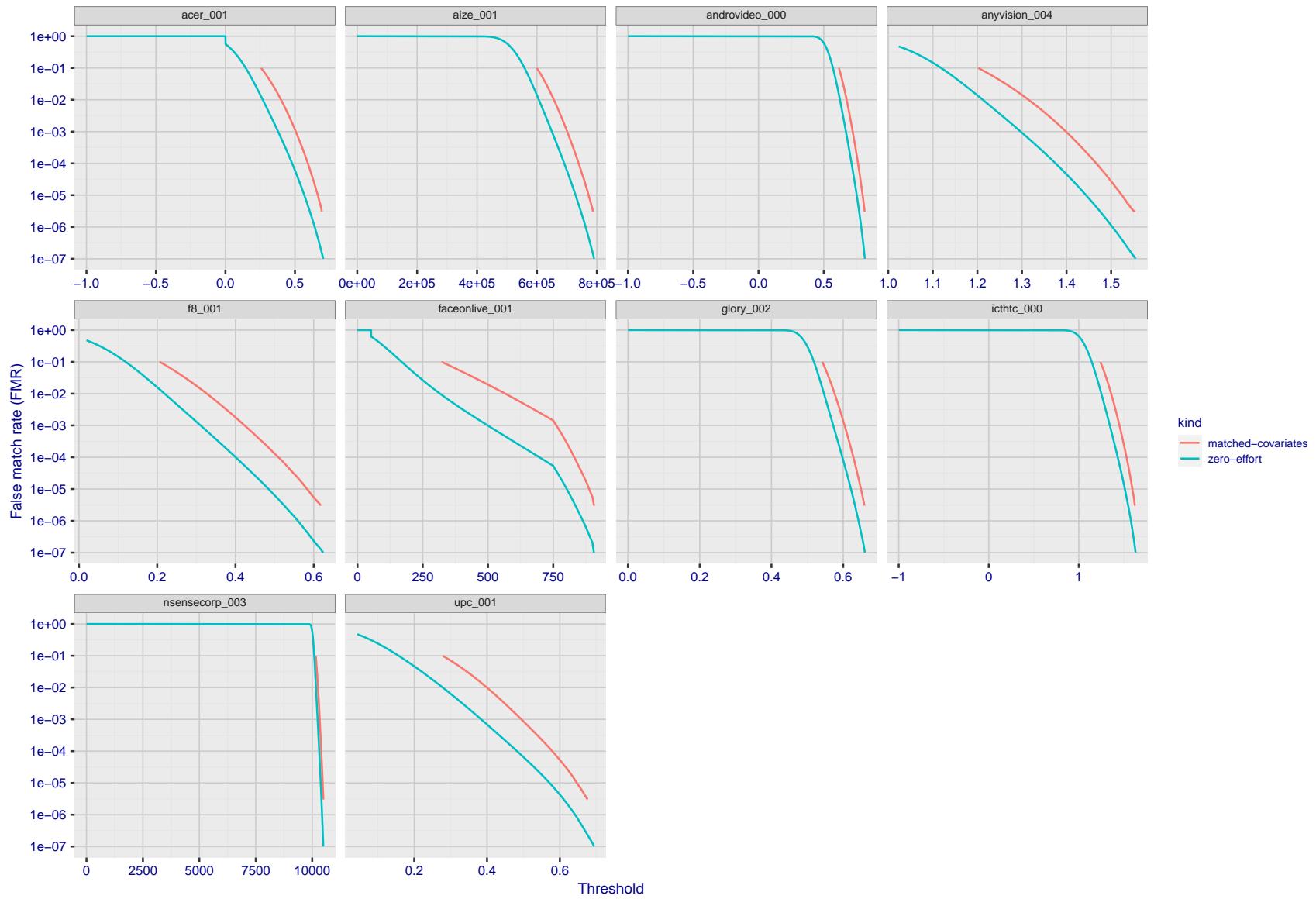


Figure 211: For the visa images, the false match calibration curves show FMR vs. threshold,  $T$ . The blue (lower) curves are for zero-effort impostors (i.e. comparing all images against all). The red (upper) curves are for persons of the same-sex, same-age, and same national-origin. This shows that FMR is underestimated (by a factor of 10 or more) by using a zero-effort impostor calculation to calibrate  $T$ . As shown later (sec. 3.6), FMR is higher for demographic-matched impostors.

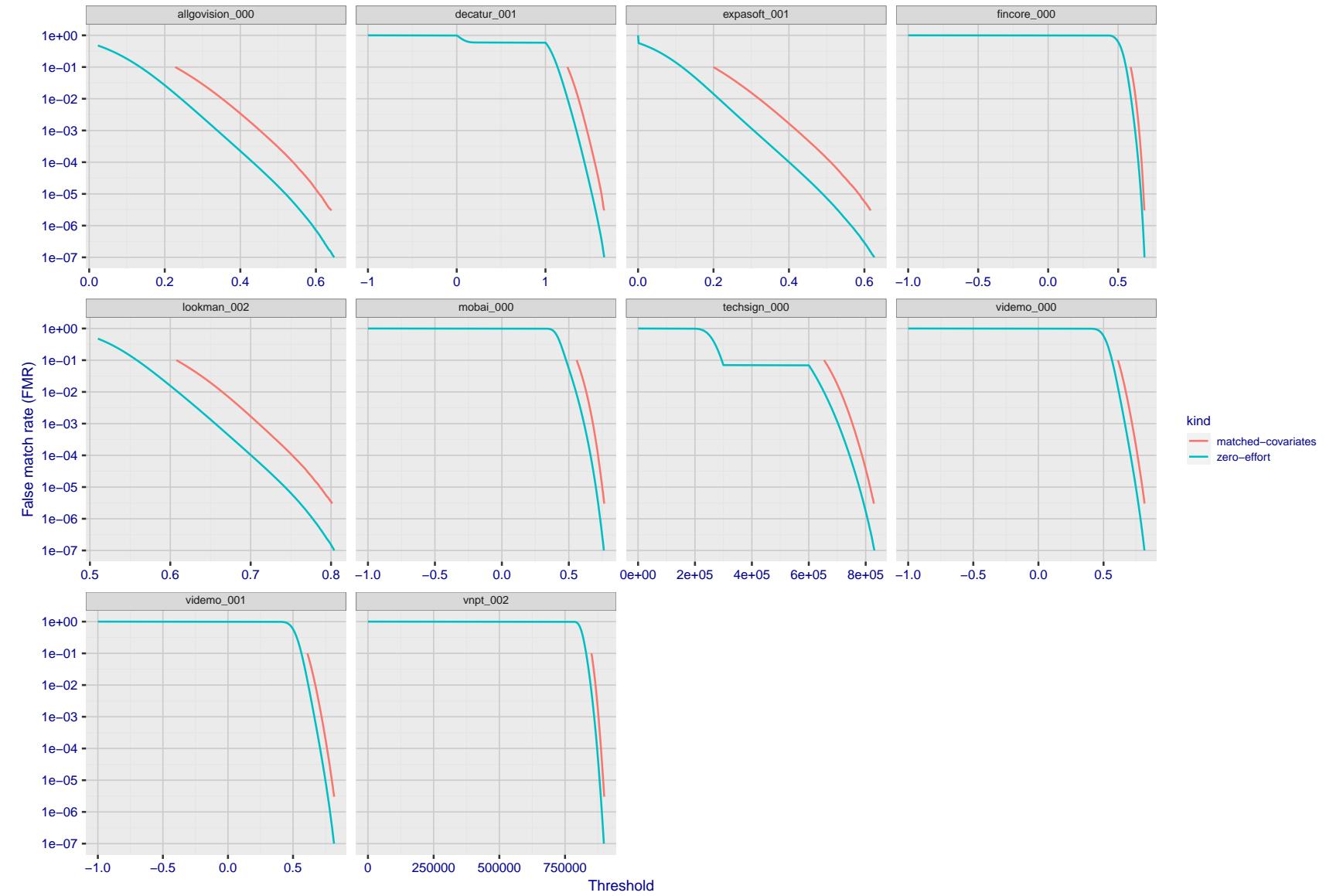


Figure 212: For the visa images, the false match calibration curves show FMR vs. threshold,  $T$ . The blue (lower) curves are for zero-effort impostors (i.e. comparing all images against all). The red (upper) curves are for persons of the same-sex, same-age, and same national-origin. This shows that FMR is underestimated (by a factor of 10 or more) by using a zero-effort impostor calculation to calibrate  $T$ . As shown later (sec. 3.6), FMR is higher for demographic-matched impostors.

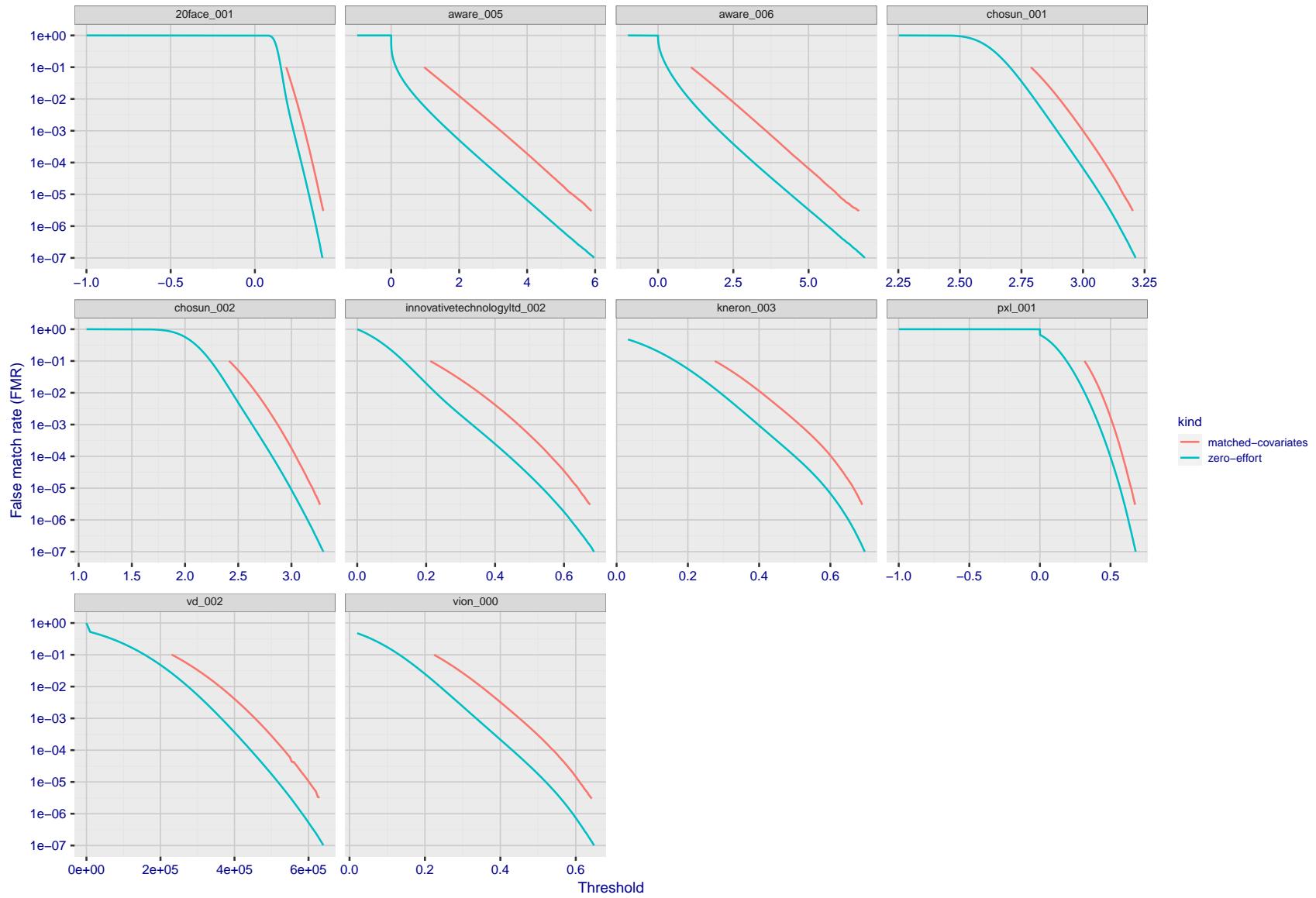


Figure 213: For the visa images, the false match calibration curves show FMR vs. threshold,  $T$ . The blue (lower) curves are for zero-effort impostors (i.e. comparing all images against all). The red (upper) curves are for persons of the same-sex, same-age, and same national-origin. This shows that FMR is underestimated (by a factor of 10 or more) by using a zero-effort impostor calculation to calibrate  $T$ . As shown later (sec. 3.6), FMR is higher for demographic-matched impostors.

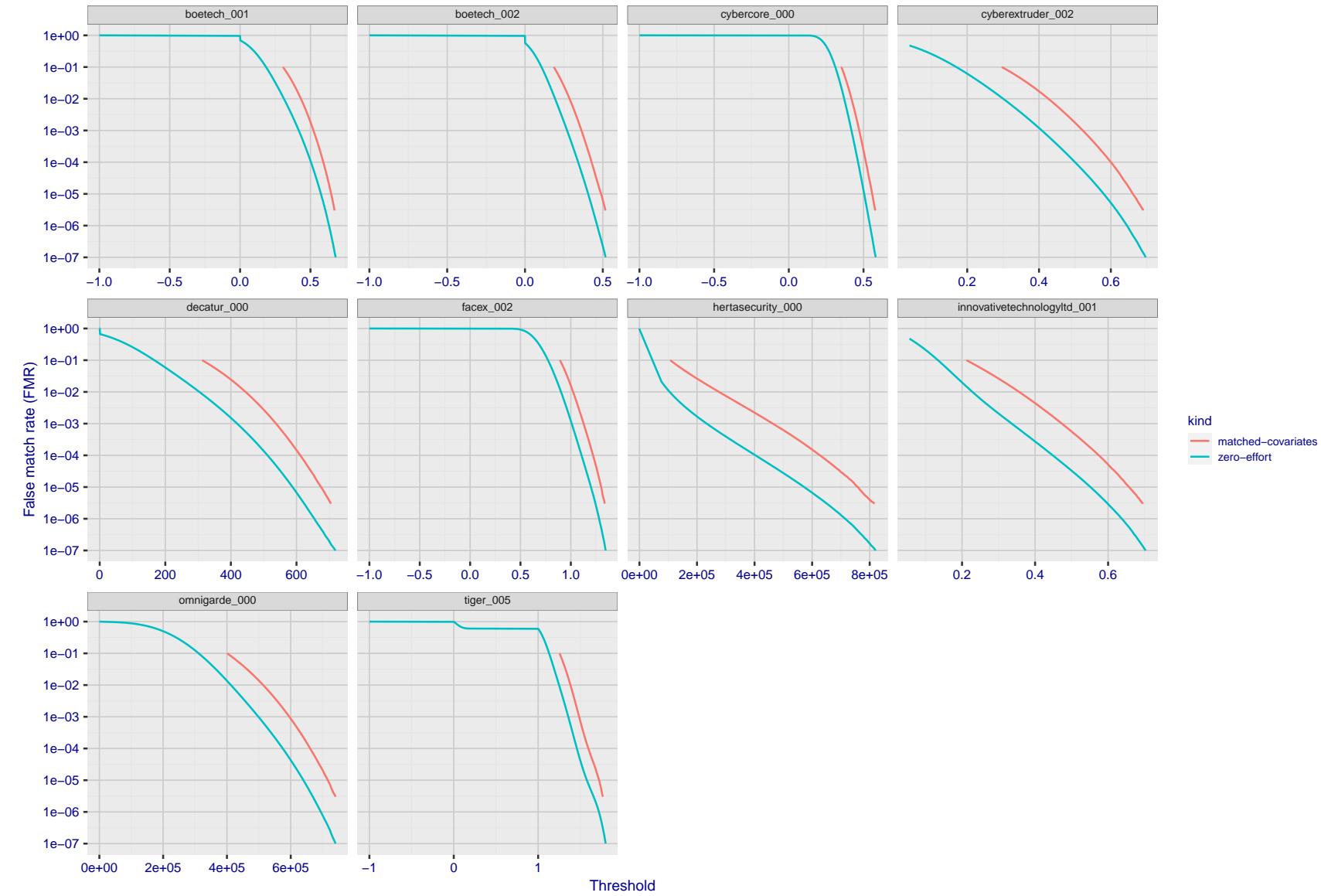


Figure 214: For the visa images, the false match calibration curves show FMR vs. threshold,  $T$ . The blue (lower) curves are for zero-effort impostors (i.e. comparing all images against all). The red (upper) curves are for persons of the same-sex, same-age, and same national-origin. This shows that FMR is underestimated (by a factor of 10 or more) by using a zero-effort impostor calculation to calibrate  $T$ . As shown later (sec. 3.6), FMR is higher for demographic-matched impostors.

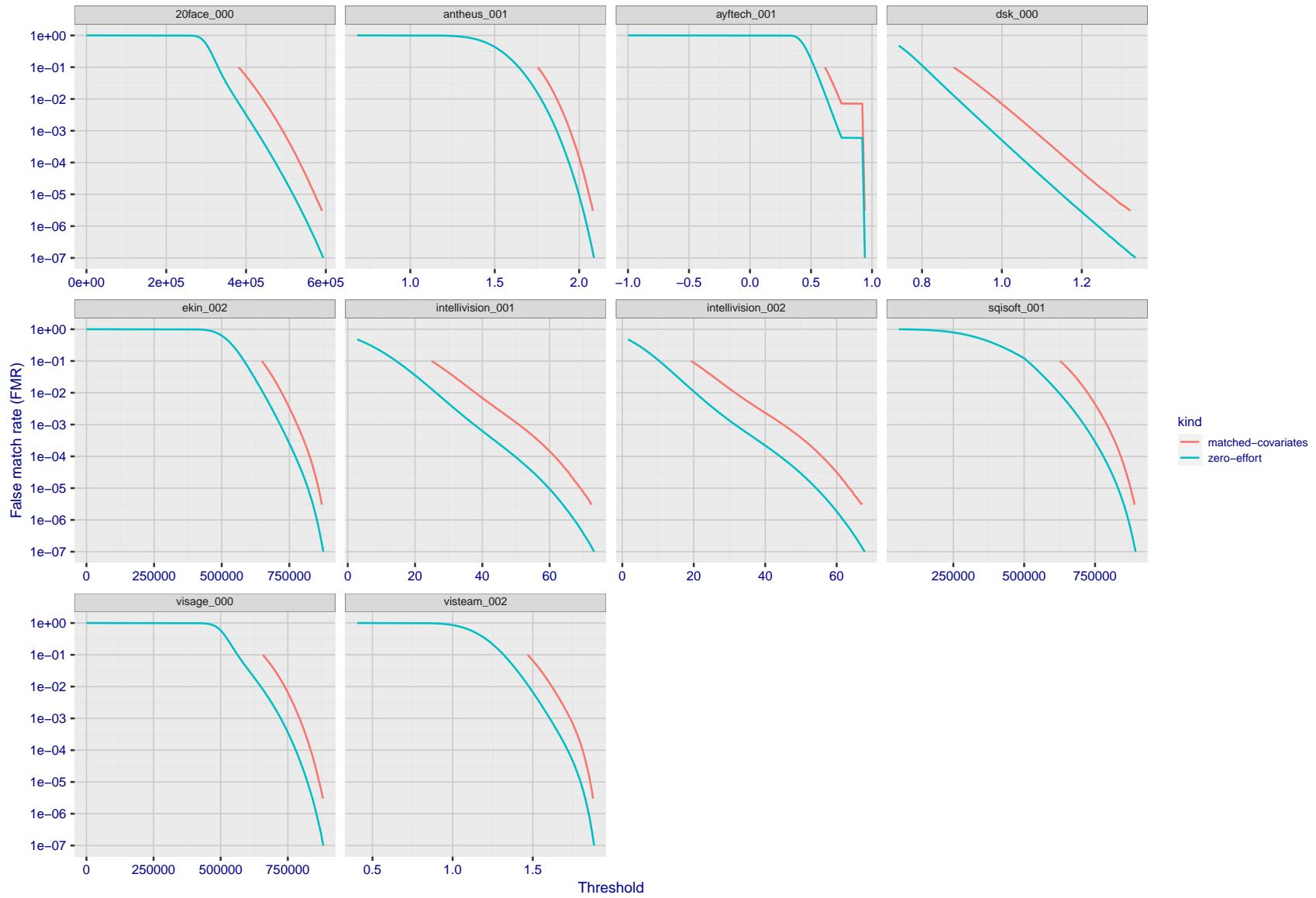


Figure 215: For the visa images, the false match calibration curves show FMR vs. threshold,  $T$ . The blue (lower) curves are for zero-effort impostors (i.e. comparing all images against all). The red (upper) curves are for persons of the same-sex, same-age, and same national-origin. This shows that FMR is underestimated (by a factor of 10 or more) by using a zero-effort impostor calculation to calibrate  $T$ . As shown later (sec. 3.6), FMR is higher for demographic-matched impostors.

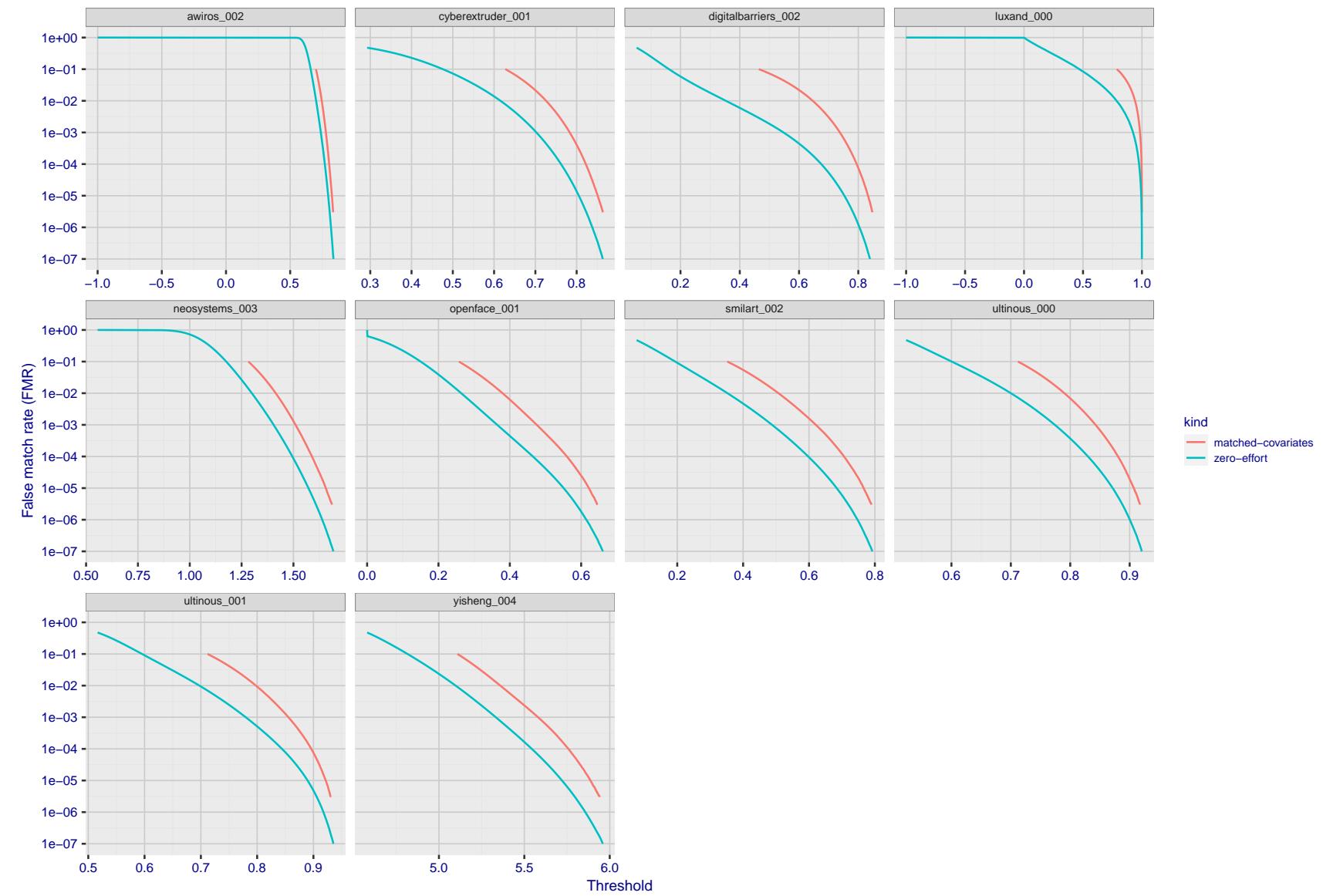


Figure 216: For the visa images, the false match calibration curves show FMR vs. threshold,  $T$ . The blue (lower) curves are for zero-effort impostors (i.e. comparing all images against all). The red (upper) curves are for persons of the same-sex, same-age, and same national-origin. This shows that FMR is underestimated (by a factor of 10 or more) by using a zero-effort impostor calculation to calibrate  $T$ . As shown later (sec. 3.6), FMR is higher for demographic-matched impostors.

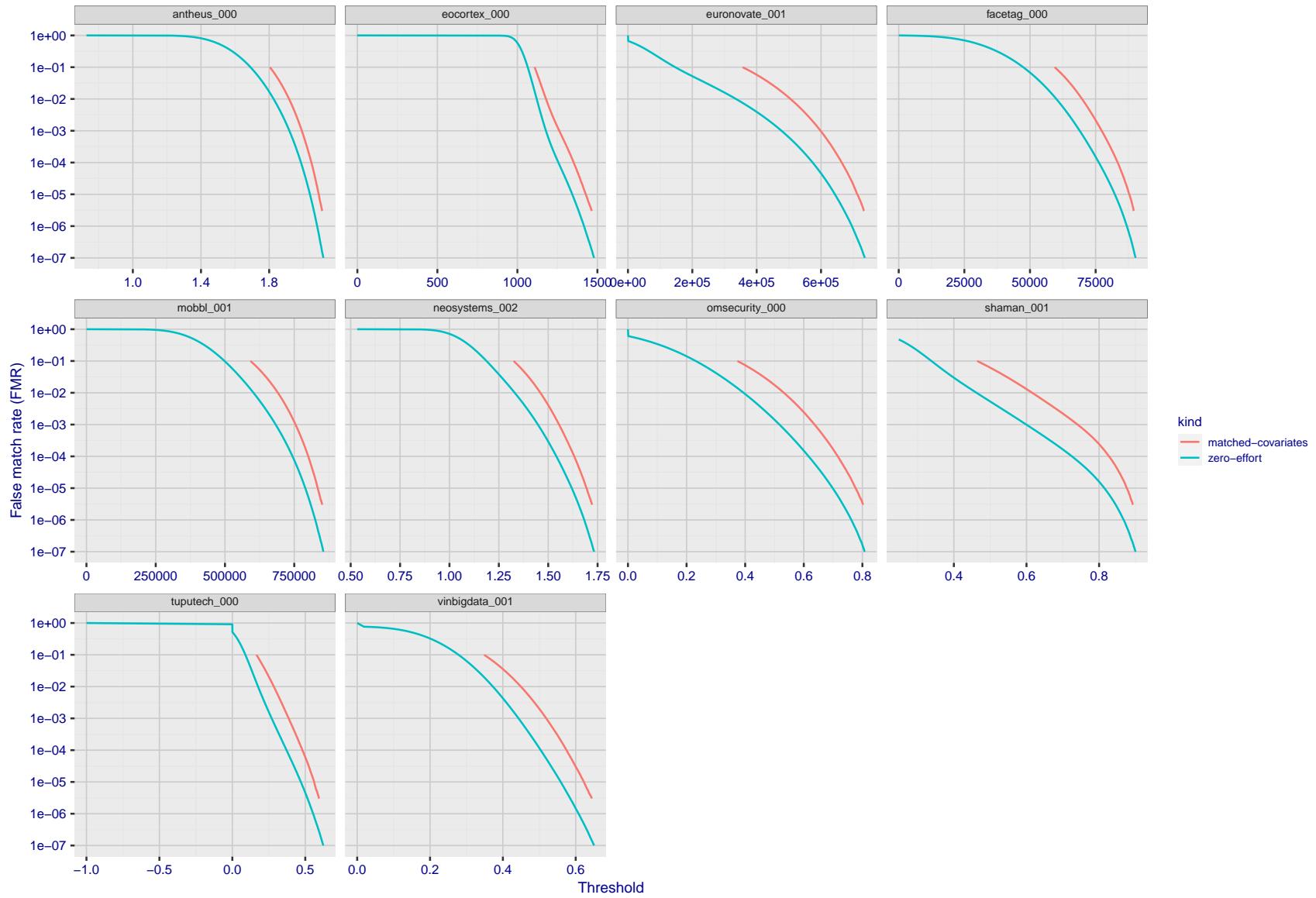


Figure 217: For the visa images, the false match calibration curves show FMR vs. threshold,  $T$ . The blue (lower) curves are for zero-effort impostors (i.e. comparing all images against all). The red (upper) curves are for persons of the same-sex, same-age, and same national-origin. This shows that FMR is underestimated (by a factor of 10 or more) by using a zero-effort impostor calculation to calibrate  $T$ . As shown later (sec. 3.6), FMR is higher for demographic-matched impostors.

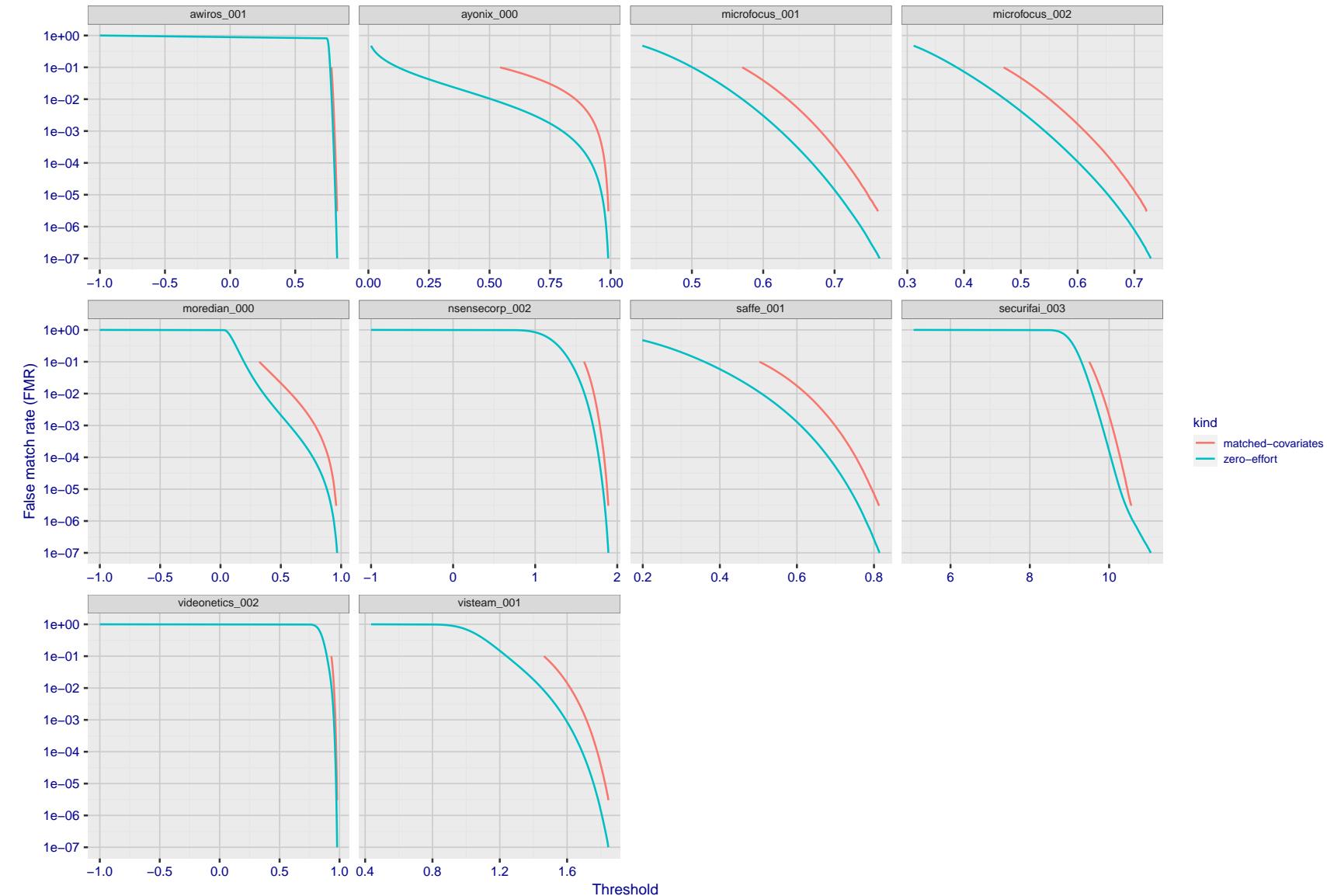


Figure 218: For the visa images, the false match calibration curves show FMR vs. threshold,  $T$ . The blue (lower) curves are for zero-effort impostors (i.e. comparing all images against all). The red (upper) curves are for persons of the same-sex, same-age, and same national-origin. This shows that FMR is underestimated (by a factor of 10 or more) by using a zero-effort impostor calculation to calibrate  $T$ . As shown later (sec. 3.6), FMR is higher for demographic-matched impostors.

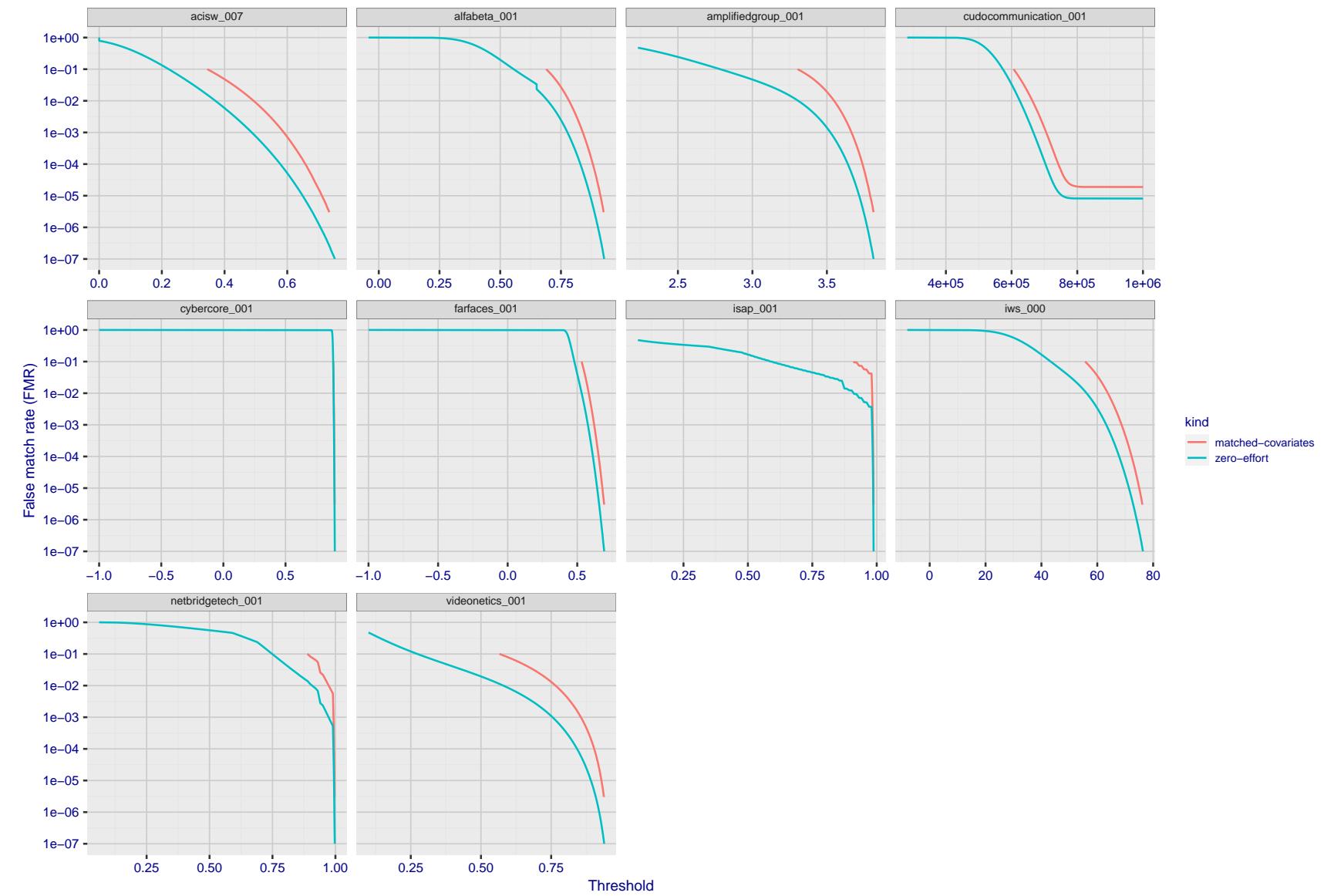


Figure 219: For the visa images, the false match calibration curves show FMR vs. threshold,  $T$ . The blue (lower) curves are for zero-effort impostors (i.e. comparing all images against all). The red (upper) curves are for persons of the same-sex, same-age, and same national-origin. This shows that FMR is underestimated (by a factor of 10 or more) by using a zero-effort impostor calculation to calibrate  $T$ . As shown later (sec. 3.6), FMR is higher for demographic-matched impostors.

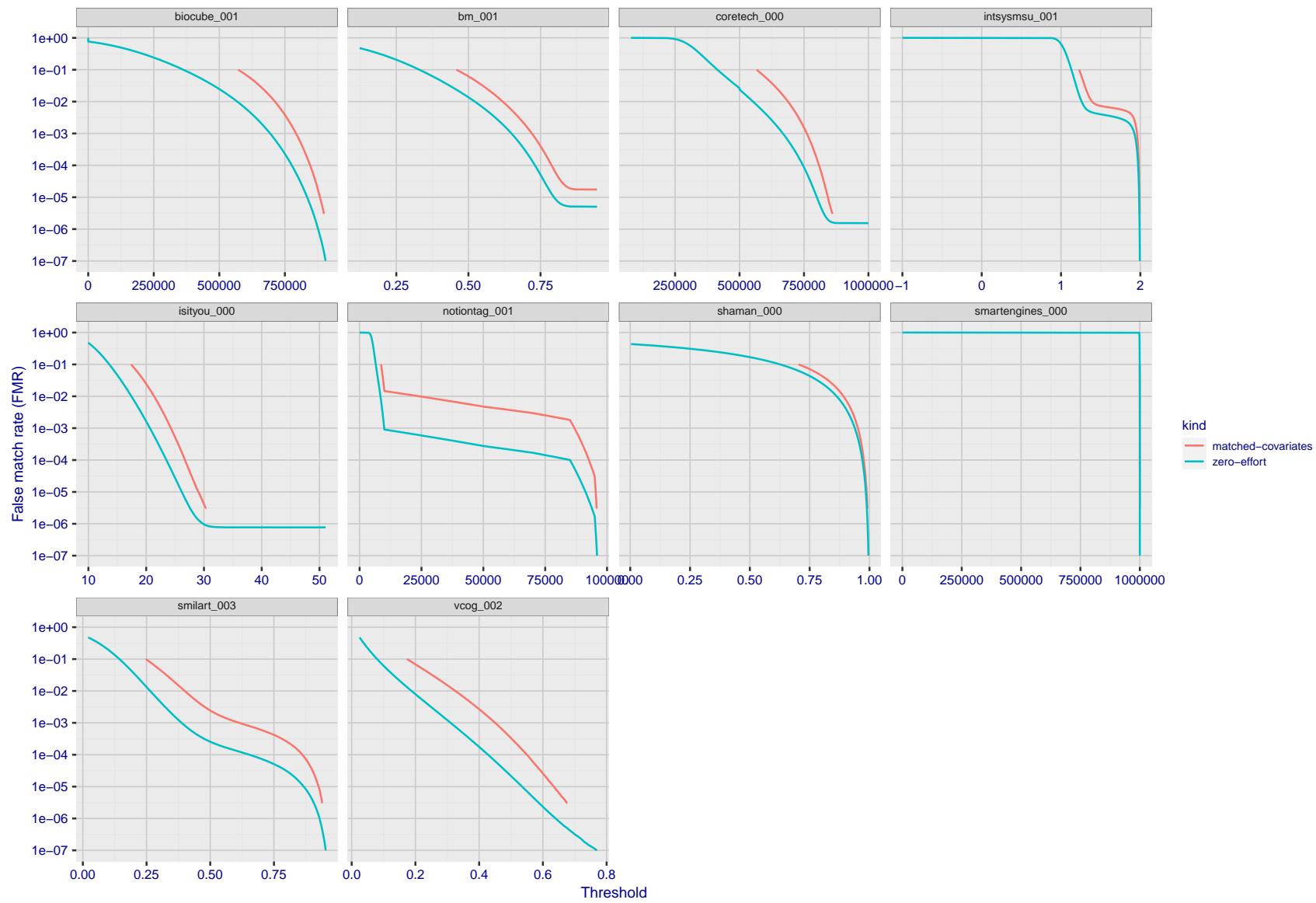


Figure 220: For the visa images, the false match calibration curves show FMR vs. threshold,  $T$ . The blue (lower) curves are for zero-effort impostors (i.e. comparing all images against all). The red (upper) curves are for persons of the same-sex, same-age, and same national-origin. This shows that FMR is underestimated (by a factor of 10 or more) by using a zero-effort impostor calculation to calibrate  $T$ . As shown later (sec. 3.6), FMR is higher for demographic-matched impostors.

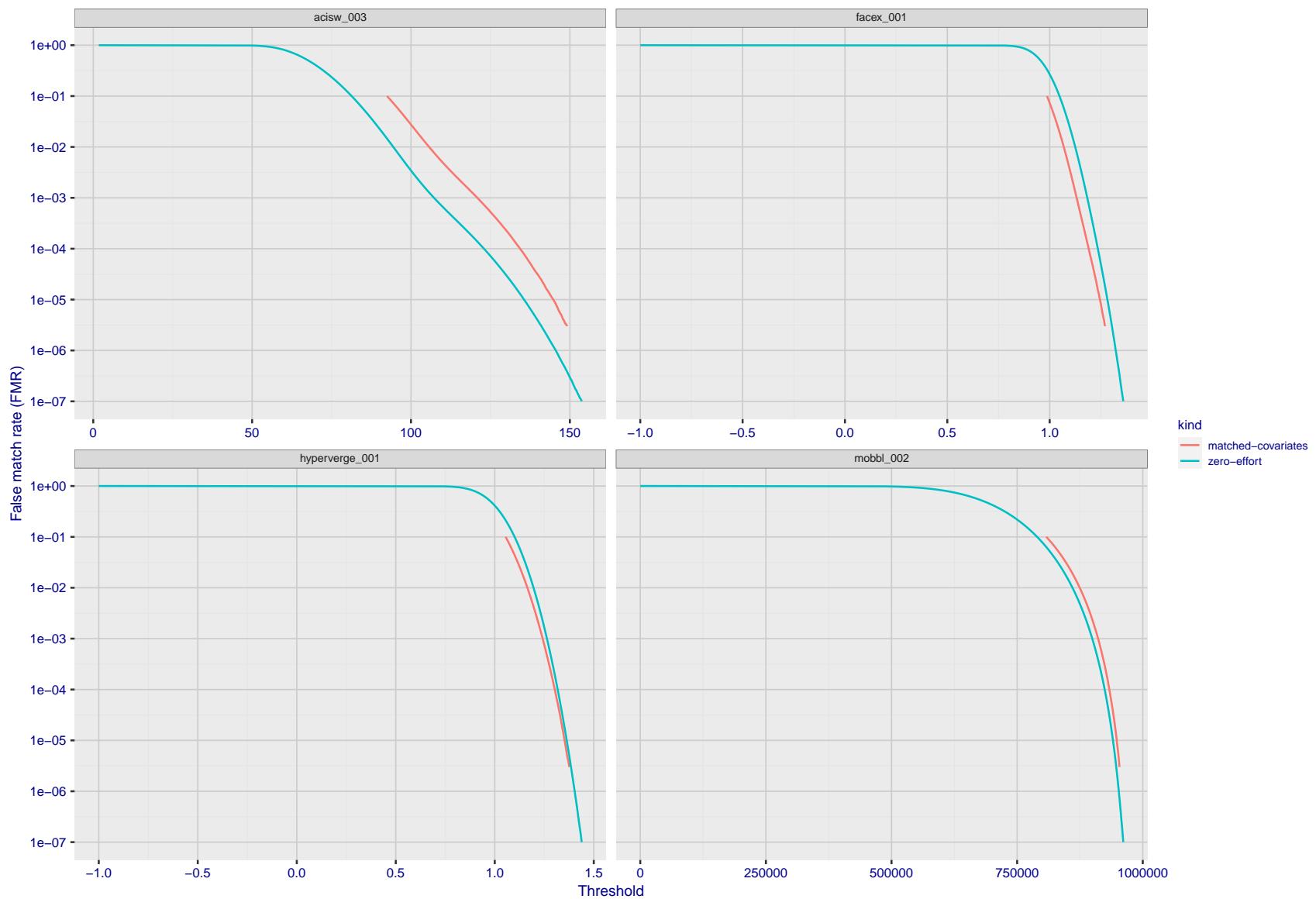


Figure 221: For the visa images, the false match calibration curves show FMR vs. threshold,  $T$ . The blue (lower) curves are for zero-effort impostors (i.e. comparing all images against all). The red (upper) curves are for persons of the same-sex, same-age, and same national-origin. This shows that FMR is underestimated (by a factor of 10 or more) by using a zero-effort impostor calculation to calibrate  $T$ . As shown later (sec. 3.6), FMR is higher for demographic-matched impostors.

## 3.5 Genuine distribution stability

### 3.5.1 Effect of birth place on the genuine distribution

**Background:** Both skin tone and bone structure vary geographically. Prior studies have reported variations in FNMR and FMR.

**Goal:** To measure false non-match rate (FNMR) variation with country of birth.

**Methods:** Thresholds are determined that give  $FMR = \{0.001, 0.0001\}$  over the entire impostor set. Then FNMR is measured over 1000 bootstrap replications of the genuine scores. Only those countries with at least 140 individuals are included in the analysis.

**Results:** Figure 253 shows FNMR by country of birth for the two thresholds.

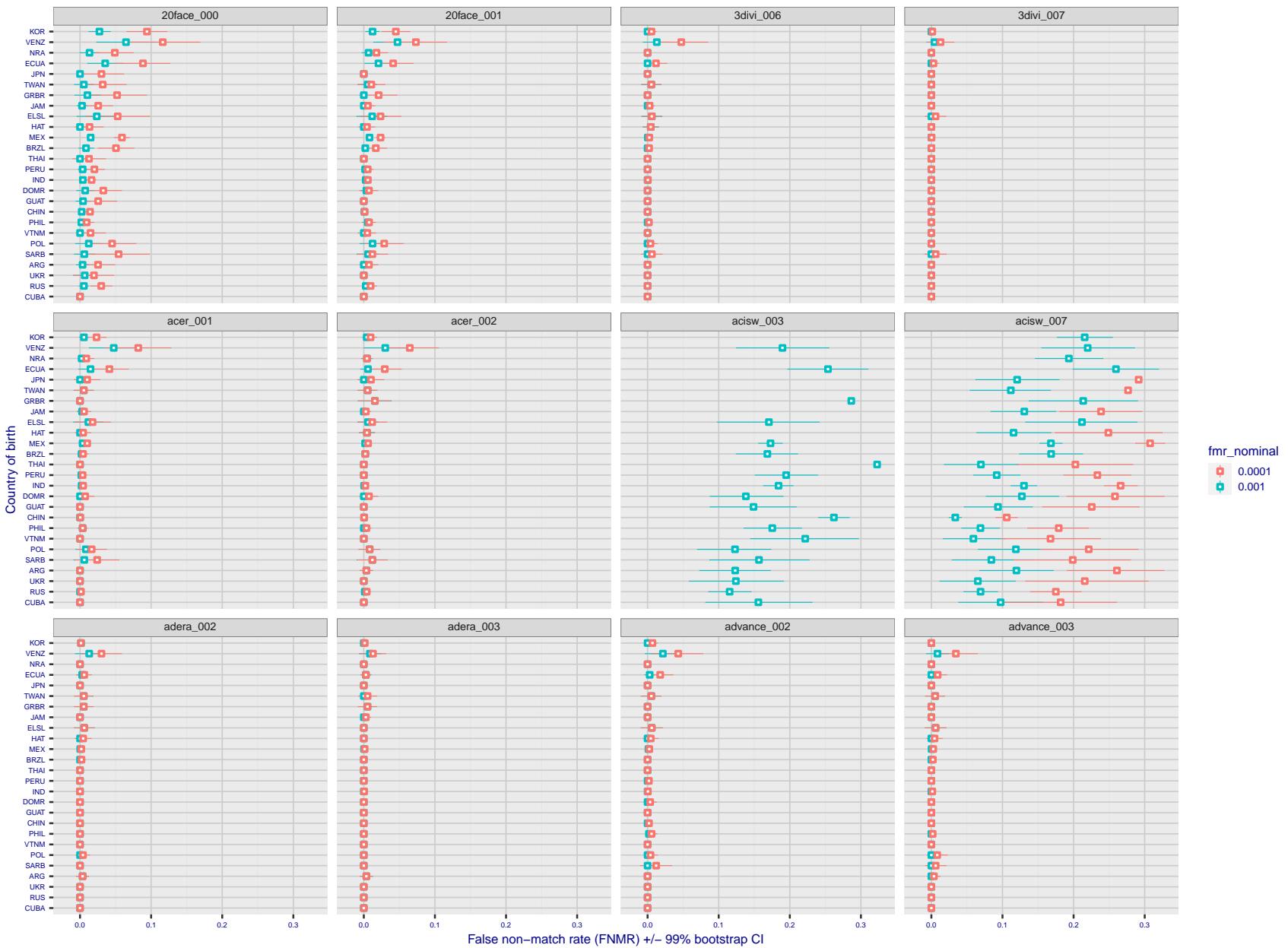


Figure 222: For the visa images, the dots show FNMR by country of birth for two globally set operating thresholds corresponding to  $FMR = \{0.001, 0.0001\}$  computed over all on the order of  $10^{10}$  impostor scores. The FMR in each bin will vary also - see subsequent impostor heatmaps in sec. 3.6.1. The figures shows an order of magnitude variation in FNMR across country of birth; these effects are likely due quality variations, then demographics like age and race. The error rates in some cases are zero, and in others the DET is flat so the error rates at the two thresholds are identical. The lines span 1% and 99% of bootstrap replicated FNMR estimates.

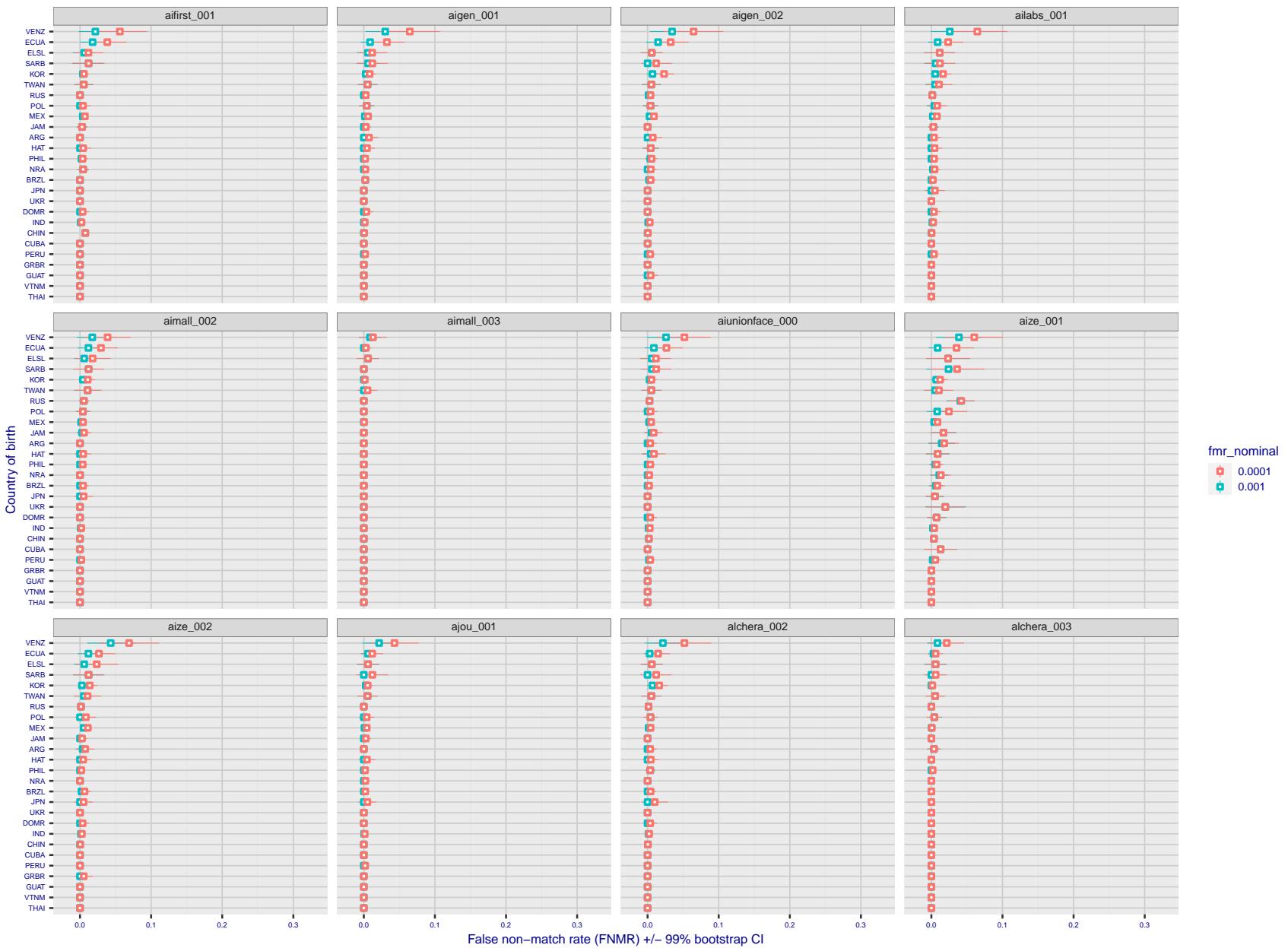


Figure 223: For the visa images, the dots show FNMR by country of birth for two globally set operating thresholds corresponding to  $FMR = \{0.001, 0.0001\}$  computed over all on the order of  $10^{10}$  impostor scores. The FMR in each bin will vary also - see subsequent impostor heatmaps in sec. 3.6.1. The figures shows an order of magnitude variation in FNMR across country of birth; these effects are likely due quality variations, then demographics like age and race. The error rates in some cases are zero, and in others the DET is flat so the error rates at the two thresholds are identical. The lines span 1% and 99% of bootstrap replicated FNMR estimates.

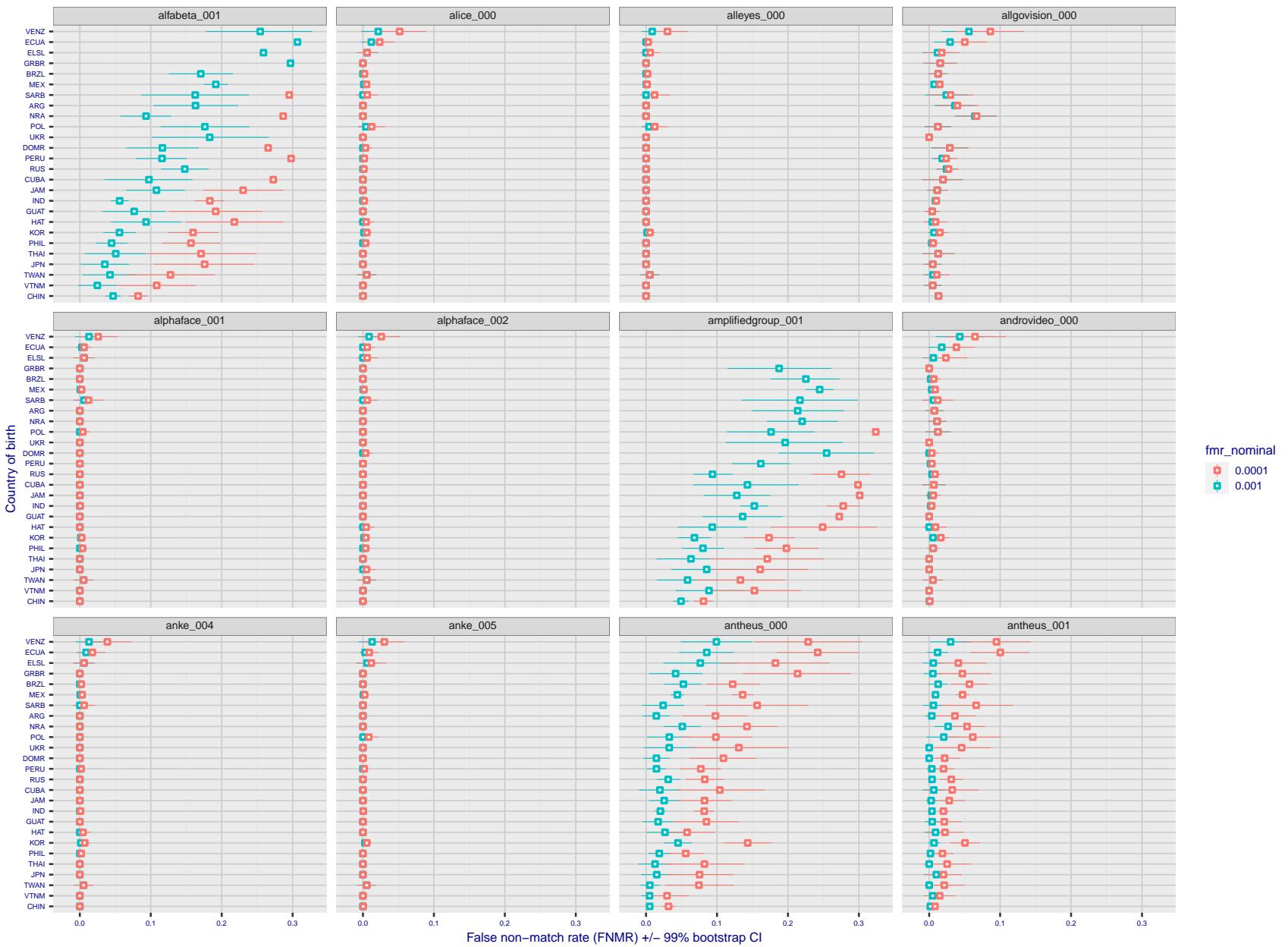


Figure 224: For the visa images, the dots show FNMR by country of birth for two globally set operating thresholds corresponding to  $FMR = \{0.001, 0.0001\}$  computed over all on the order of  $10^{10}$  impostor scores. The FMR in each bin will vary also - see subsequent impostor heatmaps in sec. 3.6.1. The figures shows an order of magnitude variation in FNMR across country of birth; these effects are likely due quality variations, then demographics like age and race. The error rates in some cases are zero, and in others the DET is flat so the error rates at the two thresholds are identical. The lines span 1% and 99% of bootstrap replicated FNMR estimates.

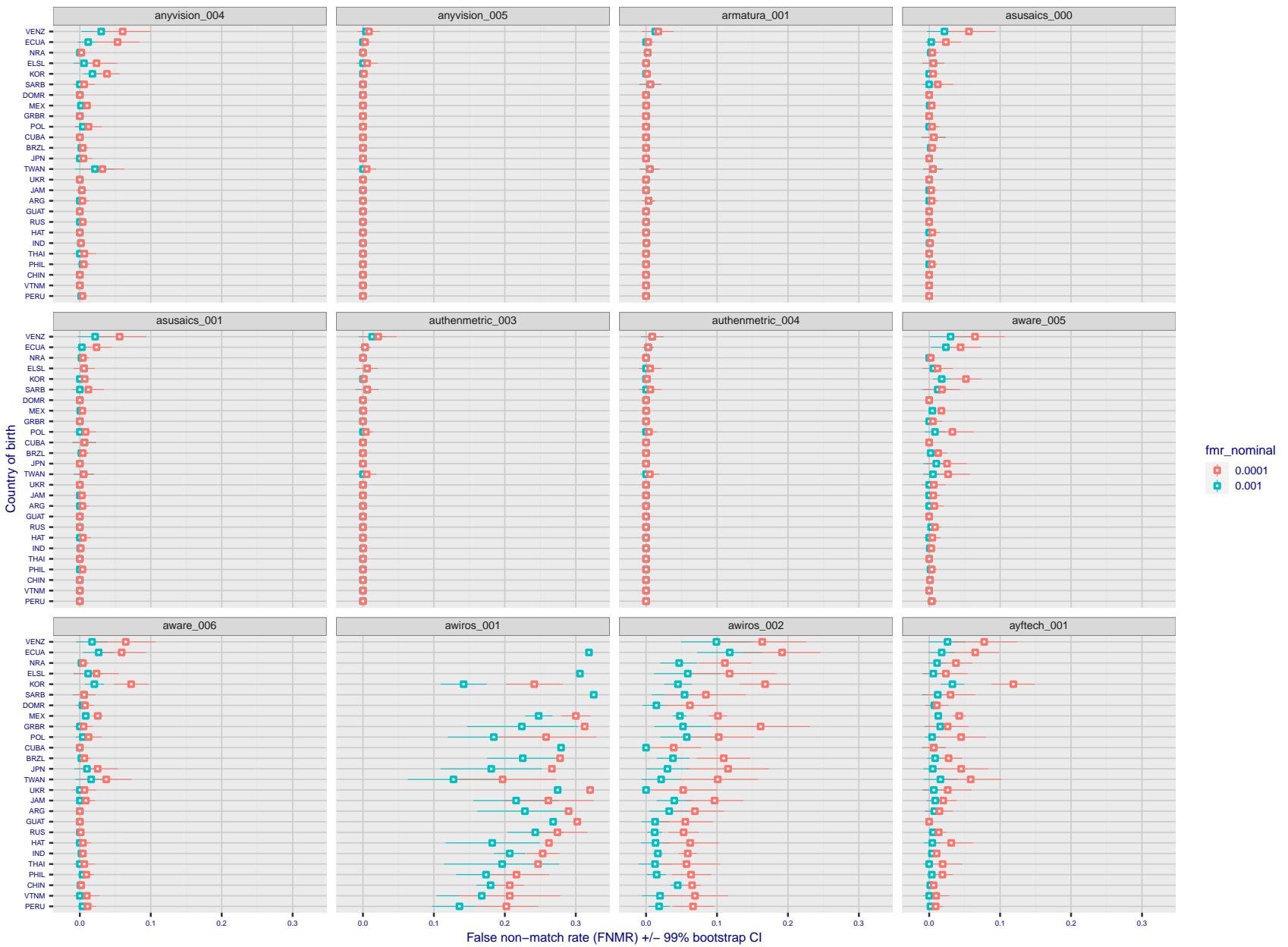


Figure 225: For the visa images, the dots show FNMR by country of birth for two globally set operating thresholds corresponding to  $FMR = \{0.001, 0.0001\}$  computed over all on the order of  $10^{10}$  impostor scores. The FMR in each bin will vary also - see subsequent impostor heatmaps in sec. 3.6.1. The figures shows an order of magnitude variation in FNMR across country of birth; these effects are likely due quality variations, then demographics like age and race. The error rates in some cases are zero, and in others the DET is flat so the error rates at the two thresholds are identical. The lines span 1% and 99% of bootstrap replicated FNMR estimates.

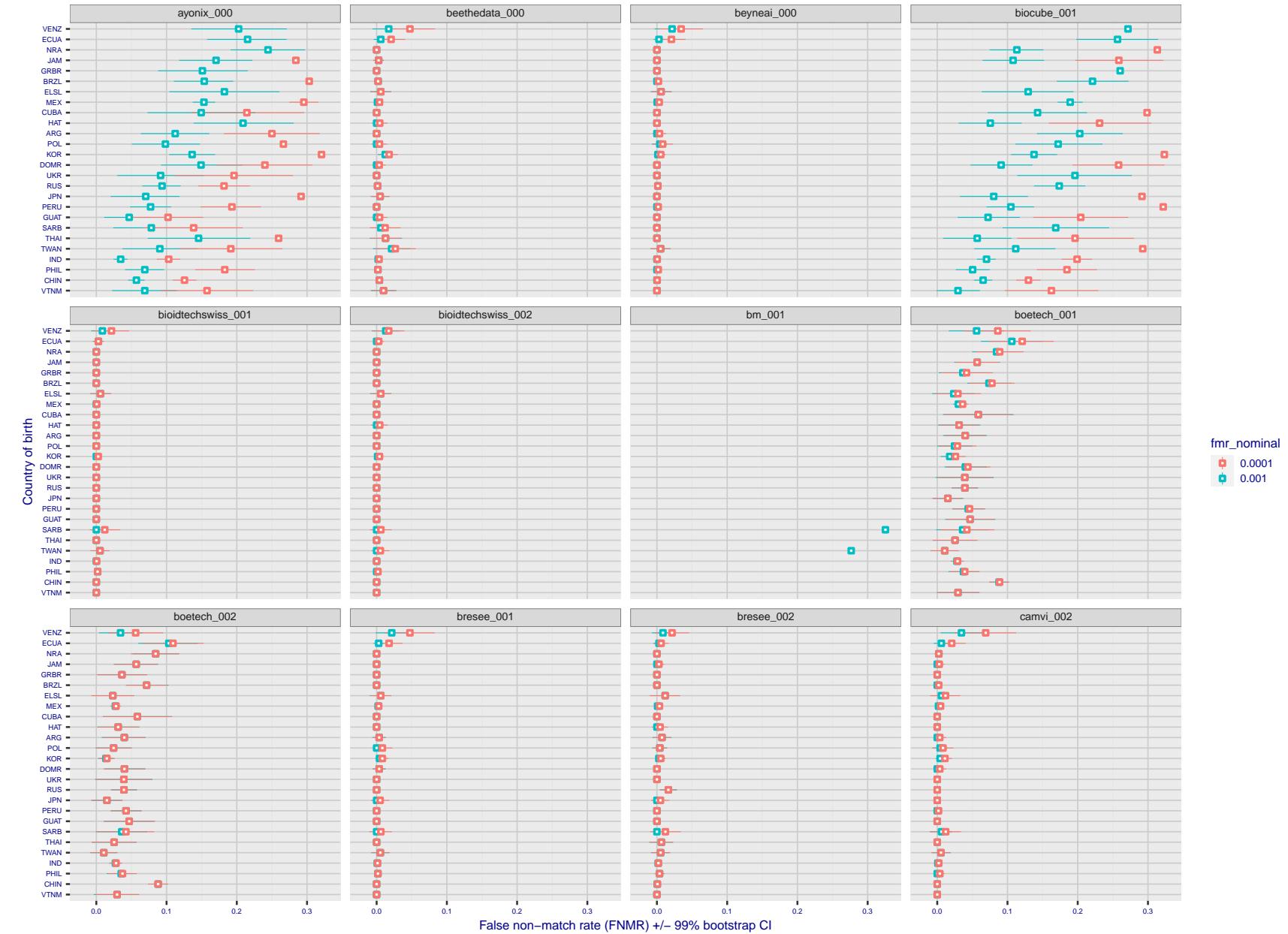


Figure 226: For the visa images, the dots show FNMR by country of birth for two globally set operating thresholds corresponding to  $FMR = \{0.001, 0.0001\}$  computed over all on the order of  $10^{10}$  impostor scores. The FMR in each bin will vary also - see subsequent impostor heatmaps in sec. 3.6.1. The figures shows an order of magnitude variation in FNMR across country of birth; these effects are likely due quality variations, then demographics like age and race. The error rates in some cases are zero, and in others the DET is flat so the error rates at the two thresholds are identical. The lines span 1% and 99% of bootstrap replicated FNMR estimates.

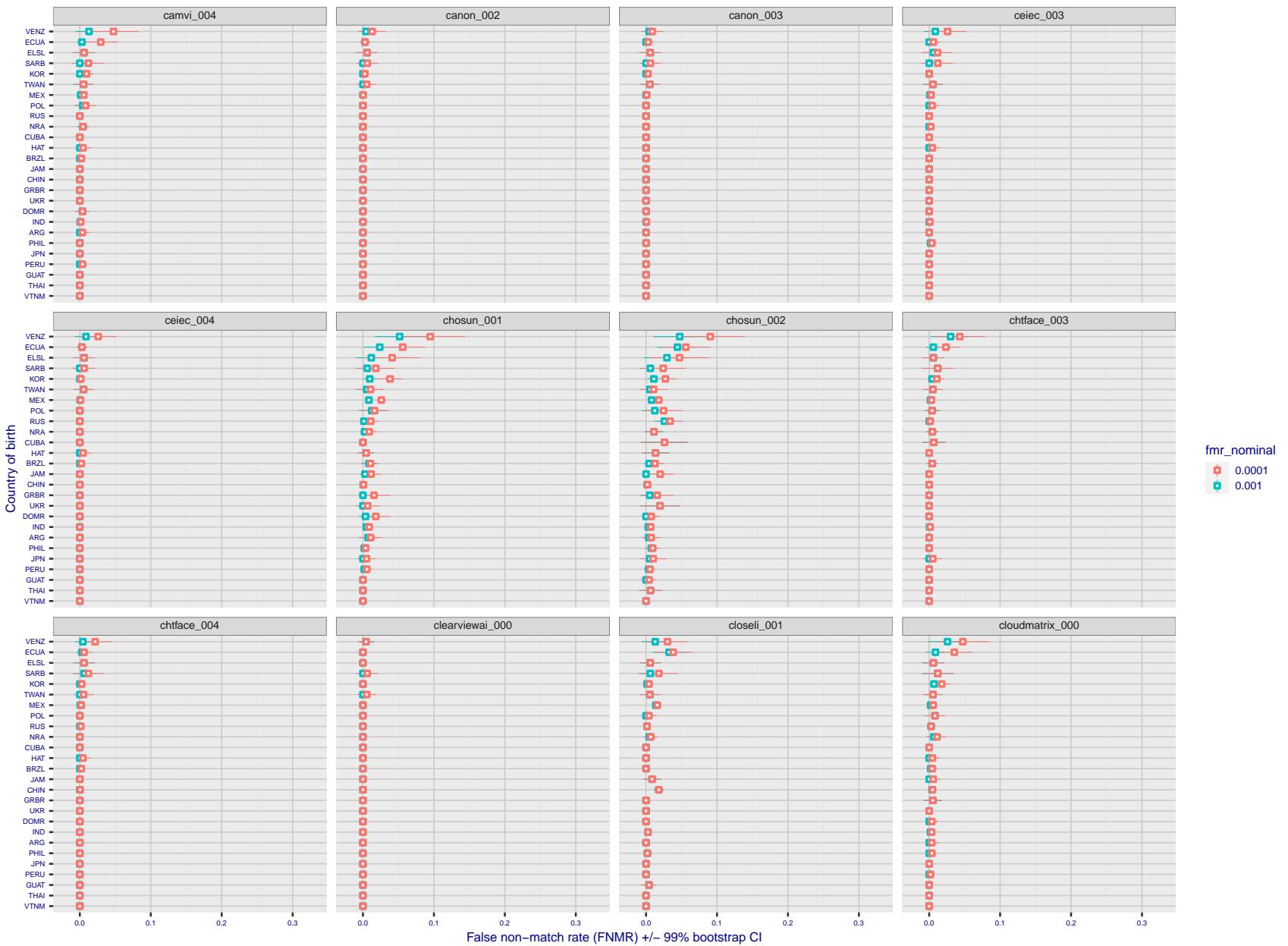


Figure 227: For the visa images, the dots show FNMR by country of birth for two globally set operating thresholds corresponding to  $FMR = \{0.001, 0.0001\}$  computed over all on the order of  $10^{10}$  impostor scores. The FMR in each bin will vary also - see subsequent impostor heatmaps in sec. 3.6.1. The figures shows an order of magnitude variation in FNMR across country of birth; these effects are likely due quality variations, then demographics like age and race. The error rates in some cases are zero, and in others the DET is flat so the error rates at the two thresholds are identical. The lines span 1% and 99% of bootstrap replicated FNMR estimates.

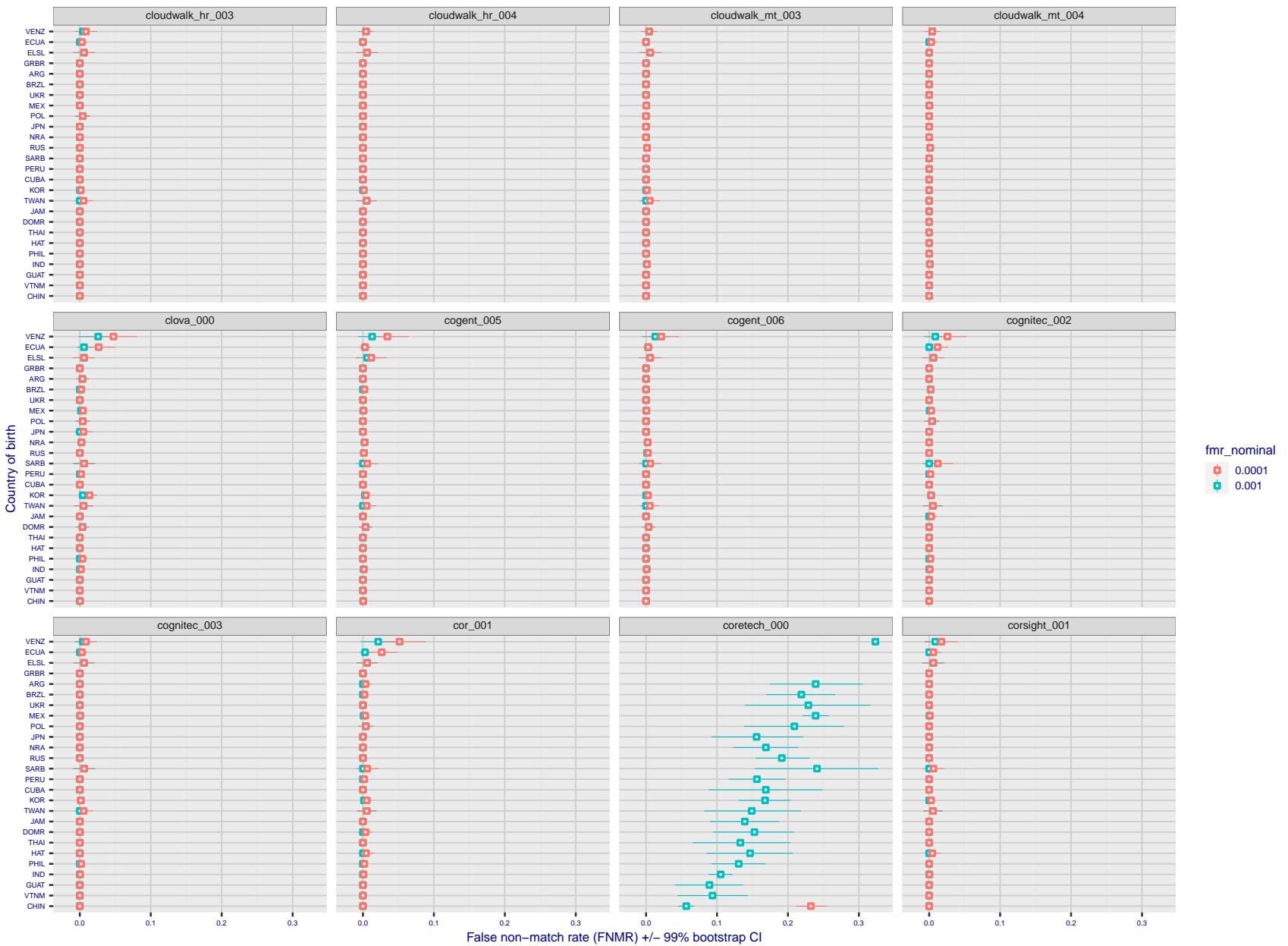


Figure 228: For the visa images, the dots show FNMR by country of birth for two globally set operating thresholds corresponding to  $FMR = \{0.001, 0.0001\}$  computed over all on the order of  $10^{10}$  impostor scores. The FMR in each bin will vary also - see subsequent impostor heatmaps in sec. 3.6.1. The figures shows an order of magnitude variation in FNMR across country of birth; these effects are likely due quality variations, then demographics like age and race. The error rates in some cases are zero, and in others the DET is flat so the error rates at the two thresholds are identical. The lines span 1% and 99% of bootstrap replicated FNMR estimates.

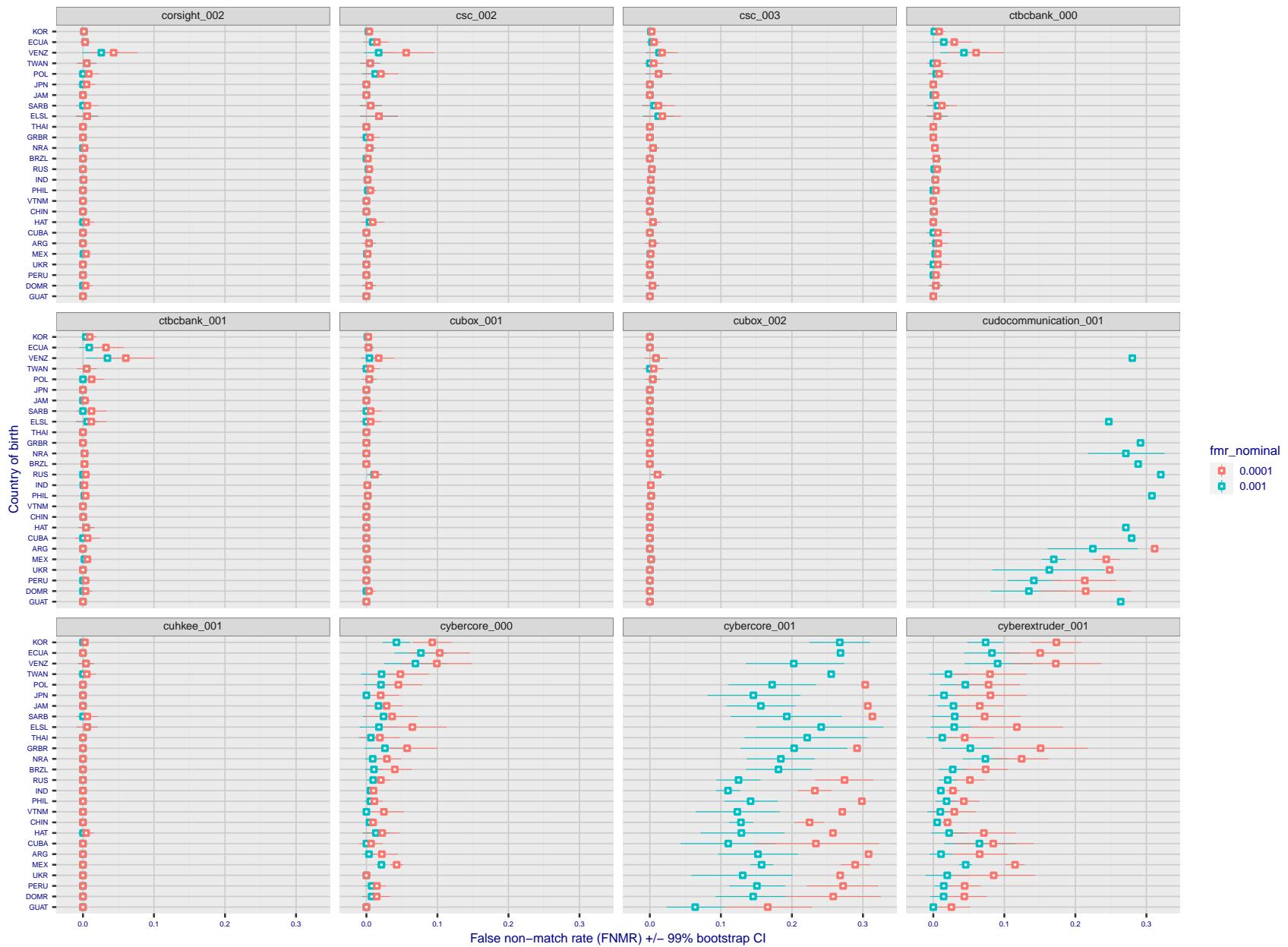


Figure 229: For the visa images, the dots show FNMR by country of birth for two globally set operating thresholds corresponding to  $FMR = \{0.001, 0.0001\}$  computed over all on the order of  $10^{10}$  impostor scores. The FMR in each bin will vary also - see subsequent impostor heatmaps in sec. 3.6.1. The figures shows an order of magnitude variation in FNMR across country of birth; these effects are likely due quality variations, then demographics like age and race. The error rates in some cases are zero, and in others the DET is flat so the error rates at the two thresholds are identical. The lines span 1% and 99% of bootstrap replicated FNMR estimates.

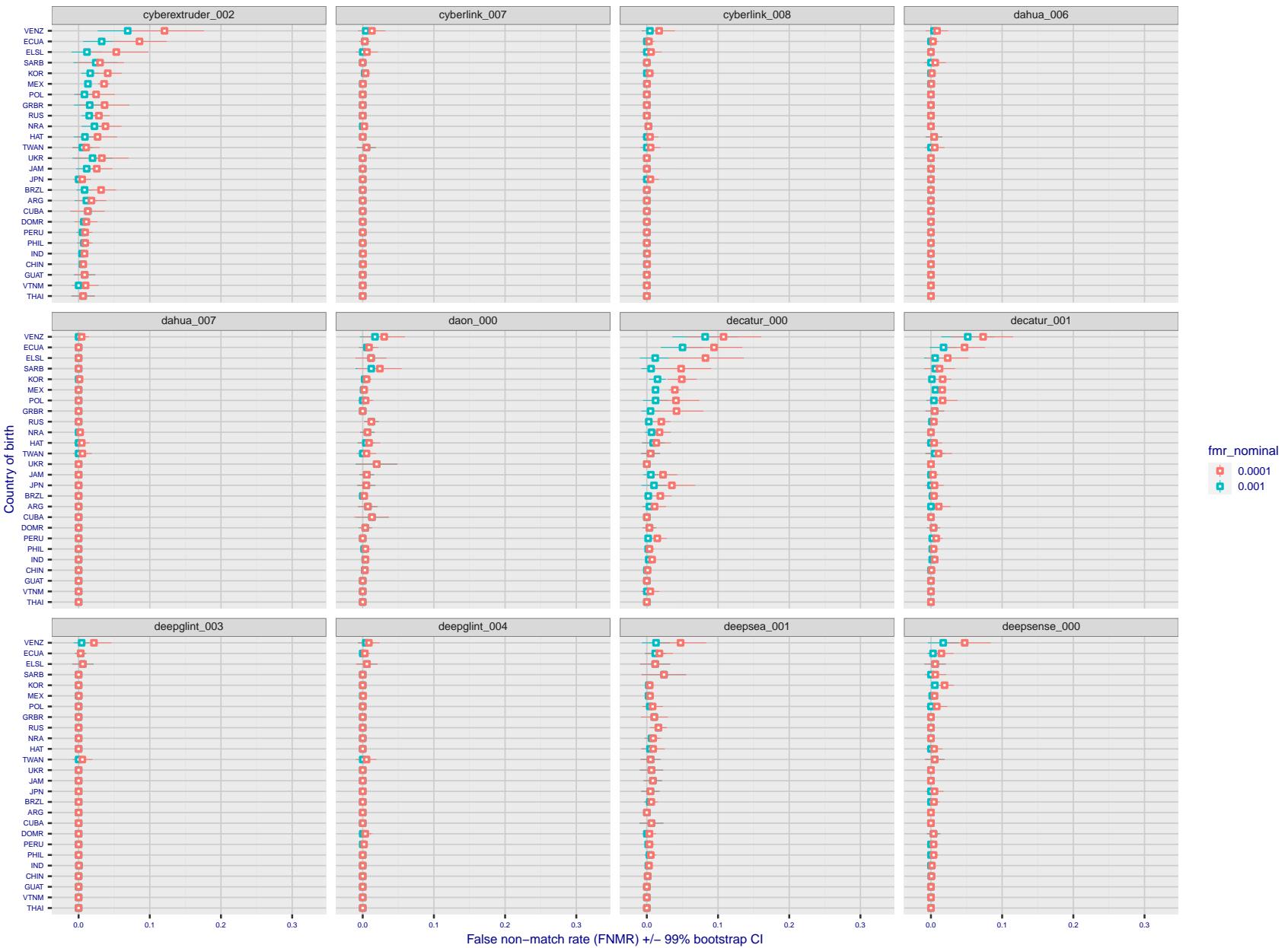


Figure 230: For the visa images, the dots show FNMR by country of birth for two globally set operating thresholds corresponding to  $FMR = \{0.001, 0.0001\}$  computed over all on the order of  $10^{10}$  impostor scores. The FMR in each bin will vary also - see subsequent impostor heatmaps in sec. 3.6.1. The figures shows an order of magnitude variation in FNMR across country of birth; these effects are likely due quality variations, then demographics like age and race. The error rates in some cases are zero, and in others the DET is flat so the error rates at the two thresholds are identical. The lines span 1% and 99% of bootstrap replicated FNMR estimates.

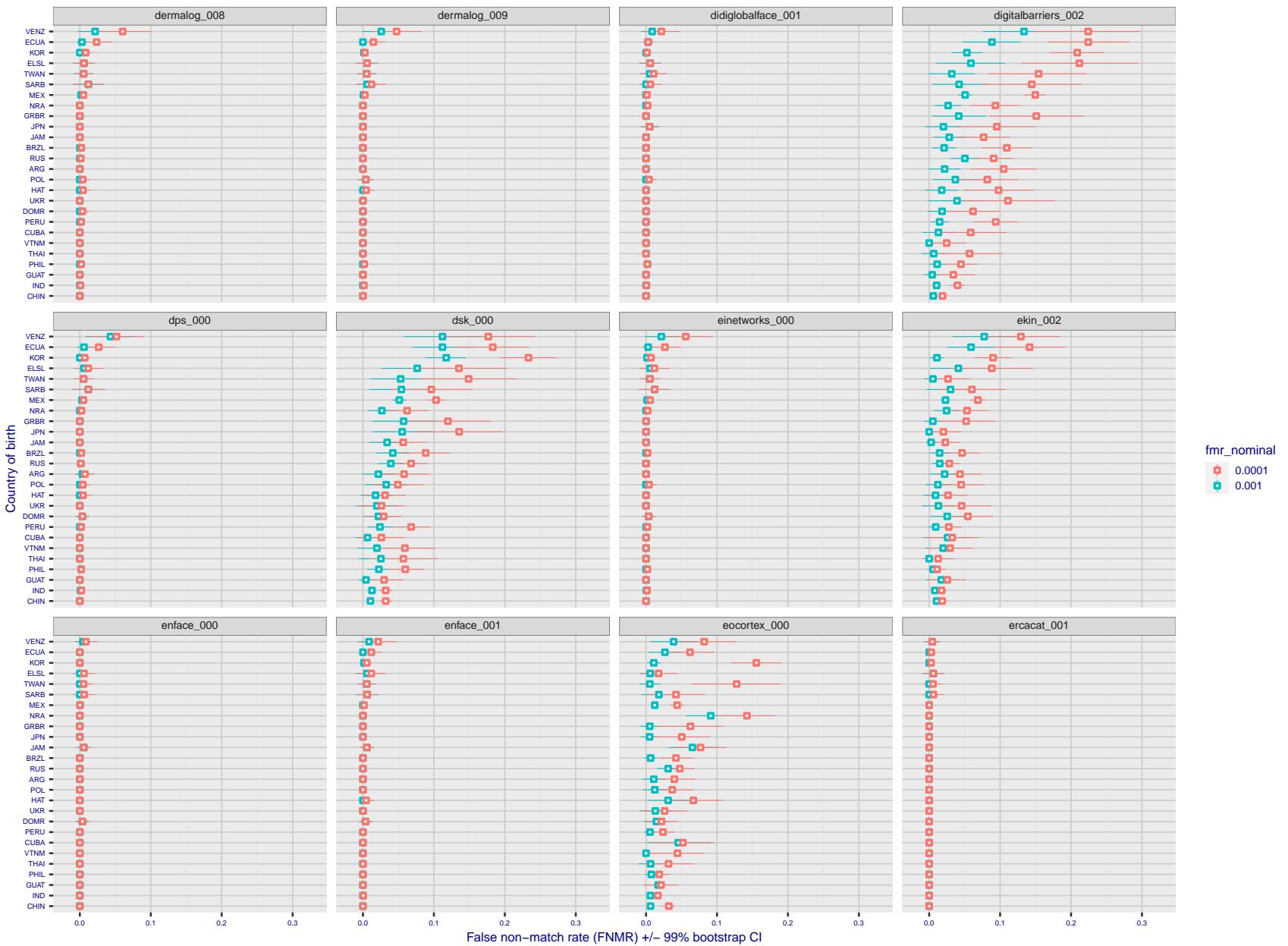


Figure 231: For the visa images, the dots show FNMR by country of birth for two globally set operating thresholds corresponding to  $FMR = \{0.001, 0.0001\}$  computed over all on the order of  $10^{10}$  impostor scores. The FMR in each bin will vary also - see subsequent impostor heatmaps in sec. 3.6.1. The figures shows an order of magnitude variation in FNMR across country of birth; these effects are likely due quality variations, then demographics like age and race. The error rates in some cases are zero, and in others the DET is flat so the error rates at the two thresholds are identical. The lines span 1% and 99% of bootstrap replicated FNMR estimates.

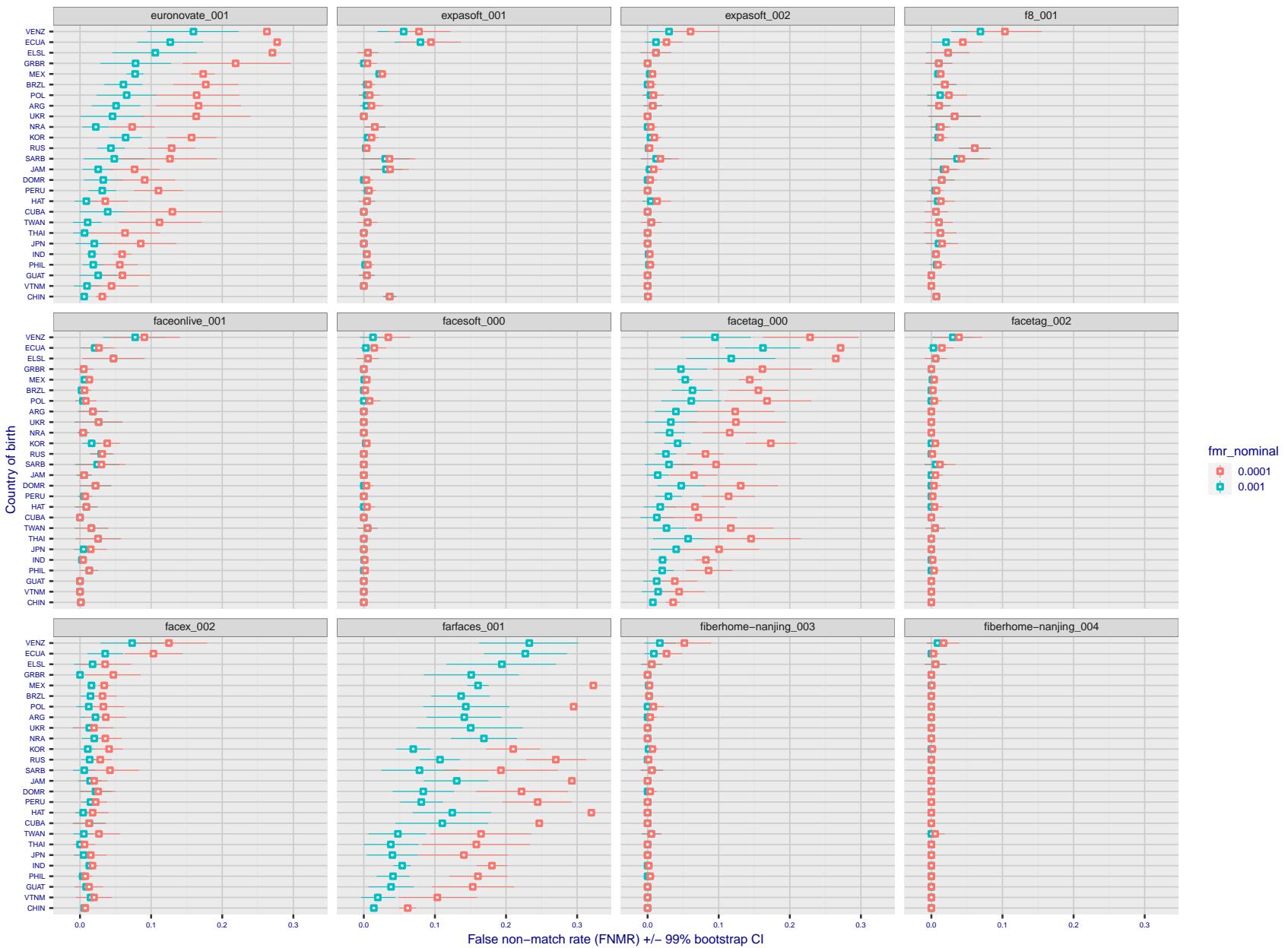


Figure 232: For the visa images, the dots show FNMR by country of birth for two globally set operating thresholds corresponding to  $FMR = \{0.001, 0.0001\}$  computed over all on the order of  $10^{10}$  impostor scores. The FMR in each bin will vary also - see subsequent impostor heatmaps in sec. 3.6.1. The figures shows an order of magnitude variation in FNMR across country of birth; these effects are likely due quality variations, then demographics like age and race. The error rates in some cases are zero, and in others the DET is flat so the error rates at the two thresholds are identical. The lines span 1% and 99% of bootstrap replicated FNMR estimates.

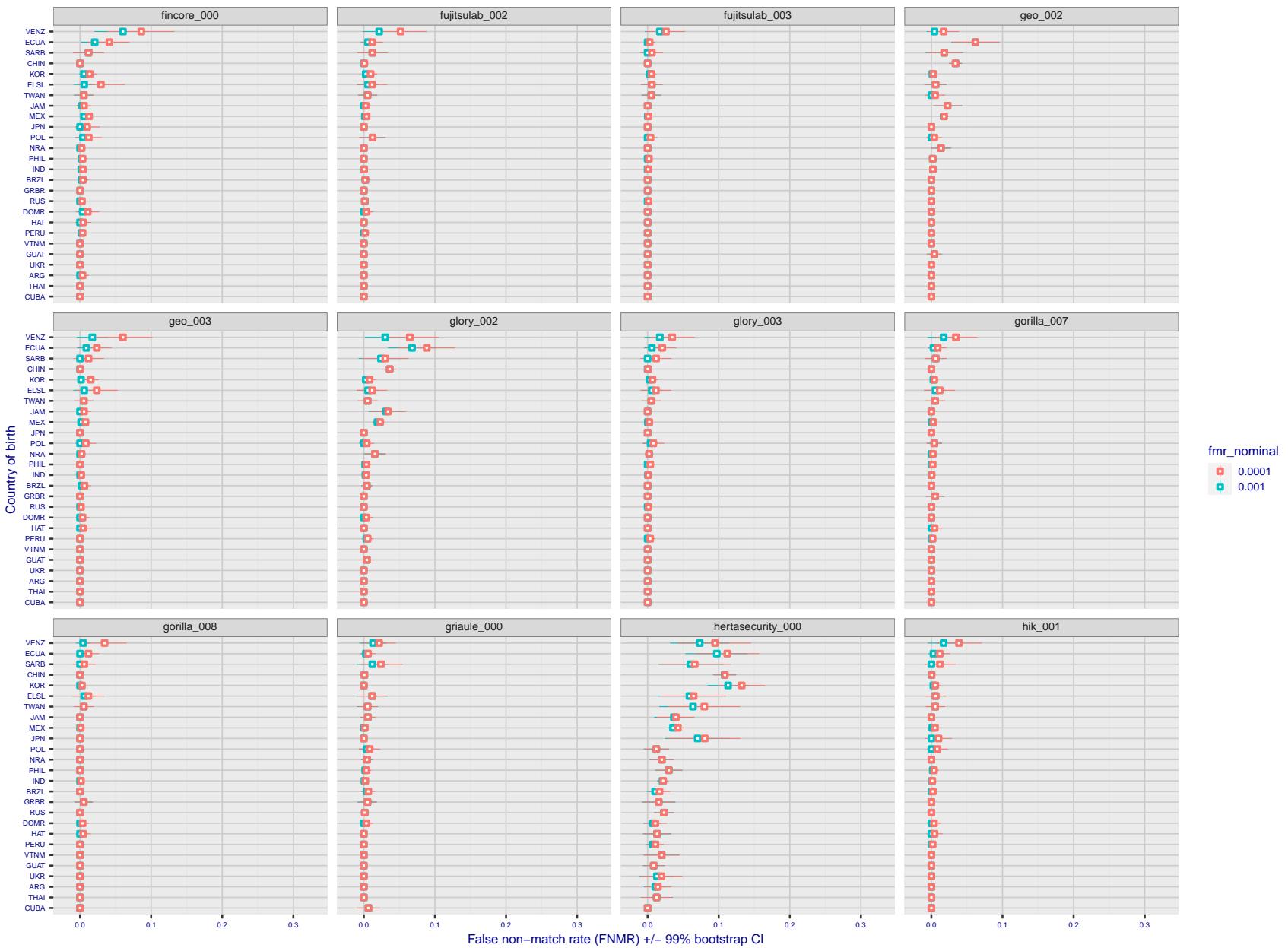


Figure 233: For the visa images, the dots show FNMR by country of birth for two globally set operating thresholds corresponding to  $FMR = \{0.001, 0.0001\}$  computed over all on the order of  $10^{10}$  impostor scores. The FMR in each bin will vary also - see subsequent impostor heatmaps in sec. 3.6.1. The figures shows an order of magnitude variation in FNMR across country of birth; these effects are likely due quality variations, then demographics like age and race. The error rates in some cases are zero, and in others the DET is flat so the error rates at the two thresholds are identical. The lines span 1% and 99% of bootstrap replicated FNMR estimates.

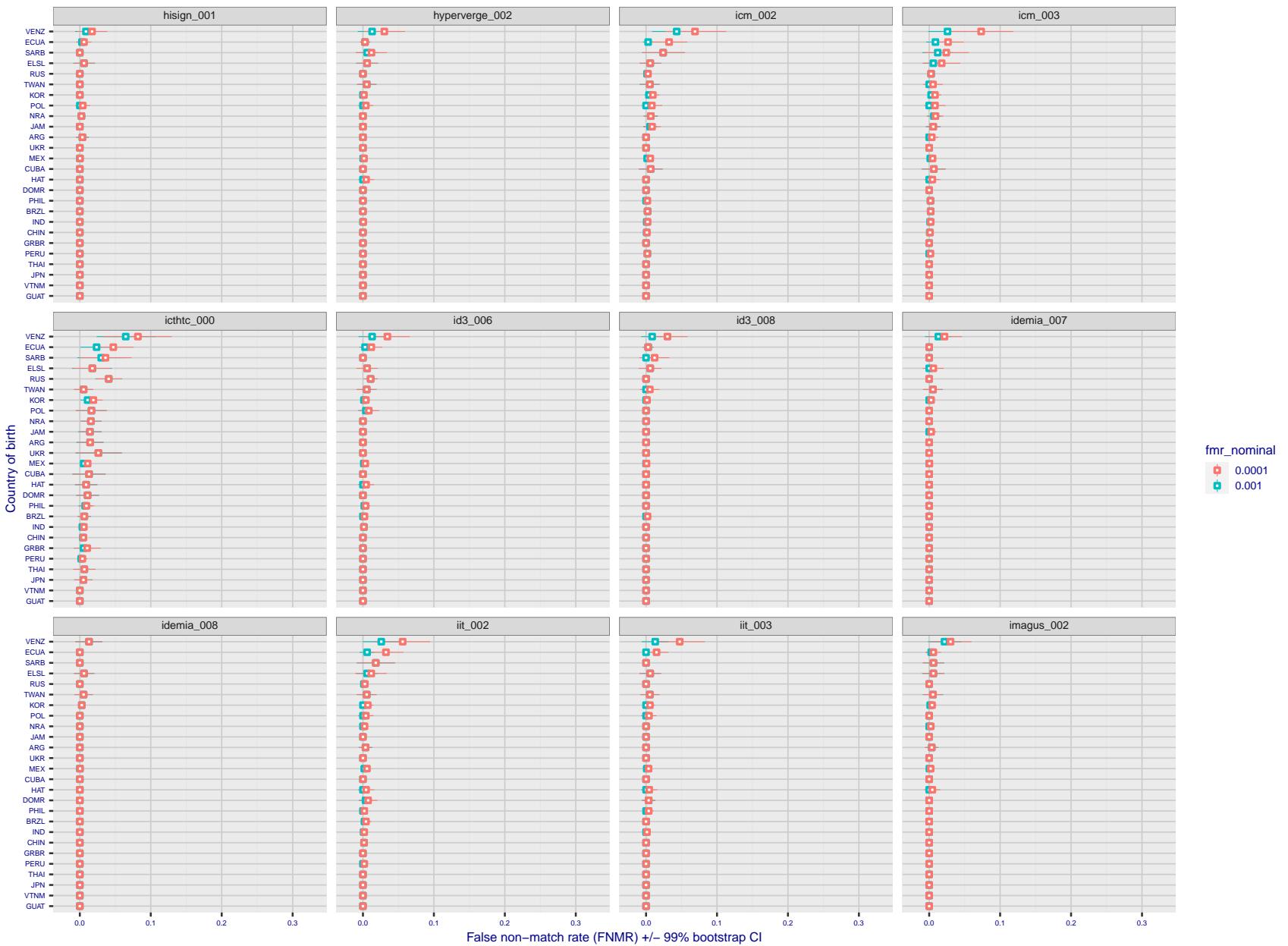


Figure 234: For the visa images, the dots show FNMR by country of birth for two globally set operating thresholds corresponding to  $FMR = \{0.001, 0.0001\}$  computed over all on the order of  $10^{10}$  impostor scores. The FMR in each bin will vary also - see subsequent impostor heatmaps in sec. 3.6.1. The figures shows an order of magnitude variation in FNMR across country of birth; these effects are likely due quality variations, then demographics like age and race. The error rates in some cases are zero, and in others the DET is flat so the error rates at the two thresholds are identical. The lines span 1% and 99% of bootstrap replicated FNMR estimates.

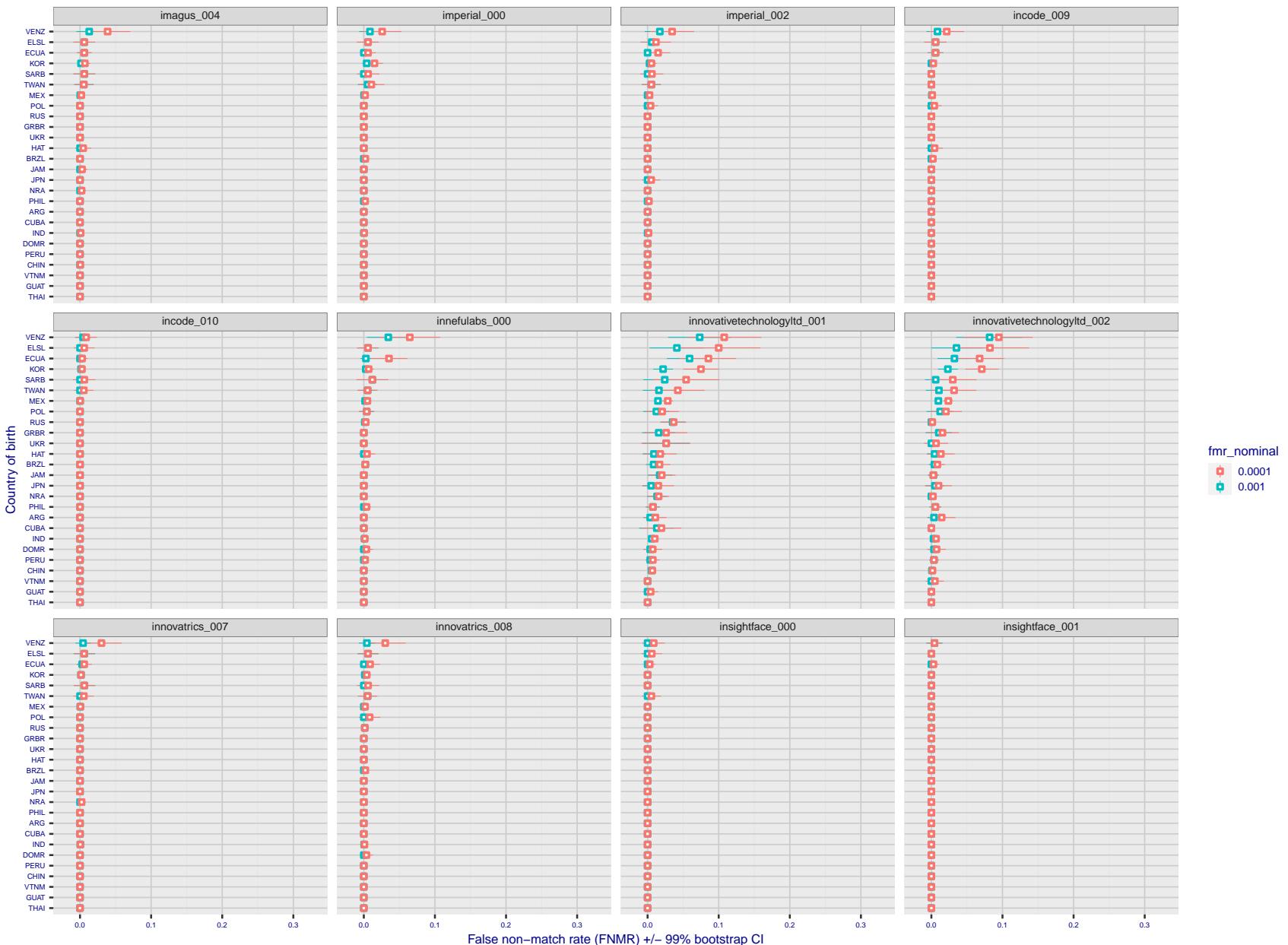


Figure 235: For the visa images, the dots show FNMR by country of birth for two globally set operating thresholds corresponding to  $FMR = \{0.001, 0.0001\}$  computed over all on the order of  $10^{10}$  impostor scores. The FMR in each bin will vary also - see subsequent impostor heatmaps in sec. 3.6.1. The figures shows an order of magnitude variation in FNMR across country of birth; these effects are likely due quality variations, then demographics like age and race. The error rates in some cases are zero, and in others the DET is flat so the error rates at the two thresholds are identical. The lines span 1% and 99% of bootstrap replicated FNMR estimates.

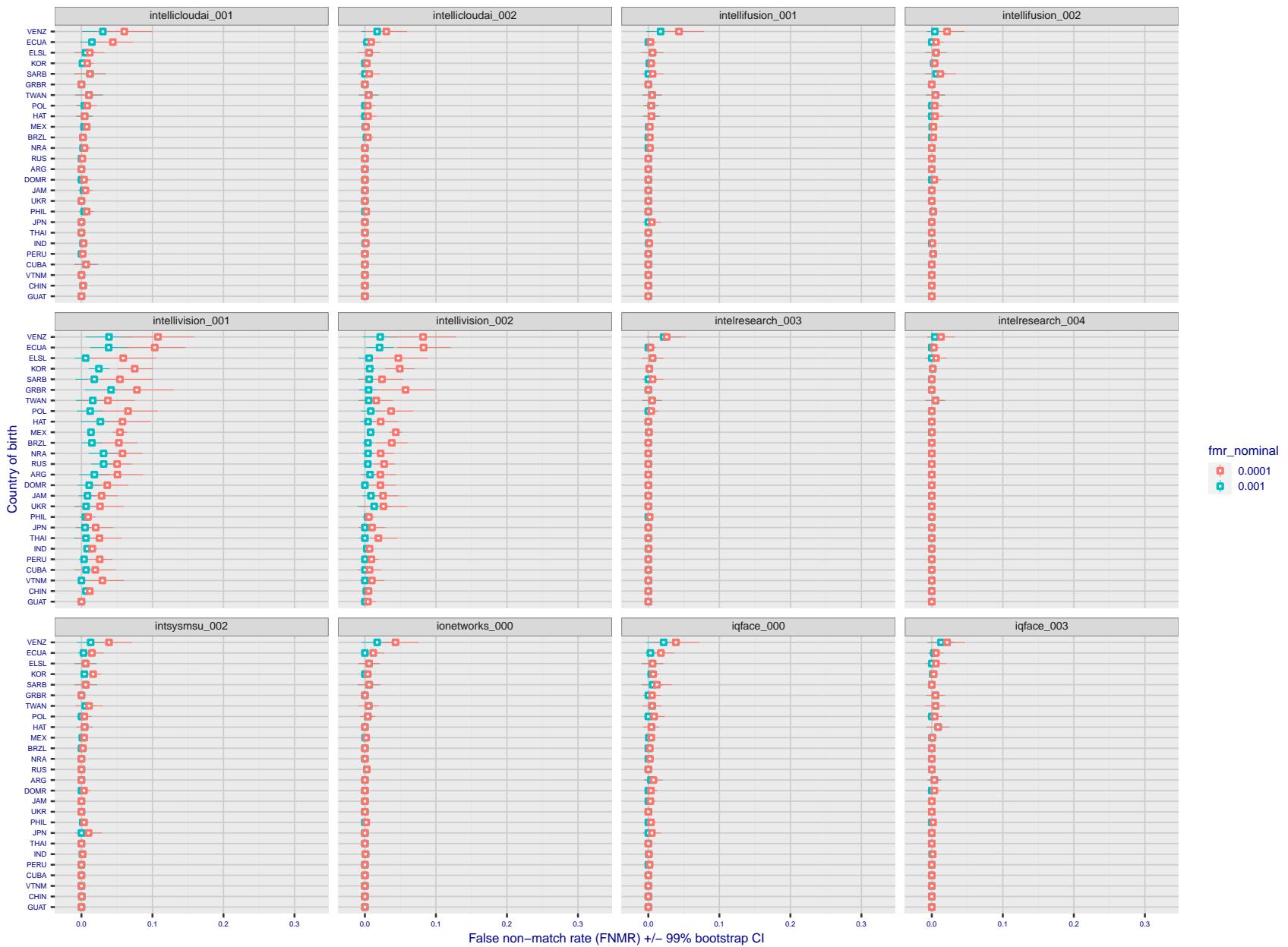


Figure 236: For the visa images, the dots show FNMR by country of birth for two globally set operating thresholds corresponding to  $FMR = \{0.001, 0.0001\}$  computed over all on the order of  $10^{10}$  impostor scores. The FMR in each bin will vary also - see subsequent impostor heatmaps in sec. 3.6.1. The figures shows an order of magnitude variation in FNMR across country of birth; these effects are likely due quality variations, then demographics like age and race. The error rates in some cases are zero, and in others the DET is flat so the error rates at the two thresholds are identical. The lines span 1% and 99% of bootstrap replicated FNMR estimates.

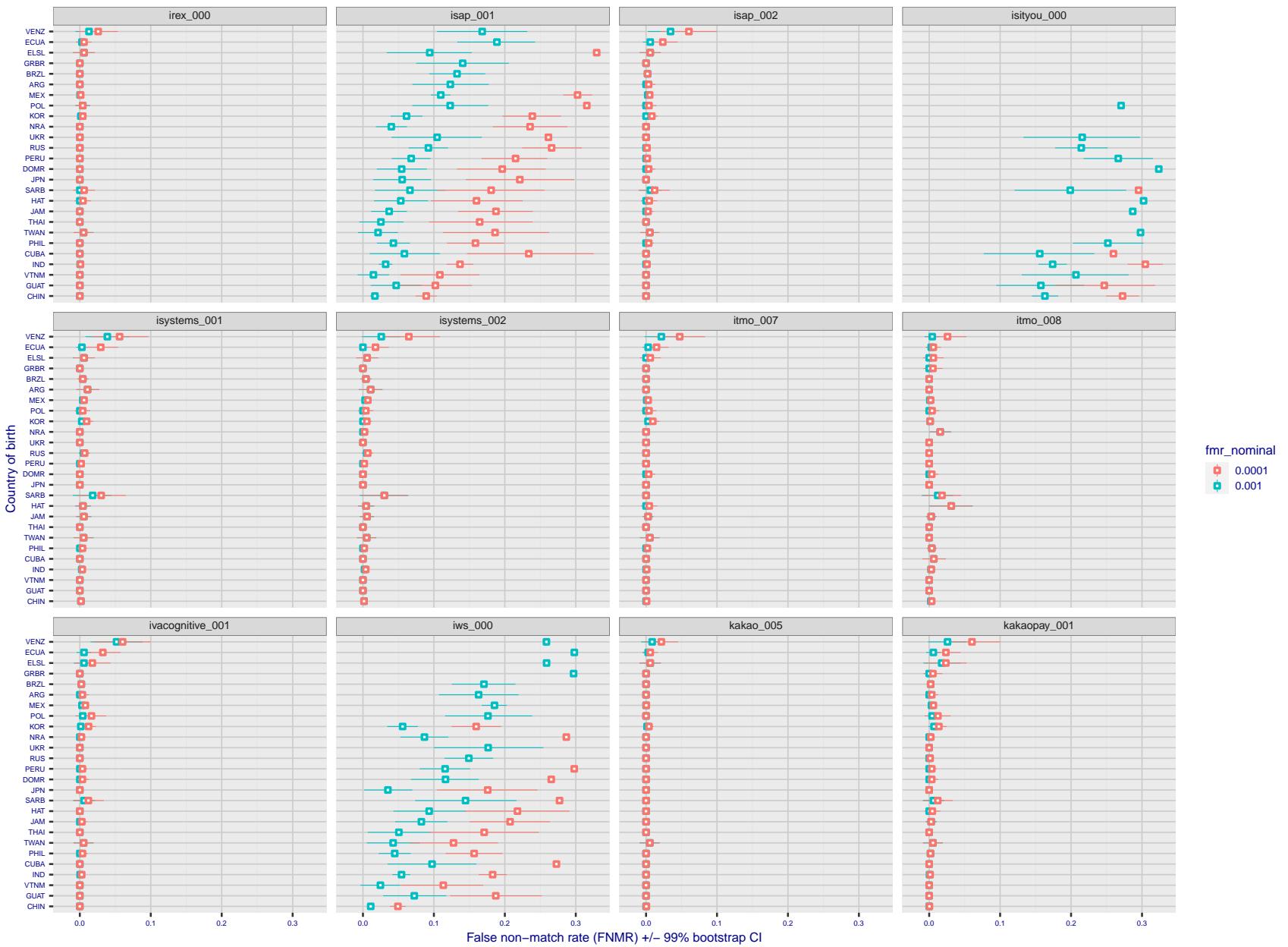


Figure 237: For the visa images, the dots show FNMR by country of birth for two globally set operating thresholds corresponding to  $FMR = \{0.001, 0.0001\}$  computed over all on the order of  $10^{10}$  impostor scores. The FMR in each bin will vary also - see subsequent impostor heatmaps in sec. 3.6.1. The figures shows an order of magnitude variation in FNMR across country of birth; these effects are likely due quality variations, then demographics like age and race. The error rates in some cases are zero, and in others the DET is flat so the error rates at the two thresholds are identical. The lines span 1% and 99% of bootstrap replicated FNMR estimates.

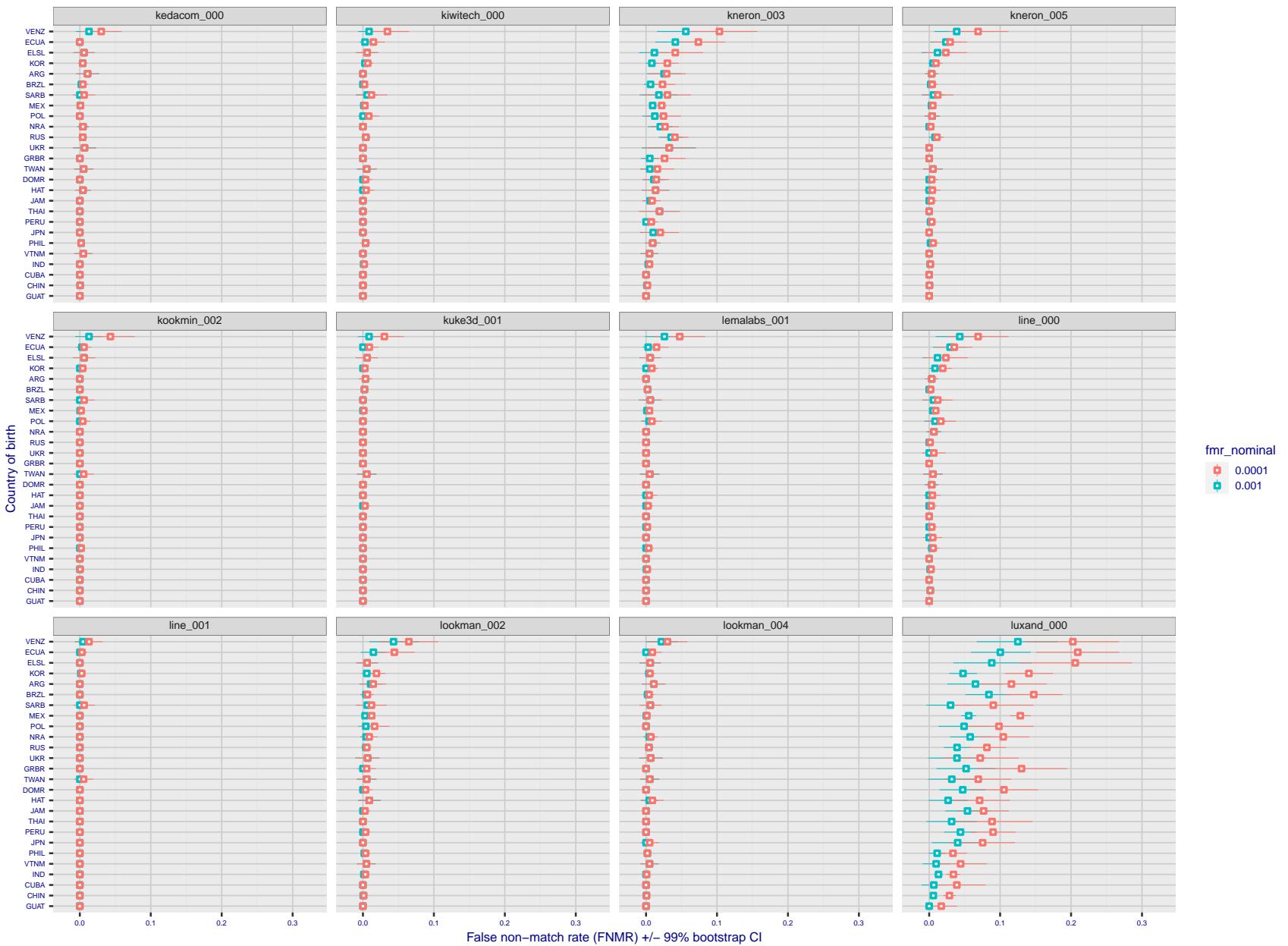


Figure 238: For the visa images, the dots show FNMR by country of birth for two globally set operating thresholds corresponding to  $FMR = \{0.001, 0.0001\}$  computed over all on the order of  $10^{10}$  impostor scores. The FMR in each bin will vary also - see subsequent impostor heatmaps in sec. 3.6.1. The figures shows an order of magnitude variation in FNMR across country of birth; these effects are likely due quality variations, then demographics like age and race. The error rates in some cases are zero, and in others the DET is flat so the error rates at the two thresholds are identical. The lines span 1% and 99% of bootstrap replicated FNMR estimates.

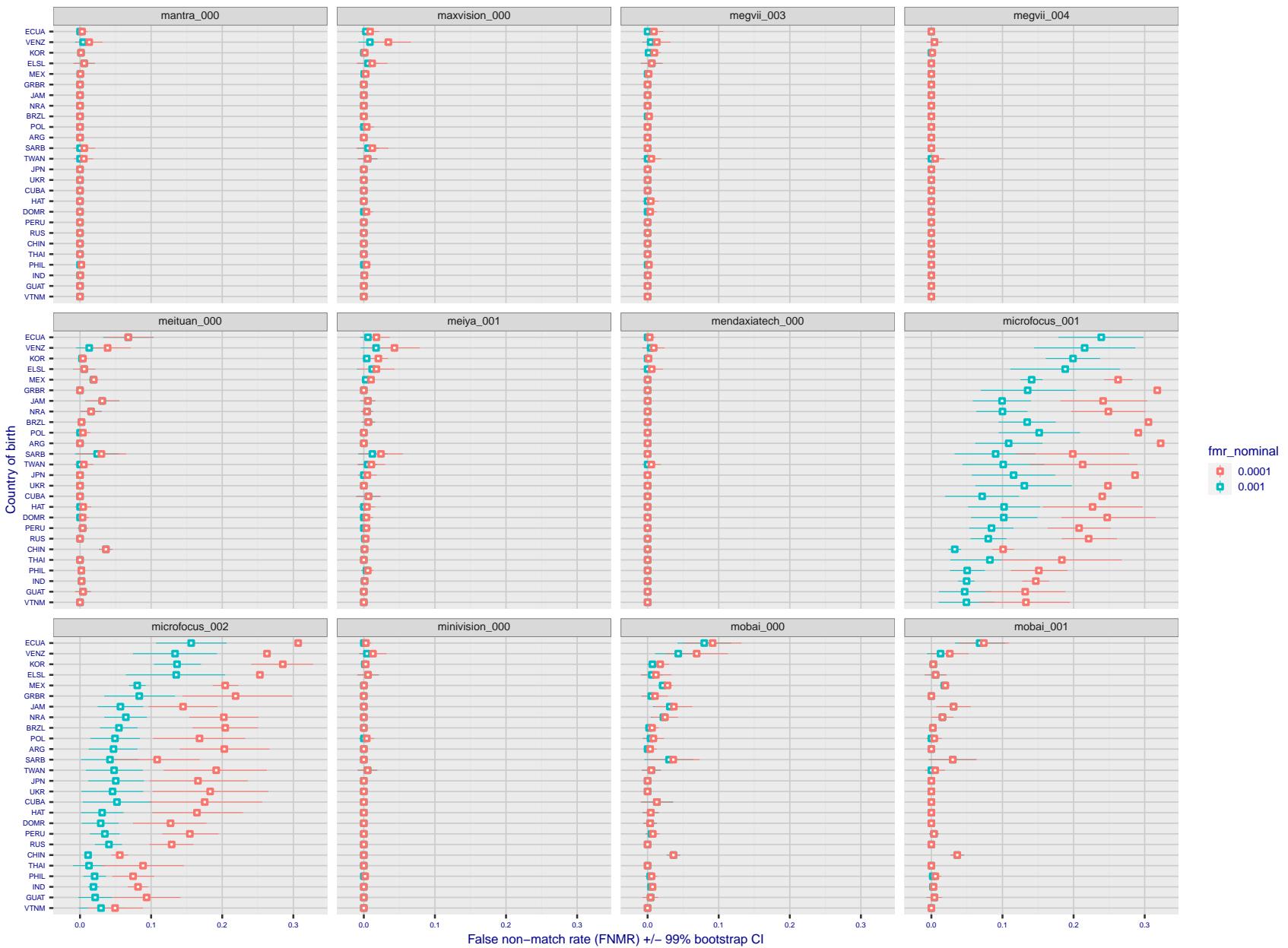


Figure 239: For the visa images, the dots show FNMR by country of birth for two globally set operating thresholds corresponding to  $FMR = \{0.001, 0.0001\}$  computed over all on the order of  $10^{10}$  impostor scores. The FMR in each bin will vary also - see subsequent impostor heatmaps in sec. 3.6.1. The figures shows an order of magnitude variation in FNMR across country of birth; these effects are likely due quality variations, then demographics like age and race. The error rates in some cases are zero, and in others the DET is flat so the error rates at the two thresholds are identical. The lines span 1% and 99% of bootstrap replicated FNMR estimates.

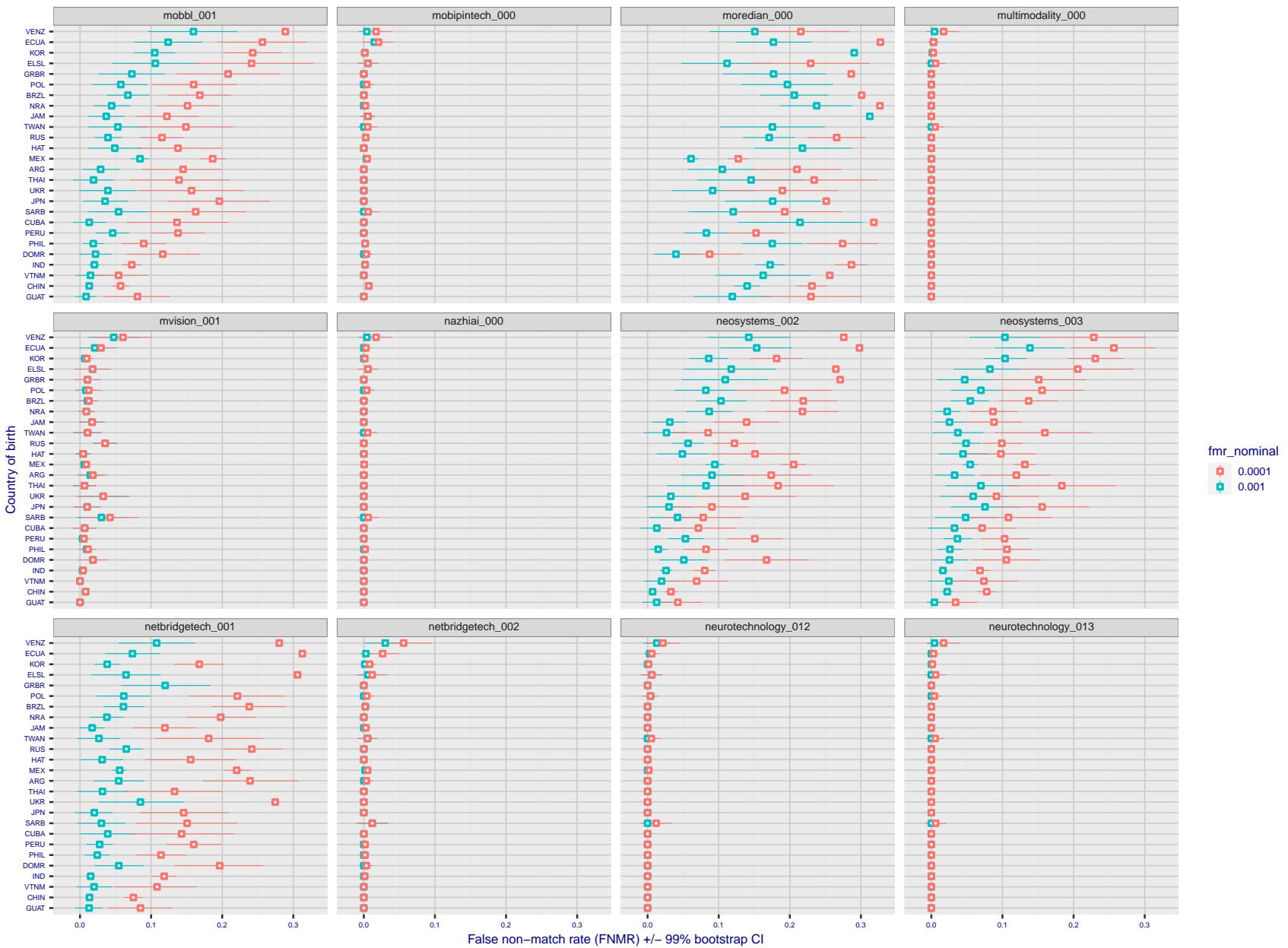


Figure 240: For the visa images, the dots show FNMR by country of birth for two globally set operating thresholds corresponding to  $FMR = \{0.001, 0.0001\}$  computed over all on the order of  $10^{10}$  impostor scores. The FMR in each bin will vary also - see subsequent impostor heatmaps in sec. 3.6.1. The figures shows an order of magnitude variation in FNMR across country of birth; these effects are likely due quality variations, then demographics like age and race. The error rates in some cases are zero, and in others the DET is flat so the error rates at the two thresholds are identical. The lines span 1% and 99% of bootstrap replicated FNMR estimates.

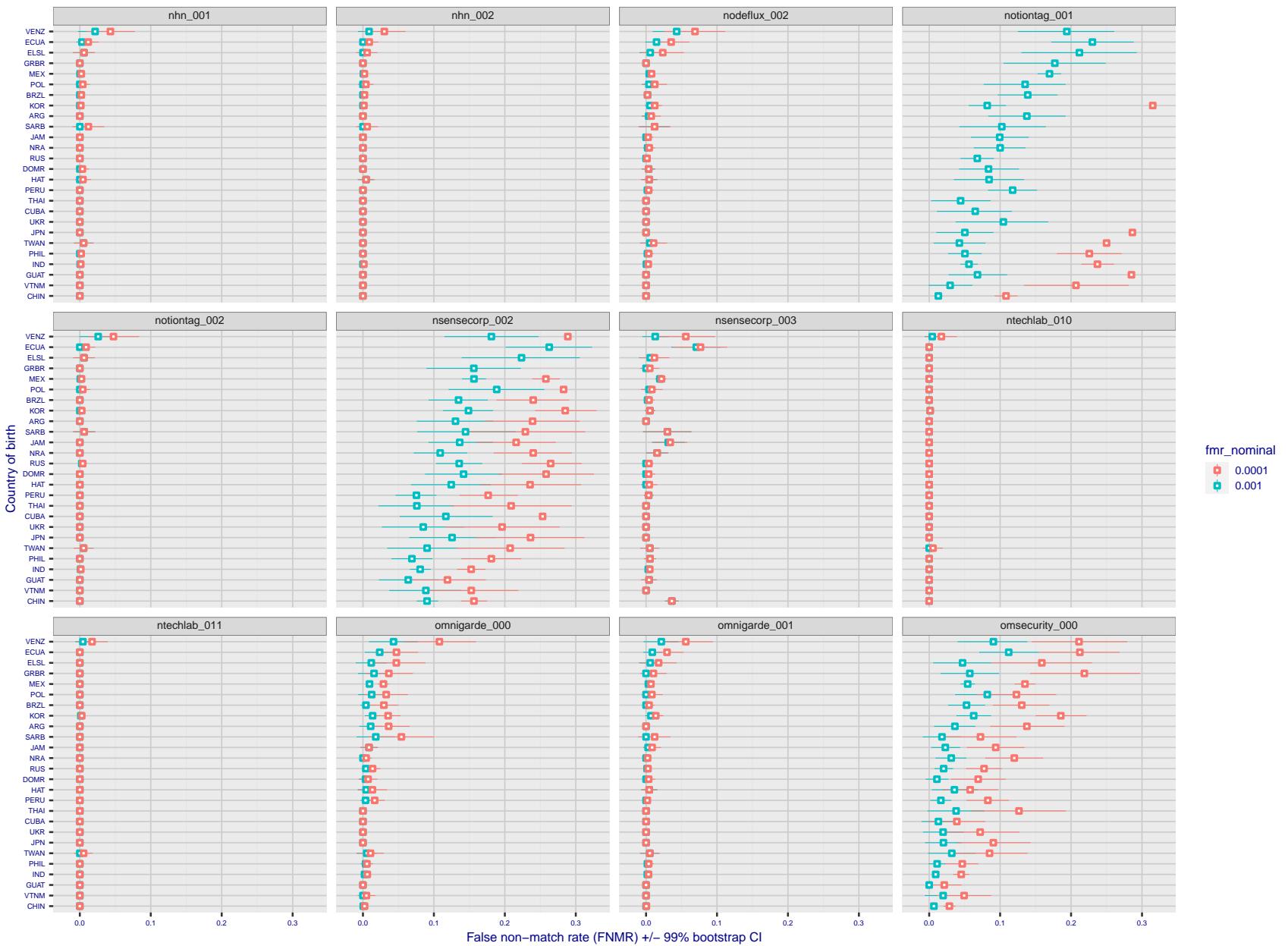


Figure 241: For the visa images, the dots show FNMR by country of birth for two globally set operating thresholds corresponding to  $FMR = \{0.001, 0.0001\}$  computed over all on the order of  $10^{10}$  impostor scores. The FMR in each bin will vary also - see subsequent impostor heatmaps in sec. 3.6.1. The figures shows an order of magnitude variation in FNMR across country of birth; these effects are likely due quality variations, then demographics like age and race. The error rates in some cases are zero, and in others the DET is flat so the error rates at the two thresholds are identical. The lines span 1% and 99% of bootstrap replicated FNMR estimates.

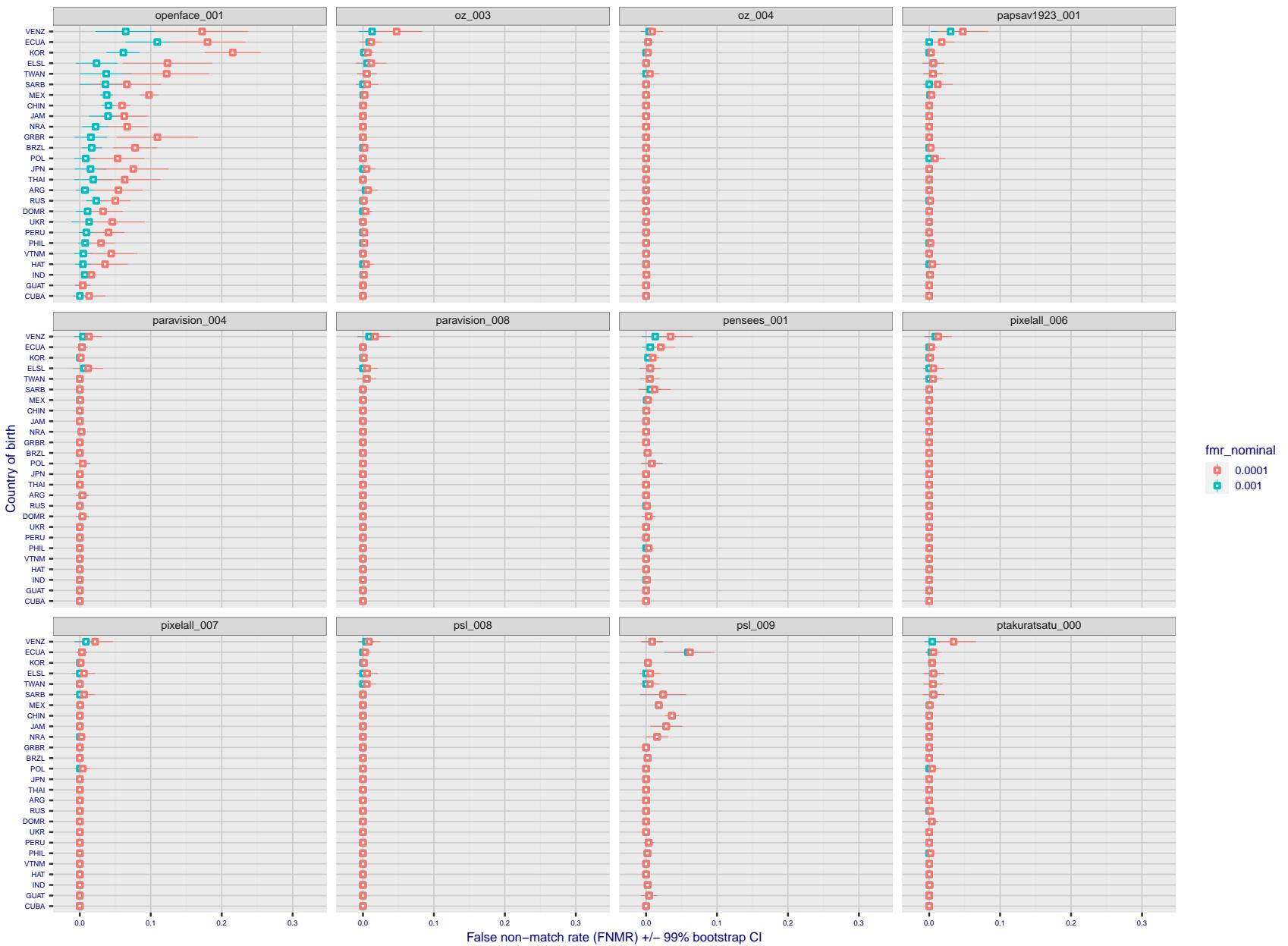


Figure 242: For the visa images, the dots show FNMR by country of birth for two globally set operating thresholds corresponding to  $FMR = \{0.001, 0.0001\}$  computed over all on the order of  $10^{10}$  impostor scores. The FMR in each bin will vary also - see subsequent impostor heatmaps in sec. 3.6.1. The figures shows an order of magnitude variation in FNMR across country of birth; these effects are likely due quality variations, then demographics like age and race. The error rates in some cases are zero, and in others the DET is flat so the error rates at the two thresholds are identical. The lines span 1% and 99% of bootstrap replicated FNMR estimates.

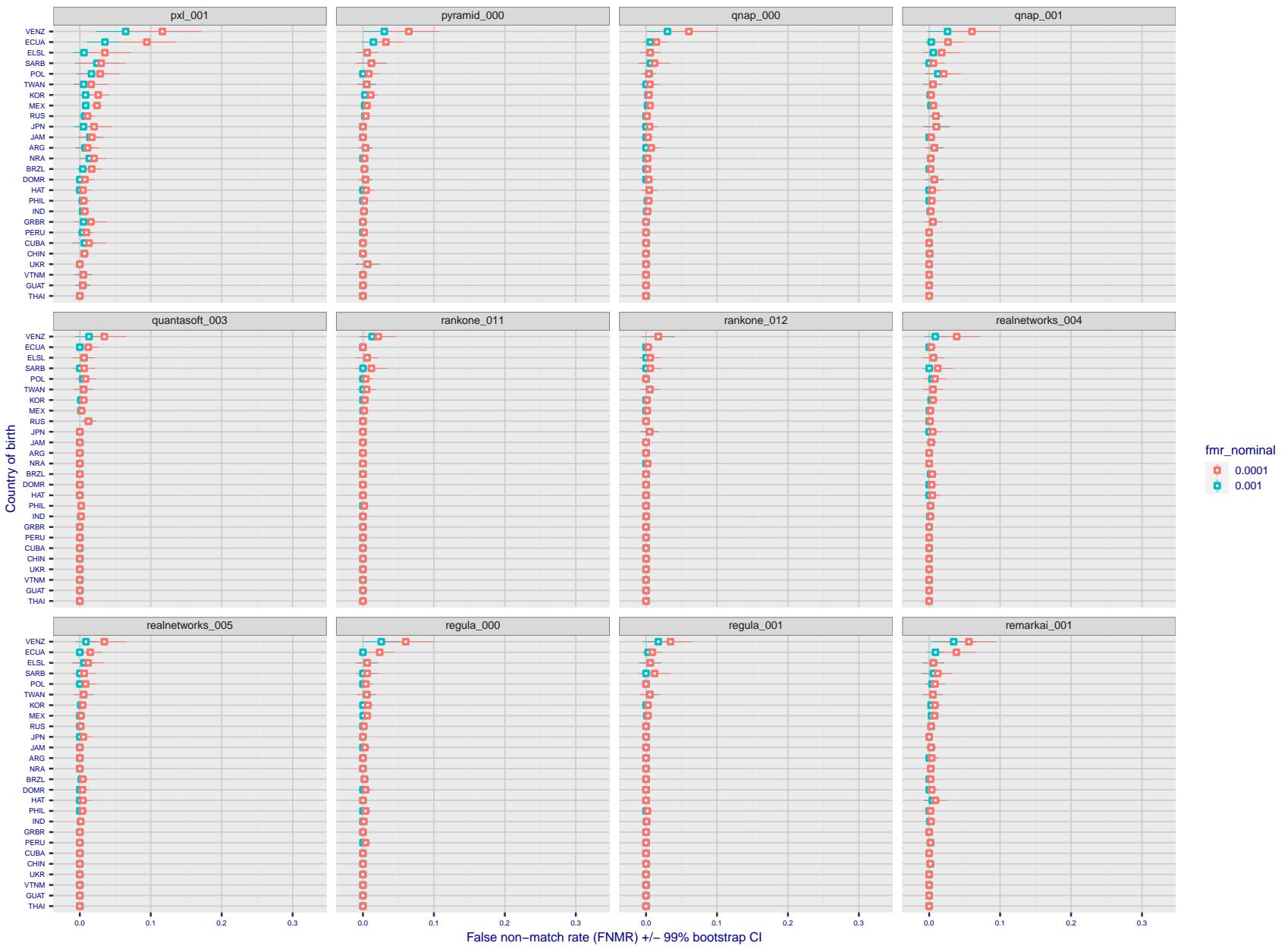


Figure 243: For the visa images, the dots show FNMR by country of birth for two globally set operating thresholds corresponding to  $FMR = \{0.001, 0.0001\}$  computed over all on the order of  $10^{10}$  impostor scores. The FMR in each bin will vary also - see subsequent impostor heatmaps in sec. 3.6.1. The figures shows an order of magnitude variation in FNMR across country of birth; these effects are likely due quality variations, then demographics like age and race. The error rates in some cases are zero, and in others the DET is flat so the error rates at the two thresholds are identical. The lines span 1% and 99% of bootstrap replicated FNMR estimates.

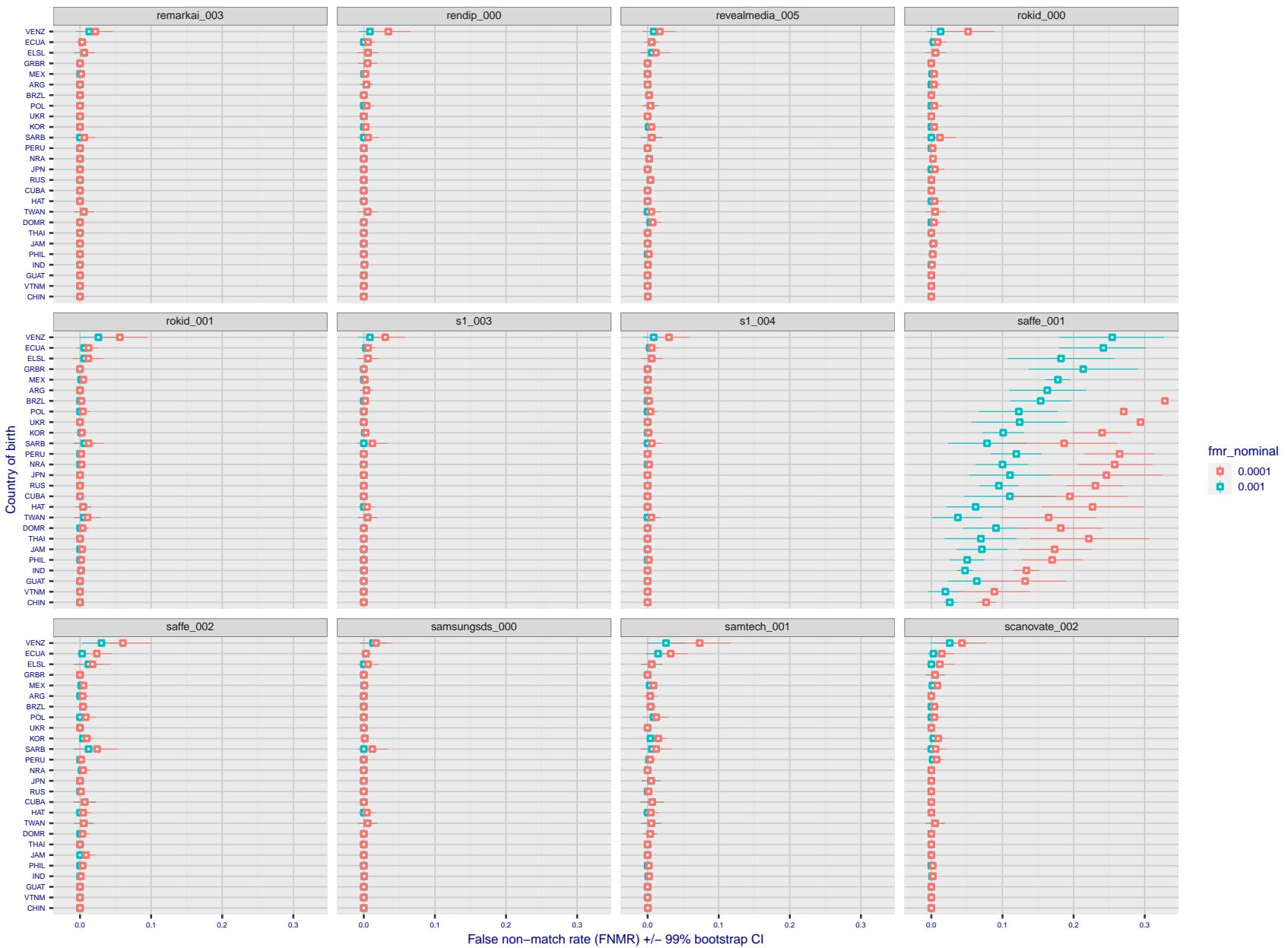


Figure 244: For the visa images, the dots show FNMR by country of birth for two globally set operating thresholds corresponding to  $FMR = \{0.001, 0.0001\}$  computed over all on the order of  $10^{10}$  impostor scores. The FMR in each bin will vary also - see subsequent impostor heatmaps in sec. 3.6.1. The figures shows an order of magnitude variation in FNMR across country of birth; these effects are likely due quality variations, then demographics like age and race. The error rates in some cases are zero, and in others the DET is flat so the error rates at the two thresholds are identical. The lines span 1% and 99% of bootstrap replicated FNMR estimates.

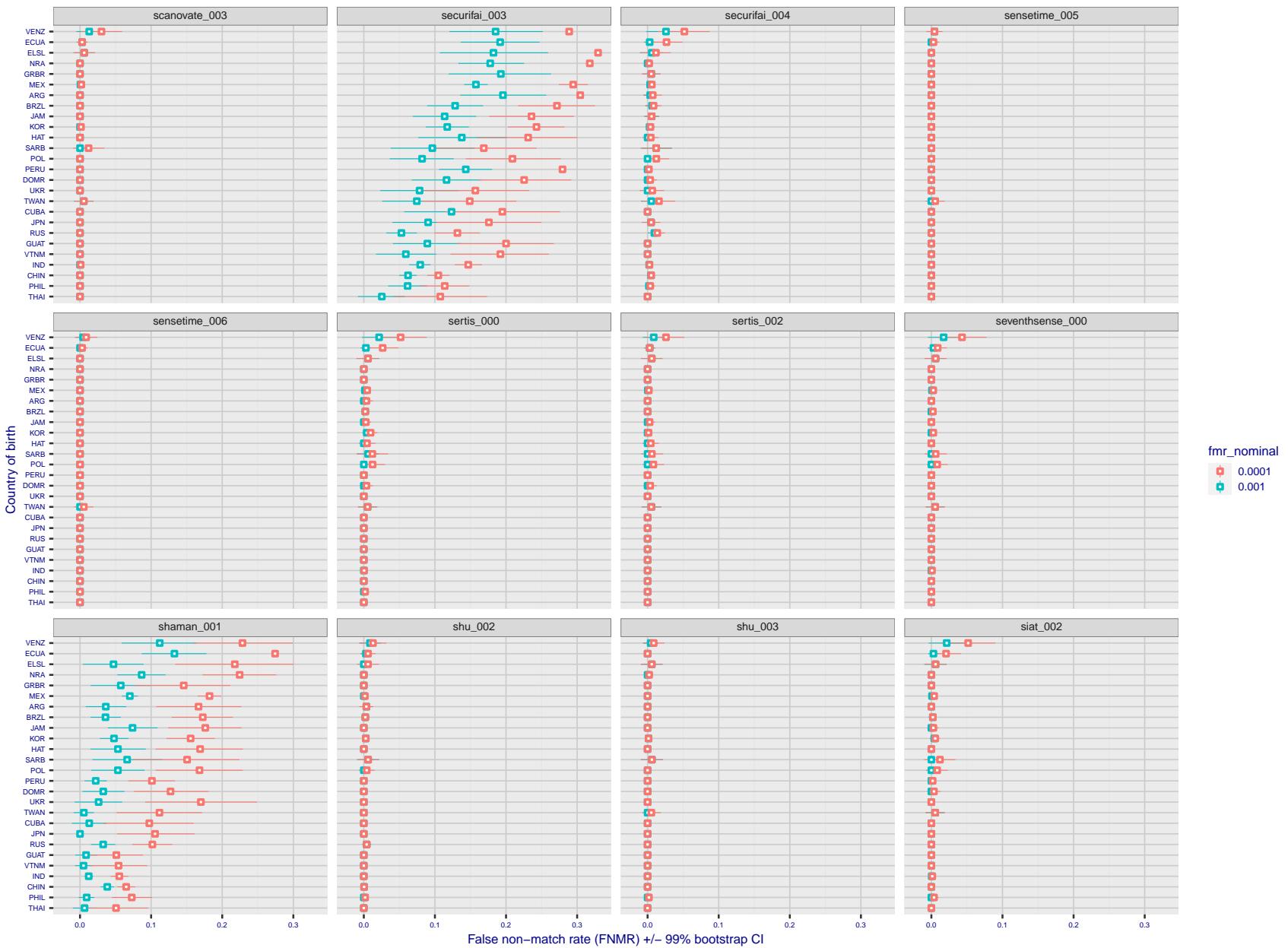


Figure 245: For the visa images, the dots show FNMR by country of birth for two globally set operating thresholds corresponding to  $FMR = \{0.001, 0.0001\}$  computed over all on the order of  $10^{10}$  impostor scores. The FMR in each bin will vary also - see subsequent impostor heatmaps in sec. 3.6.1. The figures shows an order of magnitude variation in FNMR across country of birth; these effects are likely due quality variations, then demographics like age and race. The error rates in some cases are zero, and in others the DET is flat so the error rates at the two thresholds are identical. The lines span 1% and 99% of bootstrap replicated FNMR estimates.

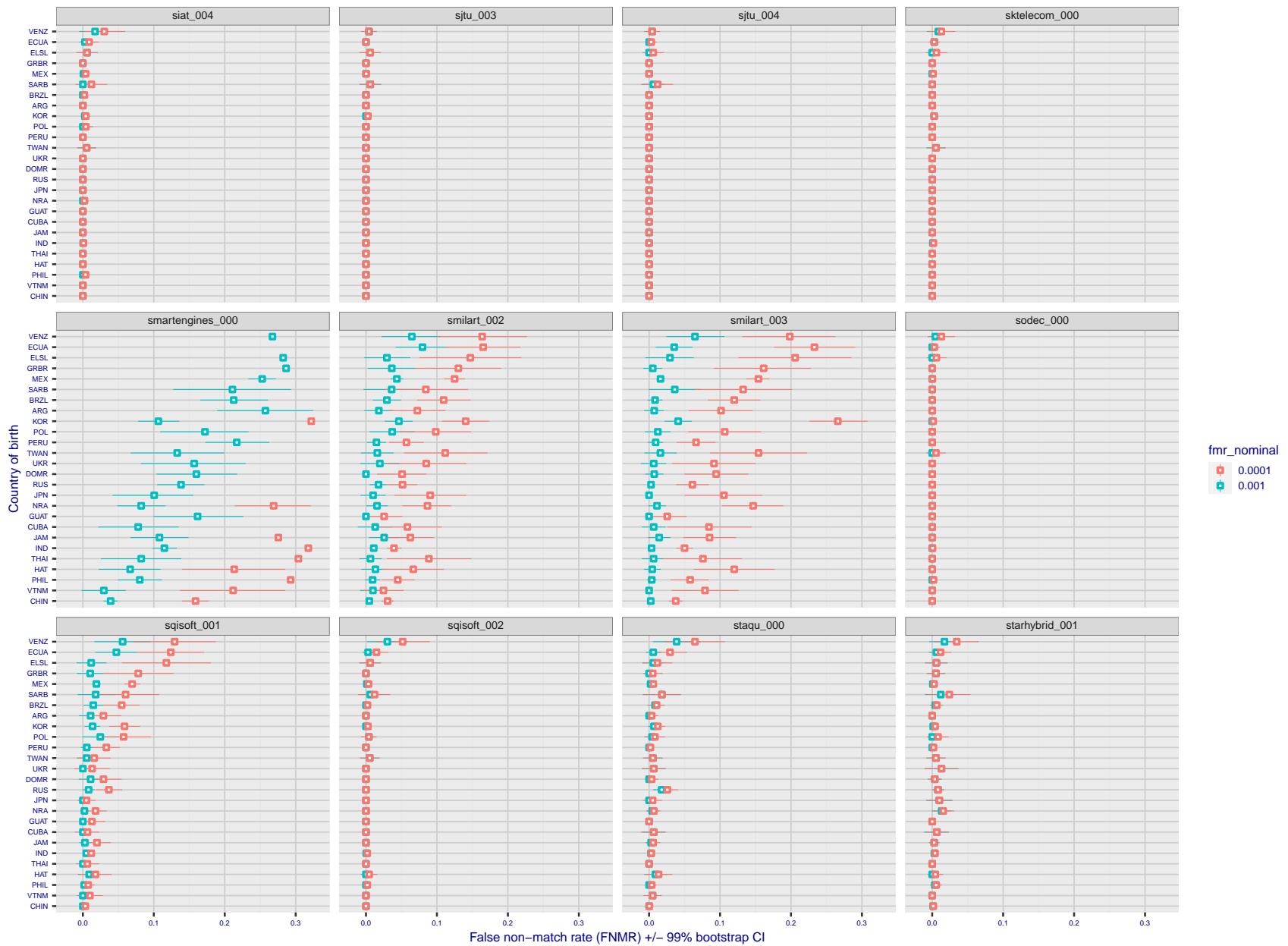


Figure 246: For the visa images, the dots show FNMR by country of birth for two globally set operating thresholds corresponding to  $FMR = \{0.001, 0.0001\}$  computed over all on the order of  $10^{10}$  impostor scores. The FMR in each bin will vary also - see subsequent impostor heatmaps in sec. 3.6.1. The figures shows an order of magnitude variation in FNMR across country of birth; these effects are likely due quality variations, then demographics like age and race. The error rates in some cases are zero, and in others the DET is flat so the error rates at the two thresholds are identical. The lines span 1% and 99% of bootstrap replicated FNMR estimates.

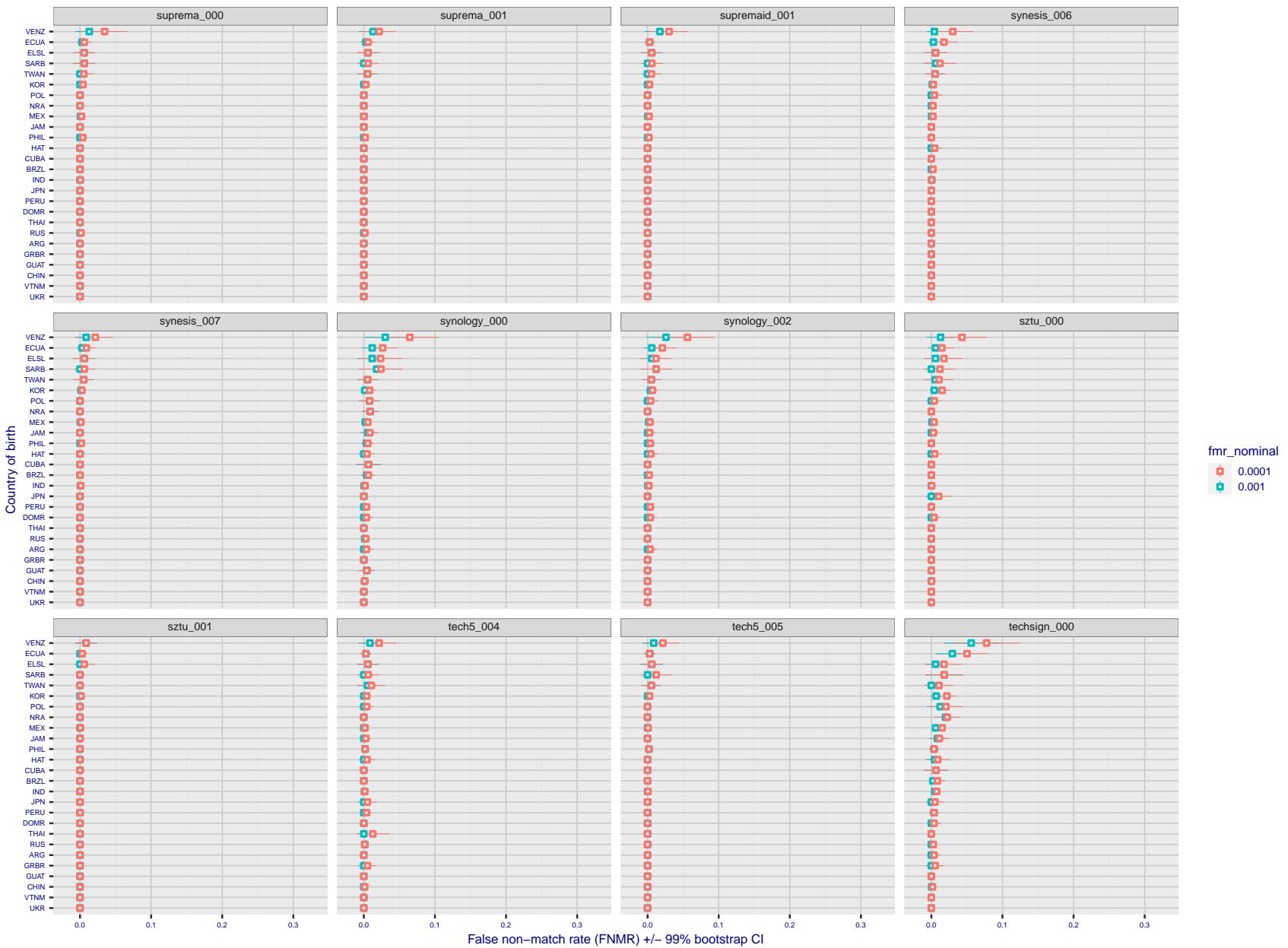


Figure 247: For the visa images, the dots show FNMR by country of birth for two globally set operating thresholds corresponding to  $FMR = \{0.001, 0.0001\}$  computed over all on the order of  $10^{10}$  impostor scores. The FMR in each bin will vary also - see subsequent impostor heatmaps in sec. 3.6.1. The figures shows an order of magnitude variation in FNMR across country of birth; these effects are likely due quality variations, then demographics like age and race. The error rates in some cases are zero, and in others the DET is flat so the error rates at the two thresholds are identical. The lines span 1% and 99% of bootstrap replicated FNMR estimates.

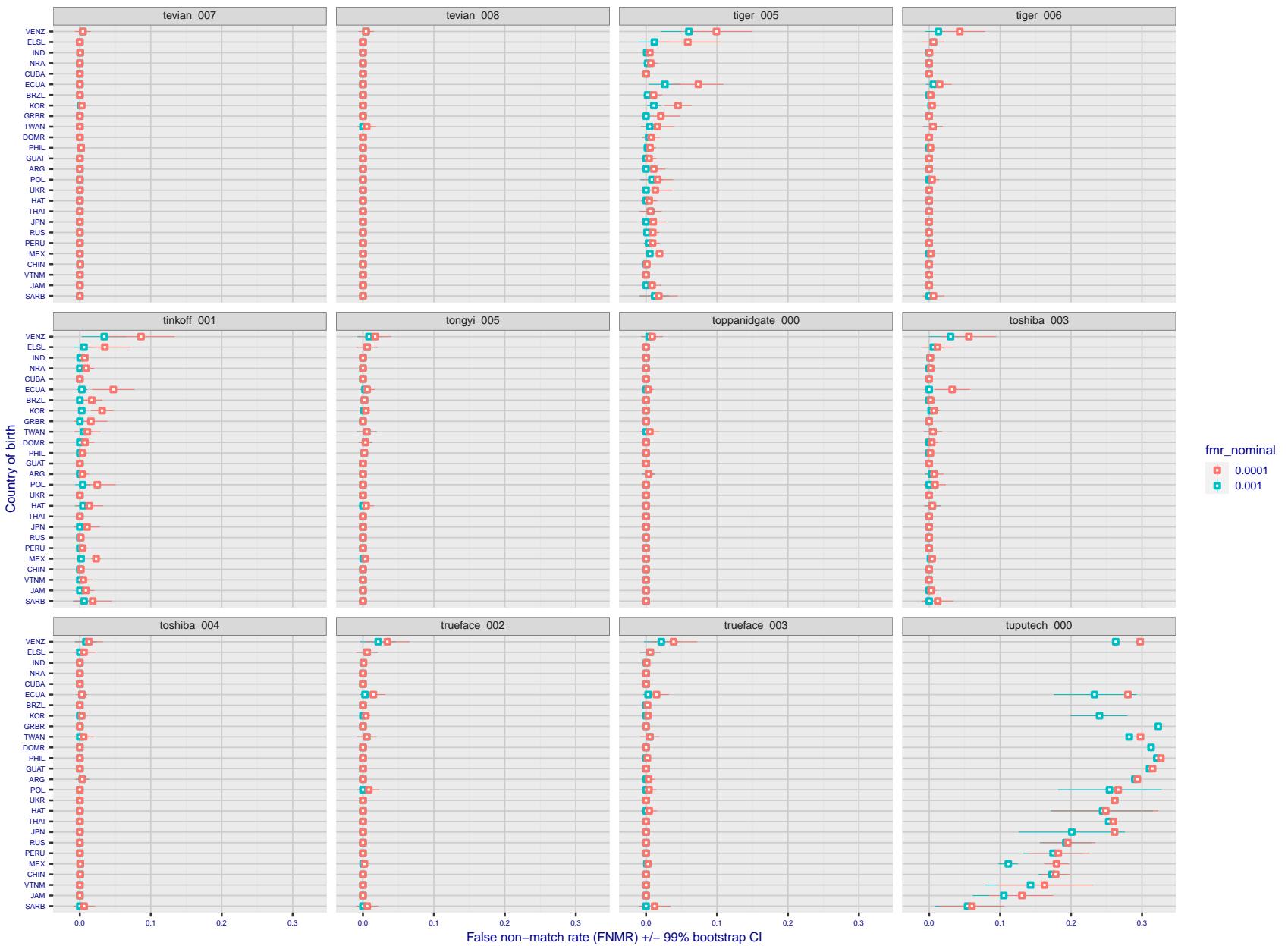


Figure 248: For the visa images, the dots show FNMR by country of birth for two globally set operating thresholds corresponding to  $FMR = \{0.001, 0.0001\}$  computed over all on the order of  $10^{10}$  impostor scores. The FMR in each bin will vary also - see subsequent impostor heatmaps in sec. 3.6.1. The figures shows an order of magnitude variation in FNMR across country of birth; these effects are likely due quality variations, then demographics like age and race. The error rates in some cases are zero, and in others the DET is flat so the error rates at the two thresholds are identical. The lines span 1% and 99% of bootstrap replicated FNMR estimates.

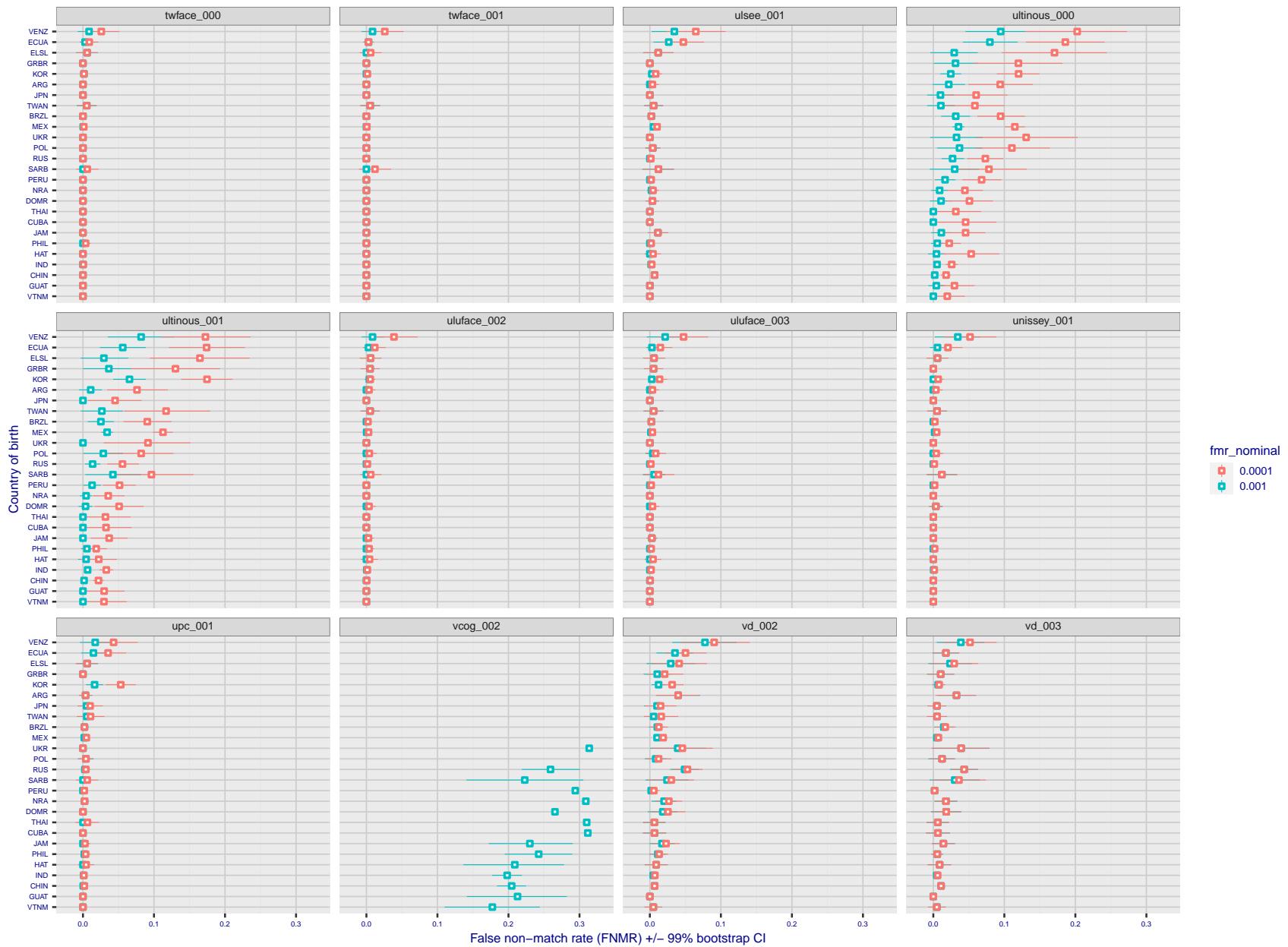


Figure 249: For the visa images, the dots show FNMR by country of birth for two globally set operating thresholds corresponding to  $FMR = \{0.001, 0.0001\}$  computed over all on the order of  $10^{10}$  impostor scores. The FMR in each bin will vary also - see subsequent impostor heatmaps in sec. 3.6.1. The figures shows an order of magnitude variation in FNMR across country of birth; these effects are likely due quality variations, then demographics like age and race. The error rates in some cases are zero, and in others the DET is flat so the error rates at the two thresholds are identical. The lines span 1% and 99% of bootstrap replicated FNMR estimates.

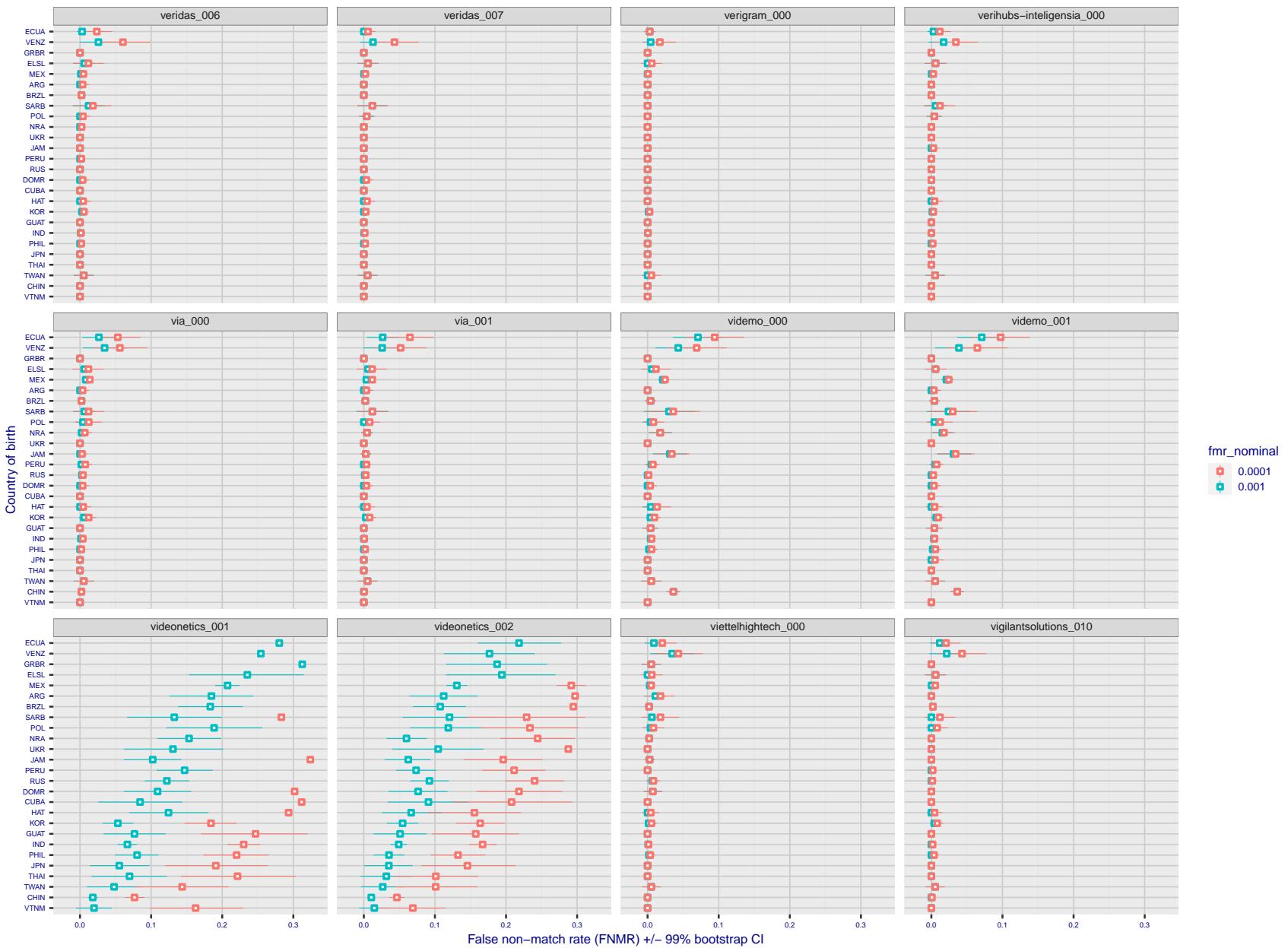


Figure 250: For the visa images, the dots show FNMR by country of birth for two globally set operating thresholds corresponding to  $FMR = \{0.001, 0.0001\}$  computed over all on the order of  $10^{10}$  impostor scores. The FMR in each bin will vary also - see subsequent impostor heatmaps in sec. 3.6.1. The figures shows an order of magnitude variation in FNMR across country of birth; these effects are likely due quality variations, then demographics like age and race. The error rates in some cases are zero, and in others the DET is flat so the error rates at the two thresholds are identical. The lines span 1% and 99% of bootstrap replicated FNMR estimates.

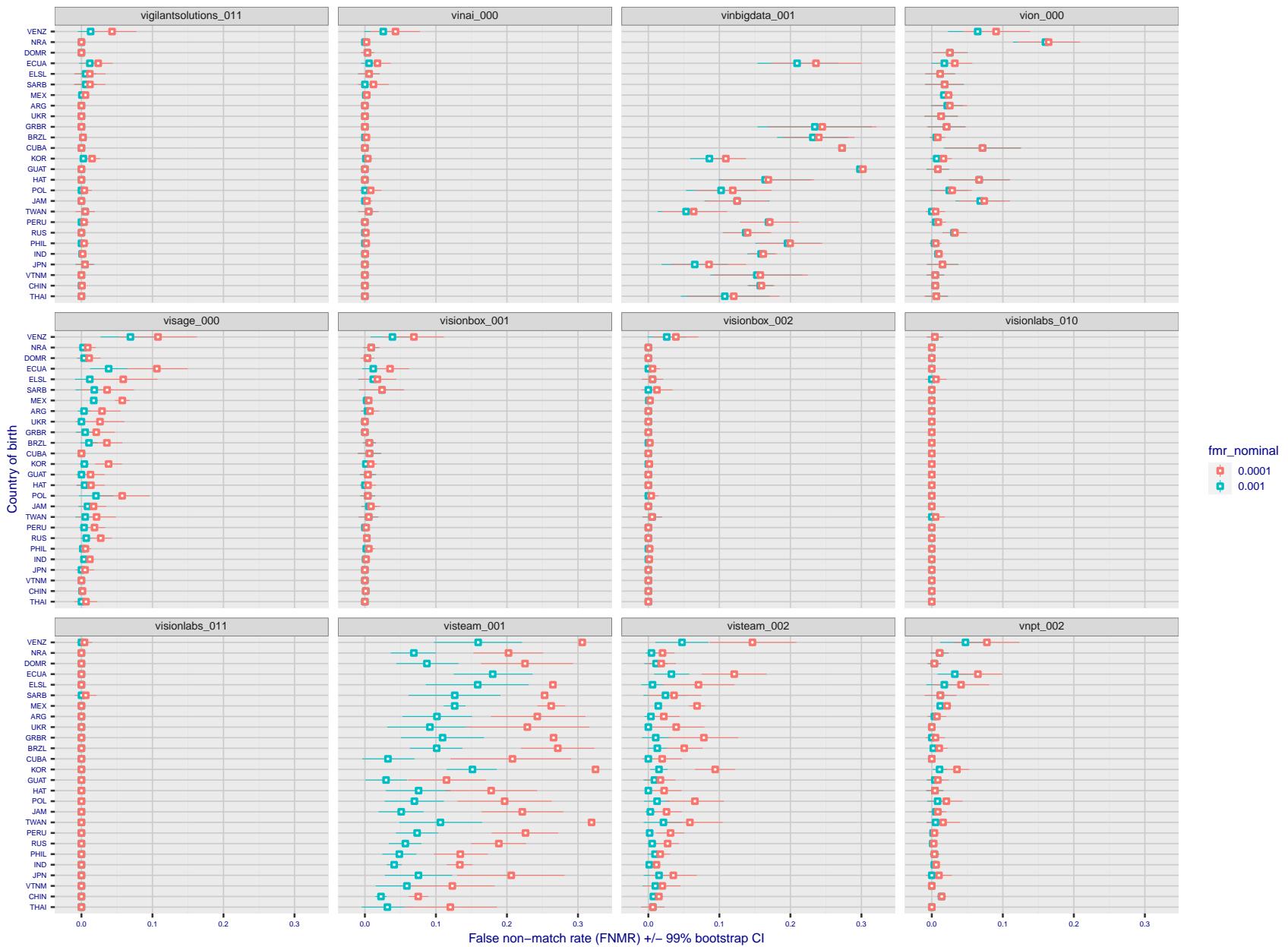


Figure 251: For the visa images, the dots show FNMR by country of birth for two globally set operating thresholds corresponding to  $FMR = \{0.001, 0.0001\}$  computed over all on the order of  $10^{10}$  impostor scores. The FMR in each bin will vary also - see subsequent impostor heatmaps in sec. 3.6.1. The figures shows an order of magnitude variation in FNMR across country of birth; these effects are likely due quality variations, then demographics like age and race. The error rates in some cases are zero, and in others the DET is flat so the error rates at the two thresholds are identical. The lines span 1% and 99% of bootstrap replicated FNMR estimates.

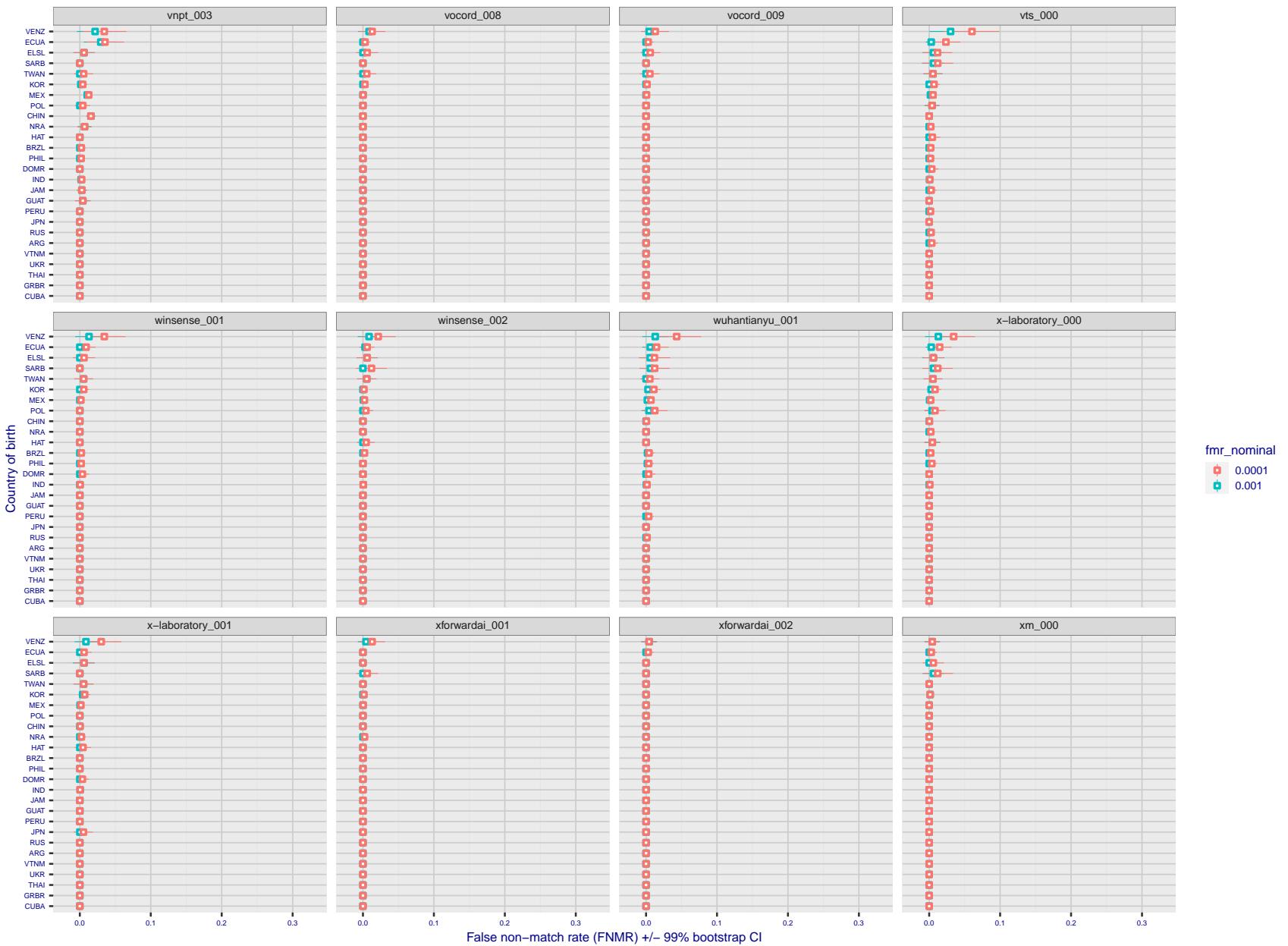


Figure 252: For the visa images, the dots show FNMR by country of birth for two globally set operating thresholds corresponding to  $FMR = \{0.001, 0.0001\}$  computed over all on the order of  $10^{10}$  impostor scores. The FMR in each bin will vary also - see subsequent impostor heatmaps in sec. 3.6.1. The figures shows an order of magnitude variation in FNMR across country of birth; these effects are likely due quality variations, then demographics like age and race. The error rates in some cases are zero, and in others the DET is flat so the error rates at the two thresholds are identical. The lines span 1% and 99% of bootstrap replicated FNMR estimates.

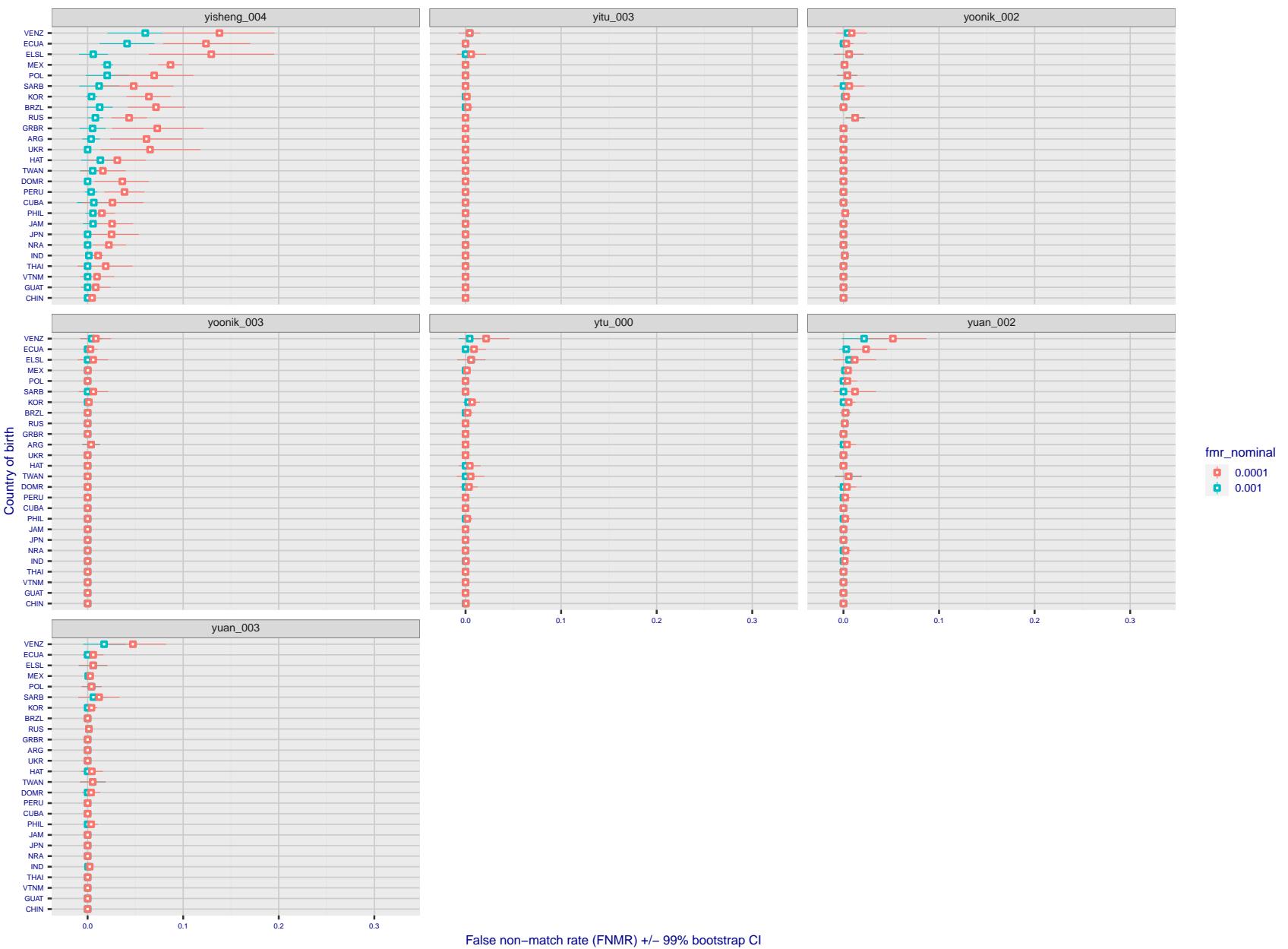


Figure 253: For the visa images, the dots show FNMR by country of birth for two globally set operating thresholds corresponding to  $FMR = \{0.001, 0.0001\}$  computed over all on the order of  $10^{10}$  impostor scores. The FMR in each bin will vary also - see subsequent impostor heatmaps in sec. 3.6.1. The figures shows an order of magnitude variation in FNMR across country of birth; these effects are likely due quality variations, then demographics like age and race. The error rates in some cases are zero, and in others the DET is flat so the error rates at the two thresholds are identical. The lines span 1% and 99% of bootstrap replicated FNMR estimates.

**Caveats:** The results may not relate to subject-specific properties. Instead they could reflect image-specific quality differences, which could occur due to collection protocol or software processing variations.

### 3.5.2 Effect of ageing

**Background:** Faces change appearance throughout life. This change gradually reduces similarity of a new image to an earlier image. Face recognition algorithms give reduced similarity scores and more frequent false rejections.

**Goal:** To quantify false non-match rates (FNMR) as a function of elapsed time in an adult population.

**Methods:** Using the mugshot images, a threshold is set to give FMR = 0.00001 over the entire impostor set. Then FNMR is measured over 1000 bootstrap replications of the genuine scores.

**Results:** For the visa images, Figure 277 shows how false non-match rates for genuine users, as a function of age group.

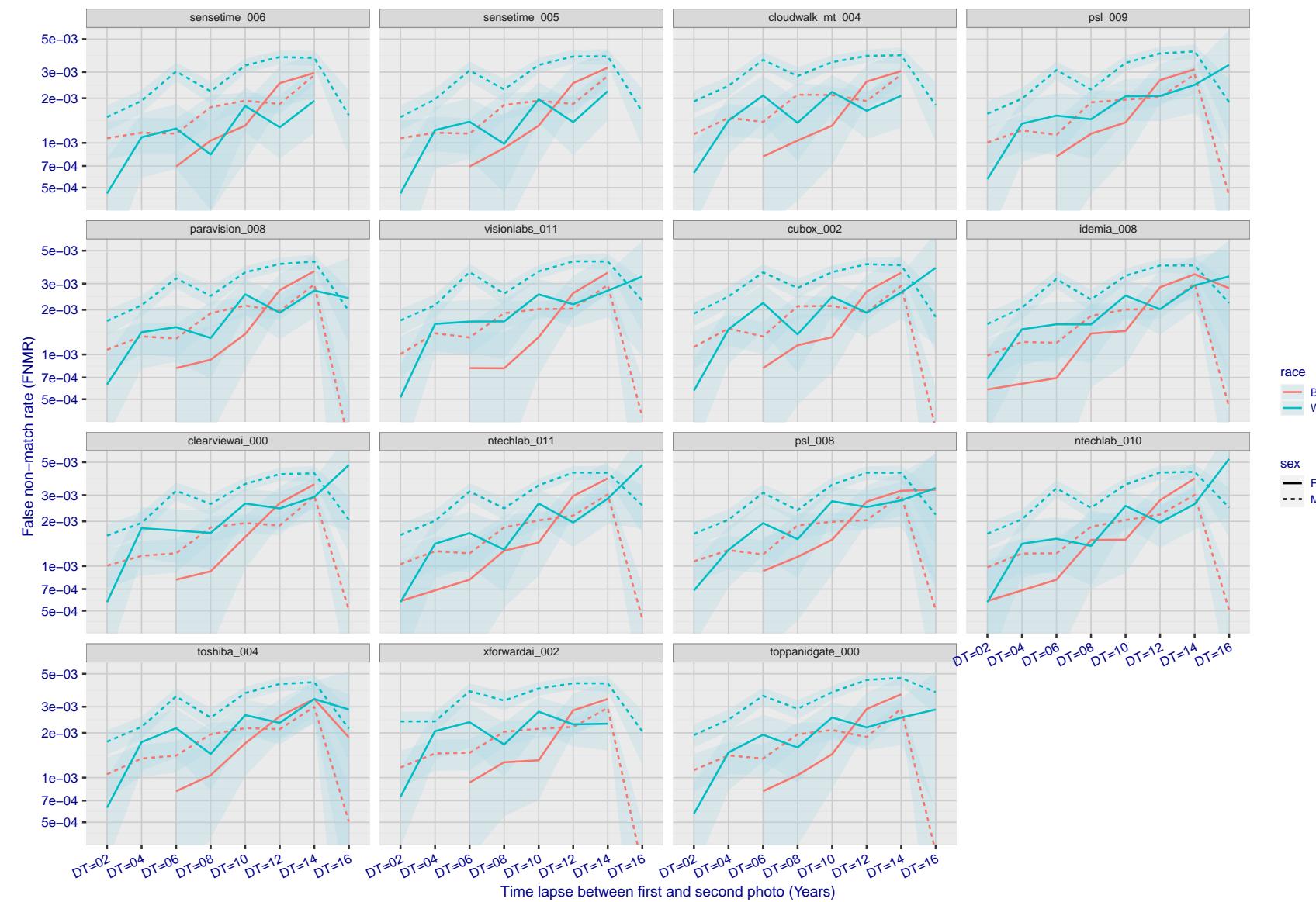


Figure 254: For the mugshot images, FNMR as a function of elapsed time between initial enrollment and second verification images. The panels appear most accurate first, and vertical scale changes on each page. The four traces correspond to images annotated with codes for black female, black male, white female, white male. The threshold is fixed for each algorithm to give  $FMR = 0.00001$  over all ( $10^8$ ) impostor comparisons. For short time-lapses, the most accurate algorithms give very few errors ( $FNMR < 0.001$ ) so that the uncertainty estimates are high.

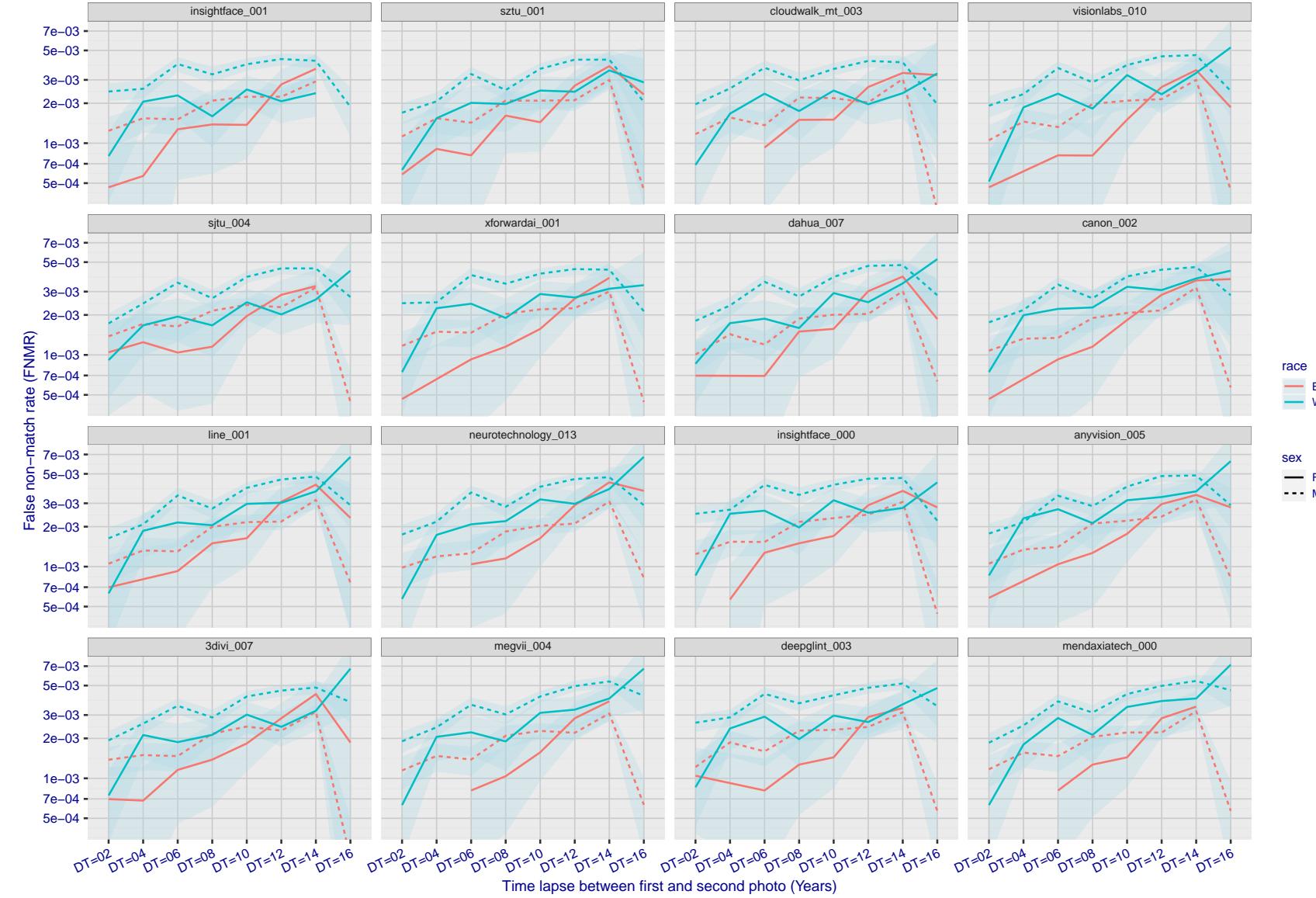


Figure 255: For the mugshot images, FNMR as a function of elapsed time between initial enrollment and second verification images. The panels appear most accurate first, and vertical scale changes on each page. The four traces correspond to images annotated with codes for black female, black male, white female, white male. The threshold is fixed for each algorithm to give  $FMR = 0.00001$  over all ( $10^8$ ) impostor comparisons. For short time-lapses, the most accurate algorithms give very few errors ( $FNMR < 0.001$ ) so that the uncertainty estimates are high.

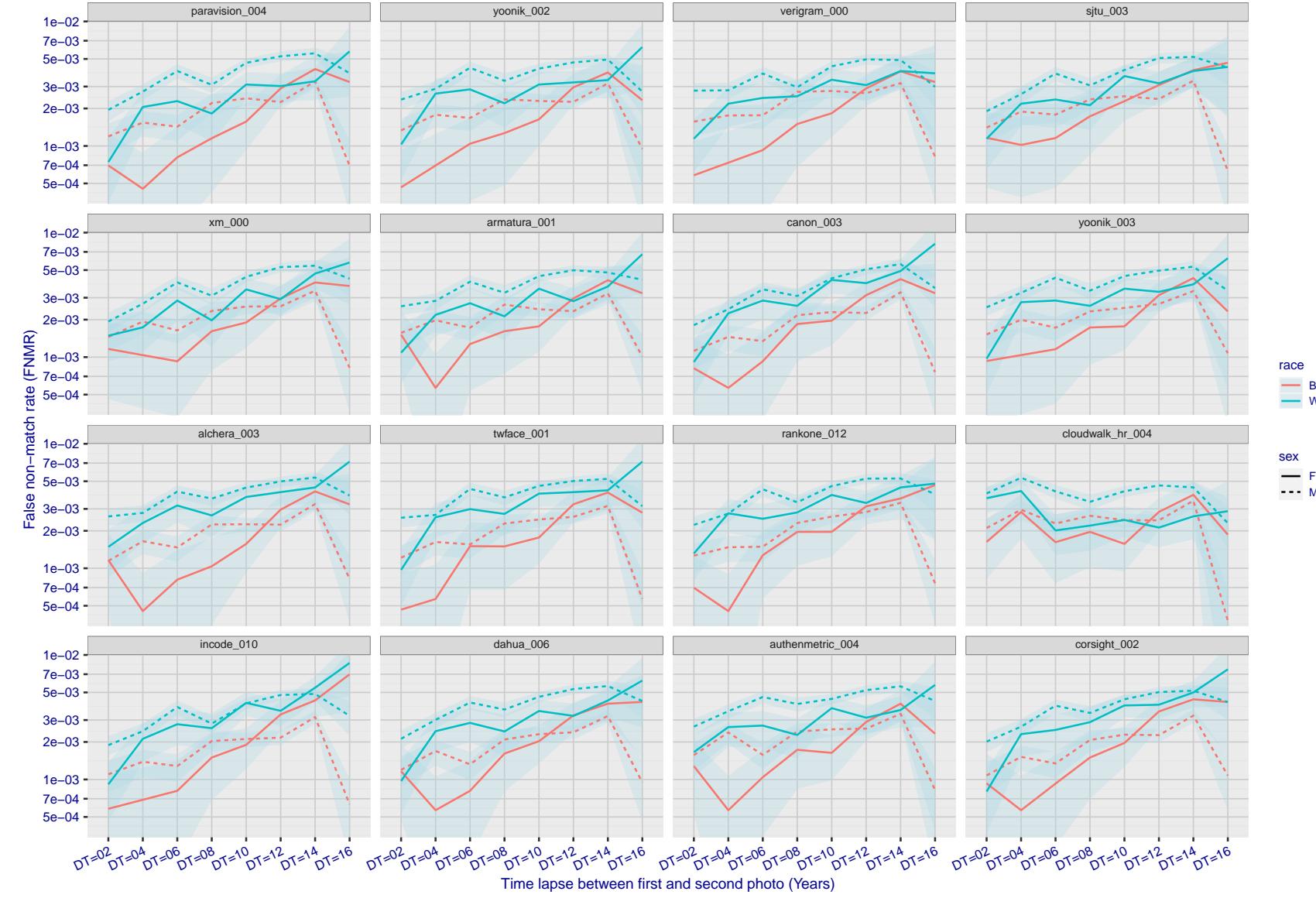


Figure 256: For the mugshot images, FNMR as a function of elapsed time between initial enrollment and second verification images. The panels appear most accurate first, and vertical scale changes on each page. The four traces correspond to images annotated with codes for black female, black male, white female, white male. The threshold is fixed for each algorithm to give  $FMR = 0.00001$  over all ( $10^8$ ) impostor comparisons. For short time-lapses, the most accurate algorithms give very few errors ( $FNMR < 0.001$ ) so that the uncertainty estimates are high.

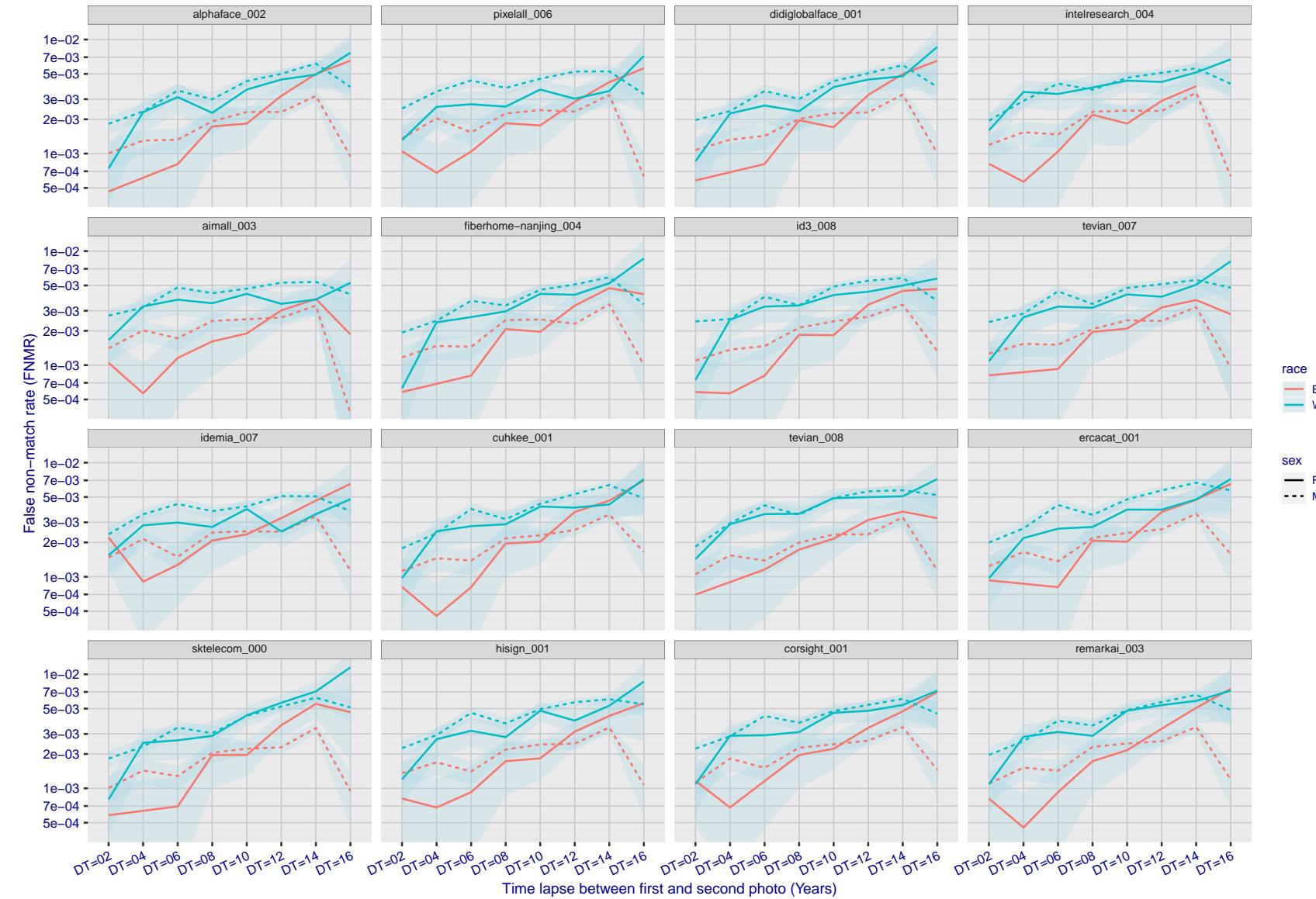


Figure 257: For the mugshot images, FNMR as a function of elapsed time between initial enrollment and second verification images. The panels appear most accurate first, and vertical scale changes on each page. The four traces correspond to images annotated with codes for black female, black male, white female, white male. The threshold is fixed for each algorithm to give  $FMR = 0.00001$  over all ( $10^8$ ) impostor comparisons. For short time-lapses, the most accurate algorithms give very few errors ( $FNMR < 0.001$ ) so that the uncertainty estimates are high.

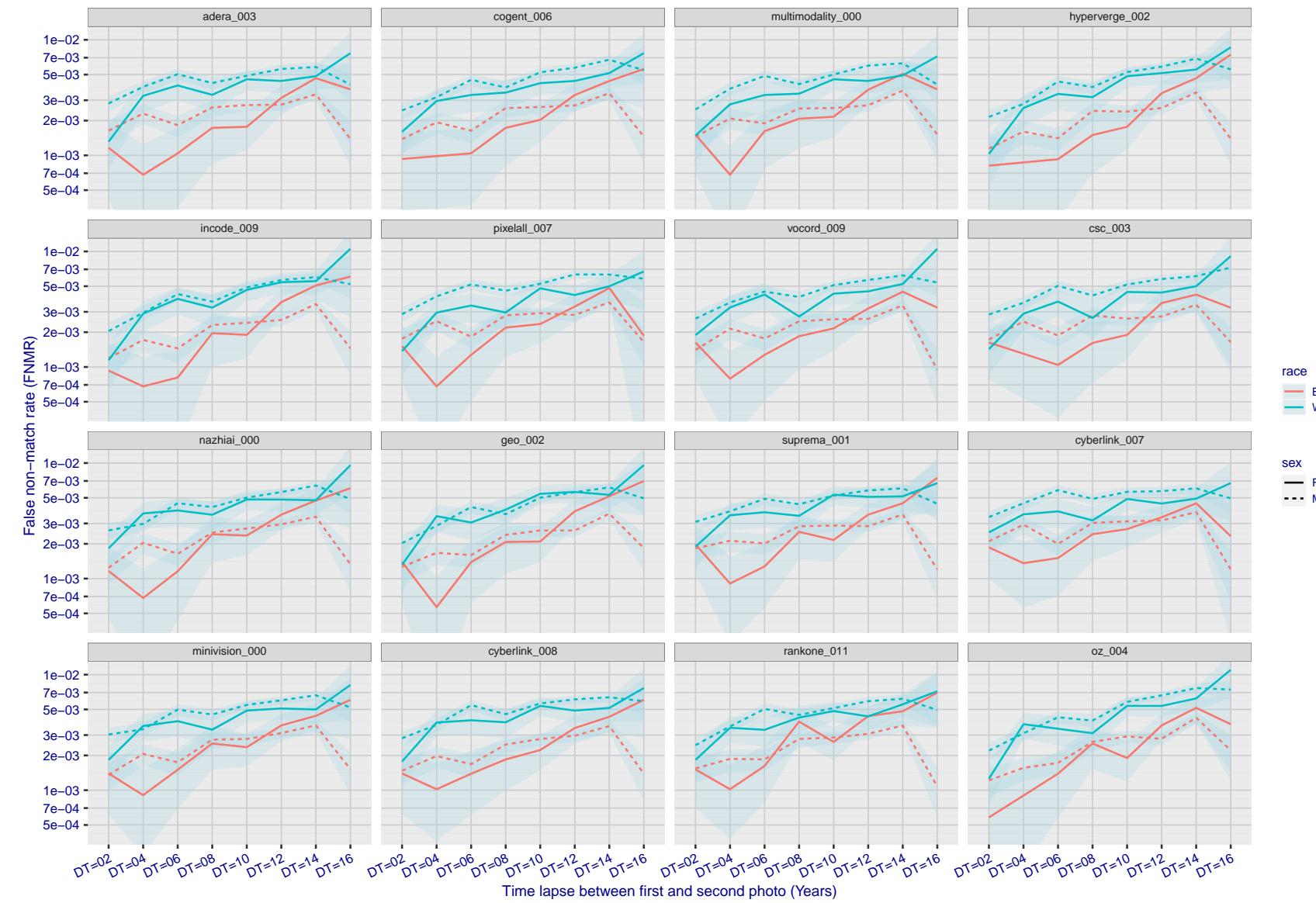


Figure 258: For the mugshot images, FNMR as a function of elapsed time between initial enrollment and second verification images. The panels appear most accurate first, and vertical scale changes on each page. The four traces correspond to images annotated with codes for black female, black male, white female, white male. The threshold is fixed for each algorithm to give  $FMR = 0.00001$  over all ( $10^8$ ) impostor comparisons. For short time-lapses, the most accurate algorithms give very few errors ( $FNMR < 0.001$ ) so that the uncertainty estimates are high.

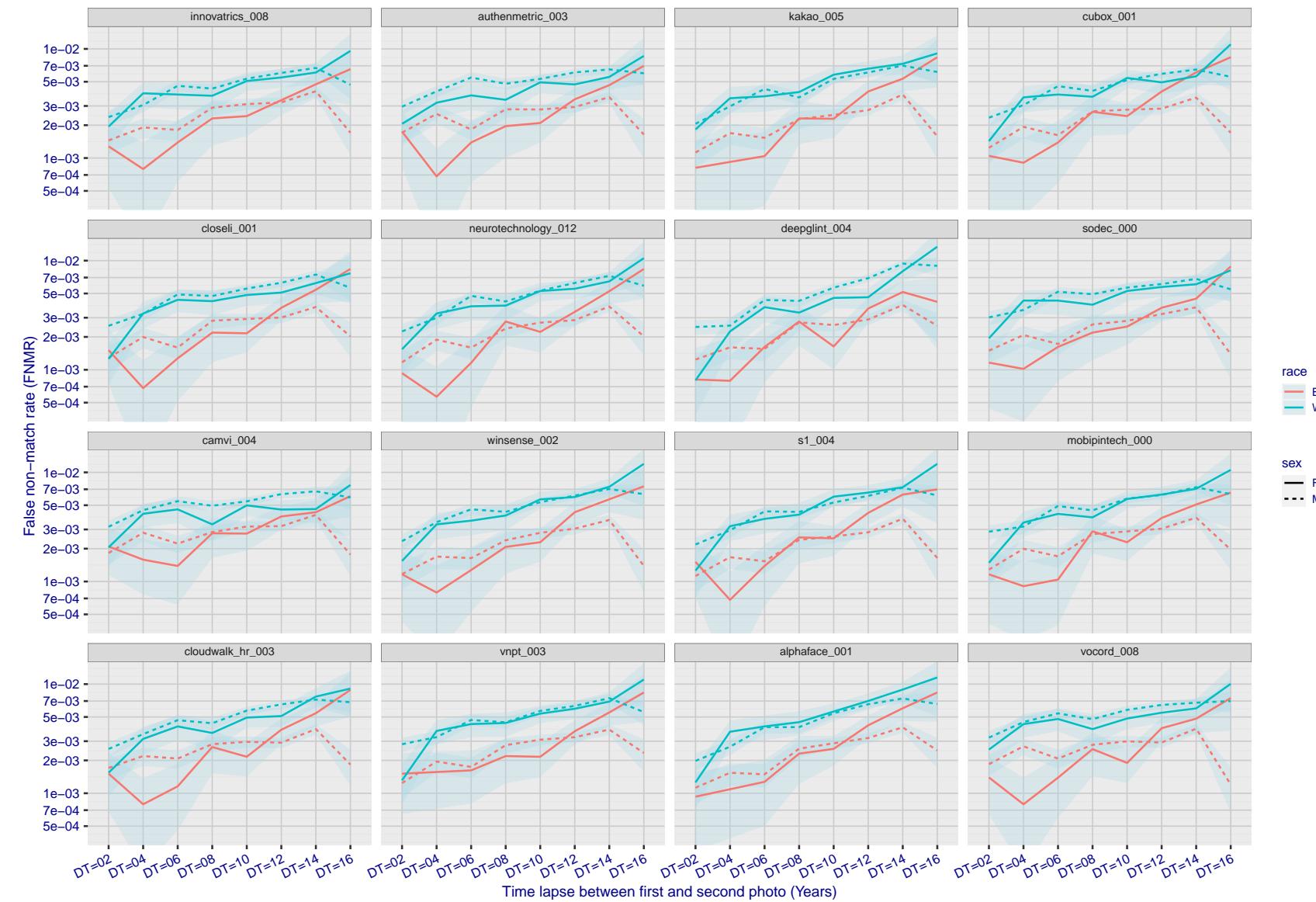


Figure 259: For the mugshot images, FNMR as a function of elapsed time between initial enrollment and second verification images. The panels appear most accurate first, and vertical scale changes on each page. The four traces correspond to images annotated with codes for black female, black male, white female, white male. The threshold is fixed for each algorithm to give  $FMR = 0.00001$  over all ( $10^8$ ) impostor comparisons. For short time-lapses, the most accurate algorithms give very few errors ( $FNMR < 0.001$ ) so that the uncertainty estimates are high.

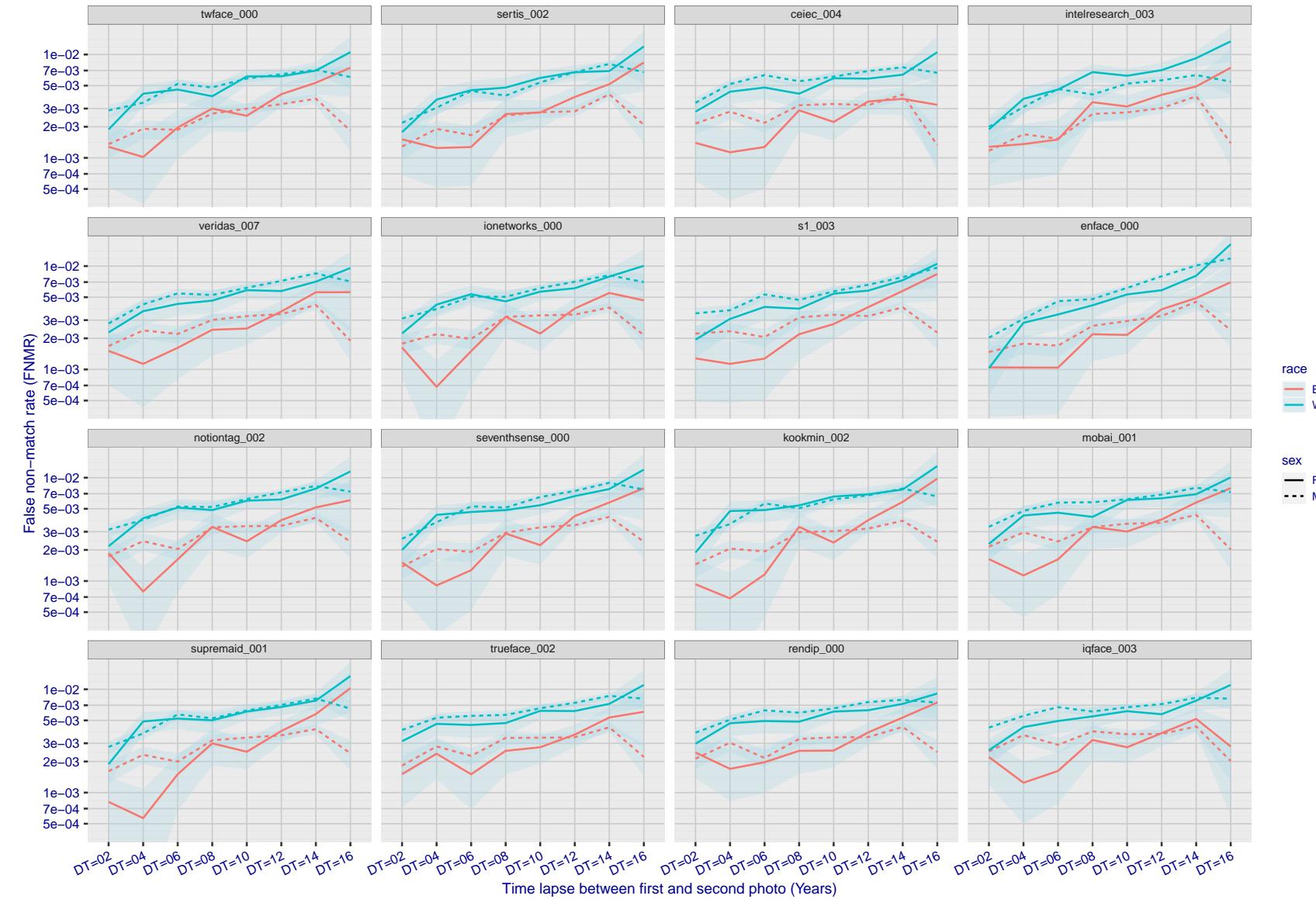


Figure 260: For the mugshot images, FNMR as a function of elapsed time between initial enrollment and second verification images. The panels appear most accurate first, and vertical scale changes on each page. The four traces correspond to images annotated with codes for black female, black male, white female, white male. The threshold is fixed for each algorithm to give  $FMR = 0.00001$  over all ( $10^8$ ) impostor comparisons. For short time-lapses, the most accurate algorithms give very few errors ( $FNMR < 0.001$ ) so that the uncertainty estimates are high.

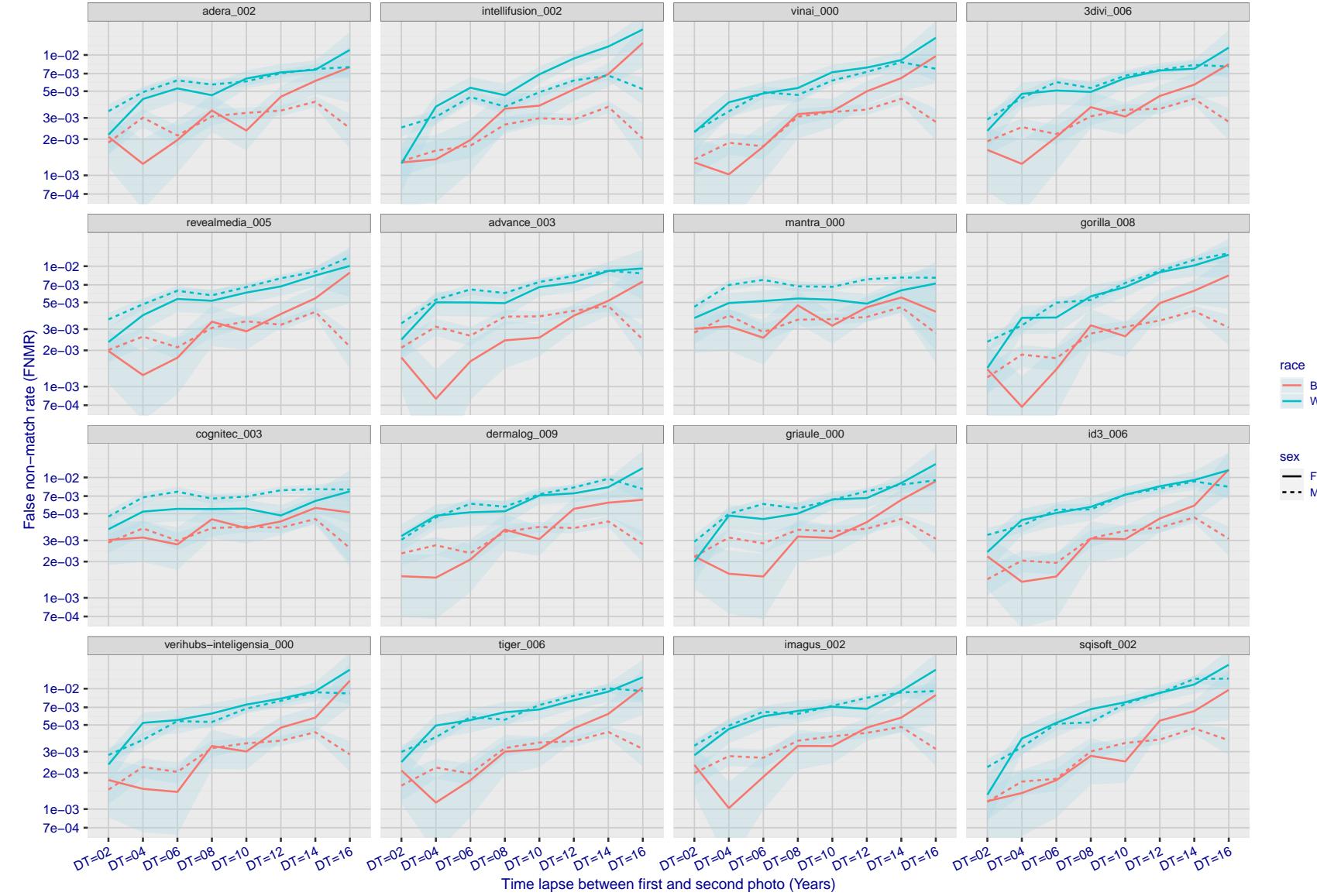


Figure 261: For the mugshot images, FNMR as a function of elapsed time between initial enrollment and second verification images. The panels appear most accurate first, and vertical scale changes on each page. The four traces correspond to images annotated with codes for black female, black male, white female, white male. The threshold is fixed for each algorithm to give  $FMR = 0.00001$  over all ( $10^8$ ) impostor comparisons. For short time-lapses, the most accurate algorithms give very few errors ( $FNMR < 0.001$ ) so that the uncertainty estimates are high.

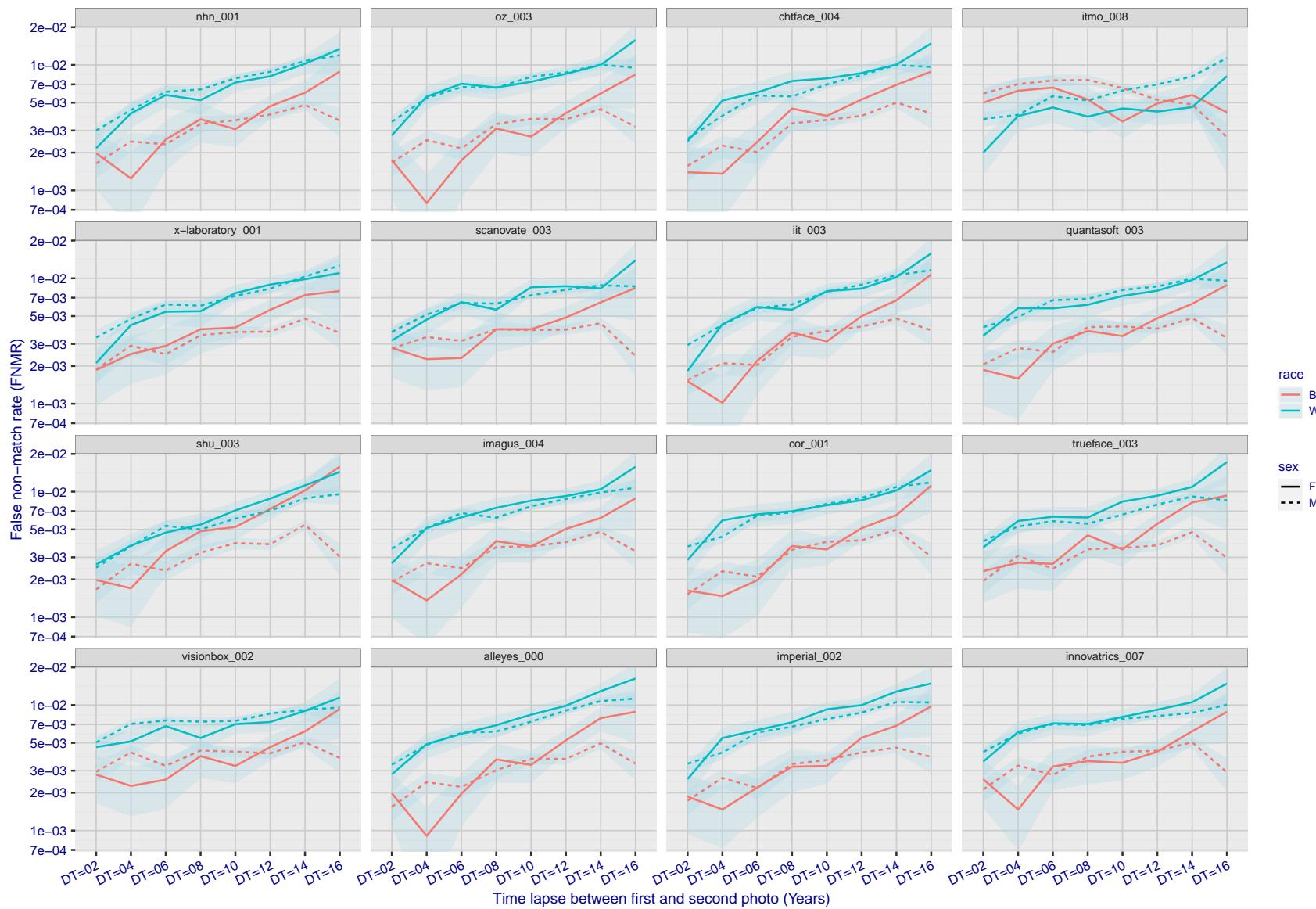


Figure 262: For the mugshot images, FNMR as a function of elapsed time between initial enrollment and second verification images. The panels appear most accurate first, and vertical scale changes on each page. The four traces correspond to images annotated with codes for black female, black male, white female, white male. The threshold is fixed for each algorithm to give  $FMR = 0.00001$  over all ( $10^8$ ) impostor comparisons. For short time-lapses, the most accurate algorithms give very few errors ( $FNMR < 0.001$ ) so that the uncertainty estimates are high.

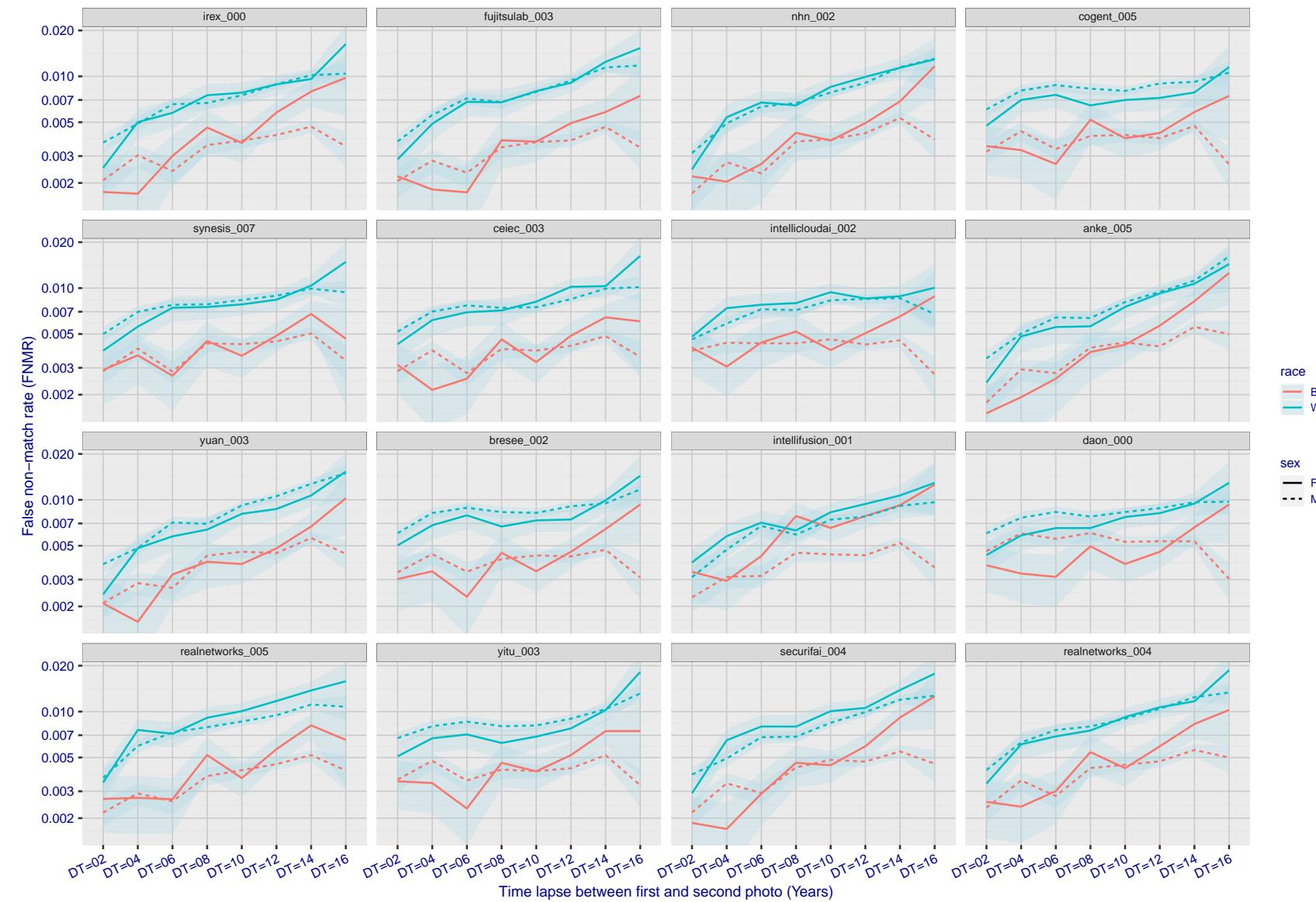


Figure 263: For the mugshot images, FNMR as a function of elapsed time between initial enrollment and second verification images. The panels appear most accurate first, and vertical scale changes on each page. The four traces correspond to images annotated with codes for black female, black male, white female, white male. The threshold is fixed for each algorithm to give FMR = 0.00001 over all ( $10^8$ ) impostor comparisons. For short time-lapses, the most accurate algorithms give very few errors (FNMR < 0.001) so that the uncertainty estimates are high.

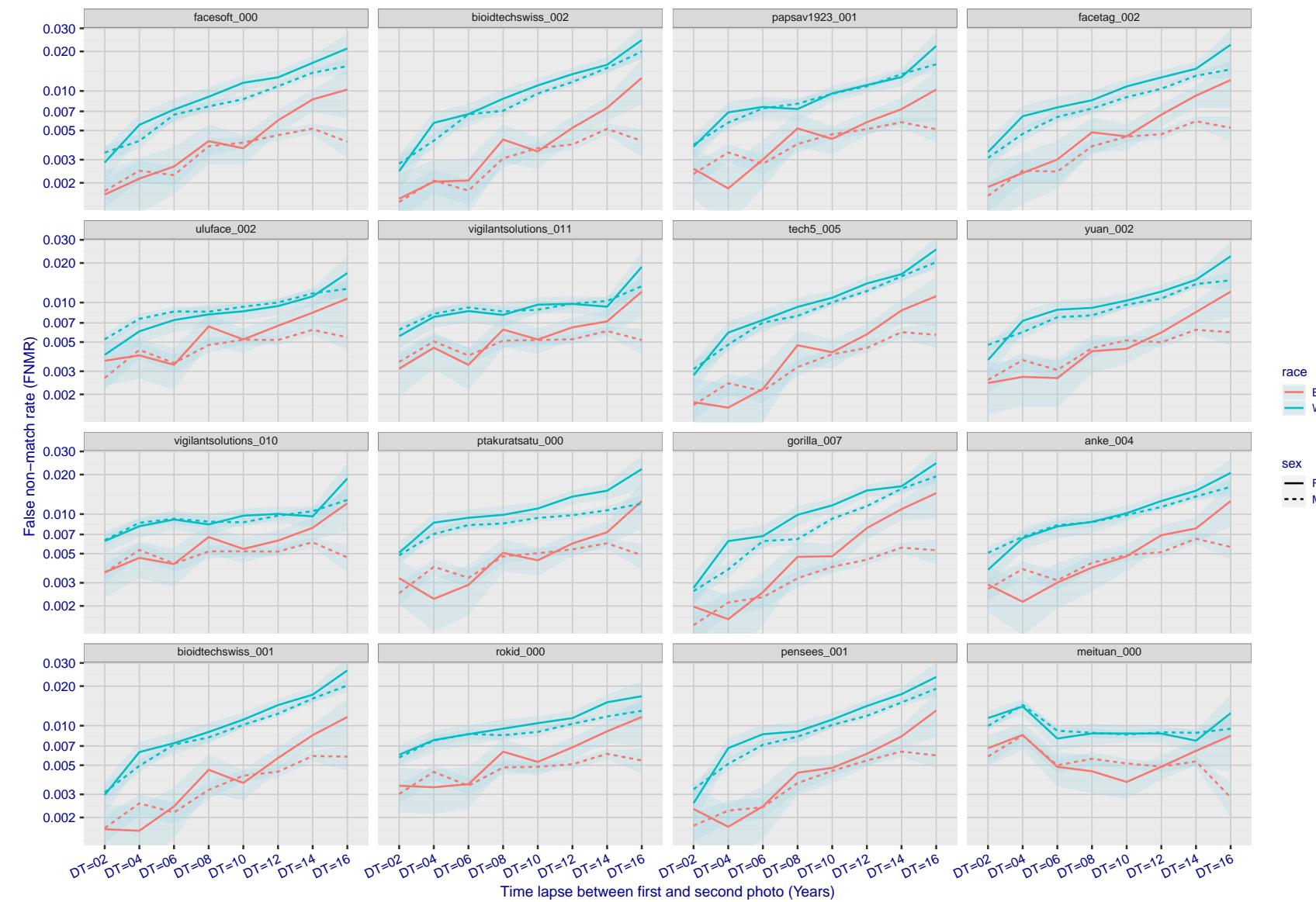


Figure 264: For the mugshot images, FNMR as a function of elapsed time between initial enrollment and second verification images. The panels appear most accurate first, and vertical scale changes on each page. The four traces correspond to images annotated with codes for black female, black male, white female, white male. The threshold is fixed for each algorithm to give FMR = 0.00001 over all ( $10^8$ ) impostor comparisons. For short time-lapses, the most accurate algorithms give very few errors (FNMR < 0.001) so that the uncertainty estimates are high.

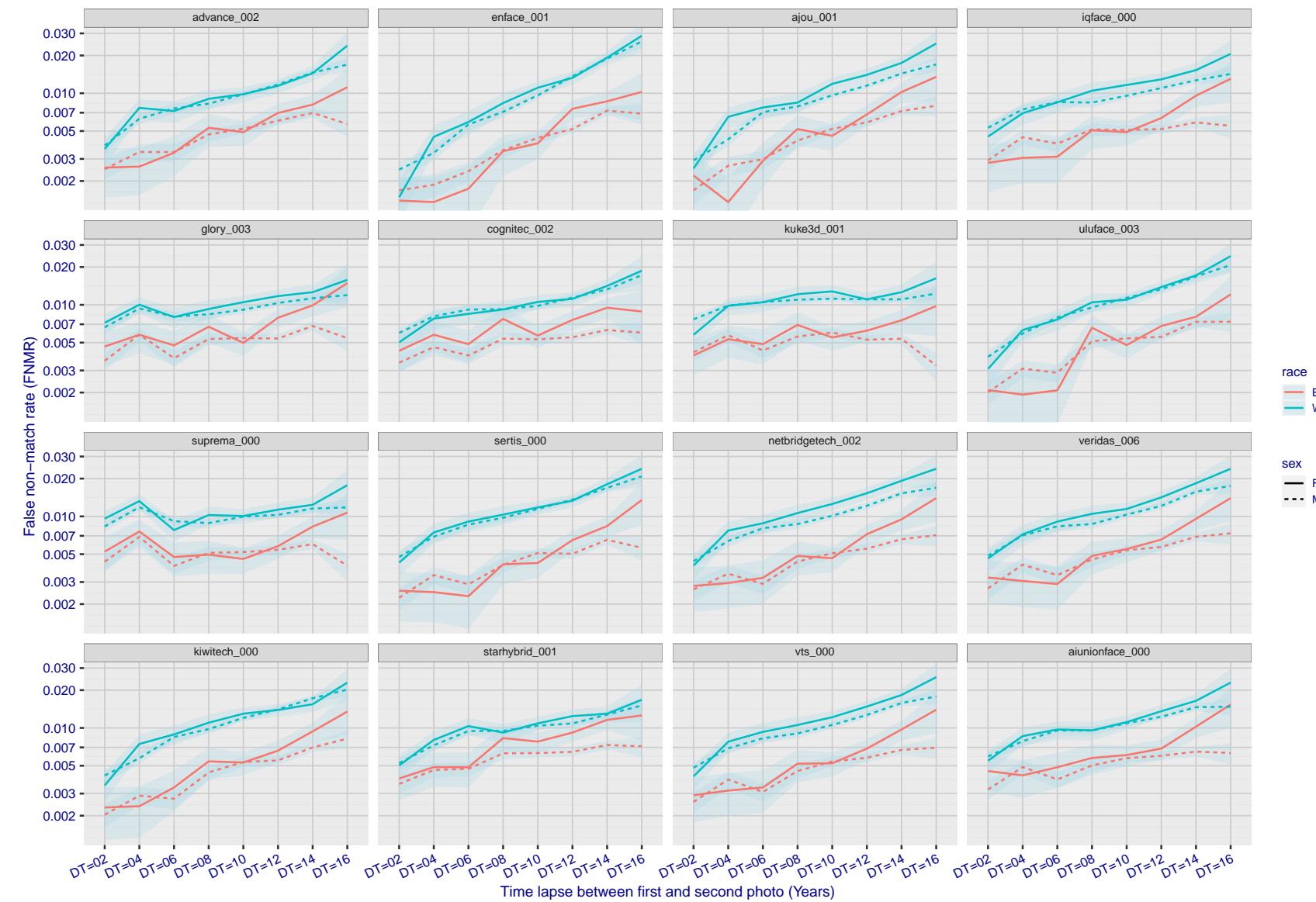


Figure 265: For the mugshot images, FNMR as a function of elapsed time between initial enrollment and second verification images. The panels appear most accurate first, and vertical scale changes on each page. The four traces correspond to images annotated with codes for black female, black male, white female, white male. The threshold is fixed for each algorithm to give FMR = 0.00001 over all ( $10^8$ ) impostor comparisons. For short time-lapses, the most accurate algorithms give very few errors (FNMR < 0.001) so that the uncertainty estimates are high.

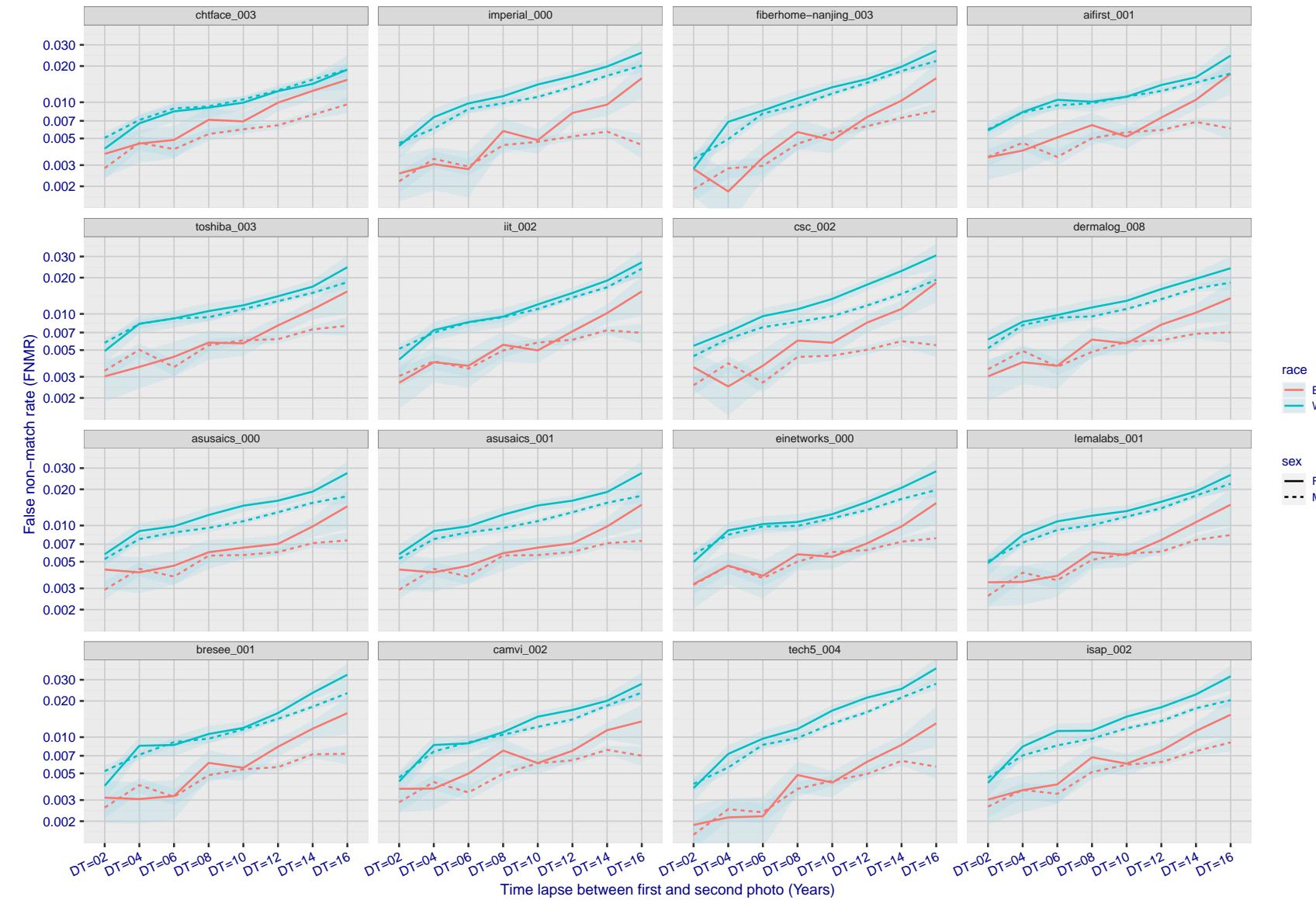


Figure 266: For the mugshot images, FNMR as a function of elapsed time between initial enrollment and second verification images. The panels appear most accurate first, and vertical scale changes on each page. The four traces correspond to images annotated with codes for black female, black male, white female, white male. The threshold is fixed for each algorithm to give FMR = 0.00001 over all ( $10^8$ ) impostor comparisons. For short time-lapses, the most accurate algorithms give very few errors (FNMR < 0.001) so that the uncertainty estimates are high.

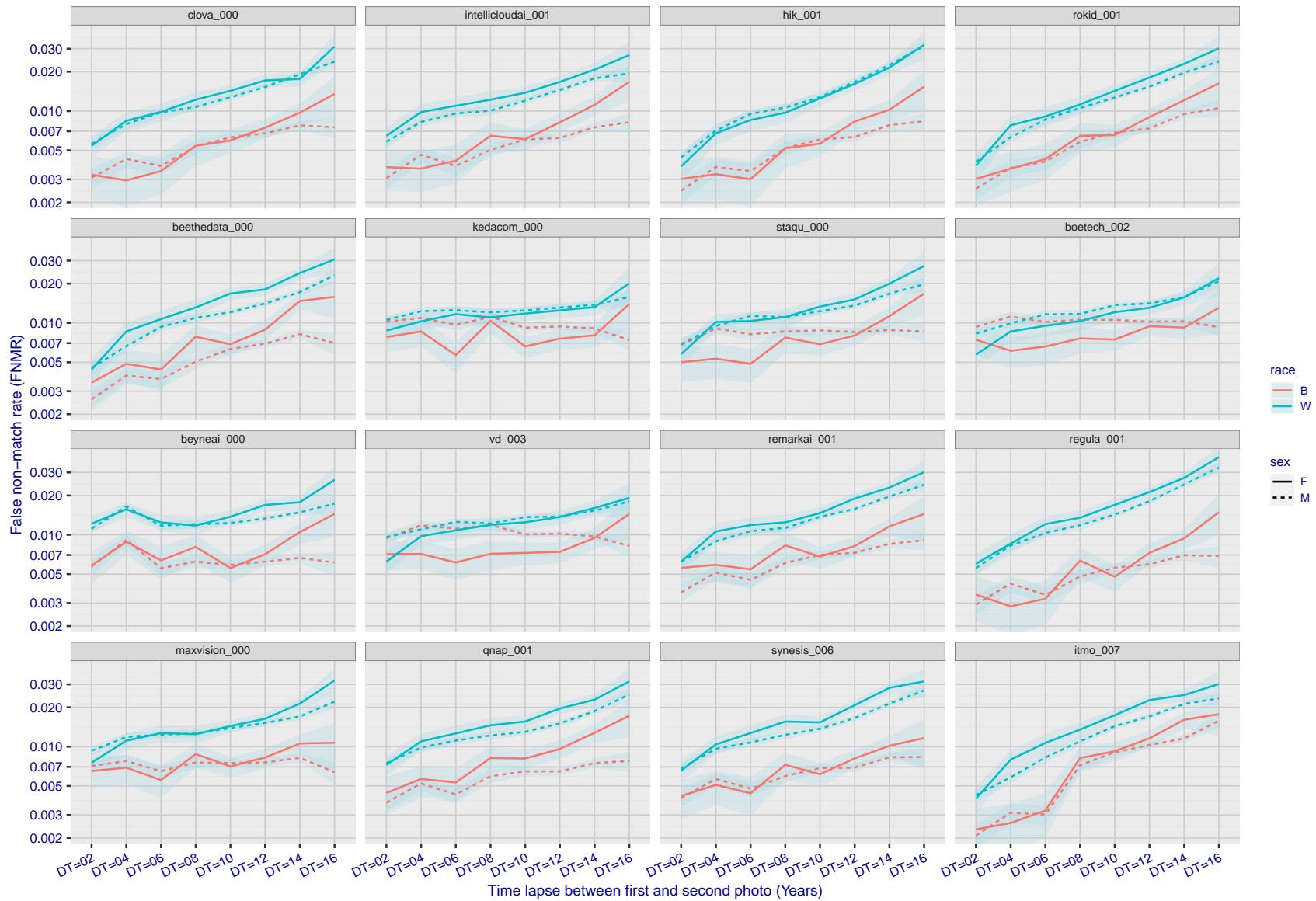


Figure 267: For the mugshot images, FNMR as a function of elapsed time between initial enrollment and second verification images. The panels appear most accurate first, and vertical scale changes on each page. The four traces correspond to images annotated with codes for black female, black male, white female, white male. The threshold is fixed for each algorithm to give FMR = 0.00001 over all ( $10^8$ ) impostor comparisons. For short time-lapses, the most accurate algorithms give very few errors (FNMR < 0.001) so that the uncertainty estimates are high.

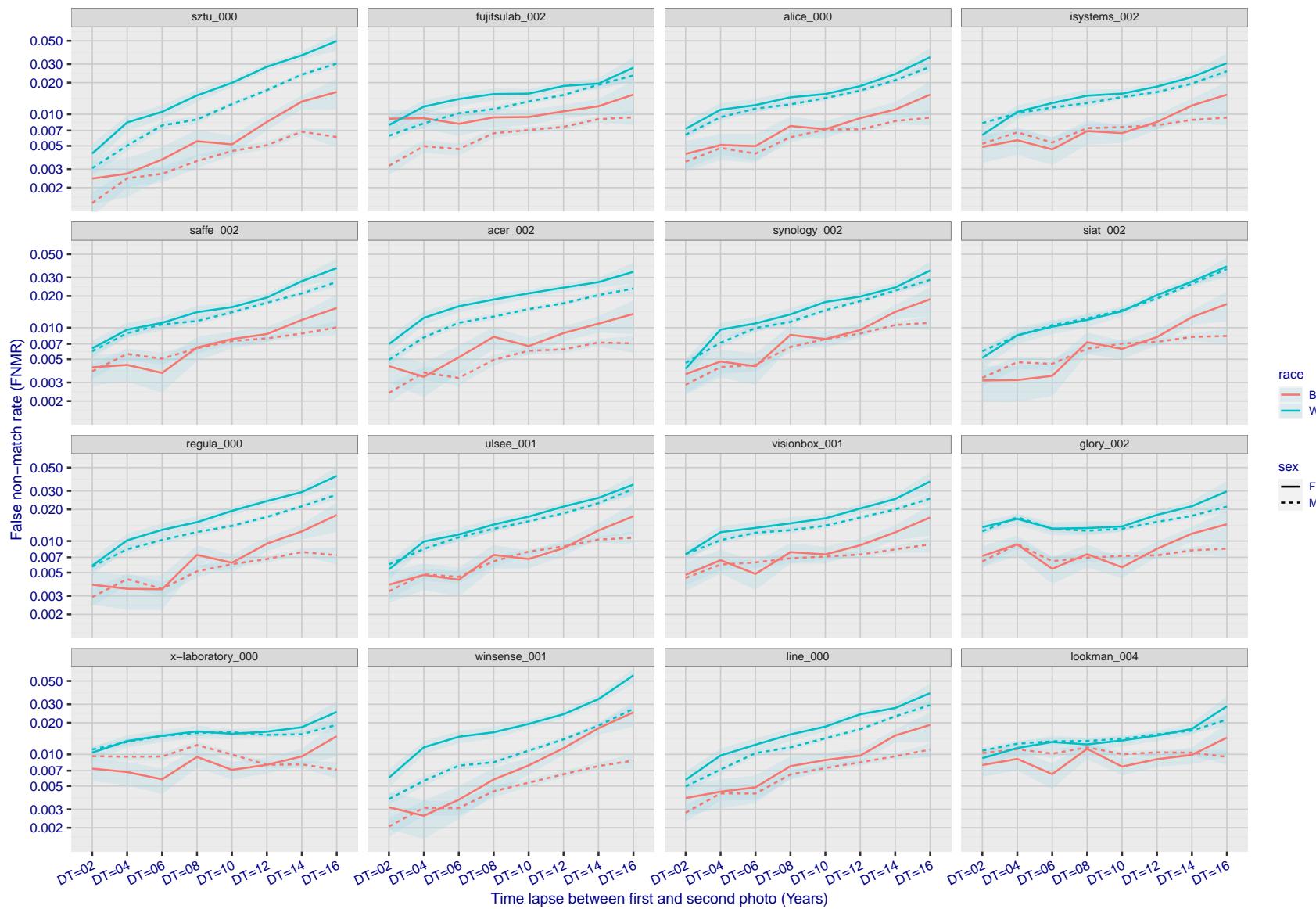


Figure 268: For the mugshot images, FNMR as a function of elapsed time between initial enrollment and second verification images. The panels appear most accurate first, and vertical scale changes on each page. The four traces correspond to images annotated with codes for black female, black male, white female, white male. The threshold is fixed for each algorithm to give  $FMR = 0.00001$  over all ( $10^8$ ) impostor comparisons. For short time-lapses, the most accurate algorithms give very few errors ( $FNMR < 0.001$ ) so that the uncertainty estimates are high.

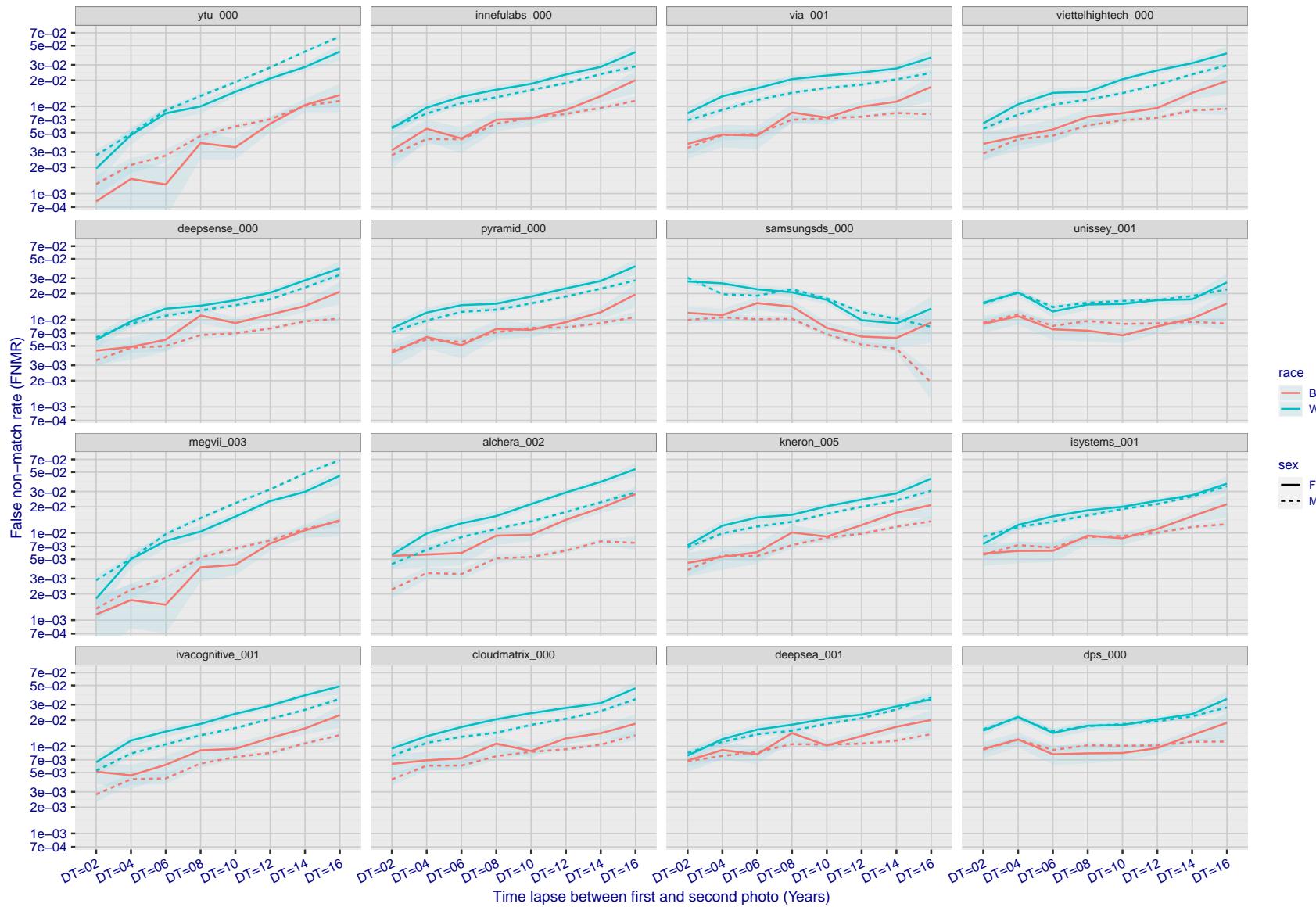


Figure 269: For the mugshot images, FNMR as a function of elapsed time between initial enrollment and second verification images. The panels appear most accurate first, and vertical scale changes on each page. The four traces correspond to images annotated with codes for black female, black male, white female, white male. The threshold is fixed for each algorithm to give  $FMR = 0.00001$  over all ( $10^8$ ) impostor comparisons. For short time-lapses, the most accurate algorithms give very few errors ( $FNMR < 0.001$ ) so that the uncertainty estimates are high.

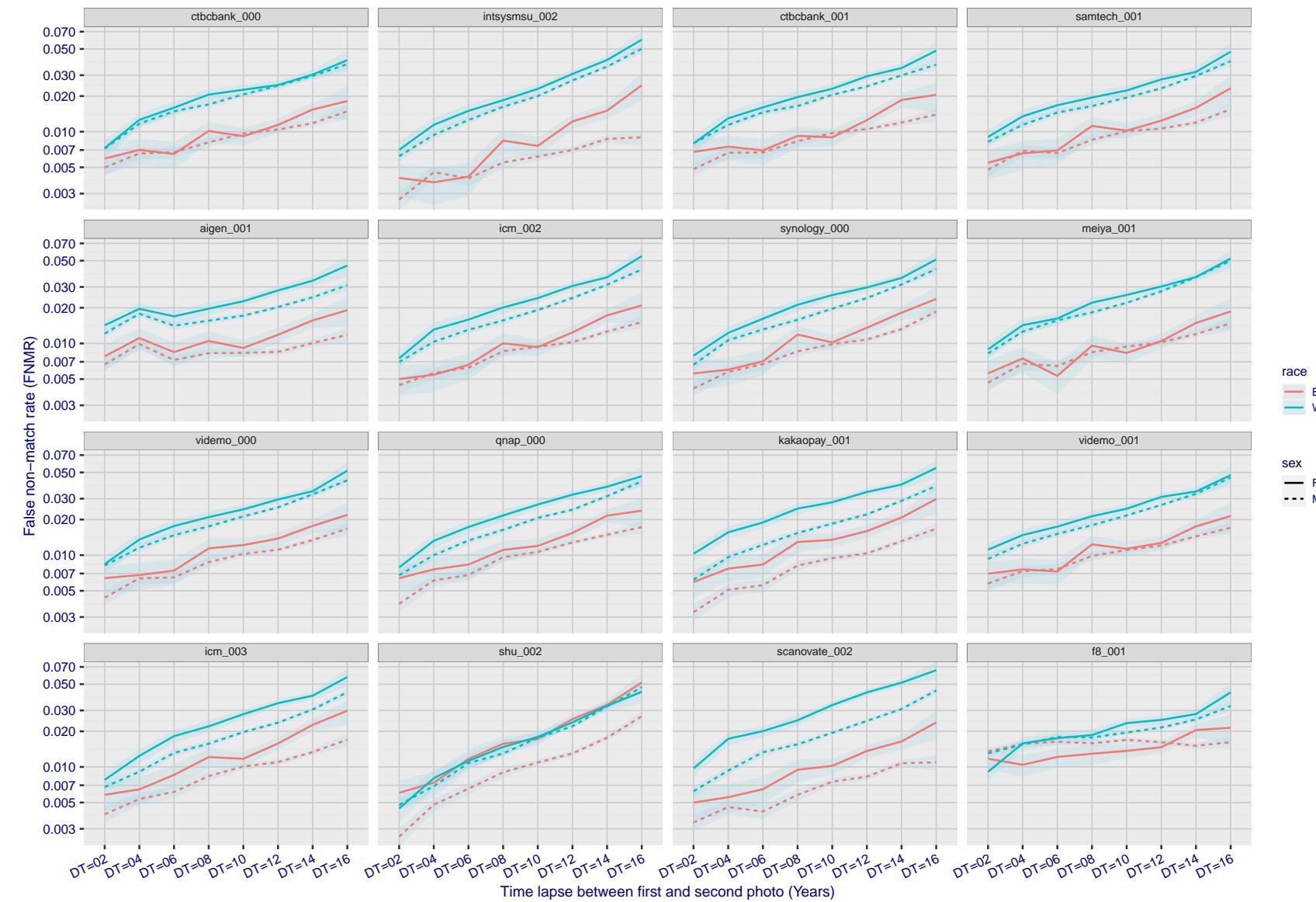


Figure 270: For the mugshot images, FNMR as a function of elapsed time between initial enrollment and second verification images. The panels appear most accurate first, and vertical scale changes on each page. The four traces correspond to images annotated with codes for black female, black male, white female, white male. The threshold is fixed for each algorithm to give FMR = 0.00001 over all ( $10^8$ ) impostor comparisons. For short time-lapses, the most accurate algorithms give very few errors (FNMR < 0.001) so that the uncertainty estimates are high.

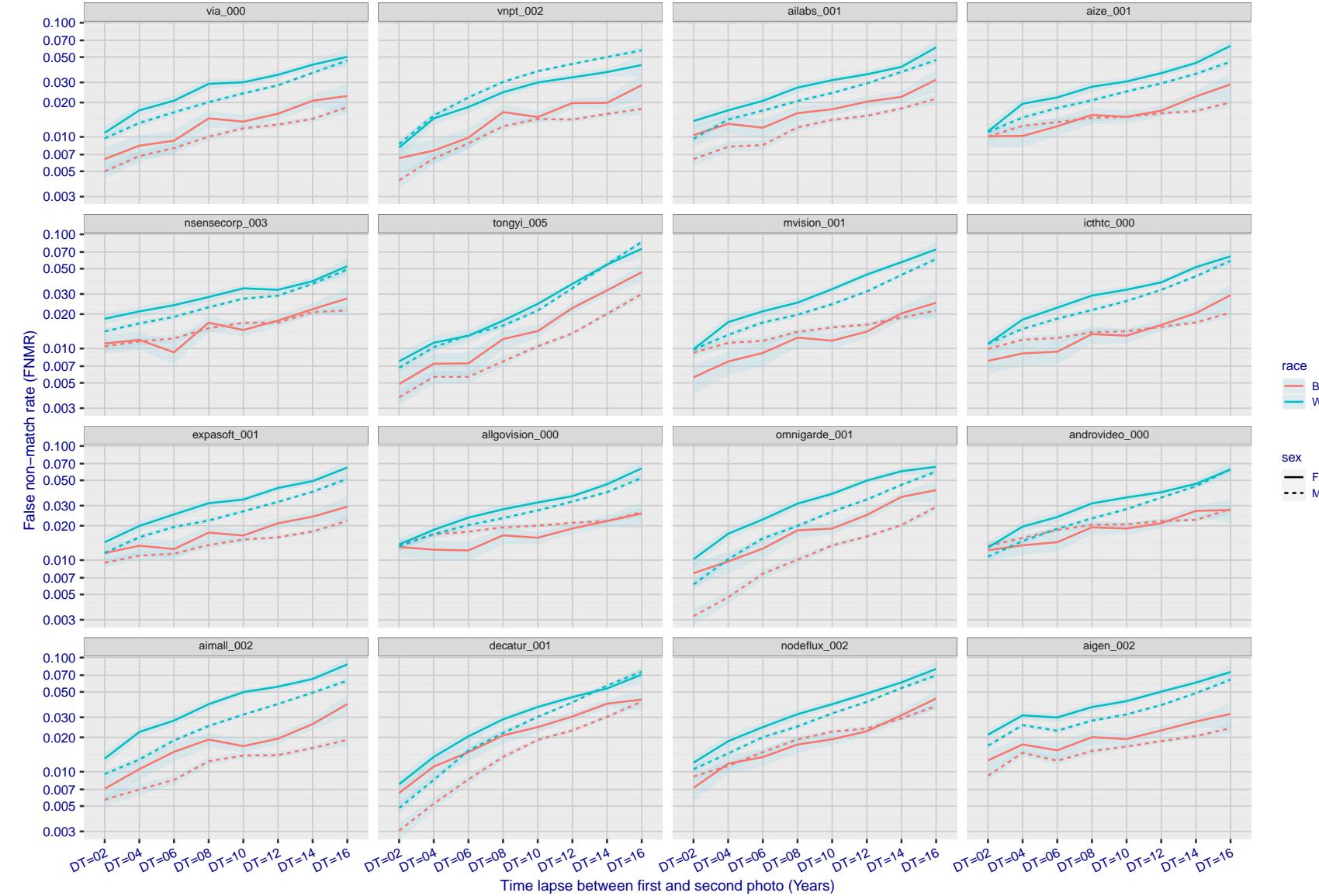


Figure 271: For the mugshot images, FNMR as a function of elapsed time between initial enrollment and second verification images. The panels appear most accurate first, and vertical scale changes on each page. The four traces correspond to images annotated with codes for black female, black male, white female, white male. The threshold is fixed for each algorithm to give FMR = 0.00001 over all ( $10^8$ ) impostor comparisons. For short time-lapses, the most accurate algorithms give very few errors (FNMR < 0.001) so that the uncertainty estimates are high.

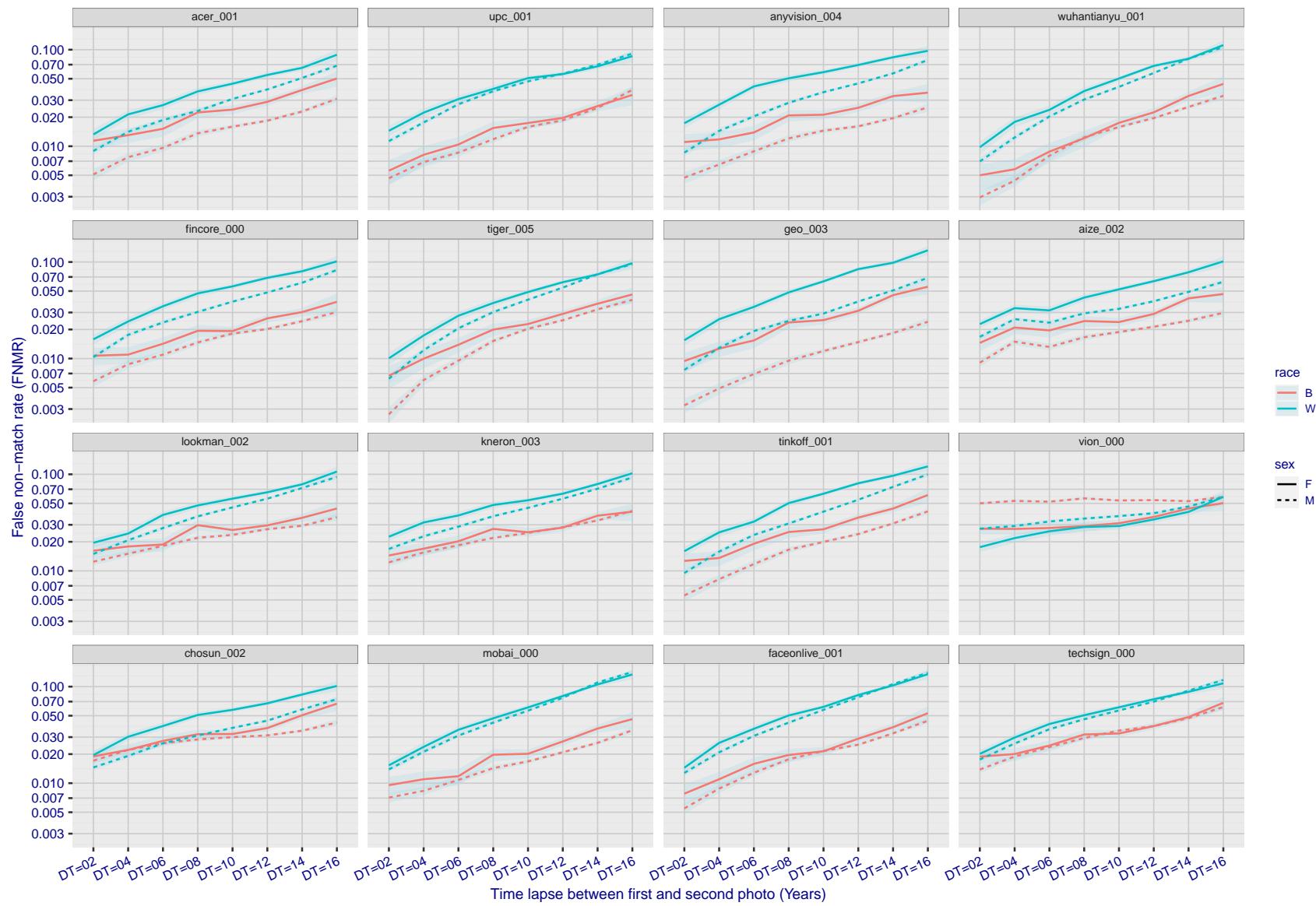


Figure 272: For the mugshot images, FNMR as a function of elapsed time between initial enrollment and second verification images. The panels appear most accurate first, and vertical scale changes on each page. The four traces correspond to images annotated with codes for black female, black male, white female, white male. The threshold is fixed for each algorithm to give FMR = 0.00001 over all ( $10^8$ ) impostor comparisons. For short time-lapses, the most accurate algorithms give very few errors (FNMR < 0.001) so that the uncertainty estimates are high.

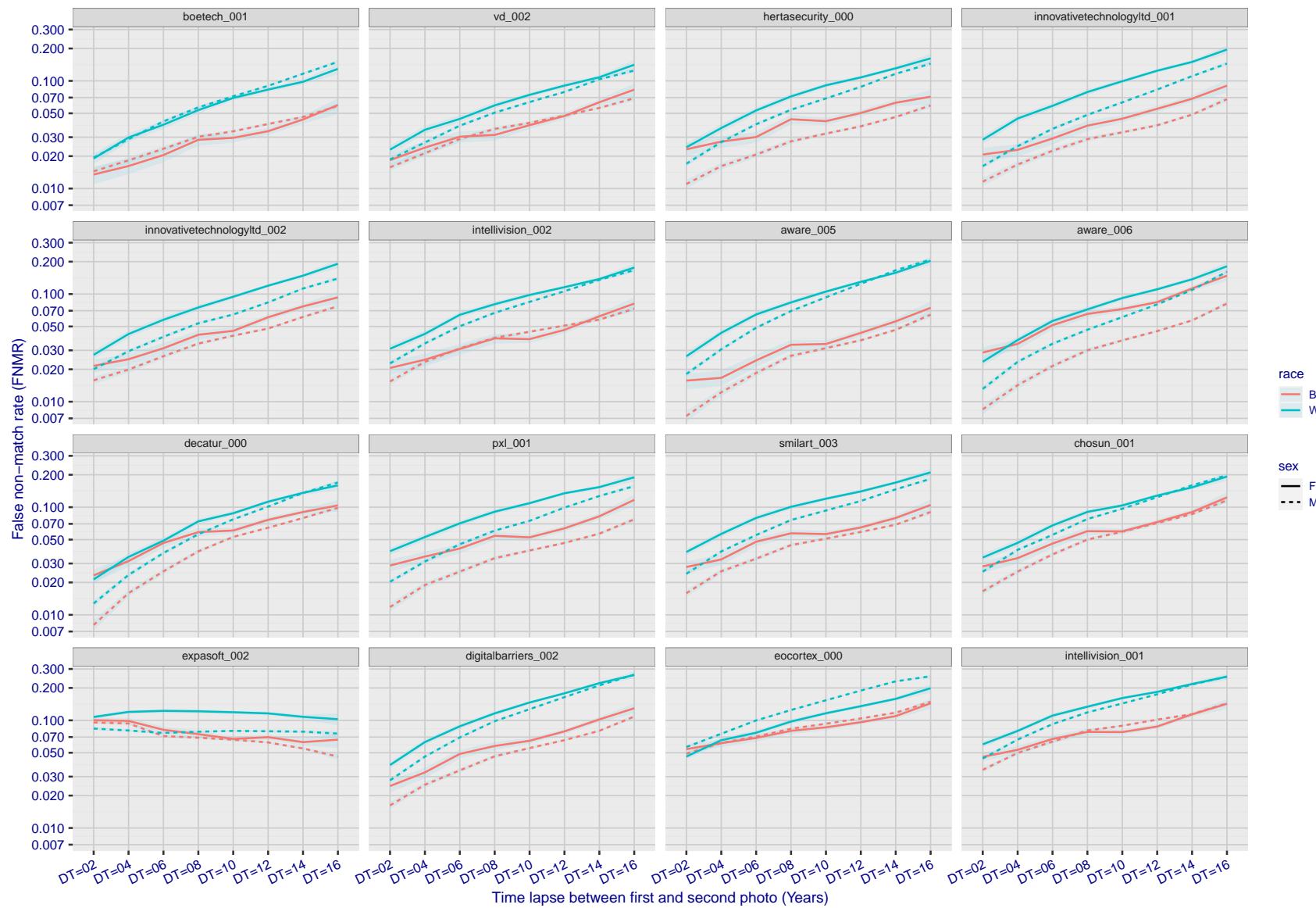


Figure 273: For the mugshot images, FNMR as a function of elapsed time between initial enrollment and second verification images. The panels appear most accurate first, and vertical scale changes on each page. The four traces correspond to images annotated with codes for black female, black male, white female, white male. The threshold is fixed for each algorithm to give  $FMR = 0.00001$  over all ( $10^8$ ) impostor comparisons. For short time-lapses, the most accurate algorithms give very few errors ( $FNMR < 0.001$ ) so that the uncertainty estimates are high.

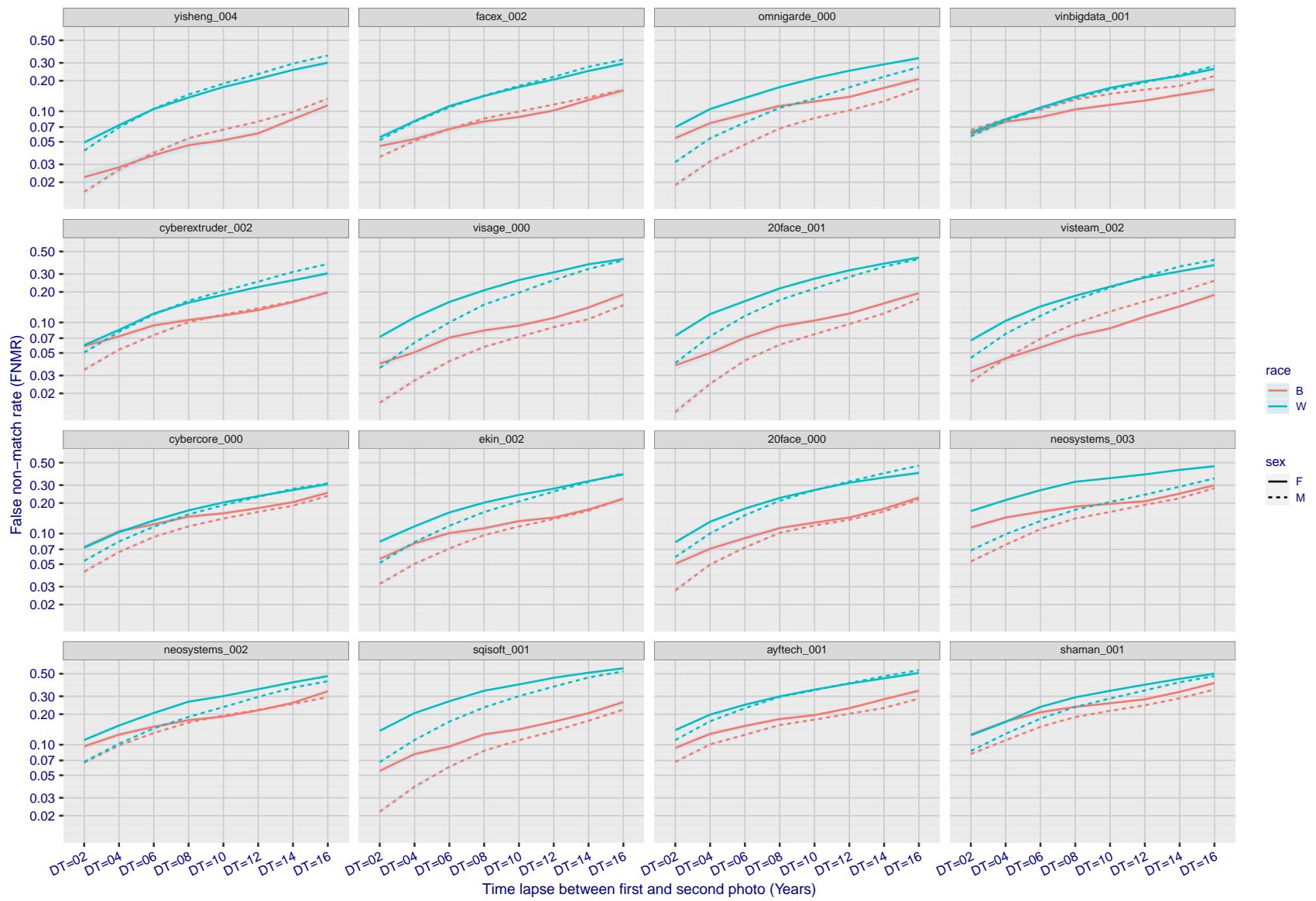


Figure 274: For the mugshot images, FNMR as a function of elapsed time between initial enrollment and second verification images. The panels appear most accurate first, and vertical scale changes on each page. The four traces correspond to images annotated with codes for black female, black male, white female, white male. The threshold is fixed for each algorithm to give  $FMR = 0.00001$  over all ( $10^8$ ) impostor comparisons. For short time-lapses, the most accurate algorithms give very few errors ( $FNMR < 0.001$ ) so that the uncertainty estimates are high.

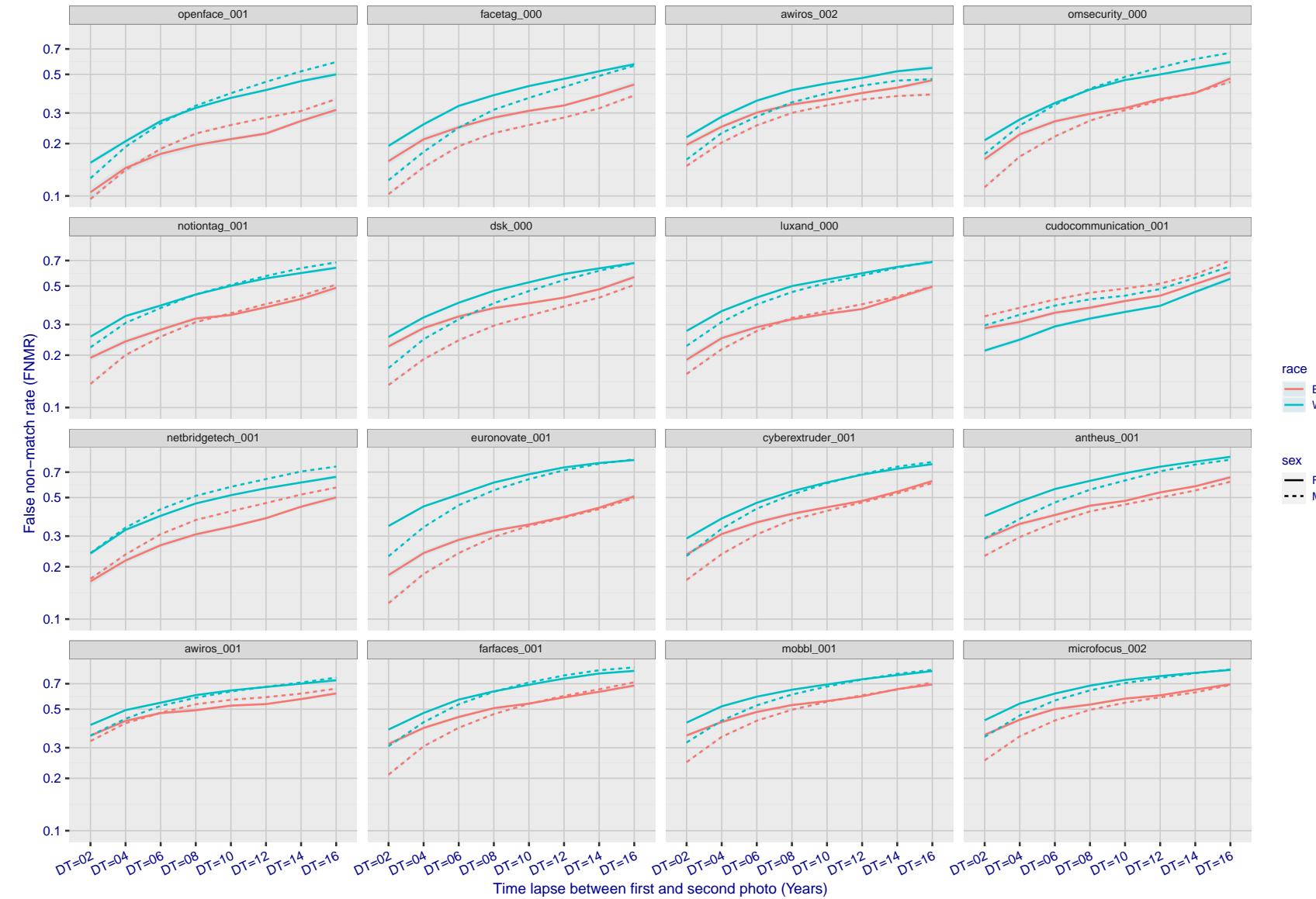


Figure 275: For the mugshot images, FNMR as a function of elapsed time between initial enrollment and second verification images. The panels appear most accurate first, and vertical scale changes on each page. The four traces correspond to images annotated with codes for black female, black male, white female, white male. The threshold is fixed for each algorithm to give FMR = 0.00001 over all ( $10^8$ ) impostor comparisons. For short time-lapses, the most accurate algorithms give very few errors (FNMR < 0.001) so that the uncertainty estimates are high.

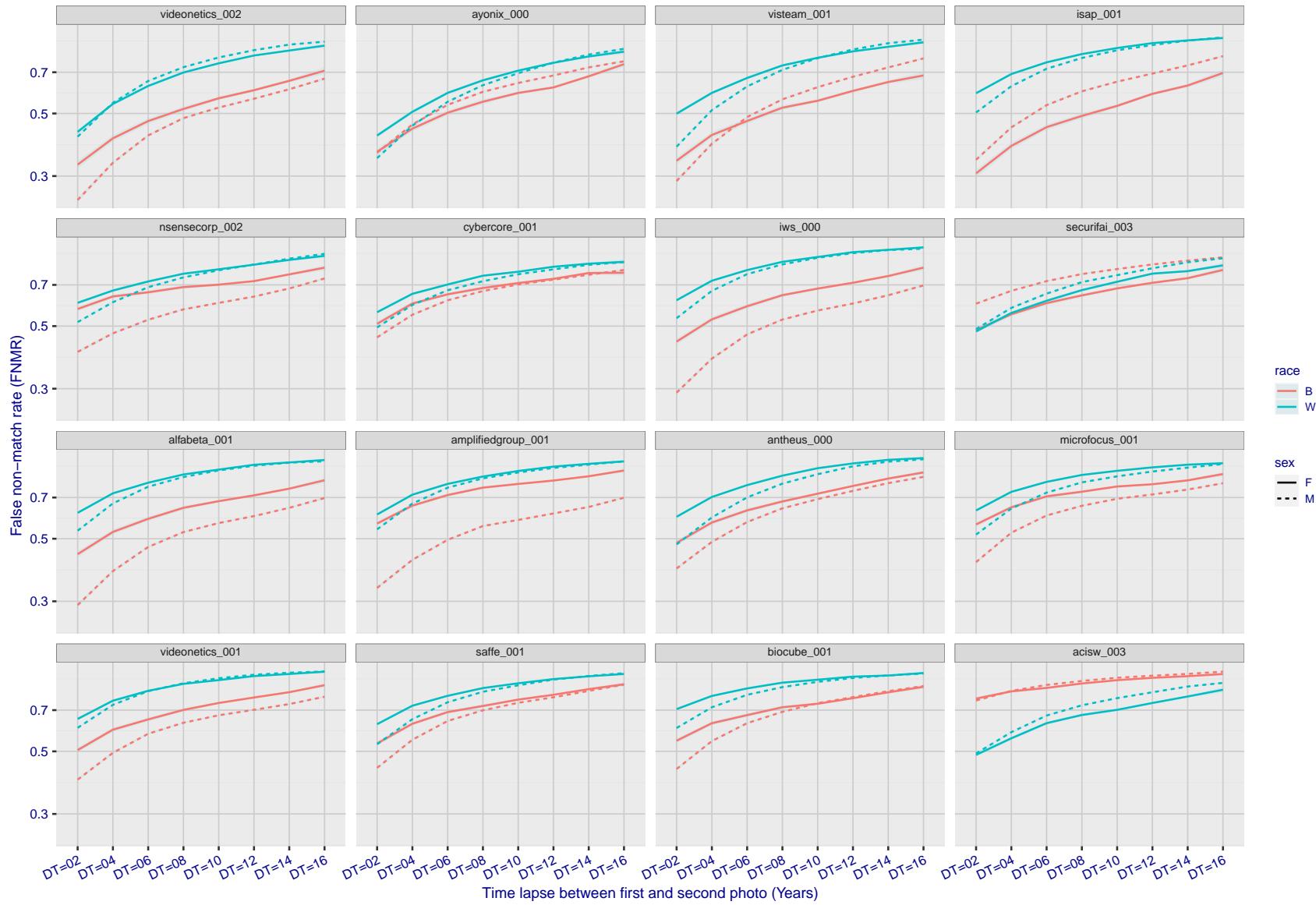


Figure 276: For the mugshot images, FNMR as a function of elapsed time between initial enrollment and second verification images. The panels appear most accurate first, and vertical scale changes on each page. The four traces correspond to images annotated with codes for black female, black male, white female, white male. The threshold is fixed for each algorithm to give FMR = 0.00001 over all ( $10^8$ ) impostor comparisons. For short time-lapses, the most accurate algorithms give very few errors (FNMR < 0.001) so that the uncertainty estimates are high.

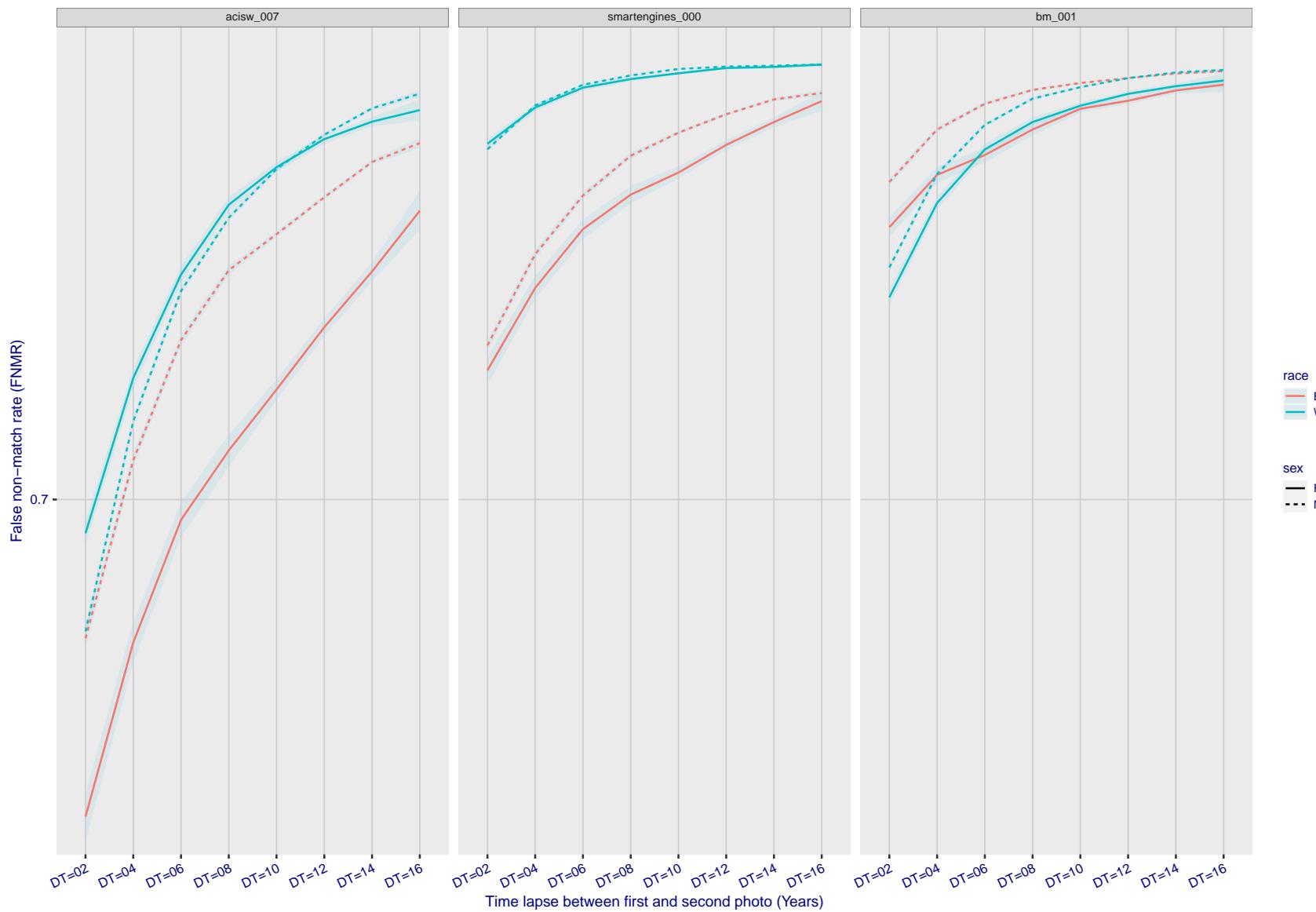


Figure 277: For the mugshot images, FNMR as a function of elapsed time between initial enrollment and second verification images. The panels appear most accurate first, and vertical scale changes on each page. The four traces correspond to images annotated with codes for black female, black male, white female, white male. The threshold is fixed for each algorithm to give FMR = 0.00001 over all ( $10^8$ ) impostor comparisons. For short time-lapses, the most accurate algorithms give very few errors (FNMR < 0.001) so that the uncertainty estimates are high.

### 3.5.3 Effect of age on genuine subjects

**Background:** Faces change appearance throughout life. Face recognition algorithms have previously been reported to give better accuracy on older individuals (See NIST IR 8009).

**Goal:** To quantify false non-match rates (FNMR) as a function of age, without an ageing component.

**Methods:** Using the visa images, which span fewer than five years, thresholds are determined that give FMR = 0.001 and 0.0001 over the entire impostor set. Then FNMR is measured over 1000 bootstrap replications of the genuine scores.

**Results:** For the visa images, Figure 309 shows how false non-match rates for genuine users, as a function of age group.

The notable aspects are:

- ▷ Younger subjects give considerably higher FNMR. This is likely due to rapid growth and change in facial appearance.
- ▷ FNMR trends down throughout life. The last bin, AGE > 72, contains fewer than 140 mated pairs, and may be affected by small sample size.

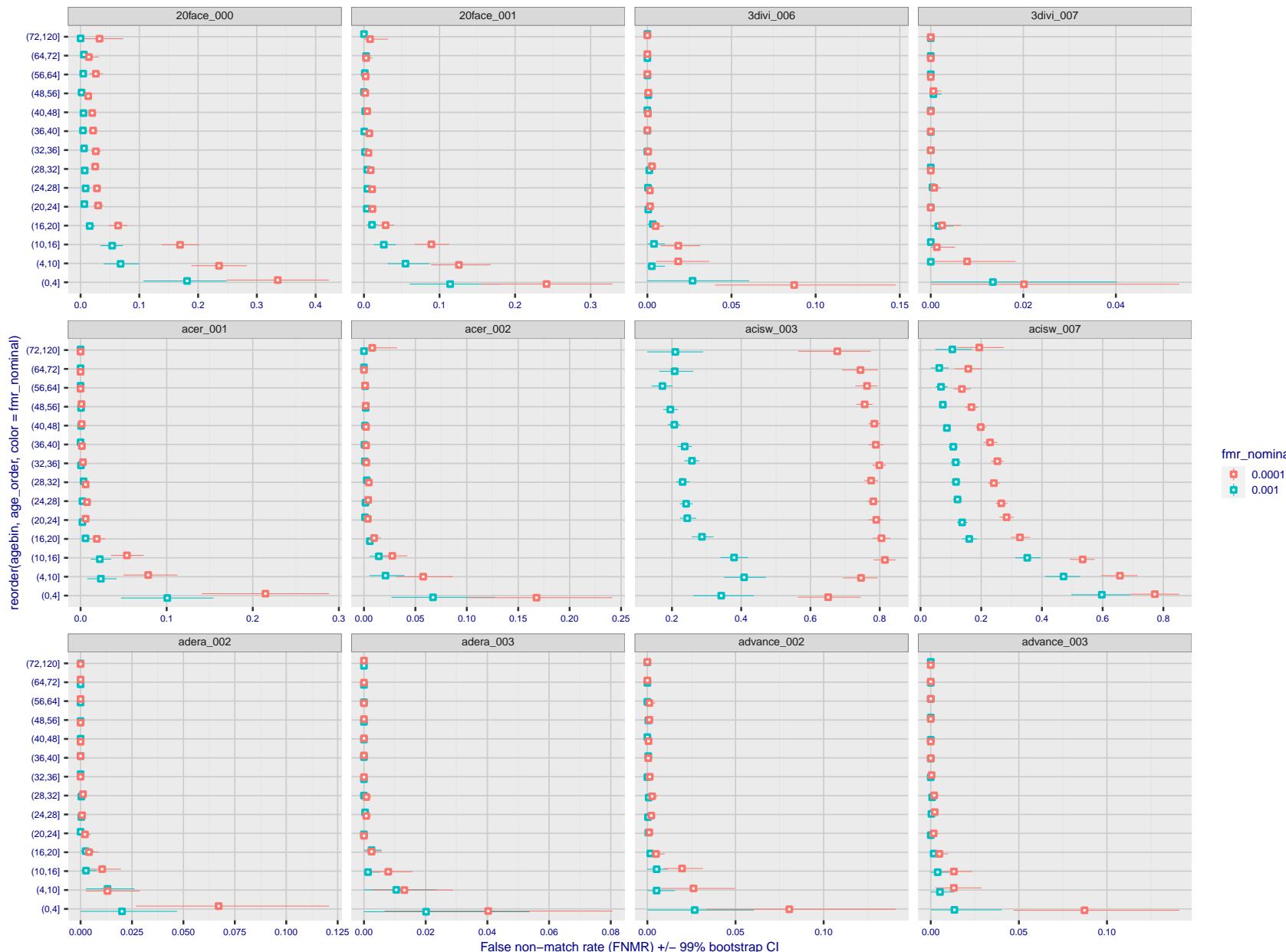


Figure 278: For the visa images, the dots show FNMR by age group for two operating thresholds corresponding to  $FMR = \{0.001, 0.0001\}$  computed over all on the order of  $10^{10}$  impostor scores. The FMR in each bin will vary also - see subsequent impostor heatmaps in sec. 3.6.2. Given a pair of face images taken at different times, we assign the comparison to the bin that is the arithmetic average of the subject's ages. This plot shows only the effect of age, not ageing. The number of comparisons in each bin is generally in the thousands, however the first and last bins are computed over 149 and 124 respectively. The error rates in some (adult) cases are zero, and in others the DET is flat so the error rates at the two thresholds are identical. The lines span 1% and 99% of bootstrap replicated FNMR estimates.

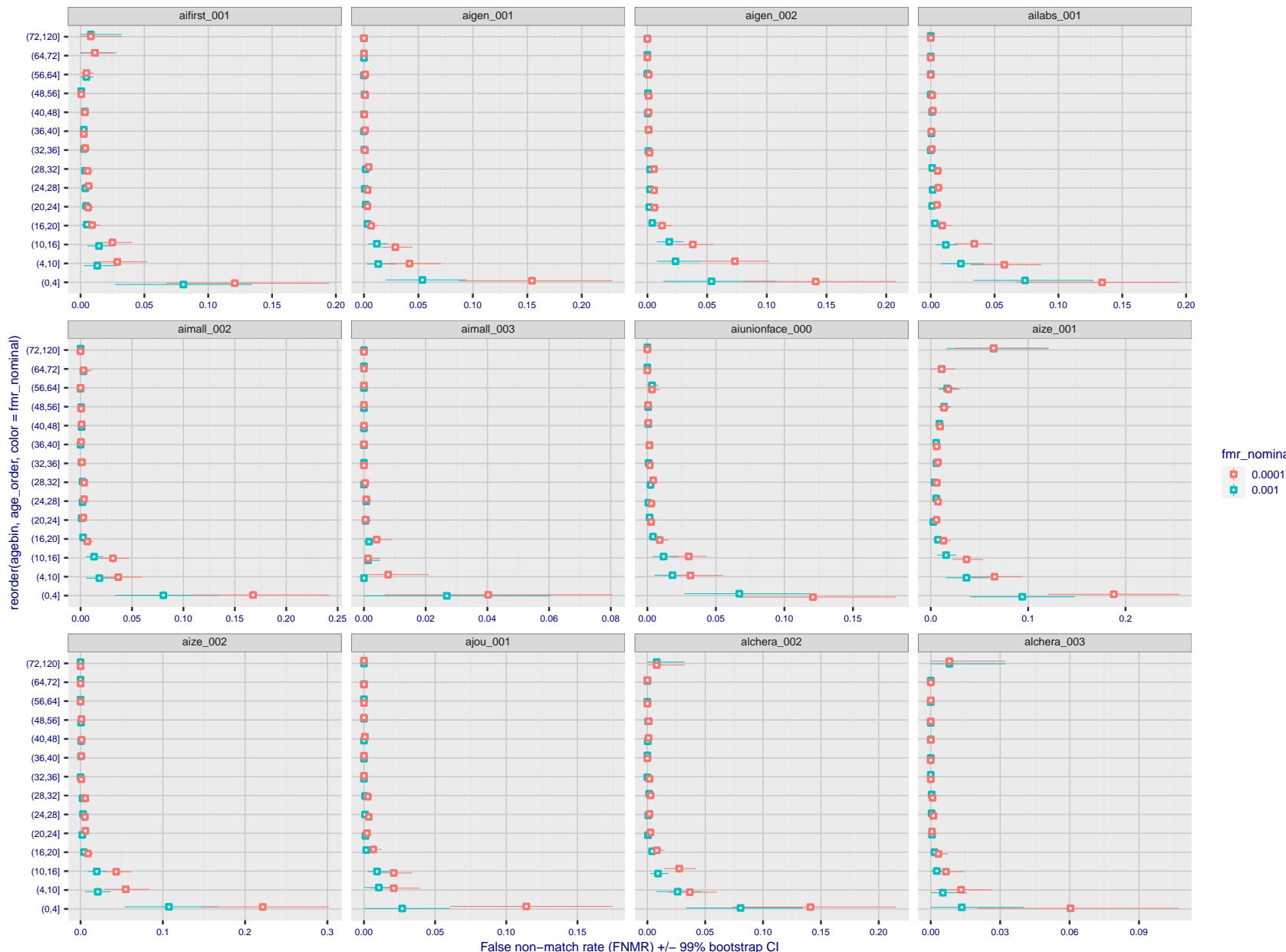


Figure 279: For the visa images, the dots show FNMR by age group for two operating thresholds corresponding to  $FMR = \{0.001, 0.0001\}$  computed over all on the order of  $10^{10}$  impostor scores. The FMR in each bin will vary also - see subsequent impostor heatmaps in sec. 3.6.2. Given a pair of face images taken at different times, we assign the comparison to the bin that is the arithmetic average of the subject's ages. This plot shows only the effect of age, not ageing. The number of comparisons in each bin is generally in the thousands, however the first and last bins are computed over 149 and 124 respectively. The error rates in some (adult) cases are zero, and in others the DET is flat so the error rates at the two thresholds are identical. The lines span 1% and 99% of bootstrap replicated FNMR estimates.

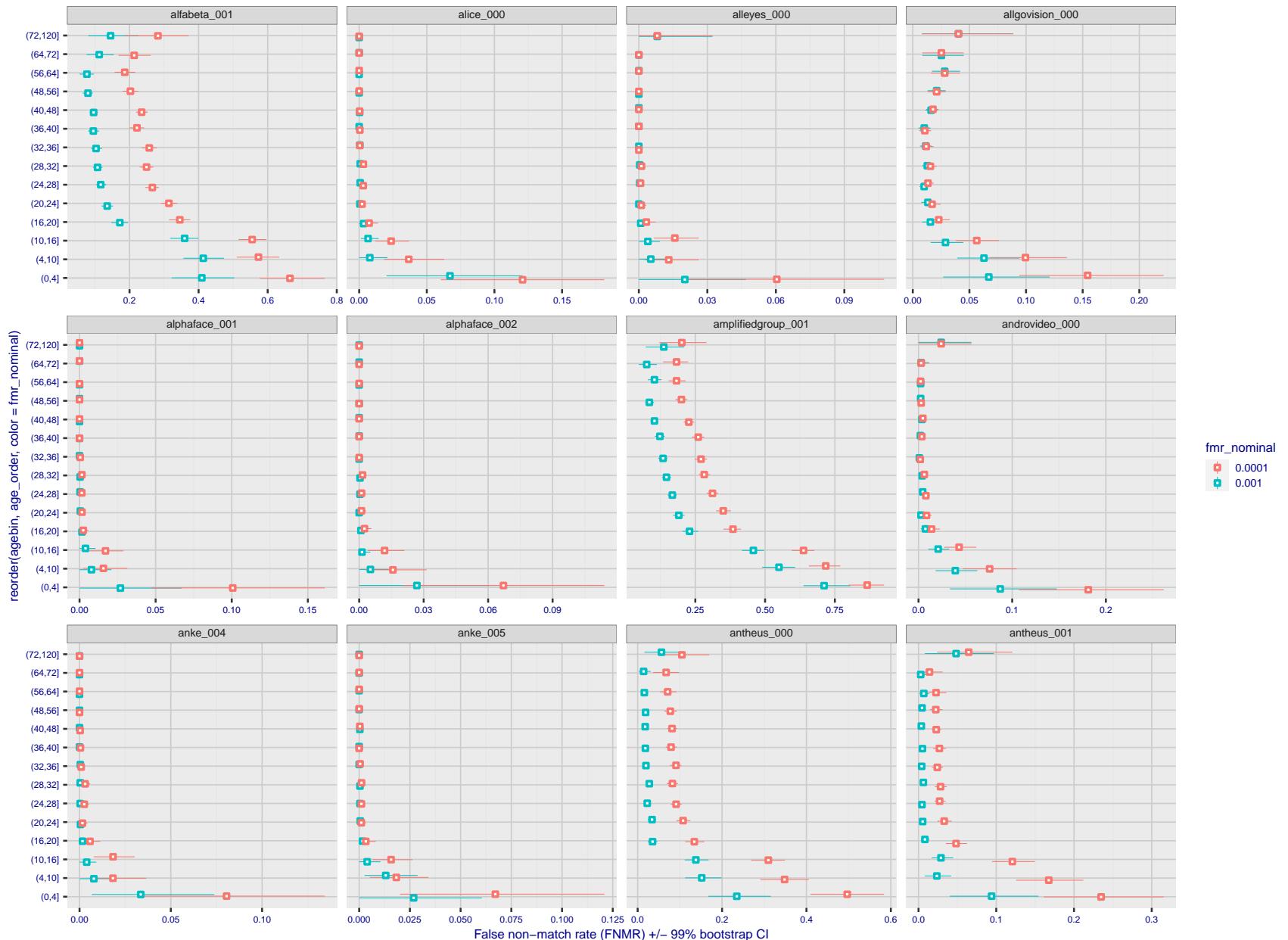


Figure 280: For the visa images, the dots show FNMR by age group for two operating thresholds corresponding to  $FMR = \{0.001, 0.0001\}$  computed over all on the order of  $10^{10}$  impostor scores. The FMR in each bin will vary also - see subsequent impostor heatmaps in sec. 3.6.2. Given a pair of face images taken at different times, we assign the comparison to the bin that is the arithmetic average of the subject's ages. This plot shows only the effect of age, not ageing. The number of comparisons in each bin is generally in the thousands, however the first and last bins are computed over 149 and 124 respectively. The error rates in some (adult) cases are zero, and in others the DET is flat so the error rates at the two thresholds are identical. The lines span 1% and 99% of bootstrap replicated FNMR estimates.



Figure 281: For the visa images, the dots show FNMR by age group for two operating thresholds corresponding to  $FMR = \{0.001, 0.0001\}$  computed over all on the order of  $10^{10}$  impostor scores. The FMR in each bin will vary also - see subsequent impostor heatmaps in sec. 3.6.2. Given a pair of face images taken at different times, we assign the comparison to the bin that is the arithmetic average of the subject's ages. This plot shows only the effect of age, not ageing. The number of comparisons in each bin is generally in the thousands, however the first and last bins are computed over 149 and 124 respectively. The error rates in some (adult) cases are zero, and in others the DET is flat so the error rates at the two thresholds are identical. The lines span 1% and 99% of bootstrap replicated FNMR estimates.

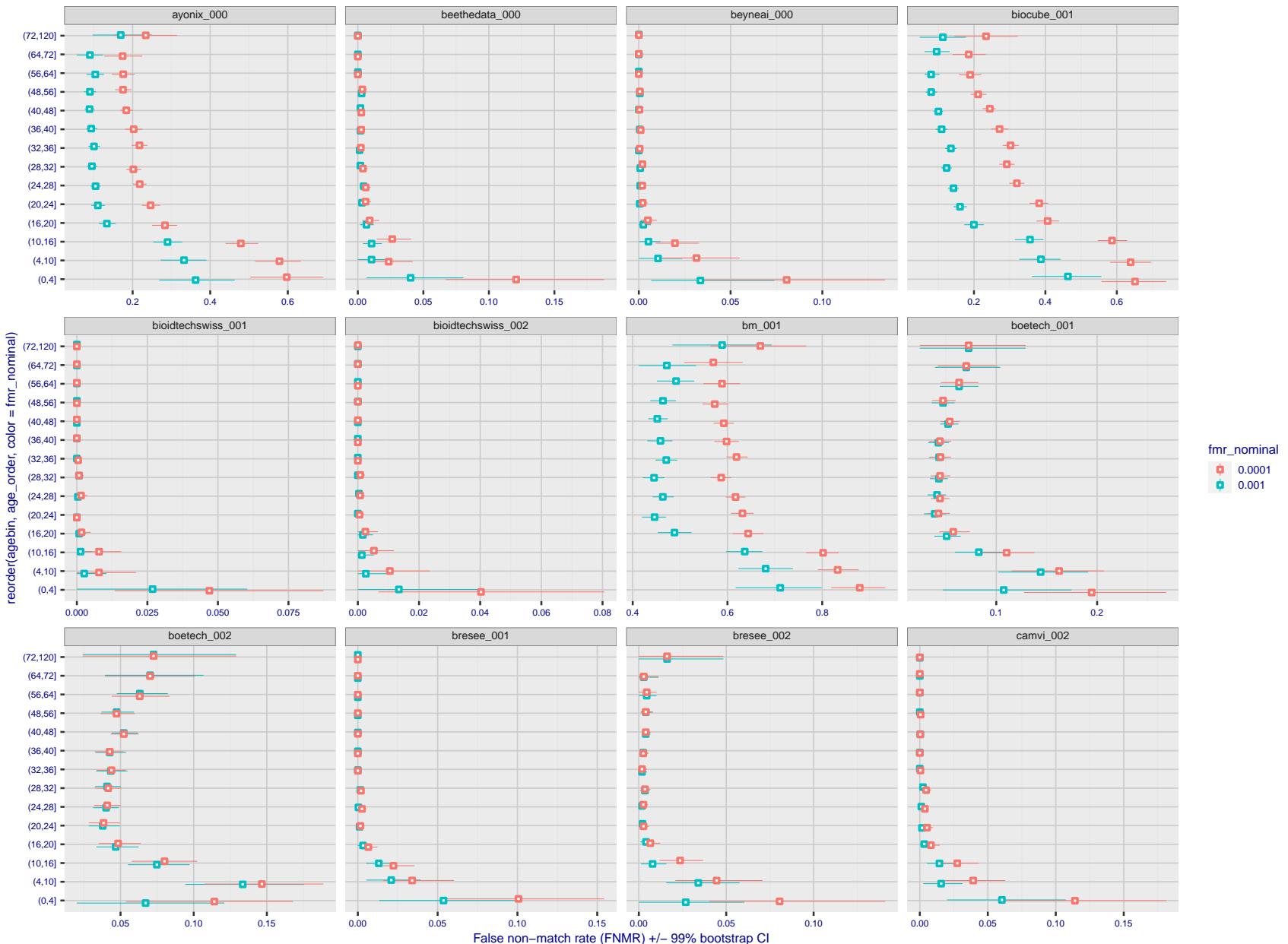


Figure 282: For the visa images, the dots show FNMR by age group for two operating thresholds corresponding to  $FMR = \{0.001, 0.0001\}$  computed over all on the order of  $10^{10}$  impostor scores. The FMR in each bin will vary also - see subsequent impostor heatmaps in sec. 3.6.2. Given a pair of face images taken at different times, we assign the comparison to the bin that is the arithmetic average of the subject's ages. This plot shows only the effect of age, not ageing. The number of comparisons in each bin is generally in the thousands, however the first and last bins are computed over 149 and 124 respectively. The error rates in some (adult) cases are zero, and in others the DET is flat so the error rates at the two thresholds are identical. The lines span 1% and 99% of bootstrap replicated FNMR estimates.

fmr\_nominal  
◻ 0.0001  
◻ 0.001

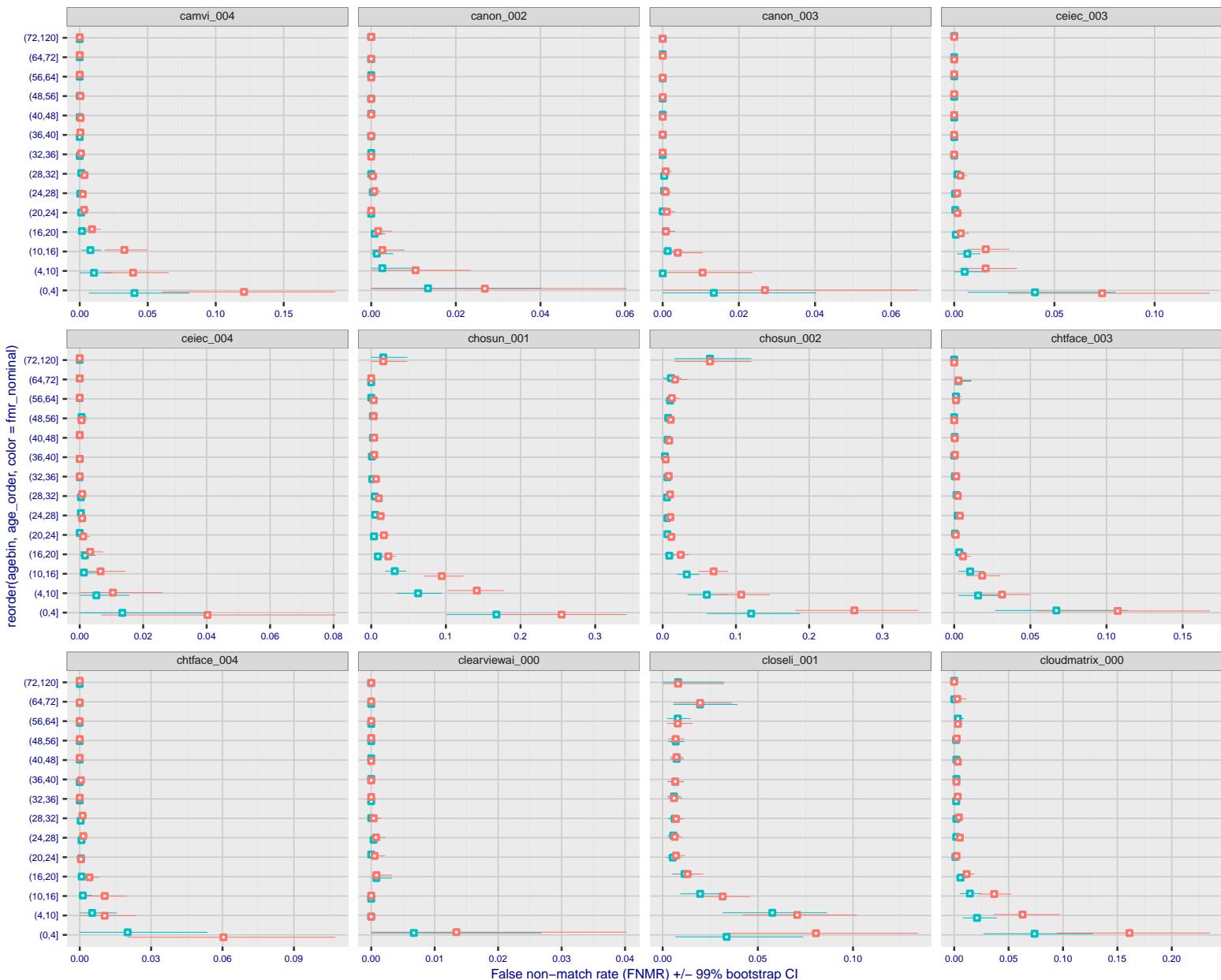


Figure 283: For the visa images, the dots show FNMR by age group for two operating thresholds corresponding to  $FMR = \{0.001, 0.0001\}$  computed over all on the order of  $10^{10}$  impostor scores. The FMR in each bin will vary also - see subsequent impostor heatmaps in sec. 3.6.2. Given a pair of face images taken at different times, we assign the comparison to the bin that is the arithmetic average of the subject's ages. This plot shows only the effect of age, not ageing. The number of comparisons in each bin is generally in the thousands, however the first and last bins are computed over 149 and 124 respectively. The error rates in some (adult) cases are zero, and in others the DET is flat so the error rates at the two thresholds are identical. The lines span 1% and 99% of bootstrap replicated FNMR estimates.



Figure 284: For the visa images, the dots show FNMR by age group for two operating thresholds corresponding to  $FMR = \{0.001, 0.0001\}$  computed over all on the order of  $10^{10}$  impostor scores. The FMR in each bin will vary also - see subsequent impostor heatmaps in sec. 3.6.2. Given a pair of face images taken at different times, we assign the comparison to the bin that is the arithmetic average of the subject's ages. This plot shows only the effect of age, not ageing. The number of comparisons in each bin is generally in the thousands, however the first and last bins are computed over 149 and 124 respectively. The error rates in some (adult) cases are zero, and in others the DET is flat so the error rates at the two thresholds are identical. The lines span 1% and 99% of bootstrap replicated FNMR estimates.

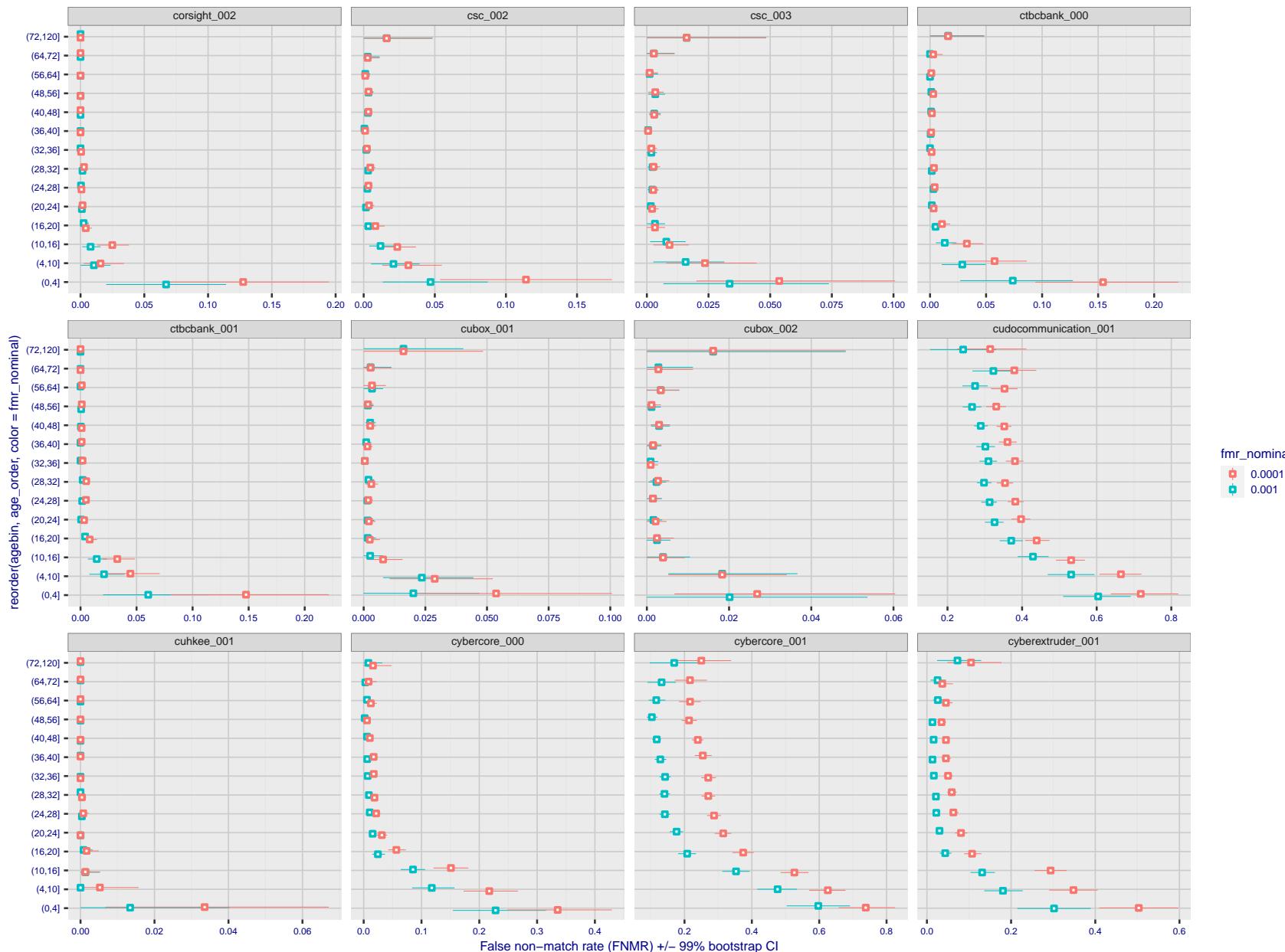


Figure 285: For the visa images, the dots show FNMR by age group for two operating thresholds corresponding to  $FMR = \{0.001, 0.0001\}$  computed over all on the order of  $10^{10}$  impostor scores. The FMR in each bin will vary also - see subsequent impostor heatmaps in sec. 3.6.2. Given a pair of face images taken at different times, we assign the comparison to the bin that is the arithmetic average of the subject's ages. This plot shows only the effect of age, not ageing. The number of comparisons in each bin is generally in the thousands, however the first and last bins are computed over 149 and 124 respectively. The error rates in some (adult) cases are zero, and in others the DET is flat so the error rates at the two thresholds are identical. The lines span 1% and 99% of bootstrap replicated FNMR estimates.



Figure 286: For the visa images, the dots show FNMR by age group for two operating thresholds corresponding to  $FMR = \{0.001, 0.0001\}$  computed over all on the order of  $10^{10}$  impostor scores. The FMR in each bin will vary also - see subsequent impostor heatmaps in sec. 3.6.2. Given a pair of face images taken at different times, we assign the comparison to the bin that is the arithmetic average of the subject's ages. This plot shows only the effect of age, not ageing. The number of comparisons in each bin is generally in the thousands, however the first and last bins are computed over 149 and 124 respectively. The error rates in some (adult) cases are zero, and in others the DET is flat so the error rates at the two thresholds are identical. The lines span 1% and 99% of bootstrap replicated FNMR estimates.



Figure 287: For the visa images, the dots show FNMR by age group for two operating thresholds corresponding to  $FMR = \{0.001, 0.0001\}$  computed over all on the order of  $10^{10}$  impostor scores. The FMR in each bin will vary also - see subsequent impostor heatmaps in sec. 3.6.2. Given a pair of face images taken at different times, we assign the comparison to the bin that is the arithmetic average of the subject's ages. This plot shows only the effect of age, not ageing. The number of comparisons in each bin is generally in the thousands, however the first and last bins are computed over 149 and 124 respectively. The error rates in some (adult) cases are zero, and in others the DET is flat so the error rates at the two thresholds are identical. The lines span 1% and 99% of bootstrap replicated FNMR estimates.

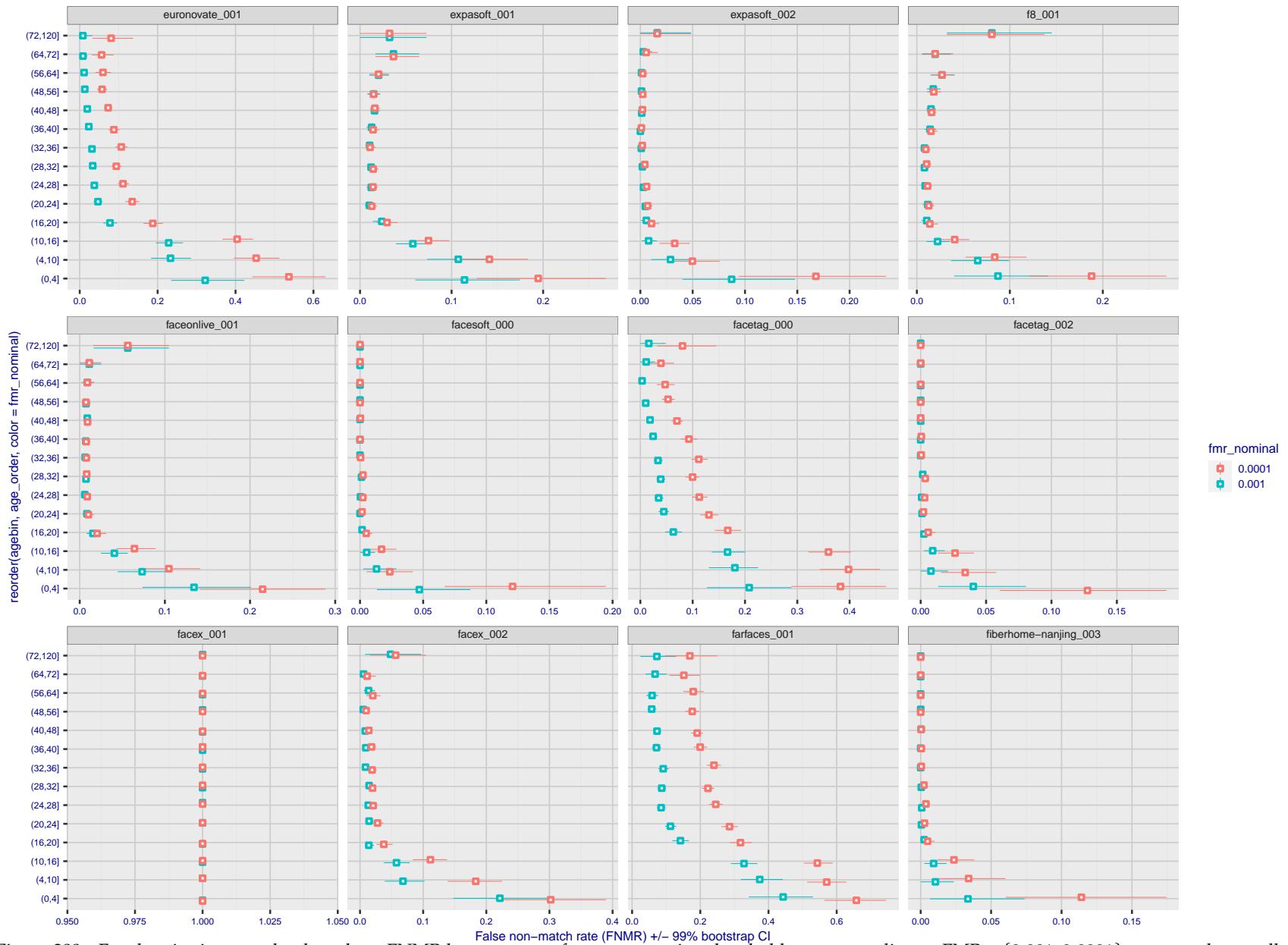


Figure 288: For the visa images, the dots show FNMR by age group for two operating thresholds corresponding to  $FMR = \{0.001, 0.0001\}$  computed over all on the order of  $10^{10}$  impostor scores. The FMR in each bin will vary also - see subsequent impostor heatmaps in sec. 3.6.2. Given a pair of face images taken at different times, we assign the comparison to the bin that is the arithmetic average of the subject's ages. This plot shows only the effect of age, not ageing. The number of comparisons in each bin is generally in the thousands, however the first and last bins are computed over 149 and 124 respectively. The error rates in some (adult) cases are zero, and in others the DET is flat so the error rates at the two thresholds are identical. The lines span 1% and 99% of bootstrap replicated FNMR estimates.

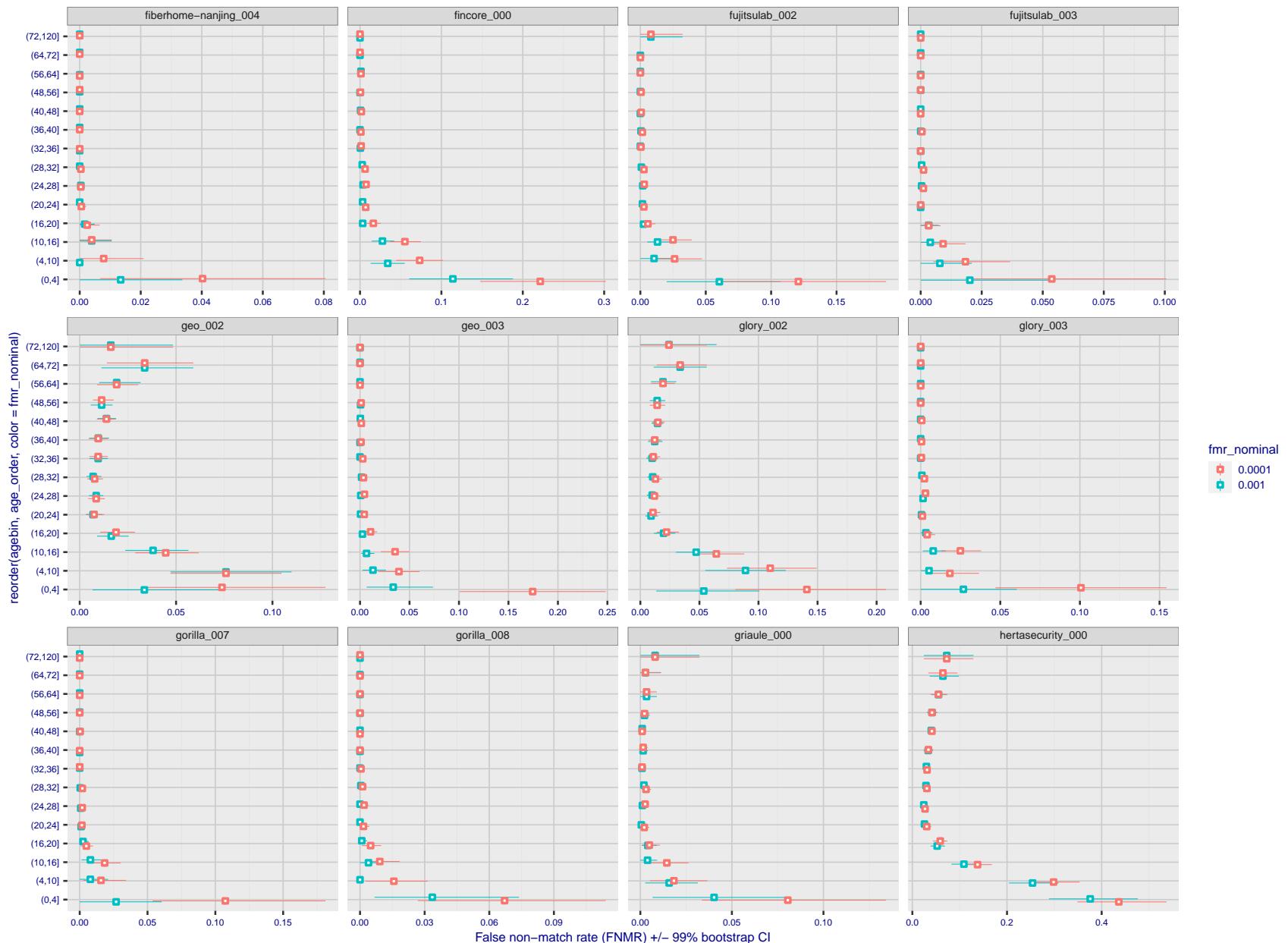


Figure 289: For the visa images, the dots show FNMR by age group for two operating thresholds corresponding to  $FMR = \{0.001, 0.0001\}$  computed over all on the order of  $10^{10}$  impostor scores. The FMR in each bin will vary also - see subsequent impostor heatmaps in sec. 3.6.2. Given a pair of face images taken at different times, we assign the comparison to the bin that is the arithmetic average of the subject's ages. This plot shows only the effect of age, not ageing. The number of comparisons in each bin is generally in the thousands, however the first and last bins are computed over 149 and 124 respectively. The error rates in some (adult) cases are zero, and in others the DET is flat so the error rates at the two thresholds are identical. The lines span 1% and 99% of bootstrap replicated FNMR estimates.

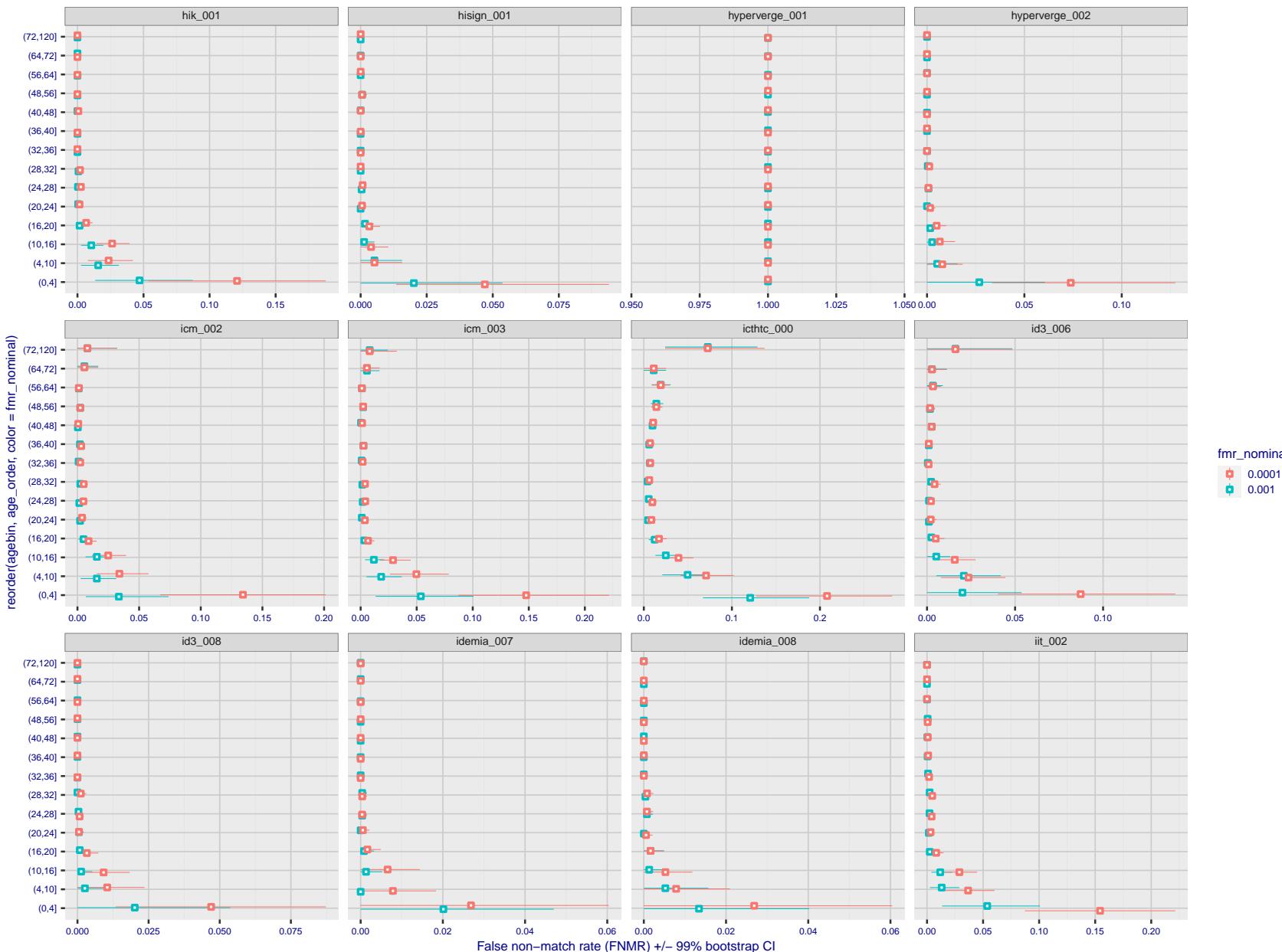


Figure 290: For the visa images, the dots show FNMR by age group for two operating thresholds corresponding to  $FMR = \{0.001, 0.0001\}$  computed over all on the order of  $10^{10}$  impostor scores. The FMR in each bin will vary also - see subsequent impostor heatmaps in sec. 3.6.2. Given a pair of face images taken at different times, we assign the comparison to the bin that is the arithmetic average of the subject's ages. This plot shows only the effect of age, not ageing. The number of comparisons in each bin is generally in the thousands, however the first and last bins are computed over 149 and 124 respectively. The error rates in some (adult) cases are zero, and in others the DET is flat so the error rates at the two thresholds are identical. The lines span 1% and 99% of bootstrap replicated FNMR estimates.

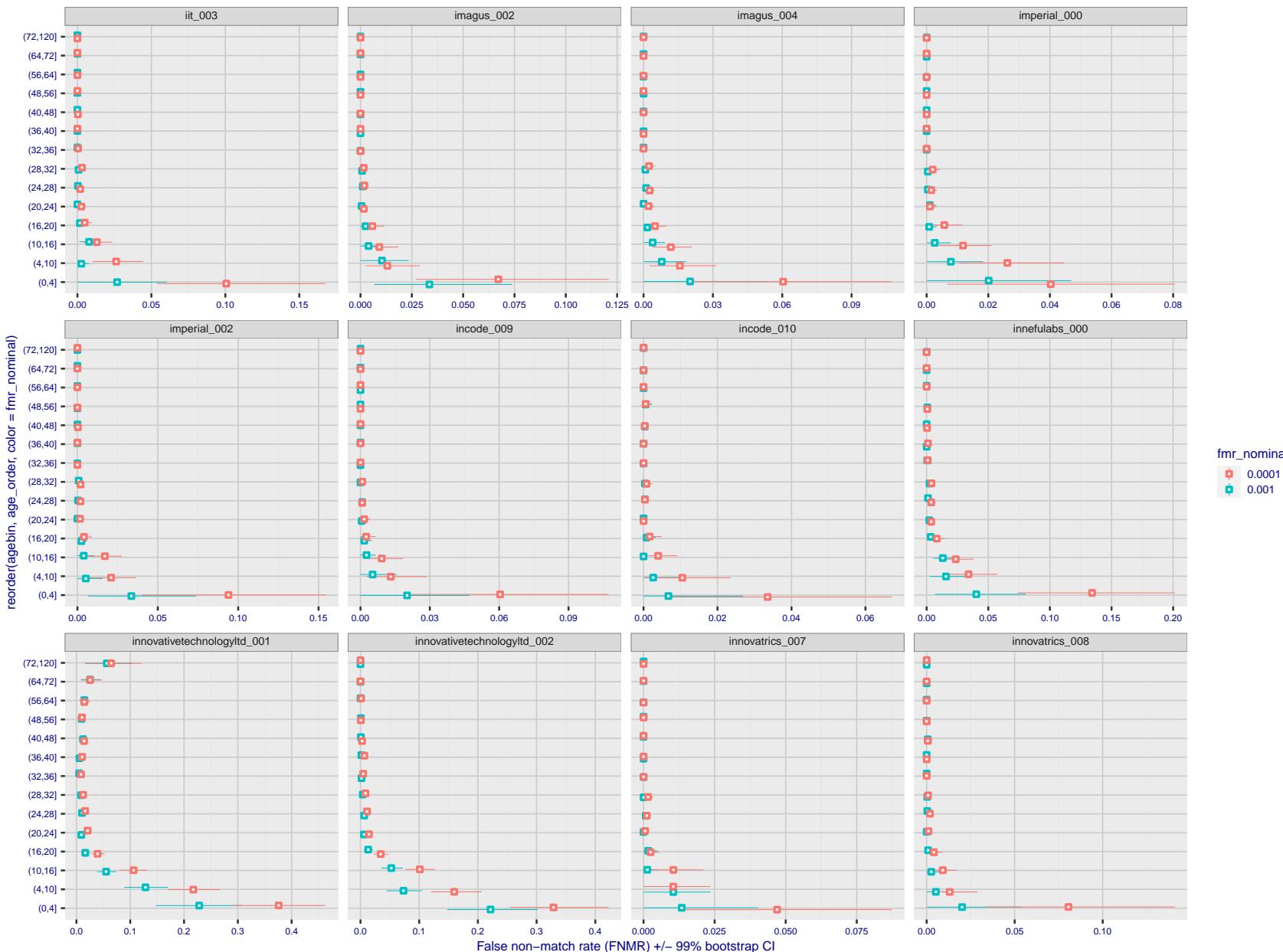


Figure 291: For the visa images, the dots show FNMR by age group for two operating thresholds corresponding to  $FMR = \{0.001, 0.0001\}$  computed over all on the order of  $10^{10}$  impostor scores. The FMR in each bin will vary also - see subsequent impostor heatmaps in sec. 3.6.2. Given a pair of face images taken at different times, we assign the comparison to the bin that is the arithmetic average of the subject's ages. This plot shows only the effect of age, not ageing. The number of comparisons in each bin is generally in the thousands, however the first and last bins are computed over 149 and 124 respectively. The error rates in some (adult) cases are zero, and in others the DET is flat so the error rates at the two thresholds are identical. The lines span 1% and 99% of bootstrap replicated FNMR estimates.

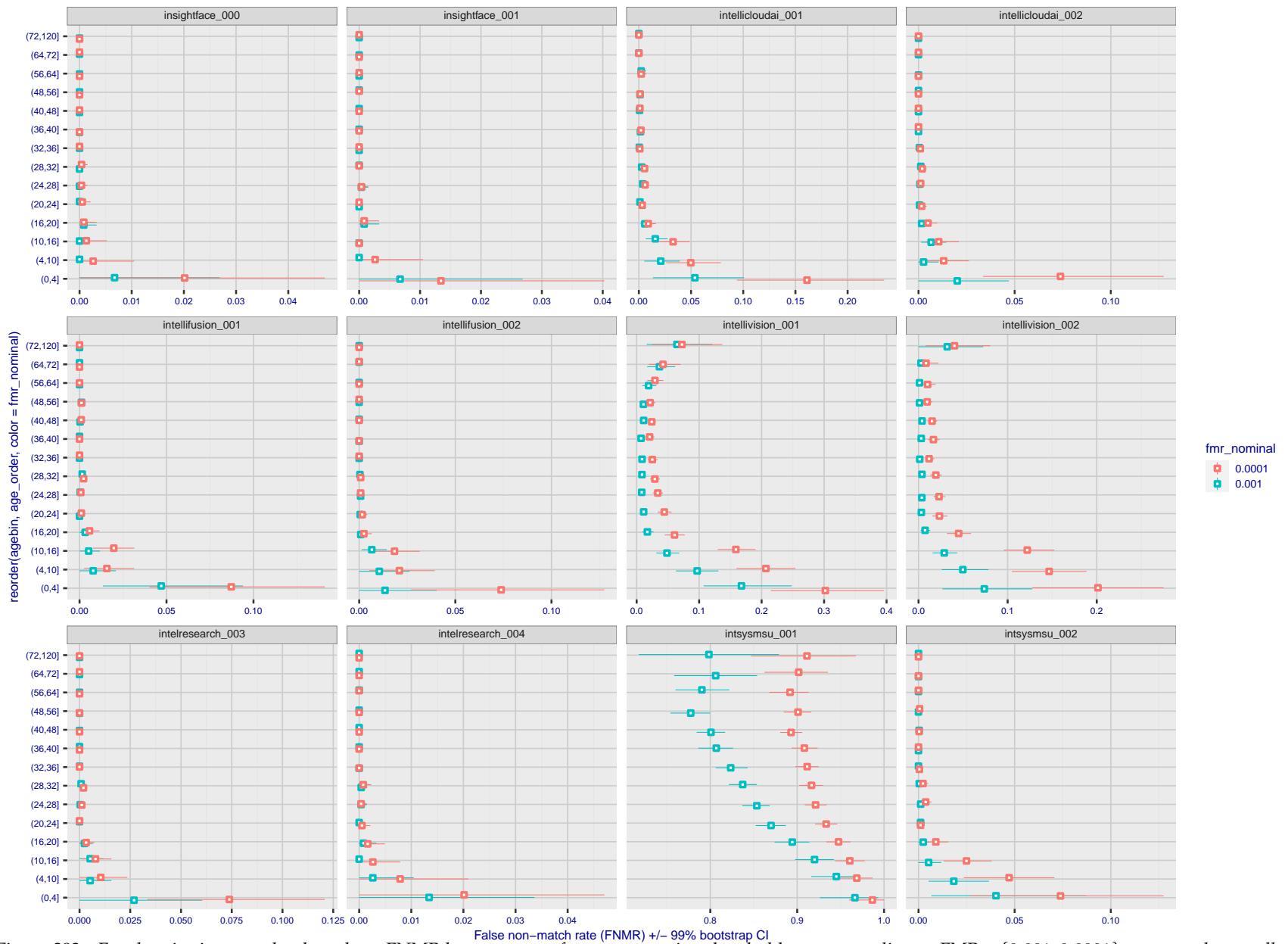


Figure 292: For the visa images, the dots show FNMR by age group for two operating thresholds corresponding to  $FMR = \{0.001, 0.0001\}$  computed over all on the order of  $10^{10}$  impostor scores. The FMR in each bin will vary also - see subsequent impostor heatmaps in sec. 3.6.2. Given a pair of face images taken at different times, we assign the comparison to the bin that is the arithmetic average of the subject's ages. This plot shows only the effect of age, not ageing. The number of comparisons in each bin is generally in the thousands, however the first and last bins are computed over 149 and 124 respectively. The error rates in some (adult) cases are zero, and in others the DET is flat so the error rates at the two thresholds are identical. The lines span 1% and 99% of bootstrap replicated FNMR estimates.

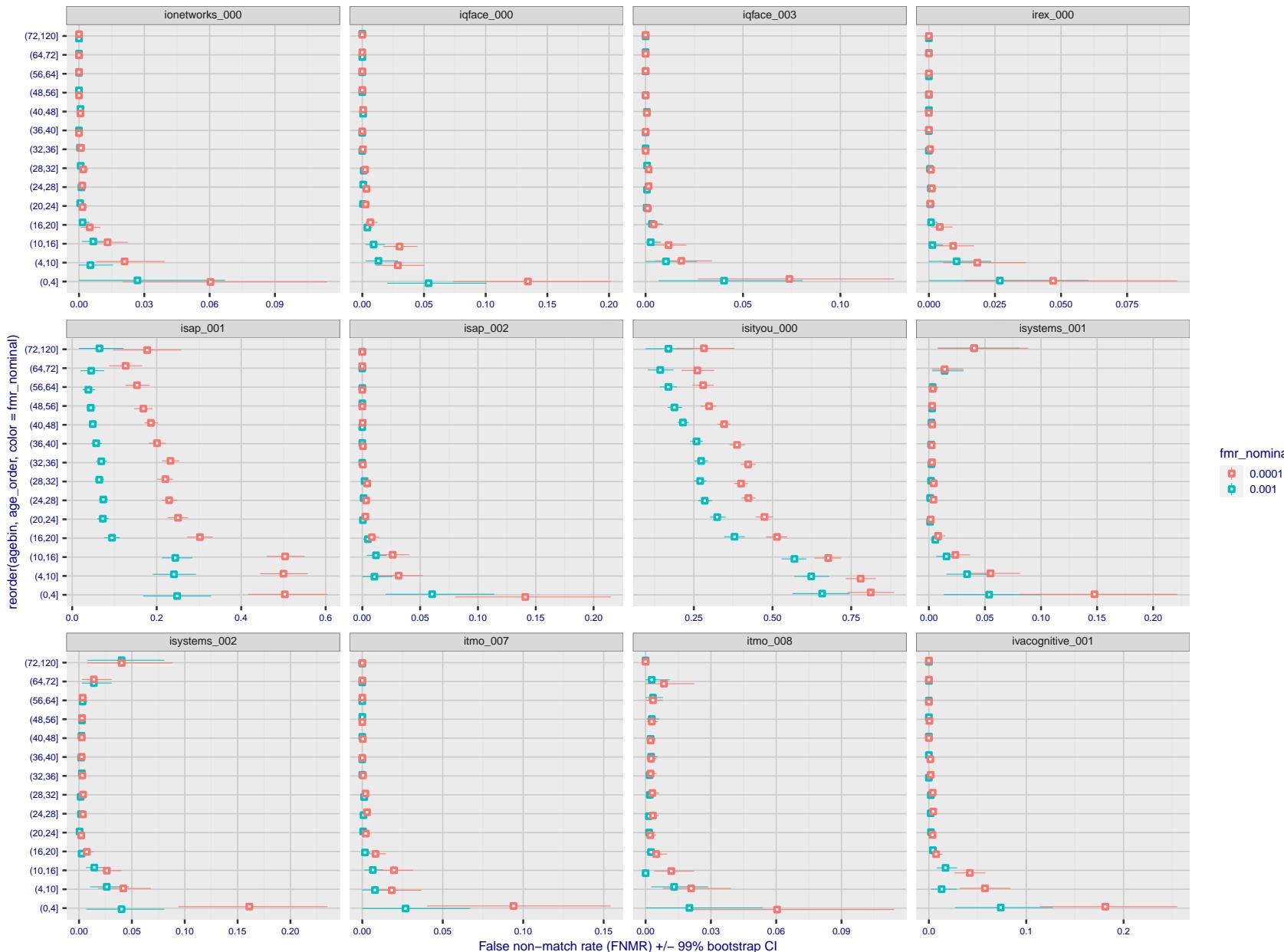


Figure 293: For the visa images, the dots show FNMR by age group for two operating thresholds corresponding to  $FMR = \{0.001, 0.0001\}$  computed over all on the order of  $10^{10}$  impostor scores. The FMR in each bin will vary also - see subsequent impostor heatmaps in sec. 3.6.2. Given a pair of face images taken at different times, we assign the comparison to the bin that is the arithmetic average of the subject's ages. This plot shows only the effect of age, not ageing. The number of comparisons in each bin is generally in the thousands, however the first and last bins are computed over 149 and 124 respectively. The error rates in some (adult) cases are zero, and in others the DET is flat so the error rates at the two thresholds are identical. The lines span 1% and 99% of bootstrap replicated FNMR estimates.

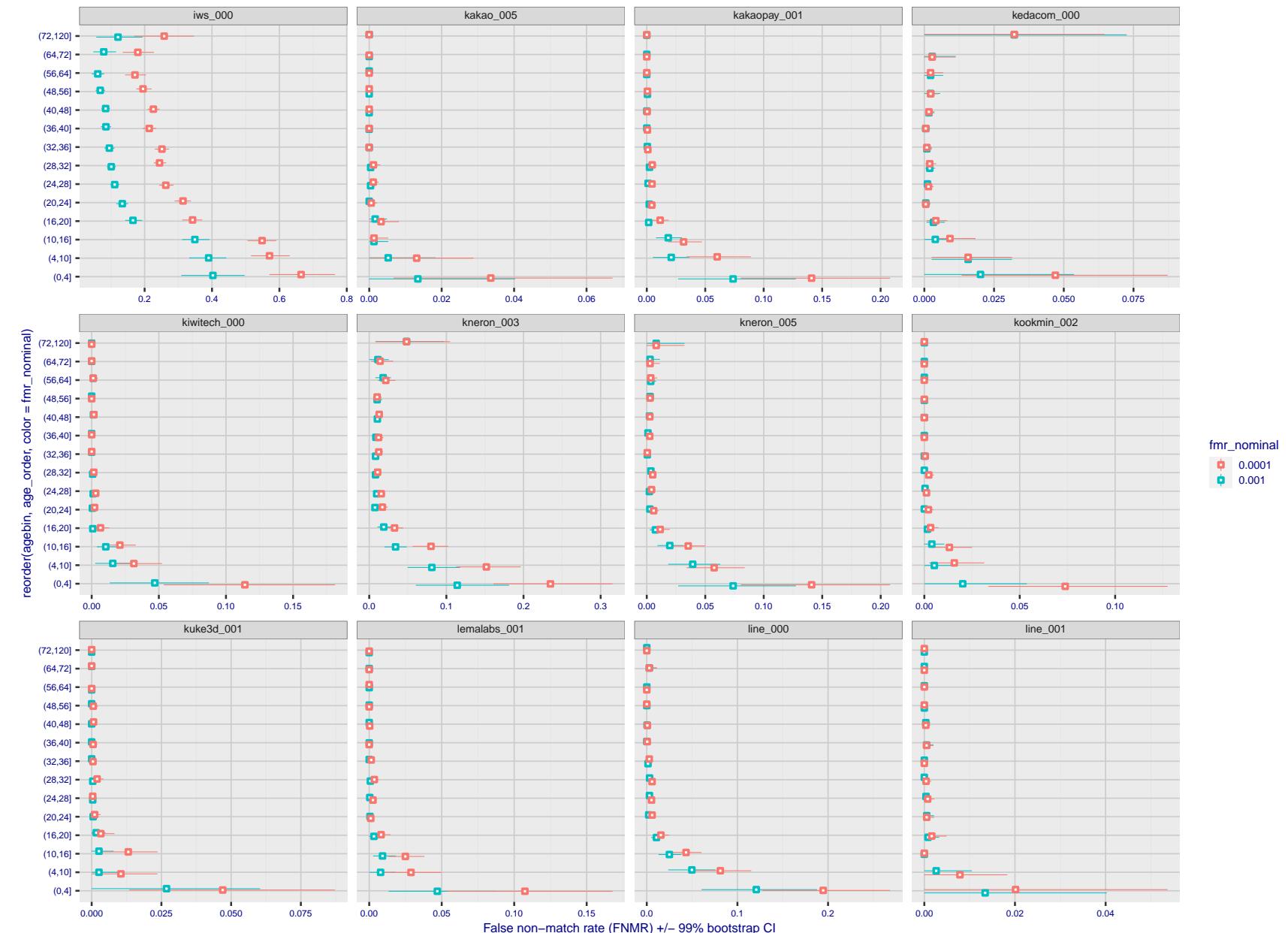


Figure 294: For the visa images, the dots show FNMR by age group for two operating thresholds corresponding to  $FMR = \{0.001, 0.0001\}$  computed over all on the order of  $10^{10}$  impostor scores. The FMR in each bin will vary also - see subsequent impostor heatmaps in sec. 3.6.2. Given a pair of face images taken at different times, we assign the comparison to the bin that is the arithmetic average of the subject's ages. This plot shows only the effect of age, not ageing. The number of comparisons in each bin is generally in the thousands, however the first and last bins are computed over 149 and 124 respectively. The error rates in some (adult) cases are zero, and in others the DET is flat so the error rates at the two thresholds are identical. The lines span 1% and 99% of bootstrap replicated FNMR estimates.

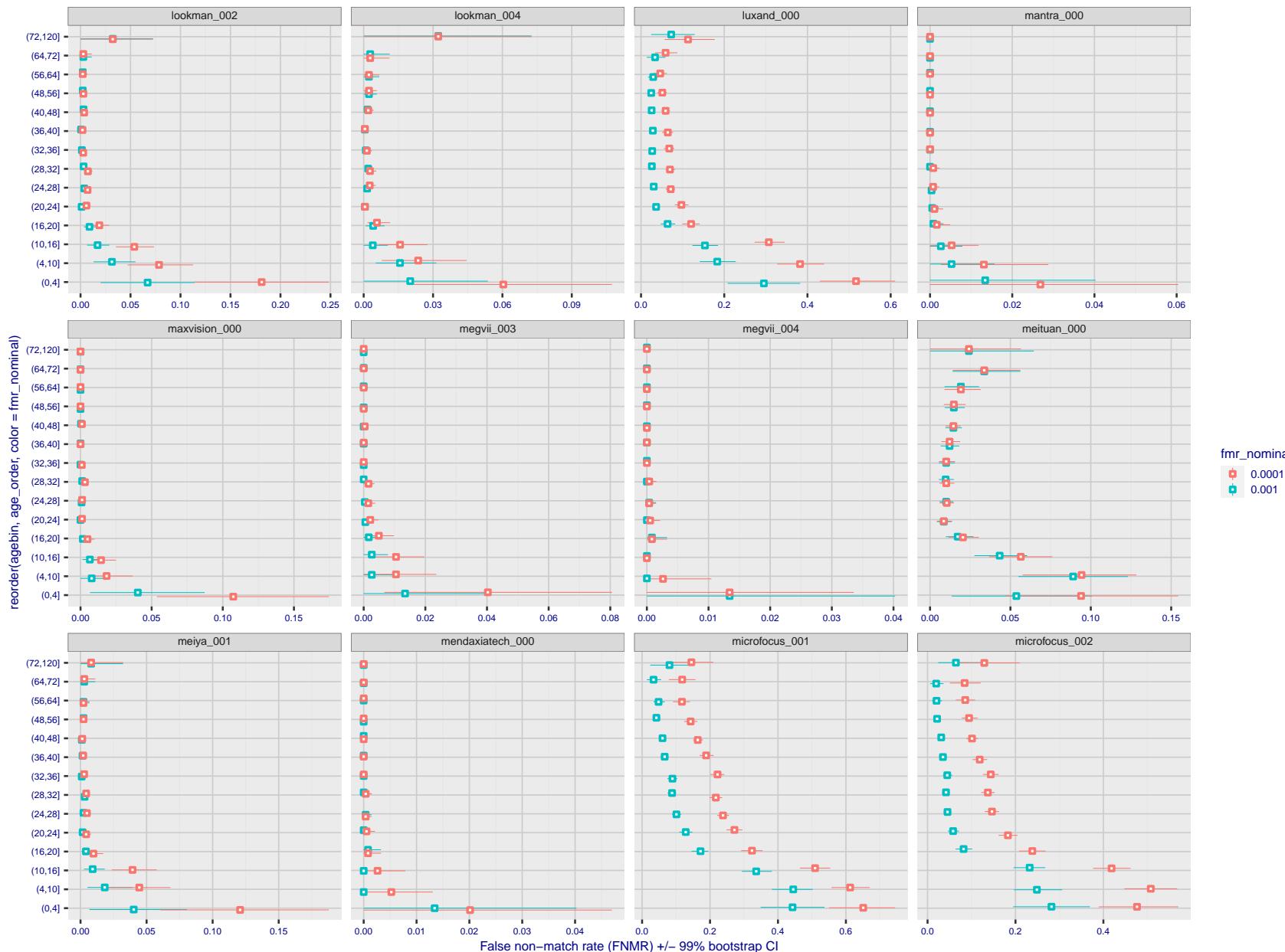


Figure 295: For the visa images, the dots show FNMR by age group for two operating thresholds corresponding to  $FMR = \{0.001, 0.0001\}$  computed over all on the order of  $10^{10}$  impostor scores. The FMR in each bin will vary also - see subsequent impostor heatmaps in sec. 3.6.2. Given a pair of face images taken at different times, we assign the comparison to the bin that is the arithmetic average of the subject's ages. This plot shows only the effect of age, not ageing. The number of comparisons in each bin is generally in the thousands, however the first and last bins are computed over 149 and 124 respectively. The error rates in some (adult) cases are zero, and in others the DET is flat so the error rates at the two thresholds are identical. The lines span 1% and 99% of bootstrap replicated FNMR estimates.

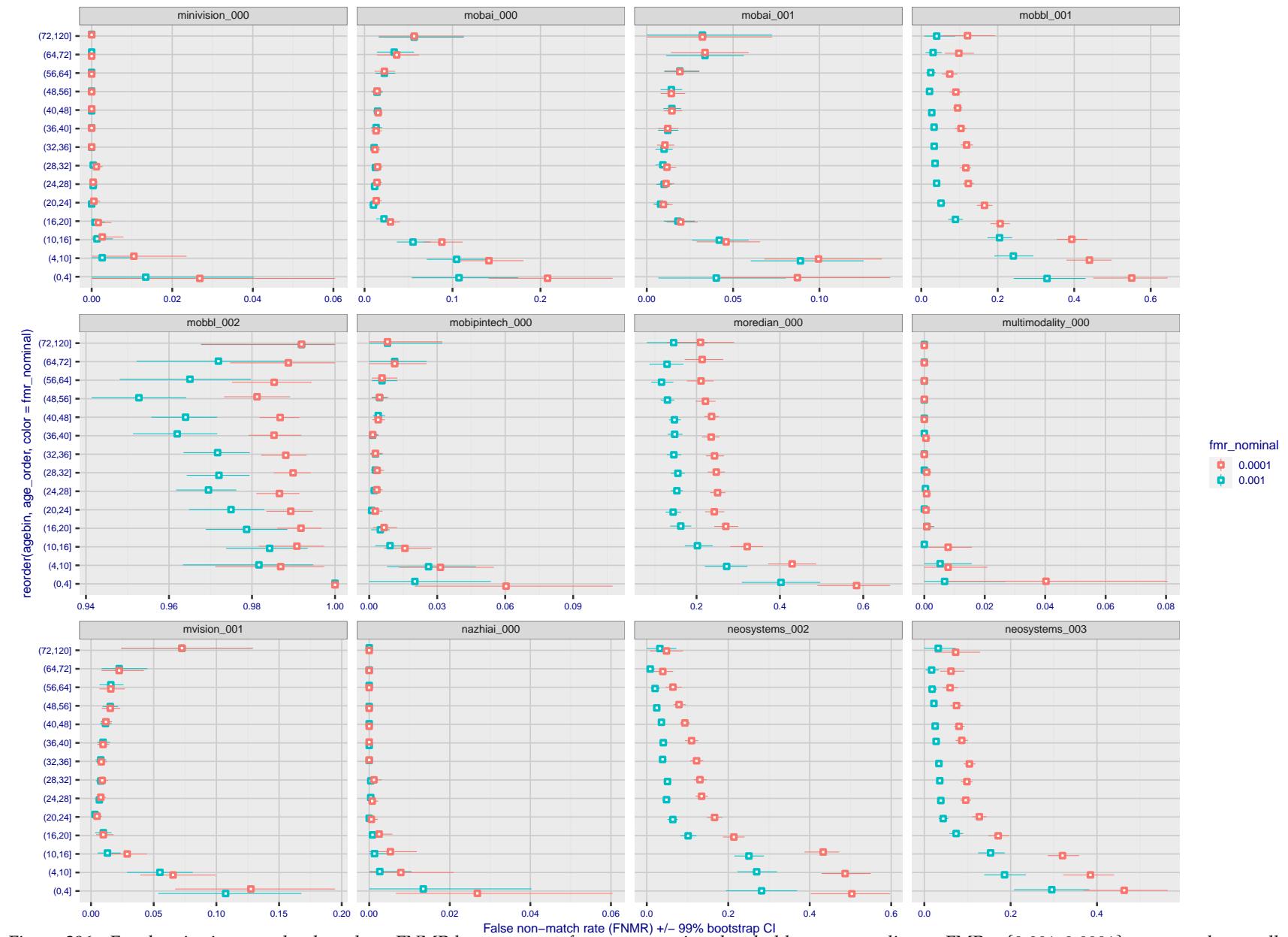


Figure 296: For the visa images, the dots show FNMR by age group for two operating thresholds corresponding to  $FMR = \{0.001, 0.0001\}$  computed over all on the order of  $10^{10}$  impostor scores. The FMR in each bin will vary also - see subsequent impostor heatmaps in sec. 3.6.2. Given a pair of face images taken at different times, we assign the comparison to the bin that is the arithmetic average of the subject's ages. This plot shows only the effect of age, not ageing. The number of comparisons in each bin is generally in the thousands, however the first and last bins are computed over 149 and 124 respectively. The error rates in some (adult) cases are zero, and in others the DET is flat so the error rates at the two thresholds are identical. The lines span 1% and 99% of bootstrap replicated FNMR estimates.

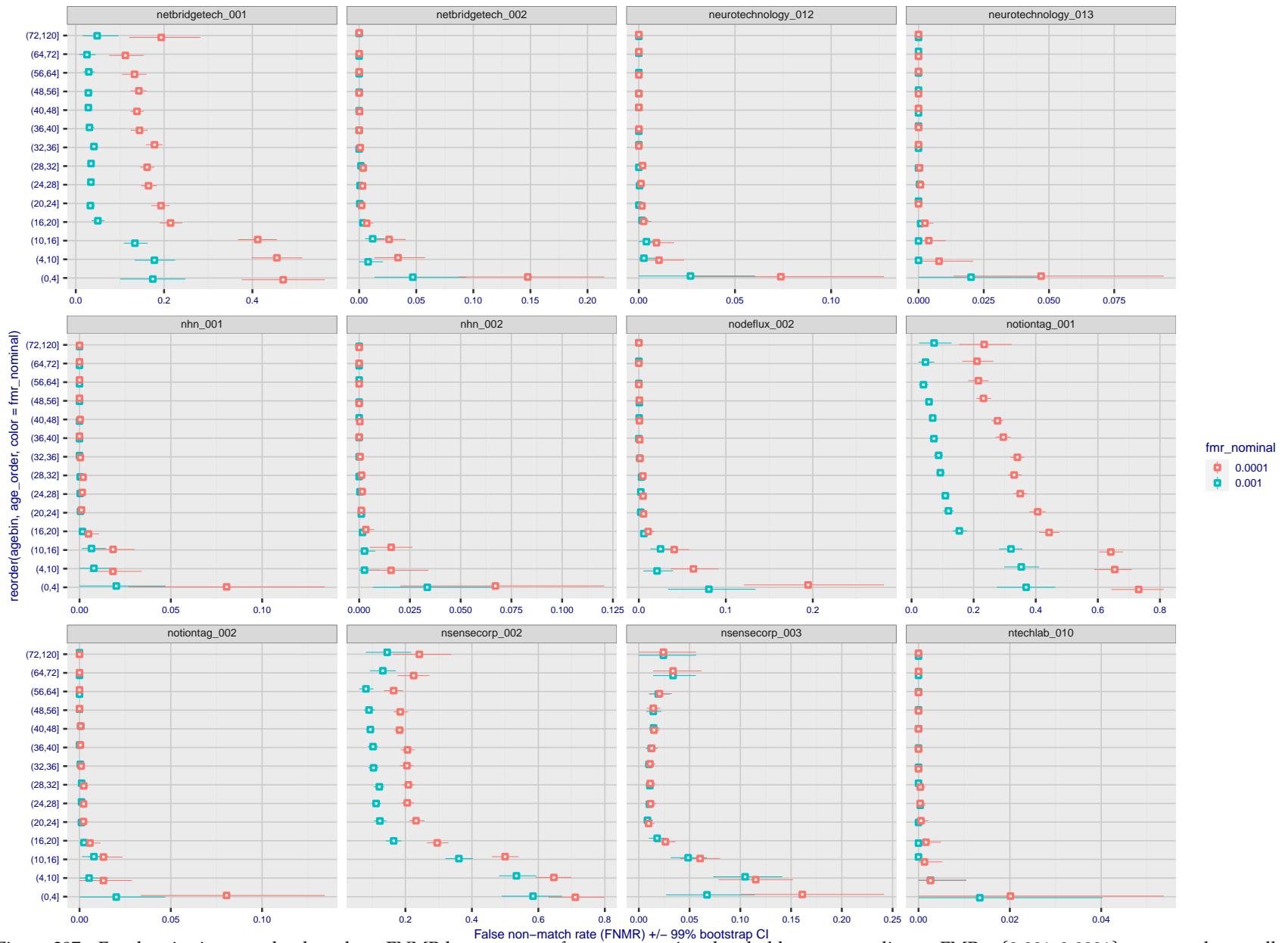


Figure 297: For the visa images, the dots show FNMR by age group for two operating thresholds corresponding to  $FMR = \{0.001, 0.0001\}$  computed over all on the order of  $10^{10}$  impostor scores. The FMR in each bin will vary also - see subsequent impostor heatmaps in sec. 3.6.2. Given a pair of face images taken at different times, we assign the comparison to the bin that is the arithmetic average of the subject's ages. This plot shows only the effect of age, not ageing. The number of comparisons in each bin is generally in the thousands, however the first and last bins are computed over 149 and 124 respectively. The error rates in some (adult) cases are zero, and in others the DET is flat so the error rates at the two thresholds are identical. The lines span 1% and 99% of bootstrap replicated FNMR estimates.

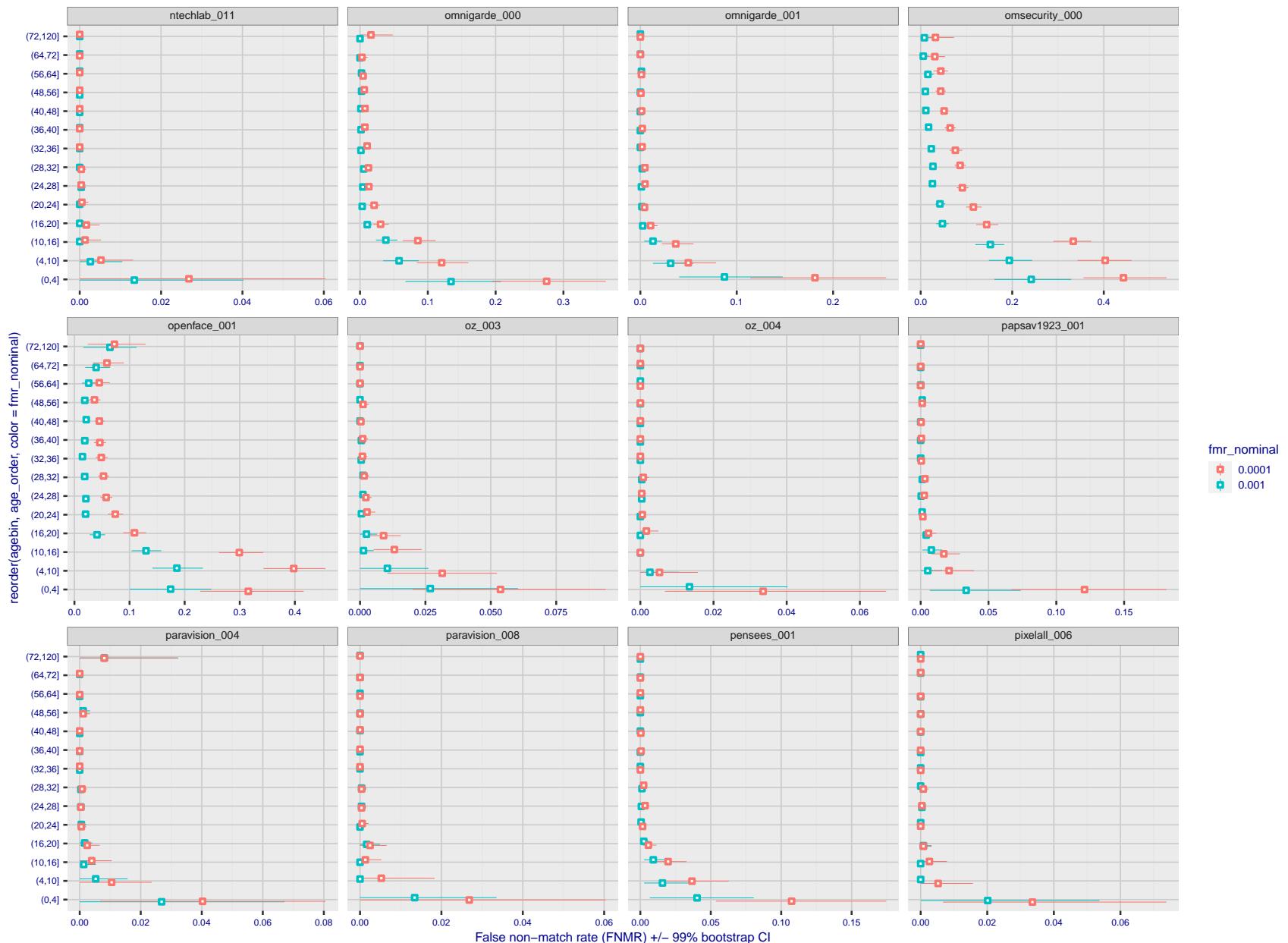


Figure 298: For the visa images, the dots show FNMR by age group for two operating thresholds corresponding to  $FMR = \{0.001, 0.0001\}$  computed over all on the order of  $10^{10}$  impostor scores. The FMR in each bin will vary also - see subsequent impostor heatmaps in sec. 3.6.2. Given a pair of face images taken at different times, we assign the comparison to the bin that is the arithmetic average of the subject's ages. This plot shows only the effect of age, not ageing. The number of comparisons in each bin is generally in the thousands, however the first and last bins are computed over 149 and 124 respectively. The error rates in some (adult) cases are zero, and in others the DET is flat so the error rates at the two thresholds are identical. The lines span 1% and 99% of bootstrap replicated FNMR estimates.



Figure 299: For the visa images, the dots show FNMR by age group for two operating thresholds corresponding to  $FMR = \{0.001, 0.0001\}$  computed over all on the order of  $10^{10}$  impostor scores. The FMR in each bin will vary also - see subsequent impostor heatmaps in sec. 3.6.2. Given a pair of face images taken at different times, we assign the comparison to the bin that is the arithmetic average of the subject's ages. This plot shows only the effect of age, not ageing. The number of comparisons in each bin is generally in the thousands, however the first and last bins are computed over 149 and 124 respectively. The error rates in some (adult) cases are zero, and in others the DET is flat so the error rates at the two thresholds are identical. The lines span 1% and 99% of bootstrap replicated FNMR estimates.



Figure 300: For the visa images, the dots show FNMR by age group for two operating thresholds corresponding to  $FMR = \{0.001, 0.0001\}$  computed over all on the order of  $10^{10}$  impostor scores. The FMR in each bin will vary also - see subsequent impostor heatmaps in sec. 3.6.2. Given a pair of face images taken at different times, we assign the comparison to the bin that is the arithmetic average of the subject's ages. This plot shows only the effect of age, not ageing. The number of comparisons in each bin is generally in the thousands, however the first and last bins are computed over 149 and 124 respectively. The error rates in some (adult) cases are zero, and in others the DET is flat so the error rates at the two thresholds are identical. The lines span 1% and 99% of bootstrap replicated FNMR estimates.



Figure 301: For the visa images, the dots show FNMR by age group for two operating thresholds corresponding to  $FMR = \{0.001, 0.0001\}$  computed over all on the order of  $10^{10}$  impostor scores. The FMR in each bin will vary also - see subsequent impostor heatmaps in sec. 3.6.2. Given a pair of face images taken at different times, we assign the comparison to the bin that is the arithmetic average of the subject's ages. This plot shows only the effect of age, not ageing. The number of comparisons in each bin is generally in the thousands, however the first and last bins are computed over 149 and 124 respectively. The error rates in some (adult) cases are zero, and in others the DET is flat so the error rates at the two thresholds are identical. The lines span 1% and 99% of bootstrap replicated FNMR estimates.



Figure 302: For the visa images, the dots show FNMR by age group for two operating thresholds corresponding to  $FMR = \{0.001, 0.0001\}$  computed over all on the order of  $10^{10}$  impostor scores. The FMR in each bin will vary also - see subsequent impostor heatmaps in sec. 3.6.2. Given a pair of face images taken at different times, we assign the comparison to the bin that is the arithmetic average of the subject's ages. This plot shows only the effect of age, not ageing. The number of comparisons in each bin is generally in the thousands, however the first and last bins are computed over 149 and 124 respectively. The error rates in some (adult) cases are zero, and in others the DET is flat so the error rates at the two thresholds are identical. The lines span 1% and 99% of bootstrap replicated FNMR estimates.

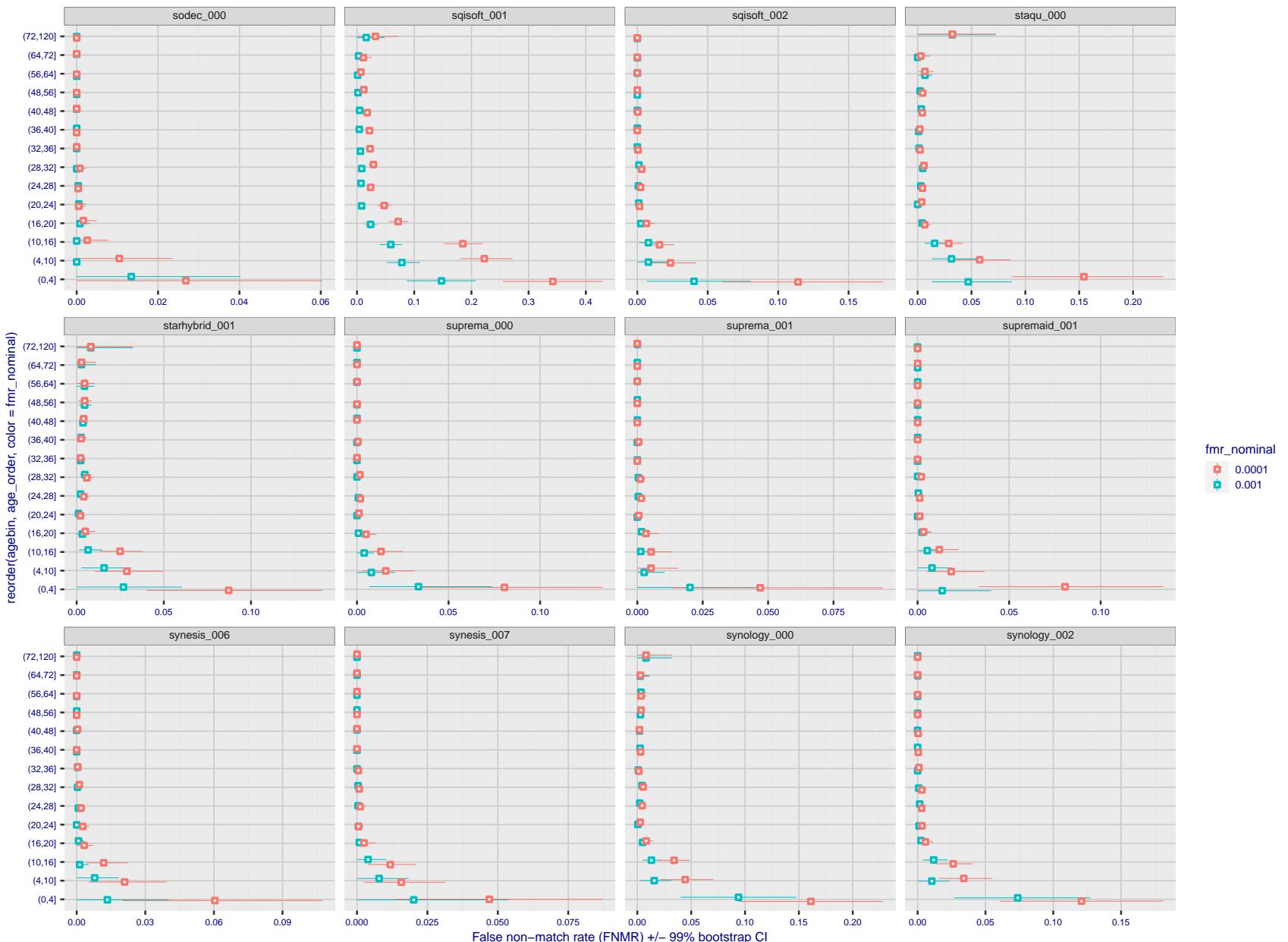


Figure 303: For the visa images, the dots show FNMR by age group for two operating thresholds corresponding to  $FMR = \{0.001, 0.0001\}$  computed over all on the order of  $10^{10}$  impostor scores. The FMR in each bin will vary also - see subsequent impostor heatmaps in sec. 3.6.2. Given a pair of face images taken at different times, we assign the comparison to the bin that is the arithmetic average of the subject's ages. This plot shows only the effect of age, not ageing. The number of comparisons in each bin is generally in the thousands, however the first and last bins are computed over 149 and 124 respectively. The error rates in some (adult) cases are zero, and in others the DET is flat so the error rates at the two thresholds are identical. The lines span 1% and 99% of bootstrap replicated FNMR estimates.

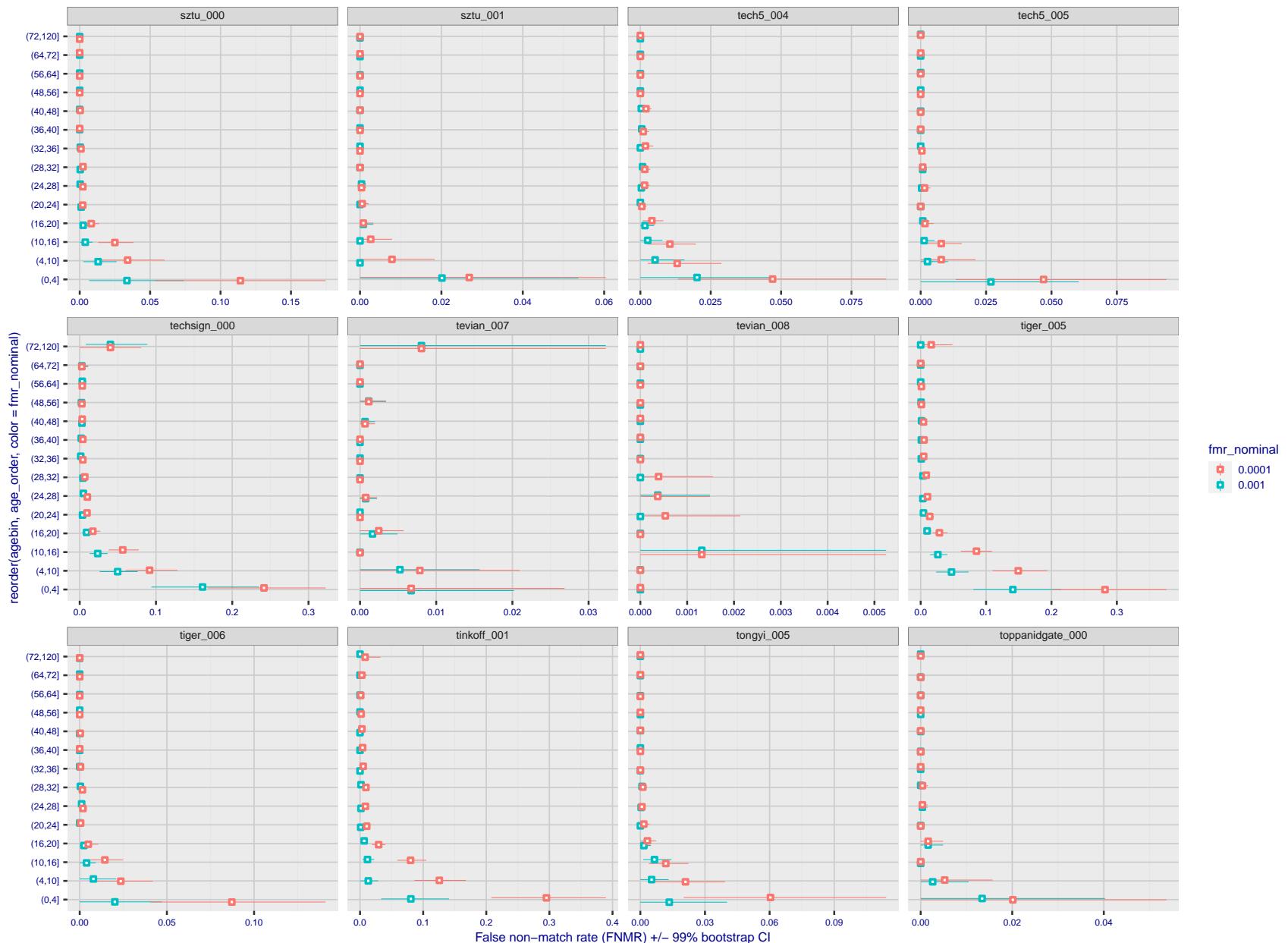


Figure 304: For the visa images, the dots show FNMR by age group for two operating thresholds corresponding to  $FMR = \{0.001, 0.0001\}$  computed over all on the order of  $10^{10}$  impostor scores. The FMR in each bin will vary also - see subsequent impostor heatmaps in sec. 3.6.2. Given a pair of face images taken at different times, we assign the comparison to the bin that is the arithmetic average of the subject's ages. This plot shows only the effect of age, not ageing. The number of comparisons in each bin is generally in the thousands, however the first and last bins are computed over 149 and 124 respectively. The error rates in some (adult) cases are zero, and in others the DET is flat so the error rates at the two thresholds are identical. The lines span 1% and 99% of bootstrap replicated FNMR estimates.

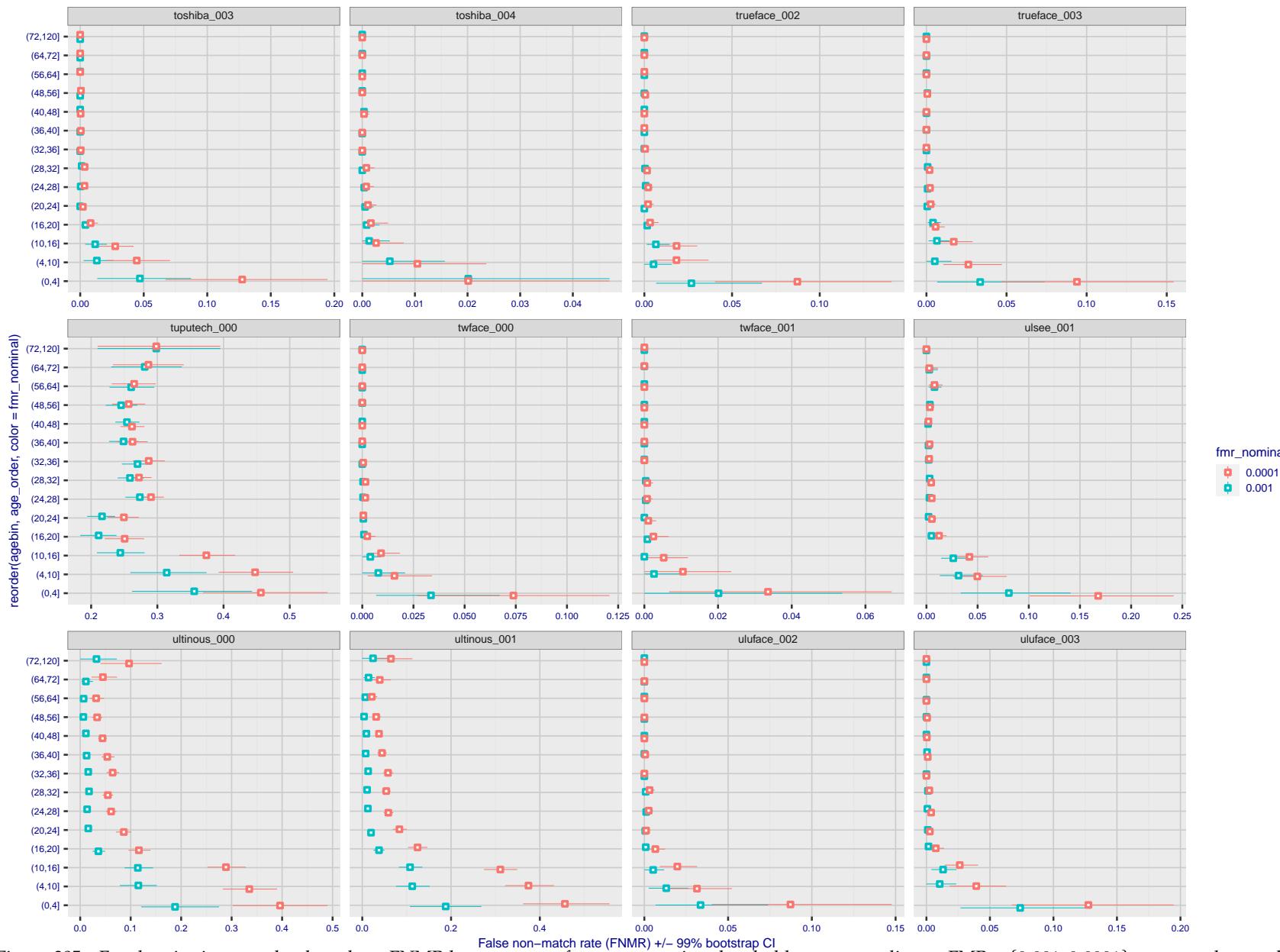


Figure 305: For the visa images, the dots show FNMR by age group for two operating thresholds corresponding to  $FMR = \{0.001, 0.0001\}$  computed over all on the order of  $10^{10}$  impostor scores. The FMR in each bin will vary also - see subsequent impostor heatmaps in sec. 3.6.2. Given a pair of face images taken at different times, we assign the comparison to the bin that is the arithmetic average of the subject's ages. This plot shows only the effect of age, not ageing. The number of comparisons in each bin is generally in the thousands, however the first and last bins are computed over 149 and 124 respectively. The error rates in some (adult) cases are zero, and in others the DET is flat so the error rates at the two thresholds are identical. The lines span 1% and 99% of bootstrap replicated FNMR estimates.

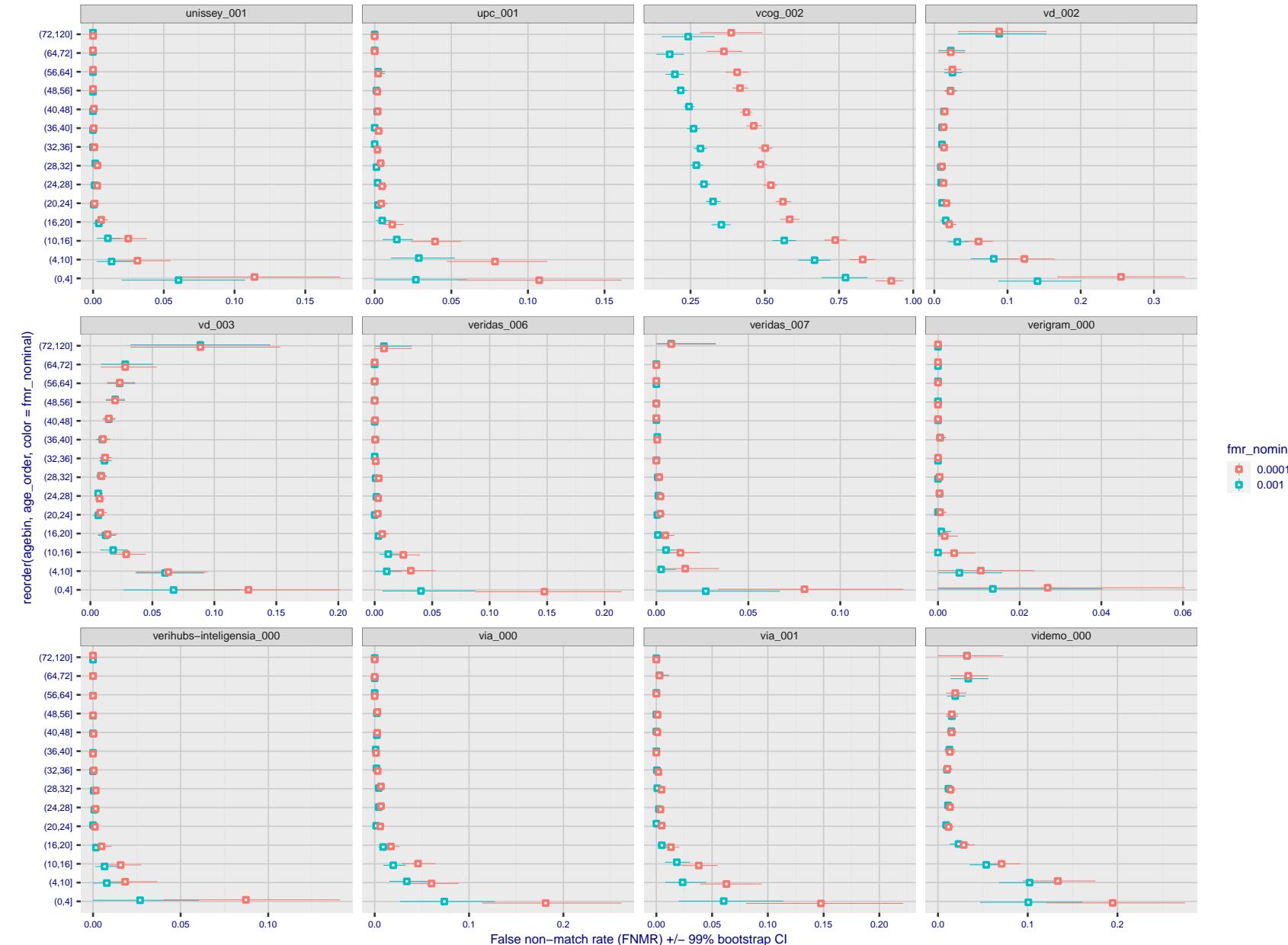


Figure 306: For the visa images, the dots show FNMR by age group for two operating thresholds corresponding to  $FMR = \{0.001, 0.0001\}$  computed over all on the order of  $10^{10}$  impostor scores. The FMR in each bin will vary also - see subsequent impostor heatmaps in sec. 3.6.2. Given a pair of face images taken at different times, we assign the comparison to the bin that is the arithmetic average of the subject's ages. This plot shows only the effect of age, not ageing. The number of comparisons in each bin is generally in the thousands, however the first and last bins are computed over 149 and 124 respectively. The error rates in some (adult) cases are zero, and in others the DET is flat so the error rates at the two thresholds are identical. The lines span 1% and 99% of bootstrap replicated FNMR estimates.

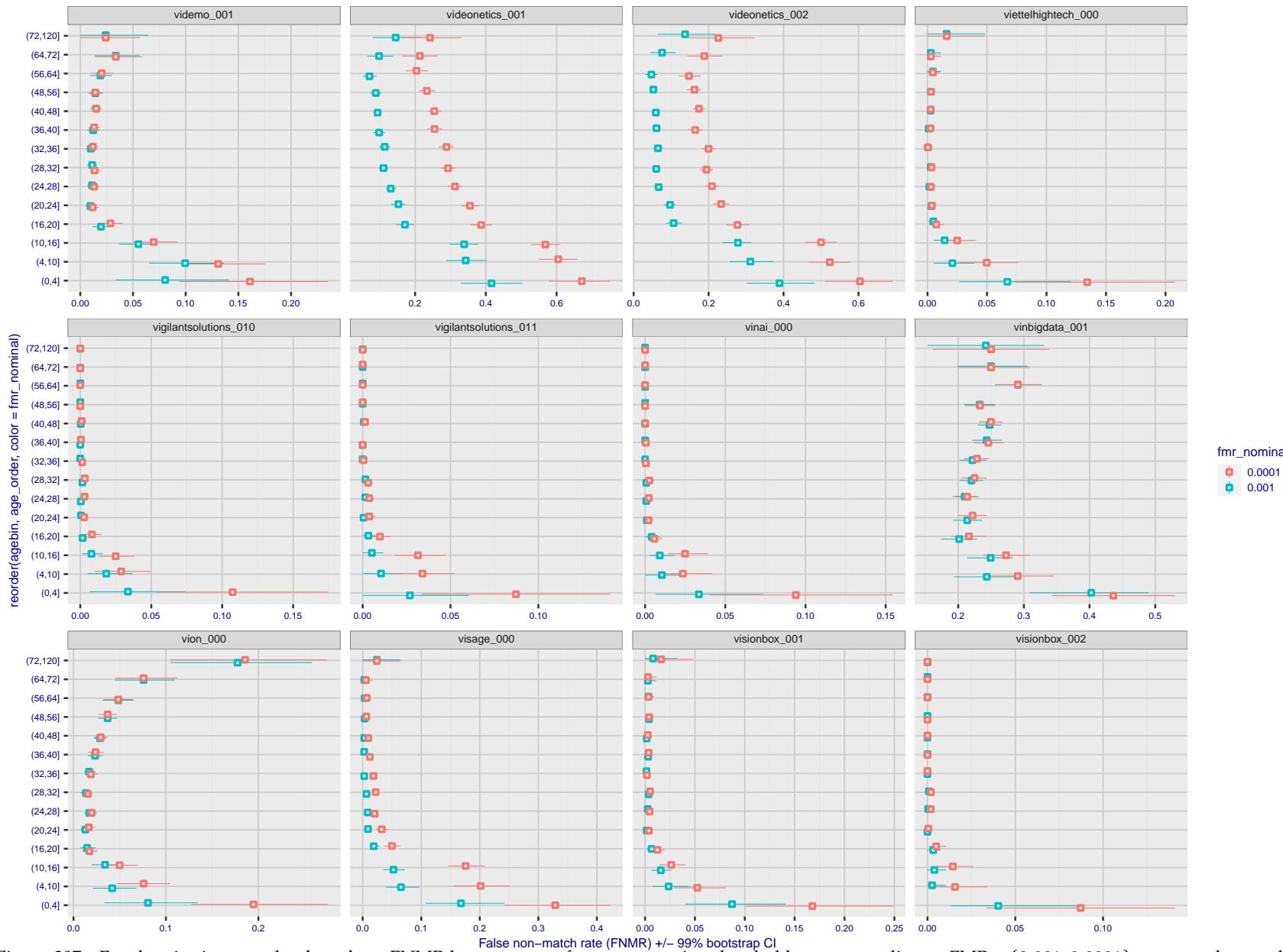


Figure 307: For the visa images, the dots show FNMR by age group for two operating thresholds corresponding to  $FMR = \{0.001, 0.0001\}$  computed over all on the order of  $10^{10}$  impostor scores. The FMR in each bin will vary also - see subsequent impostor heatmaps in sec. 3.6.2. Given a pair of face images taken at different times, we assign the comparison to the bin that is the arithmetic average of the subject's ages. This plot shows only the effect of age, not ageing. The number of comparisons in each bin is generally in the thousands, however the first and last bins are computed over 149 and 124 respectively. The error rates in some (adult) cases are zero, and in others the DET is flat so the error rates at the two thresholds are identical. The lines span 1% and 99% of bootstrap replicated FNMR estimates.

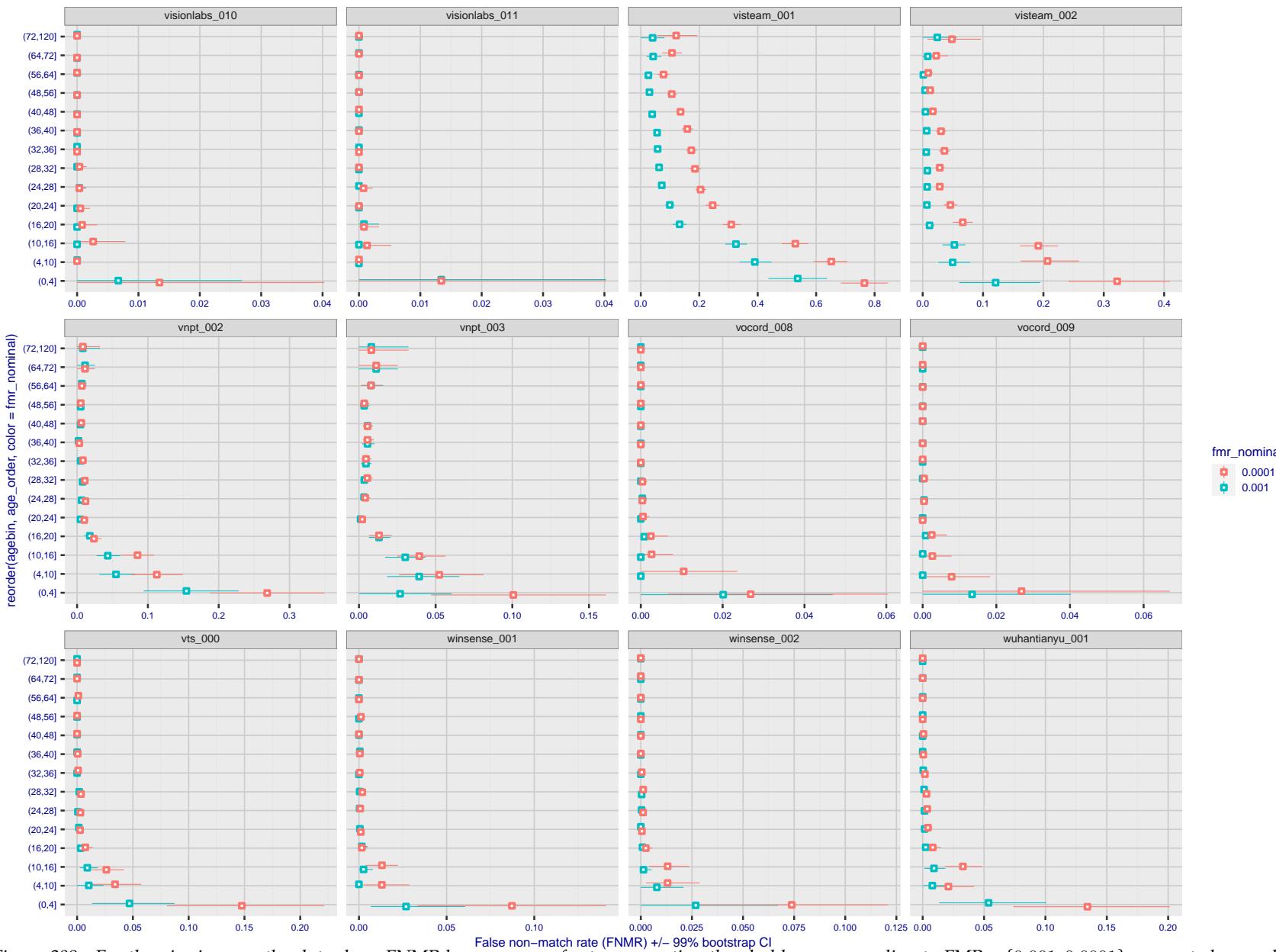


Figure 308: For the visa images, the dots show FNMR by age group for two operating thresholds corresponding to  $FMR = \{0.001, 0.0001\}$  computed over all on the order of  $10^{10}$  impostor scores. The FMR in each bin will vary also - see subsequent impostor heatmaps in sec. 3.6.2. Given a pair of face images taken at different times, we assign the comparison to the bin that is the arithmetic average of the subject's ages. This plot shows only the effect of age, not ageing. The number of comparisons in each bin is generally in the thousands, however the first and last bins are computed over 149 and 124 respectively. The error rates in some (adult) cases are zero, and in others the DET is flat so the error rates at the two thresholds are identical. The lines span 1% and 99% of bootstrap replicated FNMR estimates.

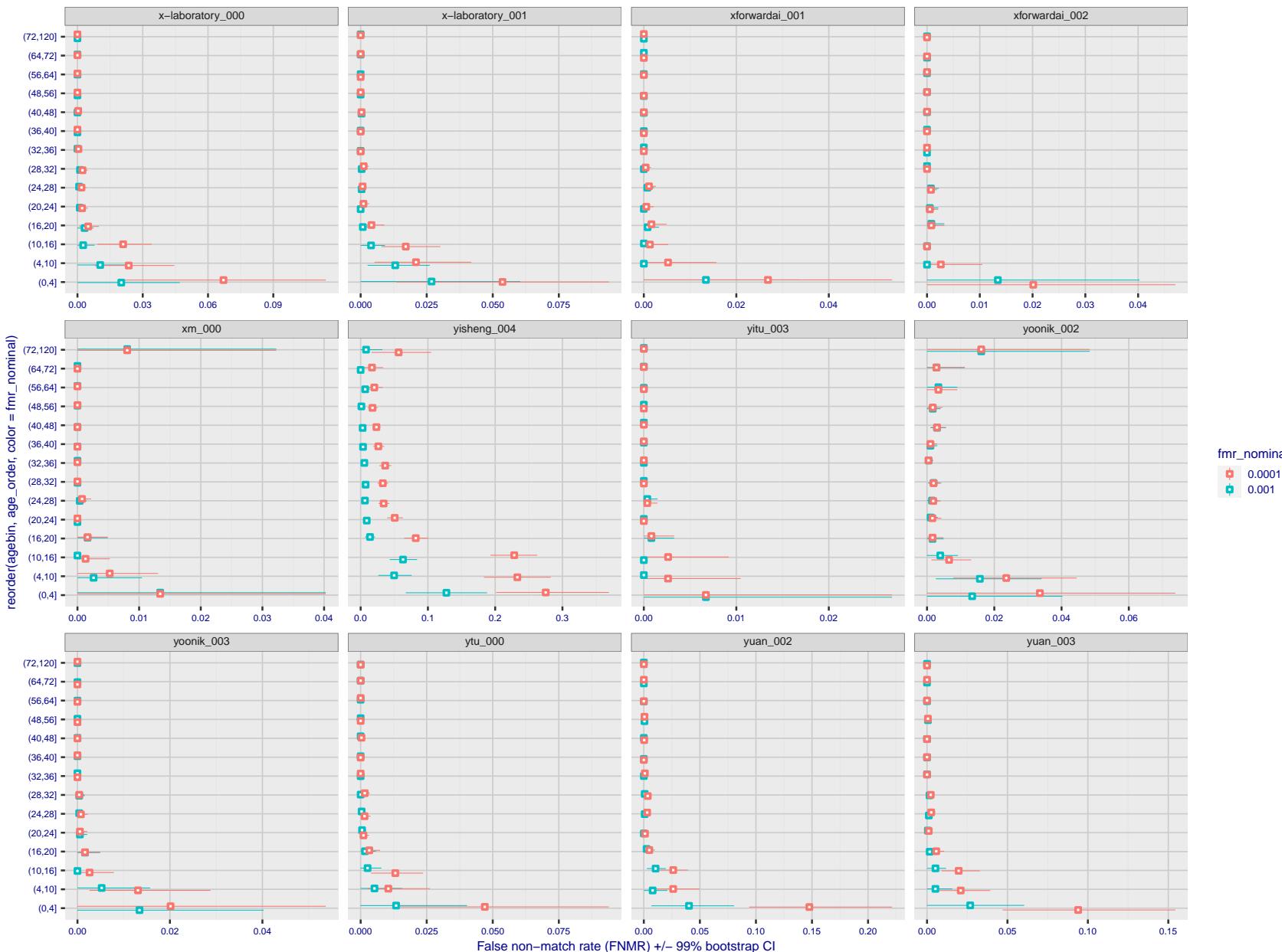


Figure 309: For the visa images, the dots show FNMR by age group for two operating thresholds corresponding to  $FMR = \{0.001, 0.0001\}$  computed over all on the order of  $10^{10}$  impostor scores. The FMR in each bin will vary also - see subsequent impostor heatmaps in sec. 3.6.2. Given a pair of face images taken at different times, we assign the comparison to the bin that is the arithmetic average of the subject's ages. This plot shows only the effect of age, not ageing. The number of comparisons in each bin is generally in the thousands, however the first and last bins are computed over 149 and 124 respectively. The error rates in some (adult) cases are zero, and in others the DET is flat so the error rates at the two thresholds are identical. The lines span 1% and 99% of bootstrap replicated FNMR estimates.

**Caveats:** None.

## 3.6 Impostor distribution stability

### 3.6.1 Effect of birth place on the impostor distribution

**Background:** Facial appearance varies geographically, both in terms of skin tone, cranio-facial structure and size. This section addresses whether false match rates vary intra- and inter-regionally.

**Goals:**

- ▷ To show the effect of birth region of the impostor and enrollee on false match rates.
- ▷ To determine whether some algorithms give better impostor distribution stability.

**Methods:**

- ▷ For the visa images, NIST defined 10 regions: Sub-Saharan Africa, South Asia, Polynesia, North Africa, Middle East, Europe, East Asia, Central and South America, Central Asia, and the Caribbean.
- ▷ For the visa images, NIST mapped each country of birth to a region. There is some arbitrariness to this. For example, Egypt could reasonably be assigned to the Middle East instead of North Africa. An alternative methodology could, for example, assign the Philippines to *both* Polynesia and East Asia.
- ▷ FMR is computed for cases where all face images of impostors born in region  $r_2$  are compared with enrolled face images of persons born in region  $r_1$ .

$$\text{FMR}(r_1, r_2, T) = \frac{\sum_{i=1}^{N_{r_1, r_2}} H(s_i - T)}{N_{r_1, r_2}} \quad (5)$$

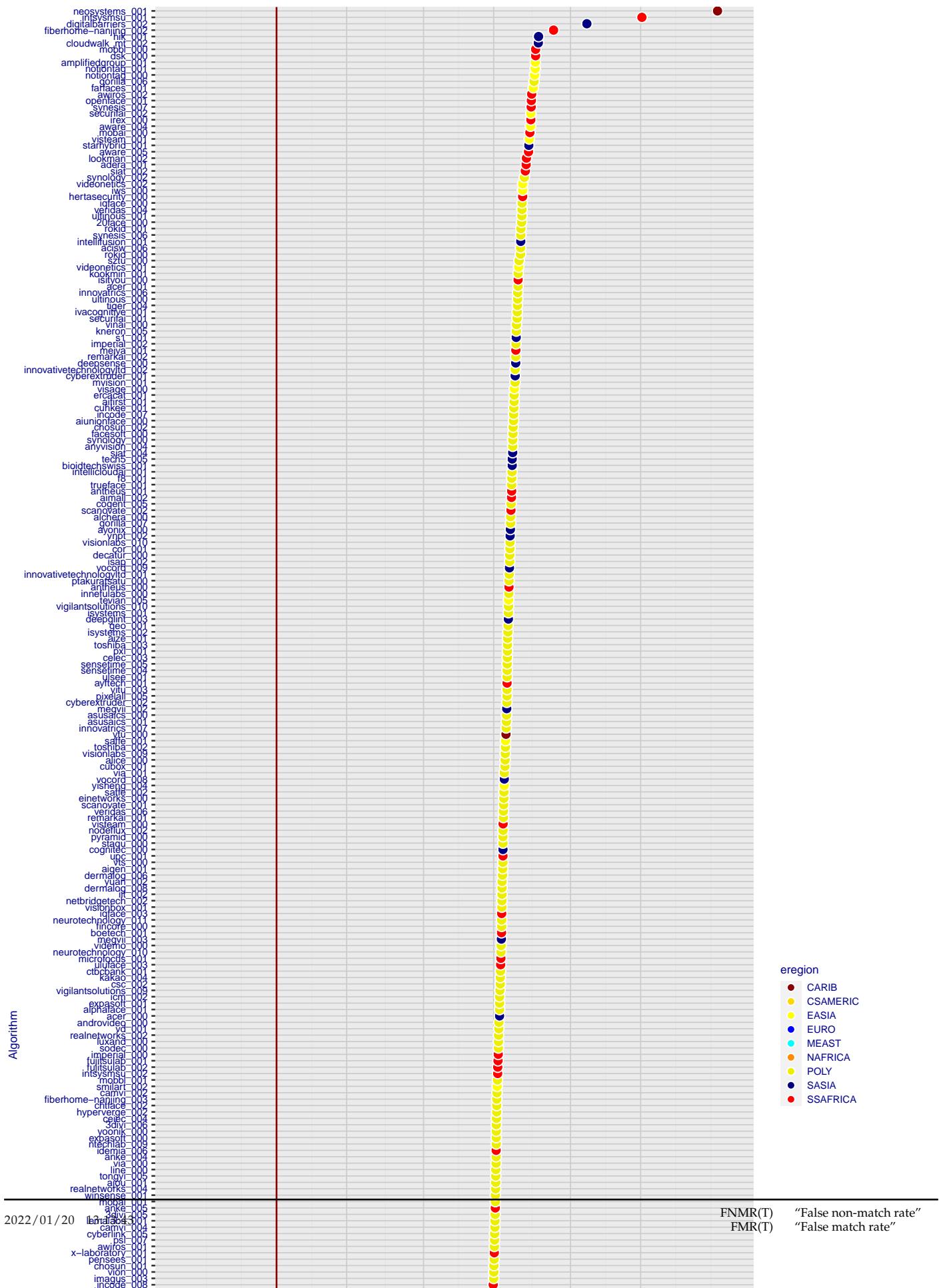
where the same threshold,  $T$ , is used in all cells, and  $H$  is the unit step function. The threshold is set to give  $\text{FMR}(T) = 0.001$  over the entire set of visa image impostor comparisons.

- ▷ This analysis is then repeated by country-pair, but only for those country pairs where both have at least 1000 images available. The countries<sup>1</sup> appear in the axes of graphs that follow.
- ▷ The mean number of impostor scores in any cross-region bin is 33 million. The smallest number of impostor scores in any bin is 135000, for Central Asia - North Africa. While these counts are large enough to support reasonable significance, the number of individual faces is much smaller, on the order of  $N^{0.5}$ .
- ▷ The numbers of impostor scores in any cross-country bin is shown in Figure ??.

**Results:** Subsequent figures show heatmaps that use color to represent the base-10 logarithm of the false match rate. Red colors indicate high (bad) false match rates. Dark colors indicate benign false match rates. There are two series of graphs corresponding to aggregated geographical regions, and to countries. The notable observations are:

- ▷ The on-diagonal elements correspond to within-region impostors. FMR is generally above the nominal value of  $\text{FMR} = 0.001$ . Particularly there is usually higher FMR in, Sub-Saharan Africa, South Asia, and the Caribbean. Europe and Central Asia, on the other hand, usually give FMR closer to the nominal value.
- ▷ The off-diagonal elements correspond to across-region impostors. The highest FMR is produced between the Caribbean and Sub-Saharan Africa.
- ▷ Algorithms vary.

<sup>1</sup>These are Argentina, Australia, Brazil, Chile, China, Costa Rica, Cuba, Czech Republic, Dominican Republic, Ecuador, Egypt, El Salvador, Germany, Ghana, Great Britain, Greece, Guatemala, Haiti, Hong Kong, Honduras, Indonesia, India, Israel, Jamaica, Japan, Kenya, Korea, Lebanon, Mexico, Malaysia, Nepal, Nigeria, Peru, Philippines, Pakistan, Poland, Romania, Russia, South Africa, Saudi Arabia, Thailand, Trinidad, Turkey, Taiwan, Ukraine, Venezuela, and Vietnam.



- ▷ We computed the same quantities for a global FMR = 0.0001. The effects are similar.

**Caveats:**

- ▷ The effects of variable impostor rates on one-to-many identification systems may well differ from what's implied by these one-to-one verification results. Two reasons for this are a) the enrollment galleries are usually imbalanced across countries of birth, age and sex; b) one-to-many identification algorithms often implement techniques aimed at stabilizing the impostor distribution. Further research is necessary.
- ▷ In principle, the effects seen in this subsection could be due to differences in the image capture process. We consider this unlikely since the effects are maintained across geography - e.g. Caribbean vs. Africa, or Japan vs. China.

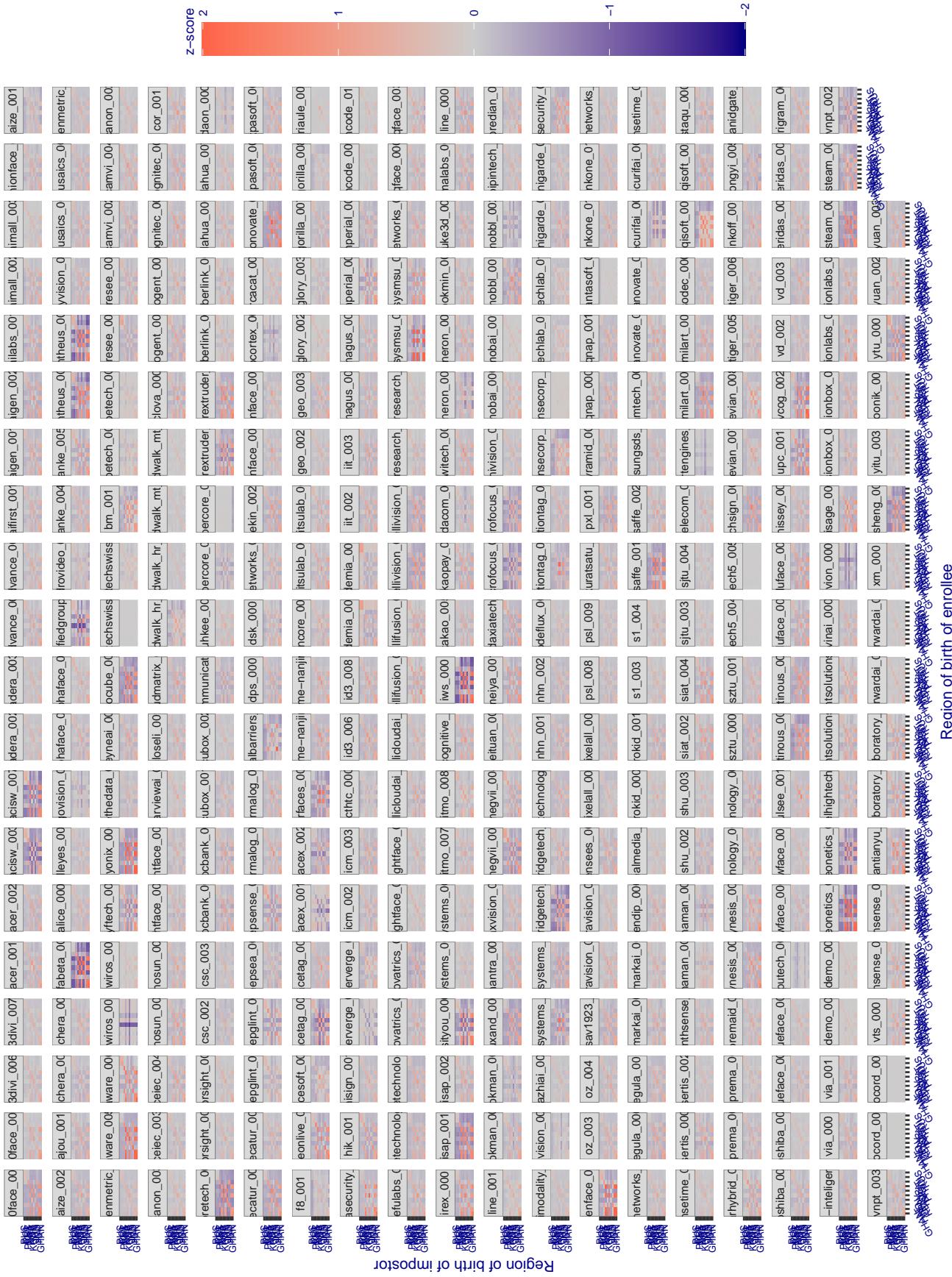


Figure 311: For visa images, the heatmap shows how the mean of the impostor distribution for the country pair (a,b) is shifted relative to the mean of the global impostor distribution, expressed as a number of standard deviations of the global impostor distribution. This statistic is designed to show shifts in the entire impostor distribution, not just tail effects that manifest as the anomalously high (or low) false match rates that appear in the subsequent figures. The countries are chosen to show that skin tone alone does not explain impostor distribution shifts. The reduced shift in Asian populations with the Yitu and Tong YiTrans algorithms, is accompanied by positive shifts in the European populations. This reversal relative to most other algorithms, may derive from use of nationally weighted training sets. The figure is computed from same-sex and same-age impostor pairs.

### 3.6.2 Effect of age on impostors

**Background:** This section shows the effect of age on the impostor distribution. The ideal behaviour is that the age of the enrollee and the impostor would not affect impostor scores. This would support FMR stability over sub-populations.

#### Goals:

- ▷ To show the effect of relative ages of the impostor and enrollee on false match rates.
- ▷ To determine whether some algorithms have better impostor distribution stability.

#### Methods:

- ▷ Define 14 age group bins, spanning 0 to over 100 years old.
- ▷ Compute FMR over all impostor comparisons for which the subjects in the enrollee and impostor images have ages in two bins.
- ▷ Compute FMR over all impostor comparisons for which the subjects are additionally of the same sex, and born in the same geographic region.

#### Results:

The notable aspects are:

- ▷ Diagonal dominance: Impostors are more likely to be matched against their same age group.
- ▷ Same sex and same region impostors are more successful. On the diagonal, an impostor is more likely to succeed by posing as someone of the same sex. If  $\Delta \log_{10} \text{FMR} = 0.2$ , then same-sex same-region FMR exceeds the all-pairs FMR by factor of  $10^{0.2} = 1.6$ .
- ▷ Young children impostors give elevated FMR against young children. Older adult impostor give elevated FMR against older adults. These effects are quite large, for example if  $\Delta \log_{10} \text{FMR} = 1.0$  larger than a 32 year old, then these groups have higher FMR by a factor of  $10^1 = 10$ . This would imply an FMR above 0.01 for a nominal (global) FMR = 0.001.
- ▷ Algorithms vary.
- ▷ We computed the same quantities for a global FMR = 0.0001. The effects are similar.

Note the calculations in this section include impostors paired across all countries of birth.

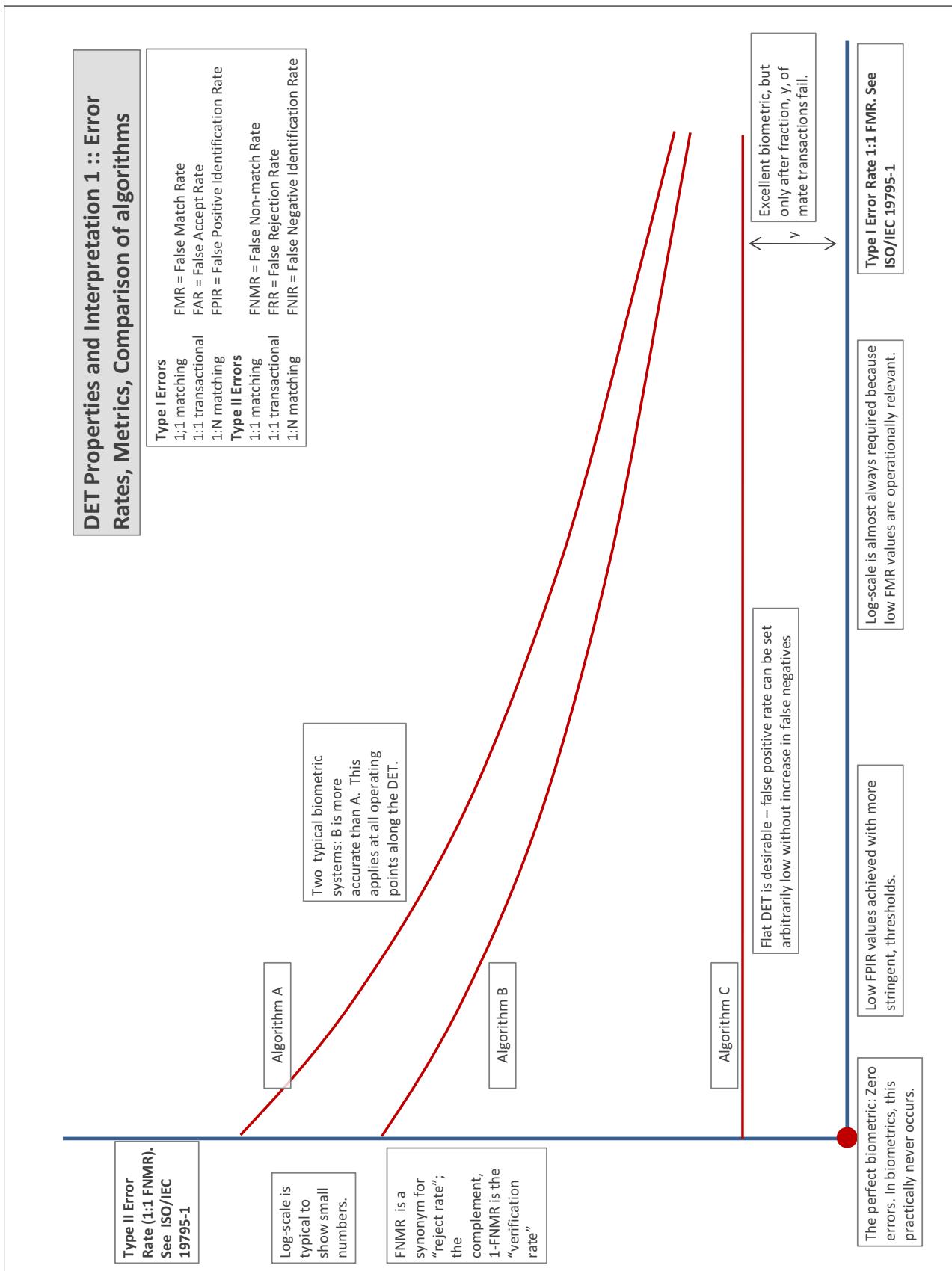
# Accuracy Terms + Definitions

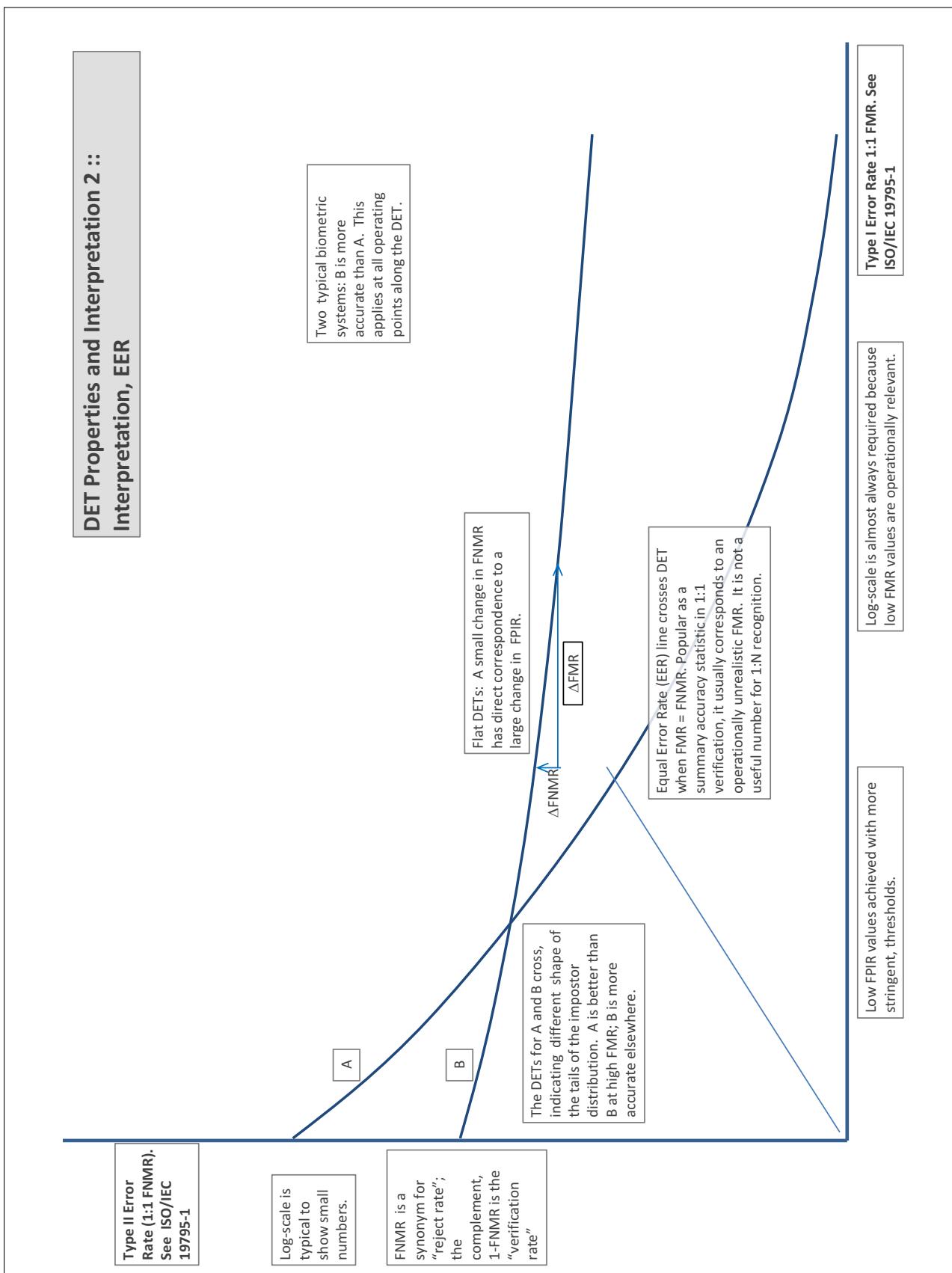
In biometrics, Type II errors occur when two samples of one person do not match – this is called a **false negative**. Correspondingly, Type I errors occur when samples from two persons do match – this is called a **false positive**. Matches are declared by a biometric system when the native comparison score from the recognition algorithm meets some **threshold**. Comparison scores can be either **similarity scores**, in which case higher values indicate that the samples are more likely to come from the same person, or **dissimilarity scores**, in which case higher values indicate different people. Similarity scores are traditionally computed by **fingerprint** and **face** recognition algorithms, while dissimilarities are used in **iris recognition**. In some cases, the dissimilarity score is a distance; this applies only when **metric** properties are obeyed. In any case, scores can be either **mate** scores, coming from a comparison of one person's samples, or **nonmate** scores, coming from comparison of different persons' samples. The words **genuine** or **authentic** are synonyms for mate, and the word **impostor** is used as a synonym for nonmatch. The words mate and nonmatch are traditionally used in identification applications (such as law enforcement search, or background checks) while genuine and impostor are used in verification applications (such as access control).

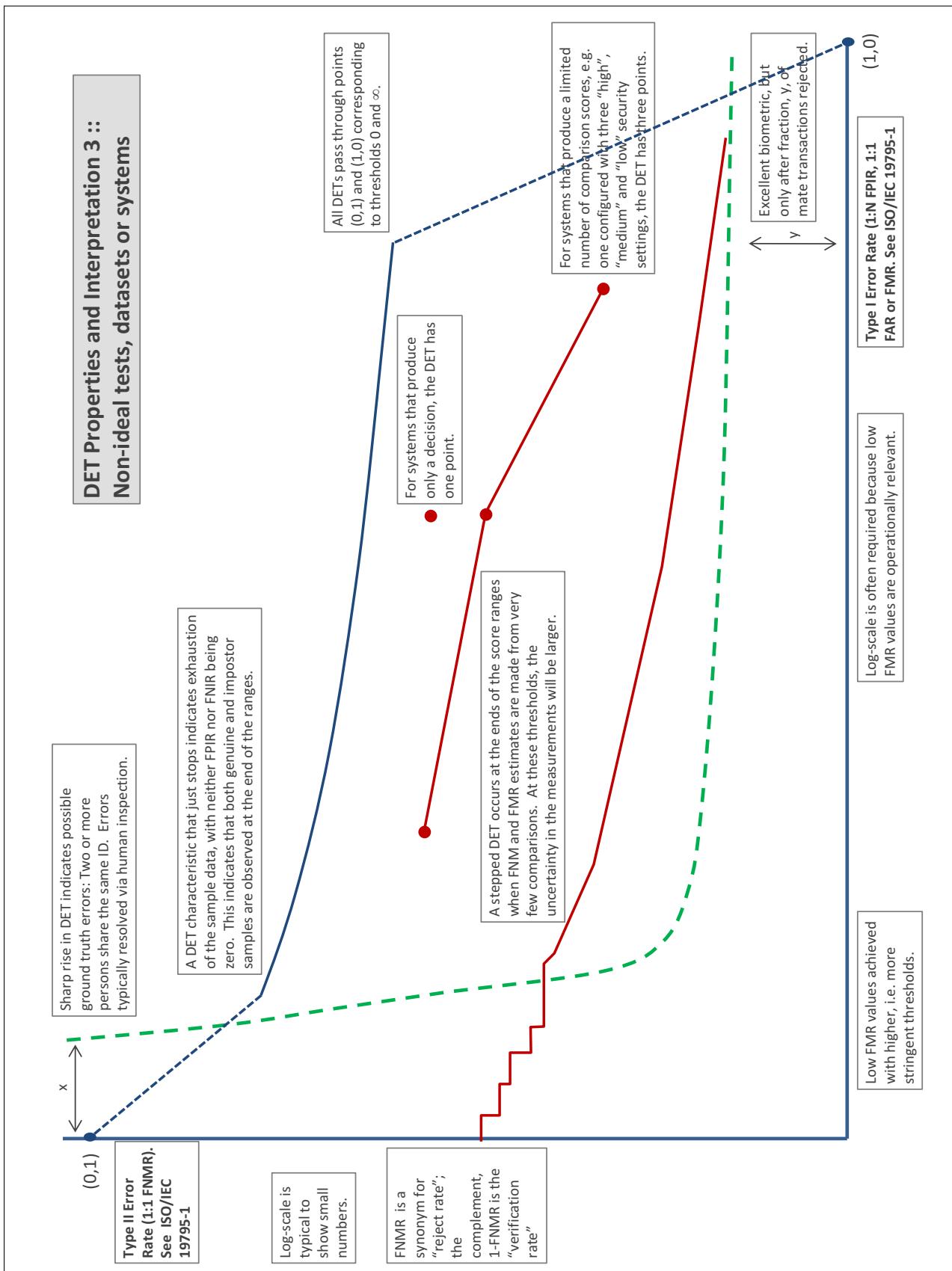
A **error tradeoff** characteristic represents the tradeoff between Type II and Type I classification errors. For verification this plots false non-match rate (FNMR) vs. false match rate (FMR) parametrically with T.

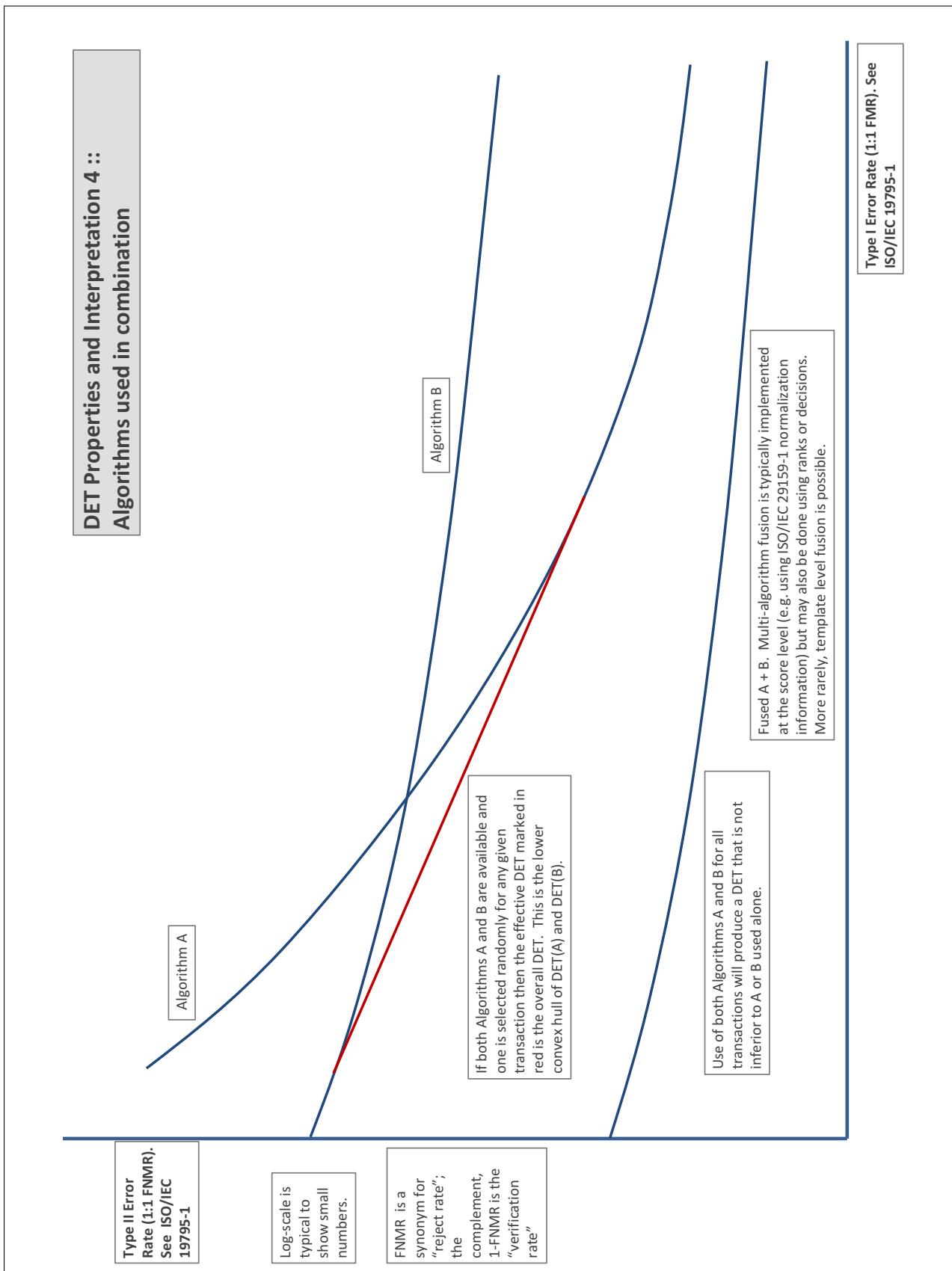
The error tradeoff plots are often called **detection error tradeoff (DET)** characteristics or **receiver operating characteristic (ROC)**. These serve the same function but differ, for example, in plotting the complement of an error rate (e.g.,  $TMR = 1 - FNMR$ ) and in transforming the axes most commonly using logarithms, to show multiple decades of FMR. More rarely, the function might be the inverse Gaussian function.

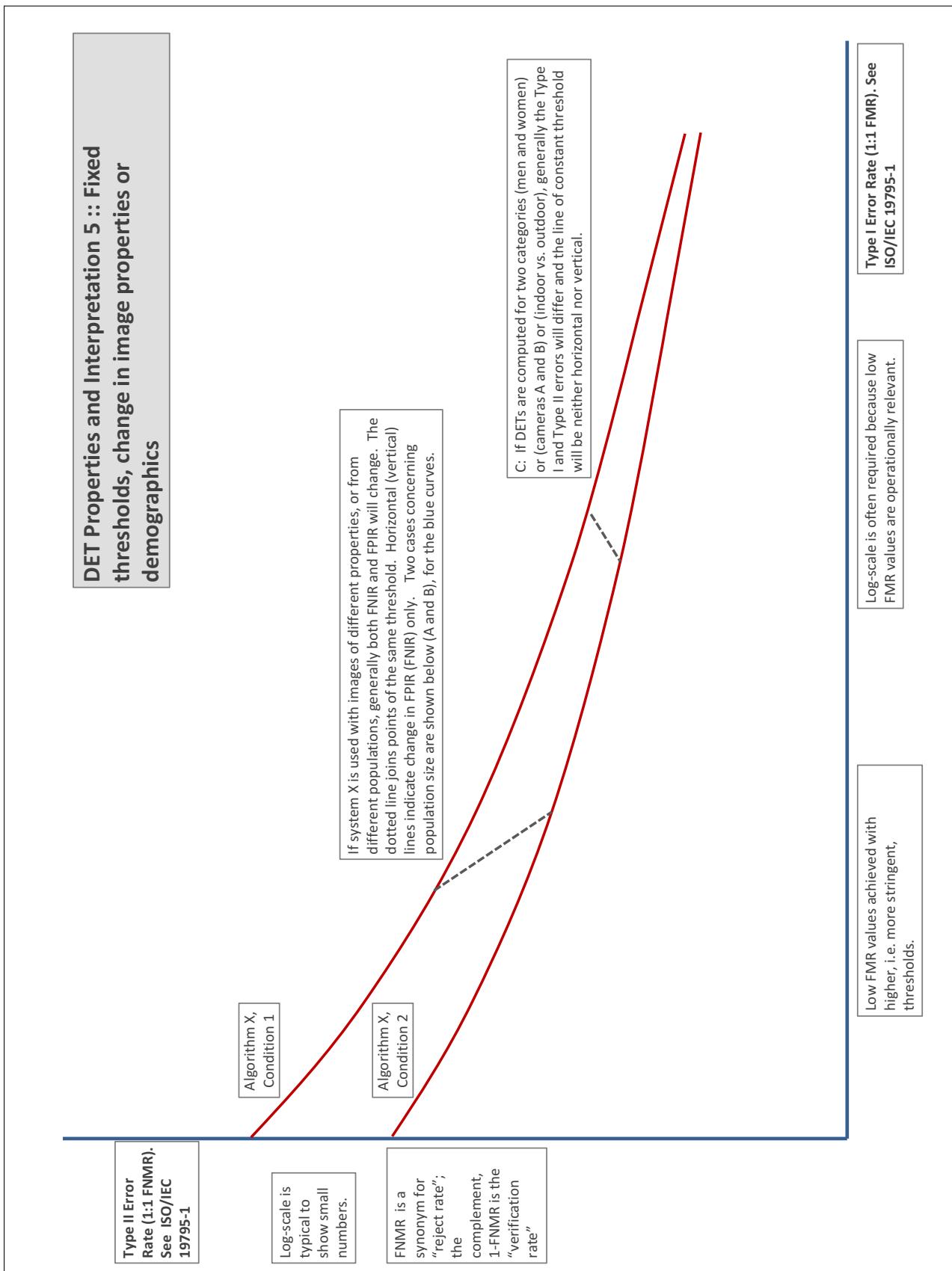
More detail and generality is provided in formal biometrics testing standards, see the various parts of [ISO/IEC 19795 Biometrics Testing and Reporting](#). More terms, including and beyond those to do with accuracy, see [ISO/IEC 2382-37 Information technology -- Vocabulary -- Part 37: Harmonized biometric vocabulary](#)











## References

- [1] P. Jonathon Phillips, Amy N. Yates, Ying Hu, Carina A. Hahn, Eilidh Noyes, Kelsey Jackson, Jacqueline G. Cavazos, Géraldine Jeckeln, Rajeev Ranjan, Swami Sankaranarayanan, Jun-Cheng Chen, Carlos D. Castillo, Rama Chellappa, David White, and Alice J. O'Toole. Face recognition accuracy of forensic examiners, superrecognizers, and face recognition algorithms. *Proceedings of the National Academy of Sciences*, 115(24):6171–6176, 2018.